To: Conmy, Robyn[Conmy.Robyn@epa.gov]
Cc: Holder, Edith[holder.edith@epa.gov];
raghuraman.venkatapathy@ptsied.com[raghuraman.venkatapathy@ptsied.com]
From: Venkatapathy, Raghuraman
Sent: Mon 2/8/2016 4:32:48 PM
Subject: FW: PCR samples- dispersant project
PCR Samples ID.docx

Hi Robyn,

Sorry, I forgot to cc you on this.

Thanks,

raghu

Raghuraman Venkatapathy
On-Site Technical Manager
Pegasus Technical Services, Inc.
On-Site Contractor to U.S. EPA
NRMRL-STD/LRPCD, MS: 443
26 W. Martin Luther King Jr. Drive
Cincinnati, OH 45268.
Phone: (513) 569 7077 (O)/(513) 549 7880 (GV)
Fax: (513) 569 7677.
e-mail: venkatapathy.raghuraman@epa.gov

raghuraman.venkatapathy@ptsied.com

From: Venkatapathy, Raghuraman
Sent: Monday, February 08, 2016 11:31
To: Elk, Michael <Elk.Michael@epa.gov>
Cc: SantoDomingo, Jorge <Santodomingo.Jorge@epa.gov>;
'raghuraman.venkatapathy@ptsied.com' <raghuraman.venkatapathy@ptsied.com>
Subject: FW: PCR samples- dispersant project

Hey Mike,

The list of samples that need to be analyzed (please see the email below for a priority list) is attached.

Thanks,

raghu

Raghuraman Venkatapathy
On-Site Technical Manager
Pegasus Technical Services, Inc.
On-Site Contractor to U.S. EPA
NRMRL-STD/LRPCD, MS: 443
26 W. Martin Luther King Jr. Drive
Cincinnati, OH 45268.
Phone: (513) 569 7077 (O)/(513) 549 7880 (GV)
Fax: (513) 569 7677.
e-mail: venkatapathy.raghuraman@epa.gov

raghuraman.venkatapathy@ptsied.com

From: Devi Sundaravadivelu [mailto:devis.255@gmail.com]
Sent: Thursday, January 21, 2016 19:05
To: Raghuraman Venkatapathy <raghuraman.venkatapathy@ptsied.com>
Cc: BOL-Zhang, Yu (zhang4y5) <zhang4y5@mail.uc.edu>
Subject: PCR samples- dispersant project

Hi Raghu,

Please find below the vials IDs for the cryo and meso samples on Day 0, 16 and 24. Since there so many samples (180 x 3), it would be great if these days are analyzed first (18 vials x 3 runs).

Day 0 : 1-3 (5 C), 4-6 (25 C)

Day 16: 88-90 (5 C), 97-99 (25 C)

Day 24: 106-108 (5 C), 115-117 (25 C)

The vial IDs were the same each time the experiments were run, the only difference is the date they were collected.

Experiment 1 was conducted with ANS and Corexit in Winter 2013.

Experiment 2 was conducted with ANS and Finasol in March 2015.

Experiment 3 was conducted with Endicott and Corexit and started in December 2015.

Please let me know if you have any questions.

Thanks,

Devi

To: Brian Robinson[Brian.Robinson@dfo-mpo.gc.ca]; Conmy, Robyn[Conmy.Robyn@epa.gov]
From: Robyn Conmy
Sent: Mon 2/1/2016 8:28:59 PM
Subject: edits to presentation
GoMRI Presentation - Robinson.pptx

Hi Brian,

I made some edits to the text on a few slides and also added some notes to some as well. We can talk about this tomorrow if you like.

Cheers,
Robyn

SURFACE VOC EMISSIONS FROM SUBSURFACE OILS RELEASES WITH AND WITHOUT DISPERSANT APPLICATION

Brian Robinson, Thomas King, Scott Ryan, Patrick Toole, Claire McIntyre, Michel Boufadel, Robyn Conmy, Haibo Niu, Kenneth Lee

[1] Fisheries and Oceans Canada, Dartmouth, Nova Scotia, Canada
[2] New Jersey Institute of Technology, Newark, New Jersey, USA
[3] US Environmental Protection Agency, Cincinnati, Ohio, USA
[4] Dalhousie University, Halifax, Nova Scotia, Canada
[5] CSIRO, Kensington, WA, Australia

Fisheries and Oceans Canada Pêches et Océans Canada

BSEE

DALHOUSIE UNIVERSITY

NJIT New Jersey's Science & Technology University

UNITED STATES ENVIRONMENTAL PROTECTION AGENCY

Presentation Outline

- Project Introduction
  - Background
  - Project Objectives
- Description of flume tank facility
  - Test Treatments
  - Experimental Protocol
- Results
- Summary and Conclusions

Introduction

- The Deepwater Horizon oil spill resulted in a large scale oil spill response effort utilizing:
  - Booming and skimming
  - In-situ burning
  - Surface dispersant spraying
  - Subsurface dispersant injection

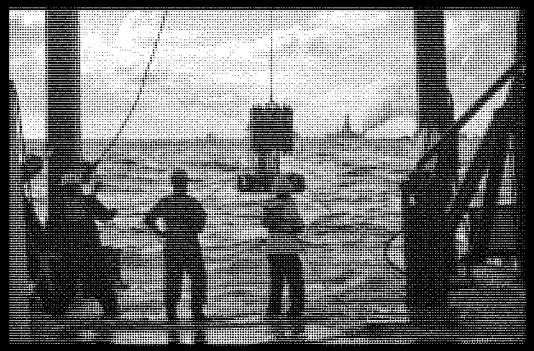

- Represented the first time dispersants had been used at depth to mitigate a wellhead blowout
- Post spill scientific research focused on gaining a better understanding of dispersant effectiveness at depth

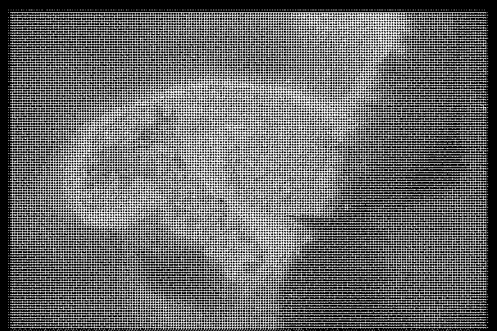

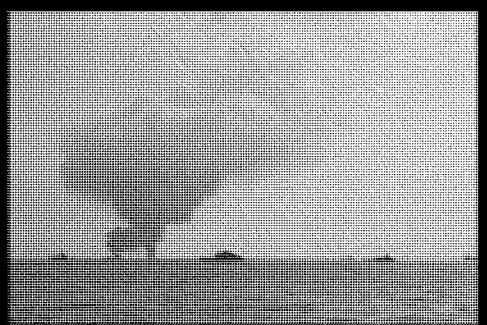

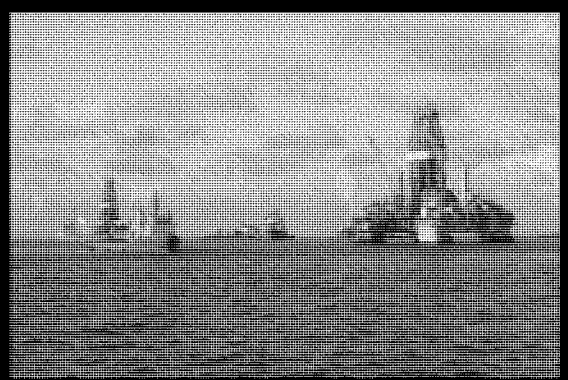

VOC Emissions from Crude Oil Spills

- Volatile Organic Compounds (VOCs) are emitted into the atmosphere as crude oil reaches the seawater surface and undergoes natural weathering
- VOCs are a human health concern
  - Acute Toxicity of airborne hydrocarbons
  - Chronic toxicity of aerosols formed as VOCs oxidize
- Very little published information on the effect of dispersant use on VOC emissions
  - Surface dispersant spraying was used to keep VOC emissions below 50 ppm (Curd 2011)

Experimental Objectives

- To measure surface VOC concentrations during flume tank studies using an underwater jet release of oil
- Component of a larger BSEE funded project:
  - Subsurface dispersant effectiveness
  - In-situ droplet size analysis
  - Evaluation crude oil fluorescence response tools
  - Numerical modelling of oil jets

Description of Facility

- Wave Tank facility has been used since 2005 for dispersant effectiveness testing
- Flume Tank was constructed in 2013 to study the transport of subsurface oil plumes
  - Inner Dimensions of 30 m x 2 m x 0.6 m
  - Operational volume of 30,000 L
  - High flow pumping system (5 cm s^{-1})

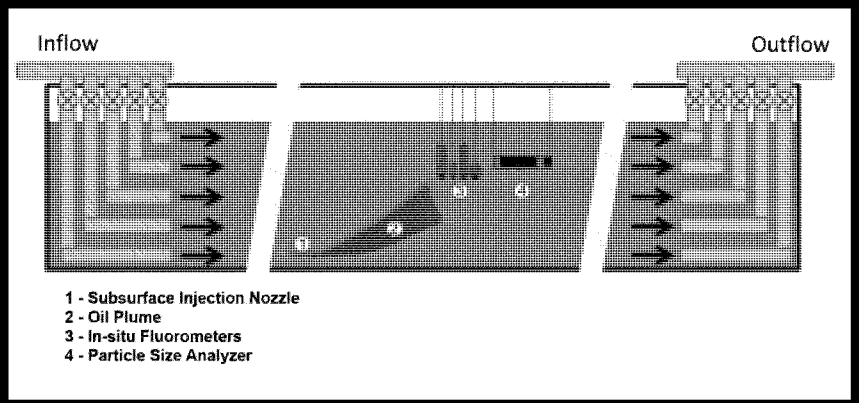

Subsurface Oil Injection System

- Underwater oil plumes are generated using a custom engineered subsurface injector
  - Stainless Steel Pressure Vessel
  - 40 psi
  - 80°C
  - 2.4 mm diameter nozzle

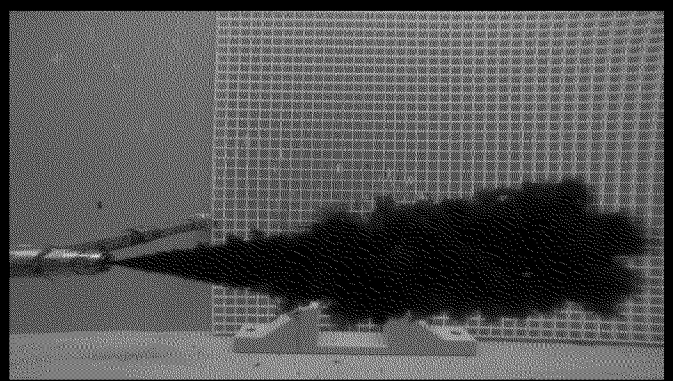

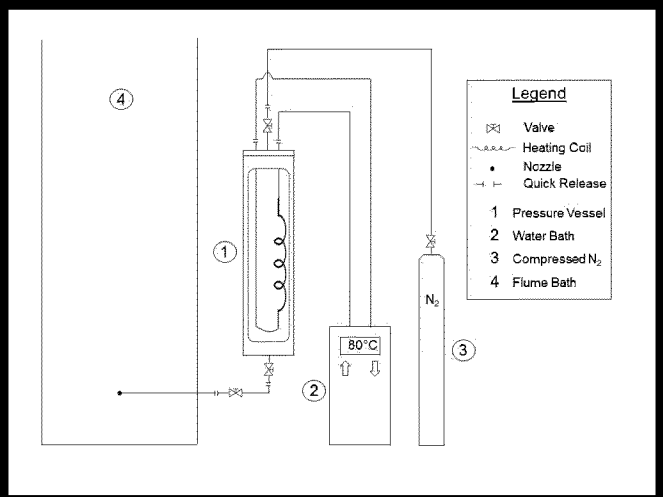

Video of Subsurface Injection

- 1-2 vidoes showing underwater injection

Experimental Treatments

- Four hydrocarbon products tested:
  - Alaska North Slope Crude (ANS)
  - Sweet Louisiana Crude (SLC)
  - Gas Condensate (CND)
  - Intermediate Fuel Oil 120 (IFO)
- All products tested with and without chemical dispersants
  - Corexit EC9500A
  - DOR 1:20, 1:100, 1:200
- Experiments conducted in triplicate in both cold (<10°C) and warm water (>10°C) seasons

Experimental Protocol

- Flume tank filled with filtered seawater
- Instruments placed in tank
  - VOC Meter – ToxiRAE Pro PID Portable Gas Detector
  - LISST Particle Size Analyzer
- Experiment started:
  - Flow turned on
  - Background collected
  - Oil injected
  - Water samples collected over 12 minutes

VOC Results – Alaska North Slope Crude

VOC Measurements

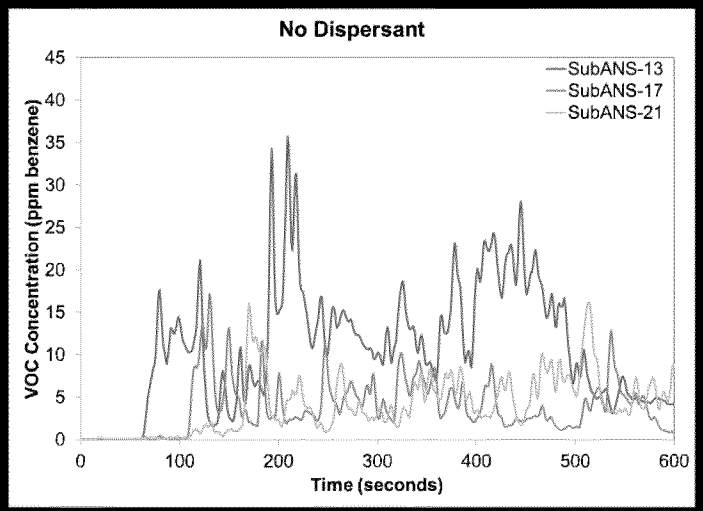

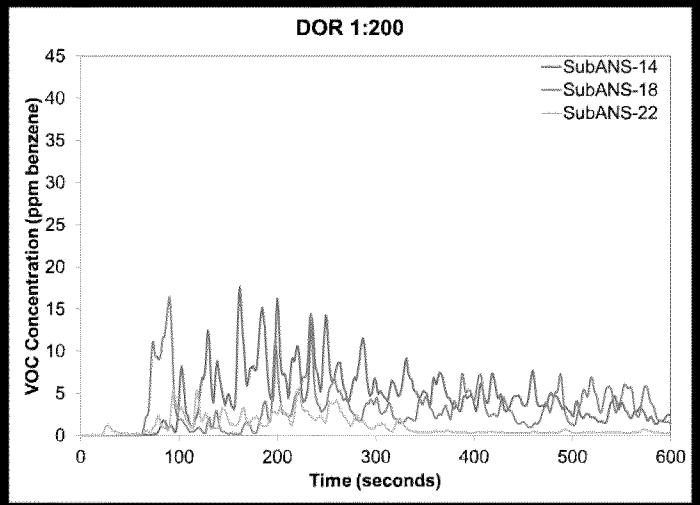

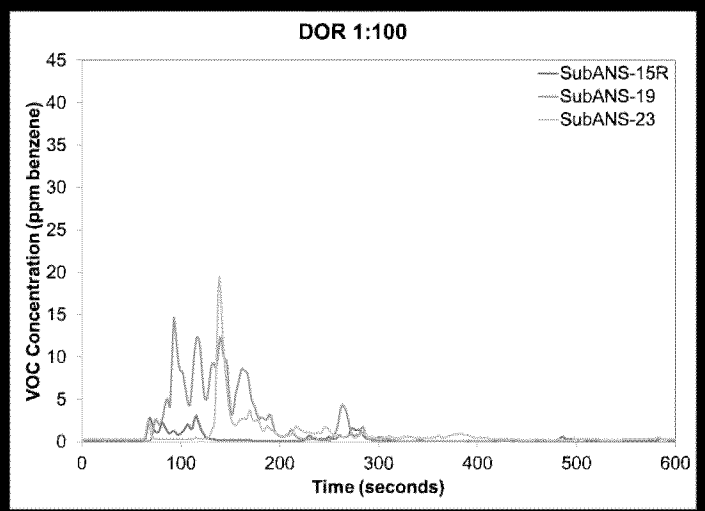

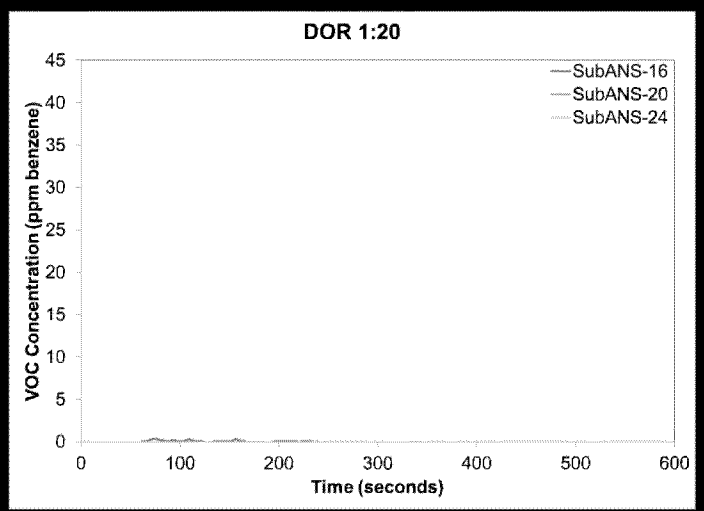

VOC Results – Sweet Louisiana Crude

VOC Measurements

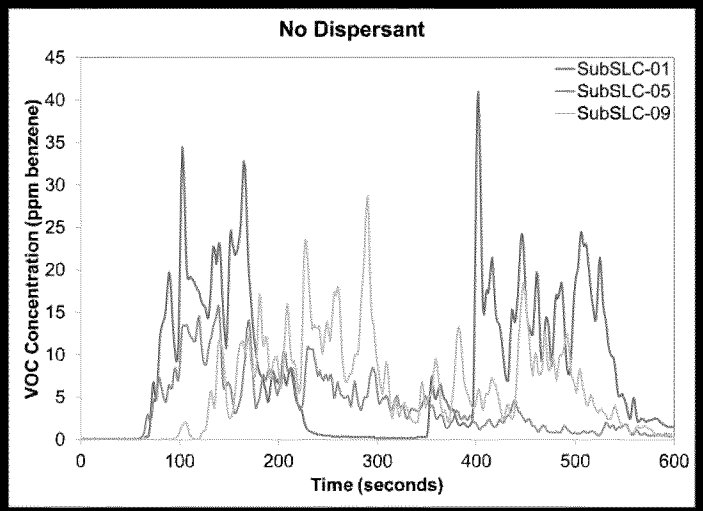

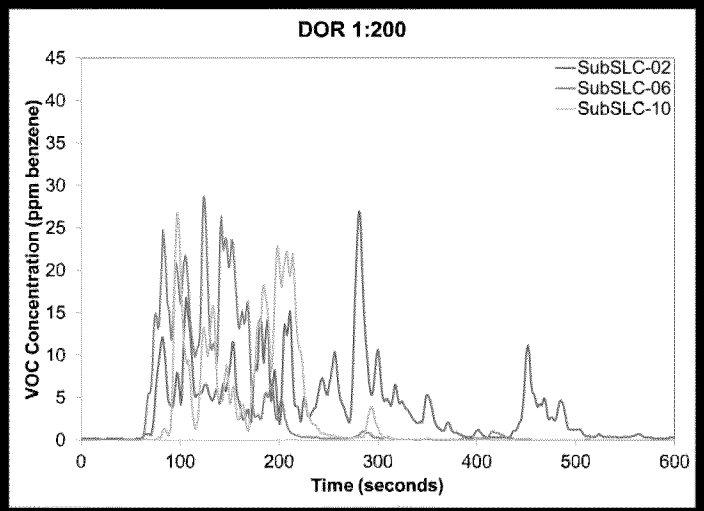

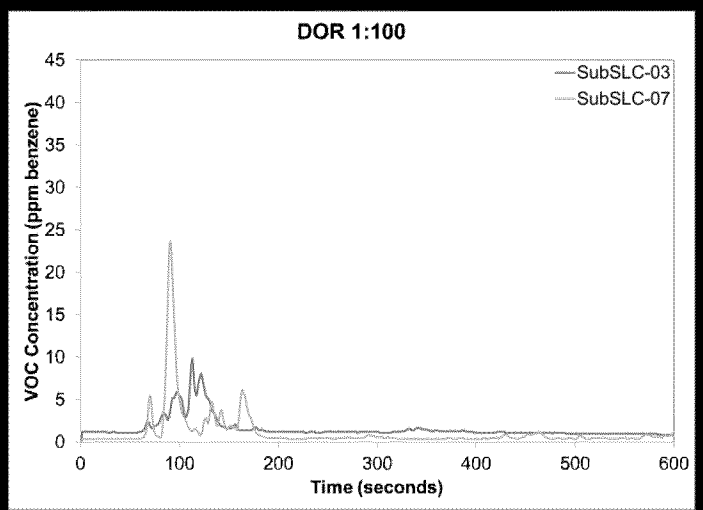

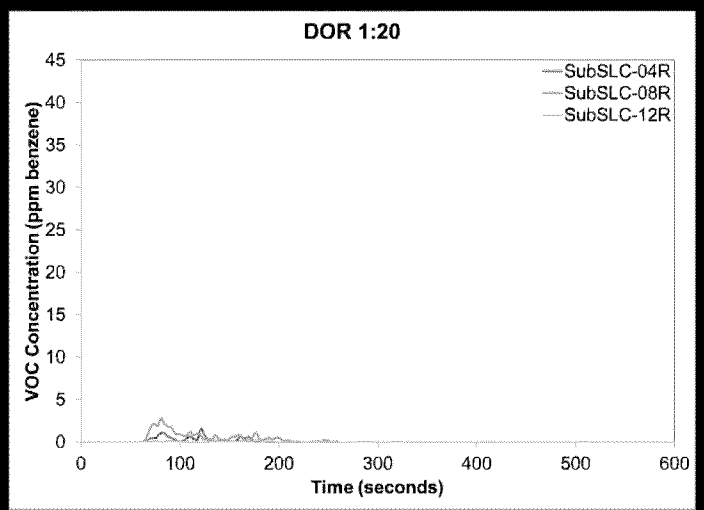

VOC Results – IFO-120

VOC Measurements

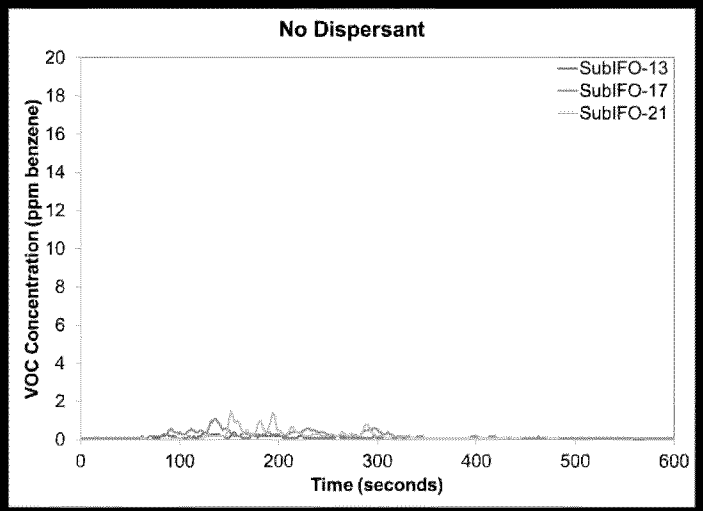

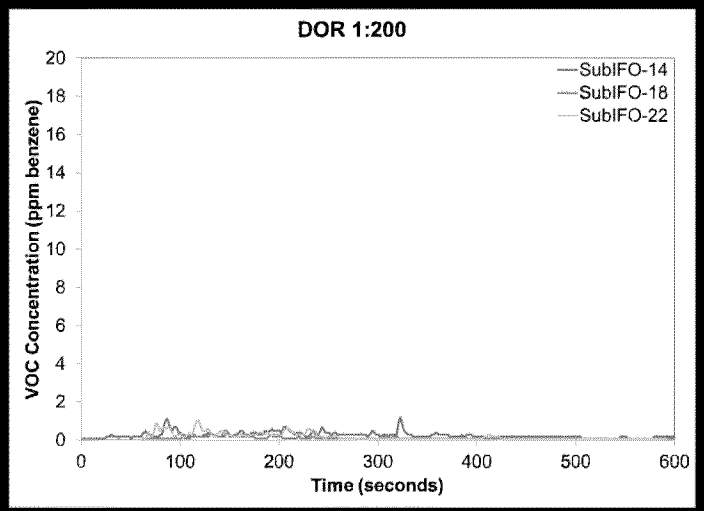

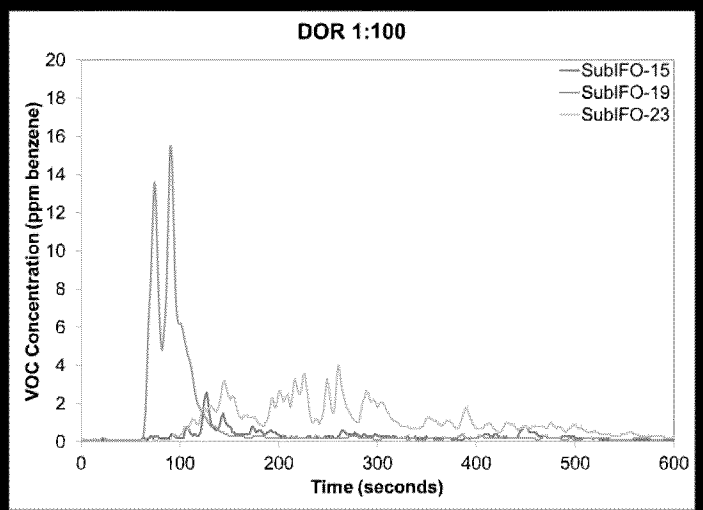

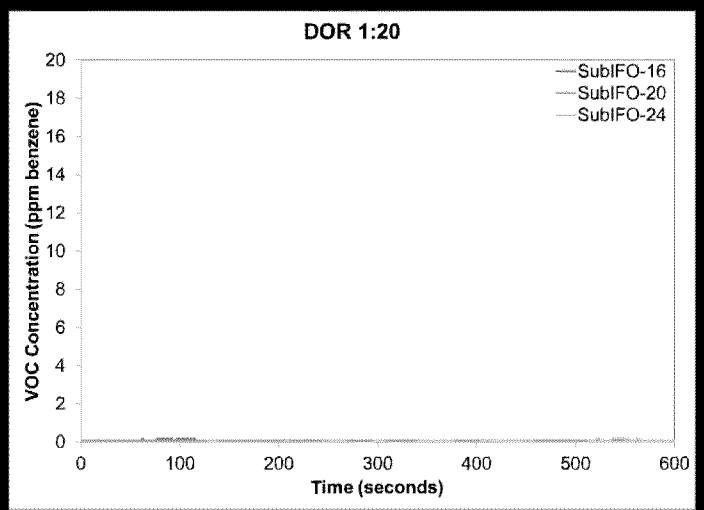

VOC Results – Gas Condensate

VOC Measurements

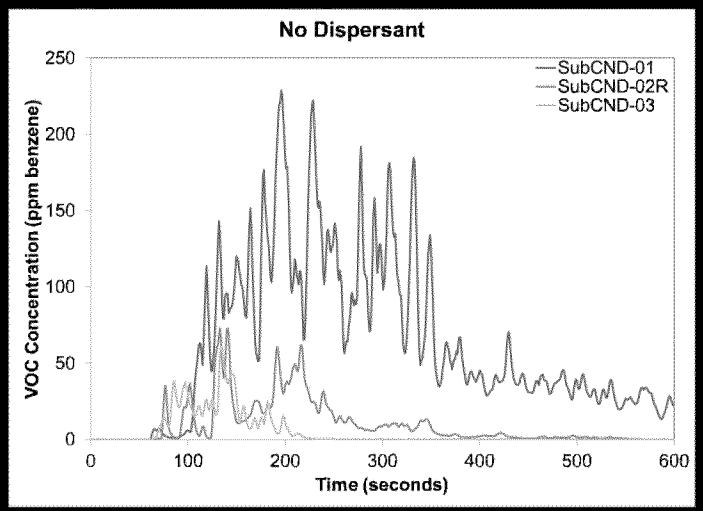

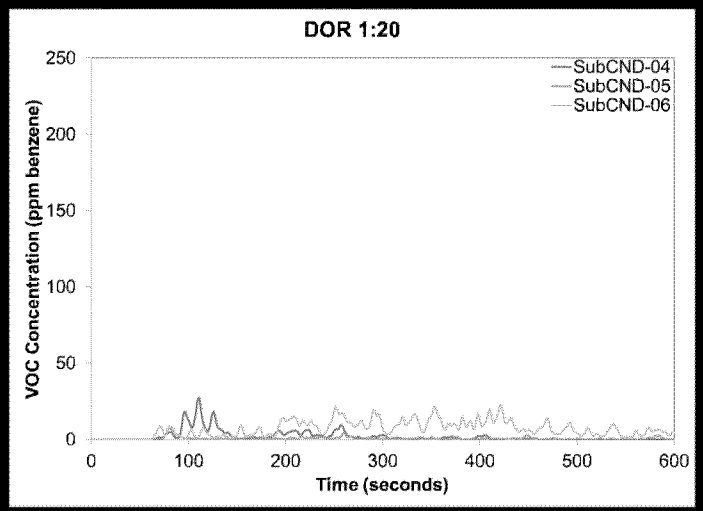

Droplet Size Results

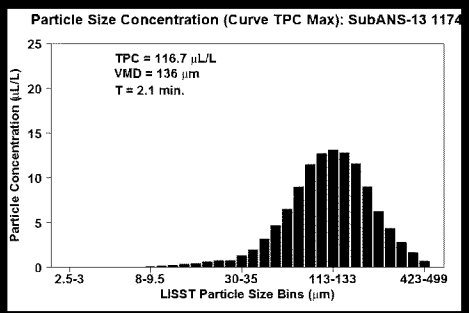

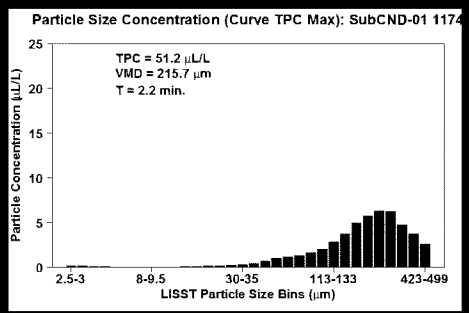

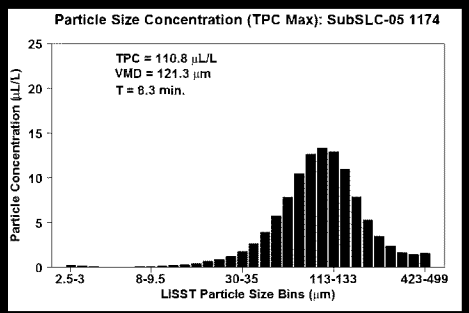

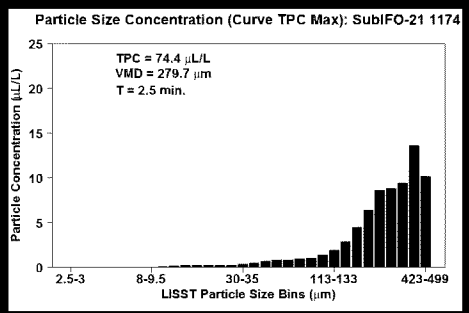

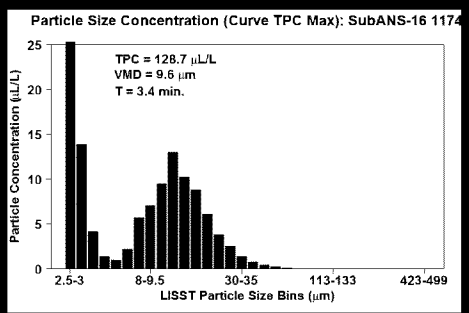

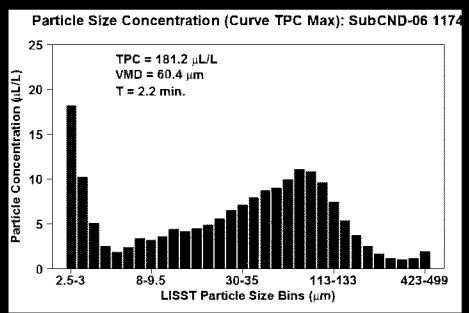

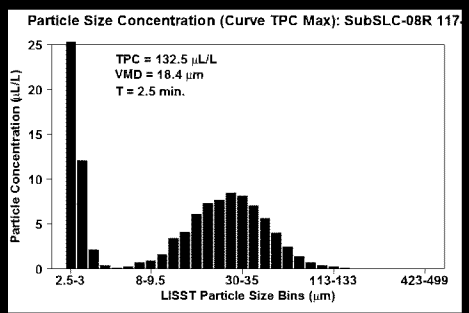

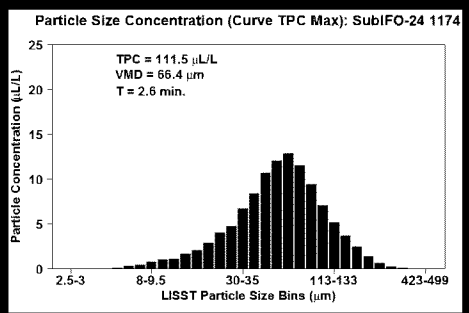

Results – BTEX Water Column Results

ANS

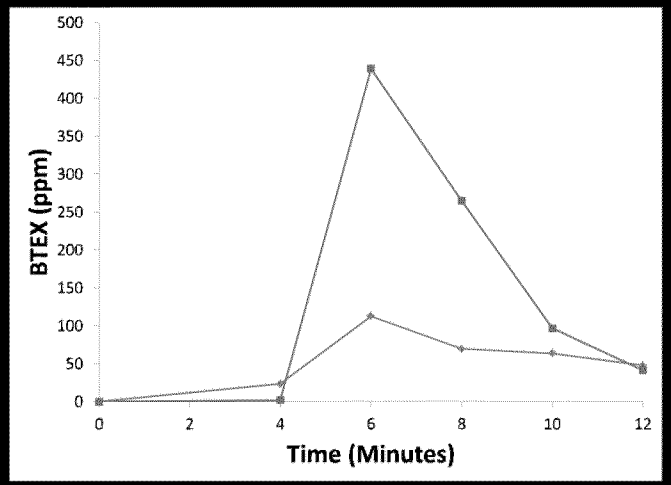

SLC

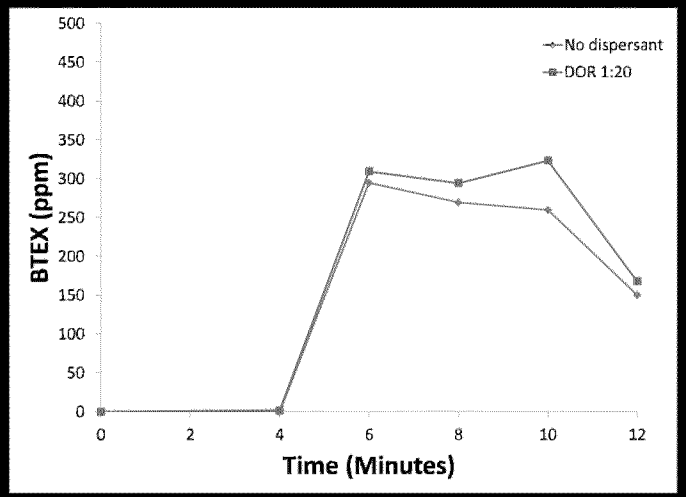

IFO-120

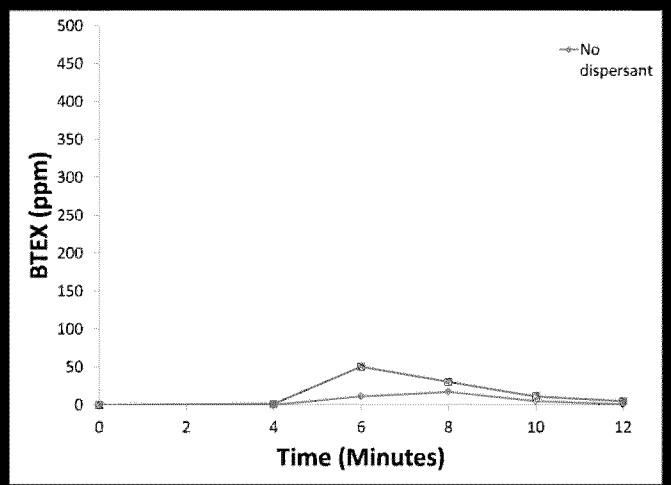

CND

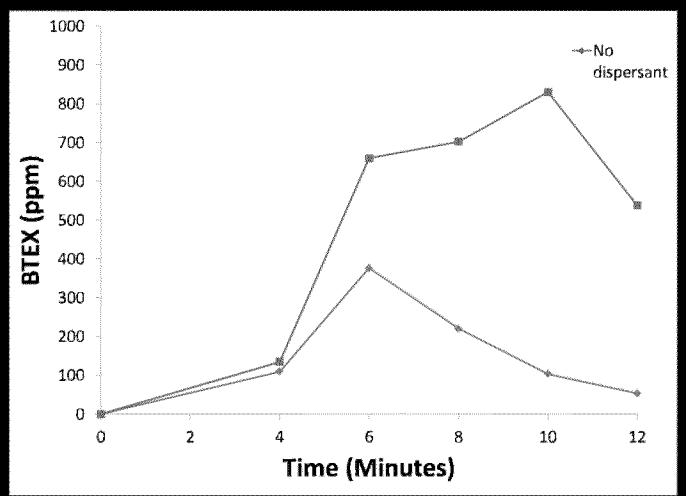

Results Summary

- VOC emissions followed the order of Gas Condensate > ANS/SLC > IFO
- Dispersant increased water column BTEX concentrations for all oils tested
- Trend of decreasing oil droplet size with increasing DOR

	Avg. Peak VOC Concentration ppm benzene, n = 3				Viscosity cst @ 15°C	Density g ml⁻¹	BTEX Content (% total)
Oil Type	No Dispersant	DOR 1:200	DOR 1:100	DOR 1:20			
ANS	23.07	13.27	12.43	0.13	18.9		2.3 %
IFO-120	1.00	0.90	7.37	0.17	2481.5		0.2 %
Condensate	121.23	--	--	19.73	0.5		13.4 %
SLC	28.53	27.5	16.75	1.53	8.2		2.4 %

Conclusion and Future Research

- VOC emissions are correlated to type of hydrocarbon product
- Regardless of the oil type, air VOC concentrations were lower for experiments with dispersant compared to those without
- Future research to focus on using Live Oil/Gas mixtures, separate dispersant injection system, surface aerosol formation and more advanced air analysis techniques

To: Conmy, Robyn[Conmy.Robyn@epa.gov]
Cc: Makram Suidan[msuidan@aub.edu.lb]; Campo Moreno, Pablo[P.Campo-Moreno@cranfield.ac.uk]; Sundaravadivelu, Devi (sundardi)[sundardi@mail.uc.edu]
From: Zhuang, Mobing (zhuangmg)
Sent: Mon 5/2/2016 3:57:45 PM
Subject: Manuscript for EPA Clearance Review
ANS_Manuscript_042716_MZ.docx
ANS_SupportingInformation_031016.docx
Manuscript_Data.xlsx
SupportingInformation_Data.xlsx

Hi Dr. Conmy,

Please find my manuscript to be submitted for EPA clearance review in the attachment. As requested, the raw data both for the manuscript and supporting information are included (the excel files in the attachment). I will also send a copy of the manuscript to Dr. SantoDomingo. Let me know if there is any question regarding my submission.

Thanks!

Regards,
Mobing Zhuang

PH.D Candidate
Department of Environmental Engineering
University of Cincinnati
Cincinnati, OH 45221

Biodegradability of Different Initial Concentrations of Alaska North Slope Crude Oil Dispersed with Corexit C9500

Mobing Zhuang[1], Gulizhaer Abulikemu[2], Pablo Campo[3*], William Platten III[4], Makram T. Suidan[5], Albert D. Venosa (retired)[4]and Robyn N. Conmy[4]

1 Department of Biomedical, Chemical and Environmental Engineering, University of Cincinnati, 2901 Woodside Drive, Cincinnati, OH 45221, USA

2 Pegasus Technical Services Inc., 46 E Hollister St, Cincinnati, OH 45219 USA

3 Cranfield Water Science Institute, Cranfield University, Cranfield, Beds, MK43 0AL, UK

4 U.S. Environmental Protection Agency, NRMRL, 26 W. MLK Drive Cincinnati, OH, 45268, USA

5 Faculty of Engineering and Architecture, American University of Beirut, Bechtel Engineering Bldg. - 3rd flr. - Room 308 P.O. Box: 11-0236 Riad El Solh 1107 2020, Beirut, Lebanon

*Corresponding author: Pablo Campo
Tel: +44 (0)1234 754332
E-mail address: p.campo-moreno@cranfield.ac.uk

ED_001324_00000209-00001

ABSTRACT

Laboratory experiments were conducted using Alaska North Slope crude oil (ANS) and the dispersant Corexit 9500 (C9500) to study the biodegradability of ANS alone, ANS dispersed with C9500 at a dispersant-to-oil ratio of 1:25. To determine the role that substrate concentration plays in biodegradation kinetics, oil loads of 1,000 and 40 ppm (v:v) were compared at 25 and 5 °C. The biodegradation rate of dioctyl sodium sulfosuccinate (DOSS), which is an anionic surfactant in C9500, by the meso culture (25 °C) was approximately an order of magnitude faster in the high concentration experiment than in the low concentration experiment. At the lower temperature, the deep-water culture cryo (5 °C) had limited ability to metabolize DOSS regardless of the initial concentrations. Uptake of oil components was favored by the presence of dispersant as C9500 shortened lag phases and enhanced biodegradation rates. Alkanes and PAHs were degraded more rapidly in the high concentration samples. In the low concentration experiment, the percentage of alkanes persisting was higher than in the high concentration experiment (8-18% vs. below 1%). No significant lag period in PAH biodegradation was observed in the high oil concentration experiment compared to the low oil concentration experiment where a lag period of 12 to 16 d was observed. The extent of biodegradation of some of the less soluble aromatics increased by 4-86% under low oil concentration conditions.

KEYWORDS

Corexit 9500, biodegradation, initial oil concentration

ED_001324_00000209-00002

INTRODUCTION

To minimize the impact of oil spills, responders adopt the Net Environmental Benefit Analysis, this is, any response technique should decrease the environmental costs rather than increase them (API, 2013). When mechanical recovery or in situ burning cannot achieve the goal of protecting shorelines from oil, the impact of using dispersants is likely outweighed by the benefits, which include keeping oil from sensitive areas and speeding up biodegradation by breaking an oil slick into small droplets (Prince, 2015). Thus, it is important to study the biodegradability of dispersants and dispersed oil under various conditions for better informed use in future applications.

In the aftermath of the Deepwater Horizon blowout in the Gulf of Mexico (GOM), comprehensive monitoring of dispersant Corexit 9500 (C9500) and hydrocarbons in both surface and subsurface environments took place. In samples collected near the Macondo well, concentrations of dioctyl sodium sulfosuccinate (DOSS), an anionic surfactant present in C9500, ranged from 0.4 to 12 μg/L (Kujawinski et al., 2011). After the spill, Gray et al. (2014) sampled at GOM different locations and detected DOSS in subsurface waters at concentrations below 40 μg/L, while in one surface water sample close to the wellhead the value exceeded 200 μg/L. In terms of oil concentration, Lee et al. (2013) pointed out that the combination of turbulence on the GOM surface and the dispersant application could rapidly decrease oil concentrations to below 100 mg/L, dropping even further over time. Hence, these researchers recommended that biodegradation tests of dispersed oil should be conducted under more dilute concentrations to mimic real conditions.

Most studies published on biodegradation of oil and dispersants prior to the Deepwater

ED_001324_00000209-00003

incident had been conducted at concentrations well-above the reported in situ levels (Operational Science Advisory Team, 2010; Prince, 2015). Several studies assessing biodegradation of oil dispersed by C9500 used initial oil and dispersant concentrations from 100 to 4,500 mg/L, with a dispersant-to-oil ratios (DOR) of 1:10, 1:20, or 1:25 (Campo et al., 2013; Lindstrom and Braddock, 2002; Zahed et al., 2010). To our knowledge, few studies have been published on oil biodegradation with initial oil and dispersant concentrations below 100 ppm (Brakstad et al., 2015; Prince et al., 2013; Venosa and Holder, 2007). Thus our objective was to determine how the initial amounts of oil and dispersant affect their biodegradation. We conducted high and low oil concentration biodegradation experiments with Alaska North Slope crude oil (ANS) and C9500 at 5 and 25 °C. C9500 is a dispersant included in the National Contingency Plan Product Schedule and was applied to both the surface and submarine environment in the GOM (Operational Science Advisory Team, 2010). The biodegradation of DOSS, dispersed ANS, and ANS alone in high and low concentration experiments at 5 and 25 °C are reported in this paper.

MATERIALS AND METHODS

Chemicals and Reagents

The U.S. Environmental Protection Agency (EPA) provided the ANS and the dispersant C9500 (Nalco Naperville, IL) used in this study. Standards for DOSS and its deuterated surrogate (D_{17}-DOSS) were obtained from Aldrich (St. Louis, MO) and Isotec (Miamisburg, OH), respectively. Acetonitrile, deionized ultra-filtered water, and mineral salts were purchased from Fisher Scientific (Pittsburgh, PA). Dichloromethane (DCM) was obtained from Tedia (Fairfield, OH). Sylon CT (Sigma-Aldrich, St. Louis, MO) was used for the deactivation of the glassware to prevent adherence of oil and biomass to the sides of the flasks. The protease

ED_001324_00000209-00004

cocktail for inhibiting enzymatic activity was also acquired from Sigma-Aldrich (St. Louis, MO).

Protease Solution Preparation

Following the instruction provided with the protease cocktail, 5 mL dimethyl sulfoxide (DMSO) was added to 1,075 mg lyophilized powder, which was previously stored unopened at -20 °C. The solution was vortexed for ten minutes before the addition of 20 mL deionized water. The resulting solution was clear. The reconstituted protease solution contained the following inhibitors: 4-(2-aminoethyl) benzenesulfonyl fluoride hydrochloride (23 mM), ethylenediaminetetraacetic acid (100 mM), bestatin (2 mM), pepstatin A (0.3 mM), and E-64 (0.3 mM).

Artificial Seawater

GP2 medium was autoclaved at 121 °C for 30 min and then used as the sterile matrix in this study (Spotte et al., 1984). The salts in the GP2 medium, dissolved in DI water, were (expressed in g/L) NaCl (21.03), $MgCl_2 \cdot 6H_2O$ (9.5), Na_2SO_4 (3.52), $CaCl_2 \cdot 2H_2O$ (1.32), KCl (0.61), KBr (0.088), $NaB_4O_7 \cdot 10H_2O$ (0.034), $SrCl_2 \cdot 6H_2O$ (0.02), $NaHCO_3$ (0.17) $FeCl_3 \cdot 6H_2O$ (0.05), $Na_5P_3O_{10}$ (0.297) and KNO_3 (2.89). The GP2 pH was ≈ 7.5.

Microbial Cultures

The original cultures were isolated from the surface water of the GOM (meso) in the vicinity of the Macondo well and water close to the plume location at a depth of 1,240 m near the wellhead (cryo) by EPA's Gulf Breeze, FL research laboratory. Enriched inocula were procured as follows: in 2-L shake flasks, 2.5 mL SLC were added to 500 mL of the original unfiltered GOM seawater supplemented with 2.8 g/L KNO_3, 0.55 g/L NaP_3O_{10}. The flasks were

ED_001324_00000209-00005

rotated (400 rpm) at 5 °C (cryo culture) and 25 °C (meso culture). The adequate growth times were 7 d for the meso culture and 17 d for the cryo culture. After these periods, cells were harvested by centrifugation (6,000 × g for 30 min at 4 °C) and the pellets preserved in 10% glycerol at -70 °C. Before shipping to EPA-Cincinnati, 1 mL of each thawed culture were added to shake flasks containing 500 mL GP2 medium fortified with 2.5 mL of SLC. The meso culture was harvested after 6 days of growth and the cryo culture after 29 days. The cultures used in the experiments of this study were grown at EPA (Cincinnati, OH) by transferring the original cultures from EPA's Gulf Breeze to GP2 medium supplemented with South Louisiana crude oil (SLC). The meso culture was harvested after 3 weeks of growth and the cryo culture after 5 weeks. The harvested culture was processed in the same fashion as mentioned previously: centrifugation (6,000 × g for 30 min at 4 °C) and the pellets preserved in 10% glycerol at -70 °C. Upon use in experiments, the cultures were defrosted at room temperature, washed with 0.85% saline solution to remove glycerol, centrifuged, and brought back up to the frozen volume.

Experimental Setup and Sampling

A summary of the experimental setup is shown in Tables S1 and S2 for the high and low oil concentration experiments, respectively. For the high concentration experiments, 6 treatments were tested at 5 and 25 °C in triplicate: C9500 dispersant alone, ANS oil alone, ANS dispersed with C9500, and the corresponding killed controls (KCs). The 5 °C experiment required 11 sampling events in triplicate (0, 2, 4, 8, 12, 16, 24, 32, 40, 48 and 56 d), while 9 events were conducted at 25 °C (0, 2, 4, 8, 12, 16, 24, 32 and 40 d). At each sampling event, triplicate shake flasks of each treatment along with KCs were sacrificed, except for the ANS alone KCs which were analyzed at the beginning and end of the experiment.

ED_001324_00000209-00006

The same treatments were included in the low concentration experiment, but both oil and dispersant concentrations were prepared at 4% of the initial loads used in the high concentration experiment. Additionally, a seventh treatment involved the use of triplicate KCs containing the enzyme protease (0.5 mL) to neutralize the enzymatic DOSS hydrolysis. This treatment was included only in the low concentration experiment. The sampling events were conducted similarly to the high concentration experiment with the exception of the protease treatment, which was sampled at 0, 12, 24, 35, 46 and 56 d and 0, 8, 18, 28, 38 and 48 d for the 5 and 25 °C experiments, respectively.

After all treatments were prepared, the appropriate cultures were spiked (0.5 mL) and the flasks were placed on orbital shakers. The shakers were operated at 200 rpm and kept in the appropriate constant temperature rooms until the expected sampling events. All KCs were sterilized by adding 1 mL sodium azide stock (50 g/L) into the 100 mL of GP2 medium.

High Concentration Treatments

To evaluate the biodegradation of dispersed oil, 2 L baffled beakers were used in which 40 μL of C9500 and 1,000 μL of ANS were added to 1,200 mL of GP2 to achieve a volumetric DOR ratio of 1:25. Subsequently, the beaker containing the mixture was shaken at 200 rpm for 10 minutes and then left stationary for an additional 10 min, then the dispersion was transferred to a 20-L continuously mixed carboy. The above procedure was repeated until the volume in the carboy reached 14 L. Subsequently, 100 mL aliquots of the mixtures were transferred to the shake flasks. The second treatment was for the evaluation of oil as the only substrate. ANS (100 μL) was added directly to shake flasks containing 100 mL sterile GP2 medium, which yielded an estimated oil concentration of 1,000 ppm by volume. The oil added to the ANS alone and

ED_001324_00000209-00007

dispersed ANS treatments aimed to result in the same oil concentration by volume. To evaluate the degradation of dispersant alone, 480 µL of C9500 was added to 14 L of sterile GP2 medium in a continuously mixed carboy; after 30 min, 100 mL aliquots of this mixture were dispensed into shake flasks for this treatment.

Low Concentration Treatments

To prepare the low concentration dispersed oil, a single batch of 1,200 mL GP2 was spiked with 200 µL ANS onto the water surface followed by addition of 8 µL C9500 onto the oil slick, which yielded a volumetric DOR of 1:25 in a 2 L baffled beaker. The shaker was started at a very slow speed and was ramped up to 200 rpm gradually. The beaker was placed on a shaker for 20 min and then remained stationary for 10 minutes. Subsequently, 3 L of the dispersion were poured into a 20 L carboy under continuous mixing and 12 L of sterile GP2 was added for dilution purposes. Overall, the oil and dispersant amounts in this treatment were approximately 4% of that in the high concentration experiment. Finally, shake flasks were filled with 100 mL aliquots of the diluted dispersed oil. Low concentration ANS alone was prepared by spiking approximately 4 µL of oil into shake flasks containing 100 mL sterile GP2, which yields an oil concentration of 40 ppm by volume (i.e., 4% of the high concentration oil alone experiment). The low concentration dispersant alone treatment was prepared in a single batch of sterile GP2 (14 L) spiked with approximately 20 µL of C9500. The batch was mixed for 30 minutes and, subsequently, 100 mL aliquots were transferred into the shake flasks.

Oil components and Dispersant Analysis

To monitor C9500 degradation, DOSS was measured by liquid chromatography tandem mass spectrometry (LC-MS/MS) following the Standard method ASTM D7730−11 (2011). The

ED_001324_00000209-00008

targeted oil components were pristane (PR), phytane (PH), normal paraffins (n-C_{10-35}) and 2-, 3- and 4-ring PAH compounds and their alkylated homologues (C_{0-4}-naphthalenes, C_{0-3}-fluorenes, C_{0-3}-dibenzothiophenes, C_{0-4}-phenanthrenes/anthracenes, C_{0-4}-napthbenzthiophenes, C_{0-2}-pyrenes, C_{0-4}-chrysenes). The concentrations of these analytes were normalized to hopane present in the oil (Prince et al., 1994). Details of oil extraction by DCM and sample preparation methods can be found elsewhere (Campo et al., 2013). For the high concentration experiment, oil analysis was conducted with a 6890 GC coupled with a 5973 mass spectrometry from Agilent (Palo Alto, CA). In the low concentration experiment, an Agilent (Palo Alto, CA) 7000 GC Triple Quad system was used. The quantification range for the single quad and triple quad mass spectrometry are 1-30 μg/L and 0.5-10 μg/L, respectively. In the case that the concentration of oil hydrocarbons is below the range, we used the quantification results as an estimation of the actual amount. The same column, a DB-5MS column (30m × 0.25mm, 0.25μm film thickness), was used to achieve chromatographic separation of analytes in both instruments. The method was a modification based on EPA Method 8270D (2007).

RESULTS AND DISCUSSION

Degradation of DOSS

High Concentration Experiment. Live samples revealed an extremely fast removal rate of DOSS at 25 °C (Fig. 1A-B, open symbols) with extents exceeding 95% after 2 d in dispersed oil (Fig. 1B) and 4 d in C9500 alone (Fig. 1A). The first order rate coefficients were -1.82 ± 0.25 d^{-1} (ANS+C9500) and -0.71 ± 0.024 d^{-1} (C9500 alone). The presence of oil enhanced DOSS biodegradation by a factor of approximately 2.6. Disappearance of DOSS was also observed in KCs at 25 °C, with zero order rates of -138 ± 7 and -221 ± 11 μg L^{-1} d^{-1} for C9500 alone (Fig.

ED_001324_00000209-00009

1C) and dispersed oil (Fig. 1D), respectively. As monooctyl sulfosuccinate (MOSS) was found in KCs, Campo et al. (2013) explained this abiotic loss in terms of hydrolysis which was confirmed by (Batchu et al., 2014). The presence of oil significantly enhanced DOSS removal in KCs ($p < 0.0001$).

In contrast with the rapid removal of DOSS at 25 °C, the biotic and abiotic processes at 5 °C were much slower. DOSS persisted for 40 d before its concentration decreased in all treatments. The difference in DOSS concentration between live samples and parallel KCs in the dispersed oil treatment was statistically insignificant at days 48 ($p = 0.078$) and 56 ($p = 0.726$). In the C9500 alone treatment, DOSS was significantly lower in live samples than in KCs at days 48 ($p = 0.0015$) and day 56 ($p = 0.023$). These results point to biodegradation as the predominant DOSS removal mechanism as opposed to hydrolysis.

ED_001324_00000209-00010

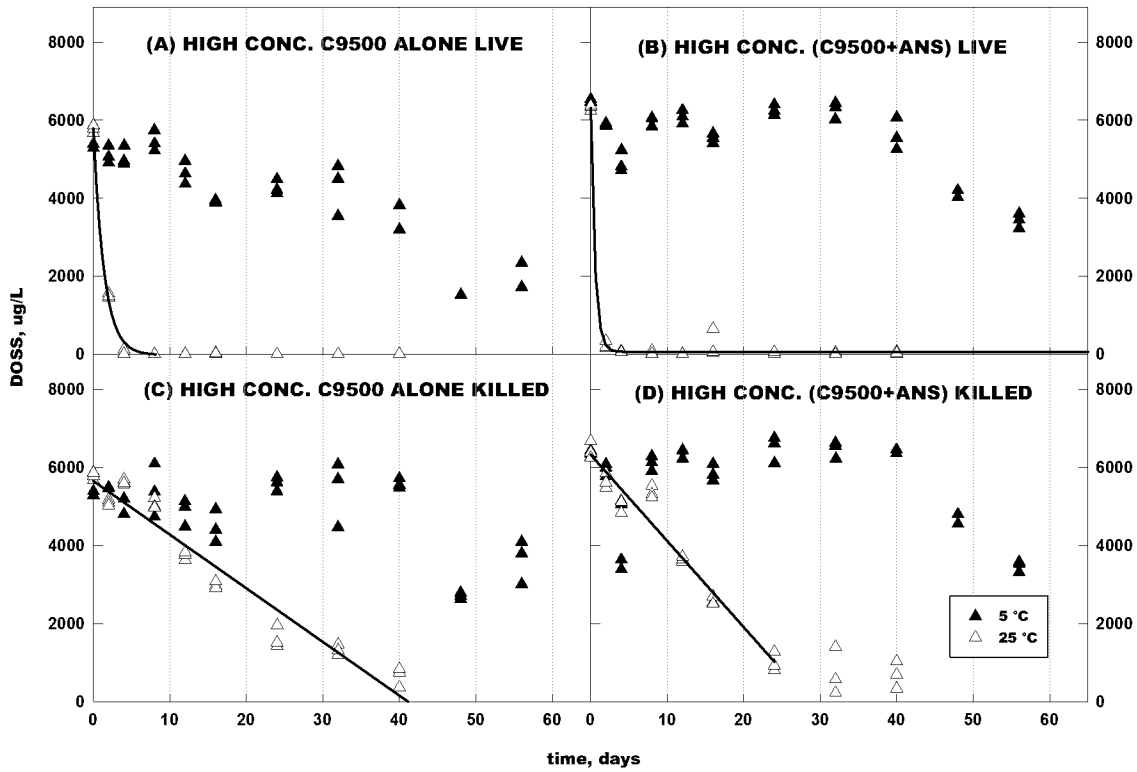

Figure 1. Disappearance of DOSS in high concentration experiment in the absence (A, C) and Presence (B, D) of ANS at 5 °C and 25 °C. Live samples are in panel A and B, whereas killed controls are in panels C and D.

Low Concentration Experiment. At 25 °C and for the dispersed oil treatment, no lag period was observed in DOSS uptake, which showed a first-order constant rate of -0.16 ± 0.015 d^{-1} (Fig. 2B). In the absence of oil (Fig. 2A), we observed an acclimation period of 2 d followed by DOSS biodegradation (-0.07 ± 0.009 d^{-1}). The presence of oil favored DOSS removal as was observed in the high concentration experiment . Removal extents over 95% for DOSS required 32 and 48 d in the presence and absence of oil, respectively. In the corresponding KCs, DOSS concentrations decreased following zero-order kinetics, with constant rates of -4.1 ± 0.3 μg L^{-1} d^{-1} (C9500 alone, Fig. 2C) and -5.1 ± 0.4 μg L^{-1} d^{-1} (C9500 and ANS, Fig. 2D).

For the high concentration experiment at 25 °C and regardless of the presence of oil, the

time series concentration of DOSS in the live samples rapidly declined to zero and clearly separated from the values measured in the corresponding KCs. In the low concentration experiment, it appeared that DOSS disappearance with time in both treatments, C9500 alone and dispersed ANS, overlapped with the abiotic losses observed in the KCs (Fig. 2). To differentiate between microbial activity and hydrolysis, we compared by a *t*-test ($\alpha = 0.05$) the average DOSS concentrations measured in live samples with those values found in the parallel KCs. Live samples significantly departed from the controls after 4 d ($p = 0.0227$) and 16 d ($p = 0.0053$) in the presence and absence of ANS, respectively. At early stages in the experiment, we could not identify the predominant removal mechanism for DOSS but, eventually, microbial uptake prevailed as the main process in terms of rate and extent.

DOSS presented a faster microbial uptake at both the higher initial concentration and temperature. Nevertheless, based on our low concentration results, it is reasonable to infer that biodegradation of DOSS at the surface of GOM might not happen as rapidly since dilution and emulsification can attenuate the concentration of dispersant. In this fashion, DOSS was detected with a reporting limit of 0.25 $\mu g\ L^{-1}$ and a highest concentration of 229 ±16 $\mu g\ L^{-1}$ in surface water samples collected 1-2 months after the spill near the Macondo well (Gray et al., 2014).

DOSS concentration remained unchanged in live samples and KCs under 5 °C and low oiling conditions (Fig. 2, closed symbols). Such finding agreed with studies by Kujawinski et al. (2011) and Gray et al. (2014) who concluded that subsurface degradation of DOSS was minimal. Campo et al. (2013) observed no hydrolysis or biodegradation of DOSS in SLC at 5 °C within 42 d.

ED_001324_00000209-00012

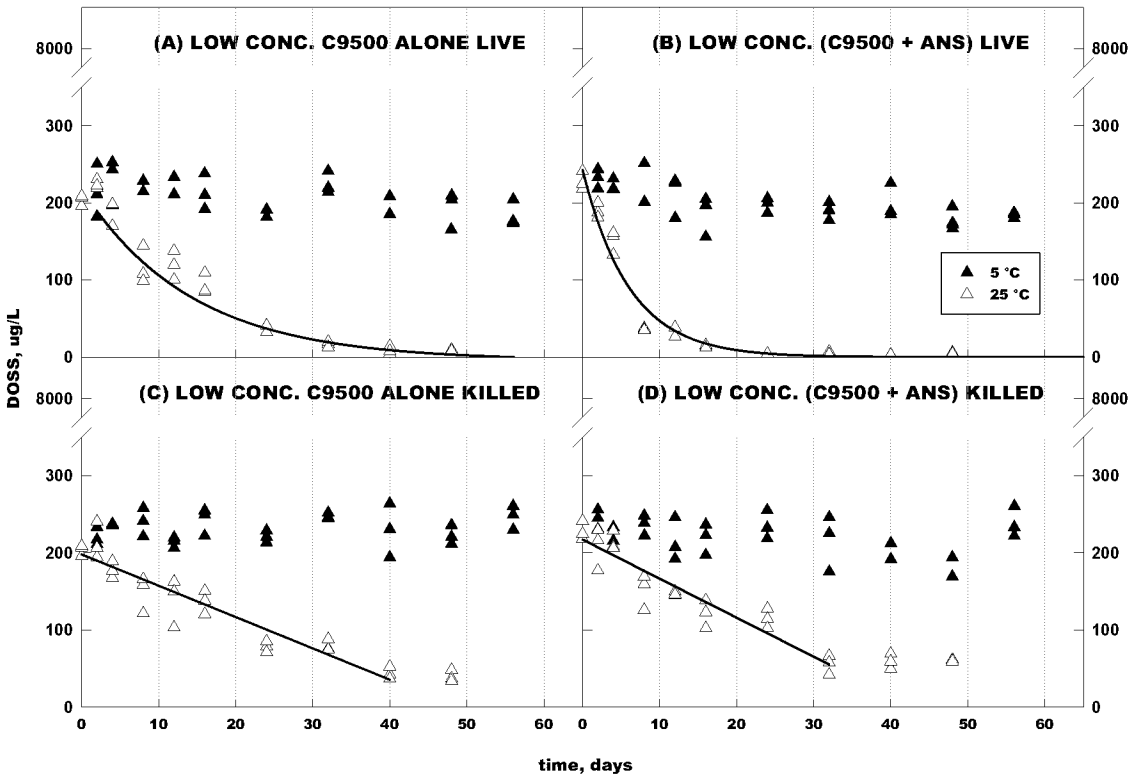

Figure 2. Disappearance of DOSS in low concentration experiment in the absence (A, C) and Presence (B, D) of ANS at 5 °C and 25 °C. Live samples are in panel A and B, whereas killed controls are in panels C and D.

We also included a series of dispersed oil KCs containing a protease cocktail (Fig. 3A), which inhibits enzymatic activity to clarify the abiotic DOSS disappearance. At 25 °C, the addition of inhibitor clearly slowed down the hydrolysis process as the zero-order rate constant in the protease KCs was -3.7 ± 0.4 μg L^{-1} d^{-1} (Fig. 3A) as opposed to -5.1 ± 0.4 μg L^{-1} d^{-1} (Fig. 3B) obtained for the regular KCs (p = 0.021). Such finding suggests the enzymatic nature of DOSS hydrolysis. Nevertheless, different enzymes may be involved in the process so that the protease cocktail could not block all of them. In the protease controls at 5 °C, DOSS persisted throughout the experiment as observed in the regular KCs for that temperature. This indicates that either the lower temperature attenuated DOSS breakdown,the cryo culture lacked the

required enzymes, or a combination of both causes.

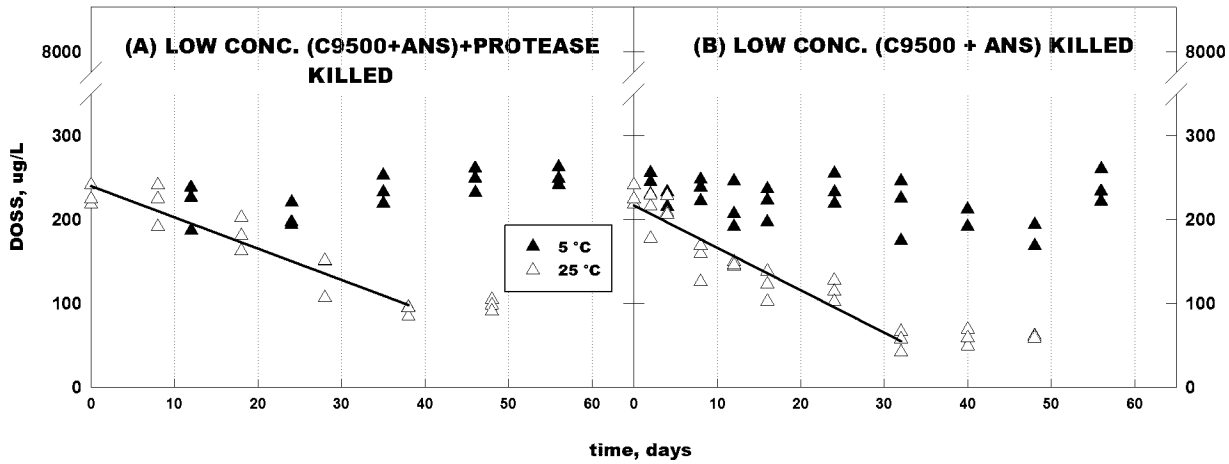

Figure 3. Disappearance of DOSS in low concentration dispersed oil killed controls in the presence (A) and absence (B) of protease at 5 and 25 °C.

Total Alkane Degradation

High Concentration Experiment. Total alkanes at both temperatures are presented in Fig. 4 A-B. At 25 °C, the meso culture metabolized the aliphatic fraction with a first-order rate constants of -0.91 ± 0.10 and -0.85 ± 0.04 d^{-1} in the absence and presence of C9500, respectively. For both treatments, the extent of removals reached 99% after 4 days. As expected, aliphatics degraded slower at 5 °C. In the dispersed oil treatment, this fraction followed first order kinetics (-0.24 ± 0.01 d^{-1}) while, for the oil alone samples, alkanes presented a linear decay during the first 8 d followed by first order kinetics of similar rate (-0.25 ± 0.03 d^{-1}). After days 16 (dispersed oil) and 24 (oil alone), the alkane extent of removal was 99% for the lower temperature.

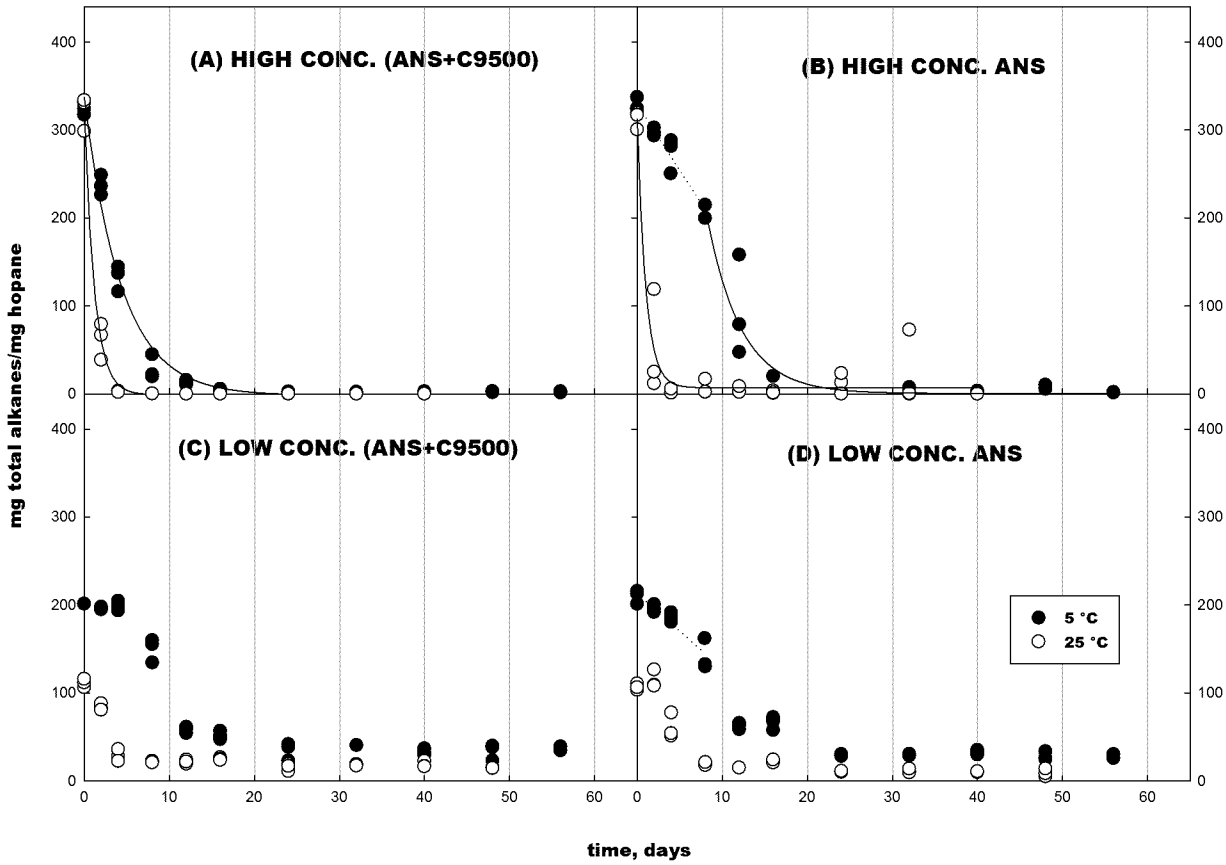

Figure 4. Biodegradation of hopane-normalized total alkanes at both temperatures in high concentration treatments (A, B) and low concentration treatments (C, D).

Low Concentration Experiment. In this experiment, the initial total alkane concentrations were considerably different at 5 and 25 °C (Fig. 4 C and D). In fact, the meso culture showed background concentrations of PAHs and hopane, the conservative biomarker to which all the target analytes concentrations are normalized. The hopane background levels were comparable to those measured in the initial oil added to the flasks. Hence, at time zero, the total alkane concentration normalized to hopane at 25 °C were almost half of the corresponding value at 5 °C.

At 25 °C, the alkane residual concentrations ranged from 8 to 18% of the initial values (Fig. 4 A and B). In the oil alone treatment, alkane biodegradation started after a lag phase of 2 d, while these organics were promptly metabolized in the dispersed oil treatment. At 5 °C, the cryo culture required 4 d for acclimation in the dispersed oil. In the absence of dispersant, after a slow and steady linear decay, fast disappearance of alkanes occurred between days 8 and 12. This suggests that C9500 reduced the length of the acclimation phase for alkane uptake.

Table 1 summarizes the actual concentrations of total alkanes (not normalized to hopane) for the first and last sampling event for both the high and low concentration experiments. It is noted that a higher alkane residual amount was observed in the low concentration experiment than the high concentration one. This was especially true considering the combination of high temperature and dispersant application, where the alkane concentrations were less than the detection limit and 142 ± 4 μg L^{-1} in the last sampling event of low concentration samples. One possible explanation is that carbon and energy sources were limited in the low concentration microcosms. Fewer microorganisms provided less microbial surface for hydrophobic compounds to interact with, which resulted in less complete degradation of alkanes.

Table 1. Average and standard deviations (sd) of total alkanes and PAHs concentration in the high and low concentration experiment at first and last sampling event.

Samples			5 °C ANS alone average (μg/L)	sd	25 °C ANS alone average (μg/L)	sd	5 °C ANS+C9500 average (μg/L)	sd	25 °C ANS+C9500 average (μg/L)	sd
High Conc.										
	Alkanes	**First**	47,400	604	43,300	9,390	24,600	973	27,200	126
		Last	201	26	36	42	186	52	0	0
	PAHs	**First**	14,500	110	13,700	3,090	7,310	323	8,790	94
		Last	3,040	281	2,470	300	1,300	74	1,270	158
Low Conc.										
	Alkanes	**First**	2,010	202	1,740	149	1,420	72	1,130	39

ED_001324_00000209-00016

	Last	216	21	83	75	225	13	142	4
PAHs	**First**	482	53	773	25	330	12	453	14
	Last	71	5	88	5	58	10	80	4

Degradation of Individual Alkanes

High Concentration Experiment. Table S3 summarizes the first-order biodegradation coefficients for individual alkanes. At 25 °C, among all the compound monitores only n-C_{10} was biodegraded faster (-2.00 vs. -1.34 d^{-1}) with the addition of dispersant. Branched alkanes exhibited similar rates regardless of the presence of C9500, although higher variability among triplicates was observed in the oil alone samples (Fig. S1 A and B). At 5 °C, consistently higher rates for n-C_{10-27} were observed in the dispersed oil treatment when compared to the oil alone treatment. Also, no lag period for the biodegradation of branched alkanes occurred when C9500 was added, whereas an 8-day lag period occurred in the absence of dispersant.

Low Concentration Experiment. As depicted in Figs. S1-5 (panels C and D), only n-C_{10-16} was completely removed at both temperatures in the low concentration experiment. In this case,a more qualitative approach was used by comparing the disappearance time. At 25 °C in the low oil concentration experiment, n-C_{10} was degraded faster in the presence of dispersant, disappearing completely before day 2, whereas in the absence of C9500, its depletion was achieved only after day 8. The biodegradation of n-C_{10} was also accelerated when C9500 was present at 5 °C, as shown in Table S4 (-0.47 vs -0.63 d^{-1}). At both temperatures, branched alkanes were not degraded faster in the presence of dispersant, as shown in Table S4 and Fig. S1 C-D.

The major mechanism of uptake of water-insoluble substrates (i.e., alkanes) is generally

ED_001324_00000209-00017

recognized as direct interaction between microbes and the hydrophobic substance (Rojo, 2009; Wentzel et al., 2007) and the effects of surfactant on such process are inconclusive (Bredholt et al., 2002; Bruheim et al., 1999; Tang et al., 1998). Both conducive and inhibitory effects of dispersant on oil biodegradation have been reported (Lindstrom and Braddock, 2002; Prince et al., 2013; Venosa and Holder, 2007). In this study, C9500 exhibited similar effects on the biodegradation of alkanes in the high and low concentration experiments. Such effects included enhancement of biodegradation rates and shortening of lag periods. Rate enhancements were more notable in the high concentration experiment, whereas C9500 clearly shortened lag phases in the lower concentration tests.

The application of dispersants to an oil slick promotes the formation of small oil droplets by decreasing the interfacial tension between oil and water (Jasper et al., 1978; Li et al., 2009; Lunel, 1995). Consequently, the total interfacial area of oil droplets for microbes to interact with is increased. In the high concentration experiment, exposure of substrates to the microbes is enough that biodegradation can initiate soon after inoculation. In this case, dispersants assisted biodegradation mainly by increasing interfacial area for microbes to interact with oil. For the low concentration experiment, the observed long acclimation phase at both temperatures, especially in the absence of C9500, was possibly due to limited exposure of alkanes to the microorganisms in the beginning. Since the oil load, appearing as an iridescent sheen, is so low, the mixing energy in the flasks could be high enough to produce similar droplet size distribution in the oil alone and dispersed oil treatments. Thus, C9500 may have shortened the lag phase in the low concentration experiment by promoting the attachment of microbes to the oil droplet.

Total Aromatics Degradation

ED_001324_00000209-00018

High Concentration Experiment. Fig. 5A-B presents total PAH biodegradation data for the high concentration experiment at both temperatures. Aromatics removals of 42 and 24% occurred by day 2 in the dispersed oil and the oil alone treatment, respectively. This difference in extent was significant ($p < 0.0001$), which indicates a positive effect of the dispersant. At 5 °C, the time for attaining maximum level of PAHs removal in non-dispersed treatment took twice as much time as in dispersed oil treatment 16 days vs. 8 days (solid symbols in Fig. 5B and 5A, respectively). The overall PAHs removals in the presence and absence of dispersant were 86% and 82%, respectively.

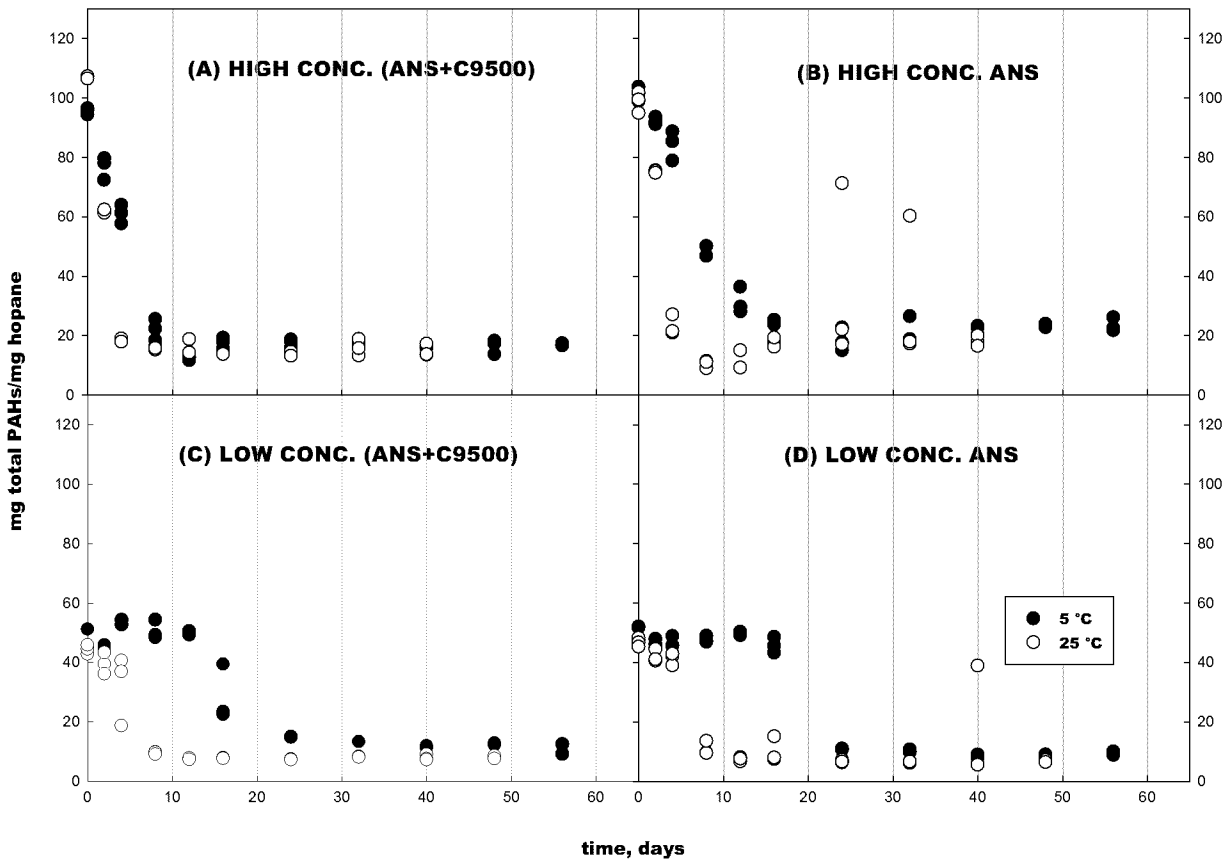

Figure 5. Biodegradation of hopane-normalized total PAHs at both temperatures in high concentration treatments (A, B) and low concentration treatments (C, D).

Low Concentration Experiment. As shown in Fig. 5C-D, when comparing the two low

concentration treatments at 25 °C (open symbols), the only difference was in one replicate of dispersed oil on day 4, which had significantly lower total PAH concentration than the parallel diluted oil alone samples. At the high temperature (open symbols), the patterns of PAH degradation were similar in the absence and presence of C9500, regardless of initial concentration. The treatment without dispersant experienced higher variability. The lag period at the low temperature (closed symbols) was longer than at 25 °C; it lasted12 and 16 days for dispersed oil and oil alone, respectively. For the sampling event on day 16, the extent of PAH removal was 20 to 50% in the replicates of dispersed oil sample, while it was negligible in the treatment without dispersant.

Transport of compounds from non-aqueous phase to aqueous phase is often the most rate-limiting step in the biodegradation of PAHs. Surfactants can enhance the dissolution of PAHs by increasing interfacial area of oil droplet and subsequently increase the bioavailability of PAHs to microorganisms (Haritash and Kaushik, 2009; Mrozik et al., 2003). The effect of C9500 on the biodegradation of total PAHs was less pronounced in the low concentration experiment than in the high concentration experiment, because this effect was observed only in one or more replicates in a single sampling event. This finding is consistent with our previous assumption about low concentration experiment: droplet size distribution in the oil alone and dispersed oil treatments are similar. Dispersion in the oil alone microcosms might have been efficient enough even without the addition surfactant, considering the mixing energy was sufficient (Kaku, 2006) and the initial presence of oil was an iridescent rainbow-colored sheen. Clearly, the comparison between our low concentration dispersed oil samples and oil alone samples indicates that dispersants had less enhancing effect on the bio-uptake of PAHs after dilution. Nevertheless, most toxicity studies on dispersed oil concluded that the presence of dispersant increased

ED_001324_00000209-00020

environmental risk for aquatic organisms living in the water column (Milinkovitch et al., 2011; Ramachandran et al., 2004), which is possibly due to their relatively high concentration of oil and dispersant in the laboratory tests.

Individual Aromatics Degradation

High Concentration Experiment. A first-order model could be used to fit the biodegradation of the individual PAHs that had a negligible fraction persisting by the end of the high concentration experiment. At both temperatures, the biodegradation rates of naphthalene, phenanthrene, fluorine, and dibenzothiophene and their homologues in the high concentration experiment were consistantly higher in the presence of dispersant (Table S5). The greatest enhancement was observed with naphthalene at 25 °C, which was 2.9-fold higher than at 5 °C (-1.94 d^{-1} vs. -0.68 d^{-1}). The surfactant likely assisted the transfer of more soluble compounds from the oil phase to the aqueous phase through the formation of small oil droplets and the resultant increase in interfacial area. Because the bio-uptake of aromatics is mostly from aqueous phase (Haritash and Kaushik, 2009; Mrozik et al., 2003), C9500 promoted the biodegradation of PAHs by increasing their bioavailability in water.

Low Concentration Experiment. Among the low concentration individual PAHs, the time-varying concentration of specific aromatics could be fitted to a first-order kinetics model (rates shown in Table S6), and the results revealed reduced rates due to dilution (low vs. high), especially when C9500 was present (i.e. naphthalene: -0.36 d^{-1} v -1.94 d^{-1}). However, we could not fit a first-order model for the other PAH compounds in the low concentration experiments because of the long lag period and the immediate and nearly complete removal after biodegradation started. As mentioned before, C9500 acted less effectively on the biodegradation

ED_001324_00000209-00021

of total PAHs in the low concentration experiment, because different PAH concentrations in parallel dispersed oil and oil alone samples was observed only at one or more replicates in a single sampling event (25 °C: day 4, 5 °C: day 16). Nevertheless, C_4-naphthalene, C_{2-4}-phenanthrene, C_{2-3}-fluorene, and naphthobenzothiophene were removed at higher extent in the low rather than in the high concentration samples (Fig. S6). The increase in removal extent for the aforementioned aromatics were 6-14%, 4-47%, 14-54%, and 55-86% respectively. Zahed et al. (2010) also observed similar enhancement of crude oil removal extent in low oiling experiments. In the low concentration experiment, the starting PAH concentrations were equal to or below the remaining residual found in the high concentration experiment, but the cultures were able to degrade the aromatic compounds to an even lower level, as shown in Table 1. The reasons are a combination of the following: (1) the alkylated structure of these compounds led to less aqueous dissolution and less susceptibility to microbial attack; (2) their aqueous uptake was primarily diffusion, for which neither energized membrane nor adenosine triphosphate was essential (Bateman et al., 1986). Taking C_2-phenanthrene for example, it was fully degraded in the low concentration experiment, whereas its removal extent ranged from 66% to 94% when the initial oil concentration was high. The enhancement in the extent of removal under diluted conditions was more remarkable at low temperature, which contributed to our conclusion that solubility was the limiting factor for those compounds to be biodegraded. Whether oil concentration is high or low, pyrene, chrysene and naphthobenzothiophene homologues persisted until the last sampling event at both temperatures, as depicted in Figs. S7 and S8. The heavy PAHs, such as chrysene, are likely to be retained on a beach for several years, according to Yin et al. (2015), who conducted research that monitors the submerged oil mats and surface residual oil balls off Alabama's beach affected by the 2010 DWH incident.

ED_001324_00000209-00022

ACKNOWLEDGMENTS

We thank Jan Kurtz and Diane Yates from EPA's Gulf Ecology Division (GED) at Gulf Breeze, FL, who collected the water samples in the GOM and performed the enrichments and provided them for our experiments. The research was a product of the U.S. Environmental Protection Agency's National Risk Management Research Laboratory (NRMRL) and was partially funded by EPA, NRMRL, Cincinnati, OH, under Pegasus Technical Services, Inc. Contract EP-C-11-006.

REFERENCES

2007. U.S. Environmental Protection Agency, EPA 8270D Semivolatile organic compounds by gas chromatography/mass spectrometry (GC/MS), 3rd. ed, Washington, D.C.

API, 2013. Net Environmental Benefit Analysis for effective oil spill preparedness and response. 2013. http://www.api.org/~/media/Files/EHS/Clean_Water/Oil_Spill_Prevention/NEBA/NEBA-Net-Environmental-Benefit-Analysis-July-2013.pdf.

Batchu, S.R., Ramirez, C.E., Gardinali, P.R., 2014. Stability of dioctyl sulfosuccinate (DOSS) towards hydrolysis and photodegradation under simulated solar conditions. Sci. Total. Environ. 481, 260-265.

Bateman, J.N., Speer, B., Feduik, L., Hartline, R.A., 1986. Naphthalene association and uptake in Pseudomonas putida. J. Bacteriol. 166, 155-161.

Brakstad, O.G., Nordtug, T., Throne-Holst, M., 2015. Biodegradation of dispersed Macondo oil in seawater at low temperature and different oil droplet sizes. Marine pollution bulletin 93, 144-152.

Bredholt, H., Bruheim, P., Potocky, M., Eimhjellen, K., 2002. Hydrophobicity development, alkane oxidation, and crude-oil emulsification in a Rhodococcus species. Can. J. Microbiol. 48, 295-304.

Bruheim, P., Bredholt, H., Eimhjellen, K., 1999. Effects of surfactant mixtures, including Corexit 9527, on bacterial oxidation of acetate and alkanes in crude oil. Appl. Environ. Microbiol. 65, 1658-1661.

Campo, P., Venosa, A.D., Suidan, M.T., 2013. Biodegradability of Corexit 9500 and dispersed South Louisiana crude oil at 5 and 25 degrees C. Environ. Sci. Technol. 47, 1960-1967.

D7730−11, A., 2011. Standard Test Method for Determination of Dioctyl Sulfosuccinate in Sea Water by Liquid Chromatography/Tandem Mass Spectrometry (LC/MS/MS). ASTM International 2011. ASTM International.

Gray, J.L., Kanagy, L.K., Furlong, E.T., Kanagy, C.J., McCoy, J.W., Mason, A., Lauenstein, G., 2014. Presence of the Corexit component dioctyl sodium sulfosuccinate in Gulf of Mexico waters after the 2010 Deepwater Horizon oil spill. Chemosphere 95, 124-130.

Haritash, A.K., Kaushik, C.P., 2009. Biodegradation Aspects of Polycyclic Aromatic Hydrocarbons (PAHs): A review. J. Hazard. Mater. 169, 1-15.

Jasper, W.L., Kim, T.L., Wilson, M.P., 1978. Droplet size distributions in a treated oil–water system., in: McCarthy, L.T., Lindblom, G.P., Walter, H.F. (Eds.), Chemical Dispersants for the Control of Oil Spills. American Society for Testing and Materials, Philadelphia, PA.

Kaku, V.J., Boufadel, M.C., Venosa, A.D., 2006. Evaluation of mixing energy in laboratory flasks used for dispersant effectiveness testing. J. Environ. Eng. Div. ASCE 132, 93-101.

Kujawinski, E.B., Kido Soule, M.C., Valentine, D.L., Boysen, A.K., Longnecker, K., Redmond, M.C., 2011. Fate of dispersants associated with the deepwater horizon oil spill. Environ. Sci. Technol. 45, 1298-1306.

Lee, K., Nedwed, T., Prince, R.C., Palandro, D., 2013. Lab tests on the biodegradation of chemically dispersed oil should consider the rapid dilution that occurs at sea. Mar. Pollut. Bull. 73, 314-318.

Li, Z., Lee, K., King, T., Boufadel, M.C., Venosa, A.D., 2009. Evaluating Chemical Dispersant Efficacy in an Experimental Wave Tank: 2—Significant Factors Determining In Situ Oil Droplet Size Distribution. 26, 1407-1418.

Lindstrom, J.E., Braddock, J.F., 2002. Biodegradation of petroleum hydrocarbons at low temperature in the presence of the dispersant Corexit 9500. Mar. Pollut. Bull. 44, 739-747.

Lunel, T., 1995. Understanding the mechanism of dispersion through oil droplet size measurements at sea., in: P. Lane (Ed.), The Use of Chemicals in Oil Spill Response. American Society for Testing and Materials, Philadelphia, PA.

Milinkovitch, T., Kanan, R., Thomas-Guyon, H., Le Floch, S., 2011. Effects of dispersed oil exposure on the bioaccumulation of polycyclic aromatic hydrocarbons and the mortality of juvenile Liza ramada. Sci. Total. Environ. 409, 1643-1650.

Mrozik, A., Piotrowska-Seget, Z., Labuzek, S., 2003. Bacterial Degradation and Bioremediation of Polycyclic Aromatic Hydrocarbons. Pol. J. Environ. Stud. 12, 15-25.

Operational Science Advisory Team, 2010. Summary report for sub-sea and sub-surface oil and dispersant detection: sampling and monitoring. Prepared for Paul F. Zukunft, U.S. Coast Guard.

Prince, R.C., 2015. Oil spill dispersants: boon or bane? Environmental science & technology 49, 6376−6384.

Prince, R.C., Elmendorf, D.L., Lute, J.R., Hsu, C.S., Halth, C.E., Senius, J.D., Dechert, G.J., Douglas, G.S., Butler, E.L., 1994. 17α(H),21β(H)-hopane as a conserved internal marker for estimating the blodegradation of crude oil. Environ. Sci. Technol. 28, 142-145.

Prince, R.C., McFarlin, K.M., Butler, J.D., Febbo, E.J., Wang, F.C., Nedwed, T.J., 2013. The primary biodegradation of dispersed crude oil in the sea. Chemosphere 90, 521-526.

Ramachandran, S.D., Hodson, P.V., Khan, C.W., Lee, K., 2004. Oil dispersant increases PAH uptake by fish exposed to crude oil. Ecotox. Environ. Safe. 59, 300-308.

Rojo, F., 2009. Degradation of Alkanes by Bacteria. Environ. Microbiol. 11, 2477-2490.

Spotte, S., Adams, G., Bubucis, P.M., 1984. GP2 medium is an synthetic seawater for culture or maintenance of marine organisms. . Zoo Biol. 3, 229-240.

Tang, W.C., White, J.C., Alexander, M., 1998. Utilization of sorbed compounds by microorganisms specifically isolated for that purpose. Appl. Microbiol. Biotechnol. 49, 117-121.

Venosa, A.D., Holder, E.L., 2007. Biodegradability of dispersed crude oil at two different temperatures. Mar. Pollut. Bull. 54, 545-553.

Wentzel, A., Ellingsen, T.E., Kotlar, H.K., Zotchev, S.B., Throne-Holst, M., 2007. Bacterial metabolism of long-chain n-alkanes. Appl. Microbiol. Biotechnol. 76, 1209-1221.

Word, J.Q., Clark, J.R., Word, L.S., 2014. Comparison of the Acute Toxicity of Corexit 9500 and Household Cleaning Products. Human Ecol. Risk Assess. 21, 19.

Yin, F., John, G.F., Hayworth, J.S., Clement, T.P., 2015. Long-term monitoring data to describe the fate of polycyclic aromatic hydrocarbons in Deepwater Horizon oil submerged off Alabama's beaches. The Science of the total environment 508, 46-56.

Zahed, M.A., Aziz, H.A., Isa, M.H., Mohajeri, L., 2010. Effect of initial oil concentration and dispersant on crude oil biodegradation in contaminated seawater. Bull. Environ. Contam. Toxicol. 84, 438-442.

ED_001324_00000209-00025

***Supporting Information**

Biodegradability of Different Initial Concentrations of Alaska North Slope Crude Oil Dispersed with Corexit C9500

Mobing Zhuang[1], Gulizhaer Abulikemu[2], Pablo Campo[3], William Platten III[4], Makram T. Suidan[5]*, Albert D. Venosa (retired)[4]and Robyn N. Conmy[4]

1 Department of Biomedical, Chemical and Environmental Engineering, University of Cincinnati, 2901 Woodside Drive, Cincinnati, OH 45221, USA

2 Pegasus Technical Services Inc., 46 E Hollister St, Cincinnati, OH 45219 USA

3 Cranfield Water Science Institute, Cranfield University, Cranfield, Beds, MK43 0AL, UK

4 U.S. Environmental Protection Agency, NRMRL, 26 W. MLK Drive Cincinnati, OH, 45268, USA

5 Faculty of Engineering and Architecture, American University of Beirut, Bechtel Engineering Bldg. - 3rd flr. - Room 308 P.O. Box: 11-0236 Riad El Solh 1107 2020, Beirut, Lebanon

*Corresponding author: Makram T. Suidan
Tel: 00961-1-347952
Fax: 00961-1-744462
E-mail address: msuidan@aub.edu.lb

ED_001324_00000210-00001

Table S1. Summary of Experimental Layout for High Concentration Experiment.

Test	Temperature	Treatment	Sampling Events	Sample Replicates	Total Experimental Units (EU)
1	5 °C	C9500 alone	11	3	33
2	5 °C	ANS dispersed by C9500	11	3	33
3	5 °C	alone	11	3	33
4	5 °C	Killed ANS control	1	3	3
5	5 °C	Killed C9500 control	11	3	33
6	5 °C	Killed ANS+C9500 control	11	3	33
				Subtotal EU's	**168**
7	25 °C	C9500 alone	9	3	27
8	25 °C	ANS dispersed by C9500	9	3	27
9	25 °C	ANS alone	9	3	27
10	25 °C	Killed ANS control	1	3	3
11	25 °C	Killed C9500 control	9	3	27
12	25 °C	Killed ANS+ C9500 control	9	3	27
				Subtotal EU's	**138**
			Total EU's for High Concentration Experiment		**306**

ED_001324_00000210-00002

Table S2. Summary of Experimental Layout for Low Concentration Experiment.

Test	Temperature	Treatment	Sampling Events	Sample Replicates	Total Experimental Units (EU)
13	5 °C	C9500 alone	11	3	33
14	5 °C	ANS+C9500	11	3	33
15	5 °C	ANS alone	11	3	33
16	5 °C	Killed ANS control	1	3	3
17	5 °C	Killed C9500 control	11	3	33
18	5 °C	Killed (ANS+C9500) control	11	3	33
19	5 °C	Killed (ANS+C9500) +Protease	6	3	18
				Subtotal EU's	**186**
20	25 °C	C9500 alone	10	3	30
21	25 °C	ANS+C9500	10	3	30
22	25 °C	ANS alone	10	3	30
23	25 °C	Killed ANS control	1	3	3
24	25 °C	Killed C9500 control	10	3	30
25	25 °C	Killed (ANS+C9500) control	10	3	30
26	25 °C	Killed (ANS+C9500) +Protease	6	3	18
				Subtotal EU's	**181**
		Total EU's for Low Concentration Experiment			**357**

ED_001324_00000210-00003

Table S3. First-order biodegradation rate coefficients and standard deviations (sd) of individual alkanes in the high concentration experiment.

Compound	5 °C ANS alone		25 °C ANS alone		5 °C ANS+C9500		25 °C ANS+C9500	
	rate (d^{-1})	sd (d^{-1})	rate (d^{-1})	sd (d^{-1})	rate (d^{-1})	sd (d^{-1})	rate (d^{-1})	sd (d^{-1})
C10	0.19	0.02	1.34	0.18	0.63	0.03	2.00	0.34
C11	0.15	0.01	1.16	0.15	0.40	0.02	1.30	0.09
C12	0.12	0.01	1.02	0.14	0.29	0.03	0.96	0.06
C13	0.11	0.01	0.94	0.14	0.27	0.03	0.91	0.05
C14	0.11	0.01	0.92	0.14	0.25	0.03	0.82	0.04
C15	0.11	0.01	0.95	0.14	0.24	0.03	0.84	0.05
C16	0.11	0.01	1.01	0.15	0.24	0.03	0.92	0.05
C17	0.11	0.01	1.08	0.16	0.24	0.03	0.97	0.06
PR	0.15	0.03	0.45	0.11	0.07	0.01	0.39	0.04
C18	0.11	0.01	1.06	0.14	0.22	0.02	0.96	0.05
PH	0.15	0.03	0.46	0.12	0.08	0.01	0.43	0.04
C19	0.11	0.01	1.05	0.14	0.22	0.02	0.97	0.06
C20	0.11	0.01	0.99	0.14	0.21	0.02	0.93	0.05
C21	0.10	0.01	0.97	0.14	0.20	0.02	0.91	0.05
C22	0.10	0.01	0.88	0.13	0.19	0.02	0.84	0.04
C23	0.09	0.01	0.84	0.13	0.18	0.02	0.79	0.04
C24	0.09	0.01	0.84	0.14	0.17	0.02	0.79	0.04
C25	0.09	0.01	0.81	0.13	0.15	0.02	0.81	0.03
C26	0.08	0.01	0.81	0.14	0.12	0.02	0.78	0.04
C27	0.08	0.01	0.74	0.13	0.11	0.01	0.71	0.05
C28	0.12	0.02	0.75	0.12	0.12	0.02	0.60	0.09
C29	0.12	0.02	0.81	0.15	0.12	0.02	0.81	0.07
C30	0.10	0.01	0.83	0.14	0.12	0.02	0.74	0.04
C31	0.09	0.01	0.81	0.14	0.09	0.01	0.61	0.05
C32	0.10	0.01	0.81	0.14	0.09	0.01	0.60	0.06
C33	0.09	0.01	0.68	0.09	0.07	0.01	0.56	0.06
C34	0.08	0.01	0.60	0.09	0.05	0.01	0.54	0.05
C35	0.07	0.01	0.53	0.09	0.04	0.01	0.58	0.04

NA: Rate not calculated because the biodegradation of noted compounds did not follow first order kinetics.

ED_001324_00000210-00004

Table S4. First-order biodegradation rate coefficients and standard deviations (sd) of individual alkanes in low concentration experiment.

Compound	5 °C ANS alone		25 °C ANS alone		5 °C ANS+C9500		25 °C ANS+C9500	
	rate (d^{-1})	sd (d^{-1})	rate (d^{-1})	sd (d^{-1})	rate (d^{-1})	sd (d^{-1})	rate (d^{-1})	sd (d^{-1})
C10	0.47	0.03	0.93	0.16	0.63	0.04	NA1	NA1
C11	0.25	0.02	0.57	0.07	0.25	0.03	0.47	0.02
C12	0.20	0.01	0.38	0.06	0.23	0.02	0.24	0.03
C13	0.18	0.01	0.42	0.06	0.21	0.02	NA2	NA2
C14	0.13	0.01	0.28	0.04	0.15	0.01	NA2	NA2
C15	0.14	0.01	0.35	0.04	0.15	0.01	NA2	NA2
C16	0.14	0.01	0.37	0.04	0.15	0.02	NA2	NA2
C17	0.13	0.01	0.36	0.04	NA2	NA2	NA2	NA2
PR	NA2	NA2	0.04	0.01	NA2	NA2	NA2	NA2
C18	NA2	NA2	0.35	0.04	NA2	NA2	NA2	NA2
PH	NA2	NA2	0.03	0.01	NA2	NA2	NA2	NA2
C19	NA2	NA2	0.32	0.04	NA2	NA2	NA2	NA2
C20	NA2	NA2	0.30	0.04	NA2	NA2	NA2	NA2
C21	NA2	NA2	0.29	0.04	NA2	NA2	NA2	NA2
C22	NA2	NA2	0.17	0.03	NA2	NA2	NA2	NA2
C23	NA2	NA2	NA2	NA2	NA2	NA2	NA2	NA2
C24	NA2	NA2	NA2	NA2	NA2	NA2	NA2	NA2
C25	NA2	NA2	NA2	NA2	NA2	NA2	NA2	NA2
C26	NA2	NA2	NA2	NA2	NA2	NA2	NA2	NA2
C27	NA2	NA2	NA2	NA2	NA2	NA2	NA2	NA2
C28	NA2	NA2	NA2	NA2	NA2	NA2	NA2	NA2
C29	NA2	NA2	NA2	NA2	NA2	NA2	NA2	NA2
C30	NA2	NA2	NA2	NA2	NA2	NA2	NA2	NA2
C31	NA2	NA2	NA2	NA2	NA2	NA2	NA2	NA2
C32	NA2	NA2	NA2	NA2	NA2	NA2	NA2	NA2
C33	NA2	NA2	NA2	NA2	NA2	NA2	NA2	NA2
C34	NA2	NA2	NA2	NA2	NA2	NA2	NA2	NA2
C35	NA2	NA2	NA2	NA2	NA2	NA2	NA2	NA2

NA1: Rate not calculated because of excessively rapid removal after acclimation.
NA2: Rate not calculated because noted compounds were persisted during the experiment.

ED_001324_00000210-00005

Table S5. First-order degradation rate coefficients and standard deviations (sd) of individual PAHs in high concentration experiment.

Compound	5 °C ANS alone		25 °C ANS alone		5 °C ANS+C9500		25 °C ANS+C9500	
	rate (d^{-1})	sd (d^{-1})	rate (d^{-1})	sd (d^{-1})	rate (d^{-1})	sd (d^{-1})	rate (d^{-1})	sd (d^{-1})
nap	0.44	0.04	0.68	0.05	0.71	0.02	1.94	0.02
C1-nap	0.23	0.02	0.60	0.04	0.41	0.03	1.84	0.04
C2-nap	0.17	0.02	0.38	0.07	0.26	0.02	0.61	0.03
C3-nap	0.27	0.02	0.35	0.10	0.20	0.02	0.40	0.05
C4-nap	0.13	0.02	0.29	0.10	0.16	0.02	0.35	0.05
phe	0.19	0.01	0.37	0.09	0.26	0.02	0.46	0.05
C1-phe	0.12	0.01	0.34	0.12	0.19	0.02	0.37	0.06
C2-phe	0.05	0.01	0.21	0.07	0.19	0.03	0.27	0.04
C3-phe	0.00	0.00	0.00	0.00	0.00	0.00	0.00	0.00
C4-phe	0.00	0.00	0.00	0.00	0.00	0.00	0.00	0.00
flu	0.19	0.02	0.37	0.10	0.26	0.02	0.44	0.05
C1-flu	0.15	0.02	0.35	0.11	0.21	0.02	0.39	0.06
C2-flu	0.05	0.01	0.20	0.07	0.11	0.01	0.27	0.04
C3-flu	0.00	0.00	0.00	0.00	0.00	0.00	0.00	0.00
dbt	0.25	0.01	0.43	0.08	0.44	0.02	0.77	0.03
C1-dbt	0.13	0.01	0.32	0.10	0.22	0.02	0.41	0.04
C2-dbt	0.04	0.01	0.17	0.06	0.11	0.01	0.26	0.04
C3-dbt	0.00	0.00	0.00	0.00	0.00	0.00	0.00	0.00
nbt	0.00	0.00	0.00	0.00	0.00	0.00	0.00	0.00
C1-nbt	0.00	0.00	0.00	0.00	0.00	0.00	0.00	0.00
C2-nbt	0.00	0.00	0.00	0.00	0.00	0.00	0.00	0.00
C3-nbt	0.00	0.00	0.00	0.00	0.00	0.00	0.00	0.00
pyr*	--	--	--	--	--	--	--	--
C1-pyr	0.00	0.00	0.00	NA	NA	0.00	NA	NA
C2-pyr	0.00	0.00	0.00	0.00	0.00	0.00	0.00	0.00
cry	0.00	0.00	0.00	0.00	0.00	0.00	0.00	0.00
C1-cry	0.00	0.00	0.00	0.00	0.00	0.00	0.00	0.00
C2-cry	0.00	0.00	0.00	0.00	0.00	0.00	0.00	0.00
C3-cry	0.00	0.00	0.00	0.00	0.00	0.00	0.00	0.00
C4-cry	0.00	0.00	0.00	0.00	0.00	0.00	0.00	0.00

NA: Rate not calculated because noted compounds were persisted during the experiment.
* Not detected in any samples.

ED_001324_00000210-00006

Table S6. First-order degradation rate coefficients and standard deviations (sd) of individual PAHs in low concentration experiment.

Compound	5 °C ANS alone		25 °C ANS alone		5 °C ANS+C9500		25 °C ANS+C9500	
	rate (d^{-1})	sd (d^{-1})	rate (d^{-1})	sd (d^{-1})	rate (d^{-1})	sd (d^{-1})	rate (d^{-1})	sd (d^{-1})
nap	NA	NA	0.29	0.05	0.43	0.09	0.36	0.03
C1-nap	NA	NA	0.24	0.03	0.44	0.09	0.28	0.03
C2-nap	NA	NA	0.17	0.04	0.40	0.09	0.21	0.04
C3-nap	NA	NA	0.18	0.04	0.31	0.06	0.20	0.04
C4-nap	NA	NA	0.13	0.03	0.15	0.02	0.14	0.02
phe	NA	NA	NA	NA	NA	NA	0.19	0.03
C1-phe	NA	NA	NA	NA	0.18	0.03	0.20	0.03
C2-phe	0.25	0.01	0.14	0.03	0.11	0.01	NA	NA
C3-phe	0.02	0.01	0.02	0.00	0.00	0.00	0.00	0.00
C4-phe	0.00	0.00	0.00	0.00	0.00	0.00	0.00	0.00
flu	NA	NA	NA	NA	0.29	0.06	NA	NA
C1-flu	NA	NA	NA	NA	0.15	0.02	0.00	0.00
C2-flu	0.29	0.03	0.14	0.03	0.21	0.01	0.00	0.00
C3-flu	0.02	0.00	0.03	0.00	0.00	0.00	0.02	0.00
dbt	NA	NA	0.00	0.00	0.31	0.11	0.00	0.00
C1-dbt	NA	NA	NA	NA	0.23	0.05	0.29	0.06
C2-dbt	0.00	0.00	0.00	0.00	0.00	0.00	0.00	0.00
C3-dbt	0.00	0.00	0.00	0.00	0.00	0.00	0.00	0.00
nbt	0.00	0.00	NA	NA	0.00	0.00	0.31	0.11
C1-nbt	0.00	0.00	0.00	0.00	0.00	0.00	0.00	0.00
C2-nbt	0.00	0.00	0.00	0.00	0.00	0.00	0.00	0.00
C3-nbt	0.00	0.00	0.00	0.00	0.00	0.00	0.00	0.00
pyr*	--	--	--	--	--	--	--	--
C1-pyr	0.00	0.00	0.00	0.00	0.00	0.00	0.27	0.07
C2-pyr	0.00	0.00	0.00	0.00	0.00	0.00	0.00	0.00
cry	0.00	0.00	0.00	0.00	0.00	0.00	0.00	0.00
C1-cry	0.00	0.00	0.00	0.00	0.00	0.00	0.00	0.00
C2-cry	0.00	0.00	0.00	0.00	0.00	0.00	0.00	0.00
C3-cry	0.00	0.00	0.00	0.00	0.00	0.00	0.00	0.00
C4-cry	0.00	0.00	0.00	0.00	0.00	0.00	0.00	0.00

NA: Rate not calculated because of excessively rapid removal after acclimation.
*Not detected in any samples.

ED_001324_00000210-00007

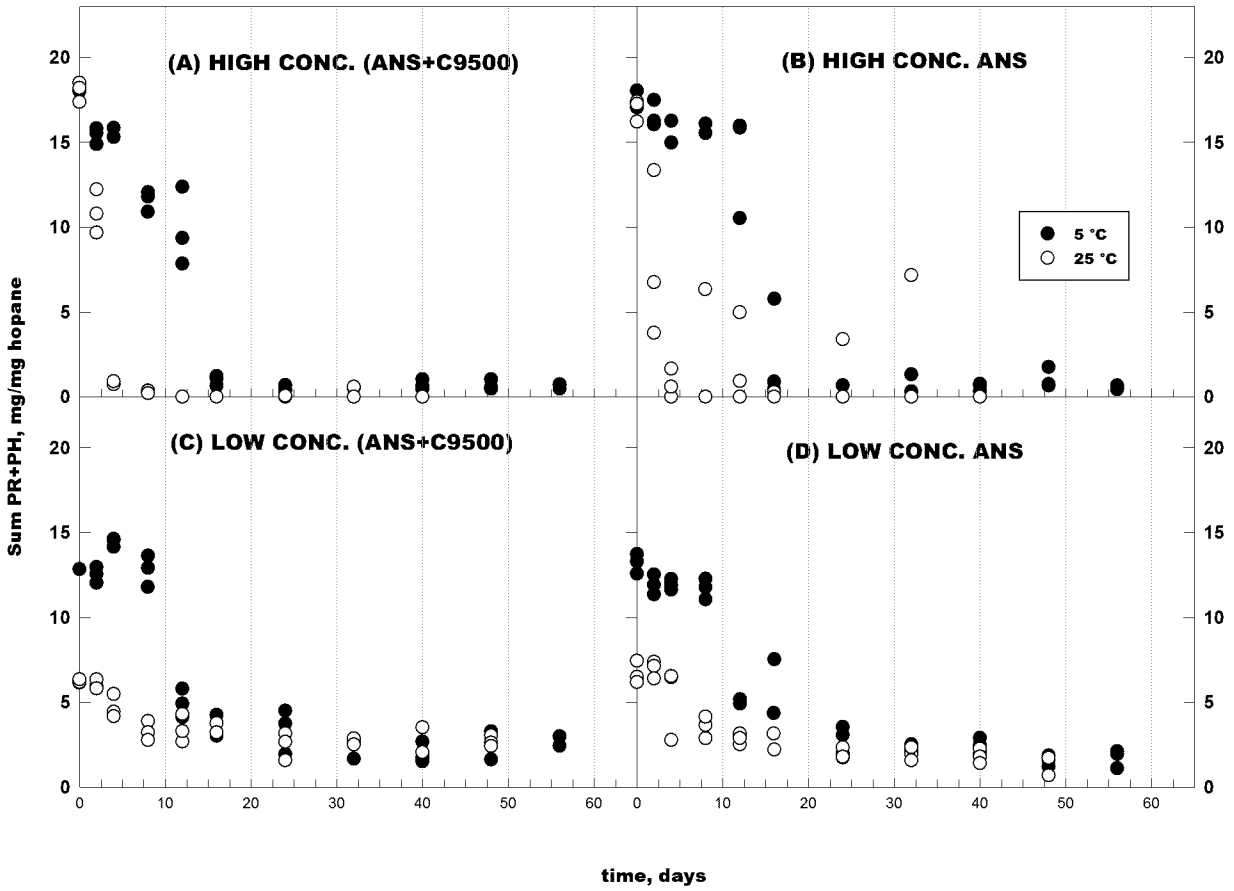

Figure S1. Biodegradation of branched alkanes in the presence (A, C) and absence (B, D) of C9500 at 5 °C and 25 °C. High concentration treatments are in panel A and B, whereas low concentration treatments are in panels C and D.

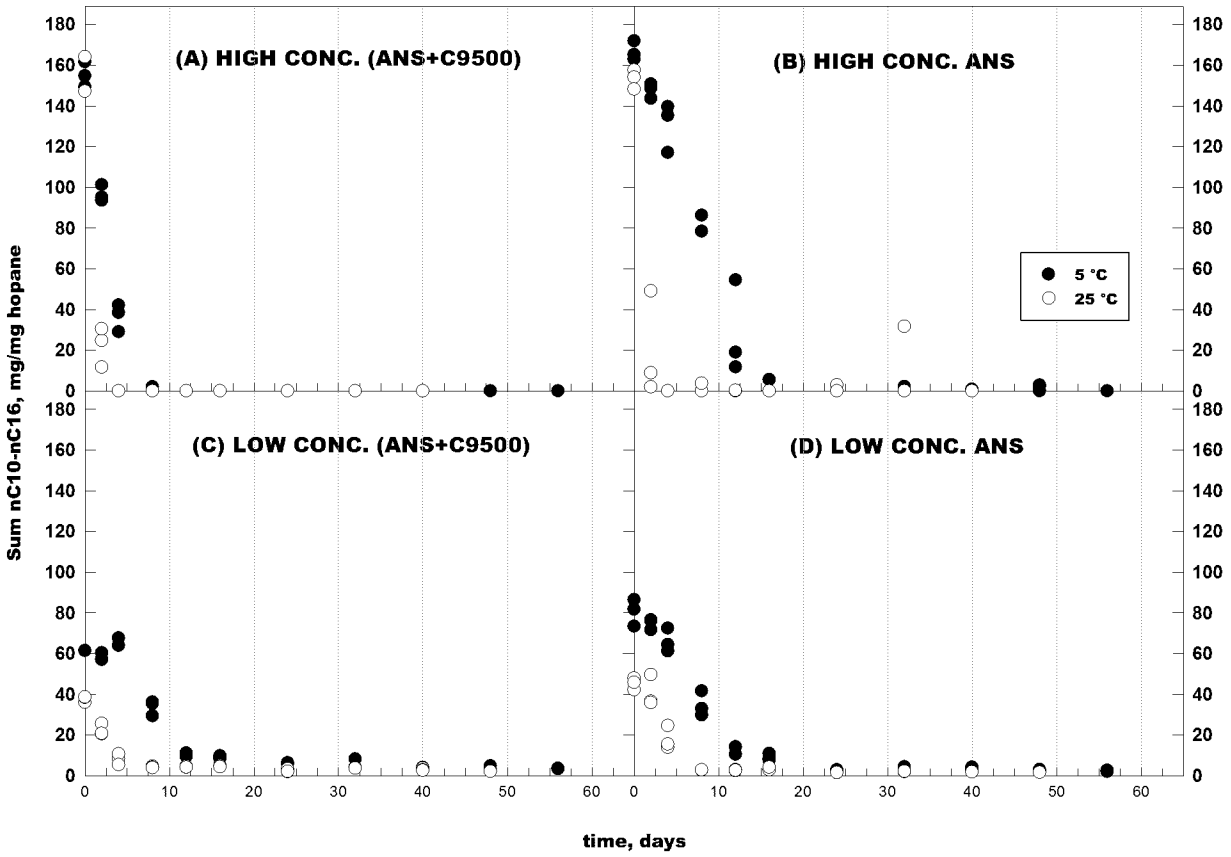

Figure S2. Biodegradation of n-alkanes (nC10-nC16) in the presence (A, C) and absence (B, D) of C9500 at 5 °C and 25 °C. High concentration treatments are in panel A and B, whereas low concentration treatments are in panels C and D.

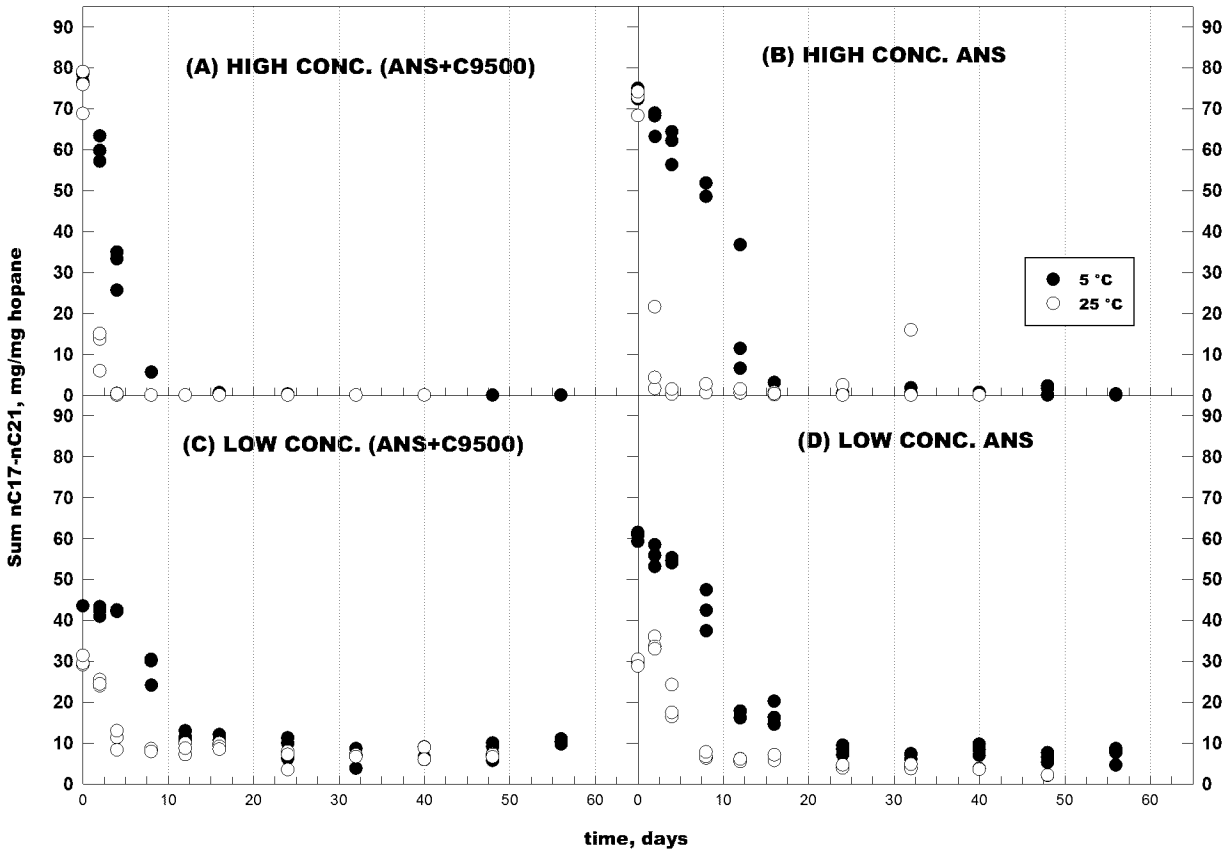

Figure S3. Biodegradation of n-alkanes (nC17-nC21) in the presence (A, C) and absence (B, D) of C9500 at 5 °C and 25 °C. High concentration treatments are in panel A and B, whereas low concentration treatments are in panels C and D.

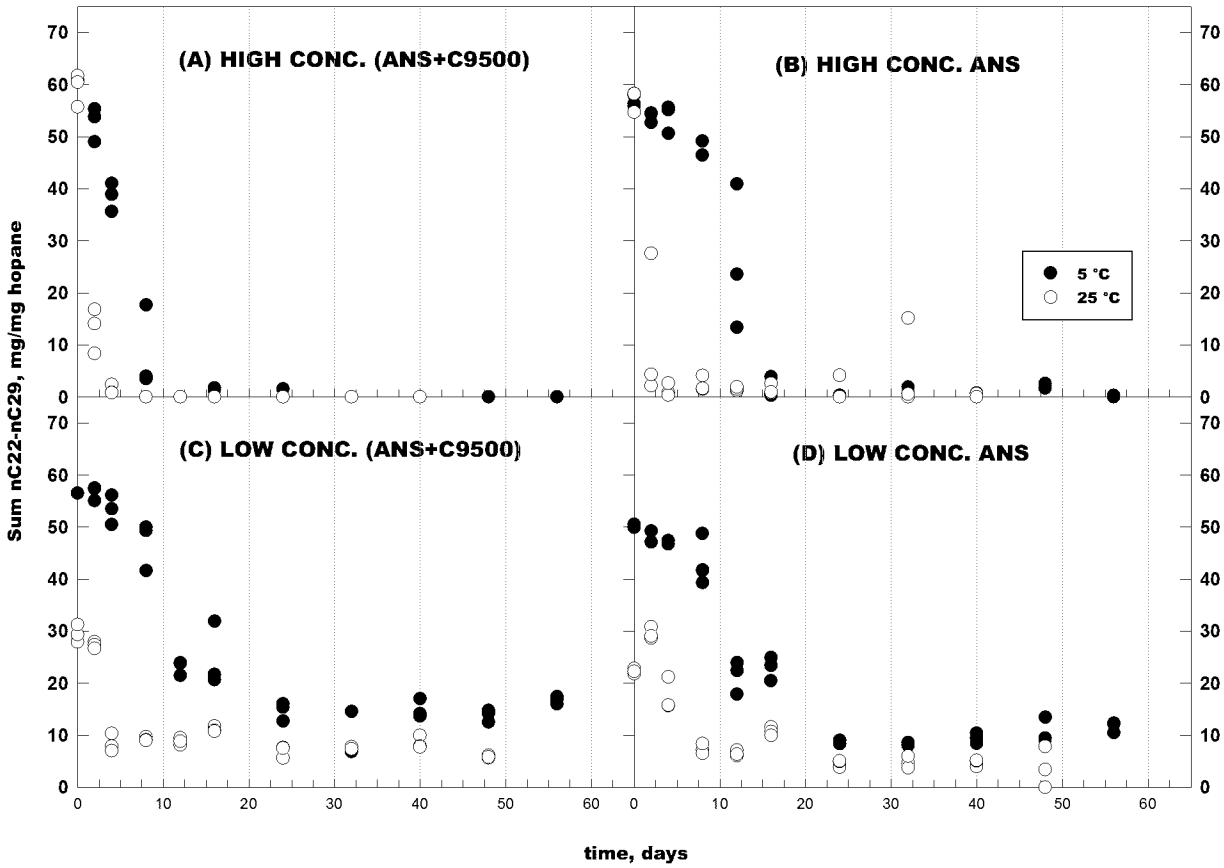

Figure S4. Biodegradation of n-alkanes (nC22-nC29) in the presence (A, C) and absence (B, D) of C9500 at 5 °C and 25 °C. High concentration treatments are in panel A and B, whereas low concentration treatments are in panels C and D.

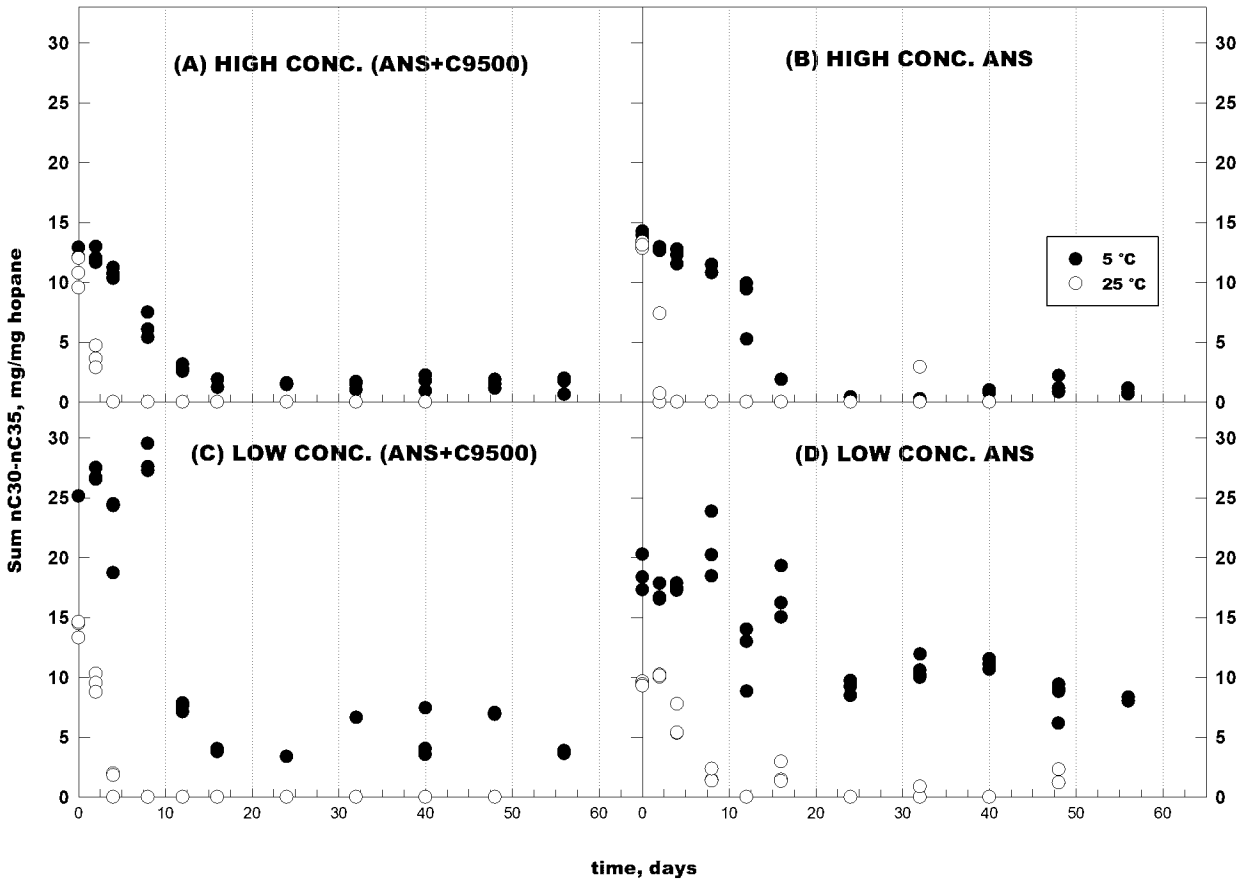

Figure S5. Biodegradation of n-alkanes (nC30-nC35) in the presence (A, C) and absence (B, D) of C9500 at 5 °C and 25 °C. High concentration treatments are in panel A and B, whereas low concentration treatments are in panels C and D.

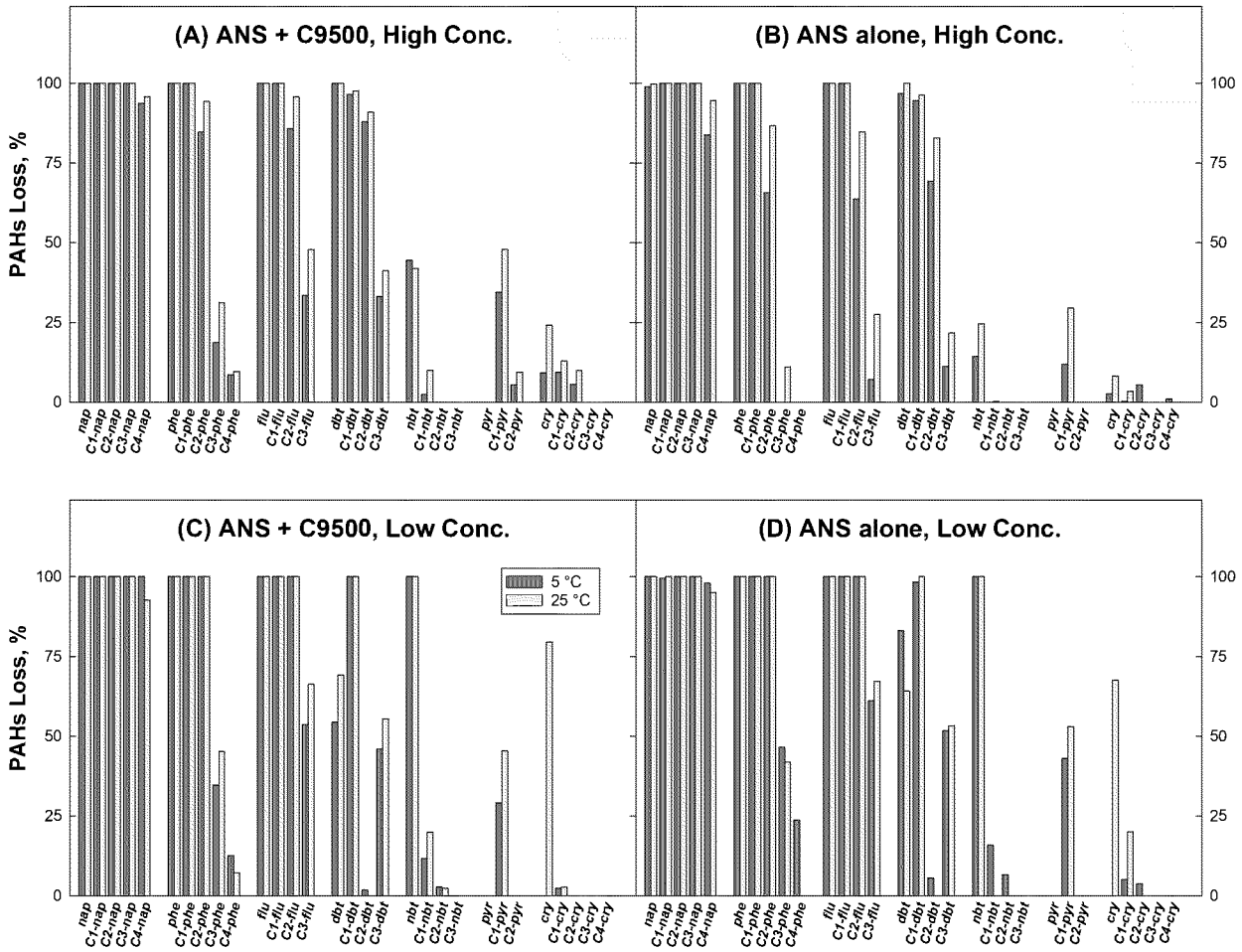

Figure S6. Loss percentage of individual PAH in the presence (A, C) and absence (B, D) of C9500 at 5 °C and 25 °C in high concentration (A, B) and low concentration (C, D) experiment.

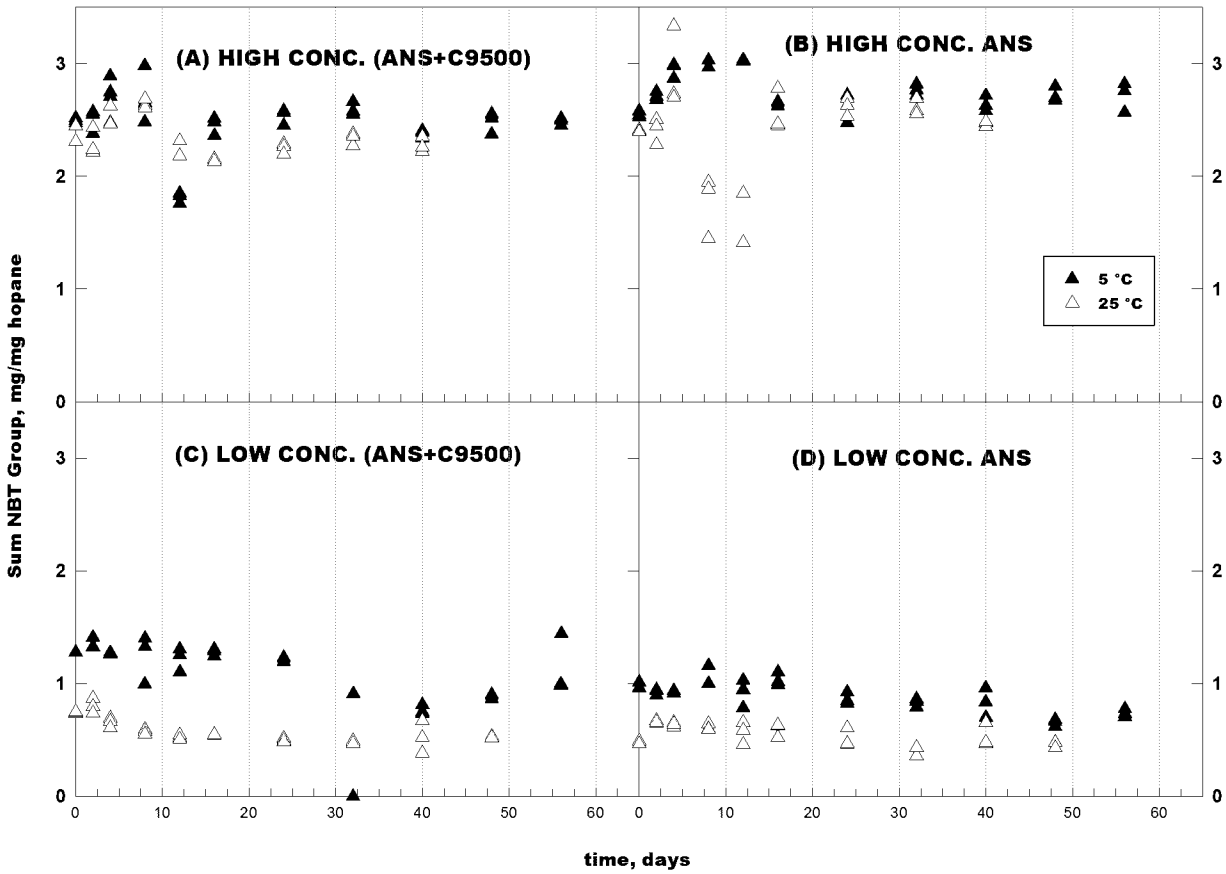

Figure S7. Biodegradation of naphthobenzothiophene homologues in the presence (A, C) and absence (B, D) of C9500 at 5 °C and 25 °C. High concentration treatments are in panel A and B, whereas low concentration treatments are in panels C and D.

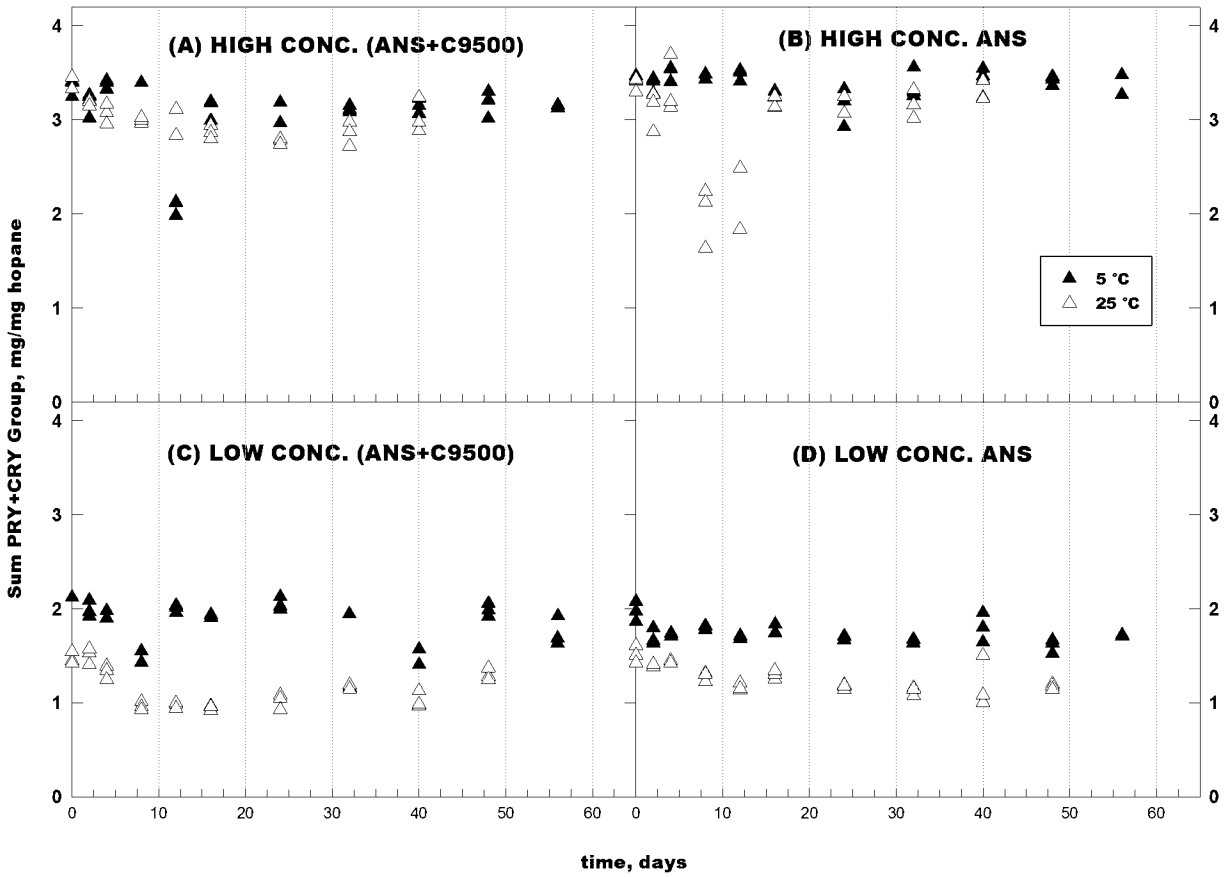

Figure S8. Biodegradation of pyrene homologues + chrysene homologues in the presence (A, C) and absence (B, D) of C9500 at 5 °C and 25 °C. High concentration treatments are in panel A and B, whereas low concentration treatments are in panels C and D.

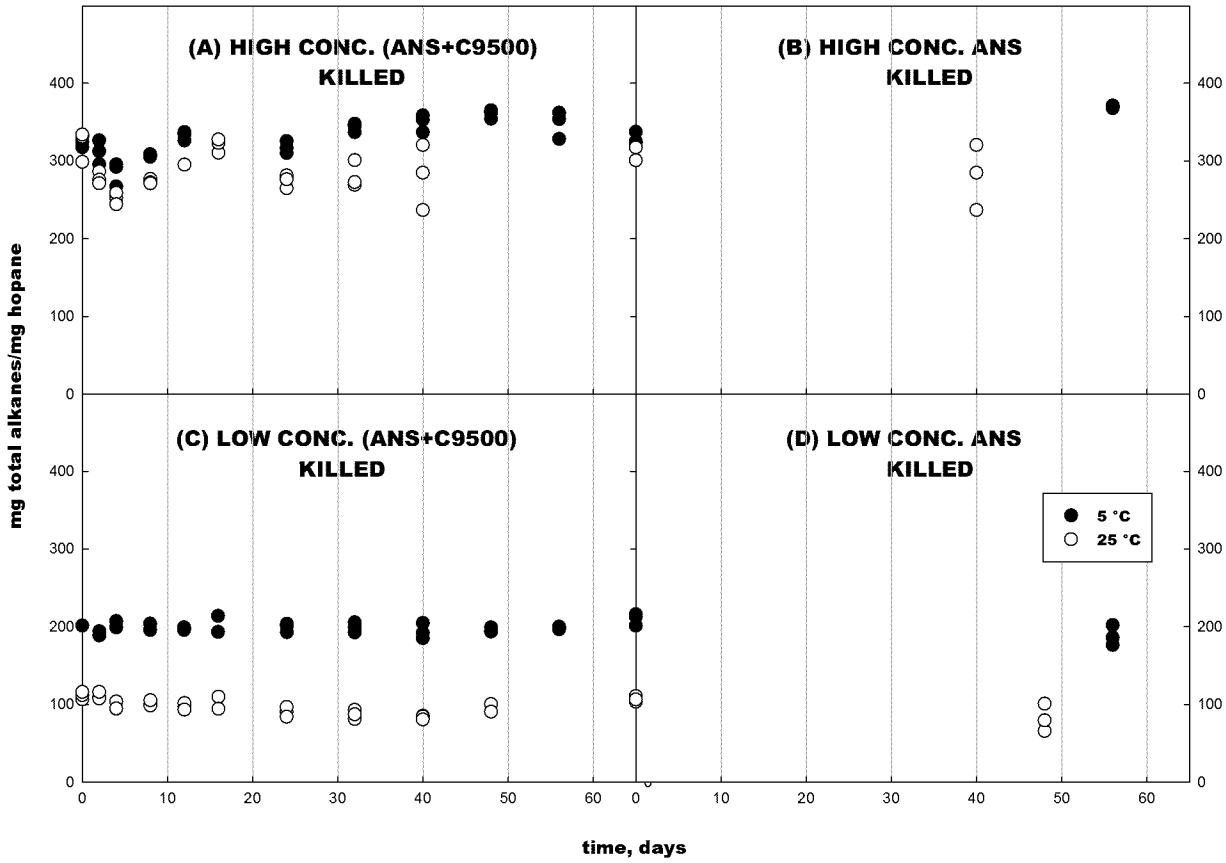

Figure S9. Biodegradation of hopane-normalized total alkanes at both temperatures in high concentration treatments (A, B) and low concentration treatments (C, D) in killed control samples.

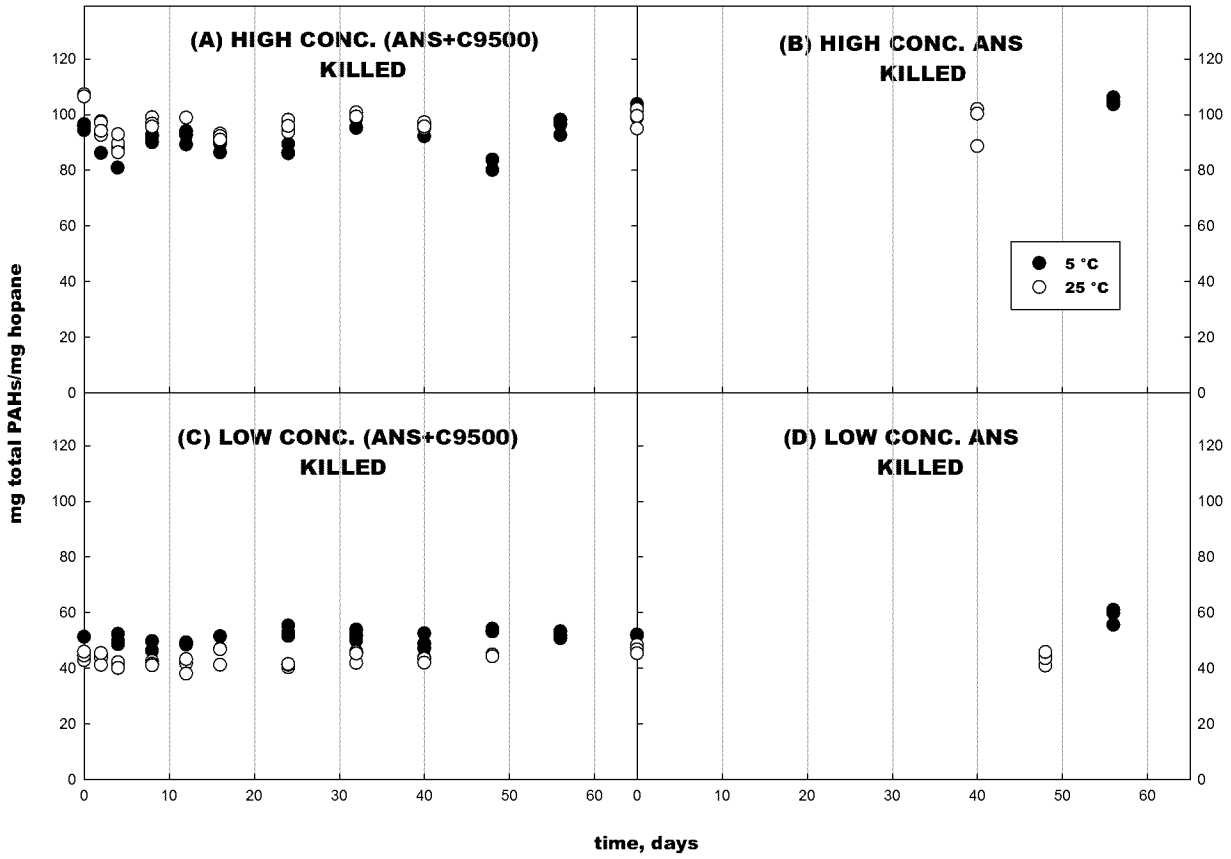

Figure S10. Biodegradation of hopane-normalized total PAHs at both temperatures in high concentration treatments (A, B) and low concentration treatments (C, D) in killed control samples.

ıdation of branched alkanes in the presence and absence of C9500 at 5 °C and 25 °C. (Hopane Normalize					
	Low Conc.				High Conc.
Time	5 °C (ANS+C9500)	5 °C ANS	25 °C (ANS+C9500)	25 °C ANS	5 °C (ANS+C9500)
0	12.84	13.73	6.15	6.48	18.05
0	N/A	13.28	6.18	6.18	18.00
0	N/A	12.57	6.34	7.44	18.14
2	12.56	11.91	5.93	7.37	15.53
2	12.03	11.35	6.34	7.12	14.88
2	12.96	12.51	5.81	6.39	15.82
4	14.56	12.25	5.48	6.46	15.84
4	14.62	11.90	4.42	6.53	15.30
4	14.14	11.62	4.16	2.76	15.30
8	11.77	11.05	3.88	3.64	12.05
8	12.91	12.27	3.22	4.13	10.91
8	13.63	11.76	2.76	2.87	11.79
12	5.78	5.17	2.67	2.51	12.34
12	4.12	4.96	4.30	3.14	7.84
12	4.91	4.93	3.28	2.87	9.34
16	4.24	7.50	3.76	3.13	1.20
16	3.21	4.34	3.20	3.16	0.64
16	3.01	7.56	3.21	2.20	1.07
24	1.94	3.06	1.57	1.73	0.68
24	4.49	3.53	3.15	2.33	0.36
24	3.73	1.98	2.66	1.77	0.42
32	2.71	1.58	2.86	1.92	0.51
32	1.66	2.12	2.50	1.57	0.56
32	N/A	2.51	N/A	2.34	0.52
40	2.67	1.99	3.51	2.26	0.63
40	1.74	2.45	2.02	1.78	1.02
40	1.51	2.89	2.05	1.40	0.45
48	3.07	1.58	3.03	1.71	0.56
48	1.61	1.85	2.61	0.68	0.47
48	3.28	1.20	2.41	N/A	1.02
56	2.46	2.10	N/A	N/A	0.73
56	2.99	1.10	N/A	N/A	0.47
56	2.49	1.94	N/A	N/A	0.69

nce of C9500 at 5 °C and 25 °C. (Hopane Normalized)		
High Conc.		
5 °C ANS	25 °C (ANS+C9500)	25 °C ANS
17.04	17.37	17.39
18.04	18.50	17.25
17.25	18.19	16.21
17.48	10.80	3.76
16.25	12.21	6.75
16.05	9.67	13.36
16.26	0.74	0.00
14.98	0.73	0.59
16.26	0.91	1.66
N/A	0.36	0.00
15.53	0.35	0.00
16.09	0.20	6.35
15.97	0.00	0.92
10.52	0.00	0.00
15.85	N/A	4.96
0.89	0.00	0.27
0.43	0.00	0.00
5.77	0.00	0.00
0.67	0.00	3.37
0.00	0.00	0.00
0.00	0.05	0.00
1.32	0.00	7.16
0.00	0.58	0.00
0.30	0.00	0.00
0.75	0.00	0.00
0.33	0.00	0.00
0.67	0.00	0.00
0.65	N/A	N/A
0.74	N/A	N/A
1.74	N/A	N/A
0.66	N/A	N/A
0.57	N/A	N/A
0.44	N/A	N/A

on of n-alkanes (nC10-nC16) in the presence and absence of C9500 at 5 °C and 25 °C. (Hopane Normaliz

	Low Conc.				High Conc.
Time	5 °C (ANS+C9500)	5 °C ANS	25 °C (ANS+C9500)	25 °C ANS	5 °C (ANS+C9500)
0	61.42	81.75	35.98	42.14	154.75
0	N/A	86.45	38.42	47.85	149.36
0	N/A	73.37	38.57	45.80	161.58
2	60.36	76.19	20.48	49.55	95.06
2	57.00	71.63	25.63	36.51	93.54
2	57.32	76.48	20.79	35.84	101.23
4	67.71	72.43	8.22	13.85	42.12
4	66.97	61.22	10.65	15.46	28.97
4	63.69	64.39	5.39	24.54	38.40
8	29.35	32.97	4.63	2.75	1.95
8	35.43	41.65	4.13	2.73	0.00
8	36.18	29.92	3.90	2.83	0.00
12	11.10	10.54	4.06	2.92	0.00
12	9.73	14.21	4.58	2.45	0.00
12	9.44	11.76	4.13	2.64	0.00
16	9.74	8.37	4.88	3.03	0.00
16	8.86	7.68	4.78	2.85	0.00
16	8.41	10.88	4.32	4.13	0.00
24	2.03	2.90	1.90	1.66	0.00
24	6.34	2.62	3.29	1.51	0.00
24	5.78	2.87	2.09	1.52	0.00
32	8.19	4.36	4.00	2.23	0.00
32	4.11	3.95	3.66	1.96	0.00
32	N/A	3.36	N/A	2.11	0.00
40	4.00	2.90	3.67	2.03	0.00
40	3.29	3.55	2.86	1.82	0.00
40	3.73	4.18	2.58	1.83	0.00
48	4.78	2.63	2.15	1.67	0.00
48	3.12	2.97	2.14	1.63	0.00
48	4.74	2.48	2.06	1.58	0.00
56	3.40	2.38	N/A	N/A	0.00
56	3.61	2.02	N/A	N/A	0.00
56	3.47	2.60	N/A	N/A	0.00

absence of C9500 at 5 °C and 25 °C. (Hopane Normalized)		
High Conc.		
5 °C ANS	25 °C (ANS+C9500)	25 °C ANS
162.85	147.15	157.53
171.87	163.96	154.04
165.17	164.03	148.16
143.61	24.70	1.89
150.68	30.45	8.83
148.62	11.66	49.04
139.59	0.00	0.00
117.09	0.00	0.00
135.23	0.00	0.00
N/A	0.00	0.00
78.39	0.00	0.00
86.17	0.00	3.70
54.49	0.00	0.00
11.66	0.00	0.00
18.81	N/A	0.22
0.00	0.00	0.00
0.00	0.00	0.00
5.49	0.00	0.00
0.00	0.00	2.88
0.00	0.00	0.00
0.00	0.00	0.00
2.09	0.00	31.65
0.00	0.00	0.00
0.00	0.00	0.00
0.00	0.00	0.00
0.70	0.00	0.00
0.00	0.00	0.00
0.00	N/A	N/A
2.08	N/A	N/A
2.83	N/A	N/A
0.00	N/A	N/A
0.00	N/A	N/A
0.00	N/A	N/A

n of n-alkanes (nC17-nC21) in the presence and absence of C9500 at 5 °C and 25 °C. (Hopane Normalize					
	Low Conc.				High Conc.
Time	5 °C (ANS+C9500)	5 °C ANS	25 °C (ANS+C9500)	25 °C ANS	5 °C (ANS+C9500)
0	43.46	60.73	29.09	29.64	78.45
0	N/A	61.43	29.45	30.40	76.47
0	N/A	59.23	31.37	28.77	78.72
2	42.29	55.83	23.96	36.01	59.76
2	40.92	53.07	25.45	33.55	57.11
2	43.27	58.39	24.42	32.98	63.32
4	42.09	55.24	11.31	16.42	34.95
4	42.50	54.50	12.97	17.45	25.61
4	42.42	53.98	8.30	24.21	33.28
8	24.08	37.34	8.22	6.29	5.62
8	30.04	47.41	8.56	6.70	0.00
8	30.42	42.35	7.88	7.78	0.00
12	12.95	16.17	7.15	6.12	0.00
12	11.45	17.67	9.91	5.44	0.00
12	10.52	16.95	8.70	6.07	0.00
16	12.03	16.27	9.97	5.94	0.58
16	10.67	14.38	9.15	5.81	0.31
16	9.49	20.25	8.44	7.05	0.00
24	6.17	8.45	3.45	4.51	0.26
24	11.25	9.43	7.92	3.87	0.00
24	9.90	7.13	7.19	4.60	0.00
32	8.63	6.09	7.07	3.87	0.00
32	3.79	7.37	6.65	3.69	0.00
32	N/A	7.18	N/A	4.79	0.00
40	9.03	6.96	8.93	3.73	0.00
40	6.48	8.35	5.91	3.61	0.00
40	6.00	9.71	5.95	3.58	0.00
48	9.08	6.51	7.28	2.06	0.00
48	5.68	7.62	7.13	2.10	0.00
48	9.97	5.19	6.58	2.12	0.00
56	9.58	8.61	N/A	N/A	0.00
56	10.99	4.58	N/A	N/A	0.00
56	10.45	7.64	N/A	N/A	0.00

nd absence of C9500 at 5 °C and 25 °C. (Hopane Normalized)		
High Conc.		
5 °C ANS	25 °C (ANS+C9500)	25 °C ANS
73.62	68.76	72.83
74.95	75.88	74.11
72.34	79.02	68.27
68.90	13.65	1.58
68.18	15.04	4.30
63.23	5.93	21.56
64.34	0.00	0.28
56.27	0.38	0.24
62.13	0.32	1.43
N/A	0.00	0.62
48.51	0.00	0.55
51.79	0.00	2.66
36.70	0.00	0.47
6.53	0.00	0.49
11.36	N/A	1.46
0.25	0.00	0.69
0.07	0.00	0.07
3.09	0.00	0.35
0.43	0.00	2.47
0.22	0.00	0.00
0.00	0.00	0.00
1.79	0.00	15.92
0.00	0.00	0.00
0.55	0.00	0.00
0.00	0.00	0.00
0.67	0.00	0.00
0.00	0.00	0.00
0.00	N/A	N/A
1.68	N/A	N/A
2.23	N/A	N/A
0.00	N/A	N/A
0.27	N/A	N/A
0.00	N/A	N/A

on of n-alkanes (nC22-nC29) in the presence and absence of C9500 at 5 °C and 25 °C. (Hopane Normaliz

	Low Conc.				High Conc.
Time	5 °C (ANS+C9500)	5 °C ANS	25 °C (ANS+C9500)	25 °C ANS	5 °C (ANS+C9500)
0	56.50	49.89	27.91	21.79	60.65
0	N/A	50.50	29.33	22.80	60.55
0	N/A	50.07	31.23	22.26	60.95
2	55.04	46.99	27.91	30.80	53.78
2	57.37	49.25	27.36	28.66	48.99
2	57.48	48.97	26.67	29.04	55.32
4	50.52	46.70	7.88	15.66	40.99
4	56.12	47.45	10.33	15.77	35.64
4	53.48	47.47	7.00	21.18	38.89
8	41.63	39.41	9.69	7.18	17.63
8	49.31	48.72	9.10	6.51	3.35
8	49.97	41.72	8.98	8.36	4.04
12	23.89	22.53	8.12	6.05	0.00
12	21.73	17.85	9.49	7.11	0.00
12	21.47	23.89	8.81	6.34	0.00
16	21.68	23.47	11.74	11.55	1.71
16	20.63	20.49	10.92	10.68	1.30
16	31.90	24.82	10.76	9.96	0.00
24	12.65	9.05	5.60	3.78	1.54
24	16.07	8.98	7.62	5.11	0.00
24	15.47	8.42	7.51	5.01	0.00
32	14.51	8.16	7.75	4.61	0.00
32	6.82	8.59	7.33	3.72	0.00
32	N/A	8.02	N/A	5.97	0.00
40	16.96	8.41	9.96	3.98	0.00
40	14.15	9.41	7.90	5.05	0.00
40	13.67	10.38	7.71	5.16	0.00
48	14.18	9.13	5.62	0.00	0.00
48	12.50	13.48	6.12	3.39	0.00
48	14.76	9.45	5.82	7.82	0.00
56	15.99	11.87	N/A	N/A	0.00
56	17.38	10.56	N/A	N/A	0.00
56	16.90	12.35	N/A	N/A	0.00

absence of C9500 at 5 °C and 25 °C. (Hopane Normalized)		
High Conc.		
5 °C ANS	25 °C (ANS+C9500)	25 °C ANS
56.30	55.69	58.25
57.97	61.68	58.21
55.87	60.44	54.68
54.42	14.06	2.15
54.53	16.77	4.29
52.69	8.32	27.57
55.61	2.37	0.80
50.66	0.85	0.33
55.12	0.79	2.62
N/A	0.00	1.47
46.43	0.00	1.61
49.10	0.00	4.09
40.94	0.00	1.14
13.37	0.00	1.47
23.50	N/A	1.89
0.27	0.00	2.57
0.52	0.00	0.73
3.86	0.00	0.92
0.28	0.00	4.12
0.25	0.00	0.00
0.00	0.00	0.00
1.88	0.00	15.12
0.00	0.00	0.00
0.69	0.00	0.52
0.00	0.00	0.59
0.73	0.00	0.00
0.00	0.00	0.00
2.55	N/A	N/A
1.66	N/A	N/A
2.20	N/A	N/A
0.00	N/A	N/A
0.27	N/A	N/A
0.00	N/A	N/A

ion of n-alkanes (nC30-nC35) in the presence and absence of C9500 at 5 °C and 25 °C. (Hopane Normali

	Low Conc.				High Conc.
Time	5 °C (ANS+C9500)	5 °C ANS	25 °C (ANS+C9500)	25 °C ANS	5 °C (ANS+C9500)
0	25.13	20.27	13.30	9.65	12.10
0	N/A	17.31	14.49	9.43	12.90
0	N/A	18.37	14.62	9.29	12.90
2	26.53	16.52	10.30	10.03	12.01
2	27.50	17.84	9.53	10.23	11.65
2	26.68	16.68	8.76	10.13	12.97
4	18.71	17.61	0.00	5.34	10.32
4	24.27	17.85	1.97	5.38	10.70
4	24.43	17.27	1.81	7.78	11.23
8	27.26	20.21	0.00	1.42	7.48
8	27.59	23.85	0.00	1.35	5.40
8	29.56	18.46	0.00	2.35	6.08
12	7.84	14.00	0.00	0.00	3.16
12	7.11	8.85	0.00	0.00	2.55
12	7.58	12.99	0.00	0.00	2.78
16	4.02	19.32	0.00	1.45	1.90
16	3.87	15.02	0.00	1.32	1.21
16	3.77	16.21	0.00	2.96	0.00
24	0.00	8.52	0.00	0.00	0.00
24	3.38	9.18	0.00	0.00	1.58
24	3.37	9.69	0.00	0.00	1.44
32	6.63	10.03	0.00	0.00	1.01
32	0.00	10.59	0.00	0.00	1.53
32	N/A	11.92	N/A	0.88	1.68
40	4.05	11.53	0.00	0.00	1.78
40	3.53	11.09	0.00	0.00	0.92
40	7.42	10.66	0.00	0.00	2.23
48	7.02	6.17	0.00	1.19	1.48
48	0.00	9.42	0.00	1.20	1.13
48	6.88	8.81	0.00	2.31	1.87
56	3.87	8.03	N/A	N/A	1.96
56	3.68	8.26	N/A	N/A	1.73
56	3.87	8.31	N/A	N/A	0.63

absence of C9500 at 5 °C and 25 °C. (Hopane Normalized)		
High Conc.		
5 °C ANS	25 °C (ANS+C9500)	25 °C ANS
13.45	9.54	12.84
14.25	10.77	13.35
13.92	12.01	13.11
12.64	3.62	0.00
12.80	4.71	0.72
12.94	2.88	7.40
12.28	0.00	0.00
11.52	0.00	0.00
12.76	0.00	0.00
N/A	0.00	0.00
10.78	0.00	0.00
11.47	0.00	0.00
9.92	0.00	0.00
5.23	0.00	0.00
9.43	N/A	0.00
0.00	0.00	0.00
0.00	0.00	0.00
1.87	0.00	0.00
0.41	0.00	0.00
0.04	0.00	0.00
0.00	0.00	0.00
0.25	0.00	2.92
0.00	0.00	0.00
0.00	0.00	0.00
0.80	0.00	0.00
0.76	0.00	0.00
0.98	0.00	0.00
2.19	N/A	N/A
0.83	N/A	N/A
1.15	N/A	N/A
0.67	N/A	N/A
0.73	N/A	N/A
1.14	N/A	N/A

idual PAH in the presence and absence of C9500 at 5 °C and 25 °C in high and low concentration experi

	Low Conc.			
Compound	5 °C (ANS+C9500)	5 °C ANS	25 °C (ANS+C9500)	25 °C ANS
nap	100	100	100	100
C1-nap	100	100	100	100
C2-nap	100	100	100	100
C3-nap	100	100	100	100
C4-nap	100	98	93	95
phe	100	100	100	100
C1-phe	100	100	100	100
C2-phe	100	100	100	100
C3-phe	35	47	45	42
C4-phe	13	24	7	0
flu	100	100	100	100
C1-flu	100	100	100	100
C2-flu	100	100	100	100
C3-flu	54	61	66	67
dbt	54	83	69	64
C1-dbt	100	98	100	100
C2-dbt	2	6	0	0
C3-dbt	46	52	55	53
nbt	100	100	100	100
C1-nbt	12	16	20	0
C2-nbt	3	7	2	0
C3-nbt	BDL	BDL	BDL	BDL
C1-pyr	29	43	45	53
C2-pyr	BDL	BDL	BDL	BDL
cry	BDL	BDL	80	68
C1-cry	2	5	3	20
C2-cry	0	4	0	0
C3-cry	BDL	BDL	BDL	BDL
C4-cry	BDL	BDL	BDL	BDL

e of C9500 at 5 °C and 25 °C in high and low concentration experiment. Unit: %

High Conc.			
5 °C (ANS+C9500)	5 °C ANS	25 °C (ANS+C9500)	25 °C ANS
100	99	100	100
100	100	100	100
100	100	100	100
100	100	100	100
94	84	96	94
100	100	100	100
100	100	100	100
85	66	94	87
19	0	31	11
9	0	10	0
100	100	100	100
100	100	100	100
86	64	96	85
34	7	48	28
100	97	100	100
96	95	98	96
88	69	91	83
33	11	41	22
45	14	42	25
2	0	10	0
0	0	0	0
0	0	0	0
35	12	48	30
5	0	9	0
9	3	24	8
9	0	13	3
6	6	10	0
0	0	0	0
0	1	0	0

BDL: below detection limit

of naphthobenzothiophene homologues in the presence and absence of C9500 at 5 °C and 25 °C. (Hopa

	Low Conc.				High Conc.
Time	5 °C (ANS+C9500)	5 °C ANS	25 °C (ANS+C9500)	25 °C ANS	5 °C (ANS+C9500)
0	1.28	1.01	0.74	0.47	2.49
0	N/A	0.96	0.75	0.49	2.52
0	N/A	0.96	0.75	0.47	2.47
2	1.33	0.90	0.87	0.67	2.55
2	1.41	0.95	0.80	0.65	2.38
2	1.33	0.94	0.74	0.66	2.57
4	1.26	0.92	0.69	0.65	2.89
4	1.28	0.92	0.67	0.61	2.75
4	1.26	0.94	0.61	0.64	2.71
8	0.99	1.00	0.59	0.64	2.65
8	1.33	1.16	0.58	0.60	2.48
8	1.40	1.00	0.55	0.59	2.98
12	1.31	0.95	0.52	0.66	1.85
12	1.25	0.78	0.54	0.46	1.83
12	1.10	1.03	0.51	0.59	1.76
16	1.31	1.10	0.55	0.52	2.48
16	1.29	0.99	0.54	0.62	2.36
16	1.25	1.01	0.55	0.63	2.51
24	1.20	0.93	0.52	0.61	2.58
24	1.24	0.82	0.50	0.46	2.45
24	1.20	0.85	0.48	0.47	2.56
32	0.91	0.86	0.49	0.43	2.55
32	0.49	0.79	0.47	0.36	2.58
32	0.00	0.84	N/A	0.43	2.66
40	0.81	0.70	0.67	0.65	2.39
40	0.75	0.83	0.52	0.47	2.34
40	0.74	0.96	0.38	0.48	2.40
48	0.89	0.63	0.53	0.48	2.55
48	0.91	0.68	0.53	0.48	2.38
48	0.87	0.66	0.52	0.43	2.51
56	1.00	0.71	N/A	N/A	2.49
56	0.99	0.78	N/A	N/A	2.51
56	1.44	0.74	N/A	N/A	2.45

and absence of C9500 at 5 °C and 25 °C. (Hopane Normalized)		
High Conc.		
5 °C ANS	25 °C (ANS+C9500)	25 °C ANS
2.58	N/A	2.41
2.54	2.31	2.39
2.53	2.45	2.39
2.71	2.43	2.50
2.75	2.21	2.44
2.68	2.24	2.28
2.99	2.48	2.73
2.87	2.46	2.70
2.98	2.62	3.33
N/A	2.63	1.45
2.97	2.61	1.95
3.03	2.69	1.89
3.02	2.18	1.41
3.02	2.31	1.85
3.03	N/A	N/A
2.62	2.15	2.78
2.66	2.13	2.45
2.66	2.13	2.46
2.63	2.29	2.69
2.47	2.26	2.63
2.72	2.20	2.53
2.82	2.27	2.69
2.72	2.38	2.58
2.77	2.35	2.55
2.72	2.22	2.47
2.58	2.35	2.44
2.63	2.26	2.48
2.70	N/A	N/A
2.67	N/A	N/A
2.80	N/A	N/A
2.57	N/A	N/A
2.81	N/A	N/A
2.75	N/A	N/A

Homologues + Chrysene Homologues in the presence and absence of C9500 at 5 °C and 25 °C. (Hopane				
	Low Conc.			
Time	5 °C (ANS+C9500)	5 °C ANS	25 °C (ANS+C9500)	25 °C ANS
0	2.12	2.08	1.45	1.61
0	N/A	1.87	1.43	1.51
0	N/A	1.98	1.55	1.43
2	1.92	1.63	1.53	1.41
2	1.97	1.67	1.58	1.38
2	2.09	1.80	1.41	1.41
4	1.90	1.71	1.39	1.42
4	1.90	1.74	1.34	1.45
4	1.98	1.74	1.25	1.43
8	1.43	1.78	1.01	1.32
8	1.43	1.82	0.96	1.23
8	1.55	1.82	0.93	1.31
12	2.02	1.71	0.99	1.21
12	1.96	1.69	1.00	1.14
12	2.04	1.68	0.94	1.15
16	1.94	1.84	0.97	1.26
16	1.91	1.75	0.92	1.30
16	1.90	1.83	0.96	1.35
24	2.03	1.71	1.08	1.19
24	2.00	1.67	1.05	1.14
24	2.13	1.71	0.93	1.18
32	1.94	1.65	1.19	1.16
32	1.16	1.64	1.15	1.08
32	N/A	1.68	N/A	1.15
40	1.57	1.65	1.13	1.50
40	1.58	1.81	0.97	1.01
40	1.41	1.96	0.99	1.09
48	2.06	1.53	1.28	1.20
48	1.99	1.64	1.37	1.18
48	1.92	1.67	1.25	1.14
56	1.64	1.71	N/A	N/A
56	1.69	1.72	N/A	N/A
56	1.93	1.73	N/A	N/A

ues in the presence and absence of C9500 at 5 °C and 25 °C. (Hopane Normalized)

High Conc.			
5 °C (ANS+C9500)	5 °C ANS	25 °C (ANS+C9500)	25 °C ANS
3.25	3.44	N/A	3.42
3.41	3.47	3.33	3.43
3.40	3.41	3.46	3.30
3.25	3.44	3.21	3.27
3.02	3.42	3.20	3.19
3.26	3.28	3.15	2.88
3.42	3.54	3.08	3.14
3.33	3.41	2.96	3.20
3.40	3.55	3.17	3.70
3.00	N/A	2.97	1.63
2.97	3.43	3.00	2.24
3.39	3.49	3.03	2.13
2.13	3.50	2.84	1.84
2.12	3.41	3.11	2.49
1.98	3.53	N/A	N/A
3.19	3.31	2.94	3.13
2.99	3.24	2.87	3.14
3.18	3.31	2.80	3.25
3.19	3.33	2.79	3.25
2.97	2.93	2.80	3.07
3.18	3.20	2.74	3.07
3.08	3.56	2.72	3.32
3.11	3.26	2.98	3.02
3.15	3.30	2.87	3.16
3.15	3.55	2.89	3.42
3.07	3.43	3.24	3.24
3.23	3.47	2.97	3.23
3.21	3.46	N/A	N/A
3.02	3.36	N/A	N/A
3.30	3.43	N/A	N/A
3.16	3.27	N/A	N/A
3.16	3.48	N/A	N/A
3.13	3.48	N/A	N/A

Biodegradation of hopane-normalized total alkanes at both temperatures in killed control samples.

	Low Conc.				
Time	5 °C (ANS+C9500) Killed	25 °C (ANS+C9500) Killed	Time	5 °C ANS Killed	25 °C ANS Killed
0	201.19	106.28	0	212.64	103.23
0	N/A	111.69	0	215.69	110.47
0	N/A	115.79	0	201.05	106.13
2	188.85	109.22	48	N/A	65.71
2	193.84	107.48	48	N/A	100.68
2	N/A	115.91	48	N/A	79.39
4	207.53	94.27	56	176.29	N/A
4	207.27	103.39	56	201.79	N/A
4	199.48	94.60	56	185.69	N/A
8	195.09	99.40			
8	N/A	98.50			
8	203.86	105.19			
12	198.66	96.99			
12	195.27	101.40			
12	N/A	92.99			
16	N/A	N/A			
16	214.10	109.66			
16	193.17	94.15			
24	203.19	90.37			
24	191.77	96.50			
24	199.14	83.84			
32	198.75	81.10			
32	205.41	92.71			
32	192.43	87.02			
40	204.58	85.19			
40	184.95	84.20			
40	191.63	80.48			
48	198.82	100.12			
48	193.92	N/A			
48	193.39	90.43			
56	200.17	N/A			
56	197.08	N/A			
56	199.21	N/A			

tal alkanes at both temperatures in killed control samples.

High Conc.				
5 °C (ANS+C9500) Killed	25 °C (ANS+C9500) killed	Time	5 °C ANS Killed	25 °C ANS Killed
324.00	298.51	0	323.27	318.85
317.28	330.78	0	337.09	316.96
332.29	333.70	0	324.56	300.42
295.42	286.23	40	N/A	284.55
326.16	275.50	40	N/A	236.64
312.15	270.97	40	N/A	320.20
266.79	252.38	56	370.83	N/A
292.12	258.68	56	368.25	N/A
295.18	244.03	56	367.53	N/A
308.75	276.45			
306.35	272.15			
304.03	270.84			
336.62	295.39			
327.41	N/A			
326.12	N/A			
310.24	310.24			
322.89	322.89			
327.34	327.34			
325.16	281.09			
309.90	264.57			
316.43	276.04			
347.30	300.82			
336.36	268.96			
344.82	272.35			
352.86	284.55			
336.53	236.64			
358.17	320.20			
353.87	N/A			
361.78	N/A			
364.63	N/A			
327.97	N/A			
353.50	N/A			
361.63	N/A			

odegradation of hopane-normalized total PAHs at both temperatures in killed control samples.

	Low Conc.				
Time	5 °C (ANS+C9500) Killed	25 °C (ANS+C9500) killed	Time	5 °C ANS Killed	25 °C ANS Killed
0	51.17	42.79	0	52.01	48.24
0	N/A	44.48	0	51.70	46.65
0	N/A	45.87	0	47.45	45.24
2	43.83	43.56	48	N/A	40.86
2	44.56	41.10	48	N/A	43.49
2	N/A	45.32	48	N/A	45.69
4	51.17	42.05	56	55.51	N/A
4	52.20	42.01	56	59.74	N/A
4	48.66	39.98	56	60.88	N/A
8	46.22	42.48			
8	N/A	41.54			
8	49.62	40.97			
12	48.41	41.65			
12	49.20	43.16			
12	N/A	37.95			
16	N/A	N/A			
16	51.37	46.72			
16	46.91	41.08			
24	55.21	40.21			
24	51.47	41.11			
24	52.73	41.41			
32	49.89	41.80			
32	53.75	45.84			
32	51.52	45.19			
40	52.46	43.77			
40	47.06	43.32			
40	48.75	41.89			
48	53.41	44.79			
48	53.12	N/A			
48	54.08	44.17			
56	50.61	N/A			
56	53.20	N/A			
56	51.10	N/A			

total PAHs at both temperatures in killed control samples.

High Conc.				
5 °C (ANS+C9500) Killed	25 °C (ANS+C9500) Killed	Time	5 °C ANS Killed	25 °C ANS Killed
95.81	N/A	0	98.86	101.86
94.35	107.21	0	103.69	99.41
96.46	106.42	0	101.52	94.89
86.13	97.04	40	N/A	101.88
97.50	92.57	40	N/A	88.57
94.17	94.08	40	N/A	100.23
80.91	89.58	56	106.09	N/A
88.91	92.81	56	103.58	N/A
87.59	86.34	56	104.57	N/A
92.66	98.93			
92.13	96.63			
89.98	95.58			
93.94	98.78			
89.18	N/A			
92.55	N/A			
86.34	93.03			
89.46	92.14			
91.11	90.89			
89.32	98.05			
86.01	93.62			
86.15	95.81			
98.48	100.70			
95.08	98.94			
95.26	99.18			
95.49	97.16			
92.12	94.93			
96.37	95.62			
146.91	N/A			
83.75	N/A			
80.01	N/A			
92.54	N/A			
98.04	N/A			
96.40	N/A			

To: Conmy, Robyn[Conmy.Robyn@epa.gov]
From: Robinson, Brian
Sent: Thur 1/28/2016 8:14:35 PM
Subject: RE: GoMRI Presentation
GoMRI Presentation - Robinson.pptx

Hi Robyn,

I'm still working on my talk, but I just wanted to send along a copy as it stands now. I've decided to make the VOC results the focus of my talk so that the overlap between our presentations is minimized. But of course there is going to be some of the same coverage – talking about the tank setup, experimental design and some droplet size data. I've thrown in a few of the videos and pictures too. Please feel free to tell me if you think there is too much overlap and I will adjust. I was planning on really selling your talk during the project objectives slide – people should stick around after the coffee break to hear more!

Let me know if you have any questions or concerns.

Brian

From: Conmy, Robyn [mailto:Conmy.Robyn@epa.gov]
Sent: January-25-16 9:51 AM
To: Robinson, Brian; Michel Boufadel
Cc: King, Thomas L
Subject: RE: GoMRI Presentation

Wonderful news Brian! And thank you for sending the fluorescence information on Friday. I am working on the issue this morning.

<>/<>/<>/<>/<>/<>/<>/<>/<>/<>/<>/<>/<>/<>/<>/<>/<>

Robyn N. Conmy, Ph.D.

Research Ecologist

USEPA/NRMRL/LRPCD

26 West MLK Drive

Cincinnati, Ohio 45268

513-569-7090 (office)

513-431-1970 (EPA mobile)

727-692-5333 (Personal mobile)

conmy.robyn@epa.gov

From: Robinson, Brian [mailto:Brian.Robinson@dfo-mpo.gc.ca]
Sent: Monday, January 25, 2016 8:47 AM
To: Michel Boufadel <boufadel@gmail.com>
Cc: Conmy, Robyn <Conmy.Robyn@epa.gov>; King, Thomas L <Tom.King@dfo-mpo.gc.ca>
Subject: RE: GoMRI Presentation

Some news to report!

I have been granted travel approval! Flights have been tentatively booked, but there is still one more layer to approval before I can confirm I will be able to attend. I'll keep you updated.

Unfortunately, Tom will most likely not be able to attend due to an illness in the family. He will let you know if things change.

Brian

From: Michel Boufadel [mailto:boufadel@gmail.com]
Sent: January-22-16 11:38 AM
To: Robinson, Brian
Cc: Conmy, Robyn (Conmy.Robyn@epa.gov); King, Thomas L
Subject: Re: GoMRI Presentation

Hi Brian,

It is really unfortunate that this is happening. Maybe Robyn could fill your time slot by presenting similar or even your results?

Michel

On Fri, Jan 22, 2016 at 10:34 AM, Robinson, Brian <Brian.Robinson@dfo-mpo.gc.ca> wrote:

Hi Michel,

I wanted to inform you that unfortunately our travel request to attend the GoMRI conference still has not been approved. Even though our request was submitted months ago, there has been a recent delay in granting travel approval which has affected a number of people, not just us.

At this late point, I would say our chances of attending the conference are slim. Even if the travel request is signed off on, we still have to go through another level of approval before our flights can be booked.

Given this, I think it will best if I withdrew my presentation giving you an opportunity to fill the time slot with another presenter. This is probably best anyways, since Robyn and my presentations were back to back and there would have been a lot of overlap.

I will have my poster completed early next week and will have it FedEx'ed to the hotel for display.

Brian

Brian Robinson

Aquatic Science Chemist
Fishieries and Oceans Canada/Government of Canada
Brian.Robinson@dfo-mpo.gc.ca
Tel: (902) 426-3639

Chimiste en sciences aquatiques
Pêches et Océans Canada/Gouvernement du Canada
Brian.Robinson@dfo-mpo.gc.ca
Tel: (902) 426-3639

--

Michel C. Boufadel, PhD, PE, BCEE, F. ASCE, D.WRE, P.Hydro.
Director, Center for Natural Resources Development and Protection (NRDP)

Professor, John A. Reif, Jr. Dept. Civil and Environmental Engineering

The New Jersey Institute of Technology

Room 435 Colton Hall

323 MLK Blvd, Newark, NJ 07102-1824

Ph: 973-596-6079

email: boufadel@gmail.com

http://civil.njit.edu/people/Boufadel.php

http://nrdp.njit.edu

To: Conmy, Robyn[Conmy.Robyn@epa.gov]; Baldwin, Maxanne[Baldwin.Maxanne@epa.gov]
From: Clark, Patrick
Sent: Mon 5/2/2016 3:38:16 PM
Subject: RE: Finasol OSR 52 Sample Request

I have no clue. I didn't see the purchase card thing. I'll have to ask..

From: Conmy, Robyn
Sent: Monday, May 02, 2016 11:33 AM
To: Baldwin, Maxanne <Baldwin.Maxanne@epa.gov>; Clark, Patrick <Clark.Patrick@epa.gov>
Subject: Fwd: Finasol OSR 52 Sample Request

Not sure how we can purchase this as they don't accept purchase cards? PR??

Sent from my iPhone

Begin forwarded message:

From: Malcolm Gore <malcolm.gore@clearcoastllc.com>
Date: May 2, 2016 at 11:19:03 AM EDT
To: "Conmy, Robyn" <Conmy.Robyn@epa.gov>
Subject: Re: Finasol OSR 52 Sample Request

Hello Robyn

This has been processed our side. We cannot accept credit cards and would ask for a check or direct transfer be made as per the invoice.

Please advise on payment timing

Thank you.

Malcolm

Malcolm Gore

President

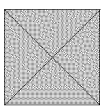

+1 832 244 1533

malcolm.gore@clearcoastllc.com

www.clearcoastllc.com

From: "Conmy, Robyn" <Conmy.Robyn@epa.gov>
Date: Thursday, April 28, 2016 at 1:02 PM
To: malcolm gore <malcolm.gore@clearcoastllc.com>
Subject: RE: Finasol OSR 52 Sample Request

Yes we have received the invoice and I have provided our purchase card holder with the information. He will be contacting your office for payment.

Cheers,

Robyn

<>/<>/<>/<>/<>/<>/<>/<>/<>/<>/<>/<>/<>/<>/<>/<>

Robyn N. Conmy, Ph.D.

Research Ecologist

USEPA/NRMRL/LRPCD

26 West MLK Drive

Cincinnati, Ohio 45268

513-569-7090 (office)

513-431-1970 (EPA mobile)

727-692-5333 (Personal mobile)

conmy.robyn@epa.gov

From: Malcolm Gore [mailto:malcolm.gore@clearcoastllc.com]
Sent: Thursday, April 28, 2016 1:43 PM
To: Conmy, Robyn <Conmy.Robyn@epa.gov>
Subject: Re: Finasol OSR 52 Sample Request

Hi Robyn

I have given the go ahead on this. Please confirm receipt of the invoice sent yesterday.

Malcolm

Malcolm Gore

President

CLEAR COAST

+1 832 244 1533

malcolm.gore@clearcoastllc.com

www.clearcoastllc.com

From: "Conmy, Robyn" <Conmy.Robyn@epa.gov>
Date: Tuesday, April 26, 2016 at 11:05 AM
To: malcolm gore <malcolm.gore@clearcoastllc.com>
Subject: RE: Finasol OSR 52 Sample Request

Thanks for the update!

<>/<>/<>/<>/<>/<>/<>/<>/<>/<>/<>/<>/<>/<>/<>/<>/<>/<>

Robyn N. Conmy, Ph.D.

Research Ecologist

USEPA/NRMRL/LRPCD

26 West MLK Drive

Cincinnati, Ohio 45268

513-569-7090 (office)

513-431-1970 (EPA mobile)

727-692-5333 (Personal mobile)

conmy.robyn@epa.gov

From: Malcolm Gore [mailto:malcolm.gore@clearcoastllc.com]
Sent: Monday, April 25, 2016 5:45 PM
To: Conmy, Robyn <Conmy.Robyn@epa.gov>
Subject: Re: Finasol OSR 52 Sample Request

Apologies for the delay Robyn

Awaiting some shipping information. Should have this to you in the morning.

Malcolm

Malcolm Gore

President

CLEAR COAST

+1 832 244 1533

malcolm.gore@clearcoastllc.com

www.clearcoastllc.com

From: "Conmy, Robyn" <Conmy.Robyn@epa.gov>
Date: Monday, April 25, 2016 at 10:05 AM
To: malcolm gore <malcolm.gore@clearcoastllc.com>
Cc: Peter Egan <peter.egan@total.com>
Subject: RE: Finasol OSR 52 Sample Request

Hello Malcolm,

Thank you for getting back with me regarding the purchase. Yes, the information below is correct, with a mail stop at room 166. Can you send to me the invoice via email so I can provide to the purchase card holder to make the purchase?

Thank you in advance,

Robyn

<>/<>/<>/<>/<>/<>/<>/<>/<>/<>/<>/<>/<>/<>/<>/<>/<>

Robyn N. Conmy, Ph.D.

Research Ecologist

USEPA/NRMRL/LRPCD

26 West MLK Drive

Cincinnati, Ohio 45268

513-569-7090 (office)

513-431-1970 (EPA mobile)

727-692-5333 (Personal mobile)

conmy.robyn@epa.gov

From: Malcolm Gore [mailto:malcolm.gore@clearcoastllc.com]
Sent: Monday, April 25, 2016 10:57 AM
To: Conmy, Robyn <Conmy.Robyn@epa.gov>
Cc: Peter Egan <peter.egan@total.com>
Subject: Finasol OSR 52 Sample Request

Hello Robin

I am writing with respect to your email below regarding a sample request of Total Finasol OSR 52.

Clear Coast is the custodian of the product stored here in Houston for Total.

I will arrange the sample as requested.

Please confirm the following:

Contact:

Robyn Conmy 513-569-7090 (office)

Deliver to:

26 West MLK Drive

Cincinnati, Ohio 45268

513-569-7090 (office)

Quantity:

2 US Gallons.

On receipt of confirmation I will get the samples drawn, packaged and dispatched.

Regards

Malcolm

Malcolm Gore

President

CLEAR COAST

+1 832 244 1533

malcolm.gore@clearcoastllc.com

www.clearcoastllc.com

From: Conmy, Robyn
Sent: Monday, April 18, 2016 10:47 AM
To: 'peter.egan@total.com' <peter.egan@total.com>
Cc: Wilson, Gregory <Wilson.Gregory@epa.gov>; Principe, Vanessa <Principe.Vanessa@epa.gov>
Subject: purchase of Finasol OSR52

Mr. Egan,

This follows up our telephone conversation of April 11.

As discussed, EPA is seeking to acquire a number of dispersant products listed on the NCP Subpart J Product Schedule for the purposes of both toxicity and efficacy testing. The product testing is intended to further inform currently proposed regulatory actions under Subpart J of the National Contingency Plan. The products will in addition be used to support our general research in the area of oil spill response.

Your product Finasol OSR52 has been identified as one of interest, as it is commonly stockpiled in the U.S. Not only could the product be encountered when presented with a response situation, but including this dispersant product in toxicity and efficacy testing studies will also allow for comparison and consistency with other existing and ongoing studies by EPA and other federal agencies. EPA's Office of Research and Development (ORD) will be conducting the dispersant studies.

At this time we are seeking 2 U.S. gallons of the product.

We appreciate your time and attention to this request.

Respectfully,

Robyn Conmy

<>/<>/<>/<>/<>/<>/<>/<>/<>/<>/<>/<>/<>/<>/<>/<>/<>/<>

Robyn N. Conmy, Ph.D.

Research Ecologist

USEPA/NRMRL/LRPCD

26 West MLK Drive

Cincinnati, Ohio 45268

513-569-7090 (office)

513-431-1970 (EPA mobile)

727-692-5333 (Personal mobile)

conmy.robyn@epa.gov

CLEAR COAST

To: Conmy, Robyn[Conmy.Robyn@epa.gov]
From: McClellan, Kim
Sent: Tue 1/26/2016 9:35:57 PM
Subject: STICS Entries

Hi Robyn,

The posters that I attached last week have been cleared. See below.

Complete Citation and Review	Brian Dyson	Devi Sundaravadivel	ORD-013921	Evaluation of Sorbent and Solidifier Properties and their Impact on Oil Removal Efficiency	Posted 1/22/2016 2:38 PM
Complete Citation and Review	Brian Dyson	Ruta Deshpande	ORD-013912	Biodegradability Of Diluted Bitumen Oil By Kalamazoo River Cultures In Freshwater	Posted 1/22/2016 2:32 PM
Complete Citation and Review	Brian Dyson	Yu Zhang	ORD-013915	Biodegradation of Finasol OSR 52 and Dispersed Alaska North Slope Crude Oil at 5 C and 25 C	Posted 1/22/2016 2:23 PM
Complete Citation and Review	Brian Dyson	Mobing Zhuang	ORD-013917	Biodegradability of Dispersed Heavy Fuel Oil at 5 and 25 C	Posted 1/22/2016 2:18 PM

As soon as I get the presentations, I will send you an email.

Thanks,

Kim

To: Conmy, Robyn[Conmy.Robyn@epa.gov]
From: Steffek, Timothy
Sent: Thur 4/7/2016 11:43:26 AM
Subject: Re: dispersant question

I have the guys at Ohmsett looking into our stock. I'll let you know what we have once they get back to me.

Timothy Steffek

Bureau of Safety & Environmental Enforcement
Oil Spill Preparedness Division
45600 Woodland Road, VAE-OSPD
Sterling, VA 20166
(703) 787-1562

On Tue, Apr 5, 2016 at 11:19 AM, Conmy, Robyn <Conmy.Robyn@epa.gov> wrote:

> Yes – the hypdersaline project. We have dwindling supplies and want to make sure we have enough.

<>/<>/<>/<>/<>/<>/<>/<>/<>/<>/<>/<>/<>/<>/<>/<>/<>/<>

Robyn N. Conmy, Ph.D.

Research Ecologist

USEPA/NRMRL/LRPCD

26 West MLK Drive

Cincinnati, Ohio 45268

513-569-7090 (office)

513-431-1970 (EPA mobile)

727-692-5333 (Personal mobile)

conmy.robyn@epa.gov

From: Steffek, Timothy [mailto:timothy.steffek@bsee.gov]
Sent: Tuesday, April 05, 2016 11:18 AM
To: Conmy, Robyn <Conmy.Robyn@epa.gov>

Subject: Re: dispersant question

for a BSEE project?

Timothy Steffek
Bureau of Safety & Environmental Enforcement
Oil Spill Preparedness Division

45600 Woodland Road, VAE-OSPD

Sterling, VA 20166

(703) 787-1562

On Tue, Apr 5, 2016 at 10:08 AM, Conmy, Robyn <Conmy.Robyn@epa.gov> wrote:

Hey Tim,

Any chance that OHMSETT has 500 ml of the following to spare?

Corexit 9500A

Finasol OSR 52

Accell Clean DWD

Dispersit SPC1000

Thanks,

Robyn

<>/<>/<>/<>/<>/<>/<>/<>/<>/<>/<>/<>/<>/<>/<>/<>/<>

Robyn N. Conmy, Ph.D.

Research Ecologist

USEPA/NRMRL/LRPCD

26 West MLK Drive

Cincinnati, Ohio 45268

513-569-7090 (office)

513-431-1970 (EPA mobile)

727-692-5333 (Personal mobile)

conmy.robyn@epa.gov

To: Conmy, Robyn[Conmy.Robyn@epa.gov]
From: Malcolm Gore
Sent: Mon 5/2/2016 3:19:03 PM
Subject: Re: Finasol OSR 52 Sample Request

Hello Robyn
This has been processed our side. We cannot accept credit cards and would ask for a check or direct transfer be made as per the invoice.
Please advise on payment timing
Thank you.
Malcolm

Malcolm Gore
President

CLEAR COAST

+1 832 244 1533
malcolm.gore@clearcoastllc.com
www.clearcoastllc.com

From: "Conmy, Robyn" <Conmy.Robyn@epa.gov>
Date: Thursday, April 28, 2016 at 1:02 PM
To: malcolm gore <malcolm.gore@clearcoastllc.com>
Subject: RE: Finasol OSR 52 Sample Request

Yes we have received the invoice and I have provided our purchase card holder with the information. He will be contacting your office for payment.

Cheers,

Robyn

<>/<>/<>/<>/<>/<>/<>/<>/<>/<>/<>/<>/<>/<>/<>/<>/<>/<>

Robyn N. Conmy, Ph.D.

Research Ecologist

USEPA/NRMRL/LRPCD

26 West MLK Drive

Cincinnati, Ohio 45268

513-569-7090 (office)

513-431-1970 (EPA mobile)

727-692-5333 (Personal mobile)

conmy.robyn@epa.gov

From: Malcolm Gore [mailto:malcolm.gore@clearcoastllc.com]
Sent: Thursday, April 28, 2016 1:43 PM
To: Conmy, Robyn <Conmy.Robyn@epa.gov>
Subject: Re: Finasol OSR 52 Sample Request

Hi Robyn

I have given the go ahead on this. Please confirm receipt of the invoice sent yesterday.

Malcolm

Malcolm Gore

President

CLEAR COAST

+1 832 244 1533

malcolm.gore@clearcoastllc.com

www.clearcoastllc.com

From: "Conmy, Robyn" <Conmy.Robyn@epa.gov>
Date: Tuesday, April 26, 2016 at 11:05 AM
To: malcolm gore <malcolm.gore@clearcoastllc.com>
Subject: RE: Finasol OSR 52 Sample Request

Thanks for the update!

<>/<>/<>/<>/<>/<>/<>/<>/<>/<>/<>/<>/<>/<>/<>/<>/<>

Robyn N. Conmy, Ph.D.

Research Ecologist

USEPA/NRMRL/LRPCD

26 West MLK Drive

Cincinnati, Ohio 45268

513-569-7090 (office)

513-431-1970 (EPA mobile)

727-692-5333 (Personal mobile)

conmy.robyn@epa.gov

From: Malcolm Gore [mailto:malcolm.gore@clearcoastllc.com]
Sent: Monday, April 25, 2016 5:45 PM
To: Conmy, Robyn <Conmy.Robyn@epa.gov>
Subject: Re: Finasol OSR 52 Sample Request

Apologies for the delay Robyn

Awaiting some shipping information. Should have this to you in the morning.

Malcolm

Malcolm Gore

President

CLEAR COAST

+1 832 244 1533

malcolm.gore@clearcoastllc.com

www.clearcoastllc.com

From: "Conmy, Robyn" <Conmy.Robyn@epa.gov>
Date: Monday, April 25, 2016 at 10:05 AM
To: malcolm gore <malcolm.gore@clearcoastllc.com>
Cc: Peter Egan <peter.egan@total.com>
Subject: RE: Finasol OSR 52 Sample Request

Hello Malcolm,

Thank you for getting back with me regarding the purchase. Yes, the information below is correct, with a mail stop at room 166. Can you send to me the invoice via email so I can provide to the purchase card holder to make the purchase?

Thank you in advance,

Robyn

<>/<>/<>/<>/<>/<>/<>/<>/<>/<>/<>/<>/<>/<>/<>/<>/<>

Robyn N. Conmy, Ph.D.

Research Ecologist

USEPA/NRMRL/LRPCD

26 West MLK Drive

Cincinnati, Ohio 45268

513-569-7090 (office)

513-431-1970 (EPA mobile)

727-692-5333 (Personal mobile)

conmy.robyn@epa.gov

From: Malcolm Gore [mailto:malcolm.gore@clearcoastllc.com]
Sent: Monday, April 25, 2016 10:57 AM

To: Conmy, Robyn <Conmy.Robyn@epa.gov>
Cc: Peter Egan <peter.egan@total.com>
Subject: Finasol OSR 52 Sample Request

Hello Robin

I am writing with respect to your email below regarding a sample request of Total Finasol OSR 52.

Clear Coast is the custodian of the product stored here in Houston for Total.

I will arrange the sample as requested.

Please confirm the following:

Contact:

Robyn Conmy 513-569-7090 (office)

Deliver to:

26 West MLK Drive

Cincinnati, Ohio 45268

513-569-7090 (office)

Quantity:

2 US Gallons.

On receipt of confirmation I will get the samples drawn, packaged and dispatched.

Regards

Malcolm

Malcolm Gore

President

CLEAR COAST

+1 832 244 1533

malcolm.gore@clearcoastllc.com

www.clearcoastllc.com

From: Conmy, Robyn
Sent: Monday, April 18, 2016 10:47 AM
To: 'peter.egan@total.com' <peter.egan@total.com>
Cc: Wilson, Gregory <Wilson.Gregory@epa.gov>; Principe, Vanessa <Principe.Vanessa@epa.gov>
Subject: purchase of Finasol OSR52

Mr. Egan,

This follows up our telephone conversation of April 11.

As discussed, EPA is seeking to acquire a number of dispersant products listed on the NCP Subpart J Product Schedule for the purposes of both toxicity and efficacy testing. The product testing is intended to further inform currently proposed regulatory actions under Subpart J of the National Contingency Plan. The products will in addition be used to support our general research in the area of oil spill response.

Your product Finasol OSR52 has been identified as one of interest, as it is commonly stockpiled in the U.S. Not only could the product be encountered when presented with a response situation, but including this dispersant product in toxicity and efficacy testing studies will also allow for comparison and consistency with other existing and ongoing studies by EPA and other federal agencies. EPA's Office of Research and Development (ORD) will be conducting the dispersant studies.

At this time we are seeking 2 U.S. gallons of the product.

We appreciate your time and attention to this request.

Respectfully,

Robyn Conmy

<>/<>/<>/<>/<>/<>/<>/<>/<>/<>/<>/<>/<>/<>/<>/<>

Robyn N. Conmy, Ph.D.

Research Ecologist

USEPA/NRMRL/LRPCD

26 West MLK Drive

Cincinnati, Ohio 45268

513-569-7090 (office)

513-431-1970 (EPA mobile)

727-692-5333 (Personal mobile)

conmy.robyn@epa.gov

To: Conmy, Robyn[Conmy.Robyn@epa.gov]
Cc: McClellan, Kim[Mcclellan.Kim@epa.gov]; Dyson, Brian[Dyson.Brian@epa.gov]; Herrmann, Ronald[Herrmann.Ronald@epa.gov]
From: Schubauer-Berigan, Joseph
Sent: Tue 9/22/2015 2:47:44 PM
Subject: Re: STICS Entries

You should thank Scott. Some of the contractor abstracts required editing. J

Sent from my iPhone

On Sep 22, 2015, at 10:45 AM, Conmy, Robyn <Conmy.Robyn@epa.gov> wrote:

Thank you all for your help getting the abstracts into STICS. I truly appreciate it. If you ever need help while away from the office, please don't hesitate to ask!

<>/<>/<>/<>/<>/<>/<>/<>/<>/<>/<>/<>/<>/<>/<>/<>/<>/<>

Robyn N. Conmy, Ph.D.

Research Ecologist

USEPA/NRMRL/LRPCD

26 West MLK Drive

Cincinnati, Ohio 45268

513-569-7090 (office)

513-431-1970 (EPA mobile)

727-692-5333 (Personal mobile)

conmy.robyn@epa.gov

From: McClellan, Kim
Sent: Tuesday, September 22, 2015 10:44 AM
To: Dyson, Brian
Cc: Herrmann, Ronald; Conmy, Robyn; Schubauer-Berigan, Joseph
Subject: RE: STICS Entries

Hi Brian,

This was taken care of last week.

Thanks,

Kim

From: Dyson, Brian
Sent: Thursday, September 17, 2015 8:11 PM
To: McClellan, Kim
Cc: Herrmann, Ronald; Conmy, Robyn
Subject: RE: STICS Entries

I can't help you with that. I entered those as a favor and was not given that information.

I think Ron Herrmann or Robyn Conmy might know.

From: McClellan, Kim
Sent: Tuesday, September 15, 2015 1:01 PM
To: Dyson, Brian
Subject: STICS Entries

Hi Brian,

All of your STICS entries are not complete. I need this additional information before these abstracts can be submitted to clearance.

You need one internal technical review (reviewer can be from inside or outside of the clearing author's Division) using EPA Form 363 + Reviewer comments for each of these abstracts.

You also need to include the Meeting Name, the Start and End Dates, the Country, State, and City of this conference.

The abstracts are listed below:

TIM Approval	Brian Dyson	Devi Sundaravadivelu	ORD-013921	Evaluation of Sorbent and Solidifier Properties and their Impact on Oil Removal Efficiency	Abstract	9/11/2015 4:43 PM
TIM Approval	Brian Dyson	Mobing Zhuang	ORD-013917	Biodegradability of Dispersed Heavy Fuel Oil at 5 and 25 C	Abstract	9/11/2015 4:28 PM
TIM Approval	Brian Dyson	Yu Zhang	ORD-013915	Biodegradation of Finasol OSR 52 and Dispersed Alaska North Slope Crude Oil at 5 C and 25 C	Abstract	9/11/2015 3:34 PM
TIM Approval	Brian Dyson	Ruta Deshpande	ORD-013912	Biodegradability Of Diluted Bitumen Oil By Kalamazoo River Cultures In Freshwater	Abstract	9/11/2015 2:57 PM

Thanks,

Kim

To: Dyson, Brian[Dyson.Brian@epa.gov]
Cc: Herrmann, Ronald[Herrmann.Ronald@epa.gov]; Conmy, Robyn[Conmy.Robyn@epa.gov]; Schubauer-Berigan, Joseph[Schubauer-Berigan.Joseph@epa.gov]
From: McClellan, Kim
Sent: Tue 9/22/2015 2:43:49 PM
Subject: RE: STICS Entries

Hi Brian,

This was taken care of last week.

Thanks,

Kim

From: Dyson, Brian
Sent: Thursday, September 17, 2015 8:11 PM
To: McClellan, Kim
Cc: Herrmann, Ronald; Conmy, Robyn
Subject: RE: STICS Entries

I can't help you with that. I entered those as a favor and was not given that information.

I think Ron Herrmann or Robyn Conmy might know.

From: McClellan, Kim
Sent: Tuesday, September 15, 2015 1:01 PM
To: Dyson, Brian
Subject: STICS Entries

Hi Brian,

All of your STICS entries are not complete. I need this additional information before these abstracts can be submitted to clearance.

You need one internal technical review (reviewer can be from inside or outside of the clearing author's Division) using EPA Form 363 + Reviewer comments for each of these abstracts.

You also need to include the Meeting Name, the Start and End Dates, the Country, State, and City of this conference.

The abstracts are listed below:

TIM ApprovalDyson	Brian	Devi Sundaravadivelu	ORD-013921	Evaluation of Sorbent and Solidifier Properties and their Impact on Oil Removal Efficiency	Abstract	9/11/2015 4:43 PM
TIM ApprovalDyson	Brian	Mobing Zhuang	ORD-013917	Biodegradability of Dispersed Heavy Fuel Oil at 5 and 25 C	Abstract	9/11/2015 4:28 PM
TIM ApprovalDyson	Brian	Yu Zhang	ORD-013915	Biodegradation of Finasol OSR 52 and Dispersed Alaska North Slope Crude Oil at 5 C and 25 C	Abstract	9/11/2015 3:34 PM
TIM ApprovalDyson	Brian	Ruta Deshpande	ORD-013912	Biodegradability Of Diluted Bitumen Oil By Kalamazoo River Cultures In Freshwater	Abstract	9/11/2015 2:57 PM

Thanks,

Kim

To: Craig Watts[craig@hydrosphere.net]
Cc: Conmy, Robyn[Conmy.Robyn@epa.gov]; Peter Meyer[pmeyer@hydrosphere.net]
From: Barron, Mace
Sent: Wed 8/24/2016 3:12:02 PM
Subject: RE: dispersants?

Thank you!

Could you send the prelim data as you have done in the past in an email?

From: Craig Watts [mailto:craig@hydrosphere.net]
Sent: Wednesday, August 24, 2016 10:06 AM
To: Barron, Mace <Barron.Mace@epa.gov>
Cc: Conmy, Robyn <Conmy.Robyn@epa.gov>; Peter Meyer <pmeyer@hydrosphere.net>
Subject: RE: dispersants?

Mace,

Good to hear from you. We have conducted all but the *Arbacia* studies on the Corexit. We plan on knocking out both *Arbacia* studies for both dispersants early next week. You should have the report for the Corexit soon. The report is written, we are just waiting on the *Arbacia* data. We are getting started on the Finasol range finders next week followed by the definitive tests.

Regards,

Craig

Hydrosphere research

Providing Environmental & Product Toxicity Testing since 1986

Craig Watts, Lab Director

Hydrosphere Research

11842 Research Circle

Alachua, FL 32615-6817

T (386) 462-7889

www.hydrosphere.net

CONFIDENTIALITY NOTICE: This message may contain privileged and confidential information from Hydrosphere Research. The information is intended to be for the use of the addressee only. Any disclosure, copying, distribution, or use of the contents by anyone but the addressee is prohibited.

From: Barron, Mace [mailto:Barron.Mace@epa.gov]
Sent: Wednesday, August 24, 2016 10:27 AM
To: Craig Watts <craig@hydrosphere.net>
Cc: Conmy, Robyn <Conmy.Robyn@epa.gov>
Subject: dispersants?

Did you receive any dispersants from us?

(Correxit and Finasol)

We don't recall getting any test data on those.

Mace

From: Craig Watts [mailto:craig@hydrosphere.net]
Sent: Tuesday, July 05, 2016 7:53 AM
To: Barron, Mace <Barron.Mace@epa.gov>
Subject: RE: electronic data?

Mace,

Sorry for the delay in getting back with you. I got started in my July 4th weekend a little early.

That is an easy request. See attached.

Glad to hear about the possibility of new work. We enjoy working with you.

Craig

From: Barron, Mace [mailto:Barron.Mace@epa.gov]
Sent: Friday, July 01, 2016 11:38 AM
To: Craig Watts <craig@hydrosphere.net>
Subject: FW: electronic data?

Craig, for the dilbit tests, you were able to use your magic and send me the attached excel sheet.

Could you do the same for the just finished crude oil tests?

I greatly appreciate it!

In future, if possible, please include an excel sheet along with the final report. We can then do LC20 analyses.

PS: in addition to the work you are currently assisting us with, I wanted to let you know there is likely to be some completely new stuff in the future (likely not till our 2017 fiscal year starts). Edie would of course get quotes from you and manage the financial aspects. I just wanted to send some love your way lol.

Mace

From: Craig Watts [mailto:craig@hydrosphere.net]
Sent: Monday, May 09, 2016 11:19 AM
To: Barron, Mace <Barron.Mace@epa.gov>
Cc: Peter Meyer <pmeyer@hydrosphere.net>
Subject: RE: electronic data?

Mace,

All is well, thanks for asking.

We did not put the survival data into spreadsheets, just the water quality values. I ran through the Word document and cut and paste into an Excel spreadsheet if that helps. There are two tabs, one for acute and the other for chronic. See attached.

Let me know if you need anything else.

Craig

From: Barron, Mace [mailto:Barron.Mace@epa.gov]
Sent: Monday, May 09, 2016 10:57 AM
To: Craig Watts <craig@hydrosphere.net>
Subject: electronic data?

Hi Craig!

I hope all is well.

We are wondering if you had the tox data from the dilbit testing in a spreadsheet format?

I know you entered the data into your tox stat program, so wondering if you could send that in an email to me?

Just trying to avoid entering the data by hand so that we can compute EC20 values for all the acute tests.

Please let me know,

Mace

To: Conmy, Robyn[Conmy.Robyn@epa.gov]
From: Malcolm Gore
Sent: Thur 4/28/2016 6:08:29 PM
Subject: Re: Finasol OSR 52 Sample Request

Great thanks.
M

Malcolm Gore
President

CLEAR COAST

+1 832 244 1533
malcolm.gore@clearcoastllc.com
www.clearcoastllc.com

From: "Conmy, Robyn" <Conmy.Robyn@epa.gov>
Date: Thursday, April 28, 2016 at 1:02 PM
To: malcolm gore <malcolm.gore@clearcoastllc.com>
Subject: RE: Finasol OSR 52 Sample Request

Yes we have received the invoice and I have provided our purchase card holder with the information. He will be contacting your office for payment.

Cheers,

Robyn

<>/<>/<>/<>/<>/<>/<>/<>/<>/<>/<>/<>/<>/<>/<>/<>/<>

Robyn N. Conmy, Ph.D.

Research Ecologist

USEPA/NRMRL/LRPCD

26 West MLK Drive

Cincinnati, Ohio 45268

513-569-7090 (office)

513-431-1970 (EPA mobile)

727-692-5333 (Personal mobile)

conmy.robyn@epa.gov

From: Malcolm Gore [mailto:malcolm.gore@clearcoastllc.com]
Sent: Thursday, April 28, 2016 1:43 PM
To: Conmy, Robyn <Conmy.Robyn@epa.gov>
Subject: Re: Finasol OSR 52 Sample Request

Hi Robyn

I have given the go ahead on this. Please confirm receipt of the invoice sent yesterday.

Malcolm

Malcolm Gore

President

CLEAR COAST

+1 832 244 1533

malcolm.gore@clearcoastllc.com

www.clearcoastllc.com

From: "Conmy, Robyn" <Conmy.Robyn@epa.gov>
Date: Tuesday, April 26, 2016 at 11:05 AM
To: malcolm gore <malcolm.gore@clearcoastllc.com>
Subject: RE: Finasol OSR 52 Sample Request

Thanks for the update!

<>/<>/<>/<>/<>/<>/<>/<>/<>/<>/<>/<>/<>/<>/<>/<>/<>/<>

Robyn N. Conmy, Ph.D.

Research Ecologist

USEPA/NRMRL/LRPCD

26 West MLK Drive

Cincinnati, Ohio 45268

513-569-7090 (office)

513-431-1970 (EPA mobile)

727-692-5333 (Personal mobile)

conmy.robyn@epa.gov

From: Malcolm Gore [mailto:malcolm.gore@clearcoastllc.com]
Sent: Monday, April 25, 2016 5:45 PM
To: Conmy, Robyn <Conmy.Robyn@epa.gov>
Subject: Re: Finasol OSR 52 Sample Request

Apologies for the delay Robyn

Awaiting some shipping information. Should have this to you in the morning.

Malcolm

Malcolm Gore

President

CLEAR COAST

+1 832 244 1533

malcolm.gore@clearcoastllc.com

www.clearcoastllc.com

From: "Conmy, Robyn" <Conmy.Robyn@epa.gov>
Date: Monday, April 25, 2016 at 10:05 AM
To: malcolm gore <malcolm.gore@clearcoastllc.com>
Cc: Peter Egan <peter.egan@total.com>
Subject: RE: Finasol OSR 52 Sample Request

Hello Malcolm,

Thank you for getting back with me regarding the purchase. Yes, the information below is correct, with a mail stop at room 166. Can you send to me the invoice via email so I can provide to the purchase card holder to make the purchase?

Thank you in advance,

Robyn

<>/<>/<>/<>/<>/<>/<>/<>/<>/<>/<>/<>/<>/<>/<>/<>

Robyn N. Conmy, Ph.D.

Research Ecologist

USEPA/NRMRL/LRPCD

26 West MLK Drive

Cincinnati, Ohio 45268

513-569-7090 (office)

513-431-1970 (EPA mobile)

727-692-5333 (Personal mobile)

conmy.robyn@epa.gov

From: Malcolm Gore [mailto:malcolm.gore@clearcoastllc.com]
Sent: Monday, April 25, 2016 10:57 AM
To: Conmy, Robyn <Conmy.Robyn@epa.gov>
Cc: Peter Egan <peter.egan@total.com>
Subject: Finasol OSR 52 Sample Request

Hello Robin

I am writing with respect to your email below regarding a sample request of Total Finasol OSR 52.

Clear Coast is the custodian of the product stored here in Houston for Total.

I will arrange the sample as requested.

Please confirm the following:

Contact:

Robyn Conmy 513-569-7090 (office)

Deliver to:

26 West MLK Drive

Cincinnati, Ohio 45268

513-569-7090 (office)

Quantity:

2 US Gallons.

On receipt of confirmation I will get the samples drawn, packaged and dispatched.

Regards

Malcolm

Malcolm Gore

President

+1 832 244 1533

malcolm.gore@clearcoastllc.com

www.clearcoastllc.com

From: Conmy, Robyn
Sent: Monday, April 18, 2016 10:47 AM
To: 'peter.egan@total.com' <peter.egan@total.com>
Cc: Wilson, Gregory <Wilson.Gregory@epa.gov>; Principe, Vanessa <Principe.Vanessa@epa.gov>
Subject: purchase of Finasol OSR52

Mr. Egan,

This follows up our telephone conversation of April 11.

As discussed, EPA is seeking to acquire a number of dispersant products listed on the NCP Subpart J Product Schedule for the purposes of both toxicity and efficacy testing. The product testing is intended to further inform currently proposed regulatory actions under Subpart J of the National Contingency Plan. The products will in addition be used to support our general research in the area of oil spill response.

Your product Finasol OSR52 has been identified as one of interest, as it is commonly stockpiled in the U.S. Not only could the product be encountered when presented with a response situation, but including this dispersant product in toxicity and efficacy testing studies will also allow for comparison and consistency with other existing and ongoing studies by EPA and other federal agencies. EPA's Office of Research and Development (ORD) will be conducting the dispersant studies.

At this time we are seeking 2 U.S. gallons of the product.

We appreciate your time and attention to this request.

Respectfully,

Robyn Conmy

<>/<>/<>/<>/<>/<>/<>/<>/<>/<>/<>/<>/<>/<>/<>/<>/<>/<>

Robyn N. Conmy, Ph.D.

Research Ecologist

USEPA/NRMRL/LRPCD

26 West MLK Drive

Cincinnati, Ohio 45268

513-569-7090 (office)

513-431-1970 (EPA mobile)

727-692-5333 (Personal mobile)

conmy.robyn@epa.gov

To: Barron, Mace[Barron.Mace@epa.gov]
Cc: Conmy, Robyn[Conmy.Robyn@epa.gov]; Peter Meyer[pmeyer@hydrosphere.net]
From: Craig Watts
Sent: Wed 8/24/2016 3:05:48 PM
Subject: RE: dispersants?

Mace,

Good to hear from you. We have conducted all but the *Arbacia* studies on the Corexit. We plan on knocking out both *Arbacia* studies for both dispersants early next week. You should have the report for the Corexit soon. The report is written, we are just waiting on the *Arbacia* data. We are getting started on the Finasol range finders next week followed by the definitive tests.

Regards,

Craig

Hydrosphere research

Providing Environmental & Product Toxicity Testing since 1986

Craig Watts, Lab Director

Hydrosphere Research

11842 Research Circle

Alachua, FL 32615-6817

T (386) 462-7889

www.hydrosphere.net

CONFIDENTIALITY NOTICE: This message may contain privileged and confidential information from Hydrosphere Research. The information is intended to be for the use of the addressee only. Any disclosure, copying, distribution, or use of the contents by anyone but the addressee is prohibited.

From: Barron, Mace [mailto:Barron.Mace@epa.gov]
Sent: Wednesday, August 24, 2016 10:27 AM
To: Craig Watts <craig@hydrosphere.net>
Cc: Conmy, Robyn <Conmy.Robyn@epa.gov>
Subject: dispersants?

Did you receive any dispersants from us?

(Correxit and Finasol)

We don't recall getting any test data on those.

Mace

From: Craig Watts [mailto:craig@hydrosphere.net]
Sent: Tuesday, July 05, 2016 7:53 AM
To: Barron, Mace <Barron.Mace@epa.gov>
Subject: RE: electronic data?

Mace,

Sorry for the delay in getting back with you. I got started in my July 4th weekend a little early.

That is an easy request. See attached.

Glad to hear about the possibility of new work. We enjoy working with you.

Craig

From: Barron, Mace [mailto:Barron.Mace@epa.gov]
Sent: Friday, July 01, 2016 11:38 AM
To: Craig Watts <craig@hydrosphere.net>
Subject: FW: electronic data?

Craig, for the dilbit tests, you were able to use your magic and send me the attached excel sheet.

Could you do the same for the just finished crude oil tests?

I greatly appreciate it!

In future, if possible, please include an excel sheet along with the final report. We can then do LC20 analyses.

PS: in addition to the work you are currently assisting us with, I wanted to let you know there is likely to be some completely new stuff in the future (likely not till our 2017 fiscal year starts). Edie would of course get quotes from you and manage the financial aspects. I just wanted to send some love your way lol.

Mace

From: Craig Watts [mailto:craig@hydrosphere.net]
Sent: Monday, May 09, 2016 11:19 AM
To: Barron, Mace <Barron.Mace@epa.gov>
Cc: Peter Meyer <pmeyer@hydrosphere.net>
Subject: RE: electronic data?

Mace,

All is well, thanks for asking.

We did not put the survival data into spreadsheets, just the water quality values. I ran through the Word document and cut and paste into an Excel spreadsheet if that helps. There are two tabs, one for acute and the other for chronic. See attached.

Let me know if you need anything else.

Craig

From: Barron, Mace [mailto:Barron.Mace@epa.gov]
Sent: Monday, May 09, 2016 10:57 AM
To: Craig Watts <craig@hydrosphere.net>
Subject: electronic data?

Hi Craig!

I hope all is well.

We are wondering if you had the tox data from the dilbit testing in a spreadsheet format?

I know you entered the data into your tox stat program, so wondering if you could send that in an email to me?

Just trying to avoid entering the data by hand so that we can compute EC20 values for all the acute tests.

Please let me know,

Mace

To: Holder, Edith[holder.edith@epa.gov]
Cc: Conmy, Robyn[Conmy.Robyn@epa.gov]; Sundaravadivelu, Devi[sundaravadivelu.devi@epa.gov]; Venkatapathy, Raghuraman[Venkatapathy.Raghuraman@epa.gov]
From: Voit, Jim
Sent: Thur 5/19/2016 4:15:31 PM
Subject: RE: Hypersalinity QAPP submission
G-LRPCD-0030110-QP-1-0 review.docx
QAPP Hypersalinity_160517_submitted QA comments.docx

Edie,

Please see the attached review of the QAPP, and let me know if there are any points which need clarification. I have also attached a commented version of the QAPP which adds some required tracking information on the cover sheet and signatures page.

Jim V.

From: Holder, Edith
Sent: Tuesday, May 17, 2016 4:43 PM
To: Voit, Jim <Voit.Jim@epa.gov>
Cc: Conmy, Robyn <Conmy.Robyn@epa.gov>; Sundaravadivelu, Devi <sundaravadivelu.devi@epa.gov>; Venkatapathy, Raghuraman <Venkatapathy.Raghuraman@epa.gov>
Subject: Hypersalinity QAPP submission

Jim,

Enclosed is a QAPP for the BSEE hypersalinity project. This project has 2 parts; research on the first part will occur here and the second part at DFO Canada. It has been requested that both parts of the project be covered under the same QAPP and not as has been done previously where DFO Canada had its own documentation. We don't have everything worked out, but we need to start work on this ASAP. We will submit an amendment to this when we have found an instrument (probably spinning drop tensiometer) that can provide us with interfacial tension measurements. Also, work on part 1 will impact decisions yet to be made regarding the work in Canada. So we will submit an amendment for Part 2 of this project at a later date.

Thanks,

Edie

Edith L. Holder

Pegasus Technical Services, Inc.

On-Site Contractor to the U.S. EPA

ORD/NRMRL/LRPCD

26 W. Martin Luther King Dr.

Cincinnati, OH 45268

Phone: 513-569-7178

Email: holder.edith@epa.gov

To: Conmy, Robyn[Conmy.Robyn@epa.gov]
From: Malcolm Gore
Sent: Thur 4/28/2016 5:43:11 PM
Subject: Re: Finasol OSR 52 Sample Request

Hi Robyn
I have given the go ahead on this. Please confirm receipt of the invoice sent yesterday.
Malcolm

Malcolm Gore
President

CLEAR COAST

+1 832 244 1533
malcolm.gore@clearcoastllc.com
www.clearcoastllc.com

From: "Conmy, Robyn" <Conmy.Robyn@epa.gov>
Date: Tuesday, April 26, 2016 at 11:05 AM
To: malcolm gore <malcolm.gore@clearcoastllc.com>
Subject: RE: Finasol OSR 52 Sample Request

Thanks for the update!

<>/<>/<>/<>/<>/<>/<>/<>/<>/<>/<>/<>/<>/<>/<>/<>/<>/<>

Robyn N. Conmy, Ph.D.

Research Ecologist

USEPA/NRMRL/LRPCD

26 West MLK Drive

Cincinnati, Ohio 45268

513-569-7090 (office)

513-431-1970 (EPA mobile)

727-692-5333 (Personal mobile)

conmy.robyn@epa.gov

From: Malcolm Gore [mailto:malcolm.gore@clearcoastllc.com]

Sent: Monday, April 25, 2016 5:45 PM
To: Conmy, Robyn <Conmy.Robyn@epa.gov>
Subject: Re: Finasol OSR 52 Sample Request

Apologies for the delay Robyn

Awaiting some shipping information. Should have this to you in the morning.

Malcolm

Malcolm Gore

President

CLEAR COAST

+1 832 244 1533

malcolm.gore@clearcoastllc.com

www.clearcoastllc.com

From: "Conmy, Robyn" <Conmy.Robyn@epa.gov>
Date: Monday, April 25, 2016 at 10:05 AM
To: malcolm gore <malcolm.gore@clearcoastllc.com>
Cc: Peter Egan <peter.egan@total.com>
Subject: RE: Finasol OSR 52 Sample Request

Hello Malcolm,

Thank you for getting back with me regarding the purchase. Yes, the information below is correct, with a mail stop at room 166. Can you send to me the invoice via email so I can provide to the purchase card holder to make the purchase?

Thank you in advance,

Robyn

<>/<>/<>/<>/<>/<>/<>/<>/<>/<>/<>/<>/<>/<>/<>/<>/<>

Robyn N. Conmy, Ph.D.

Research Ecologist

USEPA/NRMRL/LRPCD

26 West MLK Drive

Cincinnati, Ohio 45268

513-569-7090 (office)

513-431-1970 (EPA mobile)

727-692-5333 (Personal mobile)

conmy.robyn@epa.gov

From: Malcolm Gore [mailto:malcolm.gore@clearcoastllc.com]
Sent: Monday, April 25, 2016 10:57 AM
To: Conmy, Robyn <Conmy.Robyn@epa.gov>
Cc: Peter Egan <peter.egan@total.com>
Subject: Finasol OSR 52 Sample Request

Hello Robin

I am writing with respect to your email below regarding a sample request of Total Finasol OSR 52.

Clear Coast is the custodian of the product stored here in Houston for Total.

I will arrange the sample as requested.

Please confirm the following:

Contact:

Robyn Conmy 513-569-7090 (office)

Deliver to:

26 West MLK Drive

Cincinnati, Ohio 45268

513-569-7090 (office)

Quantity:

2 US Gallons.

On receipt of confirmation I will get the samples drawn, packaged and dispatched.

Regards

Malcolm

Malcolm Gore

President

CLEAR COAST

+1 832 244 1533

malcolm.gore@clearcoastllc.com

www.clearcoastllc.com

From: Conmy, Robyn

Sent: Monday, April 18, 2016 10:47 AM
To: 'peter.egan@total.com' <peter.egan@total.com>
Cc: Wilson, Gregory <Wilson.Gregory@epa.gov>; Principe, Vanessa <Principe.Vanessa@epa.gov>
Subject: purchase of Finasol OSR52

Mr. Egan,

This follows up our telephone conversation of April 11.

As discussed, EPA is seeking to acquire a number of dispersant products listed on the NCP Subpart J Product Schedule for the purposes of both toxicity and efficacy testing. The product testing is intended to further inform currently proposed regulatory actions under Subpart J of the National Contingency Plan. The products will in addition be used to support our general research in the area of oil spill response.

Your product Finasol OSR52 has been identified as one of interest, as it is commonly stockpiled in the U.S. Not only could the product be encountered when presented with a response situation, but including this dispersant product in toxicity and efficacy testing studies will also allow for comparison and consistency with other existing and ongoing studies by EPA and other federal agencies. EPA's Office of Research and Development (ORD) will be conducting the dispersant studies.

At this time we are seeking 2 U.S. gallons of the product.

We appreciate your time and attention to this request.

Respectfully,

Robyn Conmy

<>/<>/<>/<>/<>/<>/<>/<>/<>/<>/<>/<>/<>/<>/<>/<>/<>/<>

Robyn N. Conmy, Ph.D.

Research Ecologist

USEPA/NRMRL/LRPCD

26 West MLK Drive

Cincinnati, Ohio 45268

513-569-7090 (office)

513-431-1970 (EPA mobile)

727-692-5333 (Personal mobile)

conmy.robyn@epa.gov

To: Craig Watts[craig@hydrosphere.net]
Cc: Conmy, Robyn[Conmy.Robyn@epa.gov]
From: Barron, Mace
Sent: Wed 8/24/2016 2:27:19 PM
Subject: dispersants?

Did you receive any dispersants from us?

(Correxit and Finasol)

We don't recall getting any test data on those.

Mace

From: Craig Watts [mailto:craig@hydrosphere.net]
Sent: Tuesday, July 05, 2016 7:53 AM
To: Barron, Mace <Barron.Mace@epa.gov>
Subject: RE: electronic data?

Mace,

Sorry for the delay in getting back with you. I got started in my July 4th weekend a little early.

That is an easy request. See attached.

Glad to hear about the possibility of new work. We enjoy working with you.

Craig

From: Barron, Mace [mailto:Barron.Mace@epa.gov]
Sent: Friday, July 01, 2016 11:38 AM
To: Craig Watts <craig@hydrosphere.net>

Subject: FW: electronic data?

Craig, for the dilbit tests, you were able to use your magic and send me the attached excel sheet.

Could you do the same for the just finished crude oil tests?

I greatly appreciate it!

In future, if possible, please include an excel sheet along with the final report. We can then do LC20 analyses.

PS: in addition to the work you are currently assisting us with, I wanted to let you know there is likely to be some completely new stuff in the future (likely not till our 2017 fiscal year starts). Edie would of course get quotes from you and manage the financial aspects. I just wanted to send some love your way lol.

Mace

From: Craig Watts [mailto:craig@hydrosphere.net]
Sent: Monday, May 09, 2016 11:19 AM
To: Barron, Mace <Barron.Mace@epa.gov>
Cc: Peter Meyer <pmeyer@hydrosphere.net>
Subject: RE: electronic data?

Mace,

All is well, thanks for asking.

We did not put the survival data into spreadsheets, just the water quality values. I ran through the Word document and cut and paste into an Excel spreadsheet if that helps. There are two

tabs, one for acute and the other for chronic. See attached.

Let me know if you need anything else.

Craig

From: Barron, Mace [mailto:Barron.Mace@epa.gov]
Sent: Monday, May 09, 2016 10:57 AM
To: Craig Watts <craig@hydrosphere.net>
Subject: electronic data?

Hi Craig!

I hope all is well.

We are wondering if you had the tox data from the dilbit testing in a spreadsheet format?

I know you entered the data into your tox stat program, so wondering if you could send that in an email to me?

Just trying to avoid entering the data by hand so that we can compute EC20 values for all the acute tests.

Please let me know,

Mace

To: Conmy, Robyn[Conmy.Robyn@epa.gov]; Grosser, Robert[Grosser.Robert@epa.gov]; Sundaravadivelu, Devi[sundaravadivelu.devi@epa.gov]
From: Holder, Edith
Sent: Tue 8/23/2016 3:52:35 PM
Subject: hypersalinity schedule

All,

I was talking with Devi last night so have decided to publish more of the schedule. This would finish up ANS at the salinities tested thus far.

Note on the 29th we only have 5 tests instead of 6 as on June 30 we tested ANS w Finasol at 5C. The other option is to go for 7 on that day.

25-Aug	60‰	ANS	Dispersit	H25C
	60‰	ANS	Dispersit	L5C
	40‰	ANS	Dispersit	H25C
	40‰	ANS	Dispersit	L5C
	40‰	ANS	none	H25C
	40‰	ANS	none	L5C
29-Aug	40‰	ANS	Finasol	H25C
	100‰	ANS	Finasol	H25C
	100‰	ANS	Finasol	L5C
	100‰	ANS	none	H25C
	100‰	ANS	none	L5C
1-Sep	75‰	ANS	Finasol	H25C
	75‰	ANS	Finasol	L5C
	75‰	ANS	none	H25C
	75‰	ANS	none	L5C
	60‰	ANS	Finasol	H25C
	60‰	ANS	Finasol	L5C
6-Sep	60‰	ANS	none	H25C
	60‰	ANS	none	L5C
	50‰	ANS	Finasol	H25C
	50‰	ANS	Finasol	L5C
	50‰	ANS	none	H25C
	50‰	ANS	none	L5C

Then we have decisions to make. Do we want to test ANS at 125 ppt and some lower ppt. If lower, do 20 ppt now with 10 ppt and 30 ppt to follow later or just 25 ppt and 10 ppt for the lower salinities? Or do we want to run some tests on another oil.

When will the ECO leave? If after testing on Sep 22 then we have an additional 5 test days in Sep. If after testing on Sep 29, then there are 7 more test days.

We could finish testing with ANS at 10 ppt, 25 ppt, and 125 ppt by Sep. 22.

Edie

Edith L. Holder

Pegasus Technical Services, Inc.

On-Site Contractor to the U.S. EPA

ORD/NRMRL/LRPCD

26 W. Martin Luther King Dr.

Cincinnati, OH 45268

Phone: 513-569-7178

Email: holder.edith@epa.gov

To: Conmy, Robyn[Conmy.Robyn@epa.gov]
From: Steffek, Timothy
Sent: Tue 4/5/2016 3:17:30 PM
Subject: Re: dispersant question

for a BSEE project?

Timothy Steffek

Bureau of Safety & Environmental Enforcement
Oil Spill Preparedness Division
45600 Woodland Road, VAE-OSPD
Sterling, VA 20166
(703) 787-1562

On Tue, Apr 5, 2016 at 10:08 AM, Conmy, Robyn <Conmy.Robyn@epa.gov> wrote:

Hey Tim,

Any chance that OHMSETT has 500 ml of the following to spare?

Corexit 9500A

Finasol OSR 52

Accell Clean DWD

Dispersit SPC1000

Thanks,

Robyn

<>/<>/<>/<>/<>/<>/<>/<>/<>/<>/<>/<>/<>/<>/<>/<>/<>/<>/<>

Robyn N. Conmy, Ph.D.

Research Ecologist

USEPA/NRMRL/LRPCD

26 West MLK Drive

Cincinnati, Ohio 45268

513-569-7090 (office)

513-431-1970 (EPA mobile)

727-692-5333 (Personal mobile)

conmy.robyn@epa.gov

To: Conmy, Robyn[Conmy.Robyn@epa.gov]
From: SantoDomingo, Jorge
Sent: Tue 4/5/2016 2:31:39 PM
Subject: some figures
DNA data for some groups that show differences with DNA data.docx

Robyn,

I put together a few figures hoping that it will stimulate discussion on Thursday, or even before if possible. It is starting to look that there are some differences between the batches as far as the oil only samples. I have other figures comparing 5 and 25 in which some of the differences are very striking. We are putting together figures for RNA as well, which I will distribute soon.

Let me know if you have questions. I'll give you a call to go over a few notes so you can explain the figures to your students.

Thanks, jorge

To: Conmy, Robyn[Conmy.Robyn@epa.gov]
From: Holder, Edith
Sent: Mon 4/4/2016 9:57:28 PM
Subject: RE: dispersants

Current Inventory of Oil Spill Dispersants Line Items (July 2015)

date	dispersant name	quantity in lab	in use for preliminary testing
Apr-95	Corexit 9500	~ 80 mL	
Jul-97	EC9527A	~ 150 mL	
19-Dec-01	Nokomis 3-F4	1 qt.	
Aug-06	Dispersit SPC1000	~650 mL	*
undated, before 2010	JD-2000	~ 20 mL	*
undated, before 2010	Saf-Ron Gold	~ 300 mL	*
undated, before 2010	SX-100	~ 100 mL	
undated, before 2010	Corexit 9500A	~30 mL	
18-Jun-10	Corexit 9500 from Ohmsett	60 mL	*
25-Jul-13	new dispersant gel sent to AI from Tim @ ExxonMobil	~ 20 mL	
Apr-14	Finasol OSR52	1 qt.	
19-Mar-15	Nokomis 3-AA	1 pt.	*
19-Mar-15	Nokomis 3-F4	1 pt.	
9-Apr-15	FFT Solution	1 qt.	
16-Apr-15	Accell Clean DWD	1 qt.	
6-May-15	ZI-400	1 qt.	*
summer 2015	Corexit 9500 from DFO	~30 mL	

Here is the current inventory (double checked just now and added the small bottle from DFO). Even if you mix lots and add up all the Corexit we have it only equals 200 mLs. But there is enough of the other ones.

From: Conmy, Robyn
Sent: Monday, April 04, 2016 2:35 PM
To: Holder, Edith <holder.edith@epa.gov>
Subject: dispersants

I was looking for volumes of the 4 dispersants that we are using for the hypersaline DE

experiments. I found Accell clean and Finasol but not the Corexit or Dispersit. Do you kow the volume we have? The tox testing will require 400 ml of each. Given the waiver issue with Corexit and Finasol, I'm not sure how we can get more since it is for tox testing.

<>/<>/<>/<>/<>/<>/<>/<>/<>/<>/<>/<>/<>/<>/<>/<>

Robyn N. Conmy, Ph.D.

Research Ecologist

USEPA/NRMRL/LRPCD

26 West MLK Drive

Cincinnati, Ohio 45268

513-569-7090 (office)

513-431-1970 (EPA mobile)

727-692-5333 (Personal mobile)

conmy.robyn@epa.gov

To: Coolbaugh, Thomas S[thomas.s.coolbaugh@exxonmobil.com]; Bess, Amanda S[ABess@chevron.com]; victoria.broje@shell.com[victoria.broje@shell.com]; Per Johan Brandvik[PerJohan.Brandvik@sintef.no]; Conmy, Robyn[Conmy.Robyn@epa.gov]; Cooper, Cortis (CortCooper)[CortCooper@chevron.com]; Gala, William (WGala)[WGala@chevron.com]; Ken.Lee@csiro.au[Ken.Lee@csiro.au]; "\"alun.lewis4"@btinternet.com["\"alun.lewis4"@btinternet.com]; alun.lewis4@btopenworld.com[alun.lewis4@btopenworld.com]; tim.j.nedwed@exxonmobil.com[tim.j.nedwed@exxonmobil.com]; Nicolas PASSADE-BOUPAT[nicolas.passade-boupat@total.com]; Emily Hague["Hague\""@api.or]
Cc: Cox, Rob, IPIECA[Rob.Cox@ipieca.org]; Steve Potter[Steve@slross.com]
From: Ken Trudel
Sent: Fri 4/1/2016 5:07:38 PM
Subject: Re: API Dispersant Meeting Agenda
ReviewOfRecentlyPublishedOilSpillDispersantFateAndEffectsResearchPapers_DraftFinal_PDF.pdf

Hello:

Attached, as promised, is the draft report on the API/IPIECA Dispersant Research Review Project.

During our last conference call, it was agreed that I would prepare a draft final report on the project. It was to be limited in scope to the fate and effects papers, which covers off the controversial areas of microbial degradation, marine snow, effects monitoring, and toxicity testing. It is not comprehensive, but it does include many of the papers that we reviewed as a panel and some more recent papers (up to early January 2016), that I decided to include. Some papers were not included for reasons of time. As discussed in our November meeting, the sections on microbial degradation and marine snow need careful scrutiny, as my expertise in these areas is limited.

Please provide comments by the end of the day on April 20, 2016, and I will do my best to complete revisions by the end of the month.

Regards,

Ken

--
Ken Trudel
SL Ross Environmental Research Ltd.
Tel: (613) 232-1564; Fax: (613) 232-6660
200 - 1140 Morrison Drive, Ottawa, ON
CANADA, K2H 8S9
email: ken@slross.com
web site: http://www.slross.com

To: Conmy, Robyn[Conmy.Robyn@epa.gov]
Cc: Sundaravadivelu, Devi[sundaravadivelu.devi@epa.gov]
From: Holder, Edith
Sent: Thur 3/31/2016 10:10:17 PM
Subject: Draft of Hypersalinity QAPP
QAPP Hypersalinity.docx

Robyn,

Here is what we have so far. As soon as we insert information regarding the in-situ fluorometer and the tensiometer, I think we are ready to submit for review to Gune.

Edith L. Holder

Pegasus Technical Services, Inc.

On-Site Contractor to the U.S. EPA

ORD/NRMRL/LRPCD

26 W. Martin Luther King Dr.

Cincinnati, OH 45268

Phone: 513-569-7178

Email: holder.edith@epa.gov

EPA United States Environmental Protection Agency

NRMRL QUALITY ASSURANCE PROJECT PLAN

Office of Research and Development
National Risk Management Research Laboratory
Land Remediation and Pollution Control Division

EPA QA Log Number# L-20624-QP-1-1
Contract No. EP-C-15-010

Work Assignment No. WA 0-05
Determination of Biodegradability of Petroleum, with and without Dispersant

EPA NRMRL Technical Lead Person: Robyn Conmy

QA Category B

Extramural

Prepared by:
Devi Sundaravadivelu
Department of Biomedical, Chemical, and Environmental Engineering
University of Cincinnati

Under Subcontract to:
Pegasus Technical Services Inc.
Cincinnati, OH 45219

Revision Number: 1

Date: December 9, 2015

Signature and Approvals Page

QA Project Plan Title:	QA ID: L-20624-QP-1-1
NRMRL QA Tracking ID:	Determination of Biodegradability of Petroleum, with and without Dispersant
If Intramural or Extramural, EPA NRMRL Project Approvals	
Name: Technical Lead Person (TLP): **Robyn N. Conmy**	Signature/Date: ROBYN CONMY Digitally signed by ROBYN CONMY DN: c=US, o=U.S. Government, ou=USEPA, ou=Staff, cn=ROBYN CONMY, dnQualifier=0000041574 Date: 2015.12.14 12:58:53 -05'00'
Name: TLP's Supervisor: **Joe Schubauer-Berrigan**	Signature/Date: JOSEPH SCHUBAUER-BERIGAN Digitally signed by JOSEPH SCHUBAUER-BERIGAN DN: c=US, o=U.S. Government, ou=USEPA, ou=Staff, cn=JOSEPH SCHUBAUER-BERIGAN, dnQualifier=0000015734 Date: 2015.12.14 11:54:36 -05'00'
Name: QA Manager: **Jim Voit**	Signature/Date: JAMES VOIT Digitally signed by JAMES VOIT DN: c=US, o=U.S. Government, ou=USEPA, ou=Staff, cn=JAMES VOIT, dnQualifier=0000045910 Date: 2015.12.10 14:34:21 -05'00'
Name: Other EPA: **Jorge Santo Domingo**	Signature/Date: Jorge W. Santo Domingo
If Extramural, Contractor Approvals	
Name: Pegasus Project Manager **Karen Koran**	Signature/Date: Karen M Koran 12-8-15
Name: Contractor QAs: **Gune Silva/Ginger Britt**	Signature/Date: 12/08/2015
Name: UC Project Manager/WA Leader: **George Sorial**	Signature/Date: Dec 8, 2015
Name: WA Leader: **Edith Holder**	Signature/Date: 8 Dec 2015
Name: UC Team Member **Yu Zhang**	Signature/Date: Yu Zhang 12/8/2015
Name: UC Team Member **Ruta Suresh Deshpande**	Signature/Date: 12/8/2015

Justification for WA 0-05, Task 1.1 and 1.2 Quality Assurance Project Plan Amendment

An amendment to the previously approved QAPPs for WA 0-05, Task 1.1 Biodegradability of Physically and Chemically Dispersed Endicott oil and Corexit Dispersant at Two Temperatures (EPA QA Log Number: L-15045-QP-1-5, WA 3-33) and WA 0-05, Task 1.2 Biodegradability of Diluted Bitumen oil by Anderson Ferry and Kalamazoo River Cultures in Freshwater at Two Temperatures (EPA QA Log Number: L-20624-QP-1-0, WA 3-85) under Pegasus Contract EP-C-11-006 (current Contract No. EP-C-15-010) has been prepared for the U.S. Environmental Protection Agency, Land Remediation and Pollution Control Division (LRPCD). Both QAPPs have minor changes and have been combined into a single document since both experiments involve biodegradation and use similar analytical techniques.

As part of Task 1.1, the biodegradability of dispersed oil at 5 °C and 25 °C will be studied using Corexit dispersant and Endicott crude instead of Alaska North Slope crude. In the case of Task 1.2, two types of Dilbit oil biodegradability using two cultures will be studied at 5 °C and 25 °C. The original and biodegraded Dilbit samples will be analyzed using GC/MS/MS instead of GC/MS. In addition, the oils will be characterized using IATROSCAN to determine SARA (Saturates Aromatics Resins Asphaltenes) composition. The analysis for Total Petroleum Hydrocarbons (TPH) has also been added.

The following Sections were amended:
Section 1
Section 2
Section 3
Section 4
Section 5
Section 6
Section 7
Section 8
Section 9
Section 10

Table of Contents

1. Project Description and Objectives 8
1.1 Purpose of study 8
1.2 Project Objectives 9
2. Organization and Responsibilities 10
2.1 Project Organization 10
2.2 Project Schedule 13
3. Scientific Approach 14
3.1 BIODEGRADABILITY OF DISPERSED OIL 14
3.2 BIODEGRADABILITY OF DILBIT 17
4. Sampling Procedures 19
4.1 BIODEGRADABILITY OF DISPERSED OIL 19
4.2 BIODEGRADABILITY OF DILBIT 21
5. Measurement Procedures 23
6. Quality Metrics (QA/QC) 24
6.1 Critical and Non-critical Measurements 24
6.2 QA/QC Objectives 24
6.3 Internal Quality Control 25
7. Data Analysis, Interpretation, and Management 28
7.1 Data Reporting 28
7.2 Data Reduction and Validation 28
7.3 Data Summary and Analysis 28
7.4 Data Storage 29
8. Reporting 30
8.1 Monthly Reports 30
8.2 Final Report 30
9. Amendment/Revision History 31
10. List of Standard Operating Procedures 32
11. References 33

LIST OF TABLES

Table	Title	Page
Table 2.1	Organization/Title Chart	11
Table 2.2	Project Schedule	13
Table 3.1	Experimental Layout for Dispersant Experiment	15
Table 3.2	Experimental Layout for Dilbit Experiment	18
Table 4.1	Treatment and Analytical Method for Dispersant Experiment	19
Table 4.2	Experimental Sampling and Analytical Procedures to Be Used for Dispersant Experiment	20
Table 4.3	Sample Identifications for Dilbit Experiment	21
Table 4.4	Treatment and Analytical Method for Dilbit Experiment	21
Table 4.5	Sample Containers, Preservation and Holding Times for Dilbit Experiment	22
Table 5.1	Analytical Instruments for Dispersant Experiment	23
Table 5.2	Analytical Instruments for Dilbit Experiment	23
Table 6.1	Summary of Internal QC Checks for all Parameters	25
Table 7.1	Reporting Units	28
Table 9.1	Amendment/Revision History	31

LIST OF FIGURES

Figure	Title	Page
Figure 2.1	Organization Chart	12

Distribution List

Dr. Robyn N. Conmy, WACOR, U.S. Environmental Protection Agency
Mr. Jim Voit, LRPCD Quality Assurance Manager, U.S. Environmental Protection Agency
Dr. Jorge Santo Domigo, Project Support for PCR Analysis, U.S. Environmental Protection Agency
Dr. Karen Koran, Project Manager, Pegasus Technical Services, Inc.
Dr. Gune Silva, Contract Quality Assurance Manager, CB&I Federal Services LLC.
Ms. Ginger Britt, Contract Quality Assurance Manager, CB&I Federal Services LLC.
Dr. George Sorial, Manager, University of Cincinnati
Ms. Edith Holder, WA Leader, Pegasus Technical Services, Inc.
Ms. Devi Sundaravadivelu, WA Leader, University of Cincinnati
Ms. Mobing Zhuang, Project Staff, University of Cincinnati
Ms. Yu Zhang, Project Staff, University of Cincinnati
Ms. Ruta Deshpande, Project Staff, University of Cincinnati

1. Project Description and Objectives

1.1 Purpose of study

The Deepwater Horizon (DWH) incident in the Gulf of Mexico (GOM) has raised questions not only about the biodegradability of oil in deep and surface waters in that area, but also to answer concerns about the rate of biodegradation of the dispersants itself and the dispersed oil. Studying the persistence of dispersants and dispersed oil in the aquatic environments has become a high priority due to this reason. In addition to oil releases in deep waters, there is an urgent need to understand the fate of an accidental release of diluted bitumen during transportation and storage across U.S. soils. Diluted bitumen or dilbit refers to blends made from heavy crude and bitumen along with a diluent, usually condensate, for the purpose of meeting pipeline viscosity and density specifications. The most common diluent is natural gas condensate (NGC): a low-density mixture of hydrocarbon liquids. Dilbit is typically less susceptible to biodegradation; therefore, research regarding how dilbit products will further biodegrade in the environment is necessary in order to adequately characterize the fate and behavior of these products.

1.1.1 Biodegradability of Dispersed Oil

Previous research, conducted under U.S. Environmental Protection Agency (EPA) Contract No. EP-C-11-006 (WA 3-33), determined biodegradation rates of dispersants and dispersed oil at 5 and 25 °C. Nevertheless, the previous studies were conducted at substrate concentrations significantly higher than those found in field conditions. Hence, in this project, oil, dispersed oil, and dispersant will be tested at a concentration that is 4.3% of the value previously tested in the aforementioned experiments. The rationale is that, normally, in actual field trials, the concentrations of oil and dispersant never reach the levels used in laboratory experiments. The herein described approach will produce environmentally relevant data by determining oil, dispersed oil, and dispersant biodegradation rates at smaller loading concentrations. The EPA is also in need of determining what microbial cultures are responsible for biodegradation at the two temperatures and how these communities change as substrate consumption takes place.

1.1.2 Biodegradability of Diluted Bitumen

Two spills of dilbit occurred in the United Sates (U.S.) in recent times that resulted in a controversy about the transport of such oil across U.S. soil. In July 2010, a massive Enbridge, Inc. pipeline ruptured and dumped thousands of dilbit barrels into the Kalamazoo River and surrounding wetlands. The second spill occurred on March 29, 2013, on Exxon-Mobil's Pegasus pipeline in Mayflower, AK, and spill estimates range from 80,000 to 200,000 gallons. Both discharges are still being cleaned up, and the EPA's Office of Emergency Management, ORD's Program Office in Headquarters, is very concerned with discharges of dilbit because of its corrosive nature and high content of sulfur, chlorides, and abrasive sand particles. These properties induce higher risks of pipeline failure owing to sediment and chemical corrosion. Additionally, pipelines operate at high temperatures so that corrosion rates are higher, which causes an increases incidence of stress corrosion cracking. Any dilbit released into the environment could persist for a long duration since the lighter portions evaporate, leaving the heavier portions to collect debris and eventually sink into the aquatic environment, as occurred in

the Kalamazoo River incident. Once these heavy crude oils sink into the sediment, they tend to last a very long time.

As part of the previous work assignment (WA 3-85), the degradation of Canadian dilbit and Bakken oil were studied using Cold Lake Dilbit and mixed cultures that were isolated from Kalamazoo River sediments and enriched. In this research, the interaction of additional dilbits (Cold Lake 1A (taken from the tar sands at a different time from the earlier sample) and Western Canadian Select 2B) with the microbes and their potential to biodegrade will be studied.

1.2 Project Objectives

1.2.1 Biodegradability of Dispersed Oil

The overall aim of this study is to determine the biodegradation of (i) Endicott crude oil alone, (ii) Endicott oil dispersed with Corexit 9500, and (iii) Corexit 9500 dispersant alone at environmentally relevant concentrations. This goal will be achieved through the following specific objectives:

- To study the rate of biodegradation of Endicott crude oil, dispersant Corexit 9500 (C9500), and Endicott dispersed with C9500 at 5 °C and at 25 °C.
- To investigate the time-dependent changes in the microbial cultures used in the biodegradation experiments.

1.2.2 Biodegradability of Diluted Bitumen

This portion of the research aims to study the biodegradation of dilbit as a function of crude composition, temperature and microbial culture composition. The specific research goals are as follows:

- The objective of this study is to gain insight into the biodegradability of two types of dilbit oils (Cold Lake 1A and Western Canadian Select 2B) with respect to each type of microbial culture (Kalamazoo River and Anderson Ferry) at each temperature (5 C and 25 C) condition.
- These goals will be achieved by conducting a parametric study on the biodegradation rates of alkanes and PAHs present in two different dilbit oils at 5 °C and at 25 °C in fresh water exposed to two microbial cultures.

2. Organization and Responsibilities

2.1 Project Organization

Dr. Joseph Schubauer-Berrigan serves as the EPA Project Officer for EPA Contract No. EP-C-15-010. For this Work Assignment (WA), Dr. Robyn N. Conmy is the EPA WA Contract Officer Representative (WACOR) responsible for WA planning, providing technical direction related to WA activities, and ensuring that the data received from Pegasus Technical Services, Inc. (Pegasus) and the University of Cincinnati (UC) satisfy the project objectives. Mr. Jim Voit is the EPA Land Remediation and Pollution Control Division (LRPCD) Quality Assurance (QA) Manager responsible for approval of this Quality Assurance Project Plan (QAPP). Dr. Jorge Santo Domigo with EPA will be providing support for polymerase chain reaction (PCR) analysis of samples.

Dr. Karen Koran is the Pegasus Project Manager for this Off-Site WA. Dr. George Sorial with UC (a subcontractor to Pegasus for this off-site WA) is the UC Project Manager. He is also Dr. Gune Silva and Ms. Ginger Britt, with CB&I Federal Services LLC., are the Pegasus Contract QA Managers responsible for oversight of Pegasus Quality Program implementation, QA review of quality documents and deliverables, and project assessments. Ms. Devi Sundaravadivelu and Ms. Edith Holder are the UC and Pegasus WA Leaders, respectively, responsible for project planning, coordination of experiments and analyses, interpretation of the data, coordinating internal review of contract deliverables prior to submittal to EPA, and completion of the final report. Ms. Yu Zhang, Ms. Mobing Zhuang and Ms. Ruta Deshpande are UC Project Staff responsible for assisting the WA Leaders with project planning, the coordination, design, and maintenance of the experiments as well as chemical analysis and assisting with the final report.

Table 2.1 Organization/Title Chart

Name	Phone/email	Responsibilities
Dr. Joseph Schubauer-Berigan	(513) 569-7734 schubauer-berigan@epa.gov	EPA Project Officer
Dr. Robyn N. Conmy	(513) 569-7668 Conmy.Robyn@epa.gov	EPA WACOR
Mr. Jim Voit	(513) 487-2867 Voit.Jim@epa.gov	EPA LRPCD QA Manager
Dr. Karen Koran	(513) 569-7304 Koran.Karen@epa.gov	Pegasus Project Manager
Ms. Ginger Britt	(513) 782-4654 ginger.britt@CBIFederalServices.com	Pegasus Contract QA Manager
Dr. Gune Silva	(513) 569 7853 Gunadasa.Silva@CBIFederalServices.com	Pegasus Contract QA Manager
Dr. George Sorial	(513) 556-2987 sorialga@ucmail.uc.edu	UC Project Manager
Ms. Edith Holder	(513)-569-7178 Holder.Edith@epa.gov	Pegasus WA Leader
Ms. Devi Sundaravadivelu	(585)-732-4101 devis.255@gmail.com	UC WA Leader
Ms. Ruta Deshpande	(513) 556-3640 deshpars@mail.uc.edu	UC Project Staff
Ms. Mobing Zhuang	(513) 556-3640 zhuangmg@mail.uc.edu	UC Project Staff
Ms. Yu Zhang	(513) 556-3640 zhang4y5@mail.uc.edu	UC Project Staff

Figure 2.1. Organization Chart

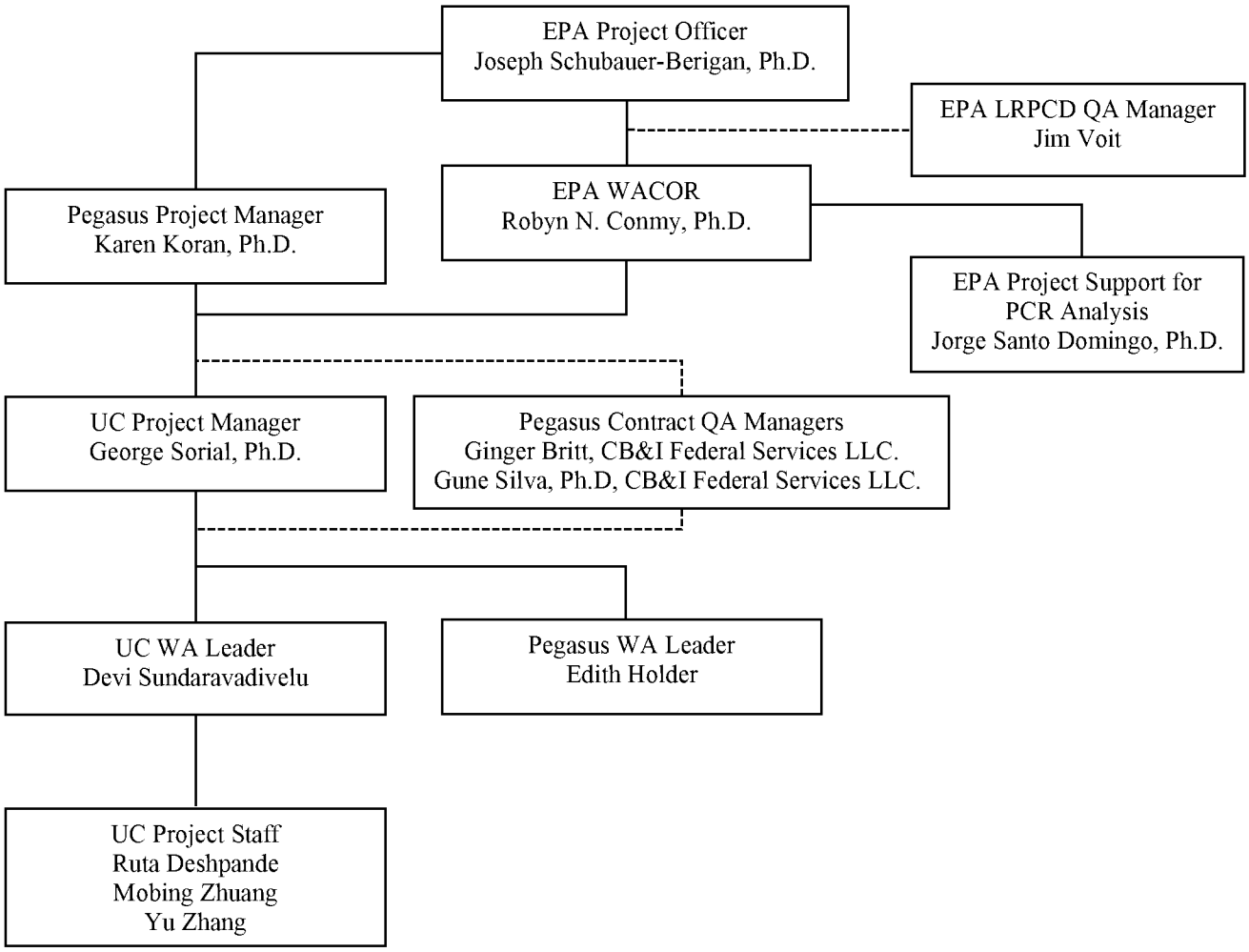

2.2 Project Schedule

The projected schedule and the main activities are shown in Table 2.2.

Table 2.2 Projected Schedule

Activity	Oct-15	Nov-15	Dec-15	Jan-16	Feb-16	Mar-16	Apr-16	May-16	Jun-16	Jul-16	Aug-16	Sep-16
QAPP Preparation												
Experimental Setup												
Sampling												
Sample Analysis												
Report Writing												
Final Report												

3. Scientific Approach

The objectives for this project will be realized by completing the biodegradation studies with (i) dispersed oil (using Endicott oil and C9500 with Gulf of Mexico cultures) and (ii) dilbit (using Cold Lake and WCS dilbits with Anderson Ferry and Kalamazoo River Cultures).

3.1 BIODEGRADABILITY OF DISPERSED OIL

3.1.1 Biodegradation study

Biodegradation studies will be conducted using Endicott oil dispersed with C9500. Additionally, degradation of Endicott and C9500 as individual substrates will also be studied. The experiments will be conducted in 250-mL shake flasks. These flasks will be rotated at 200 rpm and sterile GP2 seawater will be the matrix used in the study. Both oil and dispersant will be tested at 5 and 25 °C as described in the subsections below. Time-dependent changes in the microbial communities will be determined as well.

The critical parameters for this project will be the measured time series concentrations for oil components (alkanes and aromatics) and main component of C9500. These values will be used in the calculation of degradation rates and extents of these substances. TPH time series have a semi-quantitative value, since these data give a general idea of how the total extractable hydrocarbons evolve with time, hence this parameter is non-critical. PCR results for microbial determinations are considered non-critical as well.

3.1.2 Microbial Enrichment Studies

The EPA WACOR will provide two frozen mixed cultures of oil degrading bacteria to the UC WA Leader. These cultures were previously enriched, grown, and frozen in 5-mL vials containing glycerol by EPA's Gulf Ecology Division at Gulf Breeze, FL. The first mixed culture (denoted as cryo) was isolated from the deep sea of the GOM and enriched on South Louisiana crude oil at 5 °C. The second culture (denoted as meso) was isolated from the top 5 m of the GOM and enriched at 25 °C.

3.1.3 Experimental setup

The experiments outlined in Table 3.1 will be used for the biodegradation studies to be conducted in order to determine the biodegradation rate of Endicott crude oil and C9500. In the 5 °C test, eleven (11) sampling events will take place at 0, 2, 4, 8, 12, 16, 24, 32, 40, 48, and 56 days, while ten (10) sampling events are required at 0, 2, 4, 8, 12,16, 24, 32, 40, and 48 days in the 25 °C experiment. For both temperatures, the following treatments will be set up:

1. C9500 alone.
2. Endicott previously dispersed by C9500.
3. Endicott alone.

Additionally, killed controls (KCs) will be run in triplicates for each treatment to account for abiotic losses, if any. These KCs include all ingredients as the live microcosms (i.e., oil, dispersant, nutrients, and culture) but they will be sterilized with sodium azide (NaN_3) at a concentration of 500 mg/L per flask. In all the cases, 100 mL of autoclaved GP2 synthetic seawater will be used as the medium for microbial activity, and the orbital shakers will rotate at

200 rpm.

At a given sampling event, triplicate flasks of each treatment will be sacrificed along with those KCs having dispersed oil and C9500. For oil alone treatments, triplicates of the KCs will only be sacrificed on the final event. Before sacrificing any microcosms, 2 mL will be withdrawn from each flask containing live culture and preserved by freezing at -20 °C. These samples will be transferred to EPA -80 °C fridge as soon as possible for determination of microbial communities, which will be performed by EPA personnel at the EPA Andrew W. Breidenbach Environmental Research Center (AWBERC) under the direction of Dr. Jorge Santo Domingo. Samples will be provided to Dr. Santo Domingo by the UC WA Leader or designee for all nucleic acid-based analyses.

Table 3.1 Summary of Experimental Layout for Two Temperatures.

Test	Temperature	Treatment	Sampling Events	Sample Replicates	Total Exp. Units (EU)
1	5 °C	C9500 alone	11	3	33
2	5 °C	Endicott dispersed by C9500	11	3	33
3	5 °C	Endicott alone	11	3	33
4	5 °C	Killed Endicott control	1	3	3
5	5 °C	Killed C9500 control	10	3	30
6	5 °C	Killed Endicott + C9500 control	10	3	30
7	5 °C	Biomass Alone	1	3	3
				Subtotal EU's	**165**
8	25 °C	C9500 alone	10	3	30
9	25 °C	Endicott dispersed by C9500	10	3	30
10	25 °C	Endicott alone	10	3	30
11	25 °C	Killed Endicott control	1	3	3
12	25 °C	Killed C9500 control	9	3	27
13	25 °C	Killed Endicott + C9500 control	9	3	27
14	25 °C	Biomass Alone	1	3	3
				Subtotal EU's	**150**
				Total EU's for C9500	**315**

Finally, a second set of replicates of the oil alone and dispersed oil will be run for several of the sampling events to explore modifying the oil extraction method. There is a mandate to minimize the volume of solvent used in conducting experiments, but there is concern that lowering the volume will impact the recovery of the oil. Therefore, a comparison to the current method is necessary before a change is made. This comparison will be used to modify the method for future experiments.

3.1.4 Preparation of treatments

3.1.4.1 Dispersed oil treatment

Dispersed oil will be prepared with C9500 by making batches in the baffled flasks and compositing them in a glass carboy or bottle. The composite should be continuously mixed to keep the suspension from settling. The sterile GP2 media will be prepared by dissolving the required amounts of mineral salts in distilled water. This solution will be autoclaved at 121 °C for 30 minutes in batches of 1 liter. The concentration of each salt (expressed in g/L) will be NaCl (21.03), $MgCl_2$ $6H_2O$ (9.5), Na_2SO_4 (3.52), $CaCl_2.2H_2O$ (1.32), KCl (0.61), KBr (0.088), $NaB_4O_7.10H_2O$ (0.034), $SrCl_2.6H_2O$ (0.02), $NaHCO_3$ (0.17) $FeCl_3.6H_2O$ (0.05), $Na_5P_3O_{10}$ (0.297) KNO3 (2.89). A single dispersed oil batch will be prepared at room temperature as follows:

- Measure 1,500 mL of GP2 artificial seawater into a 2-L baffled flask.
- Pipette onto the surface 240 µL Endicott with a Brinkmann Eppendorf repeater pipette with a 1 mL tip (3 times at the 4th stop).
- Pipette 10.0 µL (1 time at 5th stop) of C9500 with a Brinkmann Eppendorf repeater plus pipette with a 100 µL tip. Thi s will give a dispersant-to-oil (DOR) volumetric ratio of 1:24.
- Cover with the foil used in autoclaving and place on shaker table.
- Start the shaker at a very slow speed to minimize sloshing and ramp it up to approximately 200 rpm.
- Agitate the flask for 20 minutes.
- Let the flask remain stationary for 10 minutes to allow undispersed oil to float to the surface. Drain the dispersed oil seawater suspension through the bottom stopcock into the carboy being careful not to disturb the top layer of undispersed oil.
- Stop draining when the liquid is still covering the opening to the stopcock. There should be about 200 mL left in the flask.
- For the next preparation, add 1,200 mL of GP2 seawater to the remaining 200 mL of dispersed oil, 200 µL Endicott oil (2 times at the 5th stop), and 8 µL C9500 (1 time at the 4th stop). Prepare 3 L of this mixture. Add 12 L of sterile GP2 for a total of 15 L.
- From the time the first batch is drained into the carboy, keep the contents of the carboy well mixed.
- Aseptically dispense 100 mL aliquots of the combined dispersed oil seawater mixture into previously silanized shake flasks.
- Add NaN_3 to the dispersed oil killed controls to a final concentration of 500 mg/L (0.5 mL of a 100 mg/mL stock solution per flask) before adding the culture.
- Incubate both live and killed culture flasks at 5 °C after adding 0.5 mL of the cryo culture; those to be incubated at 25 °C will receive 0.5 mL of the meso culture.
- Place the flasks on the orbital shaker in the corresponding constant temperature room (CTR) at 5 or 25 °C. Set the orbital shakers to 200 rpm.

3.1.4.2 Non-dispersed oil treatment

The final concentration of oil in the samples should be approximately 28 µg/L as in the dispersed oil treatment. Hence, approximately 4 µL Endicott will be pipetted (2nd stop with a 100 µL tip) into each shake flask containing 100 mL sterile GP2. The live and KC flasks will be set up in the same manner as the dispersed oil flasks discussed in the previous section.

3.1.4.3 Dispersant alone treatment

In order to evaluate the biodegradation of C9500 alone, tests will be conducted where the only substrate is the dispersant. With this purpose, a single batch of sterile GP2 (14 L) will be spiked with approximately 20 µL of C9500, to yield a similar concentration as in the dispersed oil treatment. This batch should be kept well mixed. From this stock, the experimental units (EUs) for both temperatures will be prepared by transferring 100 mL of the mix into each flask. For the 5 °C experiment, the sample inoculum is the cryo culture whereas the meso culture will be added to the 25 °C EUs. Additionally, the KCs will be sterilized by adding NaN_3 in a final concentration of 500 mg/L per flask.

3.2 BIODEGRADABILITY OF DILBIT

3.2.1 General Description

The objective will be realized by conducting microbial degradation experiments, in shake flasks for each dilbit oil type at 5 °C and 25 °C as described in the subsections below.

The critical parameter for this project will be the measured time series concentrations for oil components, i.e., alkanes and aromatics as well as Total Petroleum Hydrocarbons (TPH). These values will be used in the calculation of their degradation rates and extent.

3.2.2 Microbial Culture

Contaminated sediments from the dredging operation on the Kalamazoo River Enbridge Energy spill were mixed with Bushnell Haas Broth and dilbit as the carbon source and incubated for a month at both 5 °C (Cyro KR) and 25 °C (Meso KR). Then the enrichment cultures were washed, concentrated tenfold, and frozen with 10% glycerol at -80 °C by EPA's AWBERC personnel for use in the experiment. Anderson ferry culture was collected from Ohio River sediments, downstream of the fuel tanks at Anderson Ferry on the west side of Cincinnati, OH. This culture was enriched and frozen in October 2000. The EPA WACOR will provide these mixed cultures to the UC WA Leader.

3.2.3 Characterization of dilbit oils

Density: Densities for both the dilbit oils will be determined by weighing 1 mL of the oil.

SARA Analysis: Saturates, aromatics resins and Asphaltenes (SARA) analysis of both the dilbit oils will be done by IATROSCAN (thin layer chromatography –FID) according to SOP 7.

Alkanes and Poly aromatic hydrocarbons (PAHs): The distributions of alkanes, PAHs and conservative biomarker hopane will be characterized by GC-MS/MS (SOP 5).

3.2.4 Experimental setup

A parametric study on the biodegradation rates will be tested using each dilbit oil at 5 and 25 ± 2 °C with each respective culture. For each temperature and substrate, kinetics tests will be run in 250-mL shake flasks rotating at 200 rpm. Sterile Bushnell Hass broth (100 mL) will be the matrix used in this study. At 25 °C, triplicate bottles will be sacrificed on days 0, 2, 4, 8, 12, 16, 20, 28, 35, 42, 54, and 60; the sampling events for 5 °C will be 0, 2, 4, 8, 16, 24, 32, 40, 48, 56, 62, and 72 d. To account for abiotic losses, if any, killed controls (KC) will be run in triplicate for each temperature and will be sampled at the final event. For these KCs, the sterilant will be sodium azide (NaN_3) at a concentration of 500 mg/L per flask. The number of experimental units

(EUs) per oil, per culture for both temperatures with total sampling event, replicates and the KCs are 78 (Table 3.2.). Thus, total EUs for the entire experiment will be 312 (Oil 2 x Cultures 2x Temperature 2 x Sampling events 12x Replicates 3 + Kill Control (Oil 2 x Cultures 2 x Temperature 2 x Sampling event 1 x Replicates 3)).

Table 3.2 Summary of EUs per Oil, per Culture for both Temperatures including sampling events and replicates

Test	Temperature	Treatment	Sampling Events	Sample Replicates	Total Exp. Units (EU)
1	5 °C	Dilbit	12	3	36
2	5 °C	Killed Dilbit control	1	3	3
				Subtotal EU's	**39**
3	25 °C	Dilbit	12	3	36
4	25 °C	Killed Dilbit control	1	3	3
				Subtotal EU's	**39**
				Total EU's for Dilbit	**78**

3.2.5 Sample preparation

3.2.5.1 Matrix preparation

Bushnell Hass broth will be prepared by dissolving the required amounts of mineral salts in distilled water. This solution will be autoclaved at 121 °C and 17 psi for 15 min in batches of 1L. The concentration of each salt (expressed in g/L) will be magnesium sulfate (0.2), calcium chloride (0.02), monopotassium phosphate (1.0), dipotassium phosphate (1.0), ammonium nitrate (1.0), and ferric chloride (0.05).

3.2.5.2 Shake flasks (EU) set-up

The final oil concentration in the samples will be approximately 0.7 g/L for both temperatures. Hence, the appropriate amount of dilbit oil will be dispensed into each EU containing 100 mL of sterile broth. At 5 °C, samples and KCs will be inoculated with 0.5 mL of the cryo KR culture whereas the meso KR culture will be added to those prepared for 25 °C. These EUs will be kept on a shaker (200 rpm) in temperature rooms maintained at 5 and 25 °C.

4. Sampling Procedures

4.1 BIODEGRADABILITY OF DISPERSED OIL

4.1.1 Sampling labeling

At the beginning of every experiment, each shake flask will be labeled with temperature (5 or 25 ºC), treatment (oil, oil + dispersant, or dispersant), replicate number (1, 2, or 3), and sampling day. Liquid-liquid extracts, dispersant aliquots, and microbial subsamples for later analysis will be labeled in the same way.

4.1.2 Sampling Procedures

For any given test, three flasks will be sacrificed per treatment. Before samples are sterilized, a 2 mL-subsample will be withdrawn for further microbial characterization (PCR assays and sequencing analysis) to be conducted at EPA AWBERC. Subsequently, bacterial activity will be stopped by adding NaN_3 to every flask in a final concentration of 500 mg/L. KCs (triplicates) will also be removed for the C9500 alone and dispersed oil treatments. In tests where C9500 alone is present, a 20-mL subsample will be taken for the analysis of its main component, DOSS, by LC-MS/MS as described in SOP 6. In the flasks containing non-dispersed Endicott, the 100 mL of seawater will be extracted with methylene chloride (DCM) and the extracts will be analyzed for alkanes and aromatics by GC-MS/MS (SOP 5). Alkanes will include normal and branched aliphatics ranging in carbon number from 10 to 35 as well as pristine and phytane. Aromatics will include 2-, 3- and 4-ring PAH compounds and their alkylated homologs (i.e. C_{0-4} -naphthalenes, C_{0-3} -fluorenes, C_{0-3} -dibenzothiophenes, C_{0-4} -phenanthrenes/anthracenes, C_{0-4} -napthobenzothiophenes, C_{0-2} -pyrenes, C_{0-4} -chrysenes). Finally, in the EUs for dispersed oil with C9500, after withdrawing the 20-mL subsample for DOSS analysis, the remaining seawater will be extracted with DCM and analyzed for oil components. In addition, the total petroleum hydrocarbons (TPH) will be determined in the solvent extracts with a GC equipped with a flame ionization detector (FID) according to the EPA SW-846 Method 8015C. The SOPs for the analysis of oil components and C9500 are included in Section 10.

At each subsequent sampling event, three more EUs per treatment along with the corresponding controls will be sampled and the different target compounds analyzed.

Table 4.1. Summary of treatment and the corresponding analytical method.

Treatment	Analysis Method [Analytes]
Oil alone, currently Endicott	GC-MS/MS [Oil components]
	TPH [Total extractable hydrocarbons]
Dispersed, oil currently Endicott	GC-MS/MS [Oil components]
	TPH [Total extractable hydrocarbons]
	LC-MS/MS [Dispersant component]
Dispersant alone	LC-MS/MS [Dispersant component]

4.1.3 Sample Containers, Sample Volumes, Preservation, and Hold Times

Sample containers, sample volumes, preservation, and hold times are shown in Table 4.2.

Table 4.2. Experimental Sampling and Analytical Procedures to Be Used

Matrix	Measurement	Sampling/	Analysis Method	Sample Container/ Quantity of each Sample to be analyzed	Preservation / Storage	Holding Time
Organic solvent extract	Alkanes and Aromatics	Grab sample	SOP 5	20 mL glass vials / 1 mL	Store @ 4 °C	6 months
	TPH	Grab sample	EPA SW-846 Method 8015C	20 mL glass vials /1 mL	Store @ 4°C	6 months
Seawater / Acetonitrile	DOSS	Grab sample	SOP 6	60 mL glass vials /1 mL	Store @ 4 °C	5 days
Seawater	PCR	Grab Sample	EPA Procedure 815-B-04-001	2 mL plastic vials /2 mL	Store @ -80°C	6 months

4.2 BIODEGRADABILITY OF DILBIT

4.2.1 Sampling labeling

At the beginning of every experiment, each shake flask will be labeled with dilbit blend type (Cold Lake 1A or Western Canadian Select), temperature (5 or 25 °C), replicate number (1, 2, or 3), day (see Section 3.3) for example CLB-25-Day2-AF-1. Liquid-liquid extracts for hydrocarbon analysis will be labeled in the same way.

Table 4.3 Sample Identifications

Identification	Code Unit
Dilbit Type	Cold Lake 1A (CLB) Western Canadian Select 2B (WCS)
Microbial Culture	Kalamazoo River Culture (KMZ) Anderson Ferry culture (AF)
Temperature	5 or 25□C
Sampling Events	Day 0-72
Replicates	1-3

4.2.2 Sampling Procedures and Analytical Methods

At any given sampling day, three flasks will be sacrificed per oil and temperature. Bacterial activity will be stopped by adding NaN_3 to every flask in a final concentration of 500 mg/L. KCs (triplicates) will only be sampled at the end of the experiment. For each replicate, the 100 mL of broth will be extracted with methylene chloride (DCM) (SOP 4) and the extracts will be analyzed for alkanes and aromatics by GC-MS-MS (SOP 5) as well as for TPH by GC_FID (EPA SW-846 Method 8015C). Alkanes will include normal and branched aliphatics ranging in carbon number from 10 to 35 as well as pristine and phytane. Aromatics will include 2-, 3-, 4-, and > 4-ring PAH compounds and their alkylated homologs (i.e. C_{0-4} -naphthalenes, C_{0-3} -fluorenes, C_{0-3} -dibenzothiophenes, C_{0-4} -phenanthrenes/anthracenes, C_{0-4} -napthobenzothiophenes, C_{0-2} -pyrenes, C_{0-4} -chrysenes).

Table 4.4. Summary of treatment and the corresponding analytical method.

Substrate	Analysis Method [Analytes]
Dilbit	GC-MS/MS [Oil components]
Dilbit	GC-FID [Total Petroleum Hydrocarbons]

4.2.3 Sample Containers, Sample Volumes, Preservation, and Hold Times

Sample containers, sample volumes, preservation, and hold times are shown in Table 4.5

Table 4.5 Sample Containers, Preservation and Holding Times

Matrix	Measurement	Sampling/	Analysis Method	Sample Container/ Quantity of each Sample to be analyzed	Preservation / Storage	Holding Time
Organic solvent extract	Alkanes and Aromatics	Grab sample	SOP 5	20 mL glass vials / 1 mL	Store @ 4 °C	6 months
	TPH	Grab sample	EPA SW-846 Method 8015C	20 mL glass vials /1 mL	Store @ 4°C	6 months
Seawater	PCR	Grab Sample	EPA Procedure 815-B-04-001	2 mL plastic vials / 2 mL	Store @ -80°C	6 months

5. Measurement Procedures

The analyses will be completed with the instrumentation described in Table 5.1 and 5.2.

Table 5.1. Analytical Instruments for Dispersant Experiment (Task 1.1)

Analyses	Analytical Method	Instrument
Oil Components	SOP 5	Agilent 7890A Gas Chromatograph - 7000 MS triple quadrupole; J&W Scientific DB5-MS column (30 m × 0.25 mm, 0.25 µm)
DOSS	SOP 6	Agilent 1200 Liquid Chromatograph - 6410 MS triple quadrupole; Zorbax Eclipse XDB-C18 Rapid Resolution Column (2.1 × 50 mm, 5 µm)
TPH	EPA SW-846 Method 8015C	Agilent 6890 Gas Chromatograph- Flame Ionization Detector; J&W Scientific DB5-MS column (30 m × 0.25 mm, 0.25 µm)

Table 5.2. Analytical Instruments for Dilbit Experiment (Task 1.2)

Analyses	Analytical Method	Instrument
Oil Components	SOP 5	Agilent 7890A Gas Chromatograph - 7000 MS triple quadrupole; J&W Scientific DB5-MS column (30 m × 0.25 mm, 0.25 µm)
TPH	EPA SW-846 Method 8015C	Agilent 6890 Gas Chromatograph- Flame Ionization Detector; J&W Scientific DB5-MS column (30 m × 0.25 mm, 0.25 µm)
SARA	SOP 7	IATROSCAN MK-5 Analyzer (Iatroscan Laboratories, Tokyo)

All chemicals involved in these analytical procedures are of ACS reagent grade or equivalent unless otherwise noted. The measurement methods are summarized in the Table 5.1 and 5.2. The water quality parameters are appropriate for the matrix/analytes being tested as described in the corresponding SOPs included in Section 10. Should any method call for modifications, the EPA WA Manager will be notified before modifications are made, and the changes will be documented as amendments to this QAPP.

6. Quality Metrics (QA/QC)

Instruments/equipment will be maintained in accordance with the EPA ORD Policies and Procedures Manual, Section 13.4 *Minimum Quality Assurance (QA)/Quality Control (QC) Practices for ORD Laboratories Conducting Research* and in accordance with the SOPs and methods specified in Table 4.2 and 4.5. The quality metrics for this study are summarized below.

6.1 Critical and Non-critical Measurements

The critical measurements for this research study include:

- Oil components, alkanes and aromatics (Task 1.1 and 1.2)
- DOSS (Task 1.1 only)

The non-critical measures are:

- TPH (Task 1.1 and 1.2)
- Molecular analyses of microbial communities (Task 1.1 and 1.2)
- SARA- Saturates Aromatics Resins Asphaltenes (Task 1.2 only)

6.2 QA/QC Objectives

QA/QC objectives are listed in Table 6.1 and explained in Sections 6.2.1 to 6.2.4. For the non-critical measurements, the QC checks and criteria are described in the corresponding SOPs included in Section 10.

6.2.1 Precision

Precision objectives for all the measurements listed in Table 6.1 are presented as relative percent difference (RPD) for duplicate measurements, and as relative standard deviation (RSD, or coefficient of variance) for three or more measurements.

6.2.2 Accuracy

Accuracy objectives are listed in Table 6.1.

6.2.3 Completeness

Completeness is a measure of valid data obtained from a measurement system compared with valid data that were intended to be obtained to evaluate the performance of the system. The required level of completeness for this study is specified at 85 percent. The laboratory staff will ensure adequate completeness by minimizing mistakes that might lead to sample loss or the generation of data that is unusable for any reason.

If the rejected or missing data are randomly disbursed throughout the study and the variability is less than expected, the quality objectives established may still be achieved; however, if the rejected or missing data are not randomly disbursed, even a high degree of completeness may be inadequate for decision-making purposes.

The corrective action for incompleteness due to failure of QC requirements is statistical readjustment of the data and/or other treatment (e.g. retest or reanalysis, etc. considering the point at which the QC failure occurred).

6.2.4 Comparability

Comparability will be achieved by using the same analytical methods and data reduction/reporting methods throughout the entire course of the project including all the preliminary experiments, parametric studies, and molecular biological assays.

6.3 Internal Quality Control

Table 6.1 summarizes the QC checks of the measurements.

Table 6.1. Summary of Internal QC Checks for all Parameters

Measurement/Matrix/(SOP)	QA/QC Check	Frequency	Acceptance Criteria	Corrective Action
Alkanes & Aromatics by GC-MS-MS (critical parameter)/ Organic solvent extract / (SOP 5)	Air/Water Check	Every run	System is leak free	Make system leak free
	Solvent Blank run in SCAN MODE	Following liner change and at the start of a new run.	No contaminants of interest	Rerun fresh solvent until interfering contamination is removed.
	Autotune	Prior to calibration	Manufacture's specifications	Retune instrument
	Initial calibration (5 or 6 point curve)	Every batch and as required	% RSD of RRFs < 25%	Rerun standard curve, change standards
	Second source calibration check	After initial calibration	RRF within 25% of the average calibration FF of the initial calibration for the selected compounds	Rerun calibration check, change standard, Rerun standard curve
	Calibration check	At the beginning and end of a batch, and every 10 samples.	RRF within 25% of the average calibration FF of the initial calibration	Rerun samples since last valid calibration check, rerun standard curve, and/or change standards
	Method Blank	Every batch of extracted samples	Concentration of target compounds less than half of the reporting limit (500 µg/L for petroleum hydrocarbons)	Check for target contamination and rerun samples for the batch.
	Reagent blank	Every 10 samples	Concentration of target compounds less than half of the reporting limit (500 µg/L for petroleum hydrocarbons)	Check for target contamination and rerun samples since last valid blank

Measurement/Matrix/(SOP)	QA/QC Check	Frequency	Acceptance Criteria	Corrective Action
	Internal Standard	Every sample	50-200% of target in midrange standard	Discard data point, repeat experiment if there are insufficient data points
	Surrogate spike	Every batch	Surrogate spike recovery within 70-130%	Check standards, rerun spike
Total Petroleum Hydrocarbons by GC/FID (non-critical parameter)/ Organic solvent extract / (see EPA Method 8015C)	Single point calibration of all target compounds	Beginning of each batch used for screening (See Section 1.3 of EPA Method 80415C)	Compare to known LCS run directly after calibration. LCS must meet criteria for standard to be fit for use	Rerun standard curve, remake/run standards
	Blank	Every batch	Absence of target contaminants	Determine source of contamination. Rerun blank and sample batch
	Laboratory Control Sample	Every batch following calibration and at end of batch	75-125% of known second source standard (LCS concentration at approximate sample concentration)	Rerun standard curve, remake/run standards. Rerun samples since last valid LCS
DOSS by LC-MS-MS (critical parameter) / Seawater/ Acetonitrile/ SOP 6	Initial calibration (5 or 6 point curve DOSS)	Every batch	Linear fit if $r^2 > 0.98$ Quadratic fit if $r^2 > 0.99$	Rerun standard curve, change standards
	Analytes' retention time	Every sample	± 5% of the retention time of the analyte in a midpoint calibration standard	Rerun calibration curve and compare time shift. Rerun samples since last valid retention time
	Second source calibration check	After initial calibration	± 35% deviation from the nominal concentration of the standard	Rerun standard curve, and/or change standards
	Calibration check	At the beginning and end of a batch, every 20 samples and within 24 h after initial calibration	± 35% deviation from the nominal concentration of the standard	Rerun samples since last valid calibration check, rerun standard curve, and/or change standards
	Method Blank	At the beginning and end of a batch and every 20 samples	Less than half of the reporting limit	Check for target contamination and rerun samples since last valid blank

Measurement/Matrix/(SOP)	QA/QC Check	Frequency	Acceptance Criteria	Corrective Action
	Surrogate spike	Every sample	Spike recovery within 50-150%	Check standards, rerun spike
SARA analysis by IATROSCAN/ DCM/ (SOP 7)	Blank Scan	Every batch	Absence of target contaminants	Repeat the Blank Scan

7. Data Analysis, Interpretation, and Management

7.1 Data Reporting

All results will be reduced to the appropriate reporting units designated in the SOPs by the analyst performing the test. The reporting units for each analysis are summarized in Table 7.1. Results will be averaged and the mean and the standard deviation or the range, will be calculated.

Table 7.1 Reporting Units

Measurement	Unit	Tasks No.
Alkanes and aromatics	µg analyte/µg hopane	1.1
Alkanes and aromatics	µg/L analyte	1.2
TPH	mg/L	1.1 and 1.2
DOSS	µg/L	1.1
SARA	Relative % concentration	1.2

Calculations will be carried out on a computer and will be checked initially by the analyst for gross error and miscalculation. The calculations and data entered into computer spreadsheets will be checked by a second analyst for accuracy by printing out the calculation or data spreadsheet and checking the calculation by hand or checking each entry of data from the original. These copied spreadsheets will be initialed and dated by the second analyst doing the checking, noting the errors.

7.2 Data Reduction and Validation

Data reduction procedures are described in the related SOPs. Data will be documented in data log sheets in which sample identification, date and analyst name will be recorded. Hard copy raw data shall be archived with documentation for standard preparation and QC data (calibration check standards, analysis duplicates and analysis blanks).

Data reduction will be computerized to reduce the likelihood of transcription and calculation errors. Computerized calculations will be validated prior to use. After data are calculated in the reporting units, they will be transferred to a Microsoft Excel spreadsheet. The WA Leaders will review the reduced data to check for coherence and consistency. They will also spot check calculations all the way back to raw data logs at random, at least one per analytical method for each part of the study. Detected errors will be corrected and other data in the same set investigated before it is released to the EPA WACOR.

7.3 Data Summary and Analysis

When the experimental phase of the project has been completed, the analytical data will be analyzed statistically to show how the data will be used to support the project objectives. Table 3.1 and 3.2 describe a completely randomized design where the treatments are the two temperatures, the eleven and ten sampling days for 5 and 25 °C, and the three different substrates, i.e., dispersed oil, non-dispersed oil, and dispersant alone. The hypotheses are that, for a given temperature, (1) non-dispersed oil should be less amenable to biodegradation than the dispersed and (2) dispersant alone should experiment a faster degradation that the dispersant and crude oil mix. Additionally, it is anticipated that substrates will be degraded more quickly at 25

°C than at a lower temperature, 5 °C.

The data collected from the experiments will be summarized in two ways: (1) by conducting an analyses of variance (ANOVA) to determine if treatment and block differences exist and (2) by non-linear regression of all the data for each site and for each treatment at the end of the experiment to compare overall first-order biodegradation rates among the various treatments. If the ANOVA reveals significant differences ($p < 0.05$), then treatment differences will be evaluated by the protected least significant difference (LSD) mean separation test. These tests and ANOVA will be done on the sum total of hopane-normalized alkanes, the sum total of hopane-normalized aromatics (PAHs), and for the main component of C9500 as the dependent variables. For the non-linear regressions, an F-test will be performed to compare the slope coefficients statistically among the various treatments. For these calculations, the variance will be estimated from the sum-of-squared residuals from the fit of the first-order model to the average concentrations (over all replicates) for each treatment at each time point.

Appropriate mean comparison tests, such as the protected LSD test, will depend on whether or not the main effects and/or two-way interactions are statistically significant ($p < 0.05$).

7.4 Data Storage

Laboratory records will be maintained in accordance with Section 13.2, Paper Laboratory Records, of the Office of Research and Development (ORD) Policies and Procedures Manual. Controlled access facilities that provide a suitable environment to minimize deterioration, tampering, damage, and loss will be used for the storage of records. Whenever possible, electronic records will be maintained on a secure network server that is backed up on a routine basis. Electronic records that are not maintained on a secure network server will be periodically backed up to a secure second source storage media, transferred to an archive media (e.g., compact discs, optical discs, magnetic tape, or equivalent), or printed. Electronic records that are to be transferred for retention will be transferred to an archive media or printed, as directed by EPA.

8. Reporting

8.1 Monthly Reports

Outputs will be in the form of detailed monthly reports describing progress made in each task. Monthly reports will be prepared by the UC WA Leader, reviewed by the Pegasus Project Manager, and submitted to the EPA every month. Distribution of the monthly report to other agencies will be at the discretion of the EPA WACOR.

8.2 Final Report

A final report shall be prepared by the Pegasus/UC team summarizing the results from this study and submitted to the EPA WACOR on or before September 29, 2016. Raw data shall be provided to the EPA WACOR in the form of a Microsoft Excel spreadsheet at the conclusion of each dispersant/temperature/oil combination. The format for the data report shall be provided to the Pegasus/UC team by the EPA WACOR via written technical direction.

9. Amendment/Revision History

This section contains the revision and/or amendment history of the project QAPP.

Table 9.1 Amendment/Revision History

Revision #	Description	Effective Date
0	**Original (Contract No.: EP-C-11-006)** WA 3-33, QA ID: L-15045-QP-1-5 WA 3-85, QA ID: L-20624-QP-1-0	 12/16/2013 12/17/2014
1	**Amendment 1 (Contract No.: EP-C-15-010)** Revision to combine QAPP L-15045-QP-1-6, WA0-05 Task 1.1 with QAPP L-20624-QP-1-0 Task 1.2 under QA ID L-20624-QP-1-1. Account for changes in project objective. Included SOP for IATROSCAN.	12/09/2015

ED_001324_00000276-00031

10. List of Standard Operating Procedures

SOP	Title	File
SOP 1	Preparation of Surrogate Recovery Standard	SOP 1.docx
SOP 2	Preparation of Internal Standard Solution	SOP 2.docx
SOP 3	Preparation of Working Standard, Check Standards, and Oil Standard for GC-MS/MS	SOP 3.docx
SOP 4	Extraction of Oil from Aqueous Samples for GC-MS/MS	SOP 4.docx
SOP 5	GC-MS/MS Method for Analysis of Crude Oil Samples	SOP 5.docx
SOP 6	LC-MS/MS Method for the Analysis of Dioctyl Sulfosuccinate in Seawater	SOP 6.docx
SOP 7	IATROSCAN for SARA (Saturates Aromatics Resins Asphaltenes) Analysis of Oil Samples	SOP 7.docx
SOP 8	Total DNA Isolation	SOP 8.docx
SOP 9	Quantifying Nucleic Acids With a Nanodrop Nd-1000 Spectrophotometer	SOP 9.docx
SOP 10	Polymerase Chain Reaction (PCR)	SOP 10.docx
SOP 11	PCR Purification With QIAquick Spin Kit	SOP 11.docx

SOP 12	TOPO T/A Cloning	SOP 12.docx

11. References

U.S. Environmental Protection Agency, October 2004. Quality Assurance/Quality Control Guidance for Laboratories Performing PCR Analyses on Environmental Samples. EPA Document No. 815-B-04-001. Office of Water, Cincinnati, Ohio.

University of Cincinnati, December 2013. Category I Quality Assurance Project Plan, Amendment 2, "Biodegradability of Dispersants and Dispersed oil at Two Temperatures". EPA Contract No. EP-C-11-066. EPA QA ID: L-15045-QP-1-5.

University of Cincinnati, December 2014. Biodegradability and Persistence of Dilbit and Bakken Oil in the Environment. EPA Contract No. #P-C-11-066. EPA QA ID: L-20624-QP-1-0.

ED_001324_00000276-00033

Quality Assurance Project Plan
Category III Measurement Project

BIODEGRADABILITY OF DISPERSANT AND DISPERSED OIL AT TWO TEMPERATURES: EFFECT OF USING DILUTED OIL AND DISPERSANT

U.S. Environmental Protection Agency Contract No. **EP-C-11-006**

Work Assignment No. 3-33

Prepared for:
Albert D. Venosa, Ph.D.
Work Assignment Manager

U.S. Environmental Protection Agency
Office of Research and Development
National Risk Management Research Laboratory
26 West Martin Luther King Drive
Cincinnati, OH 45268

Prepared by:
Pablo Campo-Moreno, Ph.D.

University of Cincinnati
School of Energy, Environmental, Biological, and Medical Engineering

Under Subcontract to:

Pegasus Technical Services, Inc.
46 E. Hollister Street
Cincinnati, OH 45219

Revision 0
November 12, 2013

QUALITY ASSURANCE PROJECT PLAN APPROVAL

Concurrences:

1. Pablo Campo-Moreno, Ph.D., University of Cincinnati
   Work Assignment Leader

   _____ _____
   Signature Date

2. Steven Jones, ASQ CQA/CQE, Shaw Environmental & Infrastructure, Inc.
   Pegasus Contract Quality Assurance Manager

   _____ _____
   Signature Date

3. George Sorial, Ph.D., University of Cincinnati
   University of Cincinnati Project Manager

   _____ _____
   Signature Date

4. Karen Koran, Ph.D., Pegasus Technical Services, Inc.
   Project Manager

   _____ _____
   Signature Date

U.S. Environmental Protection Agency Approval for Implementation:

1. Albert D. Venosa, Ph.D., Work Assignment Manager

   _____ _____
   Signature Date

2. Jim Voit, LRPCD Quality Assurance Manager

   _____ _____
   Signature Date

TABLE OF CONTENTS

Section	Name	Revision	Date	Page
0.0	Approval by Project Participants	0	11/2013	2
1.0	Project Description and Objectives	0	11/2013	8
2.0	Organization and Responsibilities	0	11/2013	9
3.0	Scientific Approach	0	11/2013	12
4.0	Sampling Procedures	0	11/2013	16
5.0	Measurement Procedures	0	11/2013	18
6.0	Quality Metrics (QA/QC Checks)	0	11/2013	19
7.0	Data Analysis, Interpretation, and Management	0	11/2013	23
8.0	Reporting	0	11/2013	25
9.0	References	0	11/2013	26
APPENDIX A	Standard Operating Procedures	0	11/2013	27

APPENDIX A
List of Standard Operating Procedures (SOPs)

SOP 1	Preparation of Surrogate Recovery Standard
SOP 2	Preparation od Internal Standard Solution
SOP 3	Preparation of Working Standard, Check Standards, and Oil Standard for GC-MS/MS
SOP 4	Extraction of Oil from Aqueous Samples for GC-MS/MS
SOP 5	GC-MS/MS Method for Analysis of Crude Oil Samples
SOP 6	LC-MS/MS Method for the Analysis of Dioctyl Sulfosuccinate in Seawater
SOP 7	Total DNA Isolation
SOP 8	Quantifying Nucleic Acids With a Nanodrop Nd-1000 Spectrophotometer
SOP 9	Polymerase Chain Reaction (PCR)
SOP 10	PCR Purification With QIAquick Spin Kit
SOP 11	TOPO T/A Cloning

LIST OF TABLES

Table	Title	Page
Table 2.1	Organization/Title Chart	9
Table 2.2	Project Schedule	11
Table 3.1	Experimental Layout	13
Table 4.1	Treatment and Analytical Method	16
Table 4.2	Experimental Sampling and Analytical Procedures to Be Used	17
Table 5.1	Analytical Instruments	18
Table 6.1	Summary of Internal QC Checks for Critical Parameters	20
Table 7.1	Reporting Units	23

LIST OF FIGURES

Figure	Title	Page
Figure 2.1	Organization Chart	10

DISTRIBUTION LIST

Dr. Albert Venosa, Work Assignment Manager, U.S. Environmental Protection Agency
Mr. Jim Voit, LRPCD Quality Assurance Manager, U.S. Environmental Protection Agency
Dr. Jorge Santo Domigo, Project Support for PCR Analysis, U.S. Environmental Protection Agency

Dr. Karen Koran, Project Manager, Pegasus Technical Services, Inc.
Mr. Steven Jones, Contract Quality Assurance Manager, Shaw Environmental & Infrastructure, Inc.
Dr. George Sorial, Manager, University of Cincinnati
Dr. Pablo Campo-Moreno, Work Assignment Leader, University of Cincinnati
Ms. Mobing Zhuang , Project Staff, University of Cincinnati
Ms. Gulizhaer Abulikemu, Project Staff, University of Cincinnati

SECTION 1.0

PROJECT DESCRIPTION AND OBJECTIVES

1.1 Purpose of study

The Deepwater Horizon (DWH) incident in the Gulf of Mexico (GOM) has raised questions not only about the biodegradability of oil in deep and surface waters in that area, but also to answer concerns about the rate of biodegradation of the dispersants *per se* and the dispersed oil. Previous research conducted under U.S. Environmental Protection Agency (EPA) Contract No. EP-C-11-006, Work Assignments (WAs) 1-33 and 2-33, showed that the alkane and polycyclic aromatic hydrocarbons (PAH) fractions in the oil, dispersed oil, and dispersant biodegraded at 5 and 25 °C and the corresponding degradation rates were calculated. Nevertheless, these studies were conducted at substrate concentrations significantly higher than those found in field conditions. Hence, in this project, oil, dispersed oil, and dispersant will be tested at a concentration that is 4.3% of the value previously tested in the aforementioned WAs. The rationale is that normally, in actual field trials, the concentrations of oil and dispersant never reach the levels used in laboratory experiments. The herein described approach will produce environmentally relevant data by determining oil, dispersed oil, and dispersant biodegradation rates at smaller loading concentrations. The EPA is also in need of determining what microbial cultures are responsible for biodegradation at the two temperatures and how these communities change as substrate consumption takes place.

1.2 Project Objectives

The overall aim of this WA is to study biodegradation of oil, dispersed oil, and dispersant at environmentally relevant concentrations. This goal will be achieved through the following specific objectives:

1. To study the rate of biodegradation of Alaska North Slope (ANS) crude oil, dispersant Corexit 9500 (C9500), and ANS dispersed with C9500 at a concentration 4.3% of that used in WAs 1-33 and 2-33.
2. To measure those biodegradation rates at 5 °C and at 25 °C.

1.2_ To investigate the time-dependent changes in the microbial cultures used in the biodegradation experiments.

SECTION 2.0

ORGANIZATION AND RESPONSIBILITIES

2.1 Project Organization

Mr. Michael Moeykens and Mr. Stephen Wright serve as the EPA Project Officers for EPA Contract No. EP-C-11-006. For this WA, Dr. Albert Venosa is the EPA WA Manager responsible for WA planning, providing technical direction related to WA activities, and ensuring that the data received from Pegasus Technical Services, Inc. (Pegasus) and the University of Cincinnati (UC) satisfy the project objectives. Mr. Jim Voit is the EPA Land Remediation and Pollution Control Division (LRPCD) Quality Assurance (QA) Manager responsible for approval of this Quality Assurance Project Plan (QAPP). Dr. Jorge Santo Domigo with EPA will be providing support for polymerase chain reaction (PCR) analysis of samples.

Dr. Karen Koran is the Pegasus Project Manager for this Off-Site WA. Dr. George Sorial with UC (a subcontractor to Pegasus for this off-site WA) is the UC Project Manager. Mr. Steven Jones, ASQ CQA/CQE, with Shaw Environmental & Infrastructure, Inc., is the Pegasus Contract QA Manager responsible for oversight of Pegasus Quality Program implementation, QA review of quality documents and deliverables, and project assessments. Dr. Pablo Campo-Moreno is the UC WA Leader responsible for project planning, coordination of experiments and analyses, interpretation of the data, coordinating internal review of contract deliverables prior to submittal to EPA, and completion of the final report. Ms. Mobing Zhuang and Ms. Gulizhaer Abulikemu, WA staff, will be responsible for assisting the UC WA Leader with the design and maintenance of the experiments as well as chemical analysis.

Table 2.1 Organization/Title Chart

Name	Phone/email	Responsibilities
Mr. Stephen Wright	(513) 569-7610 Wright.Stephen@epa.gov	EPA Project Officer
Mr. Michael Moeykens	(513) 569-7196 Moeykens.Michael@epa.gov	EPA Project Officer
Dr. Albert Venosa	(513) 569-7668 Venosa.Albert@epa.gov	EPA WA Manager
Mr. Jim Voit	(513) 487-2867 Voit.Jim@epa.gov	EPA LRPCD QA Manager
Dr. Jorge Santo Domingo	(513) 569-7085 Santodomingo.Jorge@epa.gov	EPA Project Support for PCR Analysis
Dr. Karen Koran	(513) 569-7304 Koran.Karen@epa.gov	Pegasus Project Manager
Mr. Steven Jones	(513) 782-4655 Steve.S.Jones@CBIFederalServices.com	Pegasus Contract QA Manager
Dr. George Sorial	(513) 556-2987 sorialga@ucmail.uc.edu	UC Project Manager
Dr. Pablo Campo-Moreno	(513) 556-3637 campomp@ucmail.uc.edu	UC (Off-Site) WA Leader

Ms. Mobing Zhuang	(513) 556-3640 zhuangmg@mail.uc.edu	UC Project Staff
Ms. Gulizhaer Abulikemu	(513) 556-3640 abulikgr@mail.uc.edu	UC Project Staff

Figure 2.1. Organization Chart

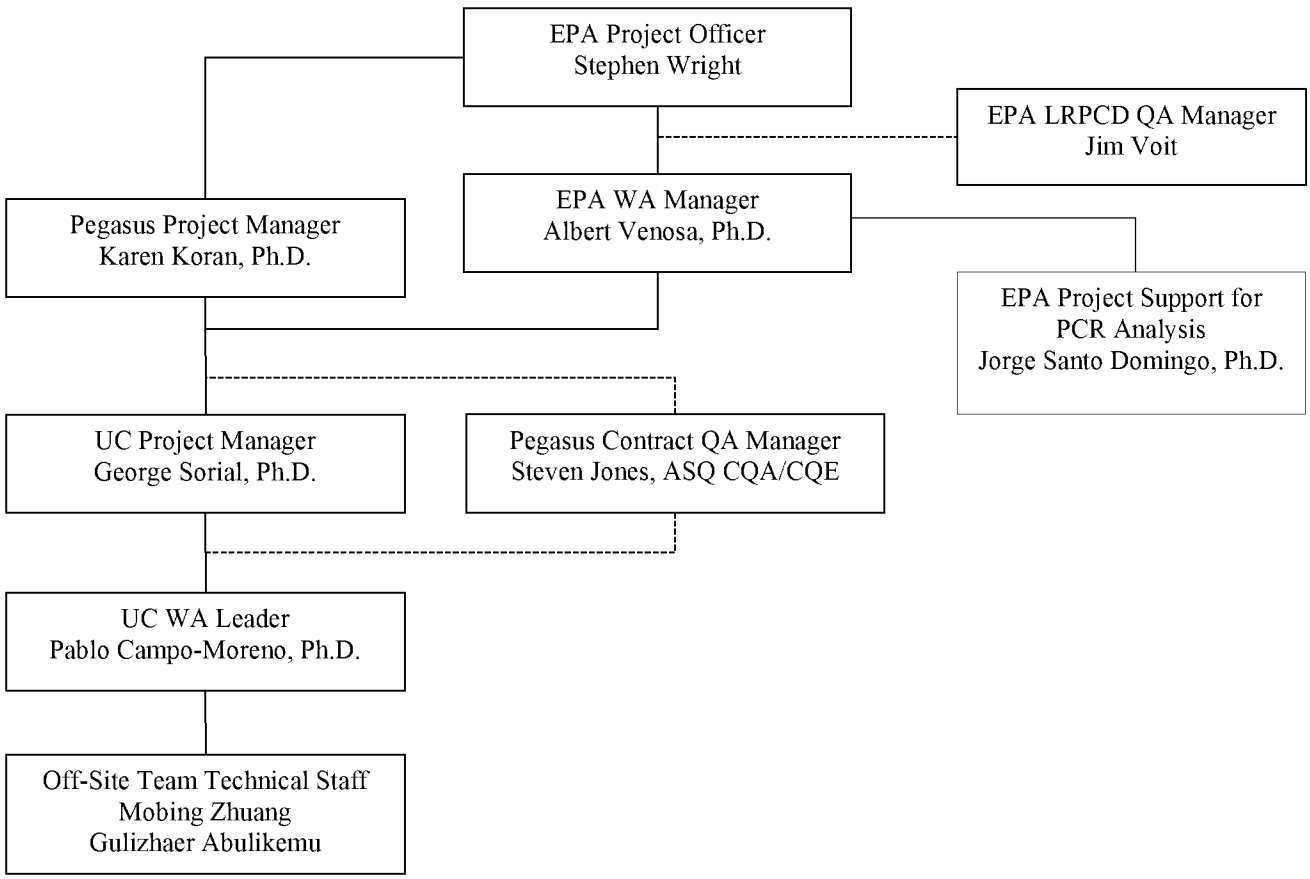

2.2 Project Schedule

The projected schedule and the main activities are shown in Table 2.2.

Table 2.2 Projected Schedule

Activity	Oct-13	Nov-13	Dec-13	Jan-14	Feb-14	Mar-14	Apr-14	May-14	Jun-14	Jul-14	Aug-14	Sep-14
QAPP Preparation												
Experimental Setup												
Sampling												
Sample Analysis												
Report Writing												
Presentation/ Manuscript												

SECTION 3.0

SCIENTIFIC APPROACH

3.1 Biodegradation study

The objectives will be realized by completing the biodegradation studies of ANS dispersed with C9500. Additionally, degradation of ANS and C9500 as only substrates will be also studied. The experiments will be conducted in 250-mL shake flasks rotating at 200 rpm and sterile GP2 seawater will be the matrix used in the study. Both oil and dispersant will be tested at 5 and 25 °C as described in the subsections below. Time-dependent changes in the microbial communities will be determined as well.

The critical parameters for this project will be the measured time series concentrations for oil components (alkanes and aromatics) and main component of C9500. These values will be use in the calculation of degradation rates and extends of these substances. TPH time series have a semi-quantitative value, since these data give a general idea of how the total extractable hydrocarbons evolve with time, hence this parameter is non-critical. PCR results for microbial determinations are considered non-critical as well.

3.2 Microbial Enrichment Studies

The EPA WA Manager will provide two frozen mixed cultures of oil degrading bacteria to the UC WA Leader. These cultures were previously enriched, grown, and frozen in 5-mL vials containing glycerol by EPA's Gulf Ecology Division at Gulf Breeze, FL. The first mixed culture (denoted as cryo) was isolated from the deep sea of the GOM and enriched on South Louisiana crude oil at 5 °C. The second culture (denoted as meso) was isolated from the top 5 m of the GOM and enriched at 25 °C.

3.3 Experimental setup

The experiments outlined in Table 3.1 will be used for the biodegradation studies to be conducted in order to determine the biodegradation rate of ANS crude oil and C9500. In the 5 °C test, eleven (11) sampling events will take place at 0, 2, 4, 8, 12, 16, 24, 32, 40, 48, and 56 days, while ten (10) sampling events are required at 0, 2, 4, 8, 12,16, 24, 32, 40, and 48 days in the 25 °C experiment. For both temperatures, the following treatments will be set up:

1. C9500 alone.
2. ANS previously dispersed by C9500.
3. ANS alone.

Additionally, killed controls (KCs) will be run in triplicates for each treatment to account for abiotic losses, if any. These KCs include all ingredients as the live microcosms (i.e., oil, dispersant, nutrients, and culture) but they will be sterilized with sodium azide (NaN_3) at a concentration of 500 mg/L per flask. The time zero (T_0) replicates for Tests 1, 2, and 3 (see Table 3.1) will serve as the same T_0 replicates for Tests 8, 9, and 10, respectively. In all the cases, 100 mL of autoclaved GP2 synthetic seawater will be used as medium for microbial activity and the orbital shakers will rotate at 200 rpm. Another set of triplicate KCs will also be

set up with an additional component, a protease enzyme, to break down or inhibit any possible enzyme or exoenzyme previously developed by the culture that may hydrolyze the surfactant dioctyl sulfosuccinate (DOSS), the active ingredient in C9500. The contents from these flasks will be periodically collected for LC-MS/MS analysis.

At a given sampling event, triplicate flasks of each treatment will be sacrificed along with those KCs having dispersed oil and C9500. For oil alone treatments, triplicates of the controls will only be sacrificed on the final event. Before sacrificing any microcosms, 2 mL will be withdrawn from each flask containing live culture and preserved by freezing at -80 °C until analysis for determination of microbial communities, which will be performed by EPA personnel at the EPA Andrew W. Breidenbach Environmental Research Center (AWBERC) under the direction of Dr. Jorge Santo Domingo. Samples will be provided to Dr. Santo Domingo by the UC WA Leader or designee for all nucleic acid-based analyses.

Table 3.1 Summary of Experimental Layout for Two Temperatures.

Test	Temperature	Treatment	Sampling Events	Sample Replicates	Total Exp. Units (EU)
1	5 °C	C9500 alone	11	3	33
2	5 °C	ANS dispersed by C9500	11	3	33
3	5 °C	ANS alone	11	3	33
4	5 °C	Killed ANS control	1	3	3
5	5 °C	Killed C9500 control	10	3	30
6	5 °C	Killed ANS + C9500 control	10	3	30
7	5 °C	Killed ANS + C9500 + Protease	5	3	15
				Subtotal EU's	**177**
8	25 °C	C9500 alone, use T_0 from line 1	9	3	27
9	25 °C	ANS dispersed by C9500, use T0 from line 2	9	3	27
10	25 °C	ANS alone, use T_0 from line 3	9	3	27
11	25 °C	Killed ANS control	1	3	3
12	25 °C	Killed C9500 control	9	3	27
13	25 °C	Killed ANS + C9500 control	9	3	27
14	25 °C	Killed ANS + C9500 + Protease	5	3	15
GP2 with ANS + C9500	**GP2 with C9500**	**GP2 with PBC**		**Subtotal EU's**	**153**
15	**12**	**7**		**Total EU's for C9500**	**330**

3.4 Preparation of treatments

Dispersed oil treatment

To make dispersed oil, the following will be carried out with C9500. The procedure involves making batches of dispersed oil in the baffled flasks and compositing them in a glass carboy or bottle. The composite should be continuously mixed to keep the suspension from settling. The sterile GP2 media will be prepared by dissolving the required amounts of mineral salts in

distilled water. This solution will be autoclaved at 120 °C for 30 minutes in batches of 1 liter. The concentration of each salt (expressed in g/L) will be NaCl (21.03), MgCl2 6H2O (9.5), Na2SO4 (3.52), CaCl2.2H2O (1.32), KCl (0.61), KBr (0.088), NaB4O7.10H2O (0.034), SrCl2.6H2O (0.02), NaHCO3 (0.17) FeCl3.6H2O (0.05), Na5P3O10 (0.297) KNO3 (2.89). A single dispersed oil batch will be prepared at room temperature as follows:

- Measure 1,500 mL of GP2 artificial seawater into a 2-L baffled flask.
- Pipette onto the surface 240 µL ANS with a Brinkmann Eppendorf repeater pipette with a 1 mL tip (3 times at the 4th stop).
- Pipette 10.0 µL (1 time at 5th stop) of C9500 with a Brinkmann Eppendorf repeater plus pipette with a 100 µL tip. This will give a dispersant-to-oil (DOR) volumetric ratio of 1:24.
- Cover with the foil used in autoclaving and place on shaker table.
- Start the shaker at a very slow speed to minimize sloshing and ramp it up to approximately 200 rpm.
- Agitate the flask for 20 minutes.
- Let the flask remain stationary for 10 minutes to allow undispersed oil to float to the surface. Drain the dispersed oil seawater suspension through the bottom stopcock into the carboy being careful not to disturb the top layer of undispersed oil.
- Stop draining when the liquid is still covering the opening to the stopcock. There should be about 200 mL left in the flask.
- For the next preparation, add 1,200 mL of GP2 seawater to the remaining 200 mL of dispersed oil, 200 µL ANS oil (2 times at the 5th stop), and 8 µL C9500 (1 time at the 4th stop). Prepare 3 L of this mixture. Add 12 L of sterile GP2 for a total of 15 L.
- From the time the first batch is drained into the carboy, keep the contents of the carboy well mixed.
- Aseptically dispense 100 mL aliquots of the combined dispersed oil seawater mixture into previously silanized shake flasks.
- Add NaN_3 to the dispersed oil killed controls to a final concentration of 500 mg/L (0.5 mL of a 100 mg/mL stock solution per flask) before adding the culture.
- Incubate both live and killed culture flasks at 5 °C after adding 0.5 mL of the cryo culture; those to be incubated at 25 °C will receive 0.5 mL of the meso culture.
- Place the flasks on the orbital shaker in the corresponding constant temperature room (CTR) at 5 or 25 °C. Set the orbital shakers to 200 rpm.

Non-dispersed oil treatment

The final concentration of oil in the samples should be approximately 28 µg/L as in the dispersed oil treatment. Hence, approximately 4 µL ANS will be pipetted (2nd stop with a 100 µL tip) into each shake flask containing 100 mL sterile GP2. The live and KC flasks will be set up in the same manner as the dispersed oil flasks discussed in the previous section.

Dispersant alone treatment

In order to evaluate the biodegradation of C9500 alone, tests will be conducted where the only

substrate is the dispersant. With this purpose, a single batch of sterile GP2 (12 L) will be spiked with approximately 16 µL of C9500, for this volume yields a similar concentration as in the dispersed oil treatment. This batch should be kept well mixed. From this stock, the experimental units (EUs) for both temperatures will be prepared by transferring 100 mL of the mix into each flask. For the 5 °C experiment, the sample inoculum is the cryo culture whereas the meso will be added to the 25 °C EUs. Additionally, the KCs will be sterilized by adding NaN_3 in a final concentration of 500 mg/L per flask.

SECTION 4.0

SAMPLING PROCEDURES

4.1. Sampling labeling

At the beginning of every experiment, each shake flask will be labeled with temperature (5 or 25 ºC), treatment (oil, oil + dispersant, or dispersant), replicate number (1, 2, or 3), and sampling day. Liquid-liquid extracts, dispersant aliquots, and microbial subsamples for later analysis will be labeled in the same way.

4.2. Sampling Procedures

At T_0 and for any given test, three flasks will be sacrificed per treatment. Before samples are sterilized, a 2 mL-subsample will be withdrawn for further microbial characterization (PCR assays and sequencing analysis) to be conducted at EPA AWBERC. Subsequently, bacterial activity will be stopped by adding NaN_3 to every flask in a final concentration of 500 mg/L. KCs (triplicates) will also be removed for the C9500 alone and dispersed oil treatments. In tests where C9500 alone is present, a 20-mL subsample will be taken for the analysis of its main component, DOSS, by LC-MS/MS as described in SOP 6. In the flasks containing non-dispersed SLC, the 100 mL of seawater will be extracted with methylene chloride and the extracts will be analyzed for alkanes and aromatics by GC-MS/MS (SOP 5). Alkanes will include normal and branched aliphatics ranging in carbon number form 10 to 35 as well as pristine and phytane. Aromatics will include 2-, 3-, 4-, and > 4-ring PAH compounds and their alkylated homologs (i.e. C_{0-4} -naphthalenes, C_{0-3} -fluorenes, C_{0-3} -dibenzothiophenes, C_{0-4} -phenanthrenes/anthracenes, C_{0-4} -napthbenzothiophenes, C_{0-2} -pyrenes, C_{0-4} -chrysenes). Finally, in the EUs for dispersed oil with C9500, after withdrawing the 20-mL subsample for DOSS analysis, the remaining seawater will be extracted with DCM and analyzed for oil components. In addition, the total petroleum hydrocarbons (TPH) will be determined in the solvent extracts with a GC equipped with a flame ionization detector (FID) according to the EPA SW-846 Method 8015C. The SOPs for the analysis of oil components and C9500 are included in Appendix B.

At each subsequent sampling event, three more EUs per treatment along with the corresponding controls will be sampled and the different target compounds analyzed.

Table 4.1. Summary of treatment and the corresponding analytical method.

Treatment	Analysis Method [Analytes]
SLC alone	GC-MS/MS [Oil components]
	TPH [Total extractable hydrocarbons]
Dispersed SLC	GC-MS/MS [Oil components]
	TPH [Total extractable hydrocarbons]
	LC-MS/MS [Dispersant component]
Dispersant alone	LC-MS/MS [Dispersant component]

4.2. Sample Containers, Sample Volumes, Preservation, and Hold Times

Sample containers, sample volumes, preservation, and hold times are shown in Table 4.2.

Table 4.2. *Experimental Sampling and Analytical Procedures to Be Used*

Matrix	Measurement	Sampling/	Analysis Method	Sample Container/ Quantity of each Sample to be analyzed	Preservation / Storage	Holding Time
Organic solvent extract	Alkanes and Aromatics	Grab sample	SOP 5 (see Appendix A)	20 mL glass vials / 1 mL	Store @ 4 °C	6 months
	TPH	Grab sample	EPA SW-846 Method 8015C	20 mL glass vials / 1 mL	Store @ 4°C	6 months
Seawater/ACN[1]	DOSS	Grab sample	SOP 6 (see Appendix A)	60 mL glass vials / 1 mL	Store @ 4 °C	5 days
Seawater	PCR	Grab Sample	EPA Procedure 815-B-04-001	2 mL plastic vials / 2 mL	Store @ -80°C	6 months

[1]ACN, acetonitrile.

SECTION 5.0

MEASUREMENT PROCEDURES

5.1 Measurement Methods

The analyses will be completed with the instrumentation described in Table 5.1.

Table 5.1. *Analytical Instruments*

Analyses	Instrument
Oil Components	Agilent 7890A Gas Chromatograph - 7000 MS triple quadrupole; J&W Scientific DB5-MS column (30 m × 0.25 mm, 0.25 μm)
DOSS	Agilent 1200 Liquid Chromatograph - 6410 MS triple quadrupole; Zorbax Eclipse XDB-C18 Rapid Resolution Column (2.1 × 50 mm, 5 μm)
TPH	Agilent 6890 Gas Chromatograph- Flame Ionization Detector; J&W Scientific DB5-MS column (30 m × 0.25 mm, 0.25 μm)

All chemicals involved in these analytical procedures are of ACS reagent grade or equivalent unless otherwise noted.

The measurement methods are summarized in the Table 5.1. The water quality parameters are appropriate for the matrix/analytes being tested as described in the corresponding SOPs included in Appendix A.

All chemicals involved in these analytical procedures are of ACS reagent grade or equivalent unless otherwise noted. Analytical instruments used for this project are listed in Table 5.1.

Should any method call for modifications, the EPA WA Manager will be notified before modifications are made, and the changes will be documented as amendments to this QAPP.

SECTION 6.0

QUALITY METRICS (QA/QC CHECKS)

Instruments/equipment will be maintained in accordance with the EPA ORD Policies and Procedures Manual, Section 13.4 *Minimum Quality Assurance (QA)/Quality Control (QC) Practices for ORD Laboratories Conducting Research* and in accordance with the SOPs and methods specified in Table 4.2. The quality metrics for this study are summarized below.

6.1 Critical and Non-critical Measurements

The critical measurements for this research study include:

1.1_ Oil components, alkanes and aromatics.
1.2_ DOSS.

The non-critical measures are:

1.1_ TPH
1.2_ Molecular Analyses of Microbial communities.

6.2 QA/QC Objectives

Quality Assurance/ Quality Control (QA/QC) objectives are listed in Table 6-1 and explained in Sections 6.2.1- 6.2.4. For the non-critical measurements, the QC checks and criteria are described in the corresponding SOPs included in Appendix A.

6.2.1 Precision

Precision objectives for all the measurements listed in Table 6-1 are presented as relative percent difference (RPD) for duplicate measurements, and as relative standard deviation (RSD, or coefficient of variance) for three or more measurements.

6.2.2 Accuracy

Accuracy objectives are listed in Table 6-1.

6.2.3 Completeness

Completeness is a measure of valid data obtained from a measurement system compared with valid data that were intended to be obtained to evaluate the performance of the system. The required level of completeness for this study is specified at 85 percent. The laboratory staff will ensure adequate completeness by minimizing mistakes that might lead to sample loss or the generation of data that is unusable for any reason.

If the rejected or missing data are randomly disbursed throughout the study and the variability is less than expected, the quality objectives established may still be achieved; however, if the rejected or missing data are not randomly disbursed, even a high degree of completeness may be inadequate for decision-making purposes.

The corrective action for incompleteness due to failure of QC requirements is statistical readjustment of the data and/or other treatment (e.g. retest or reanalysis, etc. considering the point at which the QC failure occurred).

6.2.4 Comparability

Comparability will be achieved by using the same analytical methods and data reduction/reporting methods throughout the entire course of the project including all the preliminary experiments, parametric studies, and molecular biological assays.

6.3 Internal Quality Control

Table 6-1 summarizes the QC checks of the measurements.

Table 6.1. *Summary of Internal QC Checks for all Parameters*

Measurement/ Matrix/(SOP)	QA/QC Check	Frequency	Acceptance Criteria	Corrective Action
Alkanes & Aromatics (critical parameter)/oily seawater/ (SOP 5)	Air/Water Check	Every run	System is leak free	Make system leak free
	Solvent Blank run in SCAN MODE	Following liner change and at the start of a new run.	No contaminants of interest	Rerun fresh solvent until interfering contamination is removed.
	Autotune	Prior to calibration	Manufacture's specifications	Retune instrument
	Initial calibration (5 or 6 point curve)	Every batch and as required	% RSD of RRFs < 25%	Rerun standard curve, change standards
	Second source calibration check	After initial calibration	RRF within 25% of the average calibration FF of the initial calibration for the selected compounds	Rerun calibration check, change standard, Rerun standard curve
	Calibration check	At the beginning and end of a batch, and every 10 samples.	RRF within 25% of the average calibration FF of the initial calibration	Rerun samples since last valid calibration check, rerun standard curve, and/or change

				standards
	Method Blank	Every batch of extracted samples	Concentration of target compounds less than half of the reporting limit (500 µg/L for petroleum hydrocarbons)	Check for target contamination and rerun samples for the batch.
	Reagent blank	Every 10 samples	Concentration of target compounds less than half of the reporting limit (500 µg/L for petroleum hydrocarbons)	Check for target contamination and rerun samples since last valid blank
	Internal Standard	Every sample	50-200% of target in midrange standard	Discard data point, repeat experiment if there are insufficient data points
	Surrogate spike	Every batch	Surrogate spike recovery within 70-100%	Check standards, rerun spike
Total Petroleum Hydrocarbons by GC/FID (non-critical parameter)/ oily seawater/ (see EPA Method 8015C)	Single point calibration of all target compounds	Beginning of each batch used for screening (See Section 1.3 of EPA Method 80415C)	Compare to known LCS run directly after calibration. LCS must meet criteria for standard to be fit for use	Rerun standard curve, remake/run standards
	Blank	Every batch	Absence of target contaminants	Determine source of contamination. Rerun blank and sample batch
	Laboratory Control Sample	Every batch following calibration and at end of batch	75-125% of known second source standard (LCS concentration at approximate sample concentration)	Rerun standard curve, remake/run standards. Rerun samples since last valid LCS

Measurement/ Matrix/(SOP)	**QA/QC Check**	**Frequency**	**Acceptance Criteria**	**Corrective Action**

DOSS LC-MS-MS (critical parameter) /oily seawater/ SOP 6	Initial calibration (5 or 6 point curve DOSS)	Every batch	Linear fit if $r^2 > 0.98$ Quadratic fit if $r^2 > 0.99$	Rerun standard curve, change standards
	Analytes' retention time	Every sample	± 5% of the retention time of the analyte in a midpoint calibration standard	Rerun calibration curve and compare time shift. Rerun samples since last valid retention time
	Second source calibration check	After initial calibration	± 35% deviation from the nominal concentration of the standard	Rerun standard curve, and/or change standards
	Calibration check	At the beginning and end of a batch, every 20 samples and within 24 h after initial calibration	± 35% deviation from the nominal concentration of the standard	Rerun samples since last valid calibration check, rerun standard curve, and/or change standards
	Method Blank	At the beginning and end of a batch and every 20 samples	Less than half of the reporting limit	Check for target contamination and rerun samples since last valid blank
	Surrogate spike	Every sample	Spike recovery within 50-150%	Check standards, rerun spike
PCR (non-critical parameter)/ oily seawater/ EPA Procedure 815-B-04-001	Positive control	(at least) one per PCR	Quantity (µg/µl) within 10% of control	Repeat PCR
	Negative Control	3 negative PCR tubes per PCR	No band on gel or PCR signal in 2 of 3 tubes	Repeat PCR
	Replicate PCR tubes	3-5 replicate PCR tubes per sample	N/A	N/A

SECTION 7.0

DATA ANALYSIS, INTERPRETATION, AND MANAGEMENT

7.1 Data Reporting

All results will be reduced to the appropriate reporting units designated in the SOPs by the analyst performing the test. The reporting units for each analysis are summarized in Table 7.1. Results will be averaged and the mean and the standard deviation or the range, will be calculated.

Table 7.1
Reporting Units

Measurement	Unit
Alkanes and aromatics	µg analyte/µg hopane
TPH	mg/L
DOSS	µg/L
PCR	quantity (gene copies/µL), number base pairs

Calculations will be carried out on a computer and will be checked initially by the analyst for gross error and miscalculation. The calculations and data entered into computer spreadsheets will be checked by a second analyst for accuracy by printing out the calculation or data spreadsheet and checking the calculation by hand or checking each entry of data from the original. These copied spreadsheets will be initialed and dated by the second analyst doing the checking, noting the errors.

7.2 Data Reduction and Validation

Data reduction procedures are described in the related SOPs. Data will be documented in data log sheets in which sample identification, date and analyst name will be recorded. Hard copy raw data shall be archived with documentation for standard preparation and QC data (calibration check standards, analysis duplicates and analysis blanks).

Data reduction will be computerized to reduce the likelihood of transcription and calculation errors. Computerized calculations will be validated prior to use. After data are calculated in the reporting units, they will be transferred to a Microsoft Excel spreadsheet. The UC WA Leader will review the reduced data to check for coherence and consistency. He will also spot check calculations all the way back to raw data logs at random, at least one per analytical method for each part of the study. Detected errors will be corrected and other data in the same set investigated before it is released to the EPA WA Manager.

7.3 Data Summary and Analysis

When the experimental phase of the project has been completed, the analytical data will be analyzed statistically to show how the data will be used to support the project objectives. Table 3.1 describes a completely randomized design where the treatments are the two temperatures, the

eleven and ten sampling days for 5 and 25 °C, and the three different substrates, i.e., dispersed oil, non-dispersed oil, and dispersant alone. The hypotheses are that, for a given temperature, (1) non-dispersed oil should be less amenable to biodegradation than the dispersed and (2) dispersant alone should experiment a faster degradation that the dispersant and crude oil mix. Additionally, it is anticipated that substrates will be removed in a faster way at 25 °C than at a lower temperature, 5 °C.

The analytical data collected from the experiments will be summarized in two ways: (1) by conducting an analyses of variance (ANOVA) to determine if treatment and block differences exist and (2) by non-linear regression of all the data for each site and for each treatment at the end of the experiment to compare overall first-order biodegradation rates among the various treatments. If the ANOVA reveals significant differences ($p < 0.05$), then treatment differences will be evaluated by the protected least significant difference (LSD) mean separation test. These tests and ANOVA will be done on the sum total of hopane-normalized alkanes, the sum total of hopane-normalized aromatics (PAHs), and for the main component of C9500 and JD-2000 as the dependent variables. For the non-linear regressions, an F-test will be performed to compare the slope coefficients statistically among the various treatments. For these calculations, the variance will be estimated from the sum-of-squared residuals from the fit of the first-order model to the average concentrations (over all replicates) for each treatment at each time point.

Appropriate mean comparison tests, such as the protected LSD test, will depend on whether or not the main effects and/or two-way interactions are statistically significant ($p < 0.05$).

7.4 Data Storage

Laboratory records will be maintained in accordance with Section 13.2, Paper Laboratory Records, of the Office of Research and Development (ORD) Policies and Procedures Manual. Controlled access facilities that provide a suitable environment to minimize deterioration, tampering, damage, and loss will be used for the storage of records. Whenever possible, electronic records will be maintained on a secure network server that is backed up on a routine basis. Electronic records that are not maintained on a secure network server will be periodically backed up to a secure second source storage media, transferred to an archive media (e.g., compact discs, optical discs, magnetic tape, or equivalent), or printed. Electronic records that are to be transferred for retention will be transferred to an archive media or printed, as directed by EPA.

SECTION 8.0

REPORTING

8.1 Monthly Reports

Outputs will be in the form of detailed monthly reports describing progress made in each task. Monthly reports will be prepared by the UC WA Leader, reviewed by the Pegasus Project Manager, and submitted to the EPA every month. Distribution of the monthly report to other agencies will be at the discretion of the EPA WA Manager.

8.2 Presentation/Manuscript

After completion of the experimental period (approximately 10 months), the Team will prepare a presentation for the EPAWA Manager to present to the Water Cluster review panel. In addition, the Team will write a manuscript suitable for publishing the results of the research in a peer-reviewed journal article.

SECTION 9.0

REFERENCES

U.S. Environmental Protection Agency, October 2004. Quality Assurance/Quality Control Guidance for Laboratories Performing PCR Analyses on Environmental Samples. EPA Document No. 815-B-04-001. Office of Water, Cincinnati, Ohio.

University of Cincinnati, June 2011. Category I Quality Assurance Project Plan, Amendment 2, "Biodegradability of Dispersants and Dispersed oil at Two Temperatures", Revision 0, dated June 10, 2011. EPA Contract No. EP-C-11-066. EPA QA ID: L-15045-QP-1-3.

APPENDIX A

STANDARD OPERATING PROCEDURES (SOPs)

SOP 1. Preparation of Surrogate Recovery Standards

Preparation:

Solvents: Dichloromethane (DCM), Optima (Fisher) grade or equivalent

Reagents: D36-Heptadecane (C16) (Cambridge Isotope Laboratories, Andover, MA)
D50-Tetracosane (C20) (Cambridge Isotope Laboratories, Andover, MA)
D66-Dotriacontane (C32) (Cambridge Isotope Laboratories, Andover, MA)
D10-1-Methylnaphthalene (Cambridge Isotope Laboratories, Andover, MA)
D10-Phenanthrene (Cambridge Isotope Laboratories, Andover, MA)
D10-Pyrene (Cambridge Isotope Laboratories, Andover, MA)
5β-Cholestane (coprostane) (Sigma Chemical Co., St. Louis, MO)

Equipment: Micro-spatula
Small beakers
Glass funnel
Analytical balance (0.0001g)
Vials with Teflon-lined caps
Teflon wash bottle with Optima grade DCM
Volumetric flask (250-mL), class A
Pasteur pipettes

Procedure:

1. Using a calibrated analytical balance, weigh 100 mg (0.100 g) of each reagent into separate small beakers.

2. Dissolve the reagents in their beakers by adding 10 mL DCM. Use a Pasteur pipette to transfer the solutions to a single 250-mL volumetric flask.

3. Wash the beakers 3 or 4 times with DCM. Use a Pasteur pipette to transfer each of the washings to the 250-mL volumetric flask.

4. Dilute the solution to volume with DCM.

5. Use a glass stopper to seal the flask and homogenize the solution by inverting the flask 5 or more times. The final concentration of this solution is 400 mg/L for each of the reagents.

6. Transfer the solution into 40-mL storage vials and cap with Teflon-lined caps. Label with the date of preparation, operator, sample names, and concentrations.

7. Weigh every vial and record the weight on the label. This weight is used to monitor possible evaporation during storage.

8. Store these vials at 0 °C or lower.

9. Before using, allow the solution to come to room temperature, and then shake it well.

10. Weigh the vial before using it, and compare the weight with the last weight recorded on the vial. The actual weight should be within 10% of the last recorded value.

11. If the weights are consistent, the integrity of the solution can be assumed. If not, investigate the cause.

Quality Control:

Inject 10 µL of the surrogate stock solution into 1 mL DCM. Add 10 µL of internal standard solution (see SOP 2). Analyze this solution by GC/MS using a calibrated method (see SOP 3 and 4). The expected concentration of each of the corresponding surrogate compounds is 4 ± 0.8 mg/L . If the measured value does not fall within this range, another independently prepared surrogate solution must be prepared and measured. If the measured concentration of the second surrogate solution is within the allowable tolerance range, it can be assumed that the calibration and instrument conditions are acceptable, and the first surrogate solution will be discarded. If the concentration of the second surrogate solution is also out of range, then the problem may be in the calibration or the instrument. The instrument should be cleaned and/or recalibrated until the problem is resolved.

SOP 2. Preparation of Internal Standard Solution

PREPARATION:

Solvents: Dichloromethane (DCM), Optima (Fisher) grade or equivalent

Reagents: D22 n-dencane (D22 N C10)
D34 n-Hexadecane (D34 N C16)
D42 n-Eicosane (D42 N C20)
D62 n-Triacontane (D62 N C30)
D8-Naphthalene
D10-Anthracene
D12-Chrysene
5α-Cholestane (Sigma-Aldrich, Milwaukee, WI)

All reagents but cholestane obtained from Cambridge Isotope Laboratories, Andover, MA.

Equipment: Micro-spatula
Small beakers
Glass funnel
Analytical balance (0.0001g), calibrated and checked for accuracy
Amber vials with Teflon-lined caps, labeled
Teflon wash bottle with DCM
Volumetric flask (200 mL), class A
Pasteur pipettes

PROCEDURE:

1. Using a calibrated analytical balance, weigh 100 mg (0.100 g) of each of the reagents into separate small beakers.

2. Dissolve the reagents in their beakers by adding 10 mL DCM; using a Pasteur pipette, transfer the solutions to a single 200 mL volumetric flask.

3. Wash the beakers 3 or 4 times with DCM; use a Pasteur pipette to transfer each of the washings to the 200-mL volumetric flask.

4. Dilute the solution to volume with DCM.

5. Seal the flask with a glass stopper and homogenize the solution by inverting the flask 5 or more times. The final concentration of this solution is 500 mg/L.

6. Transfer the solution into 40-mL storage vials and cap with Teflon-lined caps.

7. Label with the date of preparation, operator, sample names, and concentrations.

8. Weigh every vial, and record the weight on the label. This weight is used to monitor possible evaporation during storage.

9. Store this solution at 0°C or lower.

10. Before using, allow the solution to come to room temperature, and then shake it well.

11. Weigh the vial before using it, and compare the weight with the last weight recorded on the vial. The actual weight should be within 10% of the last recorded value. If the weights are consistent, the integrity of the solution can be assumed. If not, investigate the cause.

QUALITY CONTROL:

Inject 10 µL of the internal standard solution into 1 mL DCM. Analyze this solution by GC/MS/MS. The only peaks that appear should be the ones corresponding to the internal standards.

SOP 3. Preparation of Working Standards, Check Standards, and Oil Standards for GC/MS/MS

The following SOP applies to the preparation of working standards for GC/MS calibration, check standards, and oil standards. These standards will be used to check the consistency of the instrument prior to and during GC-MS/MS operation.

PREPARATION:

Solvent: Dichloromethane (DCM), Optima (Fisher) grade or equivalent
Stock solutions:

1. Oil analysis mix: 44 compounds, 100 mg/L in hexane/DCM (90/10), Absolute Standards, Inc., Hamden, CT, Part # 90311. For composition see Page 11 of this Appendix.

2. Surrogate solution: 400 mg/L in DCM (see SOP 1).

3. PAH mix: 9 compounds, 1,000 mg/L in DCM, Absolute Standards, Inc., Hamden, CT, Part # 90822. For composition see Page 12 of this Appendix.

4. 1,2-Benzodiphenylene sulfide solution, 2,010 mg/L in DCM, Aldrich Chem. Co., Part # 25,512-2, purity 99%. This solution is required because 1,2-Benzodiphenylene sulfide is the only commercially available source of 1,2-Benzodiphenylene, a PAH considered a target analyte in SOP 5.

5. Hopane solution (100 mg/L in isooctane).

6. Internal standard solution, 500 mg/L in DCM (see SOP 2).

7. Alaska North Slope oil (ANS).

Equipment: Glass storage vials with Teflon-lined caps (2-mL and 40-mL capacity).
Volumetric flasks, Class A, 5-mL, 10-mL, and 100-mL.
Glass syringes capable of dispensing 25-500 µL with an accuracy and precision of ± 1%, or equivalent.
Wheaton repetitive dispenser, Model 411 STEP-PETTE.
Teflon wash bottle filled with Optima grade DCM.
Pasteur pipettes.

The volumes of stock solutions required to make a 20-mg/L working standard are listed in Table 1.

Stock Standards	A	B	C	D	E	
Working standards concentration, mg/L	Oil Analysis Mix (44 compounds, 100 mg/L) µL	Aromatics Mix (9 compounds, 1000 mg/L) µL	1,2-Benzo-diphenylene sulfide (2010 mg/L) µL	Surrogate solution (100 mg/L) µL	Hopane solution (100 mg/L) µL	Volumetric Flask Volume mL
STD 20 (hopane 5)	1000	100	50	250	250	5

Procedure for Working Standards and Check Standards

1. Label a 5-mL volumetric flask as STD20
2. Add 1-2 mL of DCM to the volumetric flask.
3. With glass syringes, add the appropriate volume of stock solution A (as listed in Table 1 to the flasks labeled STD20.
4. Wash the walls of the inner neck of the flasks with several drops of DCM to rinse off the residue of the stock solution into the flasks.
5. Repeat step 3 and step 4 to dispense stock solutions B-E.
6. Dilute to volume with DCM for all the above flasks, seal with glass stoppers, and invert several times to homogenize the solutions.
7. Transfer the solution into 2-mL storage vials, and cap with Teflon-lined caps.
8. Label with date of preparation, operator, sample names, and concentrations.
9. Weigh each storage vial, and record the weight on the label. This weight is used to monitor possible evaporation during storage.
10. Store this solution at 0°C or below.
11. Before using, allow the solution to come to room temperature, and shake it well.
12. Weigh the vial before opening, and compare the weight with the last weight recorded on the vial. The actual weight should be within 10% of the last recorded value. If the weights are consistent, the integrity of the solution can be assumed. If not, investigate the cause.

Procedure for Making Oil Standards

In a 100 mL volumetric flask, weigh 0.500 g of the standard ANS, add 1 mL of surrogate solution (see SOP 1), and bring to volume with DCM. Add 1 mL of internal standard solution (see SOP 2). Follow steps 7 through 12 above, substituting 2-mL storage vials with 40-mL vials.

QUALITY CONTROL

Prepare 5 working standards by making consecutive dilutions of the 20-mg/L stock prepared. Spike the solutions with internal standard (IS) mix so that the final IS concentrations is in the middle of the desired calibration range. Analyze the working standards as described in SOP 4 on a tuned GC-MS/MS. Use the MassHunter software to calculate the average RRF and the relative standard deviation (RSD) of the RRFs for each analyte over the six concentrations. The relative response factor is defined as follows:

$$RRF = \frac{\text{area analyte}}{\text{area internal standard}} \times \frac{\text{concentration internal standard}}{\text{concentration analyte}} \qquad (1)$$

The RSD of the RRFs for all analytes should be 25% or less (EPA Method 8270).

SOP 4. Extraction of Oil from Aqueous Samples

SCOPE AND APPLICATION: This method is to be used for the extraction of crude oil and dispersed crude oil components, both alkanes and polycyclic aromatic hydrocarbons (PAH), from aqueous samples. The extracts are analyzed by gas chromatography/mass spectrometry (GC/MS) using SOP 5.

METHOD SUMMARY: A separatory funnel liquid-liquid extraction will be used to separate the oil components from seawater with methylene chloride (DCM). The extracted solvent will be concentrated and solvent exchanged into hexane ready for GC/MS analysis.

INTERFERENCES AND POTENTIAL PROBLEMS. From SW-846 Method 3500C: "Solvents, reagents, glassware, and other sample processing hardware may yield artifacts and/or interferences to sample analysis. All these materials must be demonstrated to be free from interferences under the conditions of the analysis by analyzing method blanks. Plastics, in particular, must be avoided because phthalates are commonly used as plasticizers and are easily extracted from plastic materials." Also, from our experience, oil will sorb onto rubber and plastic materials causing a loss of product so O rings, gaskets, and seals should be constructed of PTFE.

HEALTH, SAFETY, AND ENVIRONMENTAL COMPLIANCE: Gloves, lab coats, safety glasses, and fume hoods are required. Samples must be collected and disposed of through appropriate channels. The solvents may not be disposed of in a sink.

SAMPLE PRESERVATION, CONTAINERS, AND STORAGE: Upon receipt of samples, at a specific time point in the experiment, or the conclusion of the experiment, water samples should be refrigerated at 4 °C for analysis within 2 weeks. All containers should be constructed of glass, PTFE, or other DCM-resistant material. The solvent extracts should be stored in tightly sealed glass containers (serum bottles or vials) with solvent-resistant septa. They should be refrigerated at 4 °C and may be stored for up to 6 months.

APPARATUS AND MATERIALS:

1. Separatory funnels (250 mL).
2. Turbo Vap II concentration workstation by Zymark (Hopkinton, MA, USA).
3. Miscellaneous glassware, glass funnels, glass wool, Pasteur pipettes, bulbs, vials, or serum bottles with polytetrafluoroethylene (PTFE)-lined screw or crimp tops.

REAGENTS:

1. Unless otherwise noted, it is assumed that ACS reagent grade chemicals or their equivalent are used.
2. Extraction solvent: dichloromethane (DCM), CH_2Cl_2.
3. Exchange solvent: hexane, C_6H_{12}.
4. Sodium sulfate (granular, anhydrous), Na_2SO_4.
5. Tank of compressed nitrogen gas for concentration by nitrogen Turbo Vap II.
6. Surrogate standard spiking as described in SOP 1.

PROCEDURE:

1. At the specified sampling time or the end of the experiment, each experimental unit will

be removed from the experimental setup. If required, take subsamples for those analytical methods that do not require liquid-liquid extraction; after that add one mL (or a well-known volume so after concentration the recovered concentration is in the middle range of the calibration curve) of the surrogate standard spiking solution onto the sample in the flask.

2. Quantitatively transfer the sample from the shake flask to the separatory funnel. Use 60 mL of DCM to rinse the flask and transfer this rinse solvent to the separatory funnel.
3. Seal and shake the separatory funnel vigorously for 1-2 minutes with periodic venting to release excess pressure.
4. Allow the organic layer to separate from the water for a minimum of 10 minutes. Collect the solvent extract in an Erlenmeyer flask.
5. Repeat the extraction two more times using fresh portions of solvent. Combine the three solvent extracts.
6. Dry the extracts by passing it through a funnel containing a glass wool plug and approximately 10 mL of Na_2SO_4. Transfer the dried extract to the TurboVap II workstation and concentrate to 1-2 mL. Perform a solvent exchange into hexane to remove asphaltenes and quantitatively transfer to a 25-mL volumetric glass. Once the final volume is adjusted, the final extracts can be stored in glass vials sealed with screw caps and Teflon liners.
7. The hexane extracts are ready for the GC/MS injection and analysis (SOP 5).

Method Blank

For every batch of samples a method blank, consisting of 100 mL of GP2 spiked with the surrogate mix will be extracted in the same way that regular samples are treated. Only compounds used as internal standards and surrogates should be detected in these blanks.

SOP 5. GC-MS/MS Method for the Analysis of Crude Oil Samples

INSTRUMENT SPECIFICATIONS:

The instrument used in this procedure is an Agilent 7890A GC coupled with an Agielnt 7000 mass selective detector triple quadrupole and an Agilent 7693 series auto sampler. It is equipped with a DB-5 capillary column by J&W Scientific (30 m, 0.25 mm I.D., and 0.25 μm film thickness), and a split/splitless injection port operating in the splitless mode. Data acquisition occurs either in the MRM (Multi reaction monitoring) mode for quantitative analysis or in SCAN mode for qualitative analysis. In MRM mode, the dwell time of each ion is set to be 10 milliseconds. The number of ions in each ion group should be constant, yielding the same scan rate for each group.

The instrumental conditions for crude oil analysis are summarized in Table 1. Only ultra-high purity helium (99.999% pure) should be used as a carrier gas. A moisture trap, an oxygen trap, and an organic trap are connected in series to the carrier gas line before it enters the column.

TABLE 1--INSTRUMENTAL CONDITIONS FOR CRUDE OIL ANALYSIS

Instrument	Agilent 7890A Gas Chromatograph - 7000 MS triple quadrupole
Column	J&W Scientific DB5-MS column (30 m × 0.25 mm, 0.25 μm)
Carrier Gas	Helium, ultra-high purity grade (99.999%)
Inlet Temperature	300°C
Transfer Line (detector) Temperature	300°C
Oven Temperature Program	35°C for 2 minutes to 310°C at 10°C/minute for 5 min
Flow Rate	Constant flow at 1mL/min. Linear velocity: 36.2 cm/sec.
Injection Volume	1 μL
Split/splitless Mode	Splitless
Total Run Time	34.5 minutes

PROCEDURE:

Preparing the Instrument:

1. Lower the injection port temperature and the oven temperature to 50°C or less to avoid oxidation of the column.
2. Replace the liner with a clean, deactivated liner. Do not touch the liner with bare fingers.
3. Return the injection port and oven to the appropriate temperatures.
4. Wait a few minutes for the temperatures to equilibrate before using the instrument.

Tuning the MSD:

Perform an air/water check. The value reported for the relative abundance of water (*m/z* 18), nitrogen (*m/z* 28), oxygen (*m/z* 32), or carbon dioxide (*m/z* 44) should be less than 10% for a leak-free system.

Tune the MSD using the Autotune program according to the manufacturer's specifications.

Maintaining a logbook:

Maintain an instrument logbook, and make entries for each use. Include the following information in the logbook: operator name, helium cylinder tank pressure, and outlet pressure, vacuum gauge reading, any maintenance performed on the instrument (such as changing the injection port liner, gold seal, guard column, source cleaning), sequence name, data path, samples in order of injection, method information, GC column number, and the Standard Auto Tune report.

Running a Solvent Blank:

Following a liner change or at the start of a new run, an injection of a pure solvent should be run to confirm that the system is free of excessive or interfering contamination. The solvent should be analyzed in SCAN mode, using the same temperature program that is used for sample analysis. If contamination is present, additional samples of fresh solvent should be analyzed until the interfering contamination is removed.

Calibrating With a Multiple-Point Calibration Curve:

A five- or six-point calibration curve is obtained by running five or six working standards (see SOP 3) on the tuned GC-MS/MS instrument. The relative response factor (RRF) for each compound is calculated relative to its corresponding deuterated internal standard as indicated in Table 19. The relative standard deviation (RSD) of the RRFs for each compound should be less than 25%. Running an independently prepared check standard immediately after the calibration standards can validate the accuracy of the calibration curve.

Running Samples:

Once the calibration curve has been validated, samples can be analyzed. Dispense 1,000 µL of sample extract into labeled auto-sampler vials. Add 10 µL of the internal standard solution (see SOP 2) to the extract using a syringe or a positive displacement pipettor. Enter the sample ID into the sequence log table, and run the samples after the standards. Run a check standard every 10 samples to ensure the consistency of the instrument. The RRF for each compound in the check standard should be within 25% of the average RRF obtained in the initial calibration.

Quantification:

Once a calibration table has been generated, each data file is quantified using the

"Calculate and Generate" function in the MassHunter software. Individual peak integration is reviewed manually to ensure proper baseline integration. The quantification of a compound is based on the peak area of the product ion indicated in Table 3 below.

TABLE 3--TARGET COMPOUND LIST

Compound Name	Precursor Ion	Product Ion	Reference Compound for Response Factor	Internal Standard for Quantitation
N D22 C10	66	66	Internal Standard	D22 N C10
n C10	57	57	n C10	
n C11	57	57	n C11	
n C12	57	57	n C12	
n C13	57	57	n C13	
n C14	57	57	n C14	
n C15	57	57	n C15	
N D34 C16	66	66	Internal Standard	D34 N C16
n C16	57	57	n C16	
N D34 C17	66	66	N D34 C17	
n C17	57	57	n C17	
Pristane	57	57	Pristane	
n C18	57	57	n C18	
Phytane	57	57	Phytane	
n C19	57	57	n C19	
N D42 C20	66	66	Internal Standard	D42 N C20
n C20	57	57	n C20	
n C21	57	57	n C21	
n C22	57	57	n C22	
n C23	57	57	n C23	
N D50 C 24	66	66	N D50 C 24	
n C24	57	57	n C24	
n C25	57	57	n C25	
n C26	57	57	n C26	
n C27	57	57	n C27	
n C28	57	57	n C28	
n C29	57	57	n C29	
N D62 C30	66	66	Internal Standard	D62 n C30
n C30	57	57	n C30	
n C31	57	57	n C31	

N D66 C32	57	57	N D66 C32	
n C32	57	57	n C32	
n C33	57	57	n C33	
n C34	57	57	n C34	
n C35	57	57	n C35	
D8 Naphthalene	136	108	Internal Standard	D8 Naphthalene
Naphthalene	128	102	Naphthalene	
D10 1Methylnaphthalene	152	150	D10 1-Methylnaphthalene	
C1 Naphthalene	142	141	C1 Naphthalene	
C2 Naphthalene	156	141	C2 Naphthalene	
C3 Naphthalene	170	155	C3 Naphthalene	
C4 Naphthalene	184	153	C3 Naphthalene	
D10 Anthracene	188	160	Internal Standard	D10 Anthracene
D10 Phenanthrene	188	184	D10 Phenanthrene	
Phenanthrene	178	176	Phenanthrene	
C1 Phenanthrene	192	189	C1 Phenanthrene	
C2 Phenanthrene	206	189	C2 Phenanthrene	
C3 Phenanthrene	220	203	C2 Phenanthrene	
C4 Phenanthrene	234	189	C2 Phenanthrene	
Fluorene	166	165	Fluorene	
C1 Fluorene	165	163	Fluorene	
C2 Fluorene	194	179	Fluorene	
C3 Fluorene	208	193	Fluorene	
Dibenzothiophene	184	139	Dibenzothiophene	
C1 Dibenzothiophene	198	197	Dibenzothiophene	
C2 Dibenzothiophene	212	211	Dibenzothiophene	
C3 Dibenzothiophene	226	225	Dibenzothiophene	
Naphthobenzothiophene	234	202	Naphthobenzothiophene	
C1 Naphthobenzothiophene	248	215	Naphthobenzothiophene	
C2 Naphthobenzothiophene	262	245	Naphthobenzothiophene	
C3 Naphthobenzothiophene	276	274	Naphthobenzothiophene	
Fluoranthene	202	202	Fluoranthene	
D10 Pyrene	212	210	D10 Pyrene	
Pyrene	202	200	Pyrene	
C1 Pyrene	216	215	Pyrene	
C2 Pyrene	230	221	Pyrene	
D12 Chrysene	240	236	D12 Chrysene	D12 Chrysene
Chrysene	228	226	Chrysene	
C1 Chrysene	242	239	Chrysene	
C2 Chrysene	256	239	Chrysene	

C3 Chrysene	270	226	Chrysene	
C4 Chrysene	284	253	Chrysene	
5α-Cholestane	217	95	Internal Standard	5α- Cholestane
5β-Cholestane (Coprostane)	217	95	5β-Cholestane	
Hopane	191	95	Hopane	

Equation 1 is used to calculate the concentration of analytes in units of µg/l:

$$Concentration\ of\ analyte\ (\mu g / L) = \frac{A_{analyte} \times C_{istd}}{A_{istd} \times RRF} \qquad (1)$$

where $A_{analyte}$ is the peak area of the analyte,
C_{istd} is the concentration of the internal standard,
A_{istd} is the area of the internal standard,
RRF is the relative response factor, and

Some analytes are not commercially available or are extremely expensive. In such cases, the RRFs of other compounds (usually the non-alkylated parent or nearest neighbor compound) are used to quantify those analytes. These results will be reported as estimated. For example, the RRF of C3-naphthalene is used to calculate the concentrations of C3- and C4-naphthalenes. See Table 3 for details. The quantification of these alkylated PAHs is relative because it is assumed that the molecular ions of the alkylated PAHs have the same RRFs as the parent compound ions. Nevertheless, these relative concentrations are useful for monitoring the fate of these compounds during the course of any study, as long as their concentrations are measured in a consistent way throughout the study.

Concentration calculations for all target compounds are performed using MassHunter software. Data for each sample can be printed directly using a customized report template. Data can also be automatically entered into a spreadsheet within the MassHunter software. This

spreadsheet file can be opened directly in Excel and modified to perform any additional calculations needed.

QUALITY ASSURANCE QUALITY CONTROL:

The following criteria must be met before any samples are analyzed:

1. Air/water check indicates the system is leak free.
2. AutoTune pass all criteria.
3. Solvent blank scan indicates the GC-MS/MS system is free of interfering contamination.
4. Calibration curve is validated using an independently prepared check standard with a 75-125% recovery criterion.
5. A control chart of a standard oil analysis should be prepared and monitored. Concentrations of the analytes in the control chart should be no more than 25% different from their historical averages.
6. The reporting limit for the petroleum hydrocarbons analyzed by this method is 500 µg/L.

Relative response factors for analytes in the check standards inserted between every 10 samples should be no more than 25 percent different from the average RRF of those same analytes in the calibration curve. Peak shapes should be symmetrical (except for nC10, nC11, nC12, nC13, nC14, and naphthalene, which tail in this method). NC17/pristane, nC18/phytane, and phenanthrene/anthracene should be baseline separated.

SOP 6. LC-MS/MS Method for the Analysis of Dioctyl Sulfosuccinate in Sea Water[1]

1. Scope

1.1 This procedure details dioctyl sulfosuccinate (DOSS) determination in water by direct injection using liquid chromatography (LC) and detection with tandem mass spectrometry (MS/MS). This analyte is qualitatively and quantitatively determined by this method. This method adheres to single reaction monitoring (SRM) mass spectrometry.

1.2 The Detection Verification Level (DVL) and Reporting Range for DOSS are listed in Table 1.

1.2.1 The DVL is required to be at a concentration at least 3 times below the Reporting Limit (RL) and have a signal/noise ratio greater than 3:1. Figure 1 and 2 display the signal/noise ratio of the single reaction monitoring (SRM) transition.

1.2.2 The reporting limit is the concentration of the Level 1 calibration standard as shown in Table 4 for DOSS, taking into account the 50% sample preparation dilution factor.

TABLE 1. Detection Verification Level and Reporting Range

Analyte	DVL (µg/L)	Reporting Range (µg/L)
DOSS	3	10-200

1 This draft analytical procedure was developed by US EPA Region 5 Chicago Regional Laboratory (CRL) in collaboration with the Region 6 Houston Laboratory. It was first developed by CRL, July 12, 2010, and is open to improvement and discussion.

1.3 *This procedure does not purport to address all of the safety concerns, if any, associated with its use. It is the responsibility of the user of this standard to establish appropriate safety and health practices and determine the applicability of regulatory limitations prior to use.*

2. Referenced Documents

2.1 ASTM Standards:

D 1129 Terminology Relating to Water
D 1193 Specification for Reagent Water

2.2 Other Documents

EPA publication SW-846, entitled *Test Methods for Evaluating Solid Waste, Physical/Chemical Methods*

3. Terminology

3.1 Definitions:

3.1.1 Detection Verification Level, DVL, n– a concentration that has a signal/noise ratio greater than 3:1 and is at least 3 times below the Reporting Limit (RL).

3.1.2 Reporting Limit, RL, n– the concentration of the lowest-level calibration standard used for quantification.

3.2 Abbreviations:

3.2.1 CH_3CN- acetonitrile

3.2.2 ESI- Electrospray ionization

3.2.3 DOSS- dioctyl sulfosuccinate (CAS # 577-11-7)

3.2.4 LC/MS- liquid chromatography mass spectrometry

3.2.5 ppb– parts per billion, µg/L

3.2.6 mM– millimolar, 1 x 10^{-3} moles/L

3.2.7 NA– no addition

3.2.8 NH_4CO_2H- ammonium formate

3.2.9 ND– non-detect

4. Summary of Procedure

4.1 One surrogate is considered, DOSS-D34. Deuterated DOSS surrogate (DOSS-D34) recovery data are included in this SOP.

4.2 This is a performance based method, and modifications are allowed to improve performance.

4.3 In the lab, the entire collected 20-mL sample is spiked with surrogate, ammonium formate buffer solution and brought to a volume of 40 mL with acetonitrile. This prepared sample is then filtered using a syringe driven filter unit, and analyzed by LC/MS/MS. If visible oil is present, the prepared sample is allowed to settle resulting in an oil layer at the top of the 40 mL solution. A portion of the aqueous (bottom) layer is filtered, leaving the oil layer behind, through a syringe-driven filter assembly and analyzed by LC/MS/MS.

4.4 DOSS and its surrogate are identified by retention time and one SRM transition. The target analyte and surrogate are quantitated using the SRM transitions. The final report issued for each sample lists the concentration of DOSS and the surrogate recovery.

5. Significance and Use

5.1 DOSS has been identified as a possible ingredient in dispersant agents used to treat oil.

5.2 This method has been investigated for use with reagent and sea water for DOSS.

6. Interferences

6.1 Method interferences may be caused by contaminants in solvents, reagents, glassware, and other apparatuses that produce discrete artifacts or elevated baselines. All of these materials are demonstrated to be free from interferences by analyzing laboratory reagent blanks under the same conditions as samples.

6.2 All glassware is washed in hot water with detergent and rinsed in hot water followed by distilled water. The glassware is then dried and heated in an oven at 250°C for 15 to 30 minutes. All glassware is subsequently cleaned with methanol and/or 50% acetonitrile/50% water.

6.3 System contamination and surface binding are problematic as DOSS is a surface active compound. Notable DOSS is associated with the surface of glass containers after one hour. It is important to use sample containers and glassware (treatment preparation glassware, shake flasks, sampling, and analytical glassware) treated with Sylon CT or similar deactivating agent. Thorough rinsing of all lab equipment is necessary to reduce contamination. Carefully analyze blanks to ensure that the method minimizes DOSS carryover.

6.4 All reagents and solvents should be pesticide residue purity or higher to minimize interference problems.

6.5 Matrix interferences may be caused by contaminants in the sample. The extent of matrix interferences can vary considerably from sample source depending on variations of the sample matrix.

6.6 Graduated cylinder- a 50 mL cylinder was used to measure the volume of the sample and total volume. An appropriate cylinder for different sample volumes should be used to accurately measure the sample and prepared sample volumes.

7. Apparatus

7.1 LC/MS/MS System

7.1.1 Liquid Chromatography System- A complete LC system is needed in order to analyze samples. Any system that is capable of performing at the flows, pressures, controlled temperatures, sample volumes, and requirements of the standard may be used.

7.1.2 Analytical Column- Zorbax Eclipse XBD C18 analytical column 2.1 x 50 mm, 3.5 micron particle size (part no.971700-902). Any column that achieves adequate resolution may be used. The retention times and order of elution may change depending on the column used and need to be monitored.

7.1.3 Tandem Mass Spectrometer System- A MS/MS system capable of MRM analysis. Any system that is capable of performing at the requirements in this standard may be used.

7.2 Filtration Device

7.2.1 Hypodermic syringe- A Lock Tip Glass Syringe capable of holding a Millex® HV Syringe Driven Filter Unit PVDF 0.22 µm or similar may be used.

7.2.1.1 A Lock Tip Glass Syringe was used in this test method.

7.2.2 Filter– Millex® HV Syringe Driven Filter Unit PVDF 0.22 µm (Millipore Corporation, Catalog # SLGV033NS) or similar may be used.

7.2.3 Glass Pipette– Small volume pipette for sample container rinses and sample transfer.

8. Reagents and Materials

8.1 Purity of Reagents– High Performance Liquid Chromatography (HPLC) pesticide residue analysis and spectrophotometry grade chemicals shall be used in all tests. Unless indicated otherwise, it is intended that all reagents shall conform to the Committee on Analytical Reagents of the American Chemical Society. Other reagent grades may be used provided they are first determined to be of sufficiently high purity to permit their use without affecting the accuracy of the measurements.

8.2 Purity of Water– Unless otherwise indicated, references to water shall be understood to mean reagent water conforming to Type 1 of Specification D 1193. It must be demonstrated that this water does not contain contaminants at concentrations sufficient to interfere with the analysis.

8.3 Gases– Ultrapure nitrogen.

8.4 Acetonitrile (CH_3CN, CAS # 75-05-8).

8.5 Methanol (CAS # 67-56-1).

8.6 Ammonium Formate (NH_4CO_2H, CAS # 540-69-2).

8.7 2-Propanol (CAS # 67-63-0).

8.8 Dioctyl sulfosuccinate sodium salt (DOSS) (CAS # 577-11-7).

8.9 Deuterated dioctyl sulfosuccinate sodium salt (DOSS-D34, - bis(2-ethylhexyl-D17) sulfosuccinate sodium salt)

9. Hazards

9.1 Normal laboratory safety applies to this method. Analysts should wear safety glasses, gloves, and lab coats when working in the lab. Analysts should review the Material Safety Data Sheets (MSDS) for all reagents used in this method.

10. Sampling

10.1 *Sampling and Preservation*– Grab samples should be collected in 20 mL pre-cleaned and silanized glass vials with Teflon® lined septa caps demonstrated to be free of interferences. This test method is based on a 20 mL sample size per analysis. Store samples at 0°C from sample collection to sample preparation. Analyze the sample within 5 days of collection. After 7 and 10 days of storage at 0°C DOSS recoveries notably decreased (Table 12). Oil in water absorbs DOSS from water and affects surrogate analysis (Table 11). Avoid oil in samples if possible. Samples that have more than one phase may be encountered. Samples may be prepared for analysis using one or a multiple of the following options:

10.1.1 *Whole Sample**: For a 20* mL sample, add 0.2 mL of 20 ppm DOSS surrogate to the sample in the sample container. Cap the container and mix to insure homogeneity. Transfer the contents of the sample container to a graduated cylinder and record the sample volume. Subsequently, add 0.4 mL of 500 mM ammonium formate to the graduated cylinder. Rinse the sample collection vial twice with 6 to 8 mLs of acetonitrile, which is added to the prepared sample to compose ~ 50% acetonitrile solution to ensure quantitative sample transfer. Bring the prepared sample volume to 40 mL using acetonitrile, and then mix thoroughly. If different

sample sizes are used, spiking solution, ammonium formate, and acetronitrile volume shall be adjusted proportionally. The sample must be thoroughly mixed and then allowed to settle. A portion of the aqueous fraction (bottom) should be transferred to a glass syringe for filtration. Filter the sample, using a 0.22 µm PVDF filter, into an autosampler vial or another glass vial and then transfer to an autosampler vial.

10.1.2 Water Subsample*: Collect a 10 mL subsample of the water fraction (bottom) using a needle and a glass syringe. To reduce the oil exposure, invert the vial and tap gently to cause the oil move away from the septum. Insert needle through septum and collect 10 mL of the water layer; place the aliquot removed in a graduated cylinder. Then add 100 µL of 20 ppm DOSS surrogate to the sample in the graduated cylinder. Subsequently, add 0.2 mL of 500 mM ammonium formate to the graduated cylinder. Add 10 mL acetonitrile to the prepared sample to compose ~ 50% acetonitrile solution to ensure quantitative prepared sample transfer. If different sample sizes are used, spiking solution, ammonium formate, and acetronitrile volume shall be adjusted proportionally. Filter the sample, using a 0.22 µm PVDF filter, into an autosampler vial or another glass vial and then transfer to an autosampler vial.

10.1.3 Oil Subsample*: Add 1.5 mL of HPLC grade water to graduated cylinder. Collect a 0.5 mL subsample of oil (top) and place in a graduated cylinder. Then add 20 µL of 20 ppm surrogate to the sample in the graduated cylinder. Subsequently, add 40 µL of 500 mM ammonium formate to the graduated cylinder. Add 2 mL acetonitrile to the prepared sample to compose ~ 50% acetonitrile solution to ensure quantitative prepared sample transfer. If

different sample sizes are used, spiking solution, ammonium formate, and acetonitrile volume shall be adjusted proportionally. The sample should be thoroughly mixed and then allowed to settle. A portion of the aqueous fraction (bottom) should be transferred to a glass syringe for filtration. Filter the sample using a 0.22 µm PVDF filter into another vial (filtered-prepared sample).

*Note- Subsamples of water and oil fractions quantitate only the DOSS in the subsample, the DOSS concentration of subsamples may underestimate the sample DOSS concentration as a result of partitioning (Table 10) and surface binding. DOSS surrogate added to the subsample rather than the received sample and container does not indicate DOSS recovery from the total sample. Additionally, oil in samples resulted in low DOSS recovery, but resulted in higher DOSS recoveries than subsamples (Table 11).

11. Preparation of LC/MS/MS

11.1 LC Chromatograph Operating Conditions

11.1.1 The following specifications were developed for a 6410 Triple Quad Mass equipped with a 1200 Binary HPLC pump, auto sampler, column compartment, and online degasser by Agilent (Palo Alto, CA, USA). Injection volumes of all calibration standards and samples are made at 15 µL volume using a full loop injection. "Full loop" mode is the preferred technique when performing quantitative analyses. Multiple blank samples should be analyzed at the beginning of a run to remove residual DOSS from the system. The first sample analyzed after the calibration curve is a blank to ensure there is minimal DOSS carry-over. The gradient

conditions for the liquid chromatograph are shown in Table 2A. The eluent composition is A: 99% water +1% ACN with 0.1% formic acid and B: 99% ACN +1% water with 0.1% formic acid. Divert the column flow away from the electrospray source for 0 to 2.6 minutes after injection. Flow diversion to waste may be done using the mass spectrometer divert valve, divert tubing configurations vary from manual injection. Test the divert valve configuration and operation prior to analysis. Seawater samples contain nonvolatile salts; the elution from injection to 2.6 minutes after injection is diverted to waste in order to prevent mass spectrometer source contamination. If there is carry-over from one sample to another(greater than half the reporting limit) the initial percentage of acetonitrile should be raised to try and remove the carry-over. This will shorten the elution time of DOSS; therefore, it is necessary reduce the flow diversion and adjust the MRM time. Increasing the initial acetonitrile gradient concentration does not increase the DVL or reporting limit.

TABLE 2A. Gradient Conditions for DOSS Liquid Chromatography

Time (min)	Flow (mL/Min)	%A (water with 0.1% Formic)	%B (ACN with 0.1% Formic)
0-1	0.4	98	2
4	0.4	60	38
7	0.4	20	80
12	0.4	2	98
12.1	0.4	98	2

11.2 LC Sample Manager Conditions:

11.2.1 Wash Solvents– Weak wash is 4.0 mL of 50% water/50% acetonitrile. Strong wash is 2.0 mL of 60% acetonitrile/40% 2-propanol. The strong wash solvent is needed to eliminate

carry-over between injections of DOSS samples. The weak wash is used to remove the strong wash solvent. Instrument manufacturer specifications should be followed in order to eliminate sample carry-over.

11.2.2 Temperatures– Column, 35°C; Sample compartment, 15°C.

11.3 Mass Spectrometer Parameters:

11.3.1 To acquire the maximum number of data points per SRM channel while maintaining adequate sensitivity, the tune parameters may be optimized according to the instrument specifications. Each peak requires at least 10 scans per peak for adequate quantitation. This procedure will contain one surrogate, which is isotopically labeled DOSS, and DOSS which are in one MRM acquisition function to optimize sensitivity. Due to the low pKa of the sulfonate and to avoid bias associated with adducts, DOSS analysis was performed using electrospray negative ionization. Variable parameters regarding retention times, SRM transitions, and cone and collision energies are shown in Table 3. Mass spectrometer parameters used in the development of this method are listed below:

Parameter	**Settings**
Scan Mode	negative
Capillary Voltage	4.0 kV
To Waste	Until 2.6 min
Segments	3
Gas Temperature	350 °C
Gas Flow	6 L/min
Nebulizer	15 psi

TABLE 3. Retention Times, MRM transitions, and DOSS-Specific Mass Spectrometer Parameters

Compound	**Ion**	**Segment**	**Prec. ion**	**Prod. ion**	**Frag (V)**	**CE (V)**	**Multiplier (V)**
DOSS	M-	1	421	81	188	30	600

	Na						
DOSS-D34	M-Na	1	445.4	81	188	30	600

12. 12. Calibration and Standardization

12.1 The mass spectrometer must be calibrated per manufacturer specifications before analysis. In order to obtain accurate analytical values through using this test method within the confidence limits, the following procedures must be followed when performing the test method. (Prepare all solutions in the lab using Class A volumetric glassware.)

12.2 Calibration and Standardization– To calibrate the instrument, analyze six DOSS and surrogate calibration standards; the calibration standards nominal concentrations are detailed in Table 4. A calibration solution is prepared from standard materials or certified solutions. Level 6 calibration solution containing the DOSS and surrogate is prepared and aliquots of that solution are diluted to prepare Levels 1 through 5 and the DVL. The following steps will produce standards with the concentration values shown in Table 4. The analyst is responsible for recording initial component weight, calculating dilutions and preparing appropriate solutions.

12.2.1 Prepare Level 6 calibration stock standard at 200 ppb by adding to a 10 mL volumetric flask individual solutions of the following: 100 µL of DOSS and DOSS (isotopic-labeled), each at 20 ppm in 50% water/50% acetonitrile and dilute to 10 mL with a solution of 5 millimolar ammonium formate in 50% water/50% acetonitrile. The preparation of the stock standard can be accomplished using different volumes and concentrations of stock solutions as is accustomed in the individual laboratory. Depending on the prepared stock concentrations, the solubility at that concentration will have to be ensured.

12.2.2 Aliquots of Level 6 calibration stock standard are then diluted with 5 millimolar acetonitrile in 50% water/50% acetonitrile to prepare the desired calibration levels in 2 mL amber glass autosampler vials. The calibration vials must be used within 24 hours to ensure optimum results. Stock calibration standards are routinely replaced every 7 days if not previously discarded for quality control failure. Calibration standards are not filtered.

12.2.3 Inject each standard and obtain its chromatogram. An external calibration technique is used to monitor the SRM transitions of each analyte. Calibration software is utilized to conduct the quantitation of the target analytes and surrogates using the SRM transition. The quantitation method is set as an external calibration using the peak areas in ppb units. Concentrations may be calculated using the data system software to generate linear regression or quadratic calibration curves. Forcing the calibration curve through the origin is not recommended.

12.2.4 Linear calibration may be used if the coefficient of determination, r^2, is > 0.98 for the analyte (Figure 3). The point of origin is excluded and a fit weighting of 1/X is used in order to give more emphasis to the lower concentrations. If one of the calibration standards other than the high or low point causes the r^2 of the curve to be < 0.98, this point must be re-injected or a new calibration curve must be regenerated. If any calibration level result is excluded, minimally a five-point curve is acceptable but the reporting range must be modified to reflect this change.

12.2.5 Quadratic calibration may be used if the coefficient of determination, r^2, is > 0.99 for the analyte. The point of origin is excluded, and a fit weighting of 1/X is used in order to give

more emphasis to the lower concentrations (Figure 4). If one of the calibration standards causes the curve to be < 0.99, this point must be re-injected or a new calibration curve must be regenerated. At least six calibration points are required for quadratic regression. Each calibration point used to generate the curve must have a calculated percent deviation less than 25% between the nominal concentration and the regression calculated result.

12.2.6 The retention time window of the SRM transitions must be within 5% of the retention time of the analyte in a midpoint calibration standard. If this is not the case, re-analyze the calibration curve to determine if there was a shift in retention time during the analysis and the sample needs to be re-injected. If the retention time is still incorrect in the sample, refer to the analyte as an unknown.

12.2.7 A calibration check standard (midpoint) must be analyzed at the beginning and end of each run, every 20 samples, or within 24 hours after the initial calibration curve was generated (100 ppb). The end calibration check should be the same calibration standard that was used to generate the initial curve. The regression result from the end calibration check standard must have a percent deviation less than 35% from the target analyte and surrogate nominal concentration. If the results are not within these criteria, the problem must be corrected and either all samples in the batch must be re-analyzed against a new calibration curve or the affected results must be qualified with an indication that they are not within the performance criteria of the test method. If the analyst inspects the vial containing the end calibration check standards and notices that the samples evaporated, affecting the concentration, a new end calibration check standard may be made and analyzed. If this new end calibration check standard has a percent

deviation less than 35% from the calculated concentration for the target analyte and surrogate, the results may be reported unqualified.

TABLE 4. Concentrations of Calibration Standards (PPB)

Analyte/Surrogate	DVL	LV 1	LV 2	LV 3	LV 4	LV 5	LV 6
DOSS	3	10	20	60	100	150	200
DOSS-D34 (Surrogate)	3	10	20	60	100	150	200

12.3 If a laboratory has not performed the test before or if there has been a major change in the measurement system, for example, new analyst, new instrument, etc., a precision and bias study must be performed to demonstrate laboratory capability (Section 16).

12.3.1 Analyze at least four replicates of a sample solution containing the DOSS and surrogate at a concentration in the calibration range of Levels 3 to 5. The Level 4 concentration of the 6 point calibration curve was used to set the QC acceptance criteria in this method. The matrix and chemistry should be similar to the solution used in this test method. Each replicate must be taken through the complete analytical test method including any sample pre-treatment steps.

12.3.2 Calculate the mean (average) percent recovery and relative standard deviation (RSD) of the four values and compare to the acceptable ranges of the QC acceptance criteria for the Initial Demonstration of Performance in Table 5.

12.3.3 This study should be repeated until the single operator precision and mean recovery are within the limits in Table 5.

The QC acceptance criteria for the Initial Demonstration of Performance in Table 5 are preliminary until a more data and multi-laboratory study is completed. Data generated from a single-laboratory validation from reagent and sea water matrices are shown in the Precision and Bias Section 16. It is recommended that the laboratory generate their own in-house QC acceptance criteria that meets or exceeds the criteria in this standard. A Reference on how to generate QC acceptance criteria is in Method 8000B in EPA publication SW-846.

TABLE 5. Preliminary QC Acceptance Criteria

Analyte	Test Conc. (µg/L) in Reagent Water	Initial Demonstration of Performance			Lab Control Sample	
		Recovery (%)		Precision	Recovery (%)	
		Lower Limit	Upper Limit	Maximum % RSD	Lower Limit	Upper Limit
DOSS	200	50	150	30	50	150
DOSS-D34 (Surrogate)	200	50	150	30	50	150

12.4 Surrogate Spiking Solution (This draft contains DOSS-D34 data):

A surrogate spiking 50% water/50% CH_3CN solution containing DOSS-D34 is added to all samples. A stock surrogate spiking solution is prepared at 20 ppm. Spiking 200 µL of this spiking solution into a 20 mL water sample results in a concentration of 200 ppb of the surrogate in the sample. The result obtained for the surrogate recovery must fall within the limits of Table 5. If the limits are not met, the affected results must be qualified with an indication that they do not fall within the performance criteria of the test method.

12.5 Method Blank:

12.5.1 Analyze a reagent water blank with at the beginning and end of every run and every 20 samples. The DOSS measured in the blank should be less than half of the reporting limit. If the concentration of DOSS is found above this level, analysis of samples is halted until the contamination is eliminated, and a blank shows no contamination at or above this level, or the results must be qualified with an indication that they do not fall within the performance criteria of the test method. DOSS has been found to carry-over in LC systems. A rigorous washing of

the injector with stronger wash solvents has been shown to work well as described in this method.

12.6 Laboratory Control Sample (LCS):

12.6.1 To ensure that the test method is in control, analyze a LCS prepared with the DOSS. The LCS is prepared following the analytical method and analyzed with each batch of 20 samples or less. Prepare a stock matrix spiking solution in 50% water/50% acetonitrile containing the DOSS at 20 ppm. Spike 200 µL of this stock solution into 20 mL of water to yield a concentration of 200 ppb for the DOSS in the sample. The LCS result must be within the limits in Table 5. Matrix spiking solutions are routinely replaced every 7 days if not previously discarded for quality control failure.

12.6.2 If the LCS regression result is not within limits listed in Table, analysis of samples is halted until the problem is corrected, and either all samples in the batch must be re-analyzed, or the results must be qualified with an indication that they do not fall within the performance criteria of the test method.

13. Procedure

13.1 This test method is based upon a 20 mL sample size per analysis. **Any sample size may be used such as a half filled VOA vial as long as the QC spikes and sample preparation volumes are adjusted accordingly.** Samples shall be analyzed within 5 days of collection. If the samples are above 6°C when received or during storage, or not analyzed within 5 days of collection, the data is noted in the case narrative that accompanies the data.

13.2 In the laboratory, the entire 20 mL sample, collected in a 20 mL glass collection vial, is poured into a 50 mL graduated cylinder. The surrogate as described in Section 12 (added to the sample in the original sample container or graduated cylinder depending on sampling described in Section 10.1) and NH_4CO_2H are added to the sample. The vial is rinsed with two 6 to 8 mL portions of acetonitrile to collect DOSS remaining in the collection vial. These 2 portions are added to the 50 mL graduated cylinder. The samples are then diluted to 40 mL final volume with acetonitrile and mixed thoroughly. The prepared sample is filtered through the syringe-driven filter unit fitted with a PVDF filter cartridge into a glass storage vial.

13.3 For samples that are not biphasic, the entire 40 mL volume is filtered through the filtration device described in Section 7.2 and into a pre-cleaned collection vial (such as a VOA vial). A portion of that filtered sample is added to an amber glass LC vial with a Teflon®- lined cap, which is then analyzed. A new filter unit is used for each sample.

13.4 For biphasic samples, the lower aqueous layer is filtered through the filtration device described in Section 7.2 into a pre-cleaned collection vial (such as a VOA vial). The upper oil layer is left behind and is not added to the filtration device. A portion of that filtered sample is added to an amber glass LC vial with a Teflon® lined cap which is analyzed. A new filter unit is used for each sample.

13.5 The syringe must be cleaned between each filtration. It is the analyst's responsibility to ensure that the syringe is clean. A suggested method for cleaning the syringe between filtrations is to first rinse with at least 5 syringe volumes of water, followed by at least 3 volumes of 50% water/50% acetonitrile.

13.6 Once a passing calibration curve is generated, the analysis of samples may begin. An order of analysis may be: method blank, laboratory control sample, method blank, up to 20 samples, followed by an end calibration check standard and a method blank.

14. Calculation or Interpretation of Results

14.1 For DOSS and surrogate analysis, the SRM transitions are identified by comparison of retention times in the sample to those of the standards. Calibration curves are used to calculate the amounts of DOSS and surrogate. Calculate the concentration in µg/L (ppb) for each analyte. The sample concentration was diluted two-fold by the addition of surrogates, ammonium formate, acetonitrile, and target compound spike where applicable. The two-fold dilution must be accounted for when reporting the concentration. DOSS may be reported if present at or above the reporting limit. If the concentration of the analyte is determined to be above the calibration range, the sample is diluted with 5 mM ammonium formate in 50% acetonitrile/50% water to obtain a concentration near the mid-point of the calibration range and re-analyzed. This method uses one surrogate, DOSS-D34, to monitor performance and matrix affect. The surrogate recoveries are provided with all data generated from this test method.

14.1.1 A surrogate is used to monitor the performance of DOSS. If the surrogate meets the quality control criteria in this test method, the data may be reported unqualified for DOSS if all other quality control in this test method are acceptable. If the surrogate does not meet the quality control criteria of the test method, the data is qualified for DOSS.

15. Report

15.1 Determine the results in units of µg/L (ppb) in a water sample. Calculate the concentration in the sample using the linear or quadratic calibration curve. All data that does not meet the specifications in the test method must be appropriately qualified.

16. Precision and Bias

16.1 The determination of precision and bias was conducted through U.S. EPA Region 5 Chicago Regional Laboratory. **More than 50 seawater samples have been analyzed using this procedure without noticeable chromatography effect or increased pressure.**

16.2 This test method was tested by CRL on reagent and sea water. The samples were spiked with the DOSS to obtain a 200 ppb concentration of each as described in Section 12. Table 7 contains the recoveries and standard deviation (SD) for the target compound.

TABLE 7. Single-Laboratory Recovery Data in Reagent Water using chromatography conditions outlined in Table 2A and Table 2B

Precision and Accuracy Samples	Measured ppb from 200 ppb DOSS Spikes in Reagent Water					
	Table 2A			Table 2B		
	Retention time (min)	DOSS measured (ppb)	Percent Recovery	Retentio n time (min)	DOSS measured (ppb)	Percent Recovery
1	6.38	182.6	91.3%	5.41	196.1	98.0%
2	6.37	232.9	116.5%	5.41	232.8	116.4%
3	6.37	224.6	112.3%	5.41	225.8	112.9%
4	6.37	226.8	113.4%	5.41	238.9	119.5%
Average Recovery:		216.7	108.4%		223.4	111.7%
Standard Deviation:		23.0			19.0	
% Relative SD		11.5%			9.5%	

16.3 This test method was tested by CRL on Gulf of Mexico seawater. The samples were spiked with target compound as described in Section 12. Table 8 contains the recoveries for the target compound.

TABLE 8. Single-Laboratory Recovery Data in Gulf of Mexico Sea Water using chromatography conditions outlined in Table 2A and Table 2B

Precision and Accuracy Samples	Measured ppb from 200 ppb DOSS Spikes in Gulf Water					
	Table 2A			Table 2B		
	Retention time (min)	DOSS measured (ppb)	Percent Recovery	Retentio n time (min)	DOSS measured (ppb)	Percent Recovery
1	6.37	189.1	94.6%	5.4	257.2	128.6%
2	6.37	251.4	125.7%	5.4	251.4	125.7%
3	6.37	253.2	126.6%	5.41	263.0	131.5%
4	6.37	257.0	128.5%	5.4	262.4	131.2%
5	6.37	250.7	125.4%	5.4	255.0	127.5%
Average Recovery:		240.3	120.1%		257.8	128.9%
Standard Deviation:		28.7			4.9	
% Relative SD		14.4%			2.5%	

17. Keywords

17.1 Dioctyl Sulfosuccinate; Liquid Chromatography; Mass Spectrometry; Water

SOP 7. Total DNA Isolation

1.0 Scope & Application

This Standard Operating Procedure is applicable to different types of environmental samples including concrete biofilms. The commercially available kit used for this procedure: UltraClean Soil DNA kit from MoBio Laboratories (California, USA).

2.0 Summary of Method

Through various processes including mechanical and chemical lysis, precipitation of PCR inhibitors, separation via centrifugation, DNA-binding, and washing, the final elute contains DNA that can be used for PCR.

3.0 Sample Preservation, Containers, Handling, and Storage

All equipment and supplies are provided by manufacturer and are sterile. Wear gloves at all times, and change them frequently to avoid cross contamination. Following DNA isolation, the DNA may be stored at -20C until analysis.

4.0 Reagents

Proprietary reagents are provided with the kit. Solution S4 contains ethanol and is flammable.

5.0 Equipment and Supplies

Equipment needed for processing samples includes:

- Microcentrifuge (10,000 x g)
- Pipette (50ul – 500ul)
- Vortex
- Solutions S1, S2, S3, S4, S5, IRS Solution
- Spin filter units in 2ml tubes
- Collection tubes (2ml)
-

6.0 Procedure

1. Using sterile forceps, place 0.2 - 1.0 g of microbial biomass in bead solution tubes
2. gently vortex
3. add 60 µl of solution S1, vortex briefly
4. add 200 µl of solution IRS
5. vortex horizontally 10 min, max speed
6. centrifuge 10 000 g, 30 s
7. move supernatant to a new tube (about 400 µl)
8. add 250 µl of solution S2, vortex 5 s
9. incubate in +4° C, 5 min
10. centrifuge tubes 10 000 g, 1 min
11. transfer 450 µl of supernatant to a clean microcentrifuge tube

12. add 900 µl of solution S3, vortex 5 s
13. load 700 µl of sample onto spin column
14. centrifuge columns 10 000 g, 1 min, discard flow through
15. load rest of the supernatant on spin column
16. centrifuge at 10 000 g, 1 min, discard flow through
17. add 300 µl of solution S4
18. centrifuge 10 000 g, 30 s, discard flow through
19. centrifuge again 10 000 g, 1 min
20. place spin filter column to a new tube (avoid splashing any solution S4 onto spin filter)
21. add 50 µl of solution S5 to the center of the white membrane
22. centrifuge 10 000 g, 30 s
23. discard the spin filter, DNA is in tube ready for applications
24. store in -20ºC
25. Measure the DNA concentration using the instruction for the NanoDrop spectrophotometer (manual located in room 675; see attachment A.11)

Calculations
DNA may be quantified using the NanoDrop 1000 spectrophotometer or Qubit Fluorometric Quantitation. Please refer to the NanoDrop SOP or Qubit SOP.

8.0 Quality Control and Quality Assurance
QC samples required in the QA Project Plan must be followed; these may include blanks, and triplicate samples.

9.0 References
N/A

SOP 8. Quantifying Nucleic Acids With a Nanodrop Nd-1000 Spectrophotometer

1.0 Scope & Application

The NanoDrop ND-1000 is a full spectrum (220-750nm) spectrophotometer that measures 1ul samples with high accuracy and reproducibility. In addition the ND-1000 has the capability to measure highly concentrated samples without dilution.
The NanoDrop ND-1000 UV/VIS spectrophotometer can be used to measure:
- Nucleic acid concentration and quality up to 3700ng/ul (dsDNA) without dilution
- Fluorescent dye labeling density of nucleic acid microarray samples
- Purified protein analysis (A280) up to 100 mg/ml
- Bradford assay analysis of protein
- BCA Assay analysis of protein
- Cell density measurements
- General UV/VIS spectrophotometer

2.0 Summary of Method
A 1 or 2ul sample is pipetted onto the end of a fiber optic cable (the receiving fiber). A second fiber optic cable (the source fiber) is then brought into contact with the liquid sample causing the liquid to bridge the gap between the fiber optic ends. The gap is controlled to a 1mm path. A pulsed xenon flash lamp provides the light source and a spectrometer utilizing a linear CCD array is used to analyze the light after passing through the sample. The instrument is controlled by software run on a PC, and the data is logged in an archive file on the PC.

3.0 Sample Preservation, Containers, Handling, and Storage
DNA samples will be preserved at -20C, and RNA samples will be preserved at -70C.

4.0 Reagents
A 70% ethanol solution is used to clean the fiber optic ends between samples, and after completion of all sample analysis.

5.0 Equipment and Supplies
• NanoDrop ND-1000 spectrophotometer
• 70% ethanol – labeled and dated.
• Soft laboratory wipes (Kim Wipes or equivalent)
• pipette (2 -10ul)
• Pipette tips (certified RNase and DNase-free)

6.0 Procedure
1. With the sampling arm open, pipette the sample onto the lower measurement pedestal.
2. Close the sampling arm and initiate a spectral measurement using the operating software on the PC.
3. When the measurement is complete, open the sampling arm and wipe the sample from both the upper and lower pedestals using a soft laboratory wipe.
4. After measuring a large number of samples, it may be necessary to clean the areas around the upper and lower pedestals with a 5% solution of bleach – freshly prepared.
5. Results may be printed, saved to PC, or copied to electronically for archiving.

7.0 Calculations

N/A

8.0 Quality Control and Quality Assurance

All QC samples required in the QA Project Plan must be followed; these may include field blanks, trip blanks, and collection of replicate samples.

9.0 References

NanoDrop ND-1000 Spectrophotometer User's Manual V3.0.1 (rev 16-Apr-04)
Website: http://www.nandrop.com

SOP 9. Polymerase Chain Reaction (PCR)

1.0 Scope & Application

This Standard Operating Procedure is applicable to performing the Polymerase Chain Reaction (PCR) on DNA obtained from prokaryotic and eukaryotic microbiological isolates as well as from environmental samples such as potable water, biofilms, source water, and wastewater as well as enrichment cultures such as the ones associated with this study.

2.0 Summary of Method

The amplification of DNA from any given sample allows for the identification of target genes or sequences, as well as the development of clone libraries. Sample conditions may vary, particularly in environmental samples, so that no universal PCR protocol can be recommended. However, certain methods can be generalized, allowing for further optimization by the researcher.

3.0 Sample Preservation, Containers, Handling, and Storage

All equipment and supplies are provided by manufacturer and are sterile. Wear gloves at all times, and change them frequently to avoid cross contamination. Following DNA isolation, the DNA may be stored at 4C temporarily or -20C long term.

4.0 Reagents

Takara Ex Taq Polymerase, buffer, and dNTP mix (Takara Mirus Bio, Madison, WI).

5.0 Equipment and Supplies

- Thermocycler, e.g. PE9600 or equivalent
- Taq polymerase
- 10x Taq buffer (some buffers includes $MgCl_2$)
- $MgCl_2$ solution (if not included in buffer)
- dNTP's
- 25% acetamide solution or BSA
- PCR grade sterile water (autoclaved SuperQ water or equivalent)
- Primers, one forward and one reverse; varies with each experiment
- pipettes, 1000, 200, 20, and 10 ul sizes (Rainin or equivalent)
- pipet tips, with filters, 1000, 200, 20, and 10 ul sizes
- sterile 2 ml or 5 ml tubes
- PCR tubes, or strips, or 96-well plates
- PCR caps for strips or plates

Ice bucket filled with ice

6.0 Procedure

All PCR tubes, caps, pipet tips, and reagents must be sterile and DNase- and RNase- free. Wear powder-free gloves at all times. Extreme care needs to be exercised when preparing samples for PCR to avoid cross-contamination.

1. Place 10x buffer, $MgCl_2$ solution (if needed), primers, and dNTP's on ice to thaw.
2. Make 25% acetamide fresh, or store at -20*C between uses. If using stored acetamide, place on ice with other solutions to thaw.
3. Once reagents have thawed, make a master mix by placing an aliquot of each reagent (buffer, $MgCl_2$, dNTP's, acetamide, primers, and water) into a sterile tube in proportions dictated by each experiment. Close or seal the tube and place on ice. Return all reagents except water to the -20C freezer
4. Remove Taq polymerase and immediately place on ice. Remove the volume of Taq polymerase required, add to master mix in the tube, reseal the tube, and mix briefly by vortexing or swirling. Place master mix on ice and return the Taq polymerase to the freezer.
5. Aliquot the master mix into PCR tubes, strips, or 96-well plates, using a volume determined for individual protocols. Sample DNA (template) should be added to PCR tubes after the master mix to avoid cross contamination of tubes.

DNA from environmental samples used as a template for PCR should be extracted with a kit (MoBio or equivalent), or by protocols published in the peer- reviewed scientific literature. Freshly extracted DNA may be added to PCR tubes, or DNA may be stored at -20*C until needed. Frozen DNA should be thawed on ice before use. A table containing a typical recipe for PCR is included in this SOP. Further information may be obtained from Ausubel et al., 1988 or a similar protocol reference.

7. Calculations

DNA may be quantified using the NanoDrop 1000 spectrophotometer. Please refer to the NanoDrop SOP. The presence of PCR product is confirmed by agarose gel electrophoresis. Methods for gel electrophoresis are described in Ausubel et al., 1988, and in the Agarose Gel Electrophoresis SOP.

8.0 Quality Control and Quality Assurance

QC samples required in the QA Project Plan must be followed; these may include blanks, and triplicate samples. Each PCR should include a water blank as a negative control, and a positive control of template DNA known to amplify with the primer set in the reaction. Negative controls are critical for PCR as cross contamination is a constant potential problem.

9.0 References

Ausubel, F. M., R. Brent, R. E. Kingston, D. D. Moore, J. G. Seidman, J. A. Smith, and K. Struhl, eds. 1988. *Current Protocols in Molecular Biology*. John Wiley & Sons, Inc.

User's Manual, GeneAmp PCR System 9600, Applied Biosystems, Foster City, CA

PCR ASSAY MASTER MIX

PCR master mix		**date**
	one reaction (µl)	**rxn (µl)**
10X buffer	5	
dNTP mix	4	
Taq enzyme	0.25	
F primer 8F	3	
R primer 685	3	
Template	2	
H2O	32.75	
total	**50**	

The following are starting points to use when optimizing PCR conditions for each primer pair:

(1) 94C - 1 minute
(2) 94C - 30 seconds
(3) 55C - 1 minute
(4) 72C - 1 minute
(5) 30 cycles of steps 2 through 4(6) 72C - 2 minutes

SOP 10. PCR Purification With QIAquick Spin Kit

1.0 Scope & Application
Using a microcentrifuge, this protocol is designed to purify single or double stranded DNA fragments from PCR and other enzymatic reactions

2.0 Summary of Method
Fragments ranging from 100bp to 10kb are purified from primers, nucleotides, polymerases, and salts using QIAquick spin columns in a microcentrifuge. The QIAquick method relies on the selective binding properties of a silica gel membrane. DNA adsorbs to the silica membrane in the presence of high salt while contaminants pass through the column. Impurities are washed away, and the pure DNA is eluted.

3.0 Sample Preservation, Containers, Handling, and Storage
DyeEx Spin Kits will be stored dry at room temperature (15-25C). Under these conditions, these kits can be stored for up to 12 months. For longer storage, these kits can be stored at 2-8C. Do not freeze.

4.0 Reagents
All buffers are supplied with the kit. Buffer PB contains guanidine hydrochloride and isopropanol. Buffer PN contains perchlorate and isopropanol. Buffer QC contains guanidine thiocyanate. When working with these reagents, always wear a suitable lab coat, disposable gloves, and protective goggles.

5.0 Equipment and Supplies
Spin columns, collection tubes, and microcentrifuge tubes are supplied with the kits.
All centrifugation steps are performed at 750 x g in a conventional microcentrifuge.

6.0 Procedure
Note: add ethanol (96-100%) to Buffer PE before use. All centrifuge steps are at 13,000rpm (~17,900 x g) in a conventional tabletop microcentrifuge.

1. Add 5 volumes of Buffer PB to 1 volume of the PCR sample and mix.
2. Place a QIAquick spin column in a provided 2ml collection tube.
3. To bind DNA, apply sample to the QIAquick column and centrifuge for 30-60seconds.
4. Discard flow through and place the QIAquick column back in the same tube.
5. To wash, add 0.75ml Buffer PE to the QIAquick column and centrifuge for 30-60seconds.
6. Discard the flow through and place the QIAquick column back in the same tube. Centrifuge the column for an additional 1minute.
7. Place QIAquick column in a clean 1.5ml microcentrifuge tube.
8. To elute DNA, add 50ul Buffer EB or UltraPure water to the center of the QIAquick membrane and centrifuge the column for 1minute.

7.0 Calculations
The appropriate speed for individual centrifuges can be calculated as follows:

Rpm = 1000 x √750/1.12r
(r = radius of rotor in mm)

8.0 Quality Control and Quality Assurance

All QC samples required in the QA Project Plan must be followed; these may include blanks, and replicate samples.

Ensure that the elution buffer is dispensed directly onto the QIAquick membrane for complete elution of bound DNA.

9.0 References

QIAquick Spin Handbook 07/2002
QIAGEN Inc. 28159 Avenue Stanford, Valencia, CA 91355

SOP 11. TOPO T/A Cloning

1.0 Scope & Application

This standard operating protocol is applicable to cloning any sequence of DNA amplified by PCR. The DNA may be obtained from any organism or environment. Cloning DNA is carried out to produce DNA libraries for sequence analysis. This is particularly applicable to microbial ecology studies in which many environmental organisms of interest are difficult to culture.

2.0 Summary of Method

In TA cloning, the linearized plasmid vector contains single 3' thymidine overhangs. After adding fresh, purified PCR product with single 3' adenosine overhangs, topoisomerase that is covalently bound to the plasmid will ligate product and vector. After transforming competent *E. coli* with the vector and growing transformants on LB/ampicillin agar, plasmids are purified and screened to confirm the presence of the proper size insert.

3.0 Sample Preservation, Containers, Handling, and Storage

Potential problems associated with the TA cloning procedure include the recovery of an insert of an improper size and a low efficiency for the cloning reaction.

To minimize the insertion of an undesired fragment, the PCR product to be cloned should be screened carefully to ensure that it produces a single band on an agarose gel. The product should also be cleaned before cloning to remove small oligonucleotide fragments.

The efficiency of the cloning reaction can be maintained by using fresh PCR product. Once the target sequences are amplified, they immediately should be screened, purified, and ligated with the vector. PCR product may not be stored overnight before cloning; it must be cloned the same day.

4.0 Reagents

TOPO TA Cloning kit (Invitrogen).

5.0 Equipment and Supplies

- Purified PCR product (Qiagen)

A. - Agarose gels, gel box, gel buffer, and power supply
B. - sterile 0.5 ml tubes
C. - pipettes sizes 1000, 200, 20, and 10 ul (Rainin or equivalent)
D. - sterile pipet tips, with filters, sizes 1000, 200, 20 and 10 ul
E. - TOPO TA Cloning kit (Invitrogen) or equivalent

F. - LB agar plates containing 100 ug/ml ampicillin (3-4 per transformation
G. - LB broth containing 100 ug/ml ampicillin
H. - 3 ml culture tubes, pre-sterilized
I. - autoclaved toothpicks
J. - General microbiological supplies, including Bunsen burner, ethanol, plate spreaders, etc.
K. - Plasmid Preparation kit (Qiagen or equivalent)
L. - water bath set at 42 *C
M. - shaking incubator set at 37 *C
N. - non-shaking incubator set at 37 *C

6.0 Procedure

Sample Preparation

For each cloning reaction, fresh PCR product is required. The target gene or sequence should be amplified and the product purified immediately before performing the cloning reaction to obtain a high efficiency. For assistance with PCR protocols, refer to Ausubel et al., 1988 or to PCR SOP. Check the purity of the PCR product by agarose gel electrophoresis (Ausubel et al., 1988). The product should have a single band on the gel. Clean the PCR product using a purification kit (Qiagen or similar type) to remove excess dNTP's and primers.

Cloning reaction

Reagents included in the cloning kit (salt solution, sterile water, vector, and competent *E. coli*) should be thawed on ice before use. SOC medium, also included in the kit, should be warmed to room temperature before cloning.

Each cloning reaction has a total volume of 6 ul. Typically, 2 ul of fresh, purified PCR product is placed in a sterile 0.5 ml tube, along with 2 ul sterile water, 1 ul salt solution, and 1 ul TOPO vector. Mix by stirring with a pipet tip and incubate for 5 minutes at room temperature. Place reaction tube on ice and proceed with the chemical transformation of competent *E. coli* as described in the instruction manual of the Invitrogen TA cloning kit. When working with competent *E. coli*, take great care to mix them *gently* with the ligated vector, to avoid damaging the bacteria.

Analyzing transformants

Colonies that form on LB/ampicillin agar contain transformed bacteria. Isolated colonies are picked with sterile toothpicks and inoculated into sterile tubes containing 2 ml of autoclaved LB/ampicillin broth. Tubes are incubated overnight in a shaking incubator at 37 *C. One ml of grown bacteria is removed for purification using a plasmid preparation kit. The remaining bacterial culture is preserved in glycerol stock.

Purified plasmid should be analyzed by agarose gel electrophoresis, by PCR amplification, by restriction enzyme digestion, or sequencing. These methods of analysis may be used in combination. Methods for restriction enzyme digests are found in Ausubel et al., 1988, as well as the enzyme instruction sheet.

A direct observation of purified plasmid on an agarose gel determines whether or not the proper

size fragment has been inserted into the plasmid. PCR amplification with M13 primers, which are specific to the plasmid, or with primers specific to the cloned fragment, followed by agarose gel electrophoresis, also demonstrates the size of the plasmid insert. A typical PCR master mix for checking transformants is included in this SOP. Carrying out a restriction enzyme digest on the PCR product demonstrates how many plasmids contain the same or similar sequence as an insert. Doing the digest screen before sequencing the plasmid insert prevents sequencing the same fragment repeatedly. Techniques for sequencing DNA are found in Ausubel et al., 1988.

7.0 Calculations

DNA may be quantified using the NanoDrop 1000 spectrophotometer. Please refer to the NanoDrop SOP. The presence of PCR product is confirmed by agarose gel electrophoresis. Methods for gel electrophoresis are described in Ausubel et al., 1988, and in the Agarose Gel Electrophoresis SOP.

8.0 Quality Control and Quality Assurance

QC samples required in the QA Project Plan must be followed; these may include blanks, and triplicate samples. All standard microbiological practices should be observed, including use of aseptic technique and media blanks. Medium containing antibiotics should be stored at 4 *C until needed, and should be used within one to two weeks of being poured. Reagents for cloning reactions should be stored at - 20 *C or -70 *C, as indicated by the kit instructions. Freezer temperature should be monitored regularly and recorded on log sheets.

9.0 References

Ausubel, F. M., R. Brent, R. E. Kingston, D. D. Moore, J. G. Seidman, J. A. Smith, and K. Struhl, eds. 1988. *Current Protocols in Molecular Biology*. John Wiley & Sons, Inc.

User's Manual, GeneAmp PCR System 9600, Applied Biosystems, Foster City, CA

Check Transformants (analyze positive clones)

Use M13 PCR assay to confirm the presence of clones. Once the PCR assay is completed load 5µl of the reaction into agarose gel to determine the presence and size of clone inserts. The rest of the reaction will be used for sequencing experiments. Positive M13 clones are sent to Children's Hospital Core Facility, UC for sequencing. At least 20 µl of M13 PCR product are required, so if necessary bring the volume up to desired volume with sterile ddH2O. Follow A.8 protocol if sequencing at Children's.

PCR (25 µL)	per rxn	reactions
Template	2 µl	

10X	2.5µl	
4% BSA	0.4µl	
dNTP	2 µl	
Primer (25pmole/µl)	0.5 µl	
Primer (25pmole/µl)	0.5µl	
dH_2O (total 25µl)	17µl	
Tag enzyme	0.125µl	
Total	25 µl	

To: Mandsager, Kathy[kathy.mandsager@unh.edu]; chris.barker@noaa.gov[chris.barker@noaa.gov]; CJ.Beegle-Krause@sintef.no[CJ.Beegle-Krause@sintef.no]; Conmy, Robyn[Conmy.Robyn@epa.gov]; Thomas.s.coolbaugh@exxonmobil.com[Thomas.s.coolbaugh@exxonmobil.com]; fingasmerv@shaw.ca[fingasmerv@shaw.ca]; jrpayne@sbcglobal.net[jrpayne@sbcglobal.net]; wspegau@pwssc.org[wspegau@pwssc.org]; creddy@whoi.edu[creddy@whoi.edu]
Cc: nancy.kinner@unh.edu[nancy.kinner@unh.edu]
From: Khelifa, Ali (EC)
Sent: Wed 5/18/2016 7:45:23 PM
Subject: RE: state-of-science: transport and behavior group
Khelifa&So(2009).pdf
Khelifa&al(2007).pdf
Khelifa&al(AMOP2011).pdf

The three references we discussed yesterday and added in Line 257 in the draft after yesterday's session.

Khelifa, A., M.F. Fingas, B.P. Hollebone, and C.E. Brown (2007). Effects of Chemical Dispersants on Oil Physical Properties and Dispersion. In *Proceedings of the 30th Arctic and Marine OilSpill Program Technical Seminar*, Environment Canada, Ottawa, Ontario, pp. 105-116.

Khelifa A., and L.L.C. So, (2009). Effects of Chemical Dispersants on Oil0Brine Interfacial Tension and Droplet Formation. In *Proceedings of the 32nd Arctic and Marine OilSpill Program Technical Seminar*, Environment Canada, Ottawa, Ontario, pp. 383-396.

Khelifa, A., Charron, D. M., Tong, T.-S., Singh, N. R. (2011). Effects of chemical dispersants on oil-brine interfacial tension and droplet formation: New results using new high resolution imaging setup and weathed oils. In: *Proceedings of the 34th Arctic and Marine OilSpill Program Technical Seminar*, Environment Canada, Ottawa, Canada, pp. 865-879.

From: Mandsager, Kathy [mailto:kathy.mandsager@unh.edu]
Sent: May 18, 2016 3:18 PM
To: chris.barker@noaa.gov; CJ.Beegle-Krause@sintef.no; conmy.robyn@epa.gov;

Thomas.s.coolbaugh@exxonmobil.com; fingasmerv@shaw.ca; Khelifa, Ali (EC); jrpayne@sbcglobal.net; wspegau@pwssc.org; creddy@whoi.edu
Cc: Kinner, Nancy
Subject: state-of-science: transport and behavior group

Thanks for making headway on incorporating the public input into your document. Attached is the draft after yesterday's session. I'm also attaching the Weingartner et al 2013 reference for your perusal. The references that were suggested via the public input process will eventually be incorporated into the database. But please let me know if you are unable to access a particular manuscript for review.

In order to schedule a couple more meetings, please fill in all 2-hour time slots on the doodle poll that you can possibly attend. This has been tine-zone enabled for you convenience and if you could make your selection by early next week that would be helpful in order to secure these dates over our busy summer months. Thank you!

Doodle poll Here>> http://doodle.com/poll/iu423v2aywfkcyfx

Kathy Mandsager

Coastal Response Research Center

Center for Spills and Environmental Hazards

220 Gregg Hall, 35 Colovos Rd

University of New Hampshire

Durham, NH 03824

603.862.1545

Effects of Chemical Dispersants on Oil Physical Properties and Dispersion

Ali Khelifa, Merv Fingas, Bruce P. Hollebone, and Carl E. Brown
Emergencies Science and Technology Division
Environmental Science and Technology Centre, Science and Technology Branch
Environment Canada, Ottawa, ON, Canada
ali.khelifa@ec.gc.ca

Abstract

New laboratory experiments were performed to measure the effects of chemical dispersants on oil physical properties and dispersion. Specifically, the aims of this study were to measure the effects of dispersant-to-oil ratio (DOR) on the viscosity of crude oils, the brine-oil interfacial tension (IFT) and the related size distributions of oil droplets formed under various mixing conditions. Arabian Medium, Alaska North Slope and South Louisiana crude oils and Corexit 9500 and Corexit 9527 chemical dispersants were used to perform the study. Results showed a monotonous linear increase of oil viscosity with DOR. The increase is higher with the less viscous oils than with the more viscous oils. With increases in DOR from 0 to 1:5, oil-dispersant mixture viscosity is approximately 20, 30 and 40 % greater than the pure crude oilsfor Arabian Medium, Alaska North Slope, and South Louisiana crude oils, respectively. Similar results were obtained with both chemical dispersants. As reported in previous studies, application of chemical dispersants reduces the interfacial tension significantly for all values of DOR examined in the current study including a very low value of 1:200. For instance, the interfacial tension of Arabian Medium crude decreases from 20 mN/m to less than 3.6 mN/m (the detection limit of the instrument) at DOR=1:200. The results also show that an optimum DOR exists at which the IFT reduction reaches a maximum value. At this optimum DOR, the effectiveness of the chemical dispersant is at a maximum. The consequent effects of the observed IFT reductions on the resulting size distribution of oil droplets was studied using existing theories and size measurements using UV Epi-fluorescence microscopy.

1 Introduction

It is general knowledge that chemical dispersants affect oil dispersion via modification of the interfacial properties of the oil, such as oil-brine interfacial tension (IFT) (NAS, 2005). The end results of these modifications are a reduction of the size and enhancement of the concentration of oil droplets in the water column. This is well known from both laboratory and field testing. This is also illustrated by the existing theories related to the mechanics of formation of oil droplets (Hinze, 1975; Khelifa et al., 2004; Li and Garrett, 1998) and interfacial thermodynamics (NAS 2005, Liu et al., 1995). According to these theories, the reduction of IFT combined with the provision of sufficient mixing energy is one of the key ways to explain observed the reduction of droplet size of chemically treated oil (NAS, 2005). Several laboratory investigations on IFT reduction due to the application of chemical dispersants have been performed during the last few decades (Rewick et al. 1980, 1981, 1983, 1984; Mackay and Hussein, 1982; Clayton, 1993; Liu et al., 1995). All these studies showed a reduction of IFT with the addition of chemical dispersants. Factors such as oil type, dispersant type and dispersant to oil ratio (DOR) were identified as important factors affecting the magnitude of IFT reduction. However,

extrapolation of this information to practical application, such as modelling of oil droplet formation is still not well developed due, apparently, to a poor understanding of the process and the lack of representative data sets. The aim of this paper is to present new laboratory results on the effects of chemical dispersants on IFT and oil viscosity and the subsequent effects on oil droplet formation.

2 Effects on physical properties of oil

The experiments were conducted using three oils: Arabian Medium (AM), Alaska North Slope (ANS) and South Louisiana (SL) crude and Corexit 9500 and Corexit 9527 chemical dispersants. All the experiments were performed at a controlled temperature of 15 °C. The density of the oils and dispersants were measured using an Anton Parr DMA 5000 digital densitometer. The instrument was factory-calibrated. Results are shown in Table 1. Note that the dispersants are denser than any of the three oils considered in this study. Uncertainty in measurements is estimated from the standard deviation of at least eight trials of *p*-xylene at 15.0 °C. Estimated uncertainty in density measurements is ±0.002 at a 95% confidence level.

Table 1. Measured Oil Densities

Oil/Dispersant	Density (g/mL)
Alaska North Slope	0.873
Arabian Medium	0.876
South Louisiana	0.859
Corexit 9500	0.959
Corexit 9527	1.002

Oil dynamic viscosity was measured with a Thermo-Haake VT550 viscometer using NV cup-and-spindle sensors. The instrument was factory-calibrated and the calibration verified with ASTM-traceable standards (Cannon Instrument Co.) at 15.0 °C. Pure ethylene glycol (Caledon Laboratory Ltd.) is used to validate the NV method. Estimated uncertainty with this instrument is ±1.3 mPa s at a 95% confidence level. For each of the three oils, viscosity measurements are repeated in triplicate for dispersant-to-oil ratios (DOR) of 0, 1:40, 1:20, 1:10, 1:5, and dispersant only. Results are listed in Table 2. All oils show an increase of oil viscosity with DOR. As summarized in Table 2 and shown in Figure 1, results show that when DOR increases from 0 to 1:5, the viscosity of the oil-dispersant mixture increased with an increasing amount of dispersant. The relative increases ranged from about 15% with Arabian Medium and Corexit 9500 to about 43 % with South Louisiana crude and Corexit 9527 over the crude oil viscosities. The linear trend in viscosity increases with increasing DOR suggest that the viscosity of the mixture is related to a linear proportion of the less viscous crude oils and the more viscous dispersants. Both dispersants showed similar increases in oil viscosity with DOR.

Surface and oil-water interfacial tensions were measured using a Krüss K10 Tensiometer by the Du Noüy ring method. Measurements were made at 15.0 °C, maintained by an external temperature-regulating bath (Thermo Haake). Samples, aqueous phases and glassware are all maintained at 15.0 °C for a minimum of 30 minutes before measurement. The instrument was factory calibrated and instrument calibration was verified using a vendor-supplied weight. Method and operator

performance is monitored by periodic measurement of the surface and liquid/liquid interfacial tensions of *p*-xylene at 15.0 °C.

For oil/air surface tensions, the measurement ring is first zeroed in air. A small amount of sample, approximately 15 mL, is poured into a 43-mm diameter vessel (50 mL Kimax beaker). The ring is dipped into the sample to a depth of no more than 5 mm, and then pulled up such that it is just visible on the surface of the liquid. Measurement is automatically terminated when the upward pulling force on the ring just balances the downward force exerted by the liquid meniscus. The apparent interfacial tension, $\sigma_{o\text{-}a}^{APP}$, is then recorded.

Table 2. Measured Viscosities of different Oil and Dispersant Mixtures

Oil/Dispersant Mixture	**Viscosity (mPa s) for DOR by weight:**					
Fresh Oil	**0**	**1:40**	**1:20**	**1:10**	**1:5**	**dispersant only**
Alaska North Slope	17.0					
Arabian Medium	28.1					
South Louisiana	13.3					
Fresh Oil + Corexit 9500						
Alaska North Slope		17.8	18.0	20.0	23.7	
Arabian Medium		29.4	28.1	29.8	32.4	
South Louisiana		13.7	14.7	16.0	18.2	
Fresh Oil + Corexit 9527						
Alaska North Slope		17.7	17.8	20.3	22.5	
Arabian Medium		28.1	28.4	29.5	33.5	
South Louisiana		13.8	14.4	15.1	19.0	
Corexit 9500						92.9
Corexit 9527						67.5

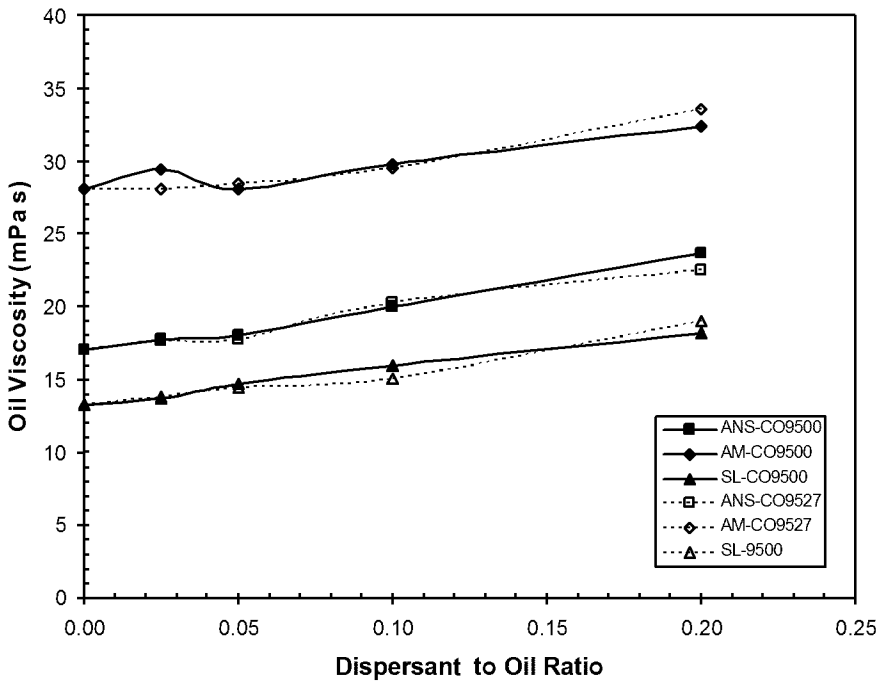

Figure 1. Measured variations of oil viscosity with dispersant to oil ratio.

For brine/oil interfacial tensions, the ring is zeroed in the sample oil at a depth of 5 mm. The ring is removed and cleaned. A 25-mL volume of water or brine is dispensed into a 43-mm diameter vessel. The ring is dipped 5 mm into the aqueous phase. A 10-mL volume of sample is carefully poured down the side of the vessel wall (creating a 10-mm thick layer of sample on the water), with great care taken so as to disturb the aqueous/oil interface as little as possible. The ring is then raised to the bottom on the interface and the system is allowed to rest for exactly 30 seconds. The measurement is started and the apparent interfacial tension is recorded, $\sigma_{o\text{-}w}^{APP}$, when the force balance is reached.

The apparent surface tension is corrected for the mass of the upper phase lifted by the ring during measurement using the Zuidema and Waters correction:

$$\sigma_{o-w} = \sigma_{o-w}^{APP}\left[0.7250 + \sqrt{\frac{1.452\sigma_{o-w}^{APP}}{D_{DN}^{2}(\rho_{\inf} - \rho_{\sup})} - \frac{1.679}{D_{DN}/D_{rw}} + 0.04534}\right] \quad (1)$$

where: $\sigma_{o\text{-}w}$ is the oil-water interfacial tension, $\sigma_{o\text{-}w}^{APP}$ is the instrument scale reading, ρ_{inf} is the density of the lower phase, ρ_{sup} is the density of the upper phase, D_{DN} is the diameter of the Du Noüy ring, and D_{rw} is the diameter of the ring wire.

Measurements are repeated in triplicate, or more, if required. The mean of at least three corrected interfacial tensions is reported as the measured value. Measured surface (oil/air) and interfacial (brine/oil) tensions for 33‰ brine are shown in Table 3 for the fresh oils. For the surface tensions (oil/air), estimated uncertainty is ±1.2 mN/m at a 95% confidence level. The limit of detection (3 times the standard deviation) is 1.8 mN/m. For the brine/oil interfacial tensions, estimated uncertainty is ±2.5 mN/m at a 95% confidence level. The limit of detection is 3.6 mN/m.

Table 3. Measured Surface (oil/air) and Interfacial (brine/oil) Tensions without Chemical Dispersants

Fresh Oil	Surface Tension (mN/m)	Brine/Oil Interfacial Tension (mN/m)
Alaska North Slope	26.4	19.0
Arabian Medium	26.5	20.0
South Louisiana	26.5	16.2

Brine/oil interfacial tensions for oils mixed with dispersants were below the detection limit, i.e. <3.6 mN/m, for all DOR values and for both dispersants (Corexit 9500 and Corexit 9527). Additional diluted mixtures with DOR of 1:200 were prepared for both dispersants and for all three oils to test further the observed effects of dispersants. No measurements of brine/oil interfacial tension could be determined even for these more dilute mixtures. As shown in Figure 2, a simple mixing test was performed with fresh South Louisiana oil and Corexit 9500 at DOR of 1:200 to quickly test these results on oil dispersion. Fresh oil and oil-dispersant mixtures were layered on the top of 33‰ brine solution in small beakers (Figure 2a) and then mixed vigorously (manually) for about one minute 1 minute. As shown in Figure 2b, even at a DOR of 1:200 oil-dispersant mixture dispersed much easier than the fresh oil. Such increase in oil dispersion, i.e. transformation of the oil layer into small droplets in the water column, relates to a reduction of the oil-water interfacial tension. Mackay and Hussein (1992) estimated (assuming exponential decay of IFT with DOR) that a 1:500 DOR of Corexit 9527 is sufficient to reduce the IFT of various crude oil to 20-fold. Liu et al. (1995) measured about a 1000-fold reduction in IFT when the DOR increases from 1:200 to 1:10. All of these results are in qualitative agreement with measurements found in the present study.

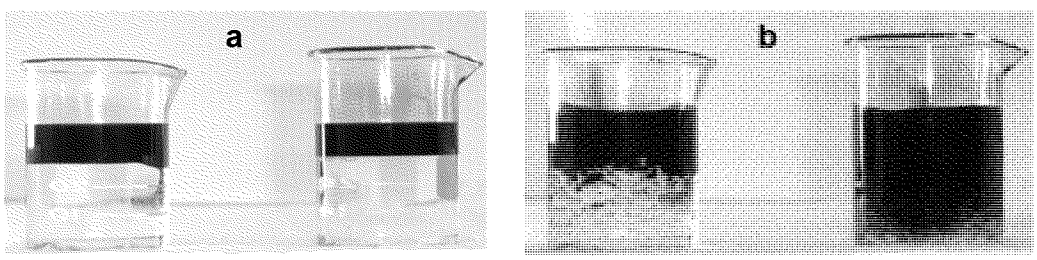

Figure 2. Simple dispersion testing: South Louisiana before (a) and after (b) 1 minute mixing. In each of these pictures, the left beaker contains no dispersant and the right one has Corexit 9500 at 1:200 DOR

3 Effects on oil dispersion

The effects of a reduction in the IFT on droplet formation can easily be illustrated using existing theories. From a thermodynamic point of view, the change in the free energy of the system after dispersion of an oil slick of thickness η to oil droplets for diameter D can be expressed by (Liu et al. 1995):

$$\Delta E = \sigma_w + \sigma_{o-w}\left(6\frac{\eta}{D} - 1\right) - \sigma_o \qquad (2)$$

where σ_w and σ_o represent surface tension of water and oil, respectively.

As such, dispersion of an oil slick into the water column requires reduction of ΔE as described in equation (2). ΔE is proportional to IFT reduction and the thickness of the slick and is inversely proportional to the size of the dispersed droplets. From the droplet formation perspective, existing theories show that IFT is a key factor that controls the size of oil droplets. This may be shown considering the model discussed by Khelifa et al. (2005) and described by equation (3). Computed reductions of maximum droplet size with the reduction of IFT are shown in Figure 3 for moderate ($1\ m^2/s^3$) and high ($10\ m^2/s^3$) kinetic energy dissipation rates ε.

$$D_{\max} = \begin{cases} 0.726\left(\dfrac{\sigma_{o-w}}{\rho_w}\right)^{3/5} \varepsilon^{-2/5} & \text{for} \quad \varepsilon \le \varepsilon_c \\ 5.2\times10^{-5}\left(\dfrac{\sigma_{o-w}}{\rho_w \upsilon_w}\right)^{3} \varepsilon^{-1}\left(\dfrac{\rho_o \upsilon_o}{\rho_w \upsilon_w}\right)^{3/8} & \text{for} \quad \varepsilon > \varepsilon_c \ \text{and}\ D_{\max} \ge \kappa \\ 3.8\times10^{-2}\left(\dfrac{\sigma_{o-w}}{\rho_w \upsilon_w}\right)\upsilon^{0.5} \varepsilon^{-1/2}\left(\dfrac{\rho_o \upsilon_o}{\rho_w \upsilon_w}\right)^{1/8} & \text{for} \quad \varepsilon > \varepsilon_c \ \text{and}\ D_{\max} < \kappa \end{cases} \tag{3}$$

where D_{max} is the maximum droplet size, σ_{o-w} oil-water interfacial tension, ρ_w water density, ρ_o oil density, ε kinetic energy dissipation rate, ν_w kinematic viscosity of water, ν_o kinematic viscosity of oil, κ Kolmogorov length scale and $\varepsilon_c = (7.2\times10^{-5})^{5/3}(\sigma_{o-w}/\rho_w\upsilon_w)^5(\ _{o-w}/\rho_w)^{-1}(\rho_o\upsilon_o/\rho_w\upsilon_w)^{5/8}$. The first expression in equation (3) is the Hinze model which is assumed to describe droplet breakup at relatively low dissipation rates. The two other expressions represent the model proposed by Li and Garrett (1998) when the dissipation rate exceeds a value defined by ε_c. Similar model was used recently by Tkalich and Chan (2002) to investigate vertical mixing of oil droplets under breaking wave conditions

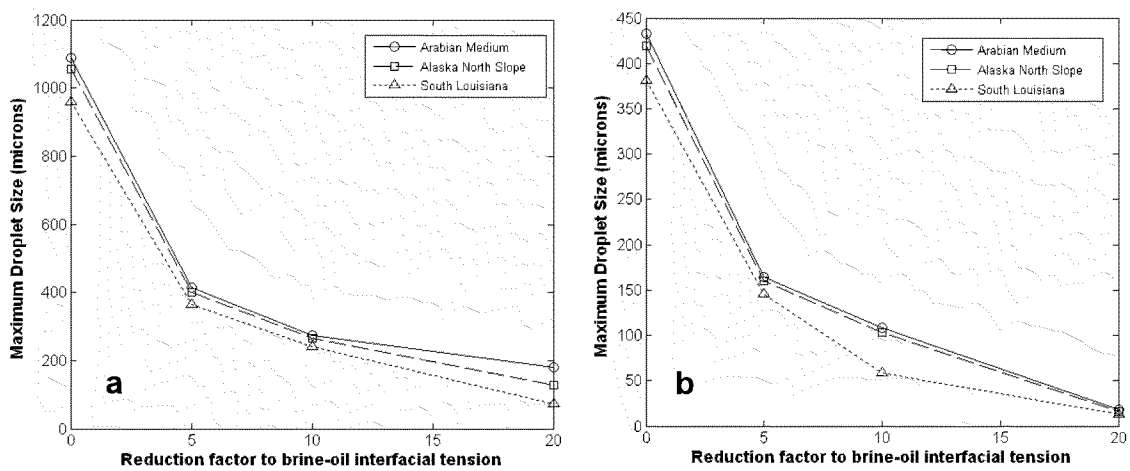

Figure 3: Calculated decrease of maximum oil droplet size with the reduction of brine-oil interfacial tension for kinetic energy dissipation rate $\varepsilon = 1\ m^2/s^3$ (a) and $10\ m^2/s^3$ (b) according to equation (3).

Further experiments were performed to measure the effects of IFT reduction on oil droplet size distribution. About 50 mg of Alaska North Slope were mixed with 250 mL of brine (33‰) in a reciprocating shaker for at least 90 minutes. Corexit 9500

was used at DOR of 0, 1:200, 1:100, 1:40, 1:20, and 1:10. While shaking, water samples were collected from the center of the suspension after about 90 minutes shaking. Each sample was analyzed immediately using UV-epi fluorescence microscopy equipped with a high resolution digital camera. The imaging setup is designed to detect oil droplets up to 0.1 μm in size.

Examples of microphotographs obtained from the imaging setup are shown in Figure 4. These microphotographs showed some interesting results about oil dispersion. The first one is that for DOR less that 1:100, the chemical dispersant has less effect on oil droplet size (Compare Figures 4e & f to 4a). The second one relates to the fact that the smallest oil droplets (generally used as an indicator of dispersant effectiveness) are not obtained at the highest DOR of 1:10 (Figure 4b), but at a DOR equal to 1:20 (Figure 4c). The third observation is that there is a good similarity between oil droplet populations obtained with DOR of 1:10 (Figure 4b) and 1:40 (Figure 4d). These observations were corroborated by visual evaluation of water turbidity (Figure 5) and quantitatively by measurements of droplet size distributions. The later was performed using an in-house image analysis program developed on the Matlab platform. A minimum of 15 frames were evaluated in the analysis depending on the concentration of oil droplets. Visual diagnosis of the six samples shown in Figure 5 clearly confirm that the 1:20 DOR provided the highest oil dispersion (highest turbidity). Water samples for DOR equal to 1:100 and less are clear and comparable to water sample without dispersant. This is further confirmation of what was observed in Figure 4. Large oil droplets resurface faster than small droplets, which makes the water samples at low DOR look cleaner than at higher DOR.

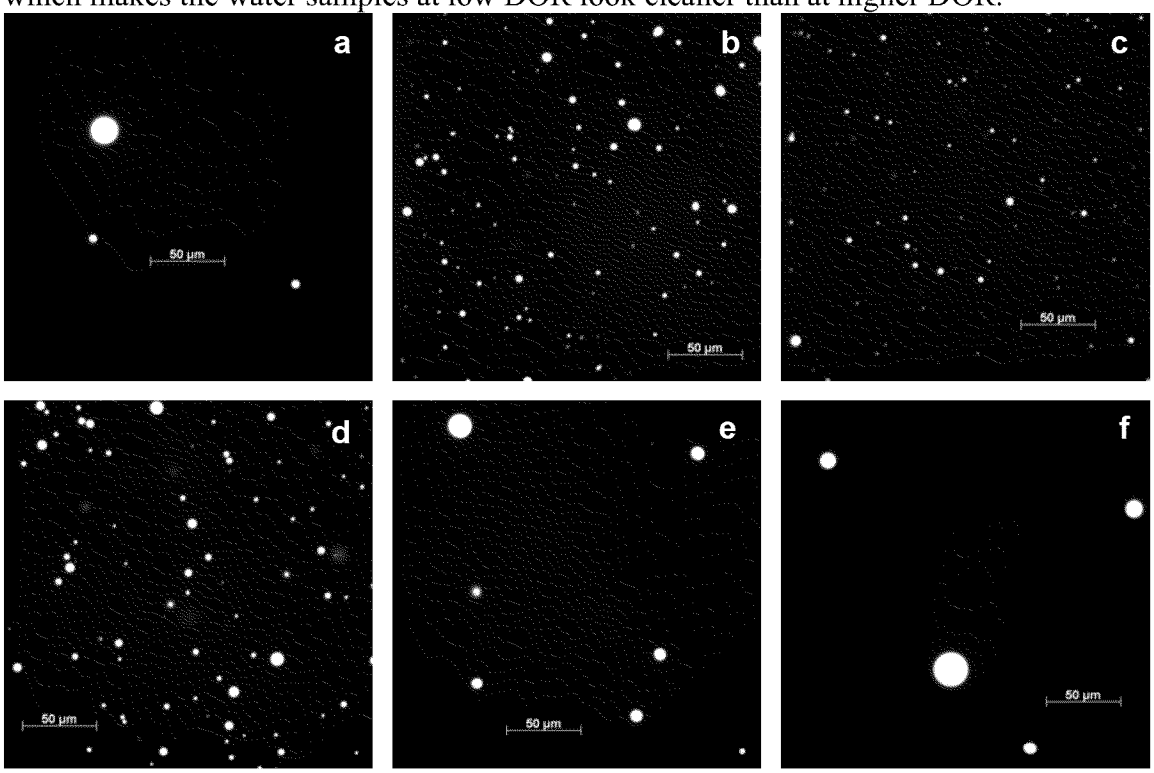

Figure 4: Microphotographs of oil droplets measured after 90 minutes while shaking using UV epi-fluorescence microscopy, Alaska North Slope crude and Corexit 9500 at various DOR: no dispersant (a), 1:10 (b), 1:20 (c), 1:40 (d), 1:100 (e), 1:200 (f).

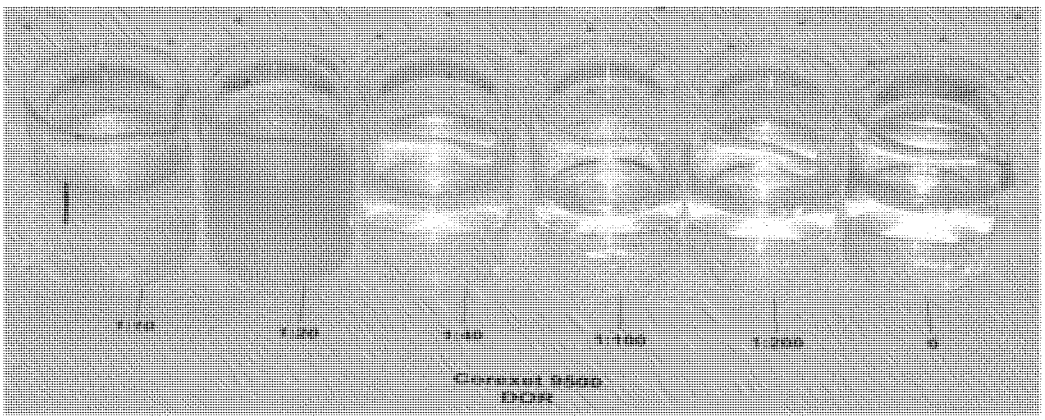

Figure 5: Water samples from different reaction chambers after overnight settling period. The ratios shown in this figure represent DOR values. Alaska North Slope crude and a shaking period of about 90 minutes. Clear water samples showed that most of the dispersed oil in the water column has resurfaced in the reaction chamber during the settling period.

One way to quantitatively investigate the observations discussed above is to measure droplet size distributions during shaking and after different settling periods. This is shown in Figure 6. All measured size distributions are shown in number concentration. Results shown in Figure 6a confirm observations made above from Figure 4. The highest concentration of small oil droplets are shown with DOR 1:20 during shaking and after the two settling periods. Size distributions measured with DOR 1:10 and 1:40 are very similar. For small DOR, size distributions measured while shaking are comparable to no dispersant conditions and include the largest droplets of about 25μm (Figure 6a). Comparison between droplet concentration in Figures 6a and 6b showed that coalescence between chemically dispersed oil droplets does occur, as more large droplets and less small droplets were measured at high values of DOR. After overnight settling period, during which large droplets have reached the water surface (Fingas and Decola, 2006), almost all size distributions are within the same size range between 0.3 and 7 μm. The high concentration of small droplets shown in Figure 6c for DOR=1:20 (higher than during shaking, Figure 6a) was not expected and is probably due to a contamination of the syringe during the sampling process.

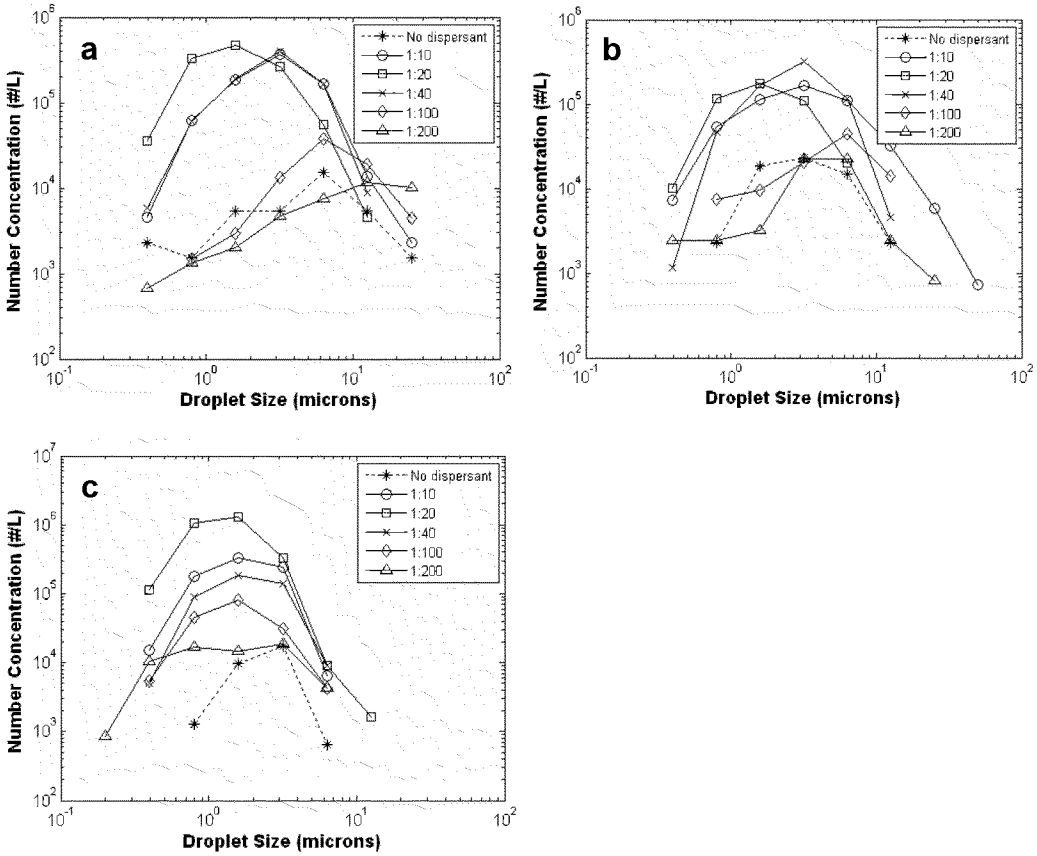

Figure 6: Measured droplet size distributions using UV epi-fluorescence microscopy, Alaska North Slope crude and Corexit 9500 at various DOR after 90 minutes shaking (a), 90 minutes settling (b), and overnight settling (c).

Overall, the measured droplet size distributions confirm the visual observations discussed above. Further confirmation is also provided in the measured variations of median droplet size with DOR (Figure 7). The smallest median diameter of less than 2 μm was obtained with DOR=1:20. At the highest DOR of 1:10, measured median droplet size is about 3.2 μm during shaking and after 90 minutes settling period. Median size is almost constant at about 1.9 μm after overnight settling regardless of DOR, except for physically dispersed oil. A significant increase (about double) of the median size was observed when the DOR increased from 0 to 1:200 (during shaking) and 1:100 after 90 minutes settling was not expected. The authors have no explanation for these results at the current time.

It is interesting to note that the results obtained in this study are also in agreement with laboratory measurements discussed by Liu et al. (1995). Both visual and quantitative investigations showed in the present study show that Corexit 9500 is more effective in dispersing Alaska North Slope crude at DOR 1:20 (or 5%) than at a higher DOR of 1:10. For the two different types of chemical dispersants employed (noted No. 2 and No. 4 in their manuscript), Liu et al. (1995) measured a maximum reduction of IFT at a DOR of 6% (or 1:17), while for the two other chemical dispersants they studied (No. 1 and No. 2), they measured a monotonous decrease of IFT with DOR. The DOR value at which the IFT reached a maximum reduction (1:20 in the present study and about 1:17 in Liu et al, 1995) is considered as the

approximate critical micelle concentration (CMC) of chemical dispersant. Apparently, this concentration is a function of the type and solubility of chemical dispersant, oil type, and oil to water ratio, but very little is known about this concentration. More laboratory measurements are needed to fully understand the effect of this parameter on dispersant effectiveness.

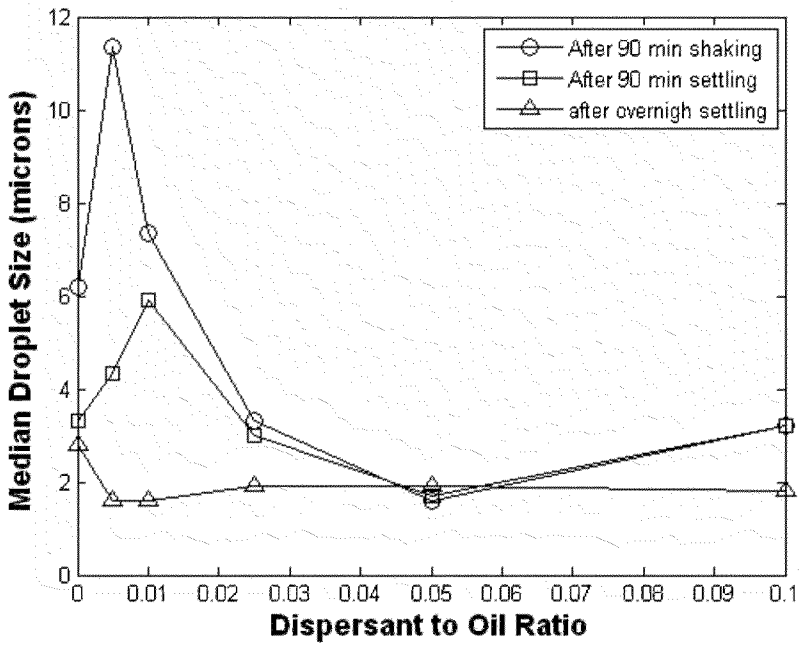

Figure 7. Median Droplet Size versus Dispersant to Oil Ratio (DOR)

4 Conclusion

Several interesting observations were made in this study. It was shown that brine-oil interfacial tension associated with Arabian Medium, Alaska North Slope and South Louisiana crudes reduces to less than 3.6 mN/m with the application of chemical dispersants Corexit 9500 and 9527, even at a low DOR value of 1:200. The Du Noüy ring method is not an appropriate method to measure small IFT values. The application of chemical dispersants increases the viscosity of the dispersant-oil mixture up to 40% over the neat crude oil. Using a high resolution imaging setup, the effect of IFT reduction on oil dispersion was measured and showed significant reduction of size and enhancement of the concentration of oil droplets, as predicted by existing theories. However, this study showed that for each mixing condition, an optimum value of DOR exists that provides for maximal dispersant effectiveness. At this optimum DOR, the IFT appeared to reach a maximum reduction, as inferred from the droplet size. This finding is in agreement with results presented in a previous study and suggests that the optimum DOR corresponds to the critical micelle concentration (CMC) of the chemical dispersant. For an Alaska North Slope/Corexit 9500 combination, the optimum DOR is 1:20. Above and below this concentration, the size of the oil droplets increases and their concentration decreases in the water column. Further investigation of IFT reduction with DOR and variations of CMC with the type and the solubility of chemical dispersant, oil type, and oil to water ratio would certainly benefit the oil spill community from a number of different perspectives. For instance, very little is known on how to integrate the effects of

chemical dispersants into oil spill models. Better quantification of this quantity is critical to a better understanding of oil-dispersant interaction. The benefit of this procedure to the actual method that looks to the reduction of droplet size distribution is that, the size reduction of chemically dispersed oil droplets is a result of a (non linear) combination of at least the chemical effects of the chemical dispersant and the physical effects dictated by the turbulent mixing.

5 Acknowledgements

Funding for this project was provided by the Coastal Response Research Center www.crrc.unh.edu

6 References

Clayton, J.R., J.R. Payne, and J.S. Farlow, "Oil Spill Dispersants: Mechanisms of Action and Laboratory Tests", *CRC Press*, Boca Raton, 1993, p. 103.

Fingas, M. and E. Decola, "Oil Spill Dispersant Effectiveness Testing in OHMSETT", Report submitted to Prince William Sound Regional Citizens' Advisory Council (PWSRCAC), Anchorage, Alaska, 47p., 2006.

Hinze, J.O., "Fundamentals of the hydrodynamic mechanism of splitting in dispersion processes", *AIChE Journal*, Vol. 8 (4), 289-295, 1955.

Khelifa, A., P.S. Hill, and K. Lee, "A Comprehensive Numerical Approach To Predict Oil-Mineral Aggregate (OMA) Formation Following Oil Spills In Aquatic Environments", in: *Proceedings of the 2005 International Oil Spill Conference*, American Petroleum Institute, Miami Beach, Florida, 2005.

Khelifa, A., P.S. Hill, and K. Lee, "Prediction of Oil Droplet Size Distribution in Agitated Aquatic Environments", in *Proceedings of the 27th Arctic and Marine OilSpill Program (AMOP) Technical Seminar*, Environment Canada, Ottawa, ON, Canada, pp. 371-382, 2004.

Li, M., and C. Garrett, "The Relationship Between Oil Droplet Size and Upper Ocean Turbulence", *Marine Pollution Bulletin*, 36(12), pp. 961-970, 1998.

Liu, H., Y. Zhang, and W. Wang, "Interfacial Properties Of Oil Spill Dispersants And Their Effects On Dispersion Effectiveness", *Acta Oceanologica Sinica*, pp. 587-593, 1995

Mackay, D. and K. Houssain, "Oil-Water Interfacial Tensions In Chemical Dispersant", *Report EE-32*, Environment Canada, Ottawa, 17p, 1982.

NAS, *Oil Spill Dispersants: Efficacy and Effects,* National Academy of Sciences, Washington, D.C., 330 p and Annexes, 2005.

Rewick, R. T., K. A. Sabo and J. H. Smith, "The Drop-weight Interfacial Tension Method for Predicting Dispersant Performance", *Oil Spill Chemical Dispersants, Research Experience and Recommendations, ASTM STP 840*, American Society for Testing Materials, Philadelphia, PA, pp. 94-107, 1984.

Rewick, R.T., K.A. Sabo, J. Gates, J.H. Smith and L.T. McCarthy, "An Evaluation Of Oil Spill Dispersant Testing Requirements", in *Proceedings of the 1981*

International Oil Spill Conference, Atlanta, Georgia, American Petroleum Institute, pp. 5-10, 1981.

Rewick, R.T., G. Jennifer, and H.S. James, "Simple Test Of Dispersant Effectiveness Based On Interfacial Tension Measurements, *Fuel*, Vol. 9, pp. 263-265, 1980.

Tkalich, P., and E.S. Chan, "Vertical Mixing of Oil Droplets by Breaking Waves", *Marine Pollution Bulletin*, 44 (11), pp. 1219-1229, 2002.

Effects of Chemical Dispersants on Oil-Brine Interfacial Tension and Droplet Formation: New Results Using New High Resolution Imaging Setup and Weathered Oils

Ali Khelifa
Emergencies Science and Technology Section, Science and Technology Branch
Environment Canada, Ottawa, ON, Canada
ali.khelifa@ec.gc.ca

Danielle Marie Charron, Tsz-Shan Tong and Nigel Roshan Singh
Faculty of Engineering, University of Waterloo
Waterloo, ON, Canada

Abstract

A research project was initiated to establish quantitative understanding of the variations of the Oil-brine interfacial tension (IFT) with chemical dispersant concentration and the resulting modifications to the size distribution of oil droplets under various mixing conditions. The first series of laboratory results obtained with three crude oils was presented by Khelifa and So (2009). This paper presents the second series of the laboratory results using weathered oils and a new high resolution imaging procedure. High values of IFT were measured using a pendant drop instrument and low values of IFT were measured with a spinning drop instrument. Undisturbed oil droplets were measured in situ (in the reaction chamber) using a new high-resolution imaging setup. In this study, Alaska North Slope (ANS) oil was used with 0, 10 and 22 % weathering conditions. Corexit 9500 was used and the dispersant-to-oil-ratio (DOR) was varied from 0 to 1:1. Mixing speed was kept constant to 2.5 Hz. Results showed remarkable reduction of IFT with DOR. The highest reductions of about 10^7, 10^6 and 10^5 % were measured with ANS oil with 0, 10 and 22% weathering, respectively. These reductions were obtained at DOR of 1:50 to 1:20 for fresh oil and at 1:10 for the weathered ANS. At a low DOR of 1:500, the reduction of IFT was about 100%.Under moderate mixing energy, measured maximum size of oil droplets decreased from about 1100 □m to 100 □m for crude ANS, 1800 □m to 130 □m for the 10% weathered ANS and 1900 □m to 230 □m for the 22% weathered ANS when the DOR was increased from 1:500 to 1:20. Overall, size distribution of chemically-dispersed oil droplets was highly affected by the DOR and oil weathering. The curves showing size distributions measured in this study were very similar in shape to those measured by Lunel and his co-workers in the field trials they conducted in early nineties. However, the size range varies with the conditions of the dispersion and the weathering intensity. This study showed that the approach to using the same droplet size distribution to model transport and fate of chemically-dispersed oil under various environmental conditions, oil types and weathering and DORs is not valid. Practical applications of the findings of this research in oil spill modelling, for instance, will be discussed

1 Background

A research project was initiated to establish quantitative understanding of oil dispersion under various oil-dispersant mixing conditions. Part of this project is to study the variations of the oil-brine interfacial tension (IFT) with chemical dispersant dosage and the resulting modifications to the size distribution of oil droplets. Variables include

oil type and weathering, dispersant-to-oil ratio (DOR) and type, temperature and mixing energy. The rational to conduct such research was discussed in details in the first paper related to the project (Khelifa and So, 2009). The needs to establish quantitative understanding of the reduction of IFT with DOR has been further emphasized during the response to the Deepwater Horizon (DWH) oil spill in the Gulf of Mexico in April 2010. Data on subsea dispersant application showed that the DOR varied from 1:1200 to 1:92. In this, 19% of the time (13 days) the DOR was less than 1:250, 34% of the time (23 days) it was between 1:150 and 1:250 and 43 % of the time (29 days) it was between 1:150 and 1:100 (FIAG, 2010). These DOR values are much smaller than the commonly referred value of 1:20. Very little is known about dispersant effectiveness at these low values of DOR. This paper discusses new laboratory results on IFT reduction and the resulting size distribution of the dispersed oil droplets for a wide range of DOR and for weathered Alaska North Slope oil. This is the second series of data generated from this project.

2 Experimental Method

The experimental method used in this study has been described in details by Khelifa and So (2009). It includes measurement of IFT using pendant drop method with KSV CAM 200 Contact Angle and Surface Tension Meter and spinning drop method with the KRÜSS Spinning Drop Tension Meter SITE100, New Brunswick Scientific Gyrotory Shaker Model G2 (orbital), and a Nikon D200 Digital Single-Lens Reflex (DSLR) camera (Figure 1). By introducing a new extension tube to the camera, the resolution of the imaging system has been enhanced by 100% compared to the previous one. It is now 2.314 □m per pixel. This allows capturing oil droplets of few microns in size. The reaction chamber consists of a 125-mL Erlenmeyer flasks filled with 80 mL of artificial seawater (salinity 33‰). The flasks were cleaned with filtered water, acetone, hexane, and DCM three times, and then allowed to dry completely prior to each test. For each experiment, 60 images were taken and analyzed using a new version of image analysis program developed on Matlab platform and Image Toolbox (Khelifa et al., 2007). Detailed description of the experimental procedure was presented by Khelifa and So (2009).

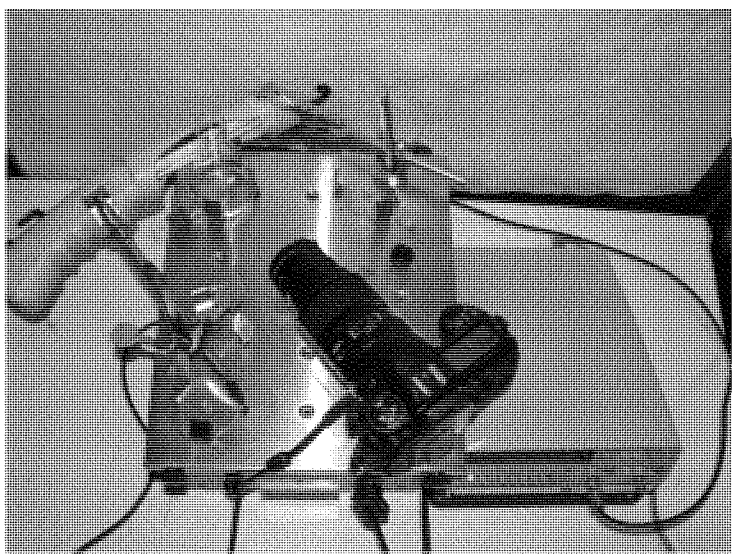

Figure 1 Imaging setup used to measure size distribution of oil droplets directly from the reaction chamber (125-mL Erlenmeyer flask) while shaking

3 Experimental Conditions

Alaska North Slope (ANS) oil was used with three weathering conditions of 0, 10 and 22.5%. The corresponding oils are referred by ANS0%, ANS10% and ANS22.5% hereafter, respectively. Physical properties of three oils are shown in Table 1. The chemical dispersant used was Corexit 9500. The dispersant-to-oil ratio (DOR) was varied from 0 to pure dispersant using 20 intermediate values, as shown in Table 2. All tests were performed in a cold room at a fixed temperature of 15°C and a constant shaking speed of 2.5 Hz (or 150 rpm). Detailed description of the physical and chemical properties of the three oils is available on the Environment Canada Oil Properties web site (Environment Canada, 2008).

Table 1 Physical properties of the oils used in this study

Properties \ Oil	ANS0%	ANS10%	ANS22.5%
Weathering (%)	0	10	22.5
Density @ 15 °C (g/L) *	866	894	919
Dynamic viscosity @ 15 °C (cP)	1.5	31.8	152
Surface tension @ 15 °C (mN/m)	26.4	28.4	30.4
Oil/brine (33‰) interfacial tension @ 15 °C (mN/m)	21.5	21.9	24.2

3 Results and Discussion

Results discussed in the following sub-sections include variations of IFT with DOR and size distribution of dispersed oil droplets.

3.1 Variations of Interfacial Tension (IFT) with Dispersant-to-oil Ratio (DOR)

Measured variations of IFT with DOR are shown on Figure 2. The corresponding numerical values are listed in Table 2. Results showed remarkable reduction of IFT with DOR for the three oils. As reported in the previous study using different crude oils (Khelifa and So, 2009), the overall trend shown by the three series of data is a rapid decrease of IFT with DOR until it reaches a minimum and then increases to reach a value close to the Corexit 9500-brine IFT. A similar trend was reported by Liu et al. (1995). However, the data do not support the exponential trend proposed by Mackay and Houssain (1982).

The effectiveness of dispersant to lower IFT is proportionally reduced with oil weathering. Reduction of IFT to a given level requires much more dispersant when applied to weathered oils than to fresh oil. For instance, reduction of IFT to 2 10^{-2} mN/m is obtained at DOR of 1:95, 1:40 and 1:20 for ANS0%, ANS10% and ANS22.5%, respectively. IFT of 6 10^{-3} mN/m is obtained at DOR of 1:90 and 1:10 for ANS0% and ANS22.5%, respectively (Table 2).

The reduction of IFT with DOR was calculated from data shown in Table 2 using the following equation:

$$IFT_{Red} = 100 \times (IFT_{Oil} - IFT_{Oil-CD}) / IFT_{Oil-CD} \quad (1)$$

where IFT_{Red} represents the reduction of IFT in %, IFT_{oil} is the oil-brine IFT without chemical dispersant, and IFT_{oil-CD} is the oil-brine IFT with chemical dispersant.

Table 2 Measured values of oil-brine interfacial tension for different DORs and the three oils. Measurements were performed with the spinning drop instrument, except for small values of DOR where the pendant drop instrument was used (rows marked with "*" in the first column). Values reported in the table are in mN/m.

DOR \ Oil	ANS0%	ANS10%	ANS22.5%
Oil only *	21.50	21.9	24.2
1:500 *	12.01	10.3	-
1:200 *	4.29	5.8	-
1:150 *	2.07	-	-
1:125 *	9.85E-01	-	-
1:100 *	1.77E-01	2.0	2.73
1:95	2.36E-02	-	-
1:90	6.17E-03	-	-
1:80	2.71E-03	-	-
1:70	1.58E-03	-	-
1:60	4.37E-04	6.0E-02	-
1:50	2.83E-04	-	-
1:40	2.18E-04	2.0E-02	0.32
1:30	2.27E-04	-	-
1:20	2.31E-04	1.98E-03	2.03E-02
1:15	3.61E-04	-	-
1:10	5.37E-04	8.99E-04	5.57E-03
1:7.5	9.05E-04	1.04E-03	-
1:5	4.20E-03	1.37E-03	6.96E-03
1:2.5	7.86E-03	3.78E-03	-
1:1	1.32E-02	6.39E-03	1.07E-02
Corexit 9500 only	1.04E-02	1.04E-02	1.04E-02

Reduction of IFT varies between about 1×10^2 and 9.8×10^6 % for ANS0%, 1×10^2 and 2.4×10^6 % for ANS10%, and up to 5.1×10^5 % for ANS22.5%. For low values of DOR up to 1:200, reductions of IFT obtained with three oils were very similar. The same remark apllies for high values of DOR of 1:05 and 1:1. The highest differences in IFT reductions were measured for DOR values between 1:100 and 1:10 (Figure 3 and Table 3). The maximum reductions were measured at a DOR of 1:40 for ANS0% and 1:10 for ANS10% and ANS22.5%. The DOR value at which the IFT reached a maximum reduction (1:10 and 1:40 in this study, 1:20 and 1:40 obtained with different crude oils in Khelifa and So, 2009 and about 1:17 in Liu et al., 1995) is considered to be the approximate critical micelle concentration (CMC) of the chemical dispersant. This concentration is a function of chemical dispersant type and solubility, oil type, and oil-to-water ratio, but very little is known on how this concentration varies with oil type and dispersant type.

Mackay and Houssain (1982) estimated (assuming exponential decay of IFT with DOR) that a DOR of 1:500 for Corexit 9527 is sufficient to reduce the IFT of various crude oils by 20-fold. This estimation is about 10 times higher than the measured values shown in Table 3 for ANS0% and ANS10% oils. Liu et al. (1995)

measured about a 1000-fold reduction in IFT when DOR increases from 1:200 to 1:10. Measurements shown in Table 3 are about 10 times higher than this value. For a DORs as low as 1:100, the reduction of IFT was about 1.2×10^4 % for ANS0% oil, 1.0×10^3 % for ANS10% oil, and 9.5×10^2 % for ANS22.5% oil (Table 3). The data showed that the reduction of IFT is affected by oil weathering when the DOR is between 1:100 and 1:10.

Table 3 Measured reduction of oil-brine interfacial tension (equation 1) for different DORs obtained with the three oils. The values of the highest reduction are shown in bold text.

DOR \ Oil	ANS 0%	ANS 10%	ANS 22.5%
1:500	$1\ 10^2$	$1\ 10^2$	-
1:200	$4\ 10^2$	$3\ 10^2$	-
1:100	$1.2\ 10^4$	$1.0\ 10^3$	$9.5\ 10^2$
1:40	**$9.8\ 10^6$**	$1.4\ 10^5$	$8.9\ 10^3$
1:20	$9.3\ 10^6$	$1.1\ 10^6$	$1.4\ 10^5$
1:10	$4.0\ 10^6$	**$2.4\ 10^6$**	**$5.1\ 10^5$**
1:5	$5.1\ 10^5$	$1.6\ 10^6$	$4.1\ 10^5$

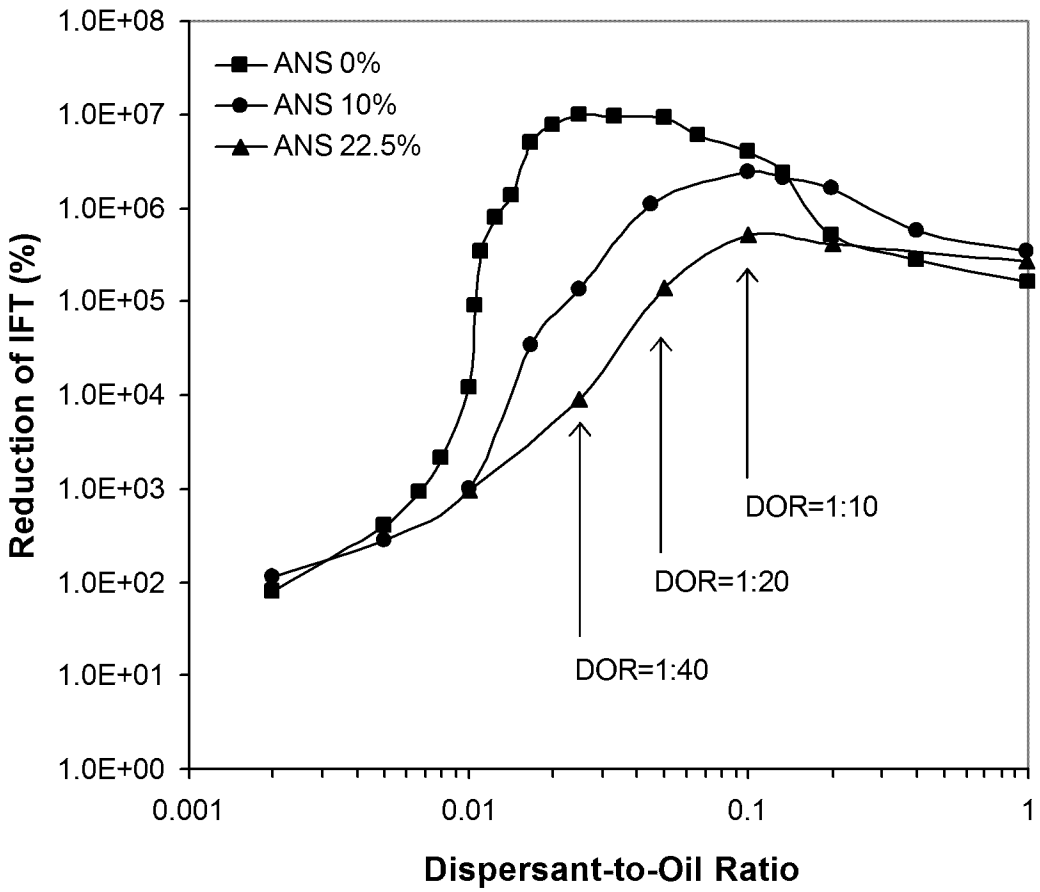

Figure 3 Reduction of oil-brine interfacial tension (equation 1) with dispersant concentration (in DOR) for the three oils

3.2 Initial Dispersion

This series of images aimed to track the breakup process of the oil-dispersant slick introduced at the free water surface during the first four seconds of mixing. As shown in Figure 4, the process that controls initial dispersion of the slick appears is affected by oil weathering. For the crude ANS (Figure 4a), the dispersion occurs in thin strings and droplets. The thickness and length of the strings increase significantly with oil weathering (Figure 4b and 4c). Oil viscosity, which increases from 1.5 to 152 cP when oil weathering increases from 0 to 22.5 %, plays a major role in the splitting process.

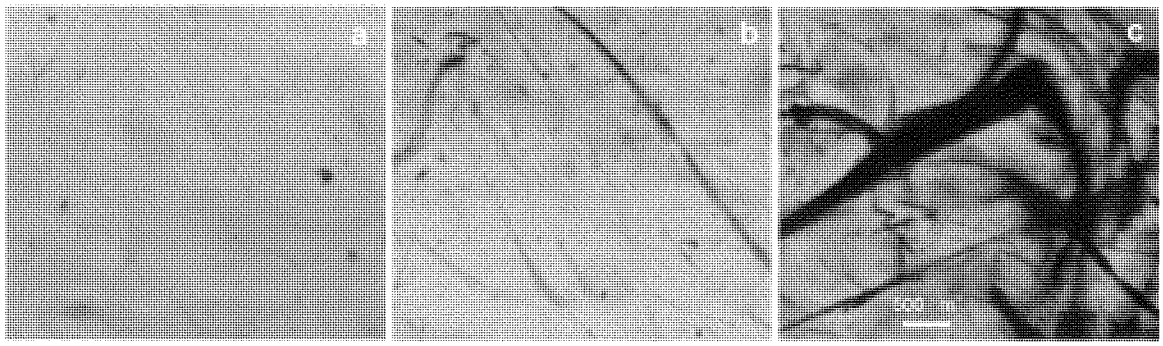

Figure 4 Images of the oil dispersion process during the first few seconds of mixing for DOR=1:40 and ANS0% (a), ANS10% (b), and ANS22.5% (c). The scale shown on image (c) applies to all images.

3.3 Size Distribution of Dispersed Oil Droplets

The measurement of droplet size was based on the analysis of several images of oil droplets taken with the DSLR camera while the reaction chamber was shaking. Samples of these images are shown on Figures 5 and 6 for DOR of 1:40 and 1:100, respectively. Systematic increase in droplet size with oil weathering and low DOR is shown. The smallest droplet population is obtained with ANS0%. No droplets were formed with oil only (no chemical dispersant). However, formation of oil droplets started with a DOR as low as 1:500.

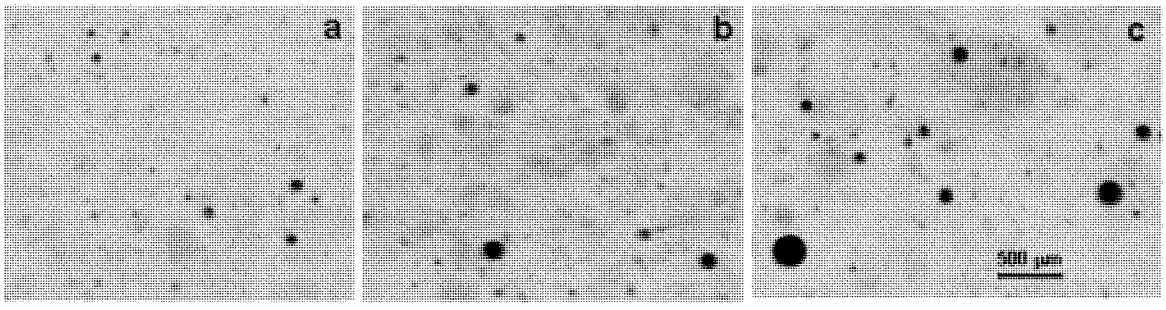

Figure 5 Images of dispersed oil droplets taken with the DSLR camera in the reaction chamber after 15 minutes of shaking using ANS oil at 0% weathering (a); 10% (b) and 22.5% (c). The scale shown on image (c) applies to all images. The experiments were performed with and Corexit 9500 at DOR of 1:40.

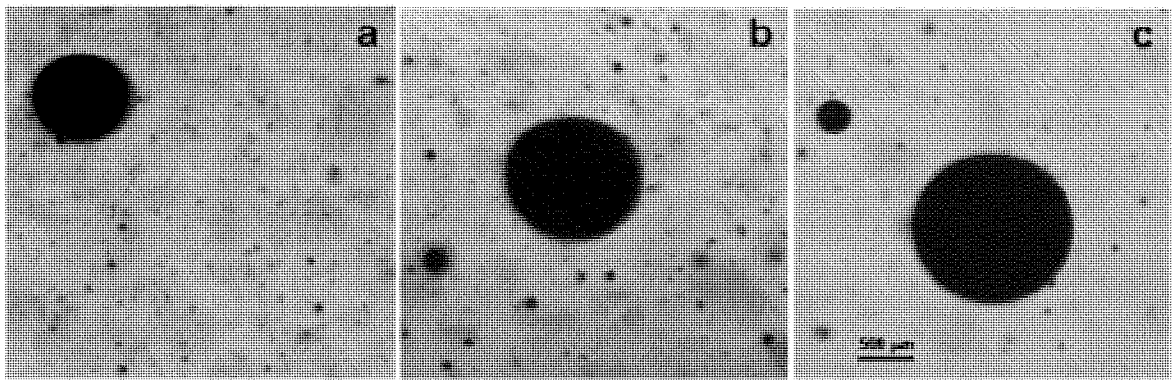

Figure 6 Images of dispersed oil droplets taken with the DSLR camera in the reaction chamber after 15 minutes of shaking using ANS oil at 0% weathering (a); 10% (b) and 22.5% (c). The scale shown on image (c) applies to all images. The experiments were performed with and Corexit 9500 at DOR of 1:100.

For each test, 50 to 60 images were analyzed to measure droplet size distribution. Effects of oil weathering on oil droplet size distribution for selected DOR values are shown on Figures 7 to 9 for DOR of 1:100, 1:40 and 1:1, respectively. For comparison, three droplet size distributions obtained from a Sea Trial reported by Lunel (1993) are also shown in all figures showing droplet size distribution. These values of the DOR were selected based on the measured reduction of IFT shown in Figures 2 and 3. At DOR of 1:100 and 1:1, small differences in size distribution are shown (Figures 7 and 9). At these DORs, the differences in the reduction of IFT measured for the three oils are small (Figures 2 and 3). Under these conditions, the main difference in the size distributions relates to the increase of the maximum size with oil weathering due to the increase of oil viscosity, as discussed below. At DOR of 1:40, the size distribution obtained with ANS22.5% shift toward larger size compared to ones obtained with ANS0% and ANS10%. The smallest oil droplets are measured with ANS0%. As shown in Figures 2 and 3, the largest difference between the three oils in IFT reduction was measured around DOR of 1:40. Size distributions measured at the highest DOR of 1:1 are very similar. They all shift towards larger sizes regardless of the level of oil weathering. This is very consistent with the measurement of IFT reduction shown in Figures 2 and 3. At high DO the IFT of oil-dispersant mixture converges to the value of pure dispersant condition regardless of oil type.

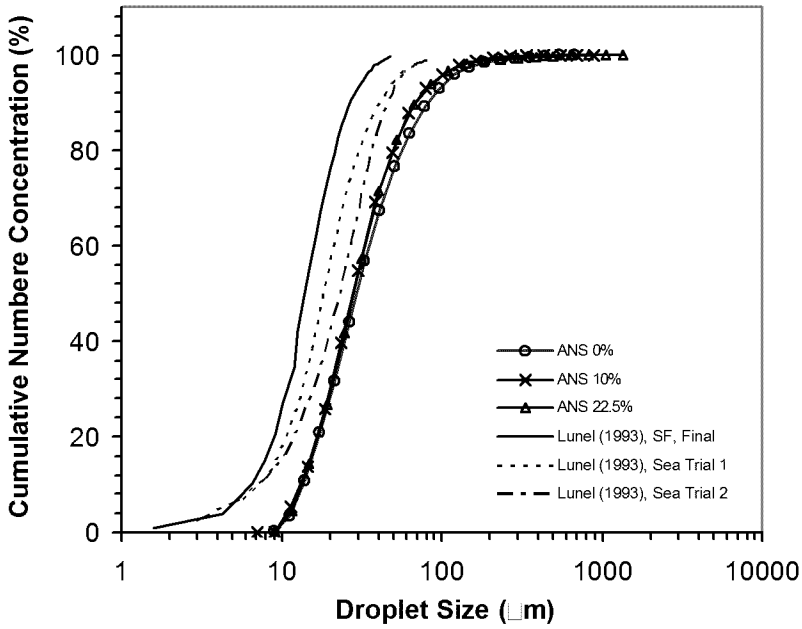

Figure 7 Size distributions of oil droplets measured from the DSLR camera images using image analysis. The experiments were conducted with ANS oil with 0, 10 and 22.5 % weathering and Corexit 9500 with 1:100 dispersant-to-oil ratio (DOR). The solid and dashed lines without symbols represent droplet size distributions obtained from Sea Trials as reported by Lunel (1993).

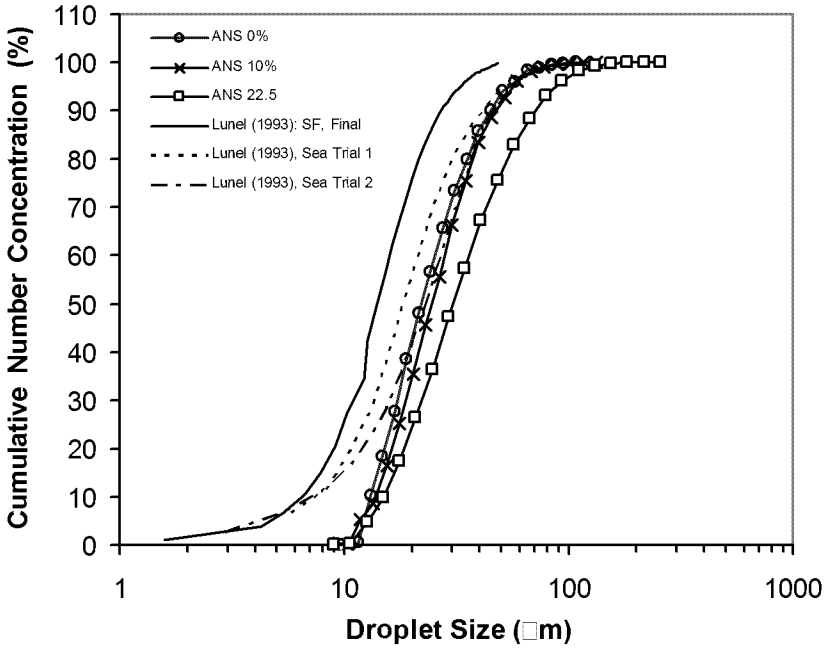

Figure 8 Size distributions of oil droplets measured from the DSLR camera images using image analysis. The experiments were conducted with ANS oil with 0, 10 and 22.5 % weathering and Corexit 9500 with 1:40 dispersant-to-oil ratio (DOR). The solid and dashed lines without symbols represent droplet size distributions obtained from Sea Trials as reported by Lunel (1993).

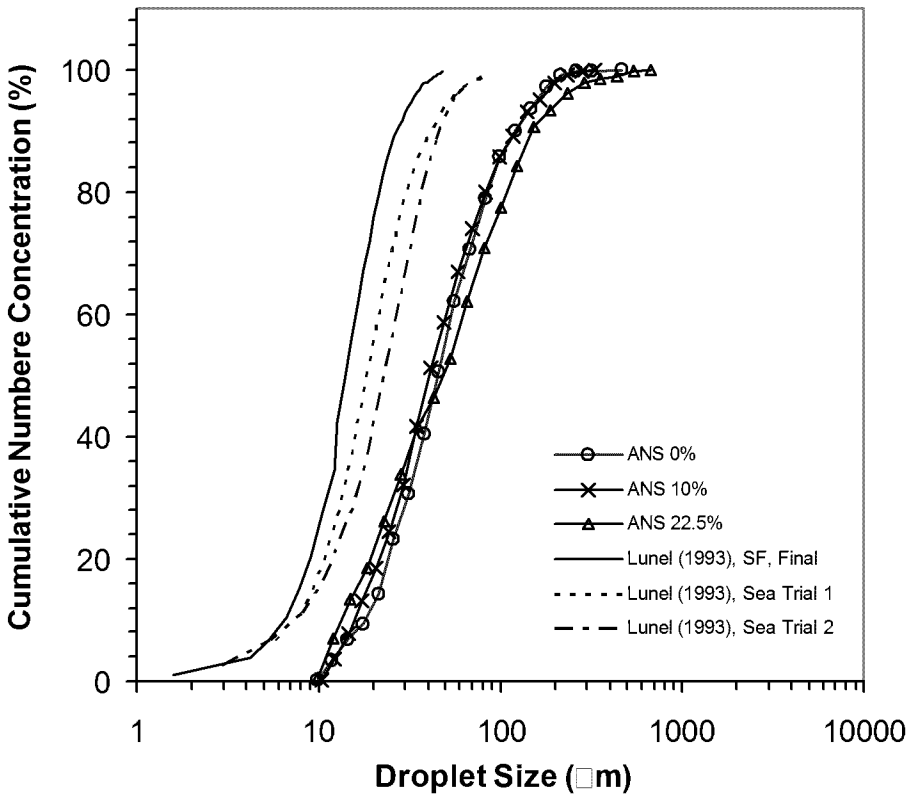

Figure 9 Size distributions of oil droplets measured from the DSLR camera images using image analysis. The experiments were conducted with ANS oil with 0, 10 and 22.5 % weathering and Corexit 9500 with 1:1 dispersant-to-oil ratio (DOR). The solid and dashed lines without symbols represent droplet size distributions obtained from Sea Trials as reported by Lunel (1993). (Note: the size distribution of ANS 22.5% was calculated using a limited number of images compared to the two other ones)

Measured droplet size distributions with various DORs for the three oils are shown in Figures 10 to 12. As expected, results show direct correlation between droplet size, oil weathering and DOR, except for DORs above the critical micelle concentration (CMC) where the size of dispersed oil droplets start to increase with DOR. As shown in the previous study with different crude oils (Khelifa and So, 2009), the data are very consistent with the measured reductions of IFT with DOR shown in Figures 2 and 3. Also, the data show good qualitative similarity between the measured size distributions and the field data. Unfortunately, the DOR at sea in Lunel's data is not well defined and the type of dispersant used was different from Corexit 9500.

The low end of all size distributions seems to be affected by the resolution of the imaging system. The actual setup is not capable to capture oil droplets with diameter smaller than few microns. New improvement of the imaging system is under way with the hope to double the already improved resolution. However, the larger droplets are well captured by the system, as shown in the size distributions of the droplets.

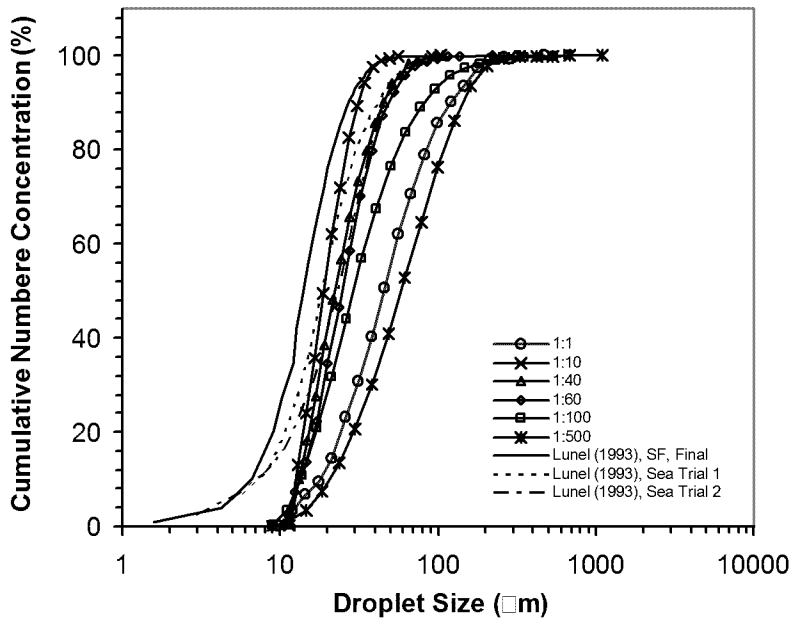

Figure 10 Size distributions of oil droplets measured from the DSLR camera images using image analysis. The experiments were conducted with ANS oil with 0 % weathering and Corexit 9500 and diverse dispersant-to-oil ratio (DOR). The solid and dashed lines without symbols represent droplet size distributions obtained from Sea Trials as reported by Lunel (1993).

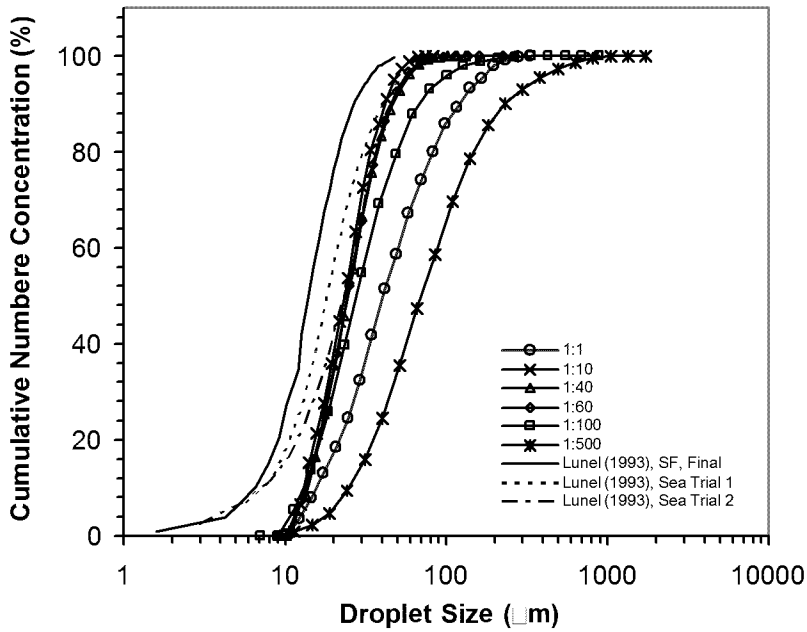

Figure 11 Size distributions of oil droplets measured from the DSLR camera images using image analysis. The experiments were conducted with ANS oil with 10 % weathering and Corexit 9500 and diverse dispersant-to-oil ratio (DOR). The solid and dashed lines without symbols represent droplet size distributions obtained from Sea Trials as reported by Lunel (1993).

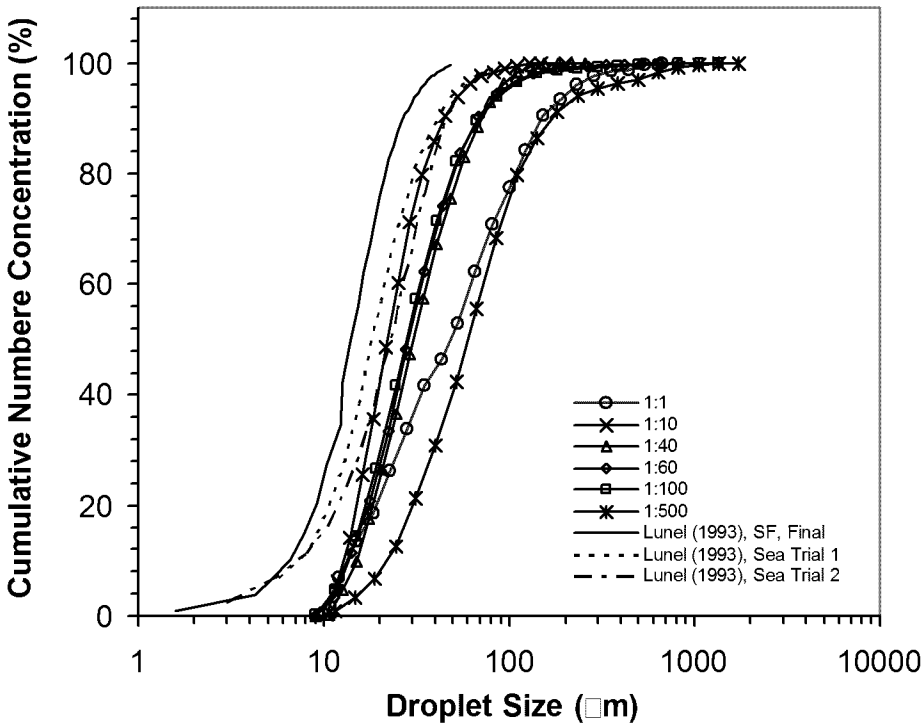

Figure 12 Size distributions of oil droplets measured from the DSLR camera images using image analysis. The experiments were conducted with ANS oil with 22.5 % weathering and Corexit 9500 and diverse dispersant-to-oil ratio (DOR). The solid and dashed lines without symbols represent droplet size distributions obtained from Sea Trials as reported by Lunel (1993). (Note: the size distribution of ANS 22.5% was calculated using a limited number of images compared to the two other ones)

The maximum size of oil droplet is an important parameter for both practical applications of chemical dispersant and theoretical predictions of droplet population (Hinze, 1955, 1975; Li and Guarrett, 1998, Khelifa et al., 2004). The data on droplet size were analyzed to show variations of the maximum size of dispersed oil droplets with DOR and oil weathering. However, there is no consensus on how to estimate this parameter from a population of oil droplet measured at a specific time under dynamic equilibrium conditions. In a dispersion process, such equilibrium is reached when breakup of large oil droplets is balanced by the coalescence process of small droplets to reform the large droplets. As such, the largest droplet that exists at a specific time of the dispersion may be larger than the maximum droplet that survives the breakup process. For this, the maximum droplet size D_{max} of the droplet population was estimated by: 1) the largest droplet in the population, 2) the size of the droplet that is larger than 95% of the population noted by D95%, and 3) the average of the upper 5% of the population. Results are shown on Figure 13. Many lessons can be drawn from these results. The obvious one relates to the large difference between the numerical values obtained with the three estimators of the maximum droplet size. The largest droplet size, the average upper 5% and the D95% varied between 145 and

1860 □m, 65 and 758 □m and 46 and 338 □m, respectively, when the DOR was varied between 1:500 and 1:1. While the data obtained using the three different estimators are quite different in magnitude, their variations with DOR are similar. They all show exponential decrease with DOR up to 1:10. For DOR larger than 1:10, the three methods show exponential increase of the maximum size of the droplet. This increase is in agreement with the increase of IFT measured at high DORs (Figures 2 and 3).

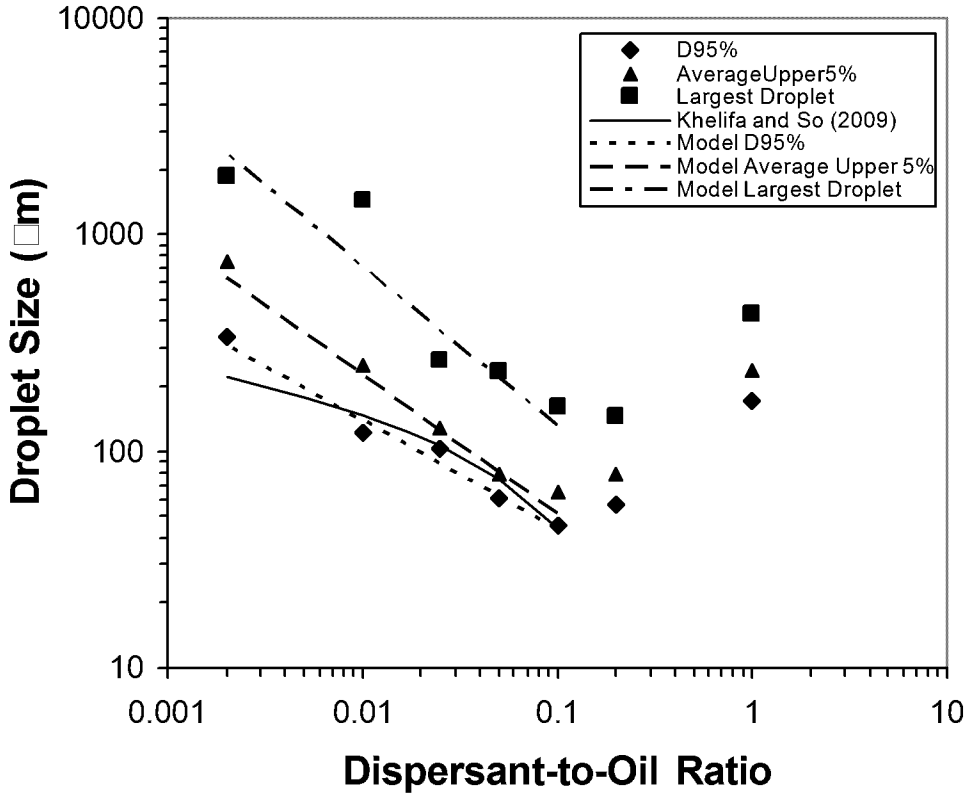

Figure 13 Maximum droplet size measured from the DSLR camera images using image analysis. The experiments were conducted with ANS oil with 22.5 % weathering and Corexit 9500 and diverse dispersant-to-oil ratio (DOR). The solid represent the relationship reported by Khelifa and So (2009) and the dashed lines are best fits models for D95% (14*DOR^-0.5), Dmax (24*DOR^-0.74) and average size of the upper 5% (12*DOR^-0.64) for data with DOR up to 1:10 (0.1 on the figure).

The best fits for the data obtained with the three estimators are as follows:

Largest droplet size $= 24\ DOR^{-0.74}$
Average of the upper 5% $= 12\ DOR^{-0.64}$
D95% $= 14\ DOR^{-0.50}$

A previously established empirical relationship by Khelifa and So (2009) is also shown by the solid line on Figure 13. They used the largest droplet approach to estimate the maximum droplet size and their relationship was based on logarithmic fitting. Compared with the new data, the previous relationship under estimate the largest droplet size measured in this study. Initially, this was related to fact that the

previous relationship was established with crude ANS oil, while the new data were generated with ANS22.5. A closer look to the previous data showed that, contrary to what is mentioned in Khleifa and So (2009), all the data related to droplet size were not in micrometer. They were in pixels and were not scaled with the resolution factor of 5.4 μm/pixel. This low resolution corresponds to the first version of the imaging system used in this paper. As noted above, this resolution has been enhanced to 2.314 μm/pixel in this study. In other words, the estimate largest droplet size shown by the solid line in Figure 13 should be multiplied by a factor of 5.4 to take into account image scaling in the previous data. Because this is a linear scaling, it will not change the shape of the solid line. The new data shown on Figure 13 are represented better with the power law shown by the discontinued lines.

4 Conclusion

This paper discussed the second part of an ongoing R&D project aimed at providing quantitative understanding of oil dispersion. The first part of the study discussed in Khelifa and So (2009) used crudes oils, while this study used weathered oils. Findings from the both studies showed that the approach of separating the direct effects of chemical dispersants on oil properties, specifically oil-brine interfacial tension, and the effects of mixing on dispersion of chemically treated oil is valid for the tested crude and weathered oils. Under constant mixing conditions, the reduction of the maximum oil droplet size that overcomes the breakage process with dispersant concentration is dictated by the effects of chemical dispersant on oil properties. It correlates well with the dispersant-to-oil ratio (DOR) up to the critical micelle concentration (CMC). This good correlation is due to the reduction of interfacial tension (IFT) with DOR, as stated in most of the existing theories.

The findings of this study also showed that the efficacy of chemical dispersant to reduction the IFT decreases with oil weathering. To reduce IFT to certain level, higher dosages of dispersant are required for weathered oils compared to crude oils. The translation of such effect to the resulting size distribution is shown in the previous study. However, oil weathering also affects the viscosity of the oil and the dispersion process. Additional testing is required to establish a clear correlation between oil weathering, IFT reduction and the properties of the resulting dispersed droplets under constant mixing energy. This will be address in the third part of the project.

5 Acknowledgements

The authors would like to thank Benjamin Fieldhouse, Bruce Hollebone, Mike Landriault, and Lloyd Gamble of the Emergencies Science and Technology Section (ESTS) for their technical help in conducting this research. Many thanks also to Natalie Jones of ESTS for her valuable input during the preparation of this paper.

6 References

Environment Canada, "Oil Properties Database", http://www.etc-cte.ec.gc.ca/databases/OilProperties/oil_prop_e.html, 2008.

Federal interagency Solutions Group (FIAG), "Oil Budget Calculator – Deepwater Horizon". Technical documentation, 49p. and annexes, 2010.

Hinze, J.O., *Turbulence*, 2nd Ed., McGraw-Hill, New York, NY, 790 p., 1975.

Hinze, J.O., "Fundamentals of the Hydrodynamic Mechanism of Splitting in Dispersion Processes", *AIChE Journal*, 8 (4), pp. 289-295, 1955.

Khelifa A., and So, L.L.C., "Effects of Chemical Dispersants on Oil Brine Interfacial Tension and Droplet Formation", in *Proceedings of the Thirty-Second Arctic and Marine Oilspill Program (AMOP) Technical Seminar*, Environment Canada, Ottawa, Ontario, Vol. 1, pp. 383-396, 2009.

Khelifa, A., M.F. Fingas, B.P. Hollebone, and C.E. Brown, "Effects of Chemical Dispersants on Oil Physical Properties and Dispersion", in *Proceedings of the Thirtieth Arctic and Marine Oilspill Program (AMOP) Technical Seminar*, Environment Canada, Ottawa, ON, Canada, pp. 105-116, 2007.

Khelifa, A., P.S. Hill, and K. Lee, "Prediction of Oil Droplet Size Distribution in Agitated Aquatic Environments", in *Proceedings of the Twenty-seventh Arctic and Marine Oilspill Program (AMOP) Technical Seminar*, Environment Canada, Ottawa, ON, Canada, pp. 371-382, 2004.

Li, M., and C. Garrett, "The Relationship Between Oil Droplet Size and Upper Ocean Turbulence", *Marine Pollution Bulletin*, 36 (12), pp. 961-970, 1998.

Liu, H., Y. Zhang, and W. Wang, "Interfacial Properties of Oil Spill Dispersants and their Effects on Dispersion Effectiveness", *Acta Oceanologica Sinica*, pp. 587-593, 1995.

Lunel, T., "Dispersion: Oil Droplet Size Measurements at Sea", in *Proceedings 1993 Oil Spill Conference*, American Petroleum Institute, Tampa, FL, pp. 794-795, 1993.

Mackay, D. and K. Houssain, "Oil-Water Interfacial Tensions in Chemical Dispersant", Manuscript Report EE-32, Environmental Protection Service, Environment Canada, Ottawa, ON, 17 p., 1982.

Hoffmann, W.C., "Field-collected and AGDISP-predicted Spray Flux from an Aerial Application", *Journal of ASTM International* 3:1, pp.1-12, 2006.

Hoffmann, W.C., W.E. Bagley, B.K. Fritz, Y. Lan, and D.E. Martin, "Effects of Water Hardness on Spray Droplet Size Under Aerial Application Conditions", *Appl. Eng. Agric.;* 24:1, pp.11-14, 2008.

Markarian, R.K., J.P. Nicolette, T.R. Barber, and L.H. Giese, *A Critical Review of Toxicity Values and and Evaluation of the Persistence of Petroleum Products for Use in Natural Resources Damage Assessment*, Publication 4594, American Petroleum Institute, Washington, D.C., 1995.

Mokeba, M.L., D.W. Salt, B.E. Lee, and M.G. Ford, "Computer Modeling of the Meteorological and Spraying Parameters that Influence the Aerial Dispersion of Agrochemical Sprays", *Int. J. Biometeorology,* 41:4, pp. 194-199, 1998.

Nedwed, T., J.R. Clark, G.P. Canevari, and R. Belore, "New Dispersant Delivered as a Gel," in *Proceedings of 2008 International Oil Spill Conference*, American Petroleum Institute, Washington, D.C., 2008.

Singer, M.M., S. George, S. Jacobson, I. Lee, L.L. Weetman, R.S. Tjeerdema, and M.L. Sowby, "Comparison of Acute Aquatic Effects of the Oil Dispersant Corexit 9500 with Those of Other Corexit Series Dispersants", *Ecotoxicology and Environmental Safety,* 35: pp. 183-189, 1996.

Teske, M.E., and H.W. Thistle, "A Simulation of Release Height and Wind Speed Effects for Drift Minimization", *Trans. ASAE,* 42:3, pp. 583-591, 1999.

Teske, M.E., H.W. Thistle, and G.G. Ice, "Technical Advances in Modeling Aerially Applied Sprays", *Trans. ASAE,* 46:4, pp. 985-996, 2003.

Teske, M.E., H.W. Thistle, and R.E. Mickle. "Modeling Finer Droplet Aerial Spray Drift and Deposition", *Appl. Eng. Agri.,* 16:4, pp. 351-357, 2000.

Trudel, B.K., R.C. Belore, A. Lewis, A. Guarino, and J. Mullin, "Determining the Viscosity Limits of Effective Chemical Dispersion: Relating Ohmsett Results to Those from Tests At-Sea", in *Proceedings of the 2005 International Oil Spill Conference*, American Petroleum Institute, Miami, FL, Manuscript #173, 15 p., 2005.

ED_001324_00000281-00001

Effects of Chemical Dispersants on Oil-Brine Interfacial Tension and Droplet Formation

Ali Khelifa
Emergencies Science and Technology Section, Science and Technology Branch
Environment Canada, Ottawa, ON, Canada
ali.khelifa@ec.gc.ca

Lily Lai Chi So
Nanotechnology Engineering, Faculty of Engineering, University of Waterloo
Waterloo, ON, Canada
lcso@engmail.uwaterloo.ca

Abstract

Oil-brine interfacial tension (IFT) plays a key role in the process of oil droplet formation following an oil spill in an aquatic environment. Theoretically, the maximur size of oil droplet that forms under turbulent mixing increases with IFT. As such, the reduction of IFT leads to the reduction of the size distribution of oil droplets. This has been recognized for many decades by the oil spill response community. However, the effects of chemical dispersants on the formation of oil droplets are not yet well understood. This paper presents the first results from a research project to establish quantitative understanding of the variations of IFT with chemical dispersant concentration and the resulting modifications to the size distribution of oil droplets unc various mixing conditions. High values of IFT were measured using a pendant drop instrument and low values of IFT were measured with a spinning drop instrument. Undisturbed oil droplets were measured in situ (in the reaction chamber) using a new high-resolution imaging setup. For the three crudes used in this study, Arabian Light (AL), Alaska North Slope (ANS), and Prudhoe Bay (PB), mixed with Corexit 9500, remarkable reduction of interfacial tension (IFT) with dispersant-to-oil ratio (DOR) wa measured. The highest reduction was obtained with ANS crude, where the IFT reducti ranged from 10^2 to about 10^7 % for DORs varying from 1:500 to 1:05. Maximum reductions of IFT were measured at a DOR of 1:20 for AL and PB crudes and at a DOI of 1:40 for ANS crude. For ANS crude, the maximum droplet size decreased from 220 μm to about 30 μm when DOR was increased from 1:500 to 1:10 under fixed mixi energy. Further research is ongoing to improve the imaging setup with the ultimate objective of establishing a correlation between IFT reduction and the observed decreas of the maximum oil droplet size.

1 Background

The application of chemical dispersant has been and, perhaps, will continue to be considered as a potential response option to oil spills in the aquatic environment. Extensive research has been conducted during the last decades to improve this method operationally. Several issues were addressed and could be classified in three categories application, effectiveness, and environmental impact (NAS, 2005). In reality, not all th questions were answered from previous studies. Decision-makers have been and are sti challenged by many fundamental questions regarding the application of chemical dispersants. For example, no agreement has been reached yet regarding the definition c the effectiveness of chemical dispersants to disperse an oil slick under given weather

and spill conditions. One common approach used in oil spill research is to relate dispersant effectiveness to the resulting diminution of oil droplet size distribution. While this approach provides an indication of some consequences of the application of chemical dispersant, it does not show explicitly the effects of dispersant on oil properties.

Size distribution of chemically dispersed oil is not a signature of the effects of chemical dispersant only. In fact, it is a result of the combined effects of chemical dispersant on oil properties and the mixing energy available at the spill site. Because these two controlling processes are completely independent, it is fundamental to isolate their effects on oil dispersion and, thus, on the definition of dispersant effectiveness. The first process relates to chemical dispersant and affects oil properties, while the second process relates to prevailing weather conditions during the oil spill and to air/seawater surface interaction present at the spill site.

The need to study the effects of these two processes on oil droplet formation and the related oil dispersion separately has many justifications. A main reason relates to the proper definition of dispersant effectiveness. A chemical dispersant may be effective in modifying the oil properties as wanted, but its application under certain sea state conditions may not be effective due to the lack of sufficient mixing. The second reason relates to the modelling of the fate and behaviour of chemically dispersed oil. Existing modelling approaches assume a constant droplet size distribution, obtained from past observations (Lunel, 1993), when dispersant is applied to oil slick. Obviously, this is not always a valid approach. As discussed above, size distribution of oil droplets is a function of the local mixing intensity and the effects of chemical dispersant on the physical properties of spilled oil, which are, as shown from previous studies and in this paper, a function of dispersant concentration and type.

The main effect of chemical dispersant on oil properties is the reduction of IFT (Rewick et al., 1980, 1981, 1984; Byford, 1982; Mackay and Houssain, 1982; Lewis et al., 1985; Clayton, 1993; Liu et al., 1995; Khelifa et al., 2007). Factors such as oil type, dispersant type, and dispersant-to-oil ratio (DOR) were identified as important factors affecting the magnitude of IFT reduction. However, extrapolation of this information to practical application, such as modelling of oil droplet formation, is still not well developed due to a poor understanding of the process and the lack of sufficient quantitative data sets. Theoretically, the maximum size of oil droplet that survives a given intensity of turbulent mixing increases with IFT as a power law function (Hinze, 1955; 1975; Li and Guarett, 1998; Khelifa et al., 2005). The reduction of IFT leads to the reduction of size distribution of oil droplets (Lewis et al., 1985). This has been recognized for decades by the oil spill response community and constituted the fundamental reason for the development of chemical dispersants. Mixing energy controls the breakup of oil slicks and large oil droplets to small droplets. After the breakup process, mixing will also control the coalescence of small droplets to form large droplets (Khelifa et al., 2004, 2005).

A research project has been initiated recently to quantify the effects of chemical dispersant on physical properties of crudes and weathered oils. First findings showed that IFT decreases rapidly even for DORs as low as 1:200 (Khelifa et al., 2007). It was also shown that the Du Noüy ring method is not appropriate to measure low values of IFT of chemically-treated oil. A new measurement approach based on the pendant drop and the spinning drop methods was developed to study effects of

ED_001324_00000281-00002

chemical dispersant on oil properties. This paper presents first results from a series of experiments aiming to establish quantitative understanding of the variations of IFT with the concentration of chemical dispersant and the resulting variations of the maximum size of oil droplets formed under various mixing conditions. Experimental procedure developed for this research is described in detail. The ultimate objective of this project is to develop a quantitative model that predicts the size distribution of chemically dispersed oil considering the reduction of IFT and the intensity of turbulent mixing as independent factors.

2 Experimental Method

The experimental method developed for this phase of the project includes several steps, as discussed in the following sub-sections. The steps include oil-dispersant sample preparation, measurement of IFT, and in-situ measurement of oil droplet size.

2.1 Oil-Dispersant Sample Preparation

The crude oils and the dispersant were stored at 15°C in 40-mL vials. The vials of crude oil were shaken for 5 min prior to sample preparation to ensure sufficient mixing of the oils. Each sample was prepared to be used within 12 hours. All sample were prepared in 7-mL vials and using the Mettler Toledo XS204 analytical balance. All sample vials were shaken for 2 min after preparation. The final volume of the samples was about 5 mL. All samples were stored at 15 °C. Prior to use, all sample vials were shaken for 2 min to ensure sufficient mixing.

2.2 Interfacial Tension Measurement

Measurements of IFT were made using the pendant drop method for IFT value greater than approximately 0.01 mN/m and using the spinning drop method for IFT values less than approximately 0.05 mN/m.

2.2.1 Pendant Drop Method

For the pendant drop method, the KSV CAM 200 Contact Angle and Surface Tension Meter with the temperature control unit measuring chamber C203W were used (Figure 1). The HAAKE DC50-K20 Refrigerated Circulator was used for temperature control. The Dickson Model SM325 Temperature Data Logger was used for temperature verification. The Hamilton 1001TPLT Threaded Plunger Syringe, KSV C209-22 gauge-22 straight needle and KSV C210 gauge-22 J-hooked needle were used to dispense the sample.

Disposable cuvettes were filled with deionized water for validation tests and with artificial seawater for oil-dispersant sample tests. For validation tests, the syringe was fitted with the gauge-22 straight needle; for oil-dispersant sample tests, the syringe was fitted with the gauge-22 J-hooked needle. Prior to making measurements for the sample of choice, the syringe and needle were rinsed three times with deionized water, acetone, hexane, and dichloromethane (DCM), allowed to dry completely, then rinsed two to three times with the sample. The syringe was carefully filled with the sample to 0.2 to 0.3 mL to ensure the absence of large air bubbles. The sample was dispensed slowly and images were taken when the sample appears as a pendant drop just before it detaches from the needle tip. Results are used to calculate the mean IFT and the standard deviation.

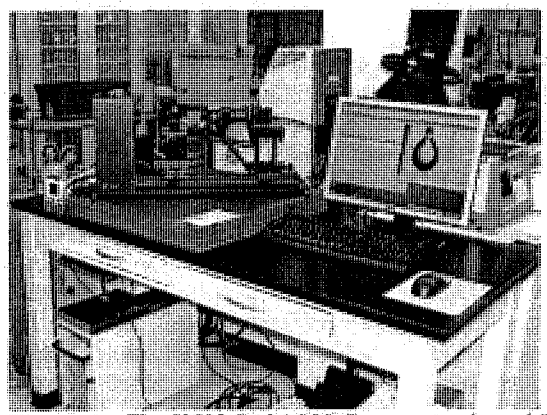

Figure 1 The KSV CAM 200 Contact Angle and Surface Tension Meter used to measure values of oil-brine interfacial tension greater than 0.01 mN/m

2.2.2 Spinning Drop Method

For the spinning drop method, the KRÜSS Spinning Drop Tensiometer SITE100 with drop shape analysis software DSA2 was used (Figure 2). The Polyscience 9102A11B Circulator was used for temperature control. The SITE100 was used for temperature verification. The Hamilton Model 701 10-μL syringe was used to inject the sample into the SITE100 capillary tube.

Prior to measurements, the syringe and needle were rinsed three times with deionized water, acetone, hexane, and DCM, allowed to dry completely, then rinsed two to three times with the sample. The syringe was carefully filled with the sample to 1 to 2 μL to ensure the absence of air bubbles and the same volume of sample was injected into the SITE100 capillary. Depending on the sample, the capillary may be stationary or rotating when the sample is injected and the rotation speed may also vary. Measurements of IFT were taken as soon as the drop elongation was stable. Each test was repeated at least three times. Results are used to calculate the mean IFT and the standard deviation.

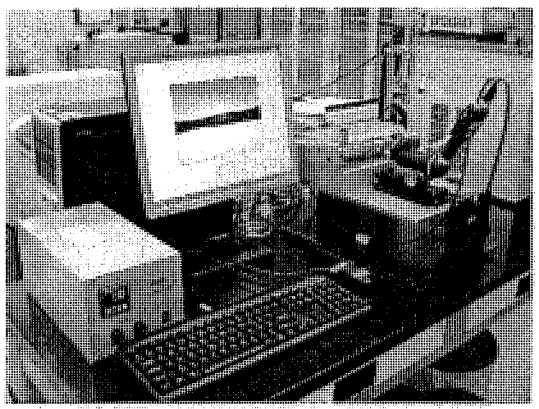

Figure 2 The KRÜSS Spinning Drop Tensiometer SITE100 used to measure small values of chemically treated oil-brine interfacial tension

ED_001324_00000281-00003

2.3 Oil-Dispersant-Seawater Mixing Procedure

The New Brunswick Scientific Gyrotory Shaker Model G2 (orbital) was used mix oil-dispersant samples in 125-mL Erlenmeyer flasks filled with 80 mL of artificial seawater (salinity 33‰). All tests were performed in a cold room at a fixed temperature of 15°C. The flasks were cleaned with filtered water, acetone, hexane, and DCM three times, and then allowed to dry completely prior to each test.

The volume of oil-dispersant samples used was calculated to ensure that a constant volume of oil was dispensed into each Erlenmeyer flask. For this study, thi volume was set to 40 μL for 1:500 dispersant-to-oil ratio (DOR) and to 16 μL for smaller DORs, based on preliminary testing. The reaction chamber was first filled with seawater and then allowed to shake for approximately 1 min prior to the injection of the sample. Immediately after injection of the sample, parafilm was use to cover the flask to prevent evaporation of the sample. The shaking speed was kept constant in this study at 2.5 Hz (or 150 rpm).

2.4 Oil Droplet Size Measurement

In the previous study, Epi-fluorescence microscopy was used to image oil droplets from a haemocytometer slide. While this method has the advantage of imaging very small droplets (less than 1 μm in size), it has two disadvantages. One disadvantage relates to the restriction of using a small sampling volume and anothe to the necessity to physically sample and disturb the oil-dispersant-seawater mixtur in the reaction chamber. These two limitations may have significant impact on the size distribution of measured oil droplets.

A new procedure was developed to measure oil droplet size distribution witho any physical sampling of the oil-dispersant-seawater mixture. This procedure is bas on imaging oil droplets from the reaction chamber directly while shaking. As show in Figure 3, a camera was placed on the shaker to eliminate relative motion betwee the reaction chamber and the camera. The imaging setup also includes a backlight, which is fixed onto the shaker. Extensive testing was performed on the selection of the camera and the related accessories to obtain sufficient magnification and good quality of the images. Results discussed in this paper were obtained by using a Nik D200 Digital Single-Lens Reflex (DSLR) camera with AF Micro Nikkor 105-mm 1:2.8 D lens, Nikon 4T Close-up lens, and Nikon 3T Close-up lens. The camera settings used in this study are listed in Table 1. The smallest droplet that can be imaged using this setup is about 5 μm in diameter.

For each test, two series of images were taken. A first series of 20 images wa taken at a rate of 5 frames per second (fps) immediately after dispensing the oil-dispersant sample into the reaction chamber. This series of images aimed to capture the breakup process of the oil-dispersant slick introduced at the free water surface. After 15 min of shaking, a second series of images was taken at a fixed rate of 1 fp to measure the droplet size distribution while the shaker is shaking and without disturbing the droplet population. All images were taken in a dark room with only a backlight to illuminate the flask. For each test, 60 images were taken and analyzed using an image analysis program developed on Matlab platform and Image Toolbo (Khelifa et al., 2007).

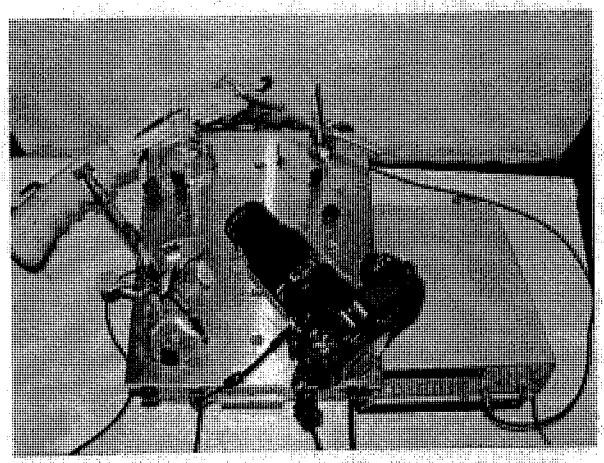

Figure 3 New imaging setup used to measure size distribution of oil droplets directly from the reaction chamber (125-mL Erlenmeyer flask) while shaking

Table 1 **Nikon D200 Digital Single-Lens Reflex Camera Settings**

Image Quality	JPEG Fine
Image Size	3872 by 2592 pixels
Lenses	Micro Nikkor 105 mm 1:2.8 D lens Nikon 4T Close-up lens Nikon 3T Close-up lens
Focus	Manual
Settings	Exposure Mode
Aperture	F 18
Shutter Speed	1/2500
ISO	High 1.0 with High ISO Noise Reduction
White Balance	8300 K

2.5 Experimental Conditions

Alaska North Slope (ANS), Arabian Light (AL), and Prudhoe Bay (PB) fresh crude oils were used to study the reduction of interfacial tension (IFT) with dispersant-to-oil ratio (DOR). Only ANS crude was used to study the variations of oil droplet size with DOR. The chemical dispersant used was Corexit 9500. DOR was varied from 0 to pure dispersant using 20 intermediate values, as shown in Table 2. Detailed description of the physical and chemical properties of the three oils is available on the Environment Canada Oil Properties web site (Environment Canada, 2008).

3 Results and Discussion

Results discussed in the following sub-sections include variations of IFT with DOR, illustration of initial dispersion of oil slick, and size distribution of dispersed oil droplets.

Table 2 Measured values of oil-brine interfacial tension for different DORs and the three crude oils. Measurements were performed with the spinning d instrument, except for small values of DOR where the pendant drop instrument was used (rows marked with "*" in the first column). Value reported in the table are in mN/m.

DOR \ Oil	AL	ANS	PB
Oil only *	18.32	21.50	28.55
1:500 *	4.92	12.01	10.05
1:200 *	1.51	4.29	2.09
1:150 *	-	2.07	-
1:125 *	2.69E-01	9.85E-01	1.48E-01
1:100 *	2.35E-02	1.77E-01	2.38E-02
1:95	-	2.36E-02	-
1:90	-	6.17E-03	-
1:80	-	2.71E-03	-
1:70	4.68E-03	1.58E-03	4.69E-03
1:60	-	4.37E-04	-
1:50	2.93E-03	2.83E-04	2.81E-03
1:40	2.29E-03	2.18E-04	1.36E-03
1:30	1.29E-03	2.27E-04	3.85E-04
1:20	6.50E-04	2.31E-04	3.36E-04
1:15	7.24E-04	3.61E-04	4.67E-04
1:10	8.17E-04	5.37E-04	7.43E-04
1:7.5	9.11E-04	9.05E-04	1.33E-03
1:5	1.14E-03	4.20E-03	2.71E-03
1:2.5	3.11E-03	7.86E-03	4.35E-03
1:1	6.46E-03	1.32E-02	7.15E-03
Corexit 9500 only	1.04E-02	1.04E-02	1.04E-02

3.1 Variations of Interfacial Tension (IFT) with Dispersant-to-oil Ratio (DO

Measured variations of IFT with DOR are shown in Figure 4. The corresponding numerical values are reported in Table 2. Results showed remarkab reduction of IFT with DOR for the three crudes. The overall trend shown by the th series of data is a rapid decrease of IFT with DOR until it reaches a minimum and then increases to reach a value close to the Corexit 9500-brine IFT. A similar trenc was reported by Liu et al. (1995). However, the data do not support the exponentia trend proposed by Mackay and Houssain (1982).

The reduction of IFT with DOR was calculated from data shown in Table 2 using the following equation:

$$IFT_{Red} = 100 \times \left(IFT_{Oil} - IFT_{Oil-CD}\right) / IFT_{Oil-CD}$$

where IFT_{Red} represents the reduction of IFT in %, IFT_{oil} is the oil-brine IFT witho chemical dispersant, and IFT_{oil-CD} is the oil-brine IFT with chemical dispersant.

Reduction of IFT varies between about 3×10^2 and 2.8×10^6 % for AL crude, 1×10^2 and 9.8×10^6 % for ANS crude, and 1×10^2 and 8.5×10^6 % for PB crude. For low values of DOR up to 1:100, reductions of IFT obtained with AL and PB crude

ED_001324_00000281-00004

were much higher than those obtained with ANS crude. The opposite trend was observed for higher values of dispersant-to-oil ratios (DORs) (Figure 5 and Table 3). The maximum reductions were measured at a DOR of 1:20 for AL and PB crudes and 1:40 for ANS crude. For the two different types of chemical dispersants employed (referred to as No. 2 and No. 4 in their article), Liu et al. (1995) measured a maximum reduction of IFT at a DOR of 6% (or 1:17), while for the two other chemical dispersants they studied (No. 1 and No. 3), they measured a monotonous decrease of IFT with DOR. The DOR value at which the IFT reached a maximum reduction (1:20 and 1:40 in this study and about 1:17 in Liu et al., 1995) is considered to be the approximate critical micelle concentration (CMC) of the chemical dispersant. This concentration is a function of chemical dispersant type and solubility, oil type, and oil-to-water ratio, but very little is known on how this concentration varies with oil type and dispersant type.

Mackay and Houssain (1982) estimated (assuming exponential decay of IFT with DOR) that a DOR of 1:500 for Corexit 9527 is sufficient to reduce the IFT of various crude oils by 20-fold. This estimation is about 7 to 20 times higher than the measured values shown in Table 3 for the three crudes. Liu et al. (1995) measured about a 1000-fold reduction in IFT when DOR increases from 1:200 to 1:10. Measurements shown in Table 3 are about 2 to 10 times higher than this value. For a DORs as low as 1:100, the reduction of IFT was about 7.8×10^4 % for AL oil, 1.2×10^4 % for ANS oil, and 12.0×10^4 % for PB oil (Table 3). The data showed that the reduction of IFT with DOR depends on the type of crude oil.

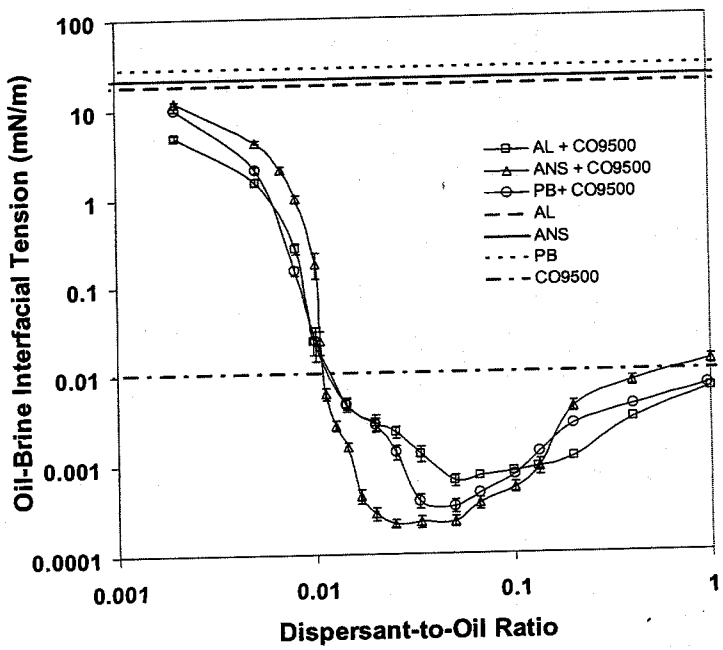

Figure 4 Measured variations of oil-brine interfacial tension with dispersant concentration (in DOR) for the three crude oils. The bars shown with each data point represent ± one standard deviation.

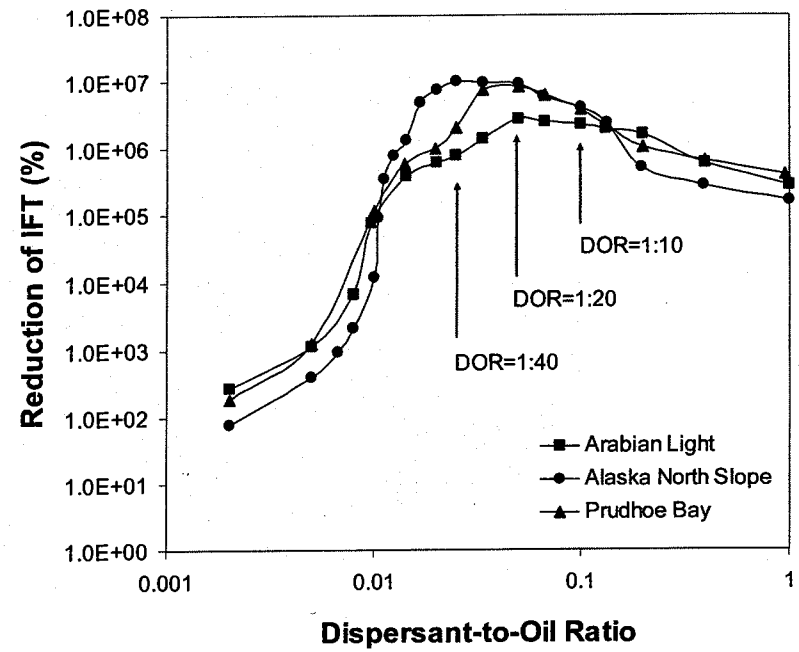

Figure 5 Reduction of oil-brine interfacial tension (equation 1) with dispersant concentration (in DOR) for the three crude oils

Table 3 Measured reduction of oil-brine interfacial tension (equation 1) for different DORs obtained with the three crude oils. The values of the highest reduction are shown in bold text.

DOR \ Oil	AL	ANS	PB
1:500	$3\ 10^2$	$1\ 10^2$	$2\ 10^2$
1:200	$11\ 10^2$	$4\ 10^2$	$13\ 10^2$
1:100	$7.8\ 10^4$	$1.2\ 10^4$	$12.0\ 10^4$
1:40	$0.8\ 10^6$	**$9.8\ 10^6$**	$2.1\ 10^6$
1:20	**$2.8\ 10^6$**	$9.3\ 10^6$	**$8.5\ 10^6$**
1:10	$2.2\ 10^6$	$4.0\ 10^6$	$3.8\ 10^6$

3.2 Initial Dispersion

As mentioned in Section 2.4, for each test, a series of 20 images was taken at rate of 5 fps immediately after dispensing the oil-dispersant sample into the reaction chamber. This series of images aimed to image the breakup process of the oil-dispersant slick introduced at the free water surface. The process that controls initia dispersion of the slick appears to be much influenced by the concentration of dispersant (DOR). As shown in Figure 6, the slick splits into small and large drople for DORs up to about 1:100 (Figure 6a and b). At a DOR of 1:60, the dispersion is dominated by the formation of elongated oil filaments that break up later on to sma oil droplets (Figure 6c). With further increase in DOR, the formation of dark cloud

ED_001324_00000281-00005

becomes dominant, along with the formation of dispersed small droplets (Figures 6d, e, and f). The turbidity of the water increases significantly and rapidly. Instead of splitting the slick into discrete oil droplets, the formation of clouds, which appears similar to a dissolution process, was observed. The process merits further investigation using a higher resolution imaging setup.

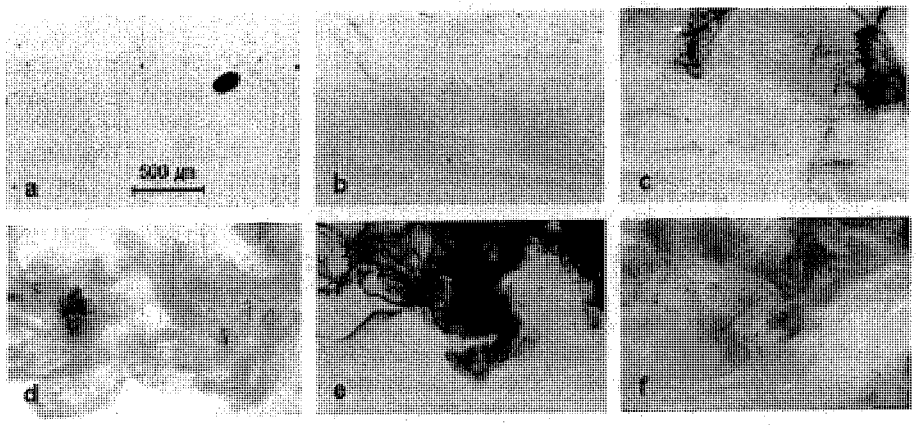

Figure 6 Images of the oil dispersion process during the first few seconds of mixing for DOR=1:200 (a), 1:100 (b), 1:60 (c), 1:20 (d), 1:10 (e), and 1:05 (f). The scale shown on image (a) applies to all images.

3.3 Size Distribution of Dispersed Oil Droplets

As mentioned in Section 2.4, the measurement of droplet size was based on the analysis of several images of oil droplets taken with the DSLR camera while the reaction chamber was shaking. Samples of these images are shown in Figure 7. Systematic decrease in droplet size and increase of their concentration is shown. The smallest droplet population is obtained at a DOR of 1:10. This is slightly different than what was found in a previous study (Khelifa et al., 2007) where a DOR of 1:20 was found to produce the smallest droplets using the same oil (ANS), but at a much higher mixing energy (using a reciprocating shaker). Mixing energy in this study was relatively low (using an orbital shaker) without significant disturbance of the water surface as with the reciprocating shaker. No droplets were formed with crude oil only (no chemical dispersant). However, formation of oil droplets started with a DOR as low as 1:500.

For each test, 60 images were analyzed to measure droplet size distribution. As expected, results show direct correlation between droplet size and DOR, except for DORs above the critical micelle concentration (CMC) where the size of dispersed oil droplets start to increase with DOR (Figure 8). For comparison, two droplet size distributions obtained from a Sea Trial reported by Lunel (1993) are also shown in Figure 8. There is a good qualitative similarity between the size distributions and the field data. For Lunel's data, the DOR at sea is not well defined and the type of dispersant used was different from Corexit 9500. However, Lunel's data are within the size range obtained in this study.

ED_001324_00000281-00006

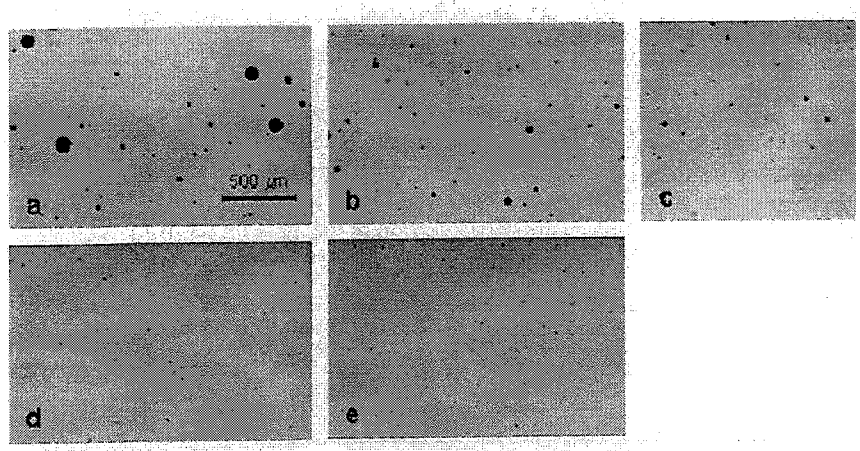

Figure 7 Images of dispersed oil droplets taken with the DSLR camera in the reaction chamber after 15 minutes of shaking for DOR=1:500 (a); 1:90 (b) 1:60 (c); 1:10 (d); and 1:5 (e). The scale shown on image (a) applies to all images. The experiments were performed with ANS crude and Corexit 9500.

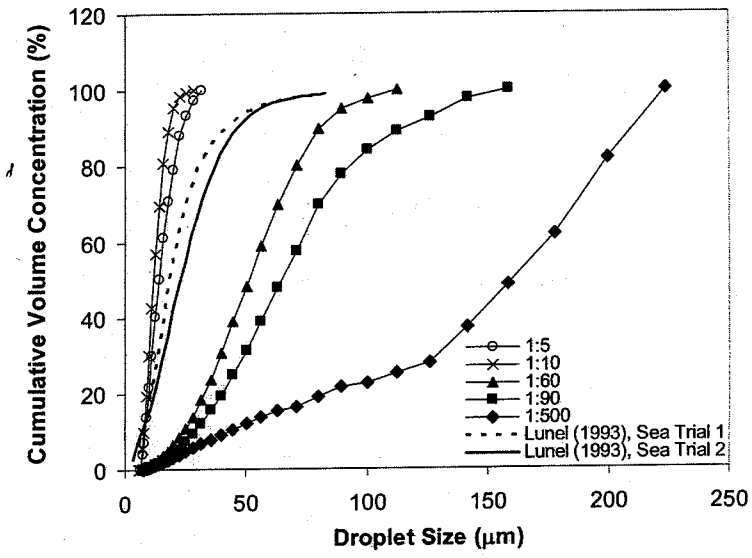

Figure 8 Distribution of droplet size measured from DSLR camera images using image analysis. The experiments were conducted with ANS crude and Corexit 9500 at different dispersant-to-oil ratios (DORs). The solid and dashed lines without symbols represent droplet size distributions obtained from Sea Trials as reported by Lunel (1993).

Size distribution obtained with the lowest dispersant-to-oil ratio (DOR) of 1:500 is somewhat different in shape than the other distributions. This difference is likely related to the limited number of droplets (larger size and less abundant than the other DORs) used to measure their size distribution. In terms of the maximum size, the data showed a strong effect of DOR, as shown in Figure 9. Measured maximum size decreases from about 220 μm to 30 μm when DOR increases from 1:500 to 1:10. Additional experiments using an improved version of the imaging setup are ongoing to validate the trend shown in Figure 9, especially at high DORs.

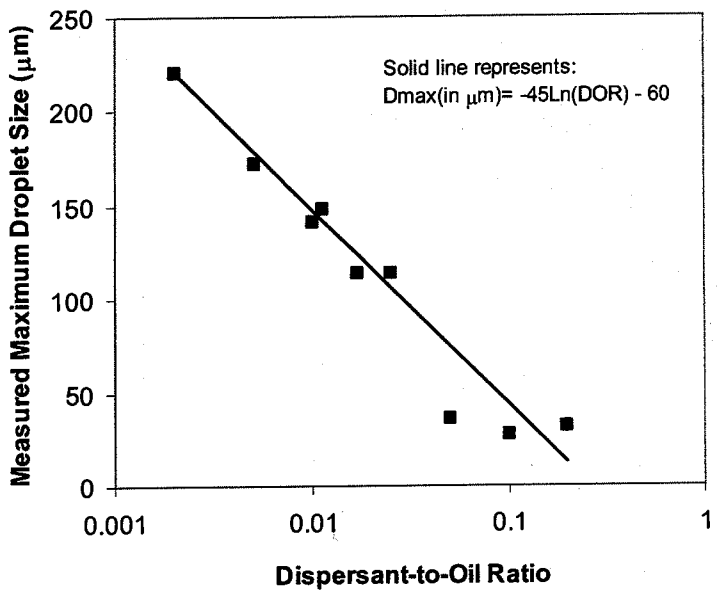

Figure 9 Maximum droplet size measured from DSLR camera images using image analysis. The experiments were conducted with ANS crude and Corexit 9500 at different DORs.

4 Conclusion

This paper discussed the first part of an ongoing R&D project aimed at providing further quantitative understanding of oil dispersion. Findings showed that the approach of separating the direct effects of chemical dispersants on oil properties, specifically oil-brine interfacial tension and the effects of mixing on dispersion of chemically treated oil, is valid. Under constant mixing conditions, the reduction of the maximum oil droplet size that overcomes the breakage process is dictated by the effects of chemical dispersant on oil properties. It correlates well with the dispersant-to-oil ratio (DOR) up to the critical micelle concentration (CMC). This good correlation is due to the reduction of interfacial tension (IFT) with DOR, as stated in most of the existing theories. As such, it appears that the reduction of IFT with dispersant concentration is an additional signature of oil composition on droplet formation, while mixing energy remains an external parameter completely independent of oil properties.

ED_001324_00000281-00007

The next steps of the project are: 1) to establish the best relationship betwee the maximum size of oil droplets and the measured IFT at different DORs and foı different levels of oil weathering and 2) to study the variations of oil droplet size mixing energy using an improved version of the imaging setup discussed in this paper. This setup has provided very encouraging results.

5 Acknowledgements

The authors would like to thank Benjamin Fieldhouse, Bruce Hollebone, M Landriault, and Lloyd Gamble of the Emergencies Science and Technology Secti (ESTS) for their technical help in conducting this research. Many thanks also to Jennifer Charles, Natalie Jones, and Patrick Lambert of ESTS for their valuable ii during the preparation of this paper.

6 References

Byford, D.C., "The Development of Dispersants for Applications at Low Temperatures", in *Proceedings of the Fifth Arctic and Marine Oilspill Program (AMOP) Technical Seminar*, Environment Canada, Ottawa, ON, Canada, pp. 239 254, 1982.

Clayton, J.R., J.R. Payne, and J.S. Farlow, *Oil Spill Dispersants: Mechanisms of Action and Laboratory Tests*, CRC Press, Boca Raton, FL, p. 103, 1993.

Environment Canada, "Oil Properties Database", http://www.etc-cte.ec.gc.ca/databases/OilProperties/oil_prop_e.html, 2008.

Hinze, J.O., *Turbulence*, 2nd Ed., McGraw-Hill, New York, NY, 790 p., 1975.

Hinze, J.O., "Fundamentals of the Hydrodynamic Mechanism of Splitting in Dispersion Processes", *AIChE Journal*, 8 (4), pp. 289-295, 1955.

Khelifa, A., M.F. Fingas, B.P. Hollebone, and C.E. Brown, "Effects of Chemical Dispersants on Oil Physical Properties and Dispersion", in *Proceedings of the Th Arctic and Marine Oilspill Program (AMOP) Technical Seminar*, Environment C Ottawa, ON, Canada, pp. 105-116, 2007.

Khelifa, A., P.S. Hill, and K. Lee, "A Comprehensive Numerical Approach to Pre Oil-Mineral Aggregate (OMA) Formation following Oil Spills in Aquatic Environments", in *Proceedings of the 2005 International Oil Spill Conference*, American Petroleum Institute, Washington D.C., paper # 214, 2005.

Khelifa, A., P.S. Hill, and K. Lee, "Prediction of Oil Droplet Size Distribution in Agitated Aquatic Environments", in *Proceedings of the Twenty-seventh Arctic ar Marine Oilspill Program (AMOP) Technical Seminar*, Environment Canada, Otta ON, Canada, pp. 371-382, 2004.

Lewis, A., D.C. Byford, and P.R. Laskey, "The Significance of Dispersed Oil Dro Size in Determining Dispersant Effectiveness Under Various Conditions", in *Proceedings of the 1985 International Oil Spill Conference*, American Petroleum Institute, Washington D.C., pp. 433-440, 1985.

Li, M., and C. Garrett, "The Relationship Between Oil Droplet Size and Upper O Turbulence", *Marine Pollution Bulletin*, 36 (12), pp. 961-970, 1998.

Liu, H., Y. Zhang, and W. Wang, "Interfacial Properties of Oil Spill Dispersants and their Effects on Dispersion Effectiveness", *Acta Oceanologica Sinica*, pp. 587-593, 1995.

Lunel, T., "Dispersion: Oil Droplet Size Measurements at Sea", in *Proceedings 1993 Oil Spill Conference*, American Petroleum Institute, Tampa, FL, pp. 794-795, 1993.

Mackay, D. and K. Houssain, "Oil-Water Interfacial Tensions in Chemical Dispersant", Manuscript Report EE-32, Environmental Protection Service, Environment Canada, Ottawa, ON, 17 p., 1982.

NAS, *Oil Spill Dispersants: Efficacy and Effects,* National Academy of Sciences, Washington, D.C., 330 p. and Annexes, 2005.

Rewick, R.T., K.A. Sabo, and J.H. Smith, "The Drop-weight Interfacial Tension Method for Predicting Dispersant Performance", *Oil Spill Chemical Dispersants: Research, Experience, and Recommendations*, T.E. Allen (ed.), ASTM STP 840, American Society for Testing Materials, Philadelphia, PA, pp. 94-107, 1984.

Rewick, R.T., K.A. Sabo, J. Gates, J.H. Smith, and L.T. McCarthy, "An Evaluation of Oil Spill Dispersant Testing Requirements", in *Proceedings of the 1981 International Oil Spill Conference*, Atlanta, GA, American Petroleum Institute, pp. 5-10, 1981.

Rewick, R.T., J. Gates, and J.H. Smith, "Simple Test of Dispersant Effectiveness based on Interfacial Tension Measurements, *Fuel*, Vol. 59(4), pp. 263-265, 1980.

ED_001324_00000281-00008

Updating the U.S. SMART Dispersant Efficacy Monitoring Protocol

Ken Trudel and Randy Belore
S.L. Ross Environmental Research
Ottawa, ON, Canada
ken@slross.com

Mark VanHaverbeke
United States Coast Guard Research and Development Center,
Groton, CT, United States

Joseph Mullin
Oil Spill Response Research, Minerals Management Service
Herndon, VA, United States

Abstract

A review of the SMART dispersant effectiveness monitoring protocol was undertaken 2007-8, involving three tasks. First, a stakeholders' workshop was held to recommend revisio SMART based on practical experience. This concluded that the three-tiered approach in SMA was appropriate, but: a) better guidance must be provided for users; b) the fluorometer histori used for monitoring of dispersed oil poses many operating challenges and should be replaced more modern instrument; and c) all U.S. government-sponsored monitoring teams must work identical instruments and operating protocols. The workshop also developed a list of characte for the new oil-analytical instrument and recommended a process for transitioning from the ol new protocol.

Second, oil behaviour monitoring data from recent OHMSETT dispersant effectivenes was analysed to verify the reliability of the SMART monitoring methods. Under SMART, instrumental methods involve comparing oil concentrations measured at a single depth under and untreated sections of the slick (SMART Ratio). Based on Ohmsett dispersant test data, th SMART Ratio was highly variable and was a poor indicator of effectiveness. On the other ha assessments based on a combination of oil concentration and oil particle size were strongly correlated with effectiveness. Specifically, when elevated oil concentrations occurred under sl the size of droplets causing the elevated oil concentration was an unambiguous indicator of effectiveness, with large droplets (VMD >83 μm) indicating low effectiveness and small drop (VMD< 83 μm) indicating high effectiveness.

Finally, commercially available, field portable instruments for measuring dispersed oil water were surveyed. The survey identified six potentially suitable submersible and field-port fluorometers and three particle-size analysers and reported key technical information for each.

1 Introduction

Effectiveness monitoring is a critical component of dispersant operations. In the Unite States in the mid 1990s, agencies developed a written dispersant effectiveness monitoring pro entitled "Special Monitoring of Applied Response Technologies (SMART)" (USCG et al., 20 and its forerunner, "Special Response Operations Monitoring Program (SROMP)[1]" (NOAA H

[1]In 1993, CAPT James Calhoun (District Chief, USCG 8th District) tasked NOAA (NOAA Scientific Support Coordinator, CDR Mike Barnhill) and the USCG Gulf Strike Team to develop a non-industry-based dispersant monitoring protocol. Barnhill, working with Charlie Henry (Louisiana State University) and members of the Gul Atlantic Strike Teams developed a two-tiered monitoring system based on visual observation and continuous in- water monitoring, called "Special Response Operations Monitoring Program" or SROMP.

2009

32nd
MOP
chnical
minar

MOP

32e
lloque
nique
de
MOP

l. 1

Volume 1

Proceedings of the Thirty-second AMOP Technical Sem on Environmental Contamination and Response

Compte rendu du trente-deuxième Colloque techniqu de l'AMOP - Contamination de l'environnement et intervention

June 9 - 11 juin 2009
Vancouver (British Columbia/Colombie-Britannique) Ca

Environment Canada Environnement Canada

Canac

ED_001324_00000281-00009

244 Evaluation of Sorbent and Solidifier Properties and their Impact on Oil Removal Efficiency

D. Sundaravadivelu
Student

Additional evaluation of sorbents and solidifiers is needed in order to increase confidence in their use for containment of oil spills. The primary focus of this project was to compare the oil removal efficiency of natural and polymeric sorbents as well as solidifiers under different environmental conditions. The physical/chemical characteristics of products were also studied and correlation of these properties with effectiveness enabled identification of characteristics that resulted in high oil uptake. Products with lower bulk powder density and large pores size had the highest oil removal efficiency. Natural sorbents, polymeric solidifiers, and polymeric sorbents had bulk densities of 0.14, 0.18-0.27, and 0.25-0.62 g cm-3, respectively. This resulted in removal efficiencies of 90, 87-65 and 40-12% for the corresponding products. Analysis of experimental data yielded empirical correlations involving certain operational variables such as application rate, product bulk density, and oil viscosity. The type of product used in a sorbent boom could greatly affect its performance. Since bulk density is a readily available measurement and can provide an approximation of product efficacy, these results could aid in evaluating and choosing high performance construction material for booms used in oil spill remediation.

266 Subsea oil plume simulations: Tracking oil droplet size distribution and fluorescence within high release jets

R. N. Conmy

Optical measurements have been used during oil spill response for more than three decades to determine oil presence in slicks and plumes. Oil surveillance ranges from simple (human eyeball) to the sophisticated (sensors on AUVs, aircraft, satellites). In situ fluorometers and particle size analyzers were deployed during the Deepwater Horizon (DWH) Gulf of Mexico oil spill to track shallow and deep subsea plumes. Uncertainties regarding instrument specifications and capabilities necessitated performance testing of sensors exposed to simulated, dispersed oil plumes. Presented here are results of 72 wave tank experiments conducted at the Bedford Institute of Oceanography. Examined were simulations of subsea releases with varying parameters such as oil release rate, oil temperature (reservoir temp ~ 80 ^oC), water temperature (<8 ^oC and >15 ^oC), oil type, dispersant type (Corexit 9500 and Finasol OSR52) and dispersant to oil ratio (DOR). Plumes of Alaskan North Slope Crude, South Louisiana Crude and IFO-120 were tracked using in situ fluorescence, droplet size distribution (DSD; LISST 100X), total petroleum hydrocarbons (TPH), benzene-toluene-ethylbenzene-xylene (BTEX) and excitation-emission matrix spectroscopy. Results offer valuable information on the behavior and dispersibility of oils over a range of viscosity and composition. Findings have implications for fate & transport models, where DSD, chemistry and fluorescence are all impacted by release variables. Research supported by the Bureau of Safety and Environmental Enforcement.

267 Simulation of Oil Dispersion under Breaking Waves

Z. Wei, R. A. Dalrymple, C. Li, J. Katz;
Johns Hopkins University, Baltimore, MD.

Water waves play an important role in the dispersal of oil in the water column and the transport of oil droplets across the air-sea interface. Although numerical studies of oil transport due to non-breaking waves were reported in literature, existing research on oil dispersion under breaking waves is still very limited. The primary focus of this study is to replicate and further analyze a oil dispersion under

breaking waves laboratory experiment, which was conducted in Department of Mechanical Engineering at Johns Hopkins University by Li & Katz, by using a mesh-free Smoothed Particle Hydrodynamics model, GPUSPH. The waves in the laboratory were generated by a piston wave maker driven by different trajectories, resulting in both spilling and plunging breakers. We first validate our numerical model by comparing the breaking wave profile with the laboratory measurements, including water surface snapshots and time-series free surface profiles at individual wave gauges. Then we investigate the impact of breaking wave forcing on oil dispersion by placing a very thin layer of oil under the waves. It is seen that: (1) qualitative agreements on the distribution of oil droplets along the water column are obtained by the numerical model, and (2) the transport of oil droplets is also influenced by the breaking wave patterns (e.g., spilling and plunging breakers). Finally, we apply the model to examine the oil dispersion difference due to the interfacial tension forces, which are varying among different types of oils.

290 Overview of the American Petroleum Institute (API) Joint Industry Task Force Subsea Dispersant Injection Project

T. Nedwed;
ExxonMobil, Houston, TX.

Oil spill response is a challenging task, especially in the case of deep water well releases. The efficiency of mechanical recovery equipment deployed at the sea surface may be reduced due to low oil encounter rates as a result of minimum oil thickness after oil slick spreading. In-situ burning may also have similar limitations. The ability to use dispersants as an oil spill response option could provide significant benefits when other response techniques have reduced efficiency. Subsea injection of dispersants offers some significant benefits for oil spill response, including access to the freshest and non-emulsified oil in a high turbulence environment, ability to reduce the volume of required dispersant by injecting it directly into the oil stream, ability to operate day and night under a wider range of weather conditions, and availability of a large water volume to rapidly decrease the concentration of a dispersed oil plume. The American Petroleum Institute has sponsored research on subsea dispersant injection for over 4 years. Project teams are looking into subsea dispersant injection effectiveness, fate and effects, subsea plume monitoring, and numerical modeling. As a result of this research, the body of knowledge regarding subsea dispersant injection has grown. Laboratory studies have demonstrated the utility of directly injecting dispersants at the source of a blowout. Work has begun to understand the biodegradation potential and toxicity of a subsea plume to deep water organisms. Additionally, progress has been made on enhancing numerical models to predict the fate of oil dispersed subsea. This presentation provides an update of the recent progress made on this research.

325 Dispersant-to-Oil Ratio and Temperature Limitations on Droplet Size Distribution in a Subsurface Oil Release

B. J. Robinson

The fate and behaviour of oil from a subsurface release was studied in a 32 m rectangular flume tank that is capable of producing current velocities of up to 5 cm/s. A series of experiments were conducted using four oil products (SLC, ANS, IFO 120, and gas condensate) and two dispersants (Corexit 9500 and Finasol OSR 52) at various dispersant-to-oil ratios (DOR: 0, 1:20, 1:100, and 1:200). Oil or oil/dispersant premixes were released into the tank using a subsurface injection system to investigate the effects of DOR and water temperature on oil droplet size distributions (DSD) measured using LISST-100x particle size analyzers. For all oil products except IFO-120, a DOR of 1:20 produced DSD plots that were bimodal shaped and the majority of the droplets were < 70 µm in size. The two dispersants, applied at DORs of

1:100 and 1:200, produced similar DSD patterns in most cases, with the exception of IFO 120. The effects of water temperature were most notable in the IFO 120 treatment, the more viscous oil. Without dispersant application, the DSD pattern revealed droplet sizes >70 µm for all oil products, where most of the submerged oil rose to the water surface. Small but non-negligible differences were observed in the dispersed oil DSD generated by the two different dispersants.

339 Experimental Determination of Oil Droplet Size Distribution in "Live Oil" under Artificial Deep Sea Conditions

K. Malone
Student

In the past years, many experiments and numerical simulations have been conducted in order to determine the oil droplet size distribution of a deep sea blowout. Though there is by now a sound understanding of the evolving size distribution of a jet of pure, "dead" crude oil, the influence of the large amounts of gasses dissolved in the oil on the droplet formation as well as the influence of high pressure is neglected in almost all experimental approaches known to date. To cover this issue, experiments were conducted the high pressure labs at the Institute of Product Development and Mechanical Engineering Design (Hamburg University of Technology) where the droplet size distribution of a "live" oil jet entering into seawater was determined under artificial deep sea conditions (high pressure up to 150 bar). The live oil consisted of Louisiana Sweet Crude oil previously saturated with methane at 160 bar. Droplet size distributions were analyzed using an endoscopic high-definition camera system. Oil droplet size distributions determined in these experiments are presented and compared to similar experiments with "dead" oil. Possible mechanisms of drop formation influenced by the dissolved methane are discussed. Preliminary results suggest that the pressure drop at the vent, which has been estimated to have been around 86 bar (1250 psi) over the DwH Blowout Preventer, might strongly influence the final droplet size in live oil while having a neglectable influence on dead oil. This research was made possible by a grant from BP/The Gulf of Mexico Research Initiative, C-IMAGE

341 Oil Droplet Formation and Effectiveness of Subsea Dispersant Injection as a Function of Hydrostatic Pressure

P. Brandvik

Experimental work described in this presentation was performed in two specialised facilities for studying subsurface releases of oil. Oil and gas were released from the base of a tower basin and oil droplets and gas bubbles were monitored by novel particle imaging techniques (Silhouette camera). The shift in oil droplets sizes towards smaller sizes was used to quantify the effect of SSDI (Subsea Dispersant Injection). The main objective of these experiments was to study possible pressure dependency of initial droplet formation and the SSDI. The first facility consists of a six meter high tower basin containing 42 000 Litres of natural sea water and is located at SINTEF in Trondheim, Norway. All experiments in this facility are performed at near ambient conditions (6 m depth). Parallel studies have been performed in a hyperbaric chamber with similar dimensions at SouthWest Research Institute (SwRI) in San Antonio, TX, USA. Comprehensive data generated at both SINTEF and SwRI will be presented and discussed. Oil droplets from comparable experiments (nozzle, oil type, flow rates, injection techniques and dispersant dosages & product) at ambient and high pressure conditions show no significant difference in sizes as a function of pressure (ambient and 175 bar or 1750 meter depth). This lack of a pressure effect was observed for both formation of large droplets from untreated oil and formation of smaller droplets by dispersant injection (1 and 2% dispersant dosage). These experiments

were performed in February 2015 and were focusing on oil droplet formation versus pressure and the effectiveness of dispersants injection. Combined releases of both oil and gas (LNG) under similar pressure conditions and dispersant injection are planned for October 2015. Initial results from these experiments might also be included in this presentation. This study was funded by the American Petroleum Institute.

369 An Oil Droplet Size Model under Subsurface Blowout Release Conditions including Application of Chemical Dispersants

Z. Li

Accurate simulation of oil droplet size distribution is of critical importance in oil spill fate and transport modeling. A novel oil droplet size model was developed that estimates oil droplet size distributions under subsurface blowout release conditions (with or without dispersant application). The oil droplet size prediction formula was developed based on non-dimensional analysis of the balance of the oil dispersion forces and the restorative forces. This new universal oil droplet size model was calibrated and validated with available oil droplet size distribution data based on comprehensive review and synthesis of available data and literature. The dispersant treated and non-treated oil droplet size data were obtained from both controlled laboratory experimental studies, such as the API- and BSEE-supported subsea dispersant injection projects, and field measurements, including the Deep Spill field trial (in Norway) and Deepwater Horizon oil spill field data. Favorable comparison of the measurement data and modeling results demonstrates that the new model provides a robust algorithm to predict blowout release oil droplet size distributions that can be used in subsequent oil fate and transport modeling.

404 Impacts of Waves on Particulate and Gaseous Emissions from Oil and Oil-Dispersant Contaminated Sea Waters

N. Afshar-Mohajer, K. Koehler, A. Rule, C. Li, J. Katz;
Johns Hopkins University, Baltimore, MD.

Crude oil spill incidents occur frequently, leaving seawater bodies with a verity of occupational, ecological and environmental issues from the local to global scale. Application of sub- surface dispersants to the oil contaminated water in order to break up the oil into smaller droplets has been gaining popularity in recent years as an intervention strategy. However, the use of dispersants may also have impacts on the generation and transport of aerosolized droplets, as well as changes in emitted gases due when subjected to natural processes such as rains, winds and waves.
In this study, systematic real-time measurements of total VOC (TVOC), particle-bound polycyclic aromatic hydrocarbons (PAH), and aerosol size distribution from 10 nm to 20 µm were conducted over a wave tank containing seawater, seawater plus crude oil, or seawater with crude oil and dispersant. All experiments were performed in triplicate using a wave tank (L = 6 m, W = 0.3 m and D = 0.6 m) and wave generation system, and sensitivity analyses were conducted on key parameters including wave type, wave frequency, dispersant to oil ratio (DOR) and crude oil contamination concentration inside the water. Results indicated that the majority of the aerosolized particles when the wave tank contained seawater only and sea water plus oil-dispersant were smaller than 15 nm (both before and after the wave generation). However, the particle mode size for the seawater plus crude oil slick was averagely 85 nm after the wave generation. Increasing the total amount of added oil-dispersant mixture from 3.5 to 10 mL led to an approximately twofold increase in the total number concentration of nano-sized particles. No obvious changes in particle mode or median sizes for both nano- and micron-sized particles was detected, but the total number concentration of nano-sized particles increased 10 to 50% after the wave was created in all contamination case scenarios. An average of 10 times increase

in TVOC concentration was observed after contaminating the sea water by 3.5 mL oil-dispersant mixture (DOR = 1:25) compared to seawater alone. Wave creation led to another 40 times increase in TVOC concentration (~ 400 times higher than the non-contaminated calm sea water). This indicates possible formation of secondary organic aerosol (SOA) in presence of the sunlight.

415 Controlled Oil-in-Water Droplet Size Distributions via Environmentally Compatible Dispersants
Z. M. Aman

Dispersants represent a chemical pathway to control oil-in-water droplet size, where adsorbed surfactants reduce water-oil interfacial tension. In the limit of low tension, minimal shear stress is required to generate small and neutrally-buoyant oil droplets in the water column. As highlighted in recent years, the current generation of dispersants primarily use ionic surfactants to increase adsorption effectiveness, which may increase environmental toxicity with limited chemical biodegradability. The current study focuses on the use of nonionic surfactants to generate oil-in-water dispersions, with a variety of hydrophilic functional groups, including carboxylic, sulphuric and acetic. Each nonionic surfactant was added to an oil-in-water dispersion at high pressure (100 bar methane) and low temperature (4 °C). Oil droplet size distributions were measured visually in a high-pressure sapphire autoclave apparatus, captured using a 2000 fps high-resolution camera. Each surfactant was compared to cases without any dispersant, and with 0.5 and 2 wt% of an ionic dispersant. The results demonstrate that nonionic surfactants may provide a pathway to control the size distribution of oil droplets in water, with decreased environmental risk relative to their ionic counterparts.

420 Advancing technology to extend the limits of particle measurements in subsea blowouts
E. J. Davies, F. Leirvik, P. Brandvik;
SINTEF Materials and Chemistry, Trondheim, NORWAY.

Measurements of the size distribution of oil droplets, gas bubbles, or the mixture of both are of critical importance in understanding the dynamics of subsea blowouts. This is due to the well-confined relationship between the turbulent energy at the release point and the resulting droplet and bubble sizes. Accurate knowledge of the particle size distribution is therefore a key requirement for predictive oil spill models. Experiments to-date have often been restricted to a limited droplet size and concentration, governed by the available instrumentation. It has therefore been necessary to scale down laboratory simulations of subsea blowouts so that the resulting droplet size distribution and concentration falls within a measureable range. Potential scaling errors in these types of experiments have created a need for extending droplet measurements to larger sizes and higher concentrations so that more realistic experimental conditions can be simulated and documented accurately. Here we present a novel telecentric silhouette-based imaging system, specifically designed for measurements of large droplets in high concentrations. The system is configured to combat the challenges associated with conventional particle measurements, and provides both images and size distributions from within a wide depth-of-field, void of position-dependent magnification errors. The ability to select from a suite of multiple techniques (e.g. LISST-100 and LISST-Holo, together with this silhouette camera) now enables accurate in-situ particle size measurements than span diameters from 5-12000µm. We show how this new measurement capability has enabled more realistic-scale experiments to be performed, which include full-scale droplet sizes.

421 Detection and Quantification of Submerged Oil Droplets by a Broadband, High-frequency Echo Sounder

S. C. Loranger, T. C. Weber;
University of New Hampshire, Durham, NH.
Student

The evolution and fate of dispersed oil droplets in the marine environment is crucial to the development of response protocols and to the assessment of risk for areas surrounding a spill. Current models of the movement of submerged oil droplets suffer from a lack of in-situ data for verification. Current in-situ measurement depends on short range instrumentation that is only capable of evaluating small segments of a spill at a time. Very high-frequency acoustics (few MHz), mass spectrometers, fluorometers and water sampling systems have very small fields of view, creating observational challenges when trying to generate a synoptic view of a spill. As an alternative, the use of broad-band high-frequency acoustics (100-500 kHz) is being explored. Broad-band high-frequency acoustics are capable of measuring and quantifying oil droplets at ranges of tens to hundreds of meters in a single measurement. The frequency-dependent acoustic response of oil droplets is dependent on the size, sound speed and density of oil droplets. Broadband high-frequency acoustic measurements of a variety of oils have been measured in the laboratory setting to quantify the droplet size dependent acoustic response of oils of varying density and sound speed. This instrumentation was able to differentiate between droplets with different radii. Results indicate that broadband high-frequency acoustics can be used to map the location of submerged oil droplets and to evaluate changes in the physical properties of oil for large areas of a spill.

460 Effects of Chemical Dispersants on Intrusion Dynamics of Oil Droplets from a Deep Ocean Blowout

D. Wang
Student

Chemical dispersants reduce interfacial tension between oil and water, producing smaller droplets. This is known directly from laboratory experiments, indirectly from surface observations during the Deepwater Horizon (DWH) spill, and theoretically from a variety of droplet size prediction models. To better understand the role of dispersants, we have been conducting laboratory experiments on the effects of droplet size on near-field oil transport. Earlier, we identified threshold diameters for droplets to detrain from the rising plume near the height of neutral buoyancy, and for them to enter an intrusion. We also provided estimates for oil transport within the intrusion for a range of conditions and droplet sizes encompassing those expected during the DWH, both with and without dispersants. The fate of oil droplets clearly depends on the depth and shape of the intrusion layer(s). While intrusion layers from multiphase plumes have been studied previously under stagnant conditions, their behavior in a current, especially a weak current, is less well understood. The common classification of plume behavior as either current-dominated or stratification- dominated, depending on the physical mechanism driving phase separation, does not consider the interplay between the two effects. To fill this gap, we are conducting additional laboratory experiments, to investigate the behavior of intrusion layers with both currents and stratification. Like our earlier experiments, we use an inverted frame of reference, using spherical glass beads with a range of diameters to simulate oil droplets and towing a carriage with the release mechanism in a salinity-stratified tank. Laser-induced fluorescence is used to measure dilution and geometrical characteristic of the intrusion. We find that a weak current creates enhanced ambient entrainment, which in turn leads to a shorter trapping height compared with the quiescent case. Complementing the experiments is a semi-empirical model that extends previous models to account for current effects, allowing more accurate prediction of average and maximum

depths of the intrusion layer. Field observations taken during the DWH are used to validate some of the analytical and experimental findings.

553 Interaction of Oil Droplets and Gas Bubbles in Blowouts: New Development of VDROP Model
L. Zhao

The interaction of oil droplets and gas bubbles in the near field of a blowout was investigated numerically in this work using the model VDROP-J, whose droplet size distribution (DSD) was thoroughly calibrated. For this purpose, a new numerical scheme is developed in VDROP-J to account for the interaction of gas bubbles and oil droplets in the blowout, giving simultaneous simulation of bubble and droplet size distribution along the discharged plume. Preliminary validation shows improvement of the modeling results compare with the one without considering the gas bubble and oil droplet interactions. The model was then used to predict the DSD and bubble size from the Deepwater Horizon blowout without and with dispersants, and for live and dead oil properties. The new model development will enhance the knowledge in subsea oil and gas blowouts.

556 Formation of Oil Particle Aggregates (OPA): Experimental Studies and Development of the OPM model
L. Zhao

Oil-particle interactions can result in oil particle aggregates (OPA), which move differently from oil droplets or particles alone. This may alter drastically the fate of oil. We conducted laboratory studies in the EPA baffled flask to evaluate the impact of the particle concentration and properties on their trapping efficiency by oil. OPA were analyzed by epifluorescence microscopy to reveal their structures. We also developed a new OPA model that requires the input of particle and oil properties and the mixing intensity. A new parameter is introduced in OPM model to account for the shape of the particles and the packing on the oil droplets, as it was found that the packing efficiency does not depend only the areas of the oil droplets and particles, but also on the particle concentration. Also a new conceptual formulation of oil-particle coagulation efficiency is introduced in the model to account for the overall behavior of the coated area on the droplet surface. Based on the new formulation, the OPM was able to closely reproduce the oil trapping efficiency both in suspended and negatively buoyant OPA. To our knowledge, the OPM is the first predictive OPA model, and thus could be used for mitigating oil spills.

626 Oil in Water Fluorescence and Backscattering Relationships
I. D. Walsh

Oil in water exists as a mixture of dissolved and droplet fractions in natural waters. Fluorometers are effective in detecting oil in water, and recent improvements in optics, electronics and instrument design have enabled a factor of five increased sensitivity in fluorescent dissolved organic matter (FDOM) sensors which respond to crude oil. The fluorescence intensity scales with oil concentration and linear calibration relationships can be derived between the fluorescence signal and oil concentration from grab samples. Because the fluorescence intensity is a function of the concentration of oil modulated by the dissolved to droplet mass ratio and the droplet size distribution, precise calibration relationships must be determined for a given oil and water mixture and will change with time. Using multiple sensors can constrain the expected calibration relationships. In particular, backscattering is an effective tool for measuring the droplet fraction of oil. We describe a series of experiments in a flume in which oil and oil and dispersant mixtures were injected under pressure into the flume. We measured backscattering with an instrument that combines backscattering with

fluorescence sensors. We evaluate the combined fluorescence and backscattering signals to investigate their relationship and compare the backscattering results with the most common current methodology of single channel fluorometers and forward scattering sensors.

655 Verifying algorithms for initial droplet formation (modified weber scaling) by performing experimental subsea releases of oil generating full-scale droplet sizes

Ø. Johansen

Experiments performed at SINTEFs Tower basin in 2011-12 lead to the development of a modified Weber scaling algorithm (Johansen et al., 2013). The main advantage with this new approach is that it also includes contributions from;
1. oil properties including viscosity
2. turbulence created by the buoyancy flux and
3. the gas void fraction
This simple numerical algorithm was quickly implemented in most operational models used to predict fate and effect of subsea oil releases for the oil industry (Socolofsky et al., 2015). After the introduction in 2013, generating additional laboratory data to verify and further develop modified Weber scaling over a wider spectrum of parameters have had a high priority. Experimental work has been performed both as a part of industry funded projects (API) and as a part of the DROPPS GOMRI consortium. This paper presents an overview of recent experimental data generated by SINTEF covering a wide range of experimental parameters: Release diameters (0.5 - 50 mm), oil flow rates (0.5 - 400 L/min), gas-void fraction (0-90%) and oil droplet sizes (untreated oil: d50: 0.03 - 6 mm, treated oil d50: 0.03 - 500 mm). Large-scale experiments performed at Ohmsett in March 2015 gave oil droplet sizes comparable to what expected from subsea release with low release velocity and low Gas to oil ratios (multiple millimetres for untreated oil). This new comparison shows a very high correlation with predictions from the modified Weber algorithm. This finding is opposed to earlier studies predicting significantly smaller droplets e.g. Paris et al. (2012), using a similar approach for estimating droplet sizes, but with calibration coefficients not representative for the high turbulence present in these combined oil and gas releases.

676 Processes and Considerations Associated with Aerosolized Oil

J. Katz, D. Murphy, C. Li, X. Xue;
Johns Hopkins University, Baltimore, MD.

Breakup of oil slicks by waves, rainfall or popping bubbles generates aerosolized droplets on the surface of the ocean, which can then be transported by winds. The present knowledge on the environmental impact of aerosolized oil is quite limited. This presentation will discuss and demonstrate several mechanisms affecting the generation of airborne droplets near the ocean surface along with available data on their size distribution. Some of the data for breaking waves and raindrop impact have been measured in recent experiments performed in our laboratory, and others have been compiled from the wealth of available information about oceanic aerosols. Introduction of dispersants drastically reduces the oil-water interfacial tension, causing a substantial decrease in the characteristic size and an increase in the number of both subsurface and airborne droplet. Continuous exposure to breaking waves also aerosolizes a fraction of the suspended subsurface droplets that have been generated by previous waves. Based on available models for particle transport in the atmosphere, under normal/moderate wind conditions, while droplet with size of 100 µm or larger are likely to settle rather quickly, a 1 µm diameter or smaller droplet is likely to remain suspended for longer periods, and carried for longer distances. Hence, plans to apply dispersants should consider the potential environmental and health impacts of aerosolized oil on communities located downstream of the oil spill.

742 Numerical Simulation of Oil Jet Underwater-CFD simulation and Trace of Individual Droplets by

Lagrangian Method

F. Gao
Student

Computational Fluid Dynamics (CFD) was used to evaluate the hydrodynamic of the horizontal oil jet experiments conducted at Ohmsett wave tank facility in USA and the Bedford Institute of Oceanography in Canada. The standard model was used to model turbulence and the Volume of Fluid (VOF) was used to model the two phases (oil and water). The profiles of the holdup (ratio of oil volume to total volume), velocity magnitude, eddy diffusivity and turbulent dissipation rate were presented. It was found that the holdup drops significantly within a close range to the jet orifice, indicating a large amount of water entrainment into the plume. The energy dissipation rate drops by orders of magnitude along the centerline, starting from 104 watt/kg to 10-4 watt/kg. Both holdup and energy dissipation values have important consequences on oil droplet breakup and coalescence. In addition, the movement of individual droplets in the discharged oil plume is tracked by coupling CFD simulations and a Lagrangian approach in which we accounted for the effect of individual oil droplet buoyancy and inertia. Accounting for the inertia of oil droplets has not been done in the oil spill literature. We found that neglecting the inertia of the droplets overestimates their rise rate as the inertia from a horizontal jet tends to propel the droplet more horizontally, and thus their rise gets delayed also by turbulent mixing. We also found that small oil droplets (e.g. d<100 μm) would mix uniformly in the plume, while those close to 500 microns tend to be above the centerline of the plume. This provides a clear guideline for interpreting the results of the LISST when measuring the droplet size distribution.

ControlNu	ReviewerF	ReviewerL	AverageSc	StandardD	ScoreValu	CommentC	Comment
244	Michel	Boufadel	0	0		Other: Not	Relevant to responding to oil spills or u
244	Thomas	King	0	0		Other: Not	relevant to this session (suggest other s
266	Michel	Boufadel	4	0	4	Positive: Novel	approach or technique that merits
266	Thomas	King	4	0	4	Positive: Novel	approach or technique that merits
267	Michel	Boufadel	3	0	3	Positive: Good	subject/relevant topic,Other: Woul
267	Thomas	King	3	0	3	Positive: Good	subject/relevant topic,Other: Woul
290	Michel	Boufadel	4	0	4	Positive: In	Provides the perspective of oil compan
290	Thomas	King	4	0	4	Positive: Important	new contribution to the field,O
325	Michel	Boufadel	4	0	4	Positive: Important	new contribution to the field,O
325	Thomas	King	4	0	4	Positive: Important	new contribution to the field,O
339	Michel	Boufadel	4	0	4	Positive: In	Advanced experimentation and seems t
339	Thomas	King	4	0	4	Positive: Important	new contribution to the field,O
341	Michel	Boufadel	4	0	4	Positive: In	Testing various dispersants on oil jets.
341	Thomas	King	4	0	4	Positive: Important	new contribution to the field,O
369	Michel	Boufadel	4	0	4	Positive: G	Provides an industry perspective
369	Thomas	King	4	0	4	Positive: Good	subject/relevant topic,Other: Woul
404	Michel	Boufadel	4	0	4	Positive: G	Senior author, Joe Katz is Keynote Spea
404	Thomas	King	4	0	4	Positive: Good	subject/relevant topic,Other: Woul
415	Michel	Boufadel	3	0	3	Positive: G	Testing various dispersants in a mixing v
415	Thomas	King	3	0	3	Positive: Good	subject/relevant topic,Other: Woul
420	Michel	Boufadel	4	0	4	Positive: G	Senior author, Brandvick is giving a talk
420	Thomas	King	4	0	4	Positive: Good	subject/relevant topic,Other: Woul
421	Michel	Boufadel	3	0	3	Positive: G	The topic is similar to the work propose
421	Thomas	King	3	0	3	Positive: Good	subject/relevant topic,Other: Woul
460	Michel	Boufadel	3	0	3	Positive: G	Focus on intrusion hydrodynamics, and
460	Thomas	King	3	0	3	Positive: Good	subject/relevant topic,Other: Woul
553	Michel	Boufadel	4	0	4	Positive: In	Recently developed model that became
553	Thomas	King	4	0	4	Positive: Important	new contribution to the field,O
556	Michel	Boufadel	4	0	4	Positive: In	Author presenting another paper on dr
556	Thomas	King	4	0	4	Positive: In	Author is presenting a paper already in
626	Michel	Boufadel	4	0	4	Positive: In	Senior author Conmy is recommended f
626	Thomas	King	4	0	4	Positive: Important	new contribution to the field,O
655	Michel	Boufadel	4	0	4	Positive: G	Same author (Brandvik) is recommende
655	Thomas	King	4	0	4	Positive: Good	subject/relevant topic,Other: Woul
676	Michel	Boufadel	4	0	4	Positive: G	Keynote speaker
676	Thomas	King	4	0	4	Positive: Good	subject/relevant topic,Other: Woul
742	Michel	Boufadel	4	0	4	Positive: N	One of the few works combining hydro
742	Thomas	King	4	0	4	Positive: Novel	approach or technique that merits

adsorm iin getirom. ent box below if applicable)
ession in comment box below if applicable)
discussion,Other: Would be best as an oral presentation
discussion,Other: Would be best as an oral presentation
d be best as a poster
d be best as a poster
tesher: Would be best as an oral presentation
ther: Would be best as an oral presentation
ther: Would be best as an oral presentation
ther: Would be best as an oral presentation
dsherdMoighlt dbretbhesbasiebrcealkuppreosfenltiaitoion droplets.
ther: Would be best as an oral presentation
ther: Would be best as an oral presentation
ther: Would be best as an oral presentation
d be best as an oral presentation
d be best as an oral presentation
kderibethisseasipostaernd he will be talking about aerosols.
d be best as a poster
dsbelbeestiaod aqpotseteect waves or a jet.
d be best as a poster
dobethbestsaemaetpopisteinr the session.
d be best as a poster
d by baeristouas gproousptesr on using acoustics to measure droplets. Seems too focused on the instrument rather than on t
d be best as a poster
dnbot tbheestdasopalpeotssizteerdistribution.
d be best as a poster
twiedeWlyouused.be best as an oral presentation
ther: Would be best as an oral presentation
dplets Wino tuhled sbaembeesstsaiso na. pAoposter would be appropriate.
tsheessioWnould be best as a poster
tdhrem: oWraoul dp rbeesbeenstta atiso an pino sthteer same session on the topic of fluorescence.
ther: Would be best as a poster
d fbore boersatl parsea spenotsattiero n. Abstract is about discussion an empirical formula.
d be best as a poster
d be best as an oral presentation
d be best as an oral presentation
dyinscaumssicio an,nOdt hdeorp: lWeot usilzdeb edi sbtersitb auts ioann oral presentation
discussion,Other: Would be best as an oral presentation

he science.

To: Conmy, Robyn[Conmy.Robyn@epa.gov]
From: Voit, Jim
Sent: Tue 3/29/2016 2:17:28 PM
Subject: RE: QAPP lookup
L15045-QP-1-5 13DEC2013.docx

Robyn,

The QAPP is attached and includes SOPs 7-10. This is an LRPCD QAPP, approved Dec 2013. I would suggest asking Jorge to confirm that these SOPs reflect current practice, and if there are any changes we should consider if our QAPP needs to be updated.

Jim V.

From: Conmy, Robyn
Sent: Tuesday, March 29, 2016 9:49 AM
To: Voit, Jim <Voit.Jim@epa.gov>
Subject: QAPP lookup

Hi Jim,

Is there a way for NRMRL staff to access QAPPs and SOPs from other groups within NRMRL? I am looking for a copy of QAPP L-15045-QP-1-5 (Dec 2013) and SOPs 7-10, pp. 75-86) which is listed under our WA through Jorge Santo Domingo's efforts.

Thanks,

Robyn

<>/<>/<>/<>/<>/<>/<>/<>/<>/<>/<>/<>/<>/<>/<>/<>/<>/<>

Robyn N. Conmy, Ph.D.

Research Ecologist

USEPA/NRMRL/LRPCD

26 West MLK Drive

Cincinnati, Ohio 45268

513-569-7090 (office)

513-431-1970 (EPA mobile)

727-692-5333 (Personal mobile)

conmy.robyn@epa.gov

IAA No. E12PG00037

Draft Final Report

Dispersant Effectiveness, In-Situ Droplet Size Distribution and Numerical Modeling to Assess Subsurface Dispersant Injection as a Deepwater Blowout Oil Spill Response Option

and

Evaluation of Oil Fluorescence Characteristics to Improve Forensic Response Tools

Submitted to:

Bureau of Safety and Environmental Enforcement
Sterling, VA

Submitted by:

Robyn N. Conmy, Ph.D.
U.S. Environmental Protection Agency
National Risk Management Research Laboratory
Land Remediation and Pollution Control Division
26 W. Martin Luther King Drive
Cincinnati, OH 45268
*Tel: 513-569-7090, Fax: 513-569-7620
Email: conmy.robyn@epa.gov

Thomas King, M.Sc.; Brian Robinson, M.Sc; Scott Ryan, M.Sc; Youyu Lu, Ph.D.;
Department of Fisheries and Oceans Canada
Center for Offshore Oil, Gas and Energy Research (COOGER)
1 Challenger Drive, Dartmouth, Nova Scotia, Canada B2Y 4A2
Tel: 902-426-4172
Tom.King@mar.dfo-mpo.gc.ca

September 30, 2015

ACKNOWLEDGEMENTS

The research presented in this report was funded by the Bureau of Safety and Environmental Enforcement (BSEE) through Interagency Agreement E12PG00037. Efforts were partially supported by the U.S. Environmental Protection Agency - Office of Research and Development (EPA ORD) and the Department of Fisheries Oceans Canada – Bedford Institute of Oceanography (DFO-BIO). This work was a highly collaborative effort and the authors would like to thank all of the contributors. The numerical modeling components are contributions by collaborators Dr. Michel Boufadel and Feng Gao (New Jersey Institute of Technology) and Dr. Haibo Niu and Linlu Weng (Dalhousie University). The high-resolution fluorescence component is a contribution of Mary Abercrombie (University of South Florida). A special thanks to all of the DFO and BDR Contracting staff who made the tank experiments possible: Patrick Toole, Claire McIntyre, Cody Sherren, Jennifer Mason, Peter Thamer, Gary Wohlgeschaffen, Susan Cobanli, and Rod Doane.

DISCLAIMER

This draft report contains scientific observations from a series of subsurface oil injection experiments and high resolution fluorescence analyses. Findings are subject to institutional review and are considered draft, thus the information provided here should not be parsed. Refrain from citing or posting until report is considered final. Upon review, approval does not signify that the contents reflect the views of the U.S. EPA, DFO Canada, or BSEE, nor does the mention of trade names or commercial products constitute endorsement or recommendation for use.

ED_001324_00000298-00002

EXECUTIVE SUMMARY

This report summarizes two projects covered under an Interagency Agreement between the Bureau of Safety and Environmental Enforcement (BSEE) and the U.S. Environmental Protection Agency (EPA) in collaboration with the Bedford Institute of Oceanography, Department of Fisheries and Oceans Canada (BIO DFO), New Jersey Institute of Technology (NJIT) and Dalhousie University. Both projects dovetail together in addressing the ability to differentiate physical from chemical dispersion effectiveness using dispersed oil simulations within a flume tank for improving forensic response monitoring tools. This report is split into separate Tasks based upon the two projects funded by BSEE:

1) Dispersant Effectiveness, In-Situ Droplet Size Distribution and Numerical Modeling to Assess Subsurface Dispersant Injection as a Deepwater Blowout Oil Spill Response Option.
2) Evaluation of Oil Fluorescence Characteristics to Improve Forensic Response Tools.

TASK A: Dispersant Effectiveness, In-Situ Droplet Size Distribution and Numerical Modeling to Assess Subsurface Dispersant Injection as a Deepwater Blowout Oil Spill Response Option.

The main objectives of work under Task A were to evaluate high velocity subsurface releases of physically and chemically dispersed oil using a flow-through wave (flume) tank.. This project addressed three issues: (1) performance evaluation of dispersants for subsurface injection into sub-sea blowouts, (2) tracking, modeling, and predicting the movement and spread of the deepwater plume and oil surfacing from deepwater blowouts, and (3) evaluating the influence of dispersant applications in reducing the concentration of volatile organic compounds emanating from the water surface. Oil dispersion experiments were conducted in the flume tank at the Department of Fisheries and Oceans Canada, Bedford Institute of Oceanography (DFO BIO), which is equipped with an underwater oil release system to simulate a high-pressure release of oil (akin to a deepwater blowout). Subsea plume simulations were generated with a pressurized underwater oil release system adapted

ED_001324_00000298-00003

from existing technology developed by Masutani and Adams (2000). To mitigate wall effects and to generate oil droplets in the size range observed at depth during the Gulf of Mexico Deepwater Horizon (GoM DWH) oil spill, a high flow-rate of oil (3.8 L/min) was released through a small diameter nozzle (2.4 mm). Although it is impossible to simulate in the tank the extreme hydrostatic pressures that exist at 1500 m water depth, underwater high-pressure release of crude oil can be simulated with and without dispersant addition. The researchers also recognize that the shallow nature of the tank does not allow for investigating the rise velocity of the droplets that would be observed in a long (`1500m) water column. Rather, the tank allows for gathering data on the differences in droplet size and distribution during physical and chemical dispersion (akin to that observed during DWH) and for observing the vertical and horizontal movement of the droplets. Although results cannot be directly scaled or translated to a deepwater spill in the ocean, results are still useful for understanding the formation and movement of oil droplets under for varying oil and dispersant type, dispersant amount and water temperature.A total of 48 core and 24 complimentary flume tank experiments were conducted to evaluate the effectiveness of dispersant injection and attenuation of the plume as a function of oil type (US EPA reference oils: ANS pipeline blend for a light-medium crude, IFO 120 for a heavy refined productand South Louisiana Crude for a light crude, and also a gas condensate), chemical dispersant type (Corexit 9500 and Finasol OSR 52), dispersant-to-oil ratio (DOR of 0, 1:20, 1:100, and 1:200; corresponding to DOR concentrations of 0, 5, 1, and 0.5%) and water temperature (< 10 °C for low temperature and > 10 ºC for higher temperature). Experiments were conducted at a fixed horizontal current flow rate of 1 cm/s (~ 1/8th of deep water flow rates in the GoM). Faster current was not permissible as it would have resulted insufficient time for collection of *in situ* measurements and discrete samples. Experiments used 80 °C oil temperature, although this is lower than the reservoir temperature for the DWH Macondo wellhead, this is as high as the experimental design would allow for safety reasons.

Time series dispersion effectiveness was evaluated by measuring dispersed oil concentrations from samples collected in the flume tank, and via *in situ* droplet size distribution analysis and fluorescence measurements. Discrete samples were collected for oil chemistry analysis of

ED_001324_00000298-00004

Total Petroleum Hydrocarbons (TPH) and Benzene-Toluene-Ethylbenzene-Xylene (BTEX) via gas chromatography coupled to a flame ionization detector (GC/FID) and gas chromatography mass spectrometry (GC/MS), employed to quantify oil concentration and partitioning of hydrocarbon compounds in seawater.

The produced Droplet Size Distribution (DSD) was determined by using Laser *In-Situ* Scattering and Transmissometry instruments (LISST-100X, type C, size range: 2.5~500 µm; Sequoia Scientific Inc. Seattle, WA) to track the full range diameters of chemically and physically dispersed oil droplets. Larger, oil droplets, whether physically or chemically dispersed, may be capable of coalescing and rising to the surface under less energetic mixing conditions. The LISST measures a range in oil droplet sizes, thus facilitating a comparison between natural (physical) and chemical dispersion efficiency of crude oil. All submersible sensors were operated with real-time data acquisition throughout each experiment. *In situ* fluorescence was monitored real-time using two Chelsea Technologies Group AquaTrackas (crude and refined oil types), one Sea Bird – Wet Labs Inc. ECO (gelbstoff type), two Turner Designs Inc. Cyclops (crude and refined oil types) and one GmBH Trios (hydrocarbon type) fluorometers. Many of the fluorescence sensors used in this study are the same models employed to track the subsea plume during the DWH oil spill and confirm dispersion effectiveness. Sensors used in this work are also ones provided as examples in the National Response Team (NRT) *Subsea Dispersant Monitoring and Assessment Interim Guidance* Document, that states "the Risk Plan should use a properly calibrated oil-specific fluorometer (e.g., Chelsea UV AQUAtracka, Turner Designs Cyclops, Wet Labs ECO, or equivalent oil-specific instrument) to enable ongoing improvements in sampling".

Also monitored during experiments was the level of Volatile Organic Compounds (VOC) above the air-water interface of the tank to evaluate concentrations from the perspective of worker safety. Cautioned are the use of these shallow water tank results, however as the short vertical water column did not allow for any stripping or dissolving of volatile compounds into the water column as would be expected during a deepwater oil release. Correlations between *in situ* fluorescence data, droplet size distribution, total particle

ED_001324_00000298-00005

concentration, and oil chemistry serve as inputs to the modeling activities of this project.

Oil droplet size distribution data from this study is essential for the improvement of oil spill trajectory and ocean circulation modeling processes to predict the fate and transport of subsurface plumes and surface oil slick movement. This has implications for improving the scientific and response community's understanding on the impacts of dispersant application at depth, ultimate fate of subsurface dispersed oil plumes and potential natural resource damages. Recent advancements in the use of numerical modelling have allowed for the prediction oil droplet sizes resulting from a subsurface release. Several different mathematical approaches have been used to determine how oil would behave flowing out of an orifice at high pressure. This includes the modified Weber Number technique (Johansen et al., 2013) and the VDROP model (Zhou et al., 2014) to predict oil droplet breakup taking into account oil viscosity and interfacial tension. However, there is a limited amount of large scale real world data to help validate the output of these models. This study provided the opportunity to further test these techniques through the use of several different oil types and treatment conditions. Results from the numerical modelling using data obtained from tank experiments are presented in Appendix G, with Part 1 using the modified Weber Number and Part 2 using VDROP. The premise for this research is that the evaluation and efficacy of chemical dispersants at depth will differ dramatically from conventional use of chemical dispersants for treating surface oil slicks. This is due to difference in mixing energy, where for surface slicks is provided mainly through naturally occurring surface waves and currents, particularly breaking waves. Monitoring of DSD is essential in differentiating between chemically and physically dispersed oil. Tank observations using underwater injection experiments provide evidence of stable dispersion that may be expected during subsea dispersant injection. Larger oil droplets, whether physically or chemically dispersed, may be capable of coalescing and rising to the surface under less energetic mixing conditions.The experimental results from this work demonstrate the chemical dispersion of oil into small droplets and help to predict the likelihood of coalescence and resurfacing of oil. Results of the project provide spill responders with critical information on the utility of subsurface dispersant application as an oil spill response option and the modeling capabilities

ED_001324_00000298-00006

that are available to predict oil trajectory during deep water blowouts. Both assist decision-making regarding countermeasures.

TASK B: Evaluation of Oil Fluorescence Characteristics to Improve Forensic Response Tools.

This project addresses the evaluation of oil fluorescence characteristics and sensor performance for improving response tools used to inform oil spill countermeasure decision-making. Fluorescence has long been used as 'one tool in the toolbox' for surface spills and used to supplement visual confirmation during response efforts. Recent oil and gas production in extremely remote locations brings an increased risk of spills in under-the-ice and/or deep-sea environments. For releases in these environs, responders will be evermore reliant on submersible sensors for plume tracking when the human eye cannot be employed. As such, the oil spill community has identified the need for better characterization of spilled oil by fluorometers.

Submersible fluorometers deployed during the 2010 Gulf of Mexico Deepwater Horizon (DWH) oil spill highlighted the challenges in ensuring selection of the optimum sensor configuration as fluorescence peaks occur over a wide nanometer range, vary in shape and wavelength position, are dependent on oil type due to chemical differences, and are affected by the addition of dispersants. This project addresses these concerns through the following objectives: (1) Characterization of oil optical properties as a function of oil type, dispersant-to-oil ratio (DOR) and concentration; (2) Generation of a comprehensive EEMs (Excitation Emission Matrix Spectroscopy) library that will be subjected to advanced statistical analyses for identification of wavelength regions best suited for oil detection; and (3) Evaluation of sensor performance through a series of experiments in a flume tank capable of static and flow-through operations, where sensor data will be validated with chemical and optical analyses.

A series of bench-scale dispersed oil-in-seawater experiments were conducted on 25 oils at 4 dispersant-to-oil ratios (DORs) using Corexit 9500 chemical dispersant. Analysis of the

ED_001324_00000298-00007

resulting 3D fluorescence excitation-emission matrix spectra (EEMs) shows oil-specific results as well as differing effects of dispersant and DORs. Results will inform the identification of optimum oil detection wavelengths in the marine environment as well as confirmation of the chemical effectiveness of dispersant application. Samples were prepared using baffled flasks to physically disperse the oil within seawater. The effect of dispersant on oil-specific fluorescence is shown, where shifts in intensity and peak wavelengths were observed. Results were compared to chemistry results of oil components.

Results of the laboratory EEMS analysis were compared to EEMS collected under Task A of this project to compare the applicability of baffled flask fluorescence to large scale mixing experiments in the flume tank.

Given recent advances with *in situ* fluorometers, enabling detection at lower UV-wavelengths, these findings help to discern wavelength regions influenced by dispersed oil within seawater, improve the interpretation of fluorescence data, and inform decision-making by responders. Findings from this project will serve to improve confidence in field data, filling operational gaps and formulating operational guidelines.

Findings: Tasks A and B

Overall findings from both tasks of this project include:

1. Addition of either Corexit 9500 or Finasol OSR 52 chemical dispersants to Alaskan North Slope (ANS), IFO 120 and South Louisiana Crude (SLC) oils decreased the Volume Mean Diameter (VMD) and shifted the Droplet Size Distribution (DSD) to smaller droplets. In general, Corexit 9500 produced smaller droplets compared to Finasol OSR 52.
2. Dispersions created without chemical dispersants or Dispersant-to-oil ratio (DOR) = 1:200 yielded VMD larger than 70 µm and exhibited unimodal DSD. Dispersions created with DOR = 1:20 yielded VMD between 2.5 to 70 µm size range with a bimodal distribution. This suggests that produced droplets from a DOR = 1:20 dispersant injection with ANS would likely remain dispersed in the presence of mixing energy given the larger proportion of small droplet sizes observed.

ED_001324_00000298-00008

3. Particle size analyses near the injection release (LISST Release) exhibited larger VMD compared to those generated further downstream from release in the tank (LISST Downstream) indicating a shift from larger to smaller droplets within the plume, with and without the presence of dispersant during the 12 minute experiments for ANS and SLC oils. This effect was not always observed with the heavier IFO 120 oil because small droplets were less predominant for this heavier oil.
4. For ANS, dispersion with < 70 um droplet VMD was observed for the DOR = 1:20 treatments at both cold and warm water temperatures. Water temperature did not appear to influence the DSD or VMD for this lighter crude oil. However, a temperature effect was observed on the Total Particle Concentration (TPC), where lower temperatures were coincident with fewer particles dispersed within the plume for a given volume of oil injected.
5. The addition of Corexit 9500 or Finasol OSR 52 to IFO 120 during warm temperature experiments resulted in a shift in DSD and a decrease in VMD; however bimodal distribution was not achieved and even DOR = 1:20 did not yield VMD less than 70 µm in most cases. At cold water temperatures, lower droplet sizes were not observed with the addition of dispersant, where DOR = 1:20 remained well above 200 µm. This suggests that dispersant addition to this oil at cold or warm temperatures would not yield droplet sizes that would likely remain in suspension.
6. For experiments conducted at water temperatures less than 5 °C, The LISST particle size analyzed yielded unexpected DSD where even a unimodal distribution was not measured. Chemistry and *in situ* fluorescence data indicate that the oil was in fact dispersed adequately. This suggests operational problems with the LISST below 5 °C, even though it is within the operating temperature of the LISST (manufacturer manual). Additional testing of the cold water temperature limits of the sensor is recommended.
7. SLC oil was more dispersible compared to ANS for treatments with and without chemical dispersant. Bimodal distribution was observed during DOR = 1:20 and some DOR = 1:100 experiments indicating that the jet release of this particular oil

ED_001324_00000298-00009

into warm water produced smaller droplets than the ANS.

8. *In situ* fluorescence serves as a good proxy for oil concentration during the subsurface injection experiments. Given the experimental design, fluorescence is better suited for correlation with particle size analysis and concentration. Heterogeneity of the produced plumes and the short time scale of experiments (~12 min) led to difficulties in correlations between the plume particle size analyses and chemistry results. This is in part due to discrete samples representing 15-30 second averages as opposed to instantaneous measures given by fluorometers and particle size analyzers.
9. VOC air monitoring was conducted above the tank at two horizontal locations during experiments. The gas condensate exhibited the highest surface VOC concentrations, followed by ANS and SLC which exhibited similar values. Lowest concentrations were observed for IFO 120 experiments. High VOC concentrations in the air were usually accompanied by lower BTEX concentrations in the water. For all oils tested, the addition of chemical dispersants (DOR = 1:20) resulted in a reduction in VOC concentrations within air compared to experiments without dispersant near the jet release location, above the tank.
10. Fluorescence Excitation Emission Matrices (EEMs) were generated for 25 oil types under varying DOR. Oils could be separated into two categories based on dispersiblity; where light, medium and heavy oils were found in each category. Fluorescence peaks are chemistry dependent and were well correlated with Total Petroleum Hydrocarbon (TPH) and Benzene-Toluene-Ethylbenzene-Xylene (BTEX) concentrations. EEMs generated from tank and Baffled Flask Test (BFT) experiments were in agreement with respect to fluorescence peak position and Fluorescence Intensity Ratio (FIR) values as an indication of dispersion effectiveness.
11. Computer programs for jet hydrodynamics, droplet size distribution, and movement of oil droplets within the jet/plume were employed where developed models were calibrated to experimental data obtained from the oil jet experiments in the flume tank. The models VDROP-J and JETLAG were used to predict the streamwise velocity

ED_001324_00000298-00010

and the holdup along the centerline of the plume, where both models were in agreement, implying that VDROP-J is capable of predicting the average droplet size distribution in the plume. In the absence of dispersant, the model VDROP-J predicted the oil DSD measured by the LISST. In the presence of dispersant, the VDROP-J model captured the overall trend of the DSD, but was challenged in capturing the peak in droplet concentration observed for 5 microns. The observed peak is could be due to tip-streaming (when at high DORs oil droplets shed filaments from their edges resulting in smaller droplets), and VDROP-J does not yet have a module for this component.

12. The Modified Weber Number approach developed by SINTEF is a recent and promising approach for predicting DSD. Previously the method has been validated by solely a light crude oil. For this project, median droplet diameters (d_{50}) and the relative droplet size (d_{50}/D) were calculated based on the measured droplet sizes obtained from the tank experiments, and the relations between d_{50}/D and modified Weber number, Reynolds number, and oil concentration were quantified. Results demonstrate that chemical dispersants tested here reduced the droplet size of ANS in both cold and warm temperatures and that dispersants tested here are more effective in reducing droplet size with ANS compared to IFO 120. A two-step Rosin-Rammler approach was found to better predict the droplet size distribution in the empirical data as indicated by higher regression coefficients.

TABLE OF CONTENTS

TASK A - Dispersant Effectiveness, In-Situ Droplet Size Distribution and Numerical Modeling to Assess Subsurface Dispersant Injection as a Deepwater Blowout Oil Spill Response

ED_001324_00000298-00011

Option.

A.1 INTRODUCTION & RELEVANCE 14
Objectives 17

A.2 EXPERIMENTAL METHODS 18
A.2.1 Flume Tank Description, Flow Calibration and Operation 18
A.2.2 Waste Water Treatment 21
A.2.3 Subsurface Oil Injection System 21
A.2.4 Submersible Sensor Deployment 25
A.2.5 VOC Air Monitoring 26
A.2.6 Discrete Water Sample Collection 27
A.2.7 Oil and Dispersant Samples 28
A.2.8 Experimental Design – Core and Complimentary Experiments 30
A.2.9 Submersible Sensor Calibration Experiments 30
A.2.10 Submersible Fluorometer and LISST Data Processing 32
A.2.11 Analytical Chemistry Analysis 33
A.2.12 Numerical Modeling 34

A.3 RESULTS & DISCUSSION 35
A.3.1 ANS Dispersion Effectiveness 35
A.3.2 IFO 120 Dispersion Effectiveness 49
A.3.3 SLC Dispersion Effectiveness 59
A.3.4 Gas Condensate Dispersion Effectiveness 64
A.3.5 Tank Dilution Series Fluorescence Measurements 66
A.3.6 VOC Air Monitoring 71
A.3.7 VDROP-J and JETLAG Numerical Plume Modeling 81
A.3.8 Weber Number Scaling Numerical Plume Modeling 83

TASK B: Evaluation of Oil Fluorescence Characteristics to Improve Forensic Response Tools.

B.1 INTRODUCTION & RELEVANCE 85
Objectives 91

ED_001324_00000298-00012

B.2 EXPERIMENTAL METHODS 94
B.2.1 Sample Preparation 94
B.2.2 Artificial Seawater Protocol 94
B.2.3 Dispersed Oil in Seawater Protocol 94
B.2.4 Spectrophotometric Analysis 95

B.3 RESULTS & DISCUSSION 99
B.3.1 Oil Fluorescence Properties 99
B.3.2 Fluorescence as a Function of Chemistry 109
B.3.3 Flume Tank & Baffled Flask EEM Comparison 114
B.3.4 PARAFAC Modeling 116

REFERENCES 155

APPENDICES (Separate Document)
APPENDIX A – Experiment Logs
APPENDIX B – Analytical Chemistry Results
APPENDIX C – Jet Release LISST Oil Droplet Size Distribution Histograms
APPENDIX D – Jet Release LISST Oil Droplet Size Distribution Time Series Contours
APPENDIX E – Submersible Fluorescence Time Series
APPENDIX F – Excitation Emission Matrix Contours
APPENDIX G – VDROP-J and JETLAG Numerical Plume Modeling Report
APPENDIX H – Weber Number Scaling Numerical Plume Modeling Report

ED_001324_00000298-00013

TASK A.1 INTRODUCTION & RELEVANCE

The 2010 Deepwater Horizon (DWH) oil spill in the Gulf of Mexico has highlighted the pressing need for a better understanding of the interaction of chemical dispersants and crude oil at ocean depth. Early in the blowout release, partial emulsification of oil was observed as it rose to the surface from 1500-m depth, and surface slicks were not continuous (JAG report, 2010). a A decision was made to inject dispersants directly at the release point as a possible means to increase efficiency of dispersion and to potentially reduce the amount of dispersant needed if applied at the air-sea interface (CRRC Report, 2010). Large quantities of chemical dispersant were applied via subsurface injection and traditional spraying from aircraft onto the surface oil slick (Oil Budget Calculator). At this workshop to discuss the use of subsurface chemical dispersants as an oil spill response option, recommendations to the RRT (Regional Response Teams) by spill response and research expert attendees were made on potential advantages of subsurface dispersant injection given the rate of continuous oil release and preliminary evidence of the dispersant efficacy from the DWH spill (CRRC 2010). Potential advantages of this application included the fact that the fresh (unweathered) oil was considered well suited for dispersion, operators were able to inject the dispersant directly into the oil stream thereby maximizing dispersant/oil contact, sufficient control of DOR (Dispersant-to-Oil Ratio) could be maintained, injection may minimize the need for surface dispersant application because of reduced oil surfacing and optimized subsurface application would likely promote formation of smaller, more stable droplets of oil, enhancing biodegradation (Lee et al., 2009).

As recommended by the interagency Unified Area Command (UAC) and on-site emergency spill response coordinators, a large-scale environmental monitoring program was implemented to detect and characterize dispersed oil based on field data and plume

ED_001324_00000298-00014

modeling outputs. This allowed for tracking the subsurface oil plume emanating from the blowout wellhead. Droplet Size Distribution (DSD) analysis using the LISST-100X Laser *in-situ* Scattering and Transmissometry System (Sequoia Scientific Inc. Seattle, WA) and fluorescence intensity from submersible fluorometers were used as an indication of Dispersion Effectiveness onboard the research vessels, where particle concentrations were monitored to evaluate oil dispersion (presence of small droplets ≤ 70 μm) based on previous studies for surface dispersant applications (Li et al., 2009b). Data analysis of the monitoring samples provided sound evidence of the presence of oil-bearing small particles both in surface waters and in the subsurface plume (Lee, 2010). Furthermore, a negative correlation between subsurface dispersant injection and low molecular weight compounds in surface waters was observed. In contrast, a strong positive correlation was observed in the subsurface. These results suggest that subsurface dispersant use may have promoted the formation of small oil droplets in the deep sea. This would likely enhance the natural weathering and dissolution of oil in the water column, thus suppressing the presence of oil organic compounds in surface waters.

Although subsurface *in situ* use of dispersants was used to counter a deepwater spill blowout, much uncertainty still exists in terms of the DE (Dispersion Effectiveness) with this type of application. For example, assumptions of the optimal DOR are based on empirical data mostly obtained from bench-scale experimental protocols that have been designed for testing at standard temperatures and pressures (STP), whereas conditions at a wellhead on the ocean floor or anywhere along a riser beneath the ocean surface could be significantly different. Hence, DOR for direct injection needs to be better understood. Although theoretical analyses and experiments suggest that jet breakup of the oil is insensitive to the absolute value of system hydrostatic pressure for incompressible liquid-liquid systems (Masutani and Adams 2000), the effects of several ambient environmental factors on subsurface dispersant effectiveness, including high release pressure, high oil temperature, low water temperature, and the presence of methane and suspended sediments in the oil plume and/or surrounding water column remain to be clarified. Improved understanding on the influence of these factors on DE and the interaction of crude oil and chemical dispersant

ED_001324_00000298-00015

under a range of turbulent regimes at depth is required for informed decision-making for future subsurface dispersant use.

For evaluating chemical dispersion effectiveness, standard laboratory tests are inherently limited in simulating real field operational performance due to space constraints that are critical for transport and dilution efficiency (NRC 2005). To address the need to evaluate chemical dispersion effectiveness under more realistic oceanographic and environmental conditions, a meso-scale wave tank capable of generating breaking and regular non-breaking wave conditions is currently in operation at the Bedford Institute of Oceanography (BIO), Dartmouth, Nova Scotia. This tank facility has been used previously to characterize the tank hydrodynamics and the efficacy of several oil dispersant formulations on dispersion of different oil types, including fresh and weathered crude oils and heavy fuel oils under breaking wave conditions (Figure 1) (Lee et al. 2009; Li et al. 2008; Wickley-Olsen et al. 2007). Mathematical modeling and experimental measurements have been used in the characterization of the fluid dynamics of the flume tank. In modeling, computer fluid dynamics software packages have been used to conduct numerical simulation of the fluid field and transport phenomena of the flume tank under both non-breaking and breaking wave conditions. Experimentally, wave gauges (WG-50) have been used to monitor wave profiling throughout the flume tank under various hydrodynamic conditions. Acoustic Doppler Velocimetry (ADV) has been employed to evaluate the *in situ* instantaneous three-dimensional velocity distribution, which is used to compute the velocity gradients and energy dissipation rates (ε) in the tank. Using this facility, previous experiments have assessed chemical dispersant effectiveness as a function of energy dissipation rate and particle size distribution (Li et al. 2009a) and demonstrated that the effectiveness of a dispersant is strongly dependent on wave conditions, dispersant type, and oil type (Lee et al. 2009). A strong correlation has been established between dispersion effectiveness and *in-situ* droplet size distribution within the hydrodynamic regime, particularly energy dissipation rate, under a variety of non-breaking wave and breaking wave conditions (Li et al. 2008; Li et al. 2009a). The flume tank has also been operated in flow-through mode to accommodate the effects of underwater currents on dispersion and dilution of oil (Li et al. 2009b; Li et al. 2010).

ED_001324_00000298-00016

Experiments have also shown the reliability of fluorescence measurements as a proxy for oil concentration within physically and chemically dispersed oil (Conmy et al., 2014). Experimental studies have also been conducted to better understand oil-mineral aggregate (OMA) formation and the influence of mineral fines on the physical and chemical dispersion of oil (Lee et al. 2009).

This report summarizes results from a project that addresses the operational performance of subsurface injection dispersant use on high pressure releases of oil within the flume tank. Developed were methods focused on monitoring subsurface oil transport by outfitting a new high-flow flume tank at the Department of Fisheries and Oceans Canada (DFO) Bedford Institute of Oceanography (BIO) facility with a new underwater high flow rate oil injection system. In this way, the efficiency of chemical dispersion during high pressure releases within the tank can be quantitatively evaluated and comparisons made to experiments with physical dispersion (without dispersant addition). This work has implications for field response options. To this end, the **objectives** of this work were to:

1) Refine existing equipment, technologies, and methodologies for subsurface dispersant application evaluation and monitoring by measuring dispersed oil concentration, fluorescence, and *in situ* oil droplet size distribution,
2) Evaluate effects of water temperature and dispersant type on dispersion efficacy and dispersed oil droplet size distribution of oil at high temperatures,
3) Evaluate dispersion effectiveness (DE) as a function of oil type and dispersant-to-oil ratio (DOR) for subsurface dispersant injection,
4) Assess the effect of dispersant application on the VOC concentration in air above the air-sea interface of the flume tank,
5) Integrate droplet size distribution into deepwater blowout transport/behavior models to enable prediction of the dispersed oil droplets under high flow subsurface release velocities.

During the DWH spill, small droplet ($d \leq 70\mu m$) concentrations were monitored to aid in evaluating oil dispersion efficiency. The particle size and distribution data obtained from the

ED_001324_00000298-00017

field monitoring program during the DWH oil spill had a significant role in supporting emergency oil spill response operations, fate and transport modeling, and impact assessment. Findings from this study will have significant implications in further supporting emergency response operations, spill transport models and assessments for future deepwater spills.

TASK A.2 EXPERIMENTAL METHODS

A.2.1 Flume Tank Description, Flow Calibration, and Operation

Oil dispersion experiments were conducted in the flow-through flume tank at BIO. The BIO flume tank is rectangular shaped with dimensions of 32 m in length x 2 m in height x 0.6 m in width. It was fabricated with carbon steel (3/16") and the interior and exterior surfaces are coated with a marine epoxy paint finish to reduce corrosion while operating under marine conditions. Two sets of manifolds consisting of five inflow and outflow pipes (each constructed of 4" PVC pipe and equipped with a ball valve so that the flow rate can be controlled) are fixed (1.1 m from the outer edges) at both ends of the tank (Figure 2). Two high flow centrifugal pumps (Magnatex 3575 Series, 3" suction, 4" discharge, 600 gpm, Houston, TX), one connected to the inflow manifold and the second connected to the outflow manifold provide a flow-through system used to generate horizontal water currents in the tank. A fiberglass holding tank is used to supply seawater for the system to ensure that a constant flow rate is maintained.

Seawater was obtained from the Bedford Basin, which is directly adjacent to the tank. Two smaller pumps (5 HP Pacer S Series Centrifugal Pump, 110 gpm, Lancaster, PA) were used to pull seawater (~50 cm below the surface) through a 3" suction hose from the Basin. A foot valve was installed at the end of the hose to maintain prime water in the line between

ED_001324_00000298-00018

fillings. Prior to entering the tank, the seawater was filtered through high-flow polypropylene bag filters (5 µm and 25 µm, Atlantic Purification, Dartmouth, NS).

During normal operations, the flume tank (30,000 L) and holding tanks (25, 000 L) were filled with filtered seawater. A stainless steel baffled was mounted (~0.5 m) in front of the influent manifold to control current flow. Flow gauges on the influent and effluent lines were monitored and valve adjustments were made to obtain a balanced flow rate, and so that the operational volume was maintained throughout the experiment. Water current velocities were measured at various depths and locations in the tank using an ADV (Nortek Vectrino+, Boston, MA) and the flow rates adjusted until the horizontal water current velocities (1 cm/s) were consistent at all measured depths.

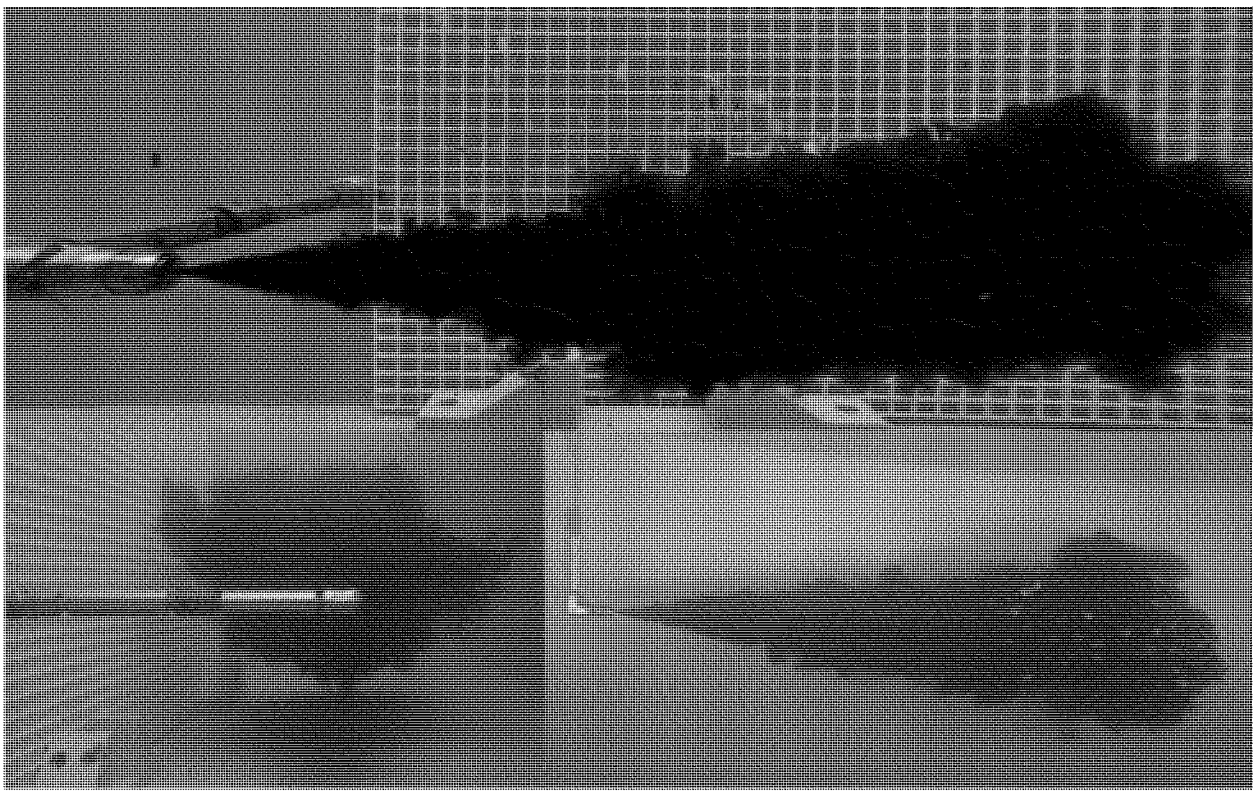

ED_001324_00000298-00019

Figure 1. Photos of subsurface oil injection at the BIO flume tank showing the formation of the subsurface oil plume.

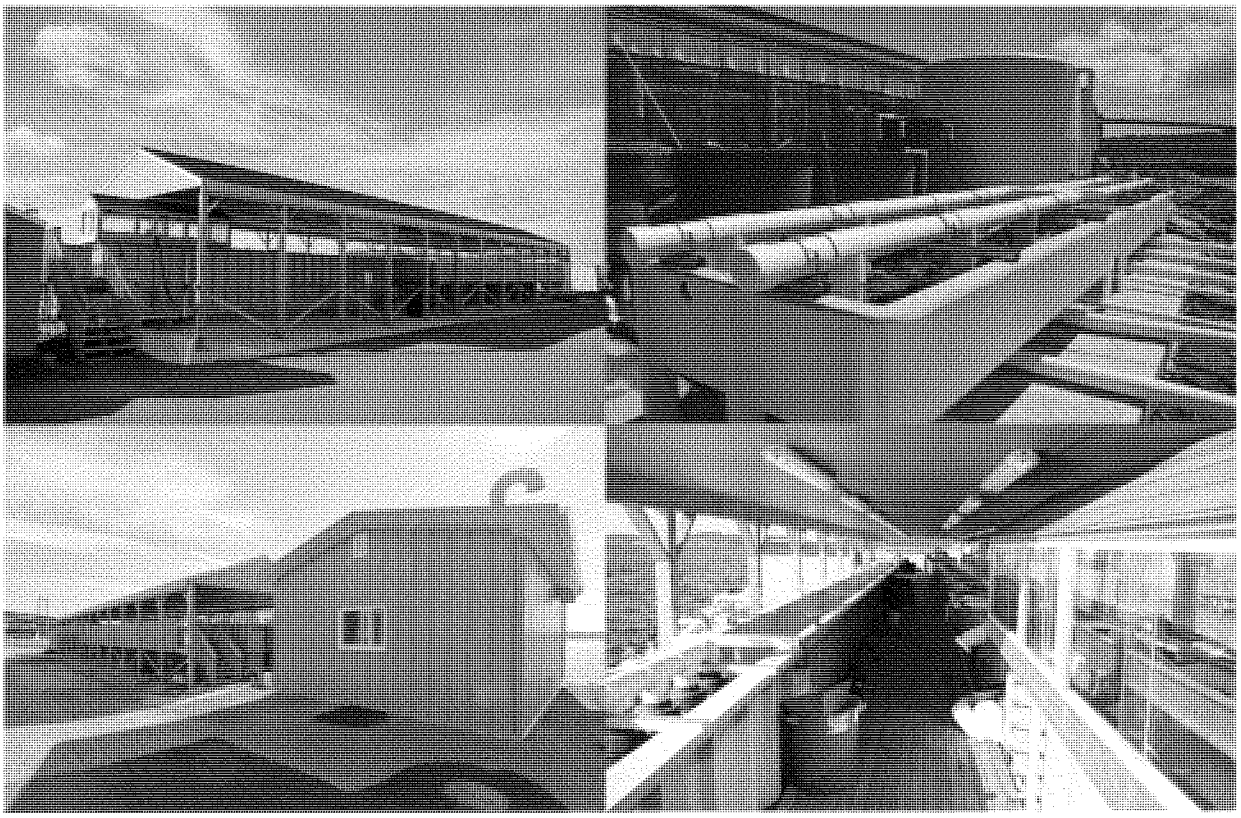

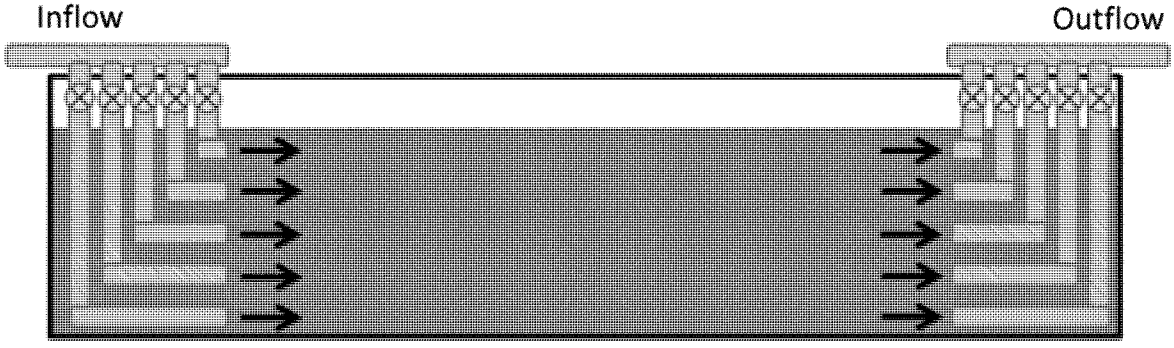

Figure 2. Photo of the DFO BIO flume tank (top) and cross-section of the tank showing the high-flow manifolds used to generate horizontal water currents (not to scale).

A.2.2 Waste Water Treatment

Oil absorbent pads (New Pig, Tipton, PA) are used to manually remove oil from the water surface. The remaining water in the tank is removed by pumping it through an effluent pipe that discharges the waste water over layers of polypropylene PomPom Oil-Mops (New Pig, Tipton, PA) that filter the waste water by removing any remaining insoluble oil prior to discharging it back into the Bedford Basin. Water samples are collected from the treated effluent and the PomPom's are changed if total petroleum hydrocarbon concentrations exceed the minimum guidelines (10 ppm) for wastewater discharge in Canada.

A.2.3 Subsurface Oil Injection System

A custom (engineered in-house) subsurface oil injection system was used to generate dispersed oil plumes in the tank (Figure 3). Briefly, the system consists of a 2 L stainless steel pressure vessel that rests in a support rack. A series of valves and pressure gauges are connected to the pressure vessel. The assembled system is fastened to the outer wall of the tank by way of a quick connect bulkhead fitting. From the same location inside the tank, the fitting connects the outer assembly to a nozzle (2.4 mm inner diameter), which extends mid-width perpendicular to the tank wall (20 cm off the bottom and 9 m downstream from the inflow manifold) and is angled at the tip, so as to direct the discharge plume downstream. Given the shallow nature of the tank, this release setup enabled using the horizontal length of the tank to capture the plume movement.

ED_001324_00000298-00021

For each experiment, oil or oil/dispersant premix is added to the pressure vessel (Figure 4A) in order to reduce the influence of any additional confounding factor of mixing effectiveness. Inside the pressure vessel is a copper coil that is connected to a water bath to permit the oil to be heated to 80°C, which takes 30 minutes. The vessel is then pressurized (40 psi for ANS, SLC and Condensate; 60 psi for IFO 120) with compressed Nitrogen. A ball valve connected to the pressure vessel is manually opened and oil is released through the subsurface nozzle into the flume tank (Figure 4B). The release time and total volume (determined by mass) of oil injected are recorded. After each experiment, the entire subsurface injector system was cleaned by flushing with toluene, acetone and fresh water prior to next experiment.

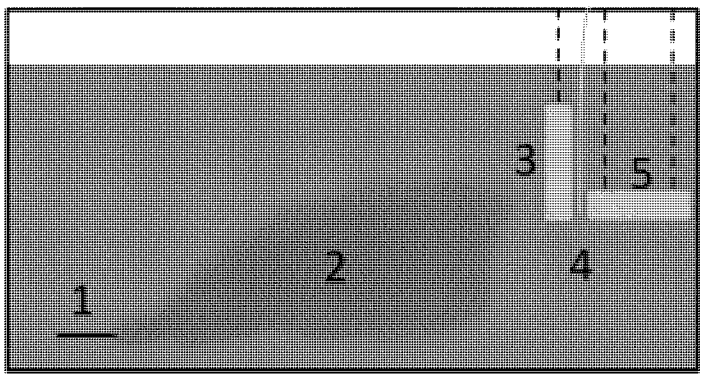

1. Subsurface Injection Nozzle
2. Oil Plume
3. Insitu fluorometers
4. Water sampling port
5. LISST

Figure 3. Schematic diagram showing the location of the subsurface injector and *in situ* instrumentation submerged within the tank.

ED_001324_00000298-00022

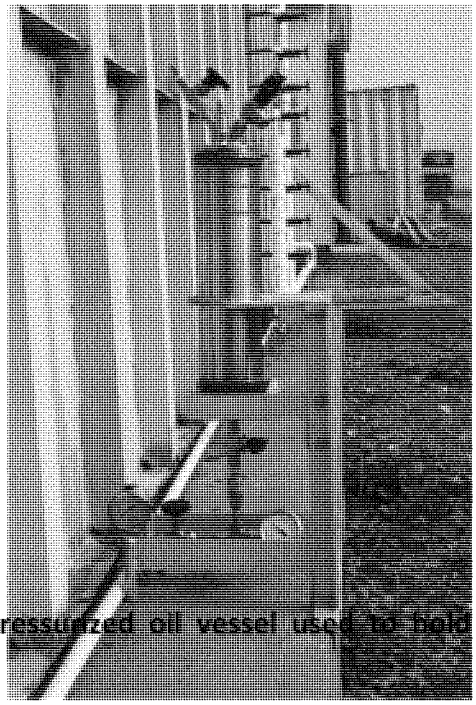

Figure 4A. Photo of the pressurized oil vessel used to hold the oil for the subsurface release.

ED_001324_00000298-00023

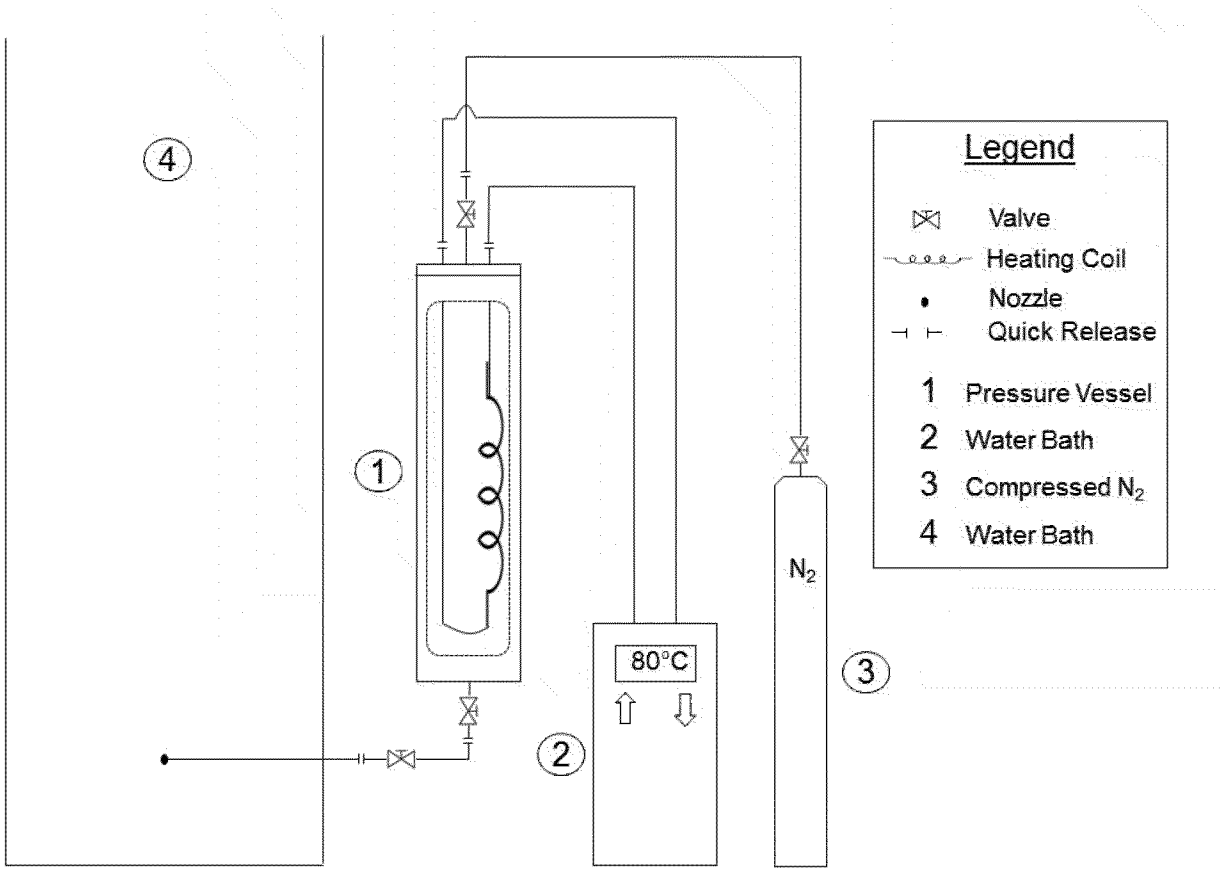

Figure 4B. Schematic diagram of the pressurized oil vessel for subsurface oil release system in the flume tank.

ED_001324_00000298-00024

A.2.4 Submersible Sensor Deployment

Fluorescence- A total of six hydrocarbon fluorometers were evaluated during this study (Table 1). The fluorometers were mounted on an aluminum frame located 4.3 m from the oil release point with their UV windows and at a depth of 0.4 m. The instruments were attached to a crosspiece support bar, so that they were all located the same distance downstream from the oil release point with the UV window pointed directly down at the bottom of the tank.

Table 1. List of hydrocarbon fluorometers used in this study.

Instrument	Excitation/Emission wavelengths
Chelsea UV AQUAtracka (Refined)	239/360nm
Chelsea UV AQUAtracka (Crude)	239/440nm
Turner Designs Cyclops (Fine Oil)	254/350nm
Turner Designs Cyclops (Crude Oil)	365/510nm
Sea Bird – WET Labs ECO-FLU	370/460nm
GmbH Trios	254/360nm

Several different data acquisition systems were used to control and collect data from the *in situ* fluorometers. The GmBH Trios was operated by the manufacturer's power supply and data acquisition system using the MSDA_DE software, which provided a real-time display of the signal intensity in calibrated units of µg/L PAH. The sampling rate was set at one reading every five seconds and raw data was saved as a .csv file. The two Turner instruments were connected to a Databank Handheld Datalogger (Turner Designs, Sunnyvale, CA), which

ED_001324_00000298-00025

powered both instruments and recorded data at a sampling rate of 1 reading every 3 seconds. The datalogger auto-gain feature cycles through settings of 1x, 10x, and 100x depending on the signal intensity. Raw data was recorded as signal intensity in mV and was offloaded from the datalogger via USB connection to a laptop and saved as a .txt file. The Sea Bird - WET Labs and Chelsea instruments were connected to a custom-built power supply and data acquisition system (Pace Scientific XR5-SE datalogger; Mooresville, NC), which collected data from the instruments at a sampling rate of one reading per second. The signal was recorded internally on the datalogger and then sent via wireless connection to a laptop in real-time display. Raw data was recorded as signal intensity in mV and offloaded as a .txt file.

Particle Size Analysis - Oil droplet size was measured *in situ* using two LISST-100X particle size analyzers (Sequoia Scientific, Seattle, WA). The instrument measures particle sizes in the range of 2.5 – 500 µm in 32 logarithmically spaced bins. The first LISST was located immediately after the aluminum frame supporting the fluorometer package at a distance of 5.1 m from the oil release point and the second LISST was located at 16.9 m from the oil release point and both at a depth of 0.4 m. Both instruments were connected via a 20 m cable to laptops running the LISST-SOP data acquisition software (v5). Prior to the start of each experiment, a background scatter file of the seawater quality in the tank was generated and used later to subtract from the final experimental data file. The instruments were operated in real-time mode with a sample acquisition rate of one measurement every three seconds.

Supplemental Measures - Weather conditions (air temperature, wind speed, wind direction, humidity, rainfall) for all experiments were recorded using a Vantage VUE Weather station (Davis Instruments, Hayward, CA). Water temperature and salinity were measured using a YSI handheld probe. Underwater video of oil droplets and the transport of the plume were captured using a GoPro Hero4 digital camera, as well as a Sony RX100 III digital camera with underwater housing.

ED_001324_00000298-00026

A.2.5 VOC Air Monitoring

Surface volatile organic compound (VOC) concentrations were monitored using handheld ToxiRAE Pro PID portable gas detectors (RAE Systems, San Jose, CA). Two detectors were used for each experiment, and they were positioned 0.4 m above the water surface at distances of 5.1 and 16.9 m from the oil release point. The detectors were calibrated using a certified 25 ppm benzene calibration gas (AirLiquide, Dartmouth, NS) according to the manufacturer's recommended procedure. Instrument drift was checked periodically against the calibration gas and recalibrated if necessary. During the experiments, the handheld meters were set to datalogging mode, which recorded VOC concentrations as ppm of Benzene every three seconds. This data was offloaded and saved as a .txt file for processing.

A.2.6 Discrete Water Sample Collection

Water samples for chemical analysis were collected at various time points throughout the experiments (Table 2). Three ¼" stainless steel tubes were attached to the aluminum fluorometer frame, so that the end of the tube was located at the same depth as the instrument UV windows (0.4 m). These were attached via peroxide cured silicon tubing (Cole Parmer, Vernon Hills, IL) to a Masterflex L/S multi-channel digital peristaltic pump (Cole Parmer, Vernon Hills, IL) which flowed to a three-way valve system. When the valve was set to bypass mode, the water in the lines was continuously primed and flowing and it could instantaneously be switched to sample mode to allow for sample collection. The pump flow rate was set to approximately 120 mL/min, and all tubing was flushed with clean seawater for 5 minutes prior to the start of any experiment. Tubing was replaced on an as needed basis. Water samples from the effluent manifolds were also collected through a 1" sampling valve at the exit of effluent pipe, which represented a depth integrated water sample prior to it entering the treatment system.

A.2.7 Oil and Dispersant Samples

Four different hydrocarbon products were tested in this study to cover a range of viscosity and physico-chemical characteristics: Two crude oils, a fuel oil, and a gas condensate.

ED_001324_00000298-00027

Samples of Alaska North Slope crude oil (ANS) and Intermediate Fuel Oil 120 (IFO 120) were obtained from BSEE. Sweet Louisiana Crude was obtained from NOAA. Gas Condensate was obtained from Exxon Mobil and originated from the Sable Offshore Energy Project. Physical properties of the samples (Table 3) were measured using an Anton Paar SVM 3000 Stabinger Viscometer (Anton Paar, Saint Laurent, QC). Supplies of chemical dispersants (Corexit 9500 and Finasol OSR 52) were purchased from the manufacturers.

Table 2. Protocol for collection of water samples for the core and complimentary experiments.

Time (min)	TPH (Tank)	TPH (Effluent)	BTEX (Tank)	BTEX (Effluent)	Fluorometry (Tank)	Fluorometry (Effluent)
Background	X		X		X	
T = 0	X	X	X			
T = 0.5	X					
T = 1.0	X		X		X	
T = 1.5	X					
T = 2.0	X	X	X		X	
T = 2.5	X					
T = 3.0	X		X			
T = 3.5	X					
T = 4.0	X	X	X	X		
T = 4.5	X					
T = 5.0	X		X	X		
T = 6.0	X	X	X	X		
T = 8.0	X	X	X	X		X
T = 10.0	X	X	X	X		
T = 12.0	X	X	X	X		

ED_001324_00000298-00028

Total # Samples/Expt	16	7	11	5	3	1
Total # of Samples Analyzed	TPH – 1725 BTEX – 1200 Fluorometry – 300					

Table 3. Physical property measurements of the oils used in this study.

Oil Type	Measurement Temperature (°C)	Density (g/mL)	Kinematic Viscosity (centistokes)
Alaska North Slope (ANS)	50	0.8529	6.4
	40	0.8600	8.3
	25	0.8704	13.1
	15	0.8777	18.9
Intermediate Fuel Oil (IFO 120)	50	0.9345	134.0
	40	0.9411	240.3
	25	0.9515	781.4
	15	0.9587	2481.5
Gas Condensate (CND)	50	0.7247	0.4
	15	0.7466	0.5
Sweet Louisiana Crude (SLC)	50	0.8219	3.2
	40	0.8291	4.0
	25	0.8733	5.8

ED_001324_00000298-00029

	15	0.8473	8.2

A.2.8 Experimental Design – Core and Complimentary Experiments

Both the flume tank and holding tanks were filled with filtered seawater as described above. Seawater temperature and salinity were recorded using a handheld probe (YSI Incorporated, Yellow Springs, OH). After the flume tank was filled, the *in situ* instrumentations including the fluorometers, LISSTs, and VOC meters were positioned in desired locations as indicated previously. The subsurface oil release system was filled with oil or oil/dispersant premix, which was heated to operating temperature. The water supply lines leading to the high flow pumps were primed and the inflow and outflow pumps were started. The system was run in recirculation mode for 10 minutes to allow current flow to stabilize in the flume tank. At a set time point prior to oil injection (5 minutes), data-logging on all instruments was started and background seawater samples were collected. After the oil was injected into the tank, the real-time readout of the fluorometer signal was monitored. Once the first spike in signal intensity was observed (usually after 2 minutes based on the fluorometer signal readout), a stopwatch was started and the first chemistry samples were collected. At this point the high flow system was switched from recirculation mode to flow through, which diverted the water flow into the effluent treatment system instead of returning it to the holding tank. The experiment ran for 12 minutes, at which point the high flow pumps were turned off and the instrument data acquisition was stopped. The tank was cleaned and drained as described above. Tank and instruments were cleaned using Big Orange Degreaser (Zep Superior Solutions, Atlanta, GA), to prevent any potential contamination between experiments. Instrument windows were cleaned using disposable alcohol wipes (Bausch and Lomb, Vaughan, ON). Water samples were returned to the lab and stored at 4°C.

ED_001324_00000298-00030

A.2.9 Submersible Sensor Calibration Experiments

The calibration experimental setup was similar to the core and complimentary experiments, except that the oil was added in a step-wise (tank dilution series measurements) fashion to the flume tank as shown in Table 4. Calibration experiments were conducted in such a way to create a series of known concentrations of dispersed oil in the flume tank. Predetermined amounts of oil and dispersant (Corexit 9500) premix were added to the tank (Alaska North Slope, ANS, crude was used at a DOR of 1:20) using the subsurface injector.

The flume tank was operated in recirculation mode and oil/dispersant premix injections occurred every 45 minutes, which provided a sufficient time for the dispersed oil concentrations to stabilize in the tank (previous testing of this system showed that hydrocarbon concentrations in the tank are homogenous after 45 minutes of recirculation). The currents created by the high flow system provided sufficient mixing energy to allow droplets generated by the subsurface injector to remain dispersed in the water column. *In situ* instrumentation was located at the same locations as all other experiments. Water samples were collected at 45 minute time intervals after each oil addition.

Upon reaching homogeneity in the tank (i.e. 45 minutes after each oil addition), the average fluorometric intensity signal collected over a 4 minute time period was calculated. Fluorometers were calibrated to manufacturer suggested units using factors provided. Triplicate water sample analysis results for TPH and BTEX were averaged that correspond with the same time points. Fluorescence and chemistry averages were regressed to generate calibration curves of TPH and BTEX vs signal intensity for oil additions ranging from 1 to 18 ppm. Higher variability at low concentrations resulted in the exclusion of some data points in the regression calculation.

Table 4. Step-wise sensor calibration experiment parameters.

Oil Addition #	Mass of Oil Added for each Addition (g)	Cumulative Oil Concentration in Tank (mg/L)

ED_001324_00000298-00031

1	9.45	0.3
2	9.45	0.6
3	12.6	1
4	63	3
5	94.5	6
6	189	12
7	189	18

A.2.10 Submersible Fluorometer and LISST Data Processing

Raw LISST data files were processed using a statistically based quality control script written using the R statistical package. In summary, this script identifies and removes "Over Range" samples (defined as 0 µL/L across all particle size bins) and outliers. Outliers are defined as any reading that is greater than the moving mean (5 data points before and after the targeted time point) of the dataset multiplied by four times the standard deviation (over the same interval as the moving mean). Due to the potential for one or more extreme outliers to skew both the moving mean and standard deviation calculations for points around them, this outlier detection routine is run iteratively, excluding previously flagged points, until no more outliers are detected. Once these QC steps have been performed the script calculates a number of parameters from the data such as Total Particle Concentration (TPC), Volume Mean Diameter (VMD), and Particle Size Concentration (PSC). It then goes on to detect the plume curve (if present) and time-normalizes the data based on that location. Data presented as Droplet Size Distribution (DSD). Plots presented include data 2 minutes before and 8 minutes after the start of the plume curve. Data from the Downstream LISST were normalized so that the plume began at t = 5 min in order to visually convey that the plume was detected in the tank roughly 3 min after detection by the LISST further upstream near point of injection release.

Similar to the LISST data, a script was used to detect outliers in data collected from the *in situ* fluorometers. Curve detection was then performed and the data was time-normalized to

ED_001324_00000298-00032

include 2 minutes of data before, and 8 minutes of data after the start of the plume curve. The baseline of the plume curve was then calculated using data points observed in the first minute preceding the start of the curve and this baseline was subtracted from the data. Finally, factory calibration factors were applied to the data values for each instrument before plotting.

A.2.11 Analytical Chemistry Analysis

Total Petroleum Hydrocarbon (TPH) Analysis - The method used for extraction and processing of TPH samples was developed by DFO in-house (Cole et al., 2007; King et al., 2015). Water samples were collected in pre-weighed 125 mL amber glass bottles and filled to approximately 90 mL. Sample bottles were weighed and a mass difference was used to determine the total volume of the collected water sample. The samples were immediately stored at 4°C until ready for further processing. Within 24 hrs of collection, 10.0 mL of dichloromethane (DCM) was added to each sample. The samples were shaken by hand for 30 seconds, and then placed on a Wheaton R2P roller (Wheaton, Millville, NJ) set at 9 rpm. After 18 hours on the roller, a Pasteur pipette was used to transfer the DCM solvent layer into a pre-weighed 15 mL graduated centrifuge tube. The solvent was then evaporated under a gentle stream of nitrogen using an N-Evap (Organomation, Berlin, MA) and topped up with DCM to a final volume of 1.00 mL. The solvent extract was transferred into an auto-sampler vial and stored at -20°C for GC-FID analysis.

Sample extracts (1 µL) were injected using an Agilent 7683 auto-sampler into an Agilent 7890B GC, using splitless injection set to oven track mode (2°C higher than the oven temperature program). The column used for separations was a Supelco MDN-5s 30 m × 250 µm × 0.25 µm (length × i.d. × film thickness). Hydrogen was used as a carrier gas with a flow rate of 3.0 mL/min. The GC oven is programmed to an initial oven temperature of 35°C, held for 2 min, followed by an increase to 320°C at 20°C/min, and held at 320°C for 10 min, with a total run time of 26.25 min. The GC flame ionization detector (FID) was operated at 320°C with the hydrogen flow set at 30 mL/min and the air flow set at 400 mL/min. An eight point

ED_001324_00000298-00033

calibration was generated using standards prepared from the appropriate crude oil stock that was used to generate the TPH samples (e.g. ANS, IFO 120, SLC or Gas Condensate). Peak quantification was performed using relative response factors. Routinely the method of extraction was tested for efficiency by a spike and recovery study. Typically, a mean percent recovery of >90% was calculated from filtered seawater spiked with crude oil. Lab and field blanks were incorporated in the method.

BTEX Analysis - EPA Method 8240 (purge and trap) was modified by running a gas chromatograph/mass spectrometer in selected ion monitoring mode to include ethylbenzene. To summarize, water samples for BTEX (benzene, toluene, ethylbenzene and [m,p & o] xylene) analysis were collected in 40 mL purge and trap vials. The vials were spiked with 40 µL of 6N HCl to serve as a preservative, so that they can be stored at 4°C for up to 14 days.

The purge and trap system was a Teledyne Tekmar Stratum PTC purge and trap concentrator equipped with a Tenax/silica gel/charcoal trap. The auto-sampler was a Teledyne Tekmar Aquatek 70-vial unit. The auto-sampler transferred a 5 mL aliquot of sample into the purge and trap chamber, where it was purged with helium for 11 minutes. During this process, the volatiles were trapped on the Tenax trap and then desorbed at 225°C for 2 min. The desorbed gases enter a heated transfer line connected to the Agilent 6890 GC injector and subsequently proceed to the GC column (Supelco MDN-5s 30 m × 250 µm × 0.25 µm length × i.d. × film thickness).

The GC oven was programmed at an initial oven temperature of 50ºC, held for 8 min, followed by an increase to 280ºC at 40ºC/min, and held at 280ºC for 2 min, for a total run time of 18 min. The gases exiting the GC column were detected by an Agilent 5973 mass selective detector (MS) used in selective ion mode (SIM) monitoring for six ions: 77, 78, 91, 92, 105 and 106 amu. BTEX standards were prepared in 40 mL purge and trap vials. Samples and standards were analyzed using this method, along with sample blanks and duplicate

ED_001324_00000298-00034

samples.

A.2.12 Numerical Modeling Methods

Refer to Appendices G and H for numerical modeling components.

TASK A.3 RESULTS

The overarching objective for this project was to evaluate the operational performance of the subsurface injection of dispersants during deepwater blowouts. Presented here are the results from a series of flume tank subsurface injection experiments where dispersion effectiveness was evaluated via response monitoring tools (fluorescence and particle size analyzers), discrete water sample chemistry analysis and VOC air monitors. The logs for all experiments conducted can be found in Appendix A. Corresponding chemistry results for each experiment are tabulated in Appendix B.

A.3.1 ANS Dispersion Effectiveness

Injection experiments were conducted using ANS crude oil, chemically dispersed with Corexit and Finasol. Regardless of warm ($\geq$ 11°C) or cold (5.4 – 10.7°C) water temperatures, the addition of the two tested dispersant lowers the VMD of ANS and shifts the DSD to smaller droplets within the plume. An example of this trend is shown in Figures 5 and 6. Note that LISST histogram plots have constrained Y-axes; thus lines that extend slightly above the top of the plot area represent values that were truncated. Plots for triplicate

ED_001324_00000298-00035

experiments for each treatment are shown in Appendices C and D. All plots represent data from the LISST positioned closest to the jet release (denoted as Jet Release LISST throughout the document) and in close proximity to the submersible fluorometers. Histograms represent the particle concentration for a given size class (Y axes). Contour plots represent the 10 minute time series of the plume, where colored contours represent the particle concentration (normalized to max value for comparison purposes), Y axes represent the droplet sizes in µm and X axes are time in minutes. These contours allow for ascertaining how the DSD shifts over the duration of the release. A second LISST positioned further downstream of release (denoted as Downstream LISST throughout the document) allows for comparing the evolution of the plume in space and time since release of the plume. For warm temperature experiments, there is a slight decrease in VMD for DOR = 1:200 and 1:100 (Corexit) compared to the no-dispersant treatment (DOR = 0), in this case ~130 µm down to ~80 µm (exact numbers are within text of the figures). A large shift in DSD is observed for the DOR 1:20 treatment, where VMD is ~ 10 µm. The cold water treatments exhibit this same trend, where VMD is ~ 10 µm for the DOR = 1:20 treatment (Figure 6). *In situ* submersible fluorescence from multiple fluorometers was recorded during experiments. Example time series for each dispersant and temperature treatment are shown in Figure 7 and illustrate the impact of dispersant at DOR = 1:20 in the plume. With DORs of 0, 1:200 and 1:100, the plumes tend to exhibit a spike in fluorescence shortly after release (within 2 min), and then a sharp decline in signal that is brought to extinction by 4 minutes. For DOR = 1:20, however, the signal remains elevated and with variability for up to 6 minutes. This indicates that more oil is remaining submerged in the plume for a longer time period. Time series fluorescence plots for triplicate experiments for each treatment are shown in Appendix E.

The Downstream LISST positioned further from the jet release and the fluorometers serves as an indication of plume evolution through the tank. Plots of the Downstream LISST DSD and VMD for all dispersant treatments for warm and cold water experiments are shown in Figures 8 and 9, respectively. Comparing these to the LISST results near the jet release

ED_001324_00000298-00036

illustrates the decrease in Total Particle Concentration (TPC; represents the maximum concentration for the entire plume) as the plume disperses through the tank (note the change of Y axis scale). Also evident is a shift to smaller particles for all DOR treatments as the plume moves through the tank. Where the decrease in TPC suggests plume dilution in the tank, the DSD shift to smaller particles suggests that within each experiment larger droplets were removed from the plume within 6 minutes of the oil release, most likely rising to the surface of the tank.

Warm water experiments conducted with ANS and Finasol OSR 52 dispersant also yield a shift in DSD towards smaller VMD for DOR = 1:20 (Figure 10). However the shift is smaller than that observed with Corexit 9500 (Figure 5), with lowest VMD on the order of ~50-60 µm. DOR = 1:200 and 1:100 treatments exhibited spikes in fluorescence signal that taper off within 3 minutes of oil release (Figure 11). Fluorescence for DOR = 1:20 Finasol OSR 52 treatments exhibited a decrease in intensity at ~4 minutes which is faster than that for treatments with Corexit 9500. The Downstream LISST exhibited a similar shift in DSD and TPC that was observed with Corexit 9500 treatments (Figures 12 and 13).

Water temperatures for experiments ranged between 5.4 – 20.8 °C. In general there was no clear trend on the influence of temperature on DSD, VMD fluorescence intensity, or oil concentrations for the time series for DOR = 0, 1:200 or 1:100 treatments. This suggests that water temperature has little effect on the dispersibility of ANS (80 °C oil temperature) when released as a jet with little or no exposure to chemical dispersant (in this case the pre-mixing process prior to release). In contrast, DOR = 1:20 experiments showed a decrease in total particle concentration (TPC) with decreasing temperature even though no effect was observed on DSD for the two temperatures. Figure 14 shows three examples of this effect, where TPC values for each DOR = 1:20 experiment are strongly correlated with temperature (Figure 15). It is important to note that for all treatments using ANS, the experiment at the lowest temperature (SubANS-10R; 5.4 °C) exhibited anomalous dispersion compared to the other DOR = 1:200 treatments (Appendices C and D). Because

ED_001324_00000298-00037

this occurred in only one experiment out of 33 experiments with ANS, it is difficult to ascribe a cause for this other than an improper jet release of oil.

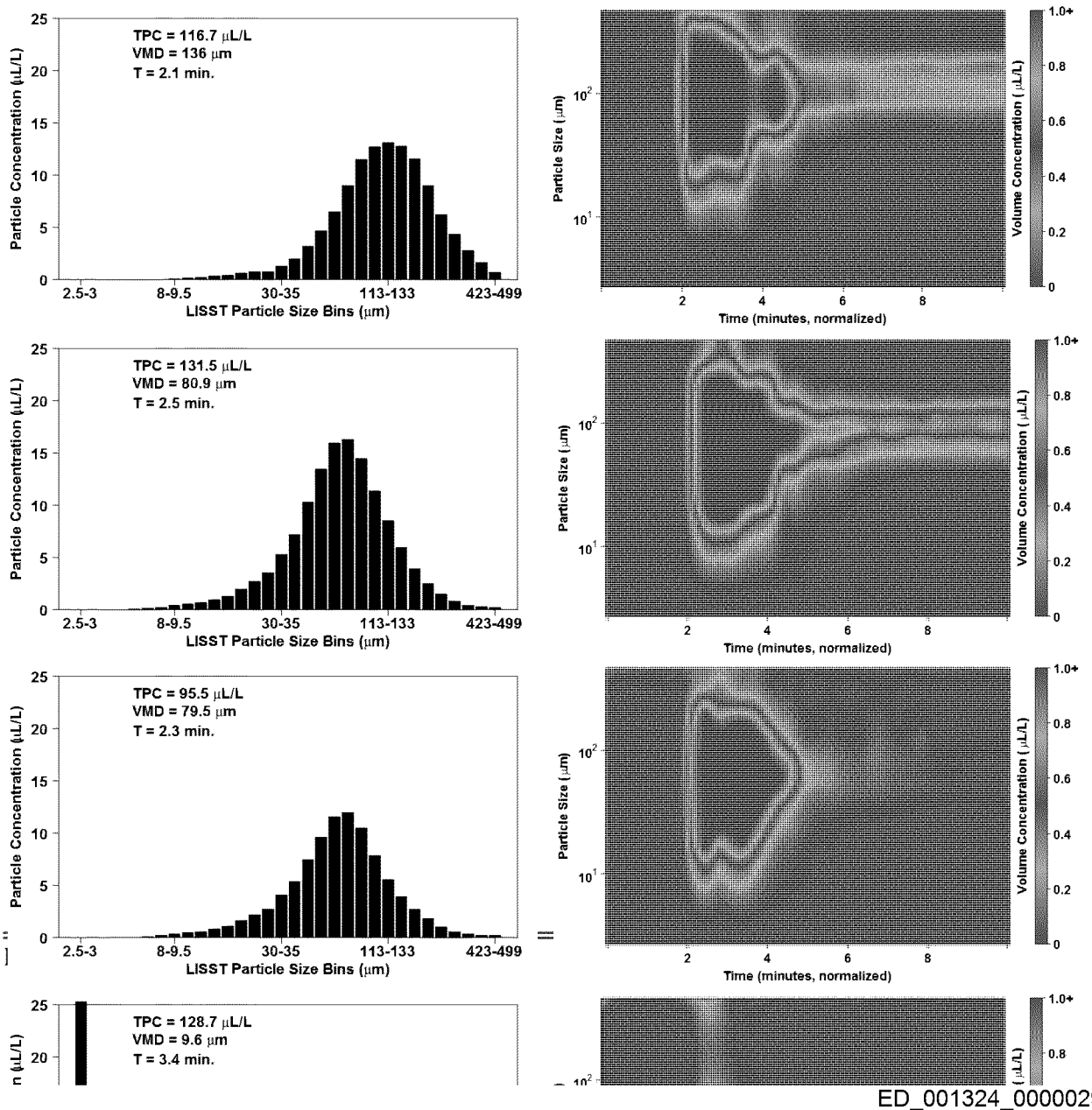

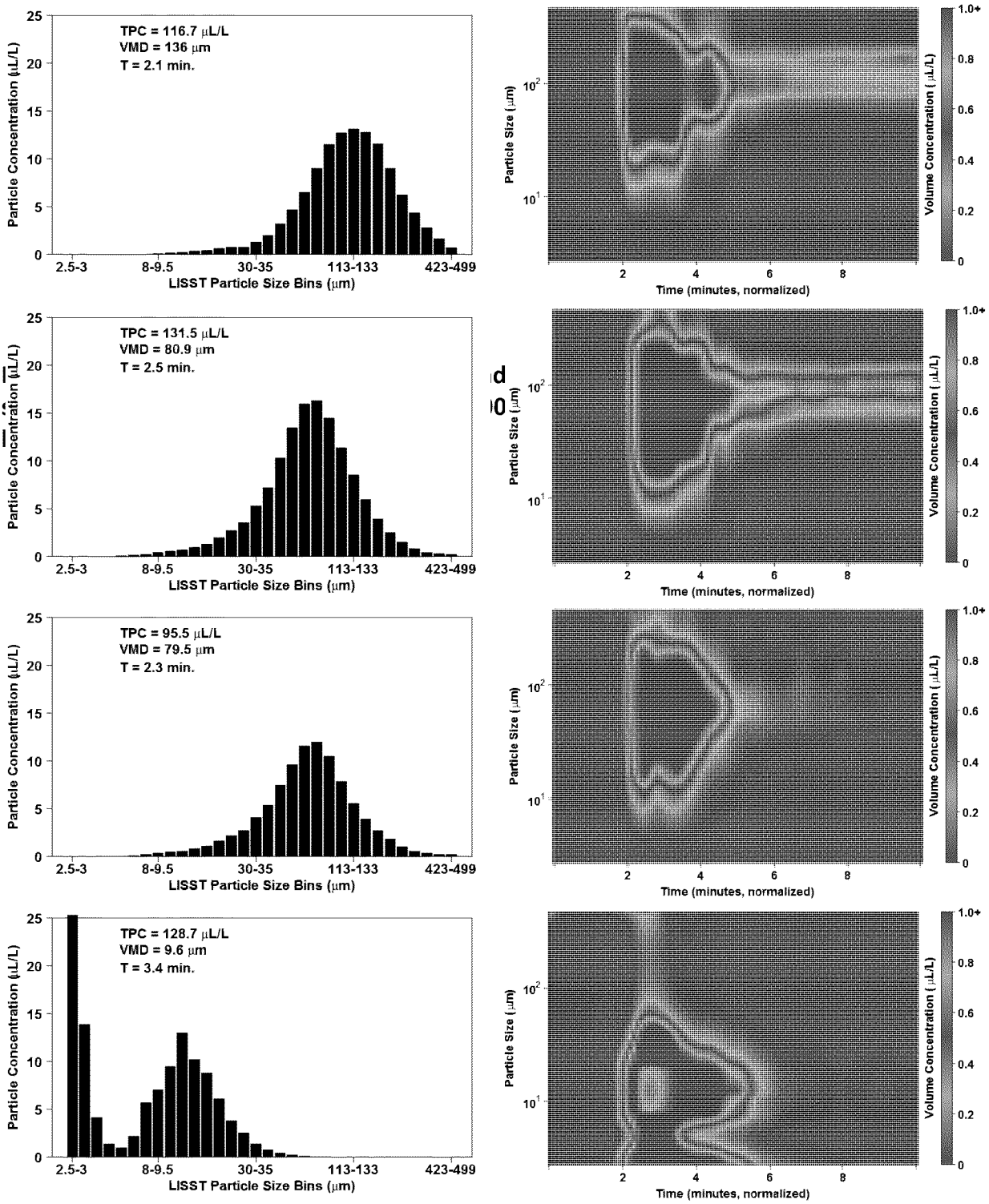
TPC = 116.7 µL/L
VMD = 136 µm
T = 2.1 min.
TPC = 131.5 µL/L
VMD = 80.9 µm
T = 2.5 min.
TPC = 95.5 µL/L
VMD = 79.5 µm
T = 2.3 min.
TPC = 128.7 µL/L
VMD = 9.6 µm
T = 3.4 min.
Particle Concentration (µL/L)
LISST Particle Size Bins (µm)
2.5-3
8-9.5
30-35
113-133
423-499
Particle Size (µm)
Time (minutes, normalized)
Volume Concentration (µL/L)
1.0+

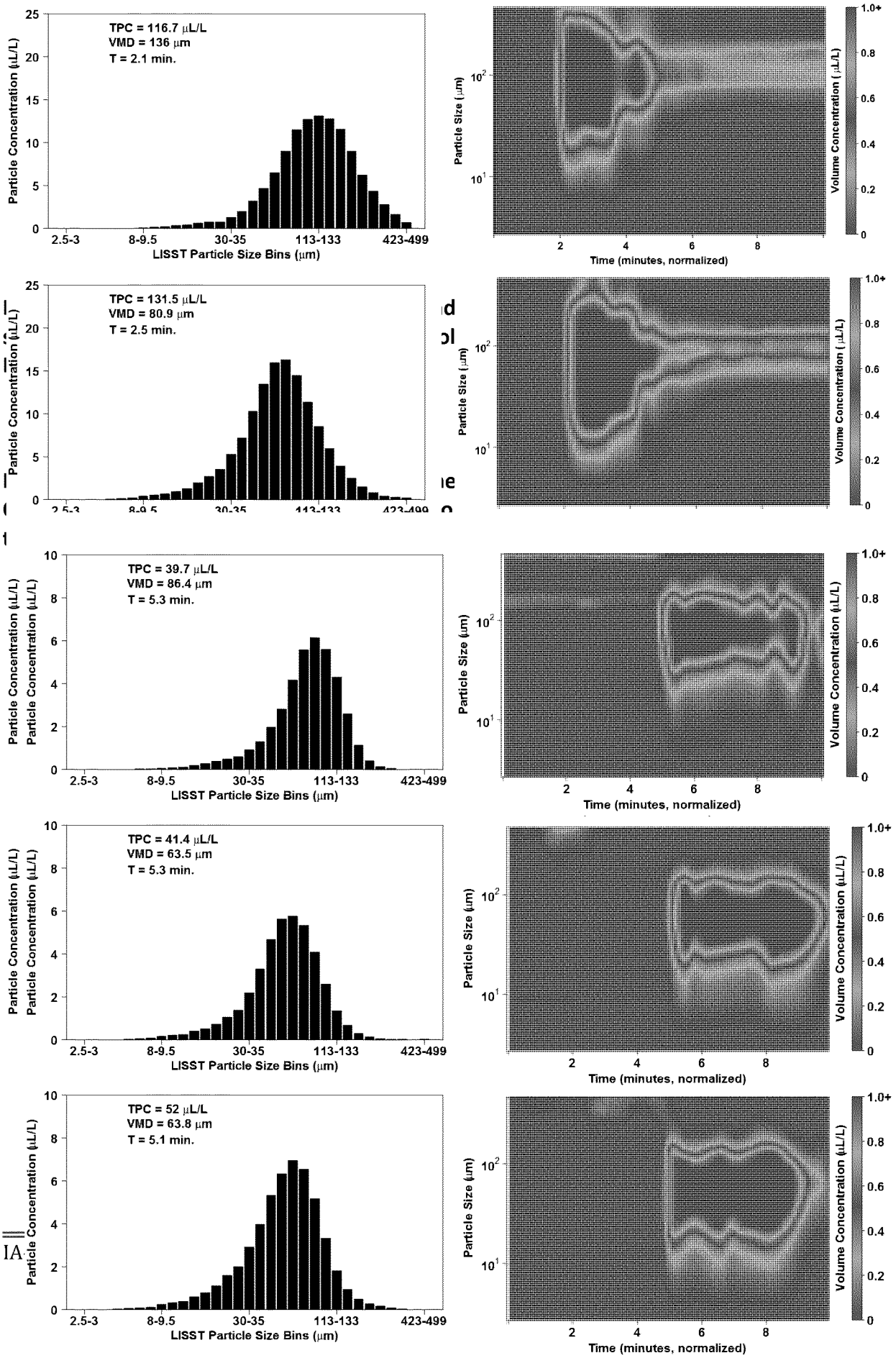
TPC = 116.7 µL/L
VMD = 136 µm
T = 2.1 min.
TPC = 131.5 µL/L
VMD = 80.9 µm
T = 2.5 min.
TPC = 39.7 µL/L
VMD = 86.4 µm
T = 5.3 min.
TPC = 41.4 µL/L
VMD = 63.5 µm
T = 5.3 min.
TPC = 52 µL/L
VMD = 63.8 µm
T = 5.1 min.
Particle Concentration (µL/L)
LISST Particle Size Bins (µm)
2.5-3
8-9.5
30-35
113-133
423-499
Particle Size (µm)
Time (minutes, normalized)
Volume Concentration (µL/L)

Figure 8. Downstream LISST DSD and VMD (left panels) and time series of concentration and particle size (right panels) for ANS and Corexit 9500 warm water treatments. From top to bottom, DOR = 0, 1:200, 1:100, 1:20.

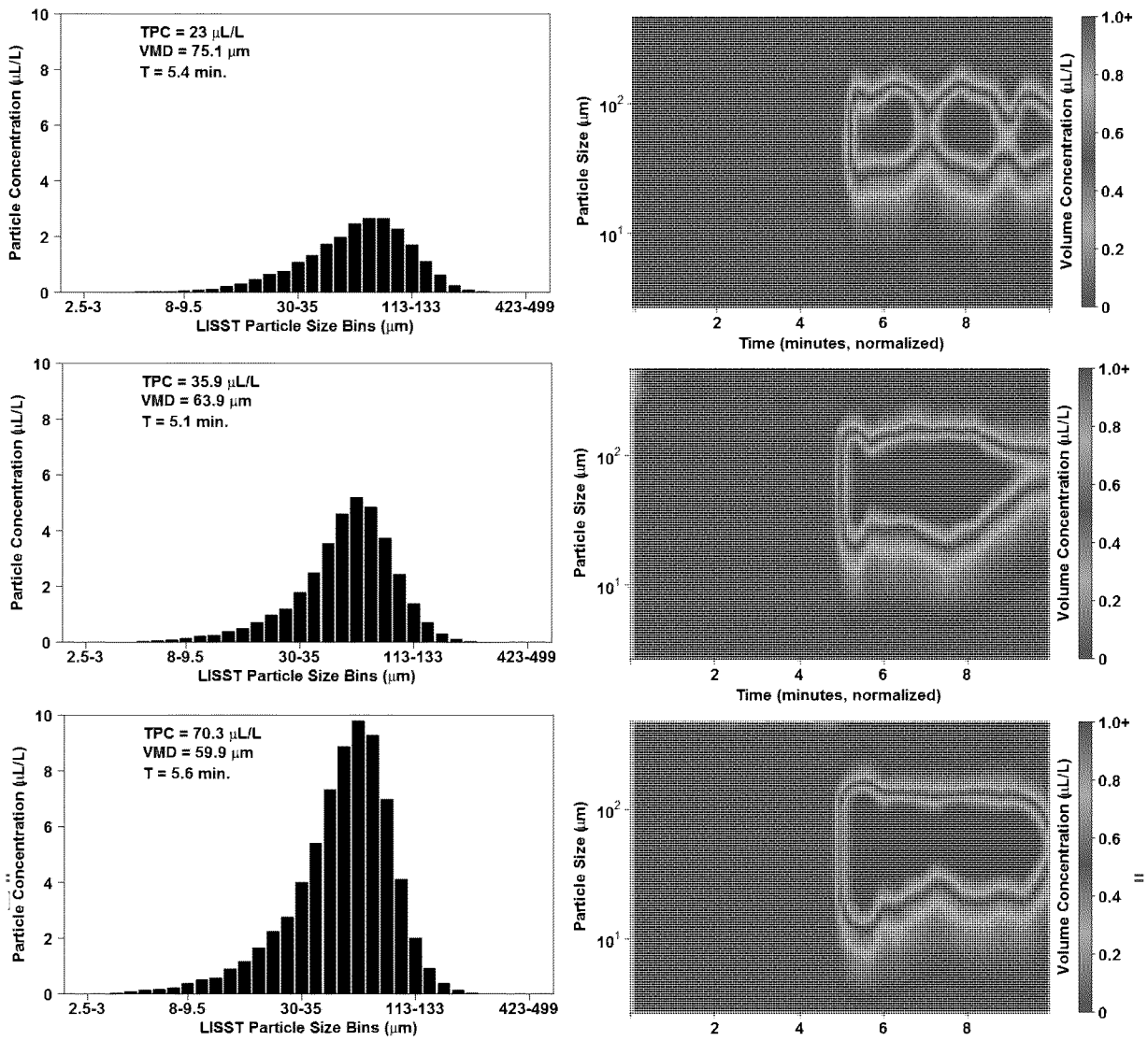

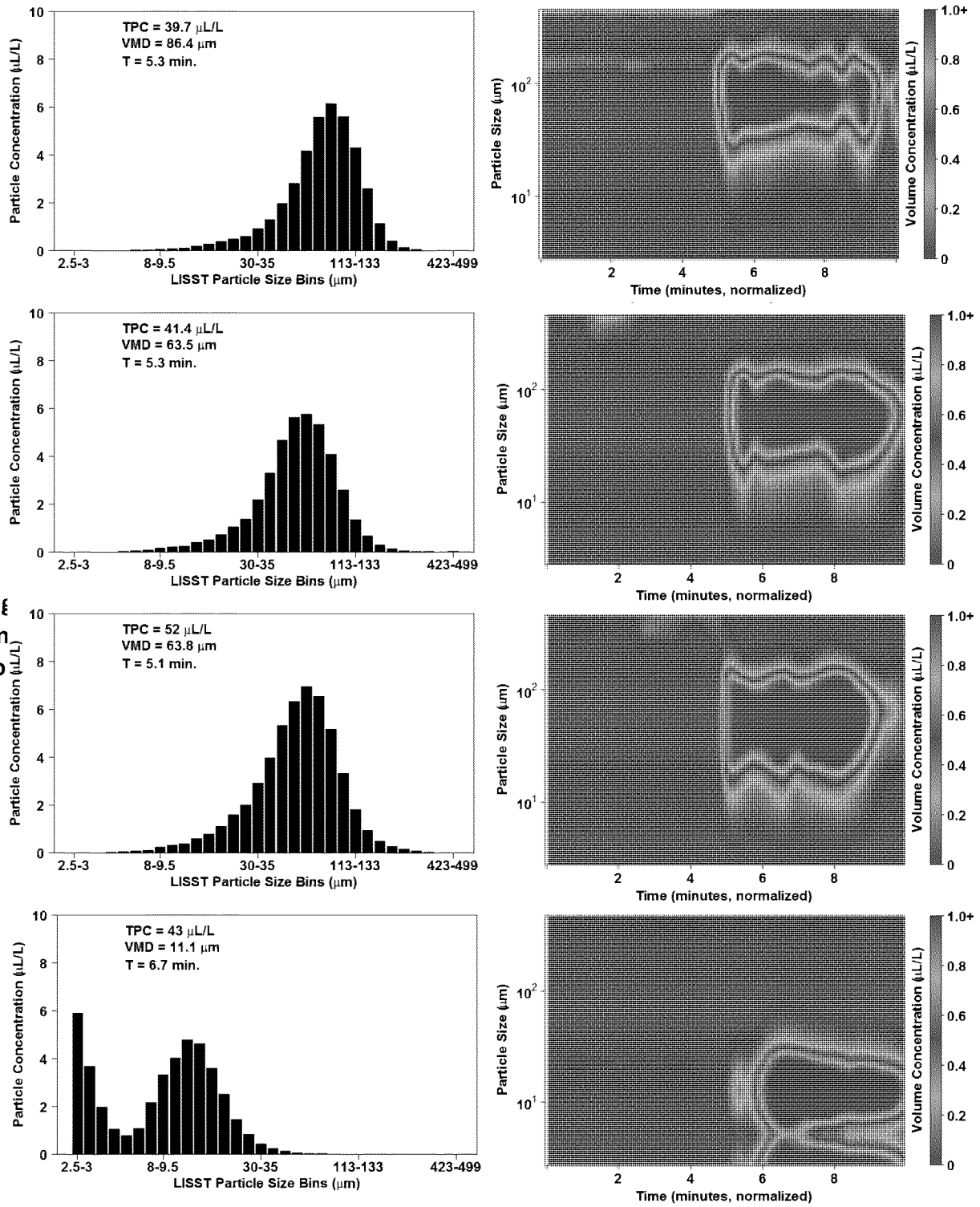
TPC = 39.7 µL/L
VMD = 86.4 µm
T = 5.3 min.
TPC = 41.4 µL/L
VMD = 63.5 µm
T = 5.3 min.
TPC = 52 µL/L
VMD = 63.8 µm
T = 5.1 min.
TPC = 43 µL/L
VMD = 11.1 µm
T = 6.7 min.
Particle Concentration (µL/L)
LISST Particle Size Bins (µm)
2.5-3
8-9.5
30-35
113-133
423-499
Particle Size (µm)
Time (minutes, normalized)
Volume Concentration (µL/L)
1.0+

Fig
an
to

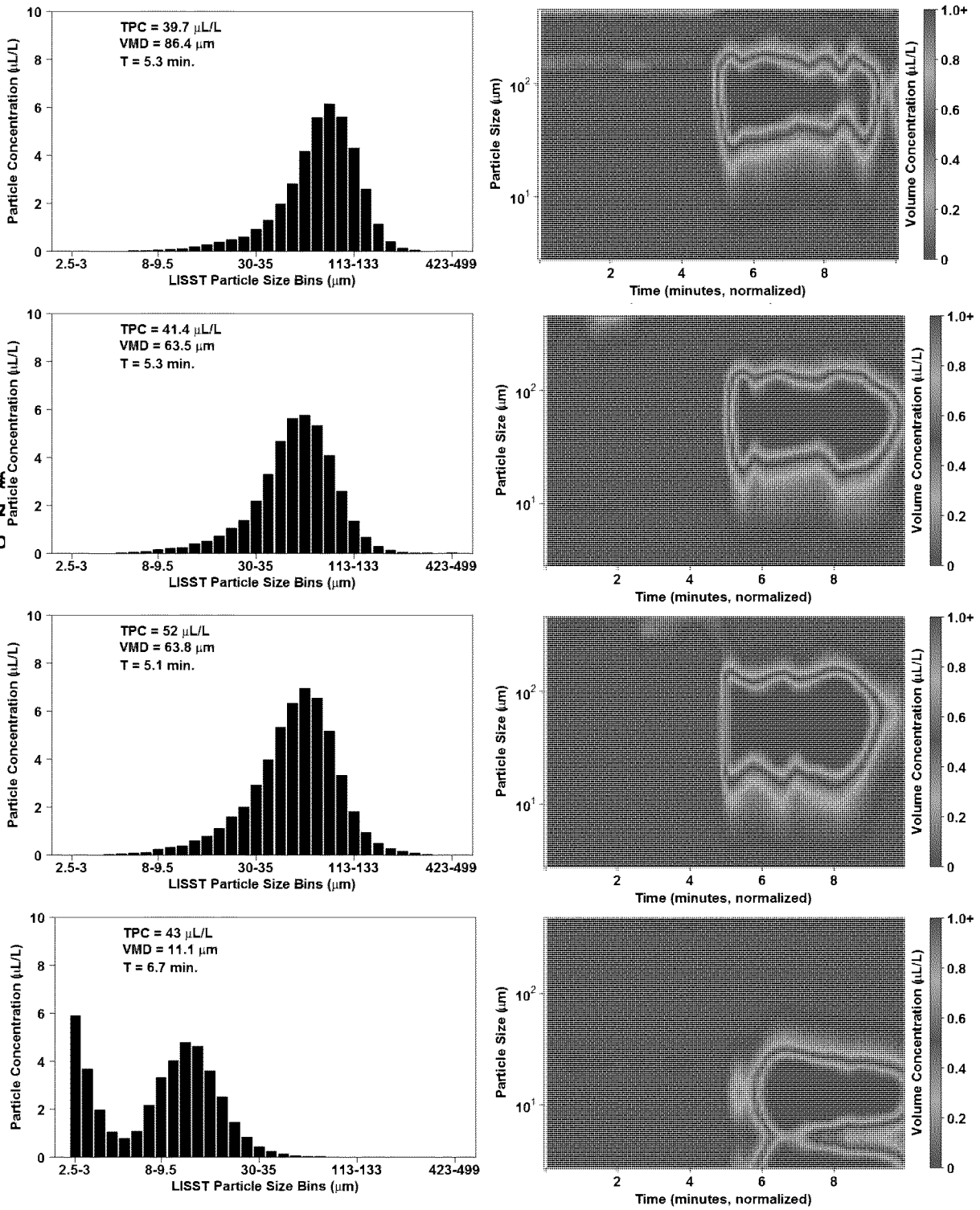
TPC = 39.7 µL/L
VMD = 86.4 µm
T = 5.3 min.
TPC = 41.4 µL/L
VMD = 63.5 µm
T = 5.3 min.
TPC = 52 µL/L
VMD = 63.8 µm
T = 5.1 min.
TPC = 43 µL/L
VMD = 11.1 µm
T = 6.7 min.
Particle Concentration (µL/L)
LISST Particle Size Bins (µm)
2.5-3
8-9.5
30-35
113-133
423-499
Particle Size (µm)
Time (minutes, normalized)
Volume Concentration (µL/L)
1.0+

Fig
siz
bo

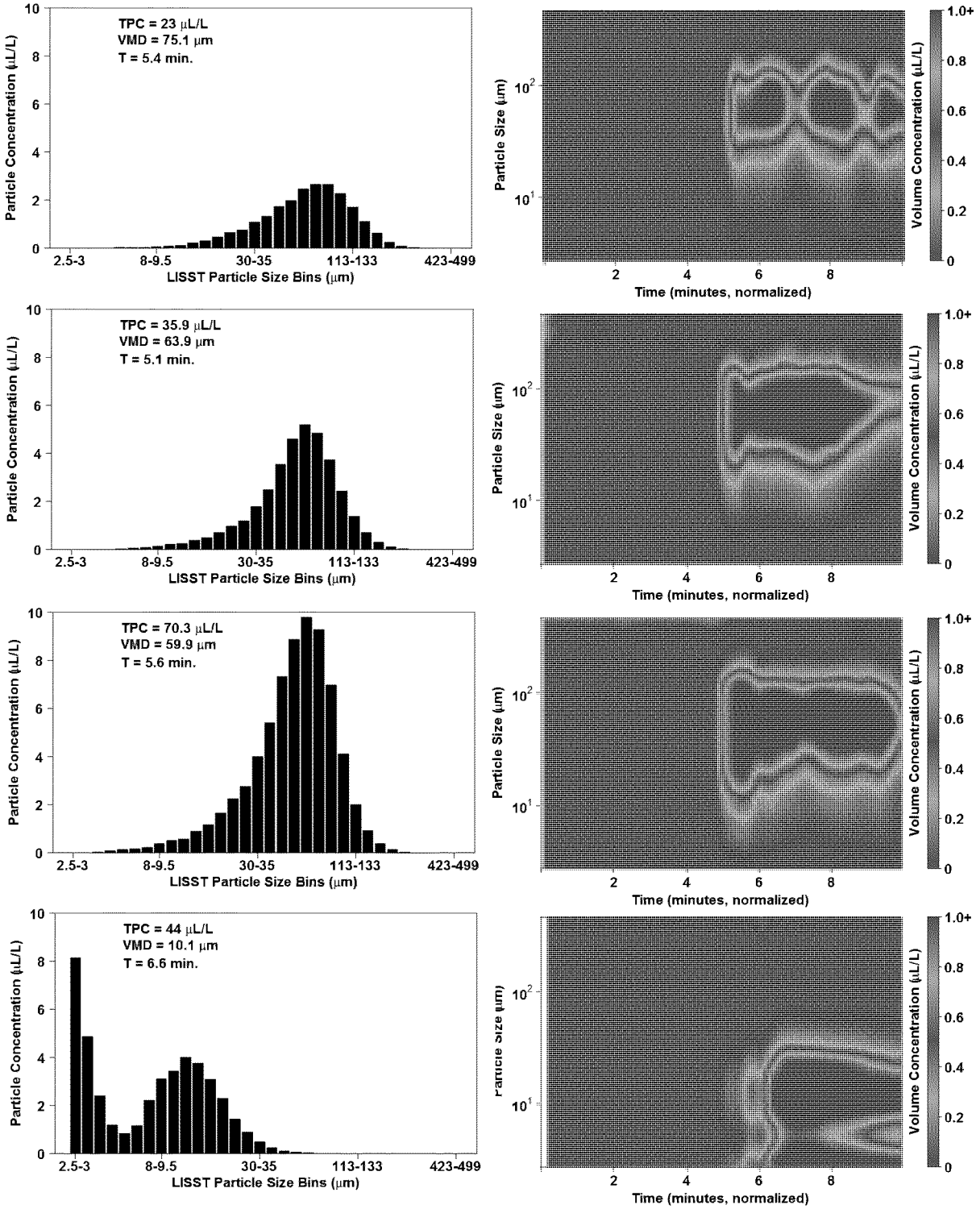
TPC = 23 µL/L
VMD = 75.1 µm
T = 5.4 min.
TPC = 35.9 µL/L
VMD = 63.9 µm
T = 5.1 min.
TPC = 70.3 µL/L
VMD = 59.9 µm
T = 5.6 min.
TPC = 44 µL/L
VMD = 10.1 µm
T = 6.6 min.
Particle Concentration (µL/L)
LISST Particle Size Bins (µm)
2.5-3
8-9.5
30-35
113-133
423-499
Particle Size (µm)
Time (minutes, normalized)
Volume Concentration (µL/L)
1.0+

Figure 12. Downstream LISST DSD and VMD (left panels) and time series of concentration and particle size (right panels) for ANS and Finasol OSR 52 warm water treatments. From top to bottom, DOR = 1:200, 1:100, 1:20.

ED_001324_00000298-00045

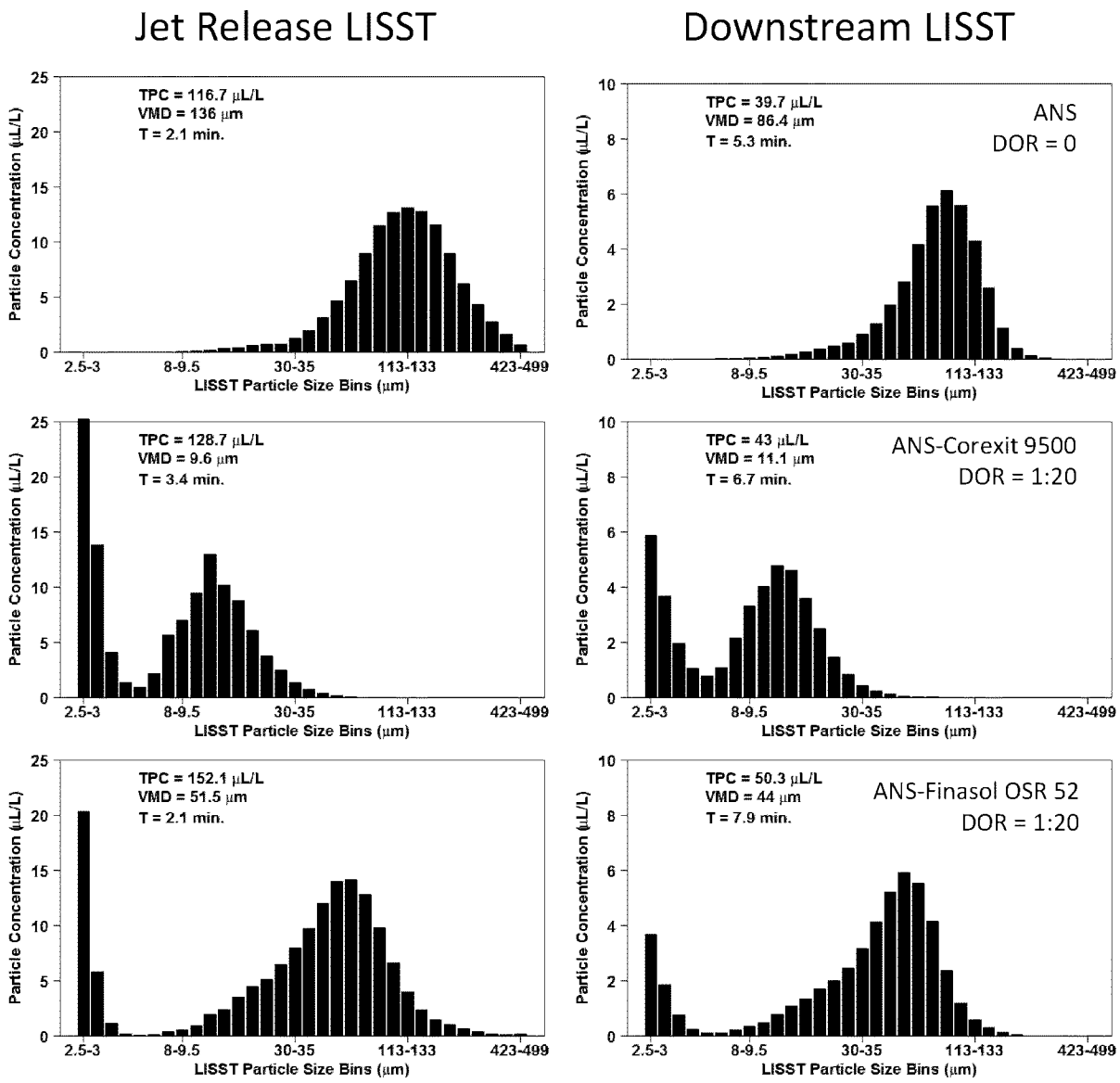

Figure 13. LISST DSD with TPC for ANS with Corexit 9500 and Finasol OSR 52 treatments. DOR = 0 (top panel); DOR = 1:20 experiments are middle and bottom panels.

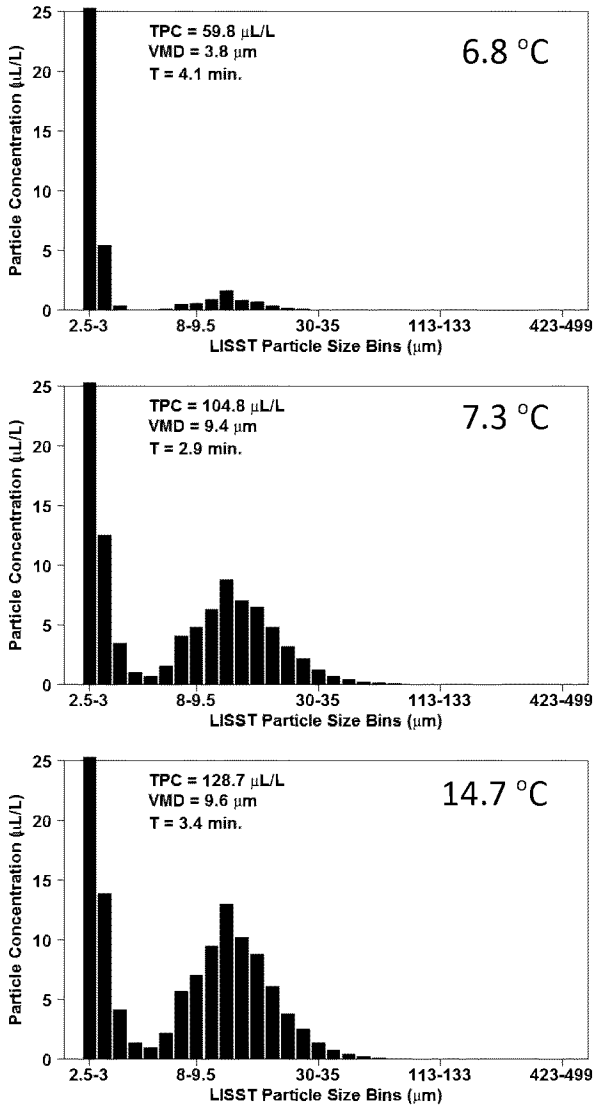

Figure 14. LISST DSD with TPC (Total Particle Concentration) for DOR = 1:20 experiments of ANS and Corexit 9500 treatments. Water temperatures increase from top to bottom panels.

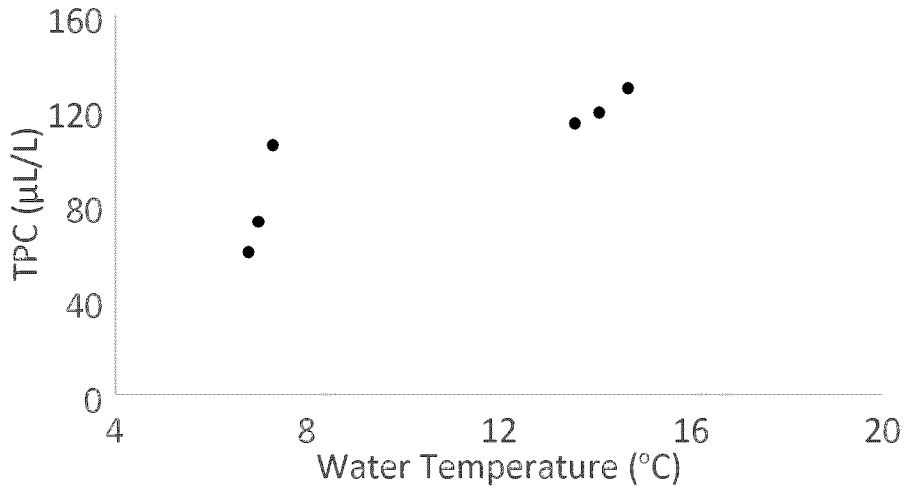

Figure 15. LISST TPC (Total Particle Concentration) for DOR = 1:20 experiments of ANS and Corexit 9500 treatments as a function of water temperature.

ED_001324_00000298-00048

A.3.2 IFO 120 Dispersion Effectiveness

Injection experiments were conducted using Intermediate Fuel Oil (IFO 120), chemically dispersed with Corexit 9500 and Finasol OSR 52. For warm water experiments, temperatures ranged between 13.5 – 16 °C for treatments with Corexit 9500 and between 17.5 – 20.3 °C for treatments with Finasol OSR 52. In the DOR = 0, 1:200 and 1:100 treatments using Corexit 9500, VMD typically remained > 200 µm (Figure 16). VMD values were smaller for DOR = 1:20 treatments (~66-120 µm), indicating a shift in DSD, but to a lesser extent than the shift observed for ANS experiments. Fluorescence data exhibited scatter and noise in the signal for all but the DOR = 1:20 treatments (Appendix E). A similar trend in DSD, VMD and fluorescence signal was observed for IFO 120 exposed to Finasol OSR 52 at warm temperatures (Figure 17), where DOR = 1:200, 1:100 and 1:20 exhibited VMD values of 376.5, 209.5 and 125.8 µm, respectively. Unlike experiments with ANS, which is less viscous and dense, IFO 120 exposed to dispersant tended to result in larger oil droplets for a given amount of dispersant added. Comparing the results of IFO 120 with the two dispersants is challenging because no triplicate experiments were conducted for Finasol OSR 52 treatments. In general, from the data collected, Finasol OSR 52 yielded higher VMD for a given DOR compared to Corexit 9500 at warm temperatures. As with ANS, the Downstream LISST measured a decrease in TPC and shift to smaller droplet sizes as the plume moved through the tank for all treatments, but to a lesser extent with DOR = 1:20 (Figures 18, 19 and 20).

For cold water experiments using IFO 120 exposed to Corexit 9500, temperatures ranged between (4.9 – 7.5 °C). At these colder temperatures a shift in DSD and VMD was not as apparent (Figure 21). For DOR = 0, 1:200 and 1:100 VMD typically remained > 223 µm but was as high as 344 µm. The DOR = 1:20 treatment exhibited VMD of 178-327 µm, suggesting that this oil was not well dispersed at cold temperatures. Fluorescence time series data were noisy for all experiments except the DOR = 1:20 (Appendix E). The Downstream LISST recorded extremely low particle concentrations, further suggesting poor

ED_001324_00000298-00049

dispersion (Figure 22). During the IFO 120 cold water treatments, one experiment resulted in an anomalous DSD histogram that was similar to one observed during one of the ANS experiments (Figure 23). In both cases, the experiments were conducted at the coldest temperatures during the course of this study (4.9 and 5 °C). Suspected as a possible cause may be the LISST instrument itself. The manual reports that the lower operating temperature for the LISTT-100X is -10 °C. However, the data suggests that our particular unit may have experienced some complications at low temperatures. This is supported by the fact that the fluorescence signal and chemistry data for these experiments indicate no anomalies. Further testing would be needed to confirm the effect of low temperatures on particle size analysis results using our instrument to rule out any potential issues with operating at temperatures between 5 and -10 °C.

One aspect to note with the IFO 120 cold water experiments is that a few of the treatments were conducted at water temperatures of ~12 °C, which overlaps with the temperatures of the warm water group. This was the result of erratic weather patterns that at times were difficult to work around. Thus, when interpreting the temperature data, caution must be exercised for these particular experiments (refer to Appendix A for temperature log), and for the interpretation in this section, they were excluded as they do not represent cold conditions.

ED_001324_00000298-00050

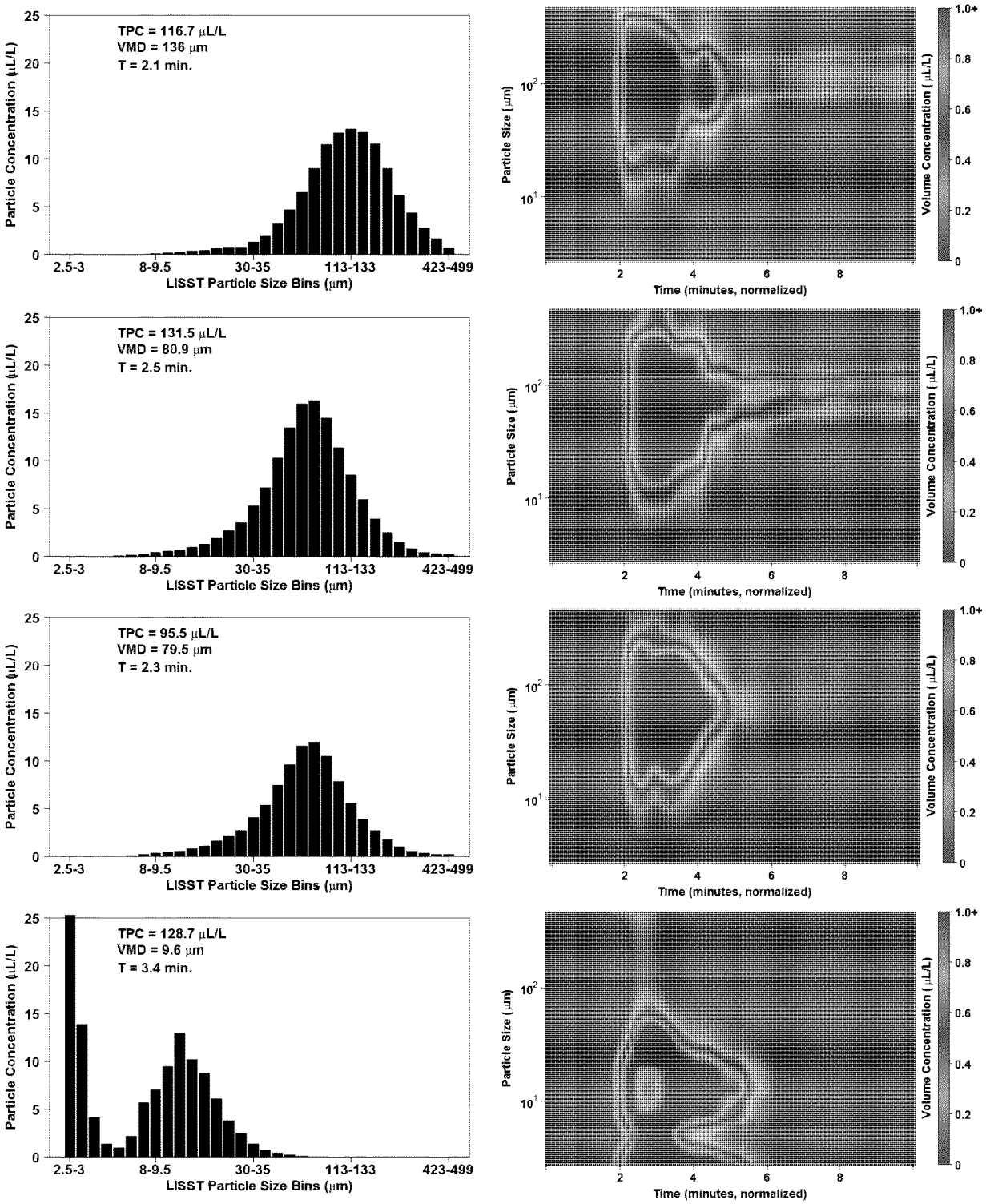
TPC = 116.7 µL/L
VMD = 136 µm
T = 2.1 min.
TPC = 131.5 µL/L
VMD = 80.9 µm
T = 2.5 min.
TPC = 95.5 µL/L
VMD = 79.5 µm
T = 2.3 min.
TPC = 128.7 µL/L
VMD = 9.6 µm
T = 3.4 min.
Particle Concentration (µL/L)
LISST Particle Size Bins (µm)
2.5-3
8-9.5
30-35
113-133
423-499
Particle Size (µm)
Time (minutes, normalized)
Volume Concentration (µL/L)
1.0+

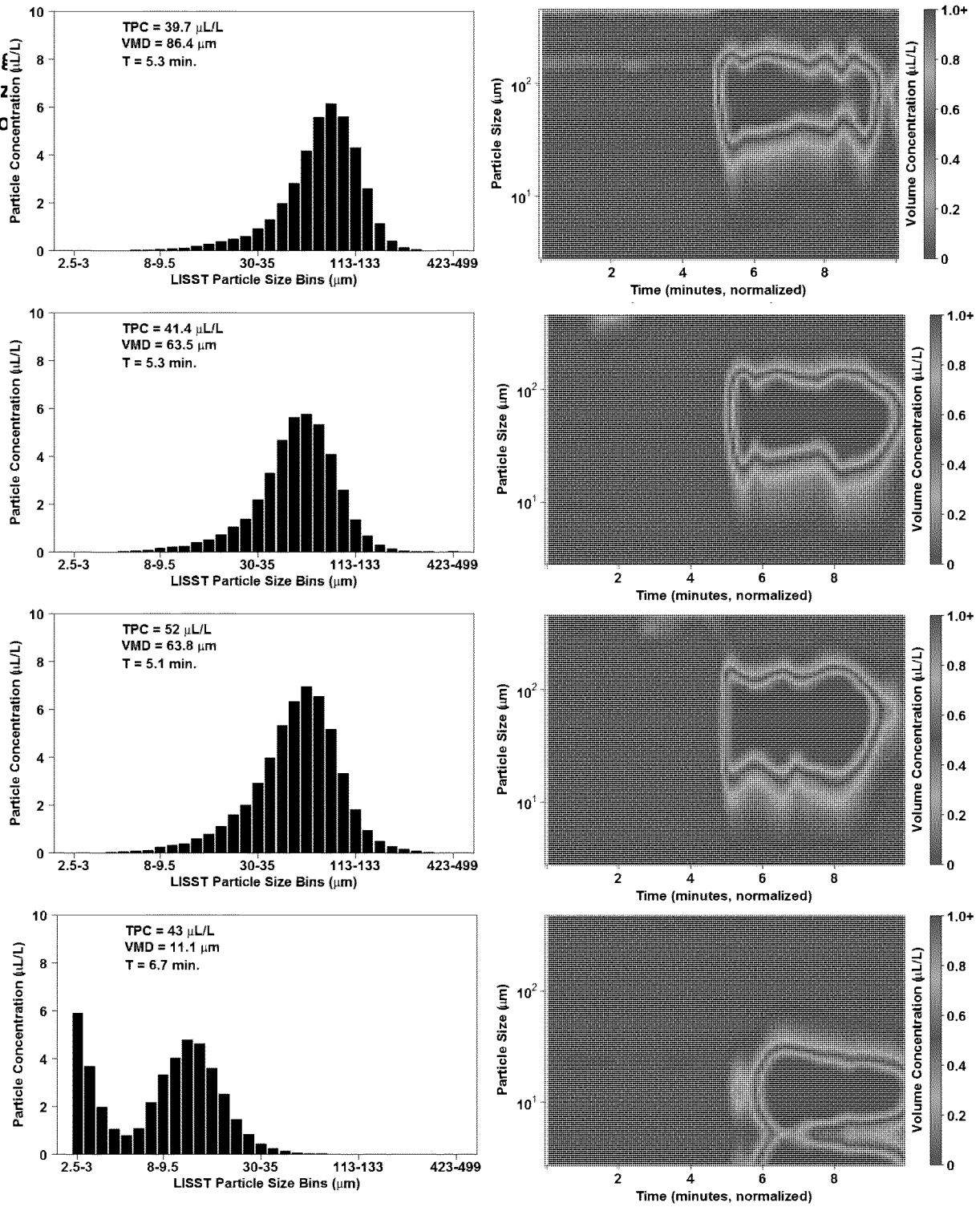

Figure 17. LISST DSD and VMD (left panels) and time series of concentration and particle size (right panels) for IFO 120 and Finasol OSR 52 warm water treatments. From top to bottom, DOR = 1:200, 1:100, 1:20.

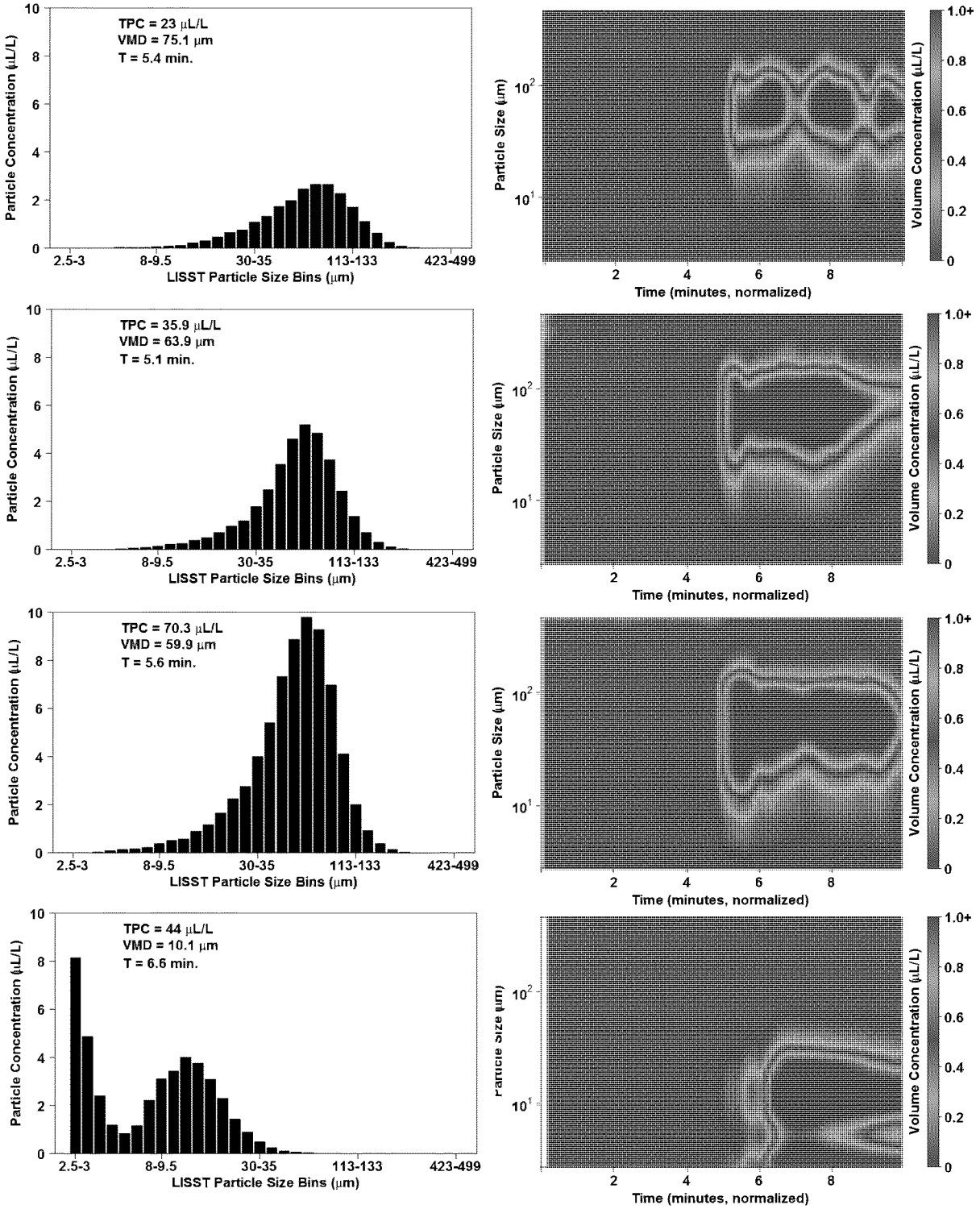
TPC = 23 µL/L
VMD = 75.1 µm
T = 5.4 min.
TPC = 35.9 µL/L
VMD = 63.9 µm
T = 5.1 min.
TPC = 70.3 µL/L
VMD = 59.9 µm
T = 5.6 min.
TPC = 44 µL/L
VMD = 10.1 µm
T = 6.6 min.
Particle Concentration (µL/L)
LISST Particle Size Bins (µm)
2.5-3
8-9.5
30-35
113-133
423-499
Particle Size (µm)
Time (minutes, normalized)
Volume Concentration (µL/L)
1.0+

Figure 18. Downstream LISST DSD and VMD (left panels) and time series of concentration and particle size (right panels) for IFO 120 and Corexit 9500 warm water treatments. From top to bottom, DOR = 0, 1:200, 1:100, 1:20.

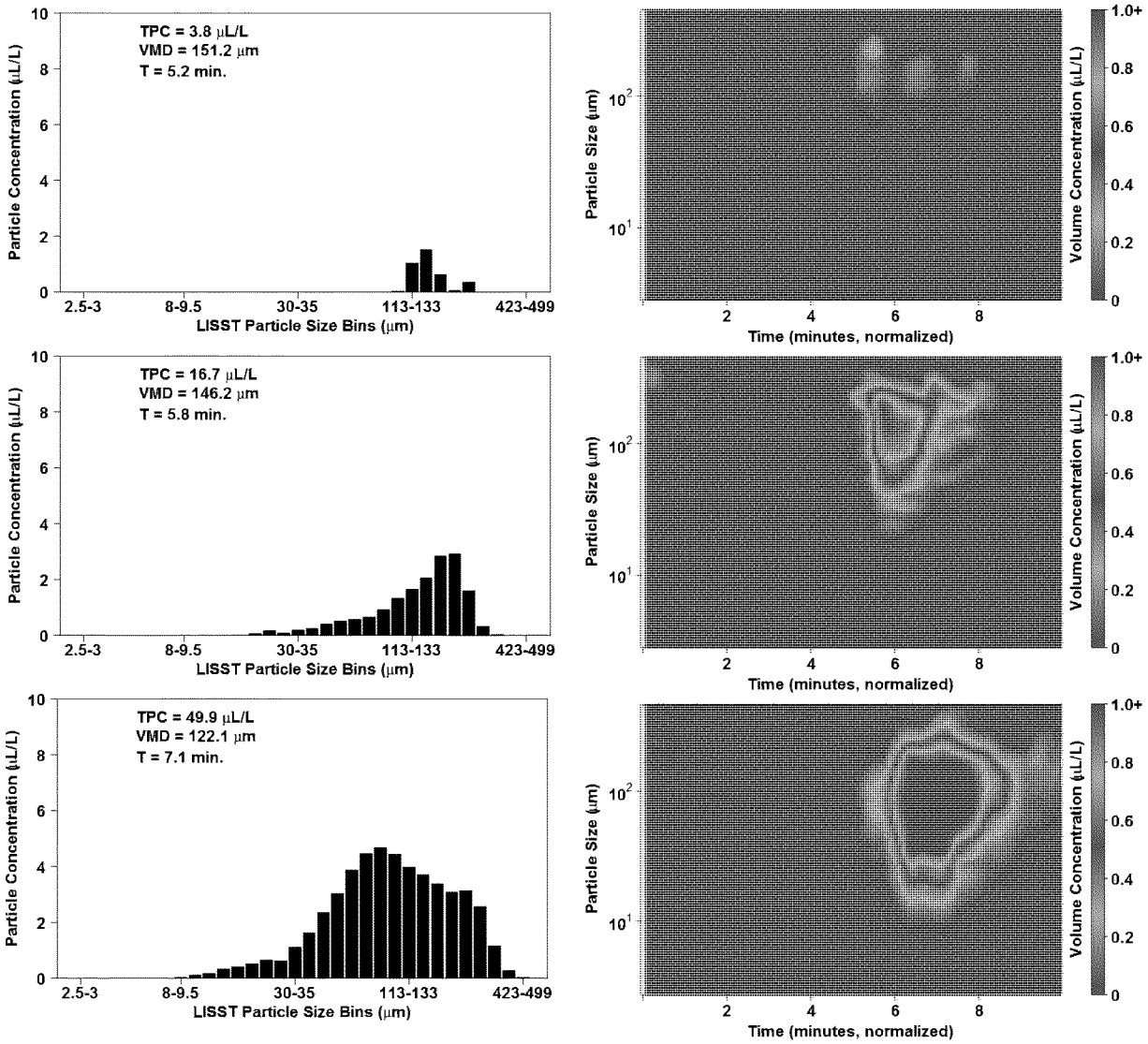

Figure 19. Downstream LISST DSD and VMD (left panels) and time series of concentration and particle size (right panels) for IFO 120 and Finasol OSR 52 warm water treatments. From top to bottom, DOR = 0, 1:200, 1:100, 1:20.

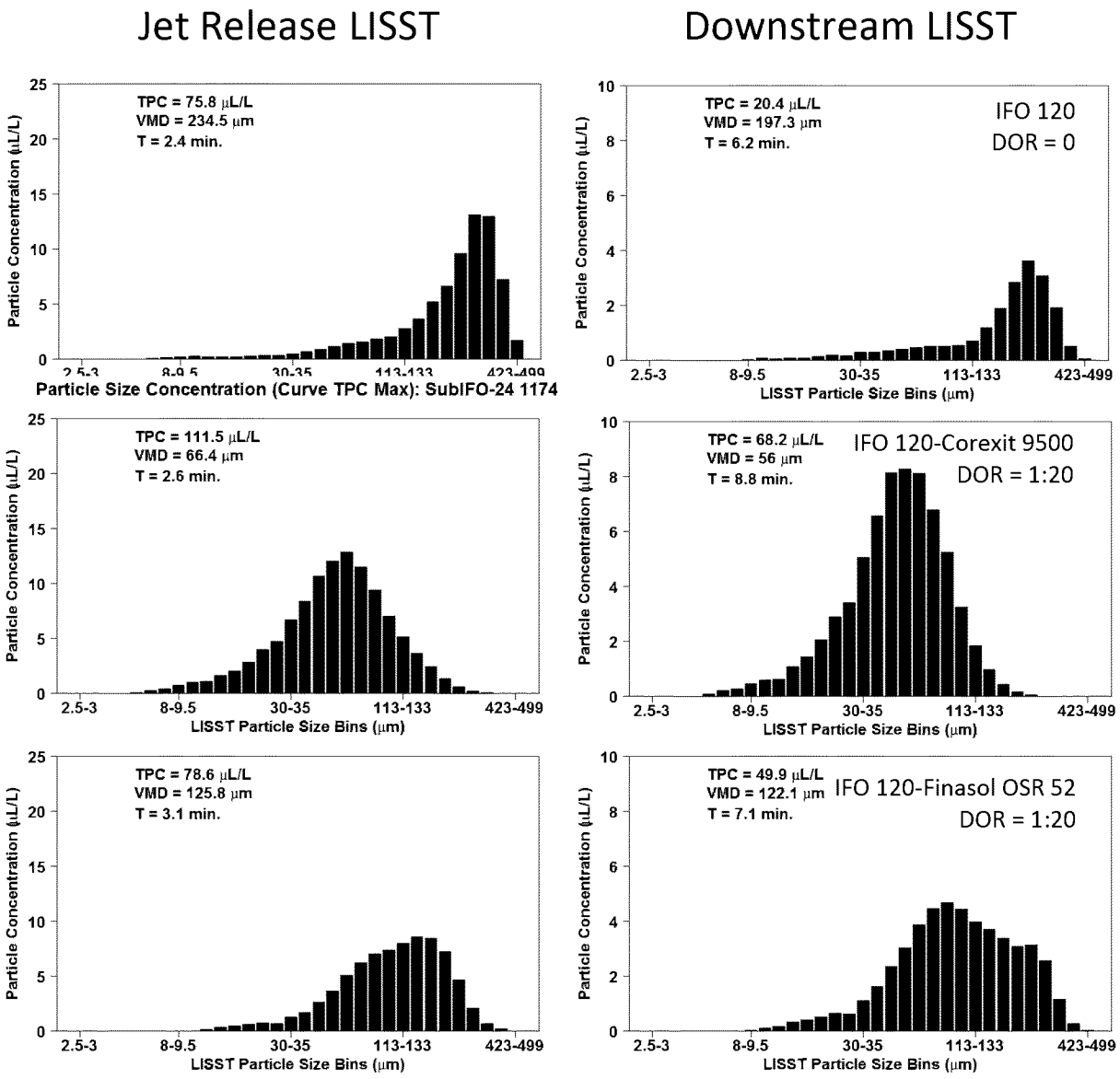

Figure 20. LISST DSD with TPC for IFO 120 with Corexit 9500 and Finasol OSR 52 treatments at warm temperatures. DOR = 0 (top panel); DOR = 1:20 experiments are middle and bottom panels.

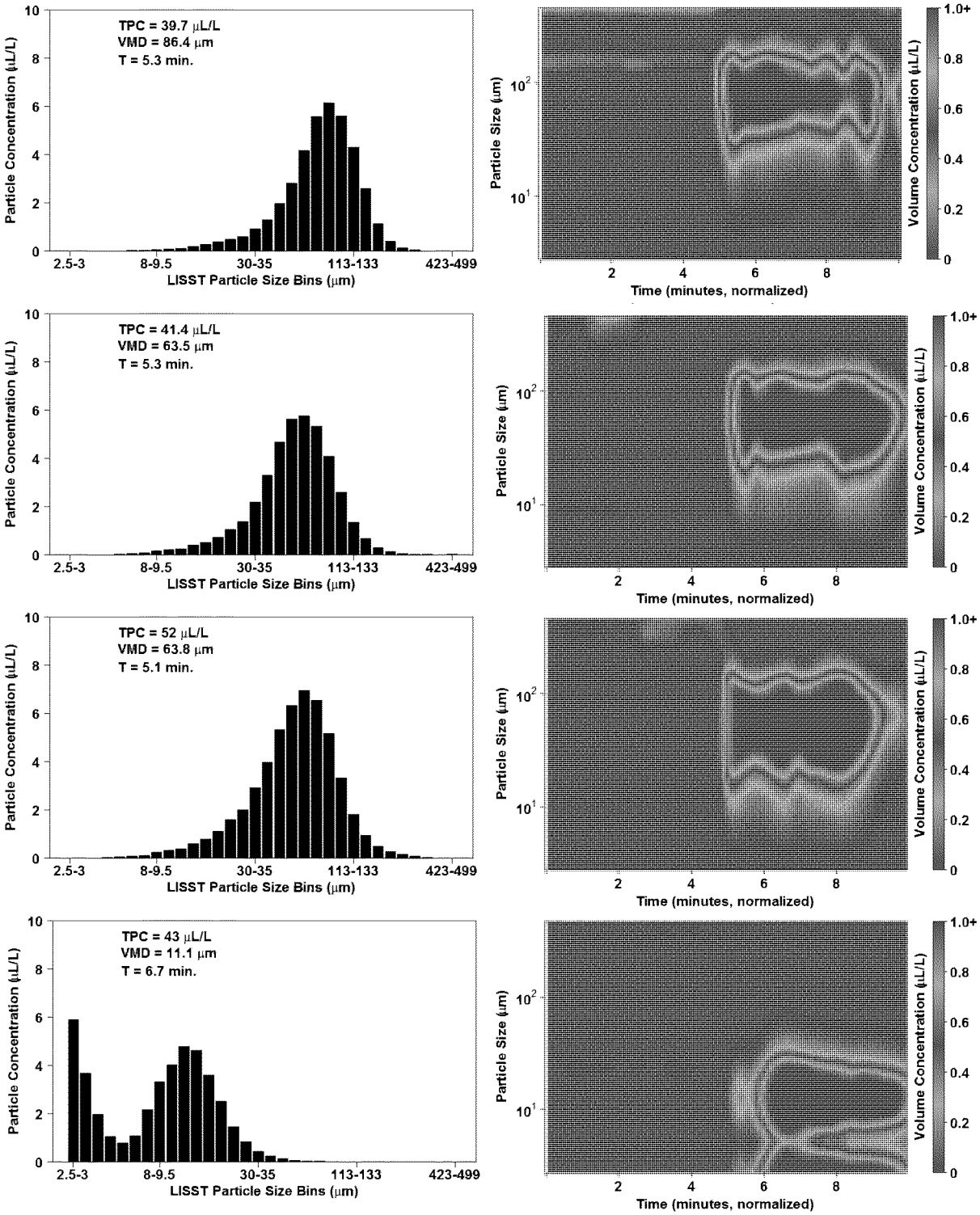
TPC = 39.7 µL/L
VMD = 86.4 µm
T = 5.3 min.
TPC = 41.4 µL/L
VMD = 63.5 µm
T = 5.3 min.
TPC = 52 µL/L
VMD = 63.8 µm
T = 5.1 min.
TPC = 43 µL/L
VMD = 11.1 µm
T = 6.7 min.
Particle Concentration (µL/L)
LISST Particle Size Bins (µm)
2.5-3
8-9.5
30-35
113-133
423-499
Particle Size (µm)
Time (minutes, normalized)
Volume Concentration (µL/L)
1.0+

Fig
siz
bo

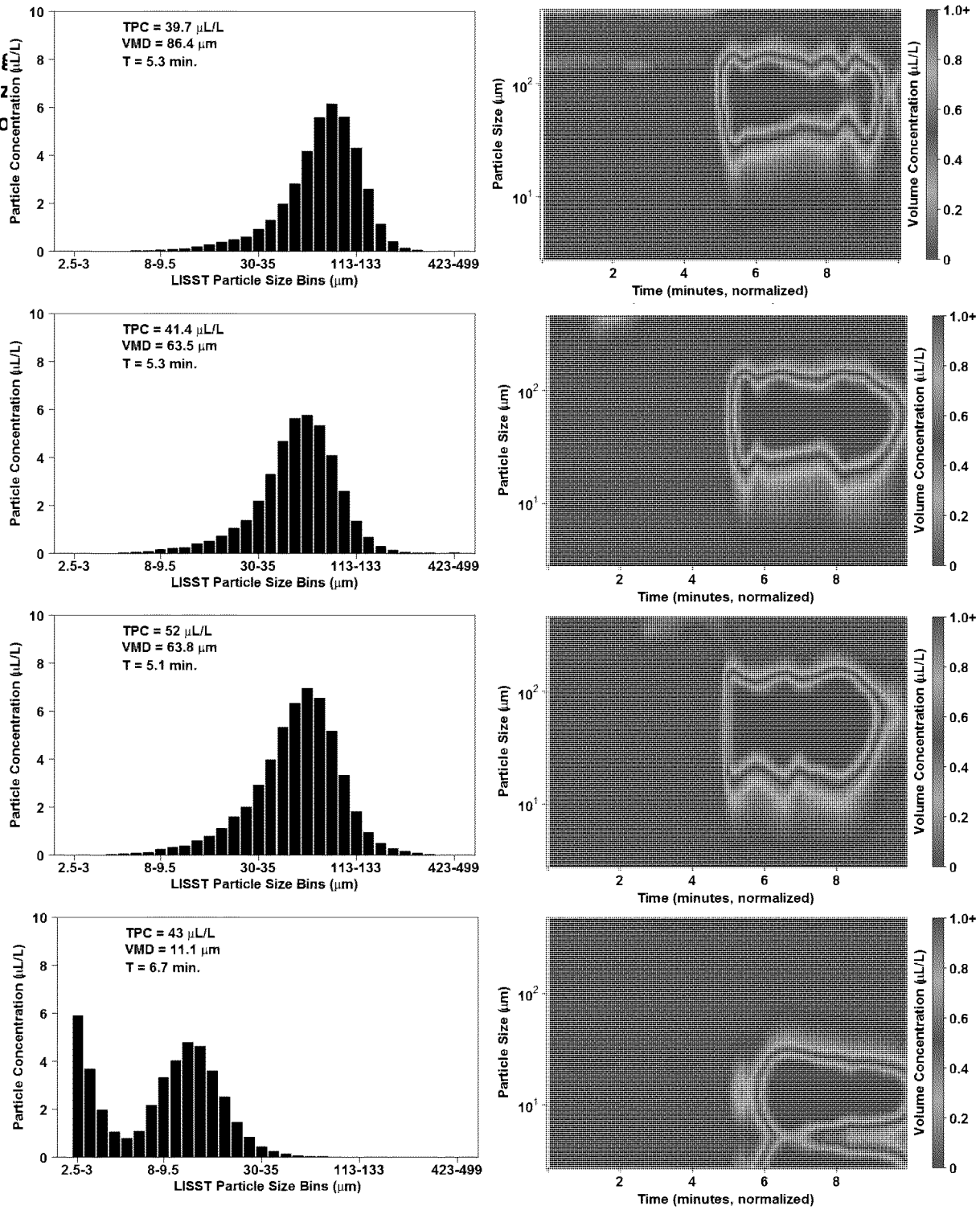
TPC = 39.7 µL/L
VMD = 86.4 µm
T = 5.3 min.
TPC = 41.4 µL/L
VMD = 63.5 µm
T = 5.3 min.
TPC = 52 µL/L
VMD = 63.8 µm
T = 5.1 min.
TPC = 43 µL/L
VMD = 11.1 µm
T = 6.7 min.
Particle Concentration (µL/L)
LISST Particle Size Bins (µm)
2.5-3
8-9.5
30-35
113-133
423-499
Particle Size (µm)
Time (minutes, normalized)
Volume Concentration (µL/L)
1.0+

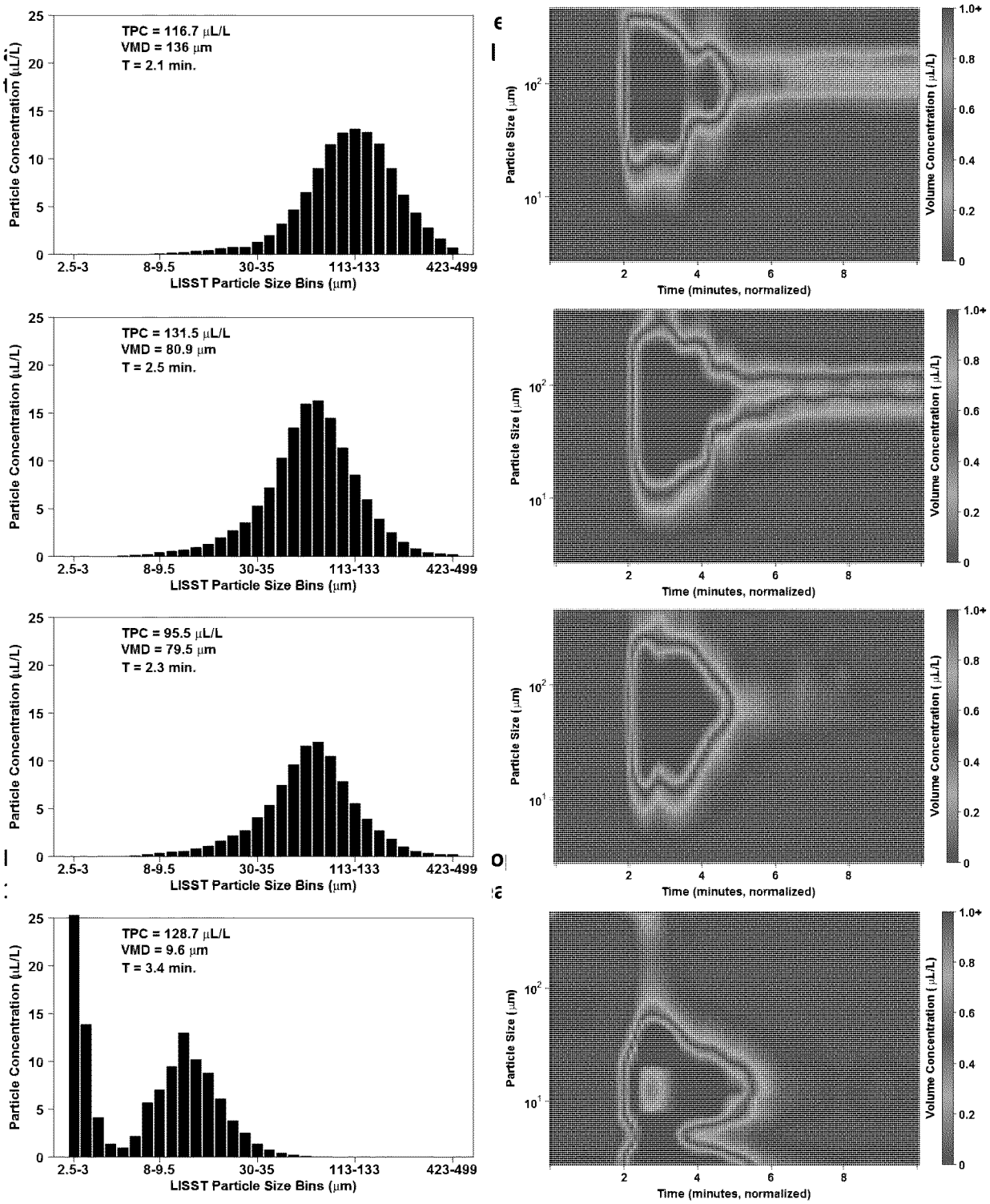
TPC = 116.7 µL/L
VMD = 136 µm
T = 2.1 min.
TPC = 131.5 µL/L
VMD = 80.9 µm
T = 2.5 min.
TPC = 95.5 µL/L
VMD = 79.5 µm
T = 2.3 min.
TPC = 128.7 µL/L
VMD = 9.6 µm
T = 3.4 min.
Particle Concentration (µL/L)
LISST Particle Size Bins (µm)
2.5-3
8-9.5
30-35
113-133
423-499
Particle Size (µm)
Time (minutes, normalized)
Volume Concentration (µL/L)
1.0+

A.3.3 SLC Dispersion Effectiveness

Experiments involving South Louisiana Crude (SLC) oil treated with Corexit 9500 were conducted for warm water conditions (16.6 – 19.6 °C) to compare dispersion between ANS and SLC. Experiments with SLC yielded higher TPC values compared to ANS results, most likely the result of slightly larger amounts of oil added to the pressure canister (~25-50 g), so comparisons shouldn't be made regarding TPC. The observed VMD of physically-dispersed SLC oil (neat; DOR = 0; ~123-148 µm) was found to be less than that of ANS (>200 µm). The addition of dispersant yielded a shift in DSD and VMD to smaller particles, where DOR = 1:200 and 1:100 exhibited diameters of ~91-108 µm, and DOR = 1:20 ranged between ~15 -21 µm, as depicted in Figure 24. The Downstream LISST results indicate smaller droplet size as the plume moves through the tank (size fractionation) and a decrease in TPC (plume dilution), further demonstrating this trend for all oils (Figures 25 and 26). The fluorescence data indicates a strong signal with little scatter for up to 4 min in these treatments (Figure 27; Appendix E). Using these results, comparisons can be made to results of SLC with Corexit 9500 from surface plume simulations (oil released into tank via pour in from flask) from Conmy et al., 2014a (and unpublished data) from those experiments. No apparent differences between DSD and VMD for DOR = 0 treatments were found. For DOR = 1:20 VMD values are similar, however, the range of droplet diameters for surface simulations is larger with particles up to 200 µm. In subsurface injection jet experiments the range of diameters is narrower, where particles > 100 µm were not observed. This suggests that the combination of the chemical dispersant tested here, elevated turbulent mixing from the jet release and higher oil temperature of 80 °C yielded smaller droplets. To discern the dominant factor controlling the difference, additional testing would need to be conducted.

ED_001324_00000298-00059

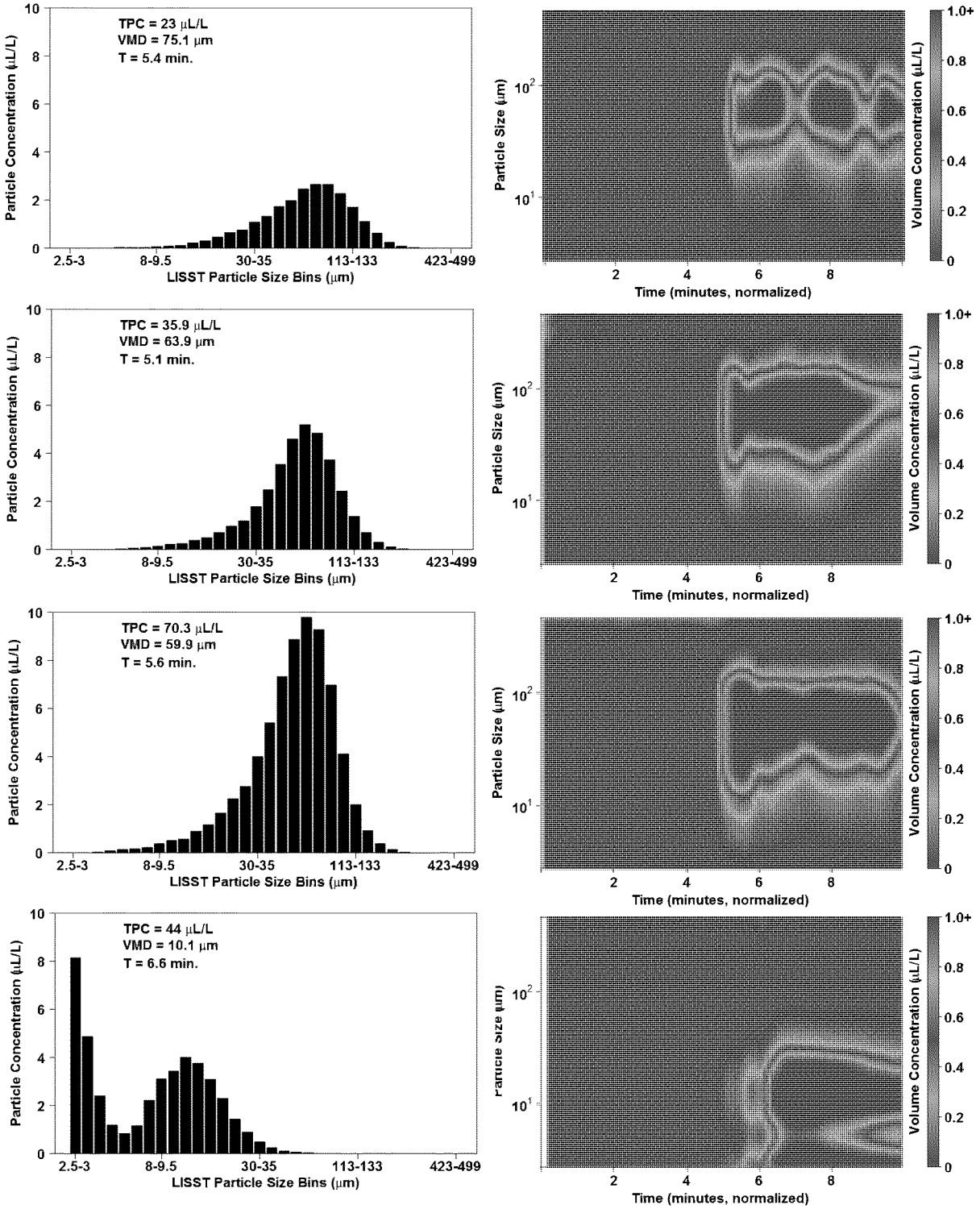
TPC = 23 µL/L
VMD = 75.1 µm
T = 5.4 min.
TPC = 35.9 µL/L
VMD = 63.9 µm
T = 5.1 min.
TPC = 70.3 µL/L
VMD = 59.9 µm
T = 5.6 min.
TPC = 44 µL/L
VMD = 10.1 µm
T = 6.6 min.
Particle Concentration (µL/L)
LISST Particle Size Bins (µm)
2.5-3
8-9.5
30-35
113-133
423-499
Particle Size (µm)
Time (minutes, normalized)
Volume Concentration (µL/L)
1.0+

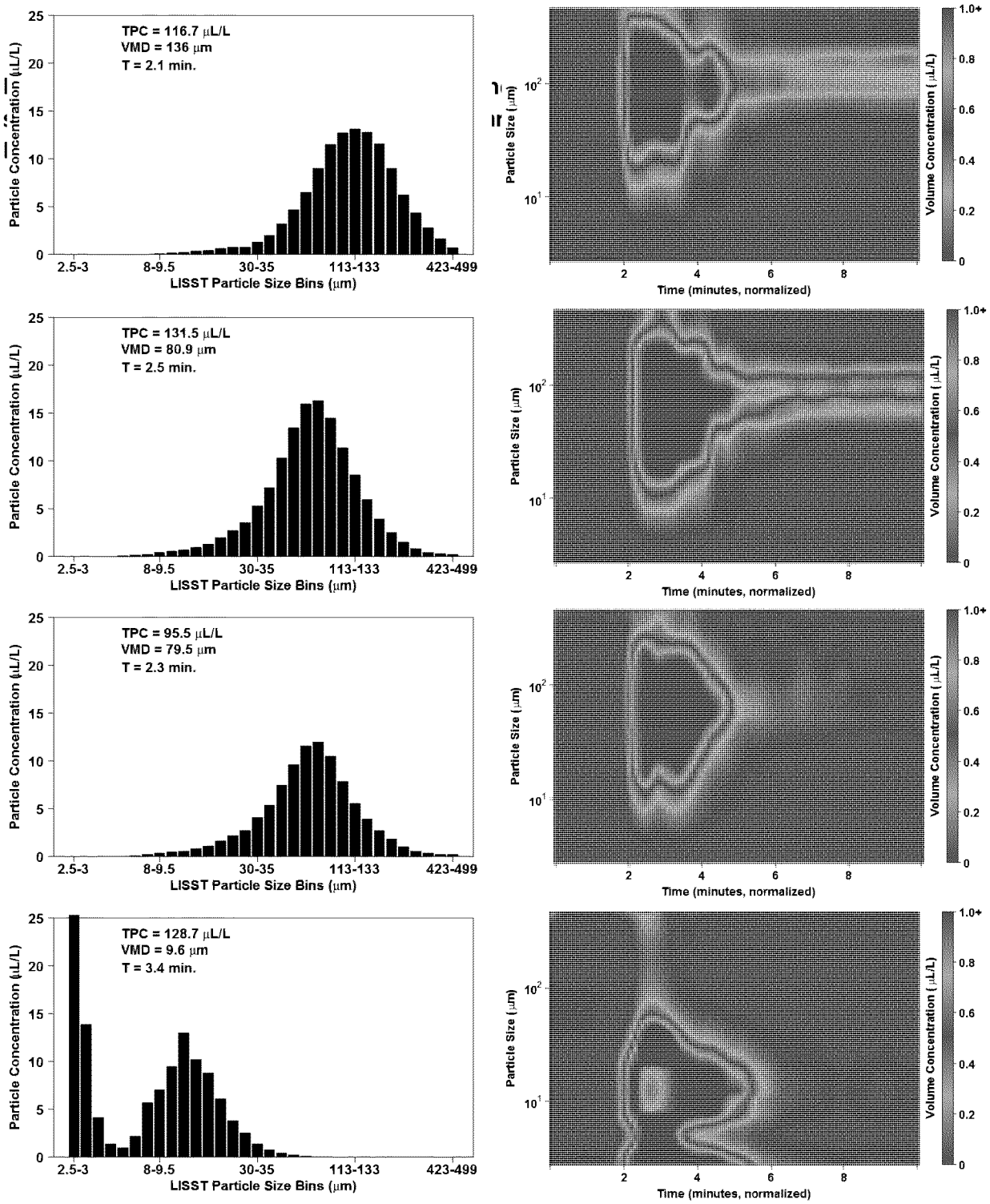
TPC = 116.7 µL/L
VMD = 136 µm
T = 2.1 min.
TPC = 131.5 µL/L
VMD = 80.9 µm
T = 2.5 min.
TPC = 95.5 µL/L
VMD = 79.5 µm
T = 2.3 min.
TPC = 128.7 µL/L
VMD = 9.6 µm
T = 3.4 min.
Particle Concentration (µL/L)
LISST Particle Size Bins (µm)
2.5-3
8-9.5
30-35
113-133
423-499
Particle Size (µm)
Time (minutes, normalized)
Volume Concentration (µL/L)
1.0+

Figure 25. Downstream LISST DSD and VMD (left panels) and time series of concentration and particle size (right panels) for SLC and Corexit 9500 warm water treatments. From top to bottom, DOR = 0, 1:200, 1:100, 1:20.

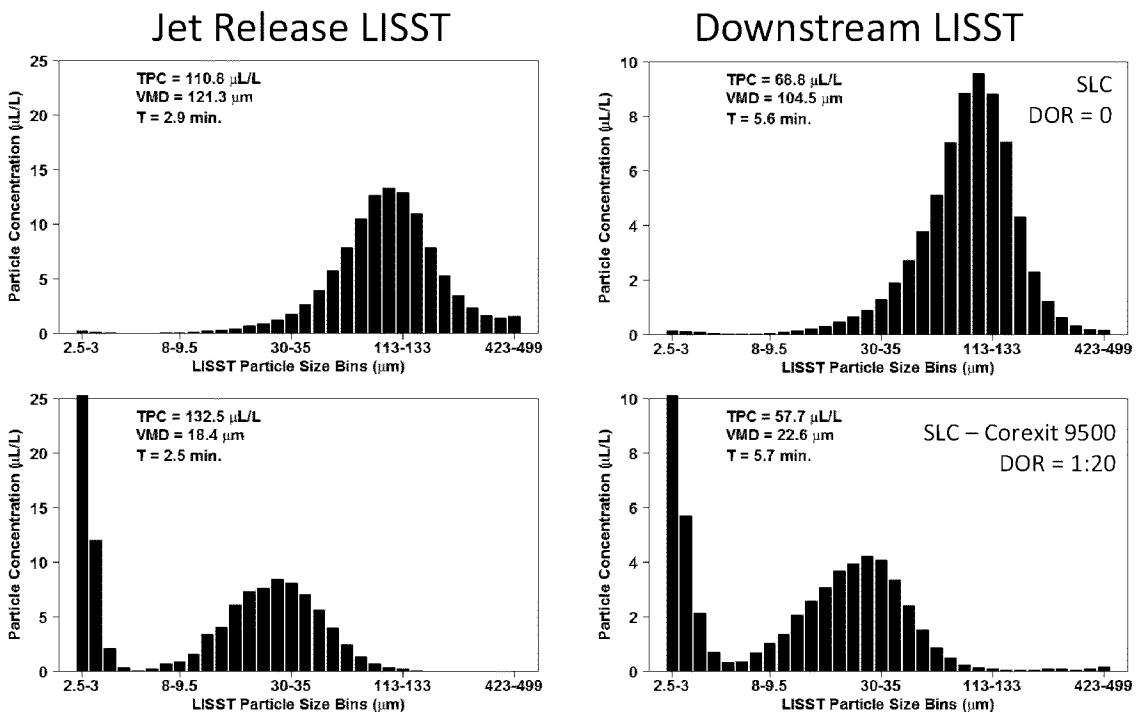

Figure 26. LISST DSD with TPC for SLC with Corexit 9500 treatments at warm temperatures. DOR = 0 (top panel); DOR = 1:20 experiments are bottom panels.

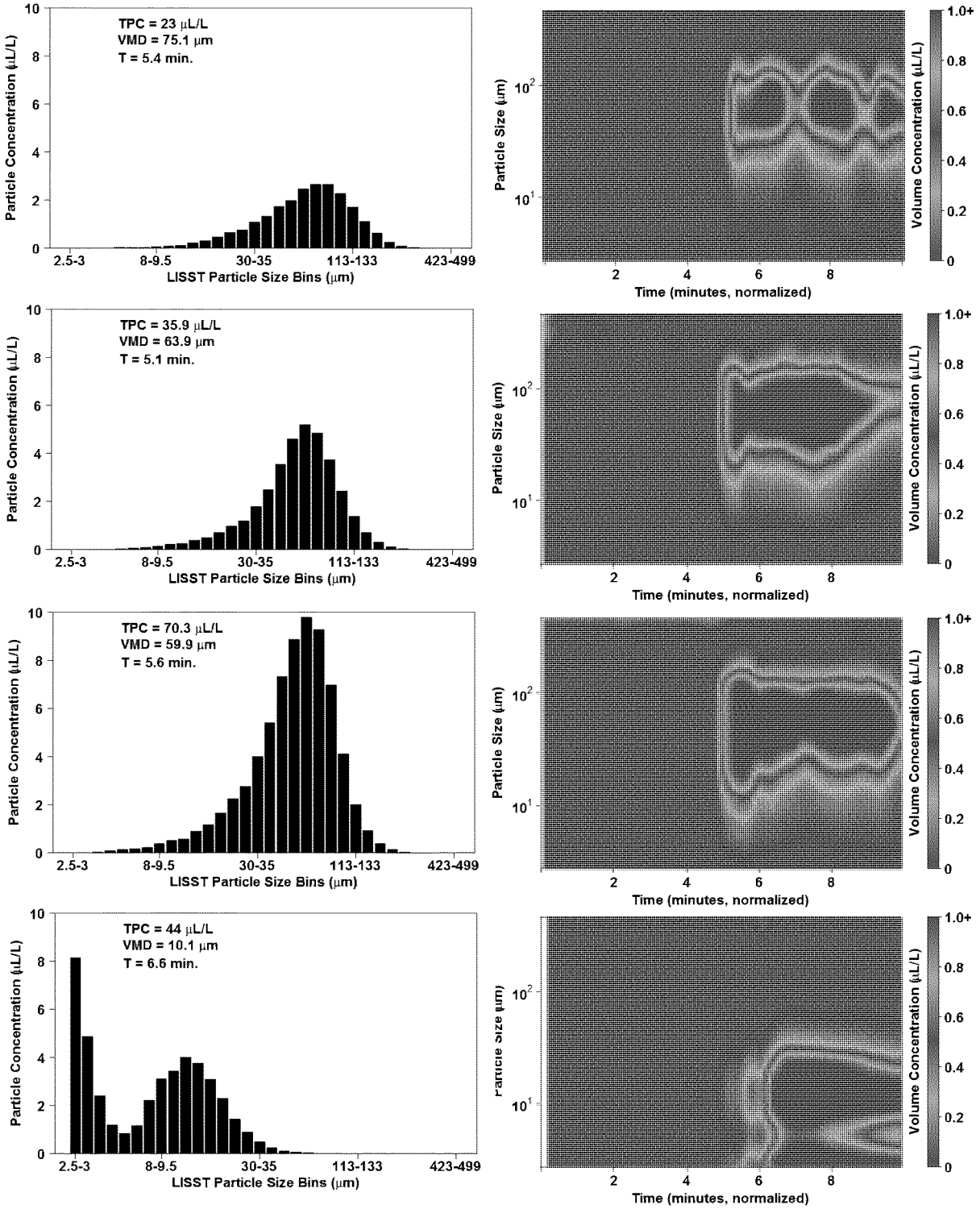
TPC = 23 µL/L
VMD = 75.1 µm
T = 5.4 min.
TPC = 35.9 µL/L
VMD = 63.9 µm
T = 5.1 min.
TPC = 70.3 µL/L
VMD = 59.9 µm
T = 5.6 min.
TPC = 44 µL/L
VMD = 10.1 µm
T = 6.6 min.
Particle Concentration (µL/L)
LISST Particle Size Bins (µm)
2.5-3
8-9.5
30-35
113-133
423-499
Particle Size (µm)
Time (minutes, normalized)
Volume Concentration (µL/L)
1.0+

Figure 27. *In situ* submersible fluorescence time series of sub-injection plume of SLC and Corexit 9500 warm water treatments. From top to bottom, DOR = 0, 1:200, 1:100, 1:20.

A.3.4 Gas Condensate Dispersion Effectiveness

Injection experiments were conducted with Gas Condensate and Corexit 9500 for warm water conditions (10 – 12 °C temperature range) and DOR = 0 and 1:20 only. The VMD for Gas Condensate with no dispersant added ranged between ~150 – 215 µm (Figure 28). With the addition of dispersant, VMD for the triplicates were 60.4, 68.2 and 170.4 µm suggesting that dispersant at DOR = 1:20 shifts the DSD to smaller particles for most experiments. The corresponding fluorescence data for these treatments indicate a strong signal with little scatter for up to 3 min in both treatments (Figure 28; Appendix E).

ED_001324_00000298-00064

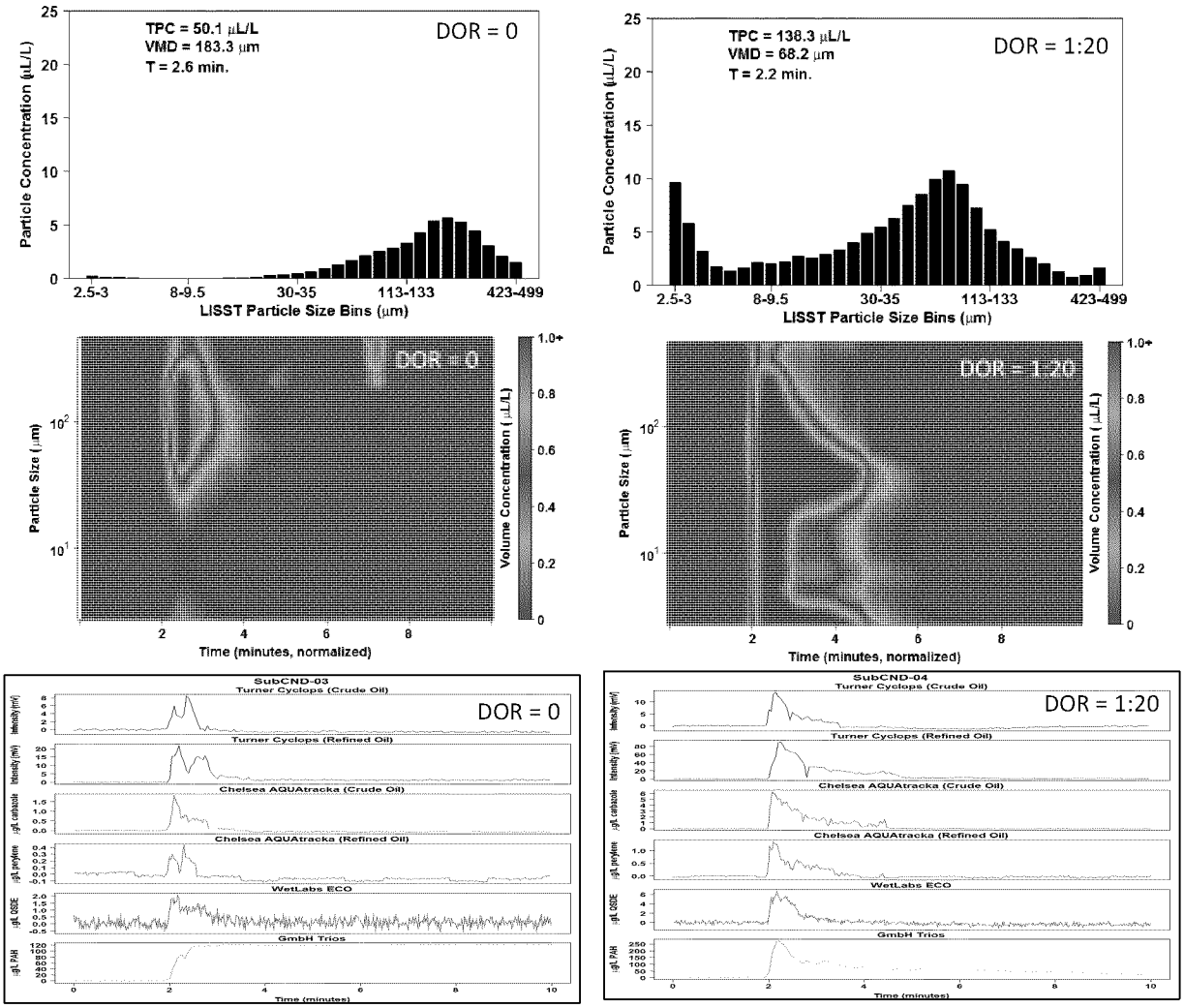

Figure 28. LISST DSD and VMD (top panels) and time series of concentration and particle size (middle panels) for Gas Condensate and Corexit 9500 warm water treatments. Left panels are DOR = 0 and right panels are DOR = 1:20.

A.3.5 Tank Dilution Series Fluorescence Measurements

Submersible fluorescence results are presented in units recommended by manufacturers and using calibration factors provided by the manufacturers. Efforts were made to correlate the fluorescence intensity with TPH and / or BTEX concentration but were not possible due to issues inherent with the discrete sample collection. In order to fill bottles for chemical analysis, a 30 second time period was needed. Due to the short time period of the experiments and the heterogeneity of the plume concentration through time (evident from the fluorescence time series), oil concentrations within the bottles represent an average over a 30 second time period that cannot be aligned with the time series data, which are generated on the time scale of seconds. Given this fact, a dilution series within the tank using ANS was conducted to provide a calibration curve for fluorometers to a known concentration of oil in a homogeneous tank akin to Conmy et al., 2014a. Calibration regression results for all submersible fluorometers can be found in Figures 29 and 30 for TPH and BTEX, respectively and regression equations are tabulated in Table 5. Strong correlations between oil concentration and fluorescence intensity were observed, suggesting that fluorescence signal may serve as a proxy for TPH or BTEX at specific time points within the tank. This is an advantage as the fluorescence is well correlated with TPC time series and employing this type of calibration may provide for chemistry estimates that can be correlated with particle / oil droplet concentrations at fine time scales within the tank during experiments. For example, comparing the TPC and fluorescence signature for ANS with and without dispersant illustrates the differences in the oil droplet concentration and dissolved oil during injection experiments and the utility of monitoring both to understanding plume dynamics (Figure 31).

ED_001324_00000298-00066

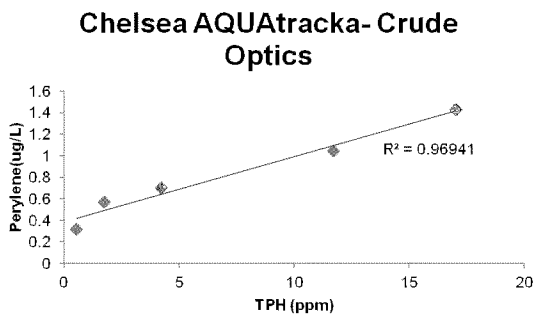
Chelsea AQUAtracka- Crude Optics
Perylene(ug/L)
TPH (ppm)
R² = 0.96941

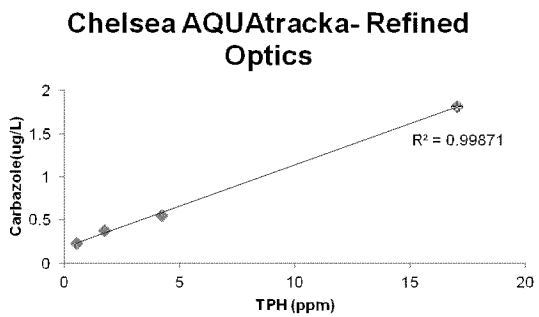
Chelsea AQUAtracka- Refined Optics
Carbazole(ug/L)
TPH (ppm)
R² = 0.99871

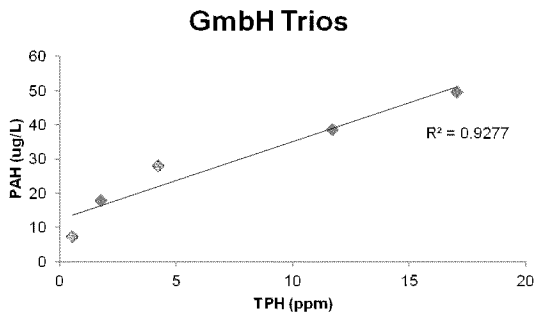
GmbH Trios
PAH (ug/L)
TPH (ppm)
R² = 0.9277

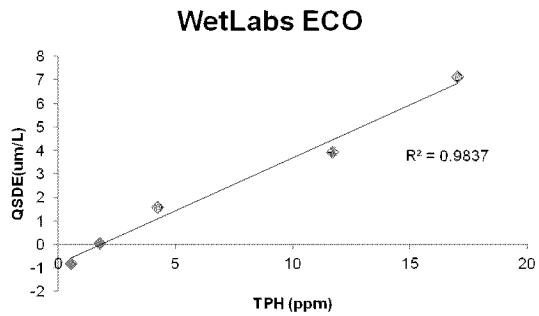
WetLabs ECO
QSDE(um/L)
TPH (ppm)
R² = 0.9837

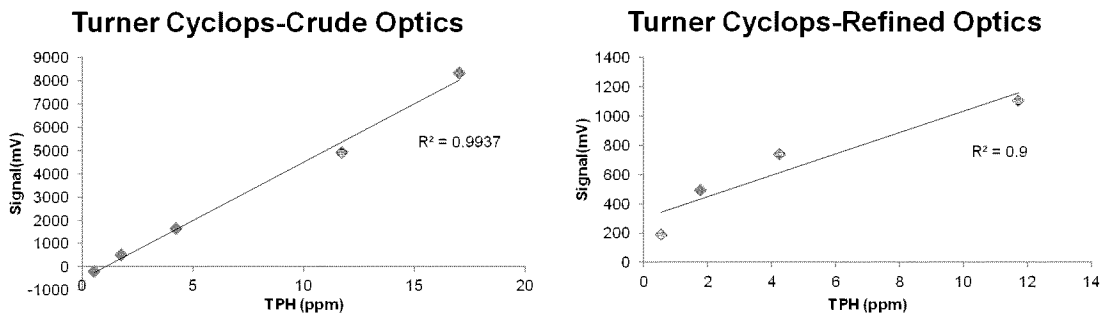

Figure 29. Calibration lines for fluorometer response vs TPH concentrations.

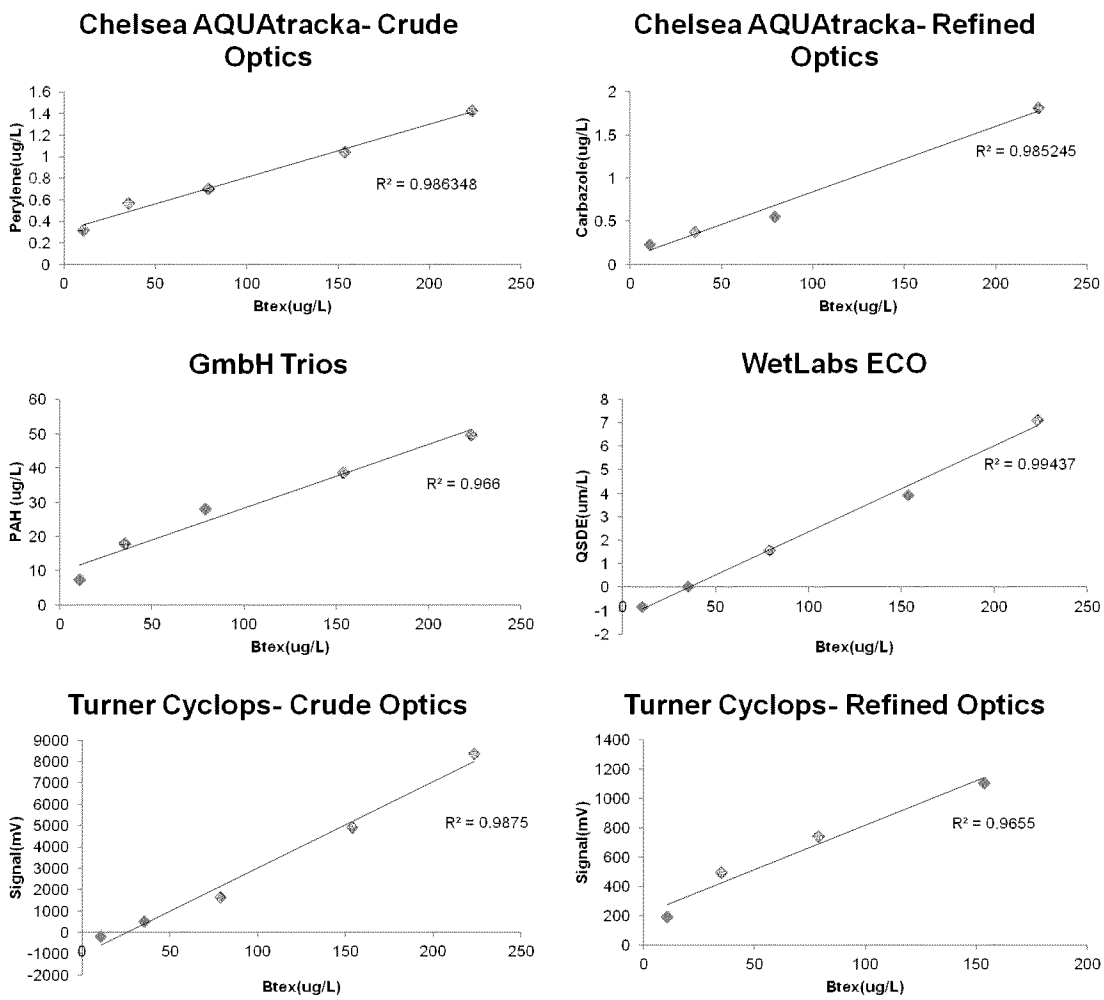

Figure 30. Calibration lines for fluorometer response vs BTEX concentrations.

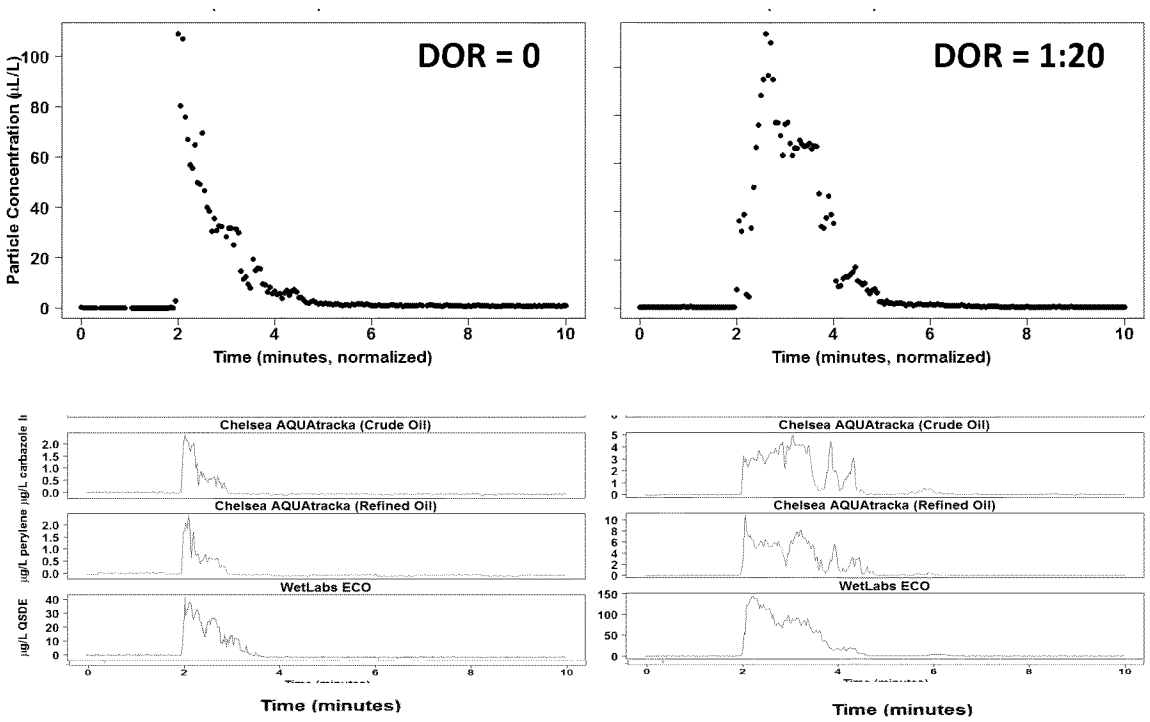
DOR = 0
DOR = 1:20
Particle Concentration (µL/L)
Time (minutes, normalized)
Chelsea AQUAtracka (Crude Oil)
Chelsea AQUAtracka (Refined Oil)
WetLabs ECO
µg/L QSDE
Time (minutes)

Figure 31. Total Particle Concentration and fluorescence time series for ANS crude oil with Corexit 9500 dispersant.

Table 5. Calibration equations for the submersible fluorometers. Data in this report have fluorescence signal in the manufacturer recommended units.

ED_001324_00000298-00070

Instrument	Factory Calibration Standard (units)	TPH Calibration Equation	BTEX Calibration Equation
Chelsea Aquatracka (Crude Optics)	Perylene (ug/L)	[TPH] = ([Perylene]-0.3834)/0.06051	[BTEX] = ([Perylene]-0.3165)/0.004922
Chelsea Aquatracka (Refined Optics)	Carbazole (ug/L)	[TPH] = ([Carbazole]-0.1804)/0.09575	[BTEX] = ([Carbazole]-0.08487)/0.007584
GmbH Trios	PAH (ug/L)	[TPH] = ([PAH]-12.288)/2.2733	[BTEX] = ([PAH]-9.559)/0.1871
Turner Cyclops (Crude Optics)	Signal (mV)	[TPH] = (Signal+320.26)/503.94	[BTEX] = (Signal+1152.2)/42.429
Turner Cyclops (Refined Optics)	Signal (mV)	[TPH] = (Signal-299.29)/73.339	[BTEX] = (Signal-212.05)/6.0593
Wetlabs ECO	QSDE (uM/L)	[TPH] = (QSDE-0.2102)/0.4362	[BTEX] = (QSDE+0.5403)/0.03697

A.3.6 VOC Air Monitoring

For all experiments the Volatile Organic Compounds (VOC) measurements exhibited higher variability compared to the in water sensor measurements. Despite the fact that a wind screen was installed at the tank facility, the effects of wind were not completely eliminated.

ED_001324_00000298-00071

The observed variability is likely caused by differences in wind speed and direction both among the triplicate experiments (typically run on the same day), and among the different treatments (which were run over days/weeks). The VOC meters were installed with the air intakes pointing down and were 0.4 m above the water surface at the top edge of the tank. This positioning helped to reduce the effects of wind, given that the tank walls acted as an additional wind blocker.

Two VOC meters were deployed above the tank, but only results from the VOC meter closest to the oil release are presented here (Jet Release VOC meter; the VOC meter directly above the fluorometer rack). Results from the second VOC meter (Downstream VOC meter) installed 11.8 m farther downstream are more variable, both in concentrations between triplicate runs and in the time it takes for airborne VOC concentrations to reach the meter. In general, readings from the second meter showed a broader plume with a lower peak VOC concentration. Due to an instrument malfunction, approximately 17 experiments are missing data from the Downstream VOC meter. All results from the Jet Release VOC meter are presented in Figures 32-39. Note that the Y-axis scale differs depending on the oil type (20 ppm for IFO, 45 ppm for ANS & SLC, 250 ppm for Gas Condensate).

Of the four different hydrocarbon products tested, experiments using the gas condensate exhibited the highest surface VOC concentrations, followed by ANS and SLC which exhibited similar values. The lowest concentrations were observed for IFO 120 experiments. Higher concentrations of VOC in the air were usually accompanied by lower BTEX concentrations in the water for each oil type (analytical chemistry results in Appendix B). Chemistry results from the water column (effluent, listed in Appendix B tables) samples help to verify the findings from the VOC meters. In general, the measured concentrations of BTEX in the effluent water samples were higher for experiments using dispersant compared to the untreated experiments. The effluent port in the flume tank during normal operation produces a depth integrated water sample which does not draw off the water surface. Therefore, oil that rises to the surface is not drawn into the effluent, and so the tank effluent can be used as a measure of how much oil was effectively dispersed into the water column.

ED_001324_00000298-00072

Regardless of the oil product tested, the use of chemical dispersants at a DOR = 1:20 resulted in a significant reduction in VOC concentrations in the air above the water compared to corresponding experiments without dispersant (summarized in Table 6). A general trend was also observed where increasing the DOR resulted in lower surface VOC concentrations near the jet release location. Due to wind effects mentioned previously, trends in VOC concentrations above the plume further down the tank could not be established.

Table 6. Summary of peak VOC concentrations at the various treatment conditions tested in this study. Values shown for ANS and IFO 120 are from the warm water season experiments.

	Avg. Peak VOC Concentration (ppm benzene), n = 3			
Oil Type	No Dispersant	DOR 1:200	DOR 1:100	DOR 1:20
ANS (Corexit 9500)	23.07	13.27	12.43	0.13
ANS (Finasol OSR 52)	23.07	16.56	7.17	2.9
IFO 120	1.00	0.90	7.37	0.17
Condensate	121.23	--	--	19.73
SLC	28.53	27.5	16.75	1.53

ED_001324_00000298-00073

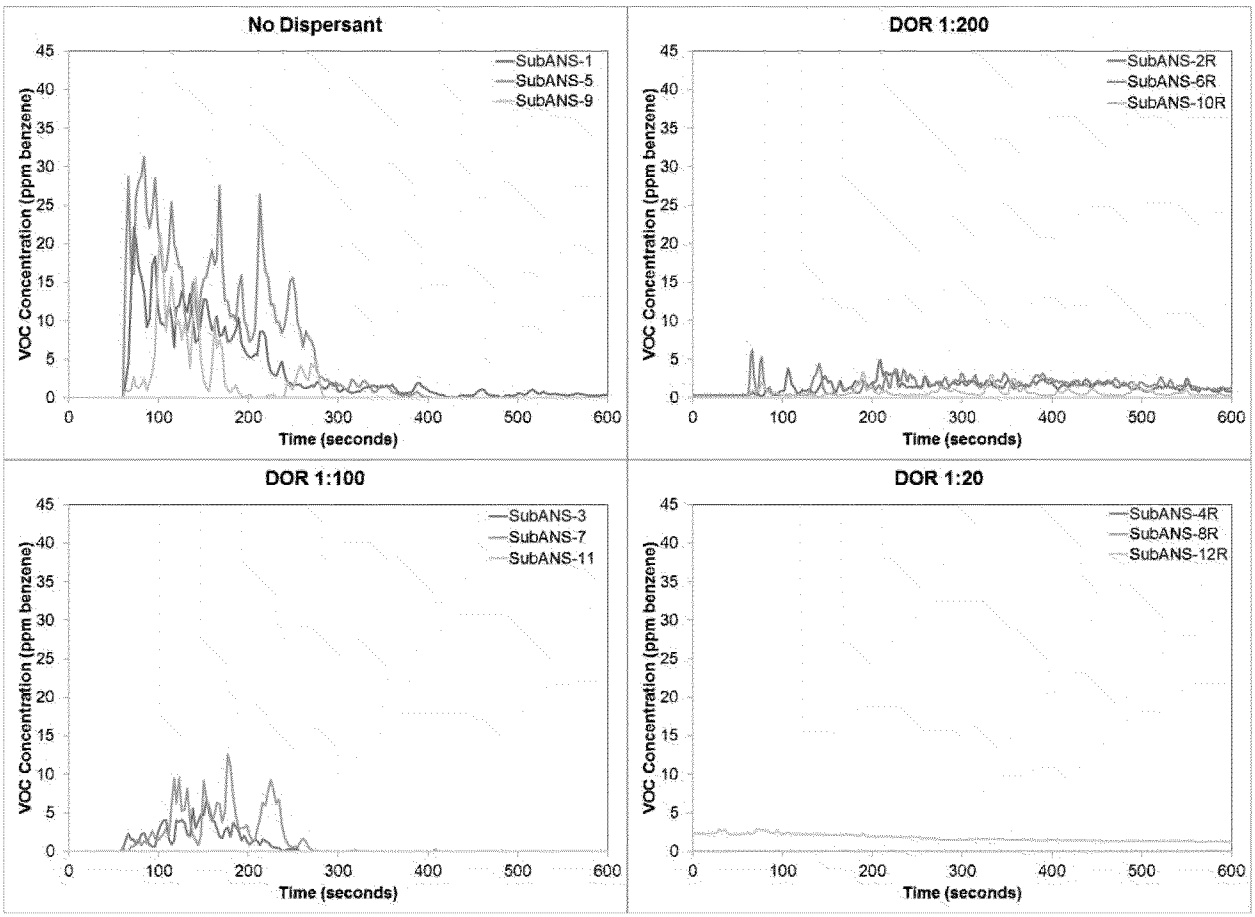

Figure 32. VOC results for subsurface injection experiments (cold water season) using Alaska North Slope crude oil and four treatment conditions (no dispersant, DOR 1:200, DOR 1:100, DOR 1:20). Replicate treatments represented by light blue, dark blue and green colored lines.

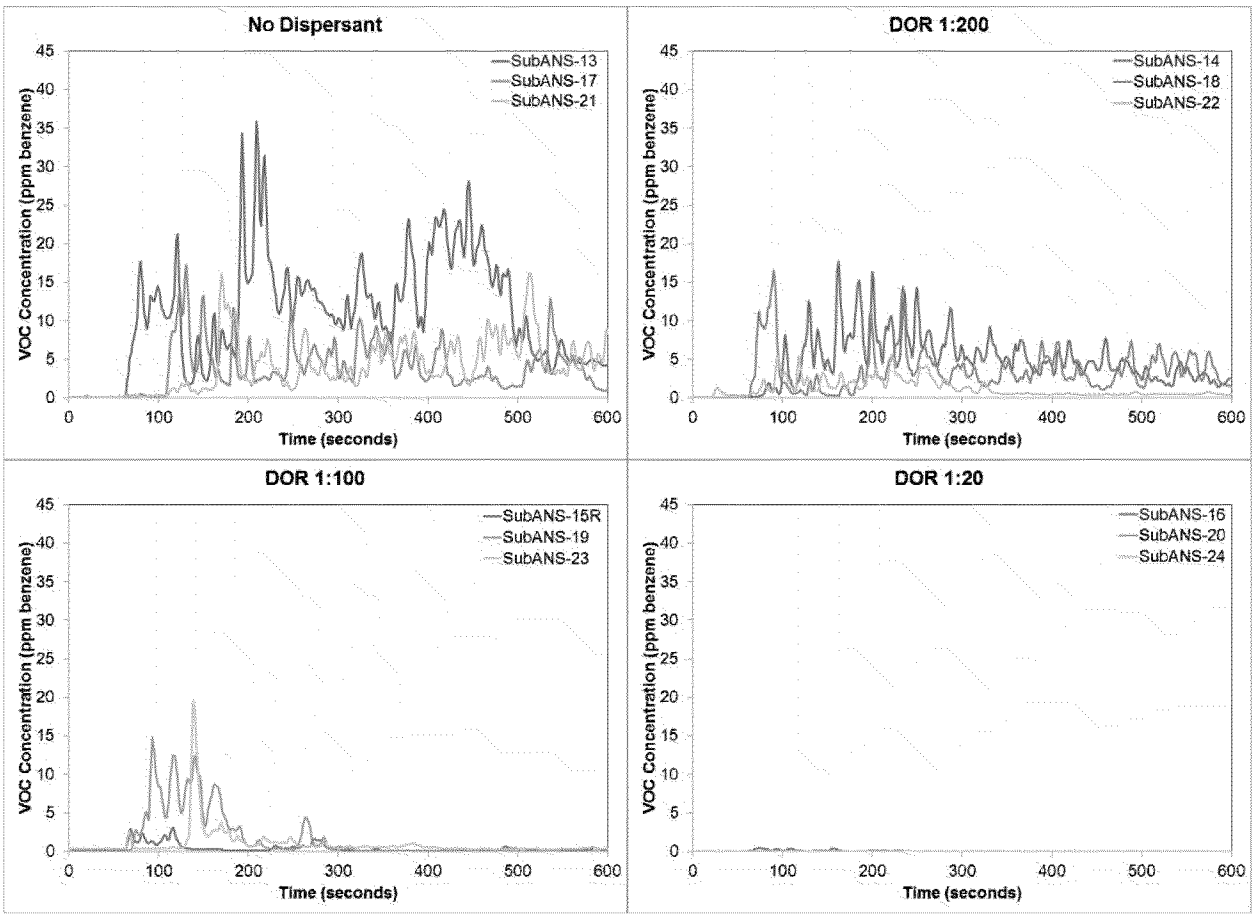

Figure 33. VOC results for subsurface injection experiments (warm water season) using Alaska North Slope crude oil and four treatment conditions (no dispersant, DOR 1:200, DOR 1:100, DOR 1:20). Corexit 9500 was used as the treating agent. Replicate treatments represented by light blue, dark blue and green colored lines.

ED_001324_00000298-00075

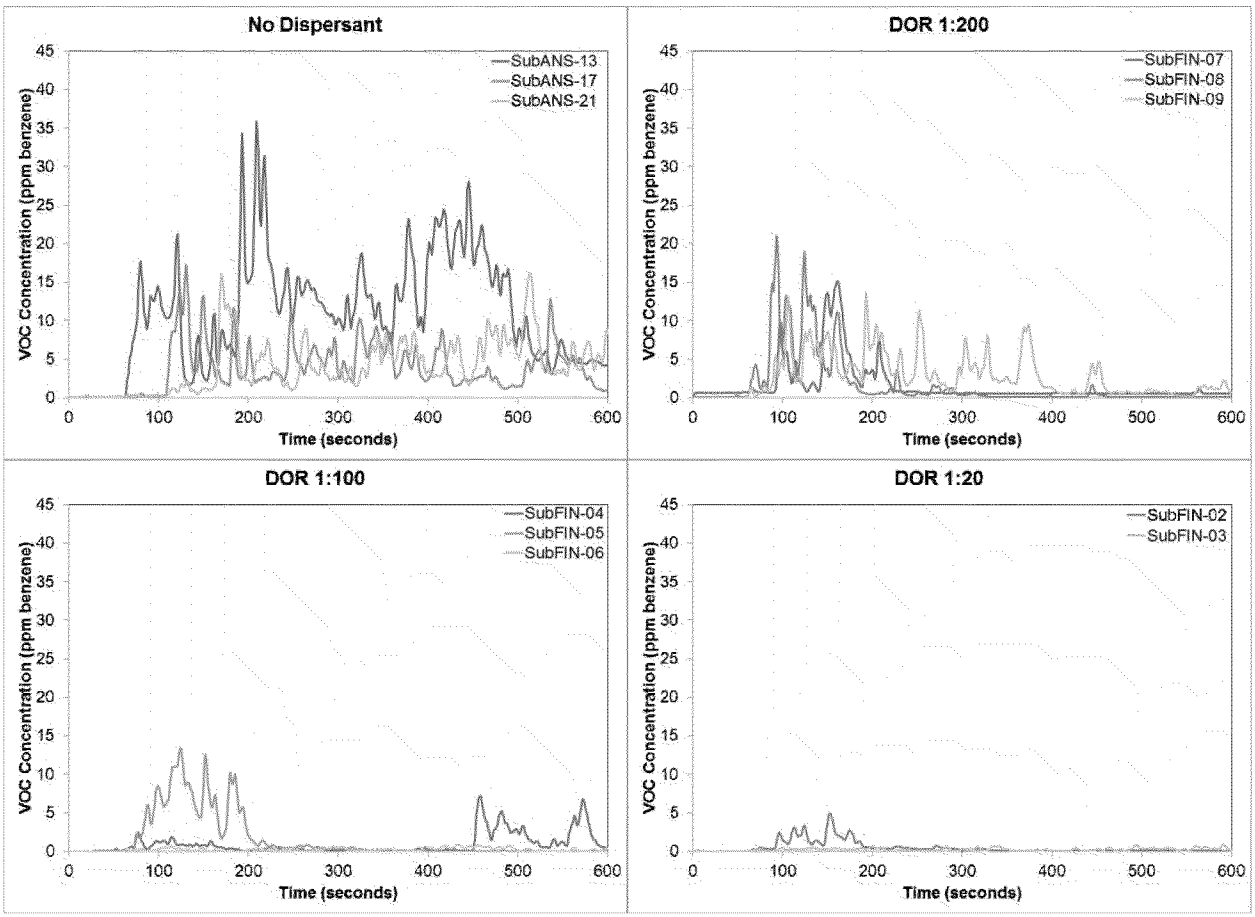

Figure 34. VOC results for subsurface injection experiments (warm water season) using Alaska North Slope crude oil and four treatment conditions (no dispersant, DOR 1:200, DOR 1:100, DOR 1:20). Finasol OSR 52 was used as the treating agent. Replicate treatments represented by light blue, dark blue and green colored lines.

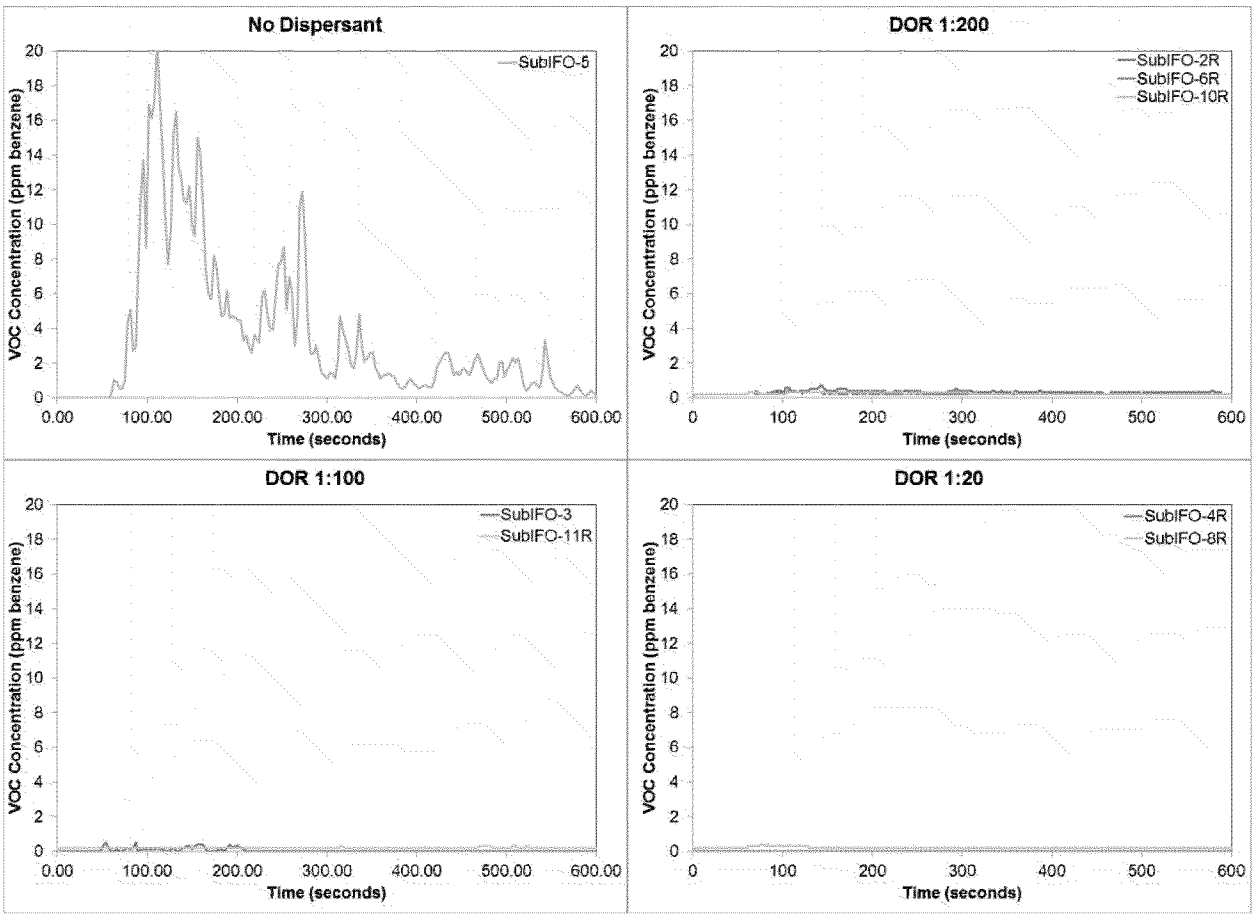

Figure 35. VOC results for subsurface injection experiments (cold water season) using IFO 120 and four treatment conditions (no dispersant, DOR 1:200, DOR 1:100, DOR 1:20). Corexit 9500 was used as the treating agent. Replicate treatments represented by light blue, dark blue and green colored lines.

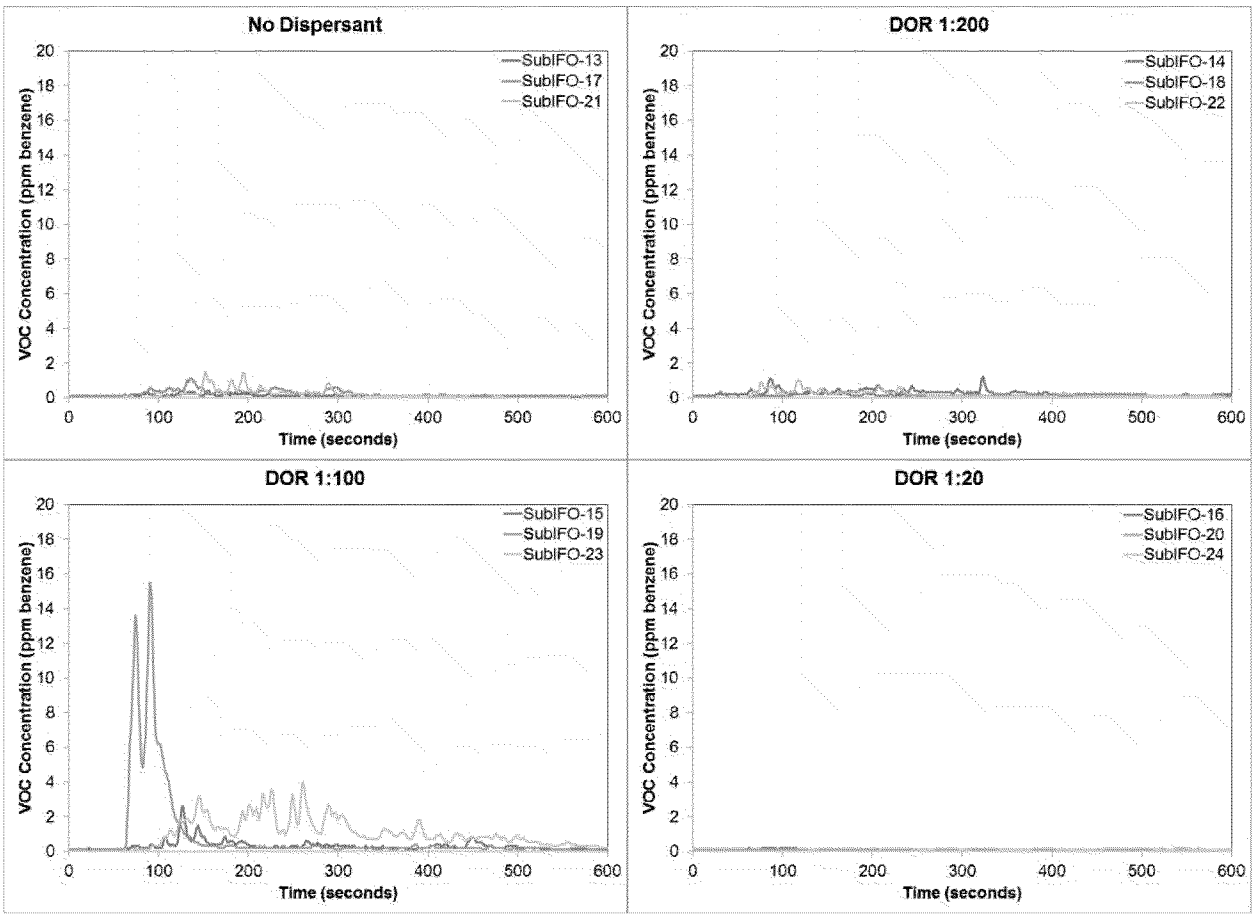

Figure 36. VOC results for subsurface injection experiments (warm water season) using IFO 120 and four treatment conditions (no dispersant, DOR 1:200, DOR 1:100, DOR 1:20). Corexit 9500 was used as the treating agent. Replicate treatments represented by light blue, dark blue and green colored lines.

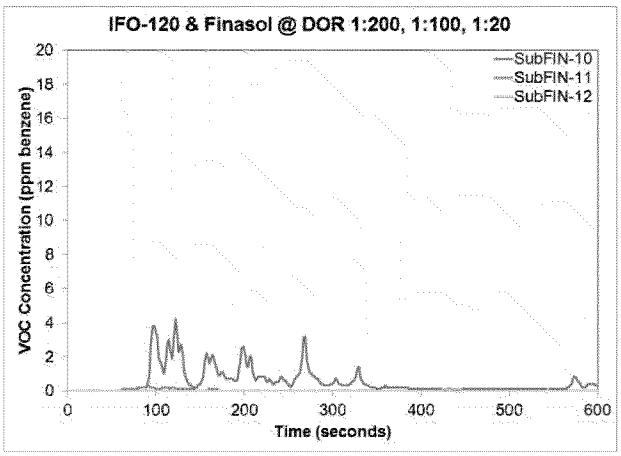

Figure 37. VOC results for subsurface injection experiments (warm water season) using IFO 120 and three treatment conditions (DOR 1:200, DOR 1:100, DOR 1:20). Finasol OSR 52 was used as the treating agent (note – these treatments were not tested in triplicate).

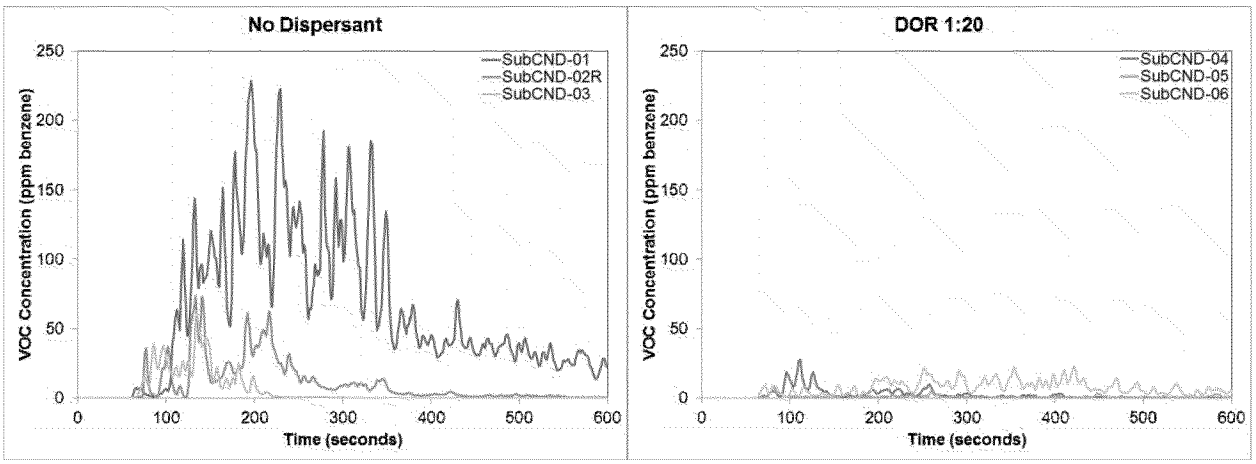

Figure 38. VOC results for subsurface injection experiments using gas condensate and two treatment conditions (no dispersant, DOR 1:20). Corexit 9500 was used as the treating agent.

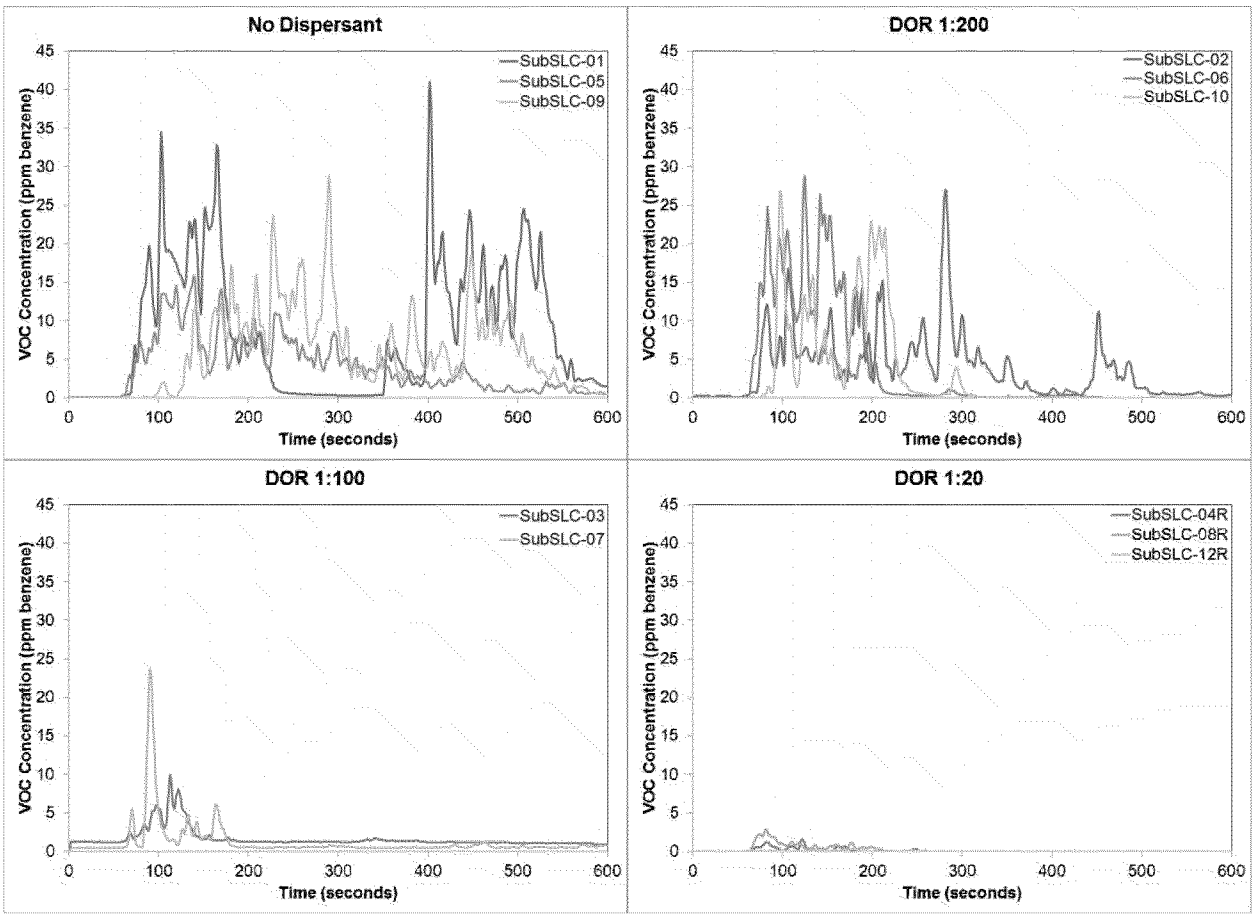

Figure 39. VOC results for subsurface injection experiments using Sweet Louisiana Crude oil and four treatment conditions (no dispersant, DOR 1:200, DOR 1:100, DOR 1:20). Corexit 9500 was used as the treating agent.

ED_001324_00000298-00081

A.3.7 VDROP-J and JETLAG Numerical Plume Modeling

Refer to Appendix G for detailed summary of the VROP-J and JETLAG numerical modeling component along with figures. Modeling the movement of oil released underwater is a challenging task due to limitations in measuring hydrodynamics in an oil-water system. Computational Fluid Dynamics (CFD) models are capable of reproducing the hydrodynamics provided they have sufficient resolution. However, current CFD models cannot predict the droplet size distribution. For this reason, we used a suite of programs to understand jet hydrodynamics, the droplet size distribution, and the movement of oil droplets within the jet/plume. The developed models were calibrated to experimental data of oil jet released underwater in the BIO tank. Based on the properties of the jet (mass flow rate 3.8 L/min through a 2.4 mm orifice), the regime of the jet is atomization, which indicates that the jet would break into small droplets. The models VDROP-J and JETLAG were used to predict the streamwise velocity and the holdup (volume of oil divided by the total volume of fluids in a control volume) along the centerline of the plume, where both models were in agreement. This implies that VDROP-J is adequate to predict the average droplet size distribution in the plume. In the absence of dispersant, the model VDROP-J predicted oil DSD that is very close to that measured by the LISST instrument. However, In the presence of dispersant premixed with the oil, the VDROP-J model captured the overall trend of the DSD, but could not capture the peak in droplet concentration observed at 5 µm. The observed peak is most likely due to tip-streaming (when at high DORs oil droplets shed filaments from their edges resulting in smaller droplets), and VDROP-J does not have such a module at this time but is considered for future development.

The computational fluid dynamics (CFD) program Fluent (www.ansys.com) was used to model the hydrodynamics of the horizontal jet experiments. The standard $k-\varepsilon$ model was used to model turbulence and the Volume of Fluid (VOF) was used to model the two phases (oil and water). The profiles of the holdup (ratio of oil volume to total volume), velocity magnitude, eddy diffusivity and turbulent dissipation rate were presented. Findings indicate that the holdup drops sharply to a few percent within 0.50 m from the source, suggesting the occurrence of water entrainment into the plume. A significant reduction in the energy

dissipation rate was also observed, by orders of magnitude along the centerline, starting from 10^4 watt/kg to 10^{-4} watt/kg. Both holdup and energy dissipation values have important consequences on oil droplet breakup and coalescence. The plume exhibited a core of high velocity and high mixing, while the edge of the plume had more or less violent conditions, which is probably due to the entrained water squishing the edges of the plume. The velocity and eddy diffusivity are needed to predict the movement of individual oil droplets. The shape of the plume was circular near the orifice, but became oblate horizontally at a centerline distance of 2.0 m, which is due to both the buoyancy of the whole plume and its inertia. This suggests that the narrow width of the tank (0.60 m) did not affect the jet hydrodynamics (otherwise the jet would be elongated in the vertical). The width of the tank had an effect on the jet dynamics only near the surface as the plume became elongated along the tank near the surface.

The CFD approach has its limitations as it smooths out the edge of the oil jet/plume, and thus does not allow for the formation of large eddies around the plume. Here, large eddy simulations (LES) were used to capture the large eddies where the movement of individual oil droplets employed a lagrangian approach. Water velocity and the eddy diffusivity were used to transport oil droplets, and the effect of individual oil droplet buoyancy and inertia were accounted for. Accounting for the inertia of oil droplets has not been done previously in the oil spill literature. Neglecting the inertia of the droplets results in overestimates of their rise rate as the inertia from a horizontal jet tends to propel the droplet more horizontally, and thus their rise gets delayed also by turbulent mixing. Results suggest that oil droplets with a diameter less than 100 µm would mix uniformly in the plume, while those close to 500 µm would tend to be above the centerline of the plume. This indicates that, when measuring the droplet size distribution using the LISST, the placement of the LISST would not affect the reading of droplets that are less than 100 microns. But the LISST needs to be placed judicially to capture particles that are 300 to 500 µm, otherwise LISST placement below the centerline would underestimate the actual droplets in that range. In contrast, LISST placement above the centerline does not allow for determining that the concentration values represent the whole cross section of the plume.

ED_001324_00000298-00083

A.3.8 Weber Number Scaling Numerical Plume Modeling

Refer to Appendix H for detailed summary of the Weber Number Scaling numerical modeling component. During the Deepwater Horizon oil spill, modeling activities for predicting oil droplet size distribution formed in subsea oil blowouts was critical given their direct influence on the fate and transport of oil in the marine environment. The community's knowledge on droplet size distributions and our capability to predict the distributions are still limited. A recent and promising approach for predicting DSD is the Modified Weber Number approach developed by SINTEF. Thus far, this method has been based on experimental results, validated by a light crude oil (Oseberg Blend crude oil). Here, this approach is validated over a range of oil types (IFO 120 and ANS) using a series of experiments conducted with a subsurface release of oil within the DFO horizontal flow tank.

Based on the measured droplet sizes obtained from the tank experiments, corresponding median droplet diameters (d_{50}) and the relative droplet size (d_{50}/D) were calculated. Accordingly, the relations between d_{50}/D and modified Weber number, Reynolds number, and oil concentration were quantified. With regression analyses, the empirical coefficients for the prediction of droplets size distribution based on the modified Weber number were determined for a certain type of oil (e.g., IFO 120 and ANS). The results indicated that chemical dispersants play an important role in reducing the droplet size of ANS in both cold and warm temperatures. The effectiveness of dispersant in reducing droplet size is higher for ANS compared to IFO 120. There may be thresholds for the dose of chemical dispersant to some oils (e.g., IFO 120) but further data analyses are needed to confirm this. There may also be over dose of dispersant to some oils (e.g., ANS) when the DOR is high, eventually affecting the droplet size distribution. Furthermore, the data indicate that the distributions of the data with $d/d_{50} <= 1$ and $d/d_{50} > 1$ are significantly varied. Therefore, a two-step Rosin-Rammler approach was introduced to more accurately predict the droplet size distribution. The regression coefficients for the two-step Rosin-Rammler are higher compared to the single step in most cases, indicating the advantage of the proposed two-step Rosin-Rammler

ED_001324_00000298-00084

approach. It should also be noted that the measured IFT for the IFO 120 and ANS with different DORs appear to be significantly different compared to the measured results from SINTEF for the modified Weber number approach, possibly due to the characteristics of different oils.

ED_001324_00000298-00085

TASK B.1 INTRODUCTION & RELEVANCE

Results presented in Task B are contribution of Mary Abercrombie of the University of South Florida and are a portion of her dissertation efforts.

BSEE's *Remote Sensing & Surveillance of Oil Spills* webpage states that "In remote sensing, a sensor other than human vision or conventional photography is used to detect or map oil spills". Thus, although certain remote sensing of oil spills is traditionally linked to detection of oil on the sea surface from above, the scope of the technology can be extended to include the detection of oil in the deep-sea and/or under-the-ice conditions using various sensors, as responders cannot use vision within the water column. As demonstrated during the 2010 Gulf of Mexico Deepwater Horizon (DWH) oil spill, oil detection by fluorescence can enable responders to discern trajectory of plumes and assess effectiveness of dispersant countermeasures (ACT, 2008; Joint Analysis Group Report, 2010). The information gained from such technologies was used to track oil in the water column and inform response strategies to protect natural resources potentially at risk; thus supporting both Net Environmental Benefit Analyses (NEBA) and Natural Resource Damage Assessments (NRDA). To advance the application of this methodology, this project evaluated fluorescence characteristics of various oils with and without dispersants to aid in the selection and refinement of *in situ* sensors for use in oil spill response operations.

The overall objective of this work was to translate oil fluorescence R&D into operational tools for oil spill response. Tabulating information on the optimum fluorescence wavelengths for oil detection as a function of oil type and DOR assists responders selecting sensors and establishing Best Practices for rapid decision making during spill response. The results of this project are timely and can be used in conjunction with the National Response Team (NRT) guidance document, Environmental Monitoring for Atypical Dispersant Operations: Including Guidance for Subsea Application and Prolonged Surface Application, for incident-specific decisions concerning monitoring subsea dispersant use. It specifically calls upon using oil-specific submersible fluorometers with laboratory and on-board ship analyses using fixed wavelength and scanning spectrofluorometers to enable improvements to monitoring sampling during

dispersant application. Findings from this project provide additional scientific information in support of implementing guidance recommendations.

Fluorescence characteristics - All fluorophores (molecules that fluoresce) have characteristic wavelengths for maximum absorption of light and characteristic wavelengths at which they emit light as fluorescence. Absorption and fluorescence can occur at either narrow or wide wavelength ranges depending on the chemistry and complexity of the fluorophores. A variety of naturally occurring fluorescent compounds occur in the ocean, from ones with narrow wavelength ranges with sharp fluorescence peak maxima (pigments, proteins) to complex compounds with wide diffuse peaks over long wavelength ranges, such as the ubiquitous Colored Dissolved Organic Matter (CDOM) or petroleum oils.

Fluorescence characteristics of complex mixtures can overlap if structurally similar compounds are shared. Such is the case with CDOM and the aromatic fraction of crude oils. Both are comprised of a variety of organic molecules and both exhibit complex, three-dimensional excitation and emission (EEM) spectra. In general, crude oils have a broad excitation peak centered in the ultraviolet spectrum (< 300 nm) and two emission peaks, one centered in the ultraviolet spectrum around 340 nm and a much larger and broader peak in the visible around 445 nm (Bugden et al., 2008). These peaks result from the single ring benzene derivatives and the "polynuclear aromatic" fraction that are particularly susceptible to UV excitation wavelengths. EEMs exhibit distinct fingerprints for different oils as illustrated by previous studies (Frank, 1978 and references therein; Bugden et al., 2008; Kepkay et al., 2008).

DWH in situ oil fluorescence - Deployment of submersible fluorometers during the DWH oil spill response illustrated the utility of this forensic tool that enabled large-scale monitoring of oil concentrations to a depth of approximately 1600 m. Co-deployment of the fluorometers alongside other response sensors [Conductivity-Temperature-Depth (CTD), Dissolved Oxygen (DO), Laser *In-Situ* Scattering and Transmissometry (LISST)] from multiple platforms (e.g. profilers) with real-time capabilities improved our understanding of the processes influencing the fate and behavior of the oil in the presence and absence of chemical dispersants. Added to this, extensive water column sampling also involved discrete sample collection for oil particle

ED_001324_00000298-00087

concentration and size, *Total* Petroleum Hydrocarbons (TPH), Volatile Organic Carbon (VOC) and other physical, chemical, biological factors. To date the in-depth reviews by the Joint Analysis Group (JAG) charged with data analysis have found that of all the variables measured, the most highly correlated in the subsea plume are *in situ* DO and oil fluorescence intensity (Joint Analysis Group Report, 2010). Such a correlation is not unexpected as laboratory tests show that enhanced oxygen utilization can result from microbial respiration in the presence of oil compounds (Venosa et al., 2002b). Beyond the underlying biochemical mechanisms however, likelihood of correlation is increased based on the fact that variables measured *in situ* at high sampling rates are better to capture plume heterogeneity. Hence, the utility of *in situ* fluorescence as a tool was ascertained early in the response due to such correlations, the high temporal and spatial resolution provided by the sensors, and also the advantages afforded by real-time capability compared to discrete analyses.

However, the multitude of submersible fluorometers used in the DWH response called to attention differences in the sensitivity and analytical capability of the instruments used due to differences in configuration of excitation and emission wavelengths, methods of calibration, sensitivity, and correlation to oil concentration (Figure 40, Table7). Many are not customized to capture oil fluorescence peak maxima, rather only a fraction of the signal (Fuller et al., 2003; Conmy et al., 2004 Conmy et al., 2014b). Furthermore, the ability of any fluorescence sensor (laboratory or field submersible) to detect oil is a function of (1) how well the sensor matches the excitation and emission wavelengths of the oil (including bandwidth of the wavelength filters or bandpasses from gratings, (2) the power of the light source, and (3) the sensitivity of the detector.

When tracking in the subsea became necessary early in the response, fluorometers used for detection of CDOM (i.e., WET Labs ECO series) were deployed on the vertical profilers as they were widely available, were capable of full ocean depth deployment and had been previously shown to detect oil in water (Wet Labs, Inc. website, www.wetlabs.com). These sensors typically have light sources that excite at wavelengths slightly longer than peak absorption by hydrocarbons and detect emission in the visible. They employ filters centered on excitation (Ex)

ED_001324_00000298-00088

and emission (Em) wavelengths at 370 and 460 nm ($ExEm_{370/460nm}$). Although the center wavelength of the filters does not capture the peak of the oil fluorescence signal, the wide bandwidth of the emission filters (120 nm Full Width at Half Max) and the broad nature of the fluorescence peaks means that CDOM sensors are capable of detecting a large portion of the visible fluorescence signal. CDOM fluorometers were used to detect oil during the response in part because of their accessibility, but also because these sensors capture some portion of the oil fluorescence peak that occurs at the longer UV wavelengths where CDOM peaks also exist.

To quell questions regarding the ability of the ECO CDOM fluorometer to detect oil in the subsea plume, calibration tests were conducted at Louisiana State University (LSU) using Mississippi Canyon 252 (MC252) source oil. They provided a means to convert raw fluorescence data to Quinine Sulfate Dihydrate Equivalents (QSDE, the standard typically used for CDOM) to ppm of oil (JAG report, 2010). The calibrations were conducted in flasks on orbital shakers at 90 revolutions per minute (rpm), where oil concentrations ranged between 1-50 ppm. Dispersant (Corexit 9500) was added at a DOR of 1:2.5 and 1:25. The response of the fluorometer was linear with respect to oil but varied as a function of DOR, with a quenching of fluorescence in the presence of more dispersant per unit oil. Results of this test indicated that the ECO sensor was a sufficient proxy for oil concentrations greater than 1 ppm. However, as the response continued and after the well was capped, oil concentrations in the subsea plume decreased as well as the magnitude of the fluorescence anomaly due to dilution and degradation of the oil, particularly at further distances from the wellhead. Concern was raised that a fluorometer with higher sensitivity for oil (one with a hydrocarbon-specific configuration) was needed. At that time, Chelsea UV Aquatrackas ($ExEm_{239/360nm}$) were deployed to track the plume in the far field of the response geographic region with the expectation (and subsequent confirmation) that it would detect fluorescence signal at lower oil concentrations.

ED_001324_00000298-00089

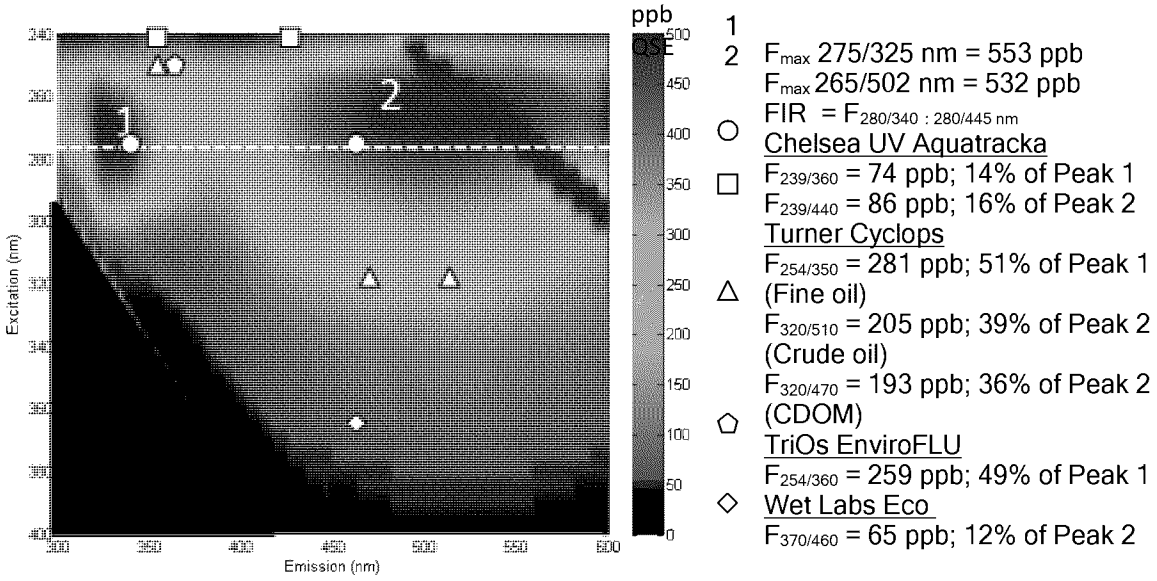

Figure 40. Fluorescence peaks of S. Louisiana sweet crude dispersed in in ppb QSE (Quinine Sulfate Equivalents). Symbols represent Fluorescence Intensity Ratio (FIR) locations and the Center Wavelength (CWL) reported by sensor manufacturers. Bandwidths (BW) are not shown.

Table 7. Sensor specifications as listed from manufacturers. Wavelengths listed as Center Wavelengths (CWL) with Full Width at Half Max (FWHM) and Bandpass (BP). Standards used

are QS (Quinine Sulfate Dihydrate), NDD Salt (Napthalene Disulfonic Disodium) and PTSA Salt (Pyrenetetrasulfonic Acid Tetrasodium) (From Conmy et al., 2014b).

Manufacturer	Instrument	Light source	Excitation λ (nm)	Emission λ (nm)	Detector	Dynamic Range
Chelsea Technologies Group	UV AQUAtracka	Xenon lamp	239 CWL	360 CWL	PMT	0.001- 10 μg/L Carbazole
	UV AQUAtracka	Xenon lamp	239 CWL	440 CWL	PMT	0.001 - 10 μg/L Perylene
Seapoint Sensors	SUVF	LED	370, 12 FWHM	440, 40 FWHM	Photodiode	0.1 - 1500 μg/L QS
TriOS, GmbH	EnviroFLU-HC, DS	Xenon lamp	254, 25 FWHM	360, 50 FWHM	Photodiode	0 - 5000 ppb Phenanthren
Turner Designs	Cyclops (Fine oil)	LED	254, 40 nm BP	350, 50 nm BP	Photodiode	0 - 10,000 ppb NDD Salt
	Cyclops (Crude oil)	LED	320, 130 nm BP	510, 180 nm BP	Photodiode	0 - 2700 ppb PTSA Salt
	Cyclops (CDOM)	LED	320, 130 nm BP	470, 60 nm BP	Photodiode	0 - 2500 ppb QS
WetLabs	WetStar	LED	370, 10 FWHM	460, 120 FWHM	Photodiode	0.100 - 1000 ppb QS
	ECO-FLU, triplet, puck	LED	370, 10 FWHM	460, 120 FWHM	Photodiode	0.01 - 500 ppb QS

Post-DWH response sensor tank testing -To address persisting uncertainties regarding sensor performance in the subsea, a team of scientists conducted experiments in June 2011 to study the dynamic range, sensitivity, and response *of in situ* fluorometers to changing excitation or emission properties of fresh and weathered MC252 oil (NOAA Science Box Award, PI: Michelle Wood; Co-PI's from EPA, NOAA, University of South Florida). The experiment was conducted within the flow-through flume tank at the BIO in Dartmouth, Nova Scotia, taking into consideration environmental factors such as wave energy and ocean currents. Experiments included the stepwise addition of oil and dispersant (DOR of 1:25; 0.3 - 12 ppm of MC252 SLC oil to the flume tank while collecting *in situ* fluorescence and droplet-size distribution data, as well as coincident discrete samples for chemistry and EEM analyses. The flume tank was operated in static mode and each addition of oil and dispersant was allowed to homogenize prior to collecting discrete samples and coincident sensor measurements to calculate the least linear squares regressions. Results indicated that all sensors tested were responsive to changes in MC252 oil concentration regardless of wavelength configuration. Linear response of the WET Labs ECO, Turner Designs Cyclops and the Chelsea Technologies Group AQUAtrackas sensors as a function of oil concentration was observed, where lowest concentrations were not below the

ED_001324_00000298-00091

detection limit of any sensor tested (Conmy et al., 2014a). Results demonstrated that all sensors exhibited a wide dynamic range of detection for MC 252 oil and were capable of detecting oil at the lowest concentration (approximately 300 ppb oil), which is significantly lower than the LSU calibration study (1 ppm) and a common misconception during the response. Differences in the detection limit between the studies may be explained by differences in the design, scale and the amount of physical dispersion of the tests, where the tank can provide mixing energies similar to those found in the field.

The 2011 study findings answered critical questions about sensor performance to detecting MC252 oil. However, the experiment highlighted the need for future studies to evaluate sensor performance using a variety of DORs and for multiple oil types. Evident from the DWH spill and post-spill research was that further R&D is needed to transfer knowledge gained through laboratory 3-D Excitation Emission Matrix (EEM) Spectroscopy into practical information for fluorescence tools used during spill response. Fluorescent properties are oil specific and investigating variations in EEMs as function of oil type and dispersant-to-oil ratios better prepares the community in identifying sensors for response options. To that end, the objectives of this project were to:

I. Generate a comprehensive EEMs database, building upon existing data at the Department of Fisheries and Oceans Canada, to provide fluorescence peak information as a function of oil type, weathering state, concentration and Dispersant-to-Oil Ratios (DORs).
II. Critically examine the database using advanced statistical methods and models to identify wavelengths best suited for oil monitoring during dispersant application and degradation.
III. Conduct flume tank experiments to determine submersible sensors capable of providing data comparable to scanning and/or fixed wavelength laboratory fluorometers for rapid deployment during response efforts.

Through this project, a comprehensive EEMs library database was generated covering a wide

ED_001324_00000298-00092

variety of oils from light to heavy fuel and crude oils and diluted bitumen. Varying DORs (1:20, 1:100, 1:200, 0) and oil concentrations were evaluated as the presence of dispersant alters EEM fingerprints. EEMs were subjected to advanced statistical analyses and models to identify wavelengths best suited for oil monitoring during dispersant application and subsequent tracking . Fluorescence is a non-destructive characterization tool that is routinely used to examine complex organic mixtures (foods, wine, medical compounds, aquatic organic matter, oils). Unlike single compound solutions, they exhibit broad, diffuse peaks that result from overlapping smaller peaks with similar chemistry. Although EEMs can be a substantial source of information on chemical composition and variability amongst samples, the high-dimensionality (intensity by emission by excitation) and nonlinearity of the data equates to difficulties in data interpretation and extraction of practical information as a characterization tool (Bieroza et al., 2010). Therefore, it is difficult to determine which underlying chemical components are responsible for which portion of the fluorescence fingerprint. Combining standard techniques for EEM analysis such as assessment of particular fluorescence peak features including peak height and wavelength position via 'peak picking' with Parallel Factor Analysis (PARAFAC) modeling results in a more comprehensive understanding of the chemical constituents. The use of advanced multivariate analyses such as PARAFAC has gained popularity as an effective means to deconvolve complex, broad peaks into their underlying smaller components (Stedmon et al., 2003; Boehme et al., 2004; Christensen et al., 2005; Stedmon and Bro, 2008). Here, we processed EEMs data with scripts in the N-way toolbox for MATLAB (Andersen and Bro, 2000) and SOLO software (Eigenvector, Inc) and used the algorithms to isolate wavelengths to best characterize an oil type. An excellent review of these chemometric techniques and applications is provided in Bieroza et al., 2010. This approach will allow for comparing oil in water mixtures for similarities and contrasting features.

Results were evaluated for the Fluorescence Intensity Ratio (FIR) technique (Bugden et al. 2008; Kepkay et al. 2008). The latter calculates the ratio at $ExEm_{280/340nm}$ to $ExEm_{280/445nm}$ as an indicator of oil dispersion. Previous studies at DFO COOGER have shown that dispersed oil fluoresces over two peaks centered on emission wavelengths of 340 nm and 445 nm, at excitation wavelength 280 nm, and that chemical dispersion enhances the emission intensity at

ED_001324_00000298-00093

450 nm (Bugden et al. 2008; Kepkay et al. 2008). Postulated is that the fluorescence intensity at $ExEm_{280/340nm}$ represents the dispersion of lower molecular weight aromatic hydrocarbons, while intensity at $ExEm_{280/445nm}$ corresponds to higher molecular weight aromatic compounds.

Finally our work addresses the disconnect that exists between fluorescence research conducted in laboratories and the collection of fluorescence data from submersible sensors. By conducting laboratory-based and tank-based experiments on the same oil type and DOR, comparisons between EEMs can be made across scales. This helps to determine how well the *in situ* sensors are aligned in detecting dispersed oil.

TASK B.2 EXPERIMENTAL METHODS

B.2.1 Sample Preparation - Twenty-five oil samples from the DFO and EPA stockpiles (covering a wide range of viscosity and oil types) were used for spectrofluorometric testing, where oil

ED_001324_00000298-00094

characteristics were tabulated for the test oils based on an extensive literature search (Table 8; Supplemental Material A). All glassware used in this study was cleaned to ensure highest analytical integrity including solvent rinsing, deionized water rinsing and baking in muffle furnace at 450˚C where appropriate. Samples were stored in 125mL amber glass bottles with PTFE-lined caps (Figure 41).

B.2.2 Artificial Seawater Protocol - Artificial seawater was used for DOR mixing to avoid interference of fluorophores found in natural seawater with oil fluorescence signal. Fresh artificial seawater was made to salinity 28 ppt and was prepared in 1 L quantity at the beginning of each experiment by adding Tropic Marin® salts (Appendix A) to 1 L ultrapure water dispensed from a Millipore Milli-Q unit (≤ 4 ppb DOM) into a 1.5 L glass beaker, covering the beaker with aluminum foil, and stirring with a magnetic stir-bar on electric stir plate for 20 minutes at room temperature (~24°C).

B.2.3 Dispersed Oil in Seawater Protocol - A series of dispersed-oil-in-seawater experiments were performed using baffled trypsinizing flasks (baffled flasks) with artificial seawater, MC252 oil and Corexit 9500 chemical dispersant (Venosa et al., 2002a). Four petroleum oil / dispersant solutions were prepared for each oil type at the following DORs: 0, 1:20, 1:100, and 1:200. Oil was pipetted into an 8.6 ml amber vial, followed by addition of the appropriate amount of Corexit 9500 chemical dispersant into the vial. Teflon-lined capped vials were shaken by hand for 60 seconds and 10 µL of dispersant / oil mixture was pipetted (Eppendorf positive displacement micropipettes, 1-20 µL) into 100 mL artificial seawater contained in each of three replicate flasks. Flasks were covered with parafilm and placed on a New Brunswick Scientific Innova 2100 platform shaker (orbit = 1.9 cm) for 12 minutes at 200 rpm. Approximately 3.5mL of the resulting dispersed-oil-in-seawater was immediately dispensed through a spigot near the bottom of each flask into three 4.0-mL UV-grade quartz cuvettes, which were immediately covered with Teflon stoppers to prevent evasion of volatile components during fluorescence analyses (Figure 42). After removal of spectrophotometric samples, additional volumes of sample were removed from the baffled flasks for extraction of total petroleum hydrocarbons (TPH) by dimethylene chloride (DCM). TPH analysis follows the same Gas Chromatography-

ED_001324_00000298-00095

Mass Spectrometry (GC-MS) method as in Task A of this project.

B.2.4 Spectrophotometric Analysis - A Horiba Scientific AquaLog spectrofluorometer was used to analyze the 25 oil types with varying DOR. A series of analyses were initially performed while varying the instrument's settings (excitation and emission increments, gain setting, integration time) in order to determine optimal settings for the entire experimental protocol. Excitation-Emission Matrices (EEMs) were generated using the following instrument parameters: 200 – 800 nm excitation (3 nm increments), 249 – 828 nm emission range (CCD detector at 534 nm, 8 pixel increments), medium gain setting and integration time of 0.1 sec. A quinine sulfate dihydrate dilution series was created consisting of: 0.5N H_2SO_4 solvent; 100 ppm 1° (primary stock) solution; 100 ppb 2° (secondary stock) solution; 1,3,5,10 and 20ppb quinine sulfate solutions. Dilutions were analyzed for fluorescence and used for cross-calibration with instrument software built-in quinine sulfate tool to convert results into Quinine Sulfate Equivalents (QSE) and demonstrate linearity of fluorescence in a dilution series. All data processing and spectral corrections follow the manufacturer's manual. Dilution series with oil concentrations between 1 – 500 ppb were also generated to determine lower detection limits for oils. EEMs are presented in Raman Units (RU).

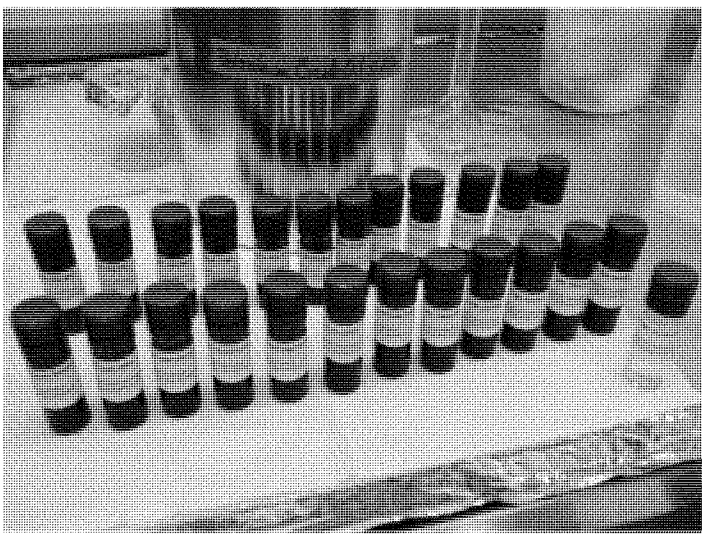

ED_001324_00000298-00096

Figure 41. Twenty-five oil samples stored in glass bottles.

Table 8. List of oil samples used for EEM analyses. Location of oil source field, as well as water depth for marine based wells, included in Supplemental Table A.

Light (API >31.1°)	Medium (API 22.3 – 31.1°)	Heavy (API <22.3°)
Arabian Light (32.2°)	Alaska North Slope (29.7°)	Access Western Blend Dilbit (21.3°)
Brent (38.2°)	Alaskan North Slope (10% weathered)	Belridge Heavy (13.6°)

ED_001324_00000298-00097

Federated (39.4°)	Heidrun (28.6°)	Cold Lake Dilbit (21.5°)
Gullfaks (32.7°)	Lago (25.0°)	Hondo (19.5°)
Hibernia (35.6°)	Mesa (30.3°)	IFO 40 (21.9°)
MC252—Discoverer Enterprise (37.2°)	Sea Rose (29.8°)	IFO 120 (18.4°)
MC252—generic (35.2°)	Vasconia (26.3°)	IFO 180 (14.1°)
Scotian Shelf Condensate (53.2°)		IFO 300
Terra Nova (33.8°)		Santa Clara(22.1°)

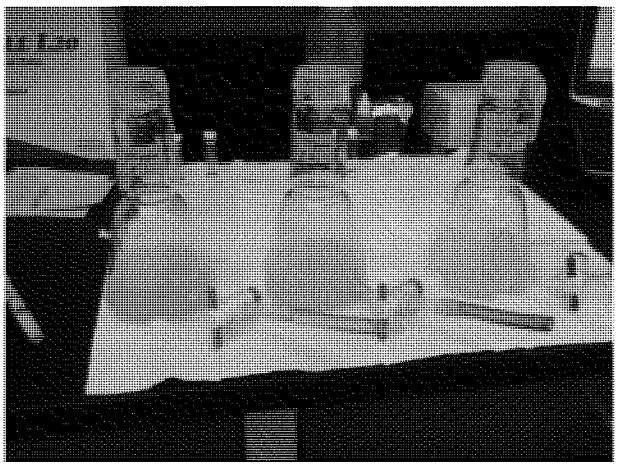

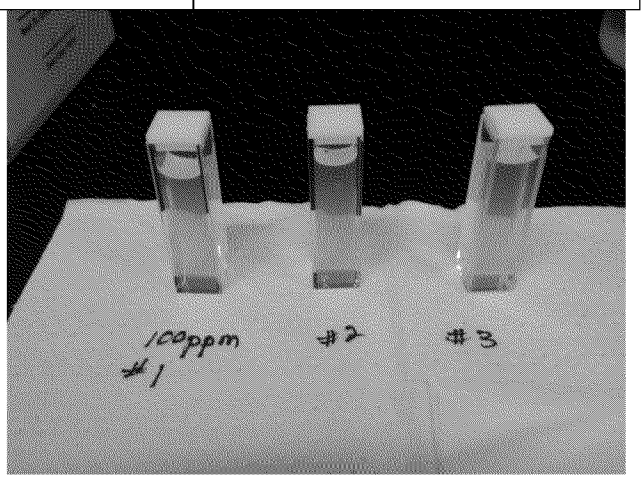

Figure 42. Trypsinizing baffled flasks containing dispersed oil in artificial seawater (left) and corresponding samples removed from each flask, ready for spectrofluorometric analysis.

ED_001324_00000298-00098

TASK B.3 RESULTS & DISCUSSION

B.3.1 Oil Fluorescence Properties

Four characteristic excitation/emission (Ex/Em) peak locations were identified: F_{max1} – F_{max4} (Figure 43) for all 25 oil types at four DORs (Figure 43). The highest intensity peak (F_{max1}) occurred, without exception, at Ex 221-239 nm/Em 335-344 nm and was paired with a blue-shifted, lower intensity peak (F_{max2}) at Ex 215-221 nm/Em 285-308 nm in all oil types.

A third broad, low-intensity peak (F_{max3}) was observed at Ex 215-305 nm/Em 418-571 nm to varying degrees across oil types, corresponding with oil categories determined by API gravity (Table 8). Light crude oils exhibited F_{max3} fluorescence at all DORs with the exception of Scotian Shelf Condensate. It is worth noting that Scotian Shelf Condensate appeared physically unlike any of the other light oils: clear in color with apparent very low viscosity. Since viscosity is largely determined by the size and relative weight of component hydrocarbons (Fingas 2011), fewer complex fluorophores would likely be present in this oil type. Fluorescence in the F_{max3} region was identified at all DORs in only one medium weight oil (Heidrun), and was not present at any DOR in one medium oil (Vasconia). Two medium-weight oils emitted measurable fluorescence in the F_{max3} region only with full dispersion (Lago and Mesa), while Sea Rose showed fluorescence at DORs 1:100 and 1:20. One medium weight oil, Alaska North Slope (both fresh and 10% weathered), exhibited unusual F_{max3} behavior, with measureable fluorescence at DOR 0, 1:100 and 1:20, but not at DOR 1:200. Finally, for the heavy weight oils, F_{max3} was almost completely absent at all DORs, with the exception of fluorescence at DOR 1:20 for Cold Lake Dilbit and IFO 40, and across all DORs for one anomalous member of this group—Access Western Blend Dilbit. By definition, a dilbits is a mixture of bitumen—essentially an extra heavy crude oil with API gravity < 10.0°—and a diluent—either a light condensate or naptha (Priaro 2016). The combination of characteristics from both oil types may account for the unusual F_{max3} fluorescence observed in this oil type. Additionally, Intermediate Fuel Oils (IFOs) are not true crude oils, but marine fuels consisting of a mixture of post-refinery heavy

ED_001324_00000298-00099

residual oil and refined diesel fuel., which may also help to explain the appearance of F_{max3} fluorescence in IFO 40. Clearly, the presence of fluorescence in the F_{max3} region , especially at DOR 1:20, appears to be closely tied to API gravity, and thus to density as well as kinematic viscosity since API gravity = (141.5/Specific Gravity) – 131.5 (Fingas, 2011). The absence of F_{max3} region fluorescence in heavy weight oils may be due to retention of energy within the large, complex hydrocarbons which make up highest density oils. Addtionally, the appearance of fluorescence in the F_{max3} region at highest DORs in the medium weight oils Lago, Mesa, and Sea Rose would also seem to suggest that the creation of smaller droplet sizes with effective dispersion leads to a decrease in reabsorption of fluorescence within droplets.

A fourth region of broad, low-intensity fluorescence (F_{max4}) was identified at Ex 269-291 nm/Em 326-353 nm, and found to be presentin all oil types at all DORs. Therefore, F_{max1} and F_{max4} oil-in-water fluorescence regions appear to be analogous to the characteristic colored dissolved organic matter (CDOM) fluorescence regions A_C (formerly A) at Ex 260/Em 400-460 and C at Ex 320-365/Em 420-470 (Coble, 2014).

In addition to maximum fluorescence intensity for all peaks (in RU), full width at half maximum (FWHM) was also recorded. Further, fluorescence intensity at Ex/Em 281/340 and 281/446 nm was recorded to enable calculation of the Fluorescence Intensity Rratio (FIR) for all samples. Optimum settings for signal collection on the HORIBA AquaLog necessitated excitation at 3 nm intervals, which accounts for the 1 nmdiscrepancy from the published FIR wavelength (Bugden, et al. 2008). Finally, fluorescence intensity at the specified Ex/Em wavelength settings of five off-the-shelf *in situ* fluorometers (Conmy et al., 2014 a & b), which were all employed in the response to the DWH spill, was recorded. Those wavelengths were also adjusted slightly to compensate for signal collection intervals on the HORIBA AquaLog. Selected results are presented in Table 9 along with results of chemical analyses, and complete fluorescence results are included as a Supplemental Table A.

Finally, EEM contour 'fingerprint' plots for all oils, which characterize each oil type and illustrate the effect of dispersant on the fluorescence properties, are presented in Appendix F. The ability to identify oil source would be particularly useful in the prevention and abatement of oil spill

ED_001324_00000298-00100

pollution. To that end, efforts to determine characteristic fluorescence fingerprints have existed since the 1970s (Frank, 1978) and have received renewed attention with the advent of improved fluorescence detection systems (Bugden, 2008).

Intensity of F_{max1} was consistently strong across oil types, with no ambiguity in peak location. The observed Ex/Em range of significant fluorescence intensity was fairly narrow with FWHM of only 37-50 nm, and little to no change in peak location with increasing DOR. Six of the nine light oil types, but just one of the seven medium oil types and one of the nine heavy oil types[1] displayed this slight increase (approximately 4.5 nm) in FWHM with maximum dispersion (DOR 1:20). One medium weight oil (Lago) and one heavy oil (Access Western Blend Dilbit) showed the same slight increase in FWHM at both DORs 1:100 and 1:20. The impact of applying the Inner Filter Effect correction tool (IFE) to fluorescence intensity was also calculated for F_{max1}. This correction utilizes the measured absorbance of the sample to correct for fluorescence emitted by fluorophores within the sample, but re-absorbed within the sample itself. Of note is that application of the IFE resulted in only a small magnification of the fluorescence signal at DORs 0, 1:200 and 1:100 for all oil types; however, there was a clear delineation between two overall categories of oil types at DOR 1:20: Oil Type I, with IFE effect > 2.5 and Oil Type II, with IFE effect < 2.5 (Table 9). This appears to be due to the increase in optical density, and thus absorbance, caused by interaction between Corexit 9500 and fully dispersed Type I oils. Photographs of four representative pre-analysis samples, along with the resulting EEMs of oil type are shown in Figure 44 to illustrate the difference in fluorescence between the types regardless of being a light, medium, or heavy crude oil.

Due to variation from laboratory to laboratory, and even differences in instrument to instrument performance from the same manufacturer, it is necessary to convert fluorescence intensity "raw counts" to a standardized unit for useful reporting purposes. Traditionally, the fluorescence community has utilized a dilution series of quinine sulfate dihydrate in weak acid to convert instrument output to Quinine Sulfate Equivalents (QSE) (Coble, 1996). However, in recent years the alternate method of reporting in Raman Units (RU) has gained favor (Murphy

[1] Increase of approximately 4.5 nm in FWHM in F_{max1} seen in light oils Arabian Light, Brent, Federated, Gullfaks, Hibernia, and Terra Nova; in medum oil Mesa; and in heavy oil IFO 120 at DOR 1:20.

ED_001324_00000298-00101

et al., 2010). Due to inherent properties of water molecules, the Raman scatter peak is a reliable feature which can be used through collecting a scan of ultra-pure water at the beginning of each day, and then using the ratio of raw counts to the area under the curve of the Raman peak (approximately 381-426 nm) to convert fluorescence to RU. As the Quinine Sulfate SRM is no longer available from NIST (National Institute of Standards and Technology), we have reported results in RU and offer a conversion factor to QSE using the highest quality quinine sulfate dihydrate readily available.

Overall, F_{max1} intensity ranged from a minimum of 39.58 RU (Access Western Blend Dilbit DOR 0) to 3090.23 RU (IFO 120 DOR 1:100). Since all of the Intermediate Fuel Oils and the Scotian Shelf Condensate showed unusual fluorescence profiles which tended to skew our results for the forementioned reasons, (see Figures 45 and 46), these will be eliminated from the remaining discussion. F_{max1} intensity within Type I oils ranged from 357.62 RU (Arabian Light DOR 1:200) to 1998.60 RU (MC252 Discoverer Enterprise DOR 1:20), while the range in Type II Oils was the overall low of 39.58 previously mentioned to a high of 1098.90 (Heidrun DOR 1:20).

While the excitation wavelength of maximum intensity for F_{max2} remained relatively consistent, the emission wavelength varied within, as well as among, oil types. The occurrence of double and triple peaks, as well as minor sub-peaks, within the F_{max2} region was fairly common. It was sometimes difficult to distinguish the F_{max2} peak from the shoulder of a very strong F_{max1} peak, especially at higher DORs. For this reason, determination of the true FWHM was sometimes problematic. For F_{max2} intensity, Type I Oils ranged from 63.95 RU (Brent DOR 1:200) to 437.32 RU (MC252 Discoverer Enterprise DOR 1:20), and Type II Oils ranged from 25.07 RU (Belridge Heavy DOR 0) to 164.07 RU (Heidrun DOR 1:20).

For oil types exhibiting an F_{max3} peak, it was most apparent at the highest DOR (1:20), and some oils exhibited a strong F_{max3} peak across all DORs (e.g., Brent, Federated). However, for those oils the F_{max3} peak at DOR 1:20 was significantly blue shifted (peak moved to lower wavelengths) from the F_{max3} location observed at lower DORs. FWHM of the F_{max3} peak was much greater than that of any other peak (145-283 nm), with the exception of the three lower DORs of Access Western Blend Dilbit (52-56 nm). Identification of highest F_{max3} intensity proved somewhat

ED_001324_00000298-00102

problematic as it tended to lie within the second order Rayleigh region, a band of high intensity light resulting from scattering by water molecules. The edge of highest intensity could also lie in this region, so determination of the true FWHM was also problematic for many oil types. Traditionally, second order Rayleigh is eliminated by simply masking this region (10-12 nm). Although algorithms have been developed to model the character of fluorescence peaks lying within (Zepp, et al. 2004; Bahram, et al. 2006), assumptions about the linearity of fluorescence must be made, and the true signal behavior cannot be known. For this reason, as our goal was to identify signals which could also be detected by *in situ* instruments, the decision was made to identify the maximum fluorescence intensity lying outside of the second order Rayleigh region rather than to try to interpolate the data.

As previously mentioned, F_{max3} intensity was not always present, and it was observed far more often in Type I Oils with a range of 2.64 RU (Arabian Light DOR 1:200) to 744.69 (MC252 Discoverer Enterprise DOR 1:20). Only four of the Type II Oils exhibited F_{max3} peaks and these ranged from 2.45 RU (Access Western Blend Dilbit DOR 0) to 174.93 RU (Heidrun DOR 1:20).

As with F_{max2}, the F_{max4} region sometimes contained double peaks. Unique spectral shapes for this region were also observed, especially in higher-density oils such as Access Western Blend Dilbit, Belridge Heavy, and Cold Lake Dilbit. FWHM ranged from 27 nm to 73 nm, for all oil types but one. The exception was Access Western Blend Dilbit, with FWHM of 77-110. Intensity at F_{max4} ranged from 33.53 RU (Arabian Light DOR 1:200) to 231.86 RU (MC252 Discoverer Enterprise DOR 1:20) in Type I Oils and from 4.93 RU (Access Western Blend Dilbit DOR 0) to 116.97 RU (Heidrun DOR 1:20) in Type II Oils.

Results of the concentration dilution series showed that the HORIBA AquaLog was consistently capable of detecting dispersed oil in artificial seawater in the three oil types tested (Alaska North Slope, IFO 120, and MC252 Discoverer Enterprise) at all four DORs down to at least 50 ppb. However, detecting dispersed oil below 100 ppb necessitated increasing the integration time to 10 sec. per scan in order to collect sufficient data, which resulted in a total analysis time of approximately 30 minutes for each sample. Since the HORIBA AquaLog scans from high to low wavelengths and much of the fluorescence signal from petroleum resides in the UV region,

ED_001324_00000298-00103

photobleaching of the sample as well as temperature effects certainly may have impacted these results.

ED_001324_00000298-00104

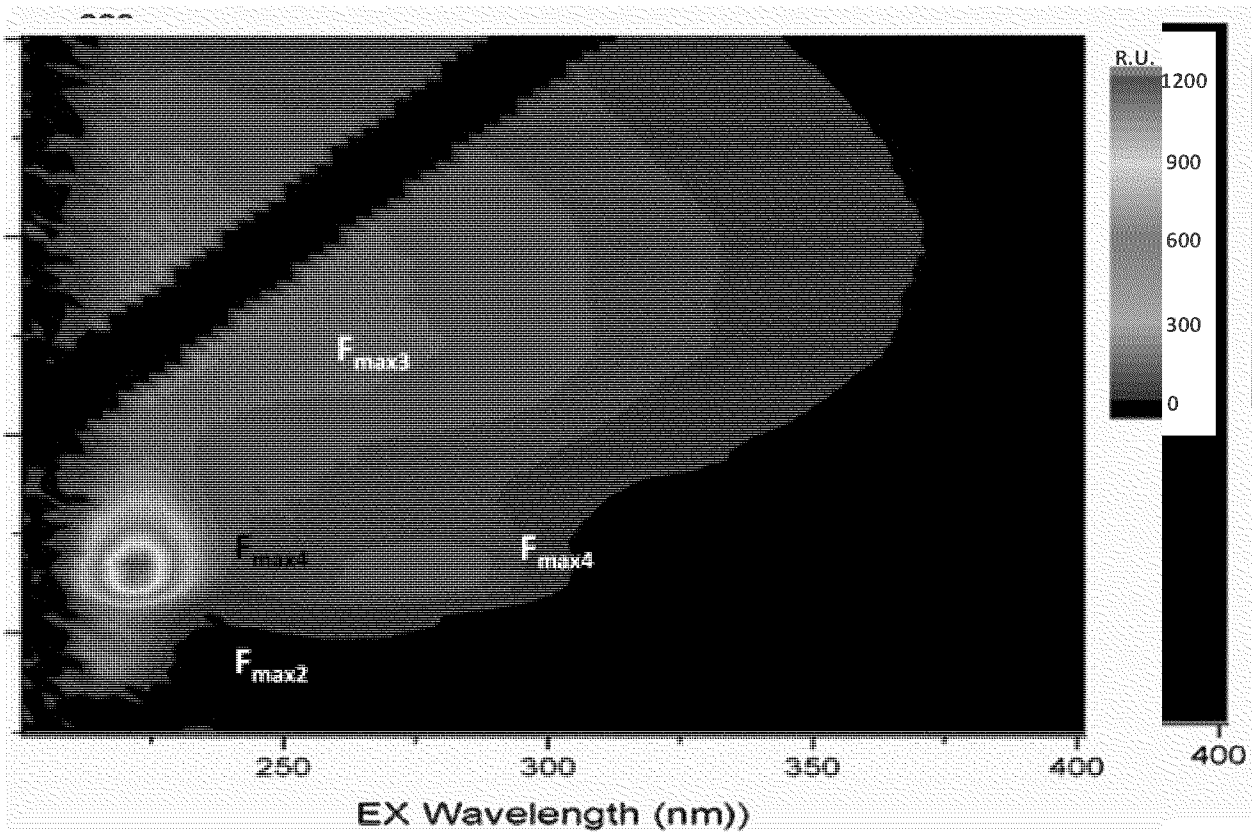

Figure 43. Alaska North Slope dispersed oil in artificial seawater at DOR 1:20 with locations of F_{max1}, F_{max2}, F_{max3} and F_{max4} indicated. Note that maximum fluorescence intensity at F_{max3} is mostly obscured by masking of second order Rayleigh scattering.

Table 9. Fluorescence and chemical characteristics of EEMs. For full table of fluorescence properties, refer to Supplemental Table A.

Type I Oils	DOR	F_{max}[1] (RU)	FIR	Alkanes (µg/L)	2-3 rings (µg/L)	4-5 rings (µg/L)	**Type II Oils**	DOR	F_{max}[1] (RU)	FIR	Alkanes (µg/L)	2-3 rings (µg/L)	4-5 rings (µg/L)
Alaska North Slope	0	697.07	21.59	375	160	8	Access Western Blend Dilbit	0	39.58	12.24	93	19	10
	1:200	715.01	37.73					1:200	46.52	14.20			
	1:100	839.60	6.87					1:100	49.84	8.97			
	1:20	1171.63	0.88	3019	566	65		1:20	60.19	1.15	258	57	38
Alaska North Slope (10% weathered)	0	812.97	22.75	545	201	14	Belridge Heavy	0	118.69	5.31	42	52	30
	1:200	831.70	21.86					1:200	161.75	5.65			
	1:100	828.06	8.98					1:100	140.96	4.93			
	1:20	1109.51	0.93	3312	598	74		1:20	147.09	3.51	44	84	52
Arabian	0	400.42	7.90	733	124	12	Cold Lake	0	120.61	20.72	155	94	23

ED_001324_00000298-00106

Light							Dilbit						
	1:200	357.62	12.06					1:200	120.65	18.01			
	1:100	426.82	2.68					1:100	125.85	13.11			
	1:20	701.75	0.39	6004	642	103		1:20	133.15	1.94	368	210	58
Brent	0	646.18	7.78	1068	183	12	Heidrun	0	902.69	4.61	382	392	43
	1:200	660.37	6.88					1:200	909.47	6.32			
	1:100	708.16	2.03					1:100	964.31	3.80			
	1:20	1098.42	0.69	5954	553	59		1:20	1098.90	0.80	684	620	82
Federated	0	574.35	3.72	1921	238	30	Hondo	0	283.04	21.99	412	84	3
	1:200	607.97	2.06					1:200	312.27	18.73			
	1:100	645.28	0.97					1:100	274.80	20.66			
	1:20	1223.17	0.37	6501	617	87		1:20	288.01	17.01	319	74	1
Gullfaks	0	937.00	5.86	762	373	26	IFO-40	0	1173.91	33.15	1324	560	172

ED_001324_00000298-00107

	1:200	934.42	5.64					1:200	1246.63	59.63			
	1:100	933.08	3.30					1:100	1338.56	42.94			
	1:20	1524.21	0.69	1943	749	61		1:20	1458.79	4.40	4354	1508	570

Hibernia	0	938.08	7.46	2289	335	24	IFO 120	0	3030.69	117.26	343	696	51
	1:200	951.49	3.22					1:200	2903.21	334.13			
	1:100	978.62	1.66					1:100	3090.23	88.73			
	1:20	1812.41	0.50	6095	635	59		1:20	2527.73	42.66	840	3097	122
MC252 (Discoverer Enterprise)	0	998.50	4.97	1578	350	30	IFO-180	0	1263.05	38.88	866	645	326
	1:200	1009.18	3.07					1:200	1394.42	42.40			
	1:100	1085.54	1.23					1:100	1703.55	5.76			

ED_001324_00000298-00108

	1:20	1998.60	0.39	3992	583	69		1:20	1532.99	12.28	2933	1986	1109
MC252 (generic)	0	857.35	4.81	1468	267	21	IFO-300	0	720.55	65.84	446	295	192
	1:200	877.78	3.11					1:200	443.51	48.50			
	1:100	964.02	0.97					1:100	465.91	75.70			
	1:20	1795.13	0.41	5093	624	68		1:20	661.50	43.02	366	248	162
MESA	0	757.84	20.04	1388	268	24	Lago	0	352.22	12.53	1289	146	18
	1:200	806.76	12.21					1:200	398.40	11.30			
	1:100	745.17	6.33					1:100	367.75	9.10			
	1:20	1107.09	1.09	4088	524	62		1:20	453.10	0.93	4221	346	52
Sea Rose	0	1145.29	10.65	1583	320	19	Santa Clara	0	157.30	23.17	209	28	0
	1:200	1223.98	7.40					1:200	147.55	27.03			
	1:10	1236.6						1:10					

ED_001324_00000298-00109

	0	3						0					
	1:20	1973.55	0.72	5903	721	70		1:20	169.39	7.39	1196	81	3
Terra Nova	0	665.50	6.81	1038	186	11	Scotian Shelf Condensate	0	946.52	43.40	447	127	0
	1:200	719.72	3.96					1:200	1408.59	51.61			
	1:100	821.24	1.47					1:100	1487.16	49.14			
	1:20	1380.34	0.40	5608	540	50		1:20	1337.98	51.42	1057	220	0
							Vasconia	0	844.93	34.44	2550	415	59
								1:200	828.37	53.23			
								1:100	835.62	29.32			
								1:20	935.79	3.64	4402	631	96

ED_001324_00000298-00110

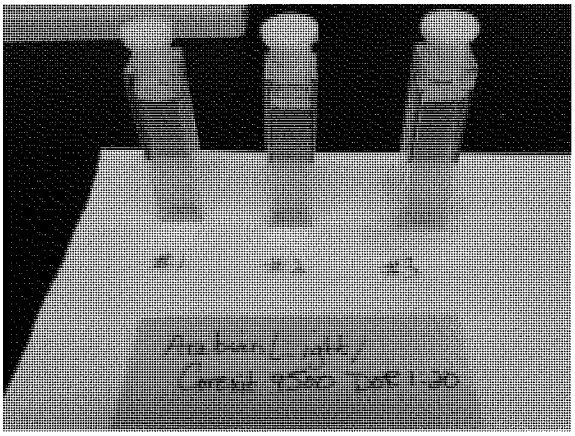

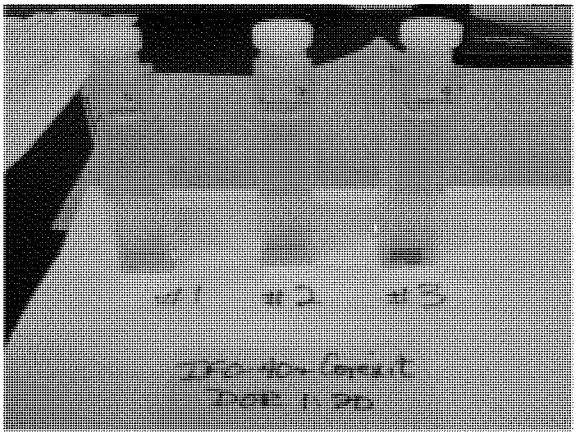

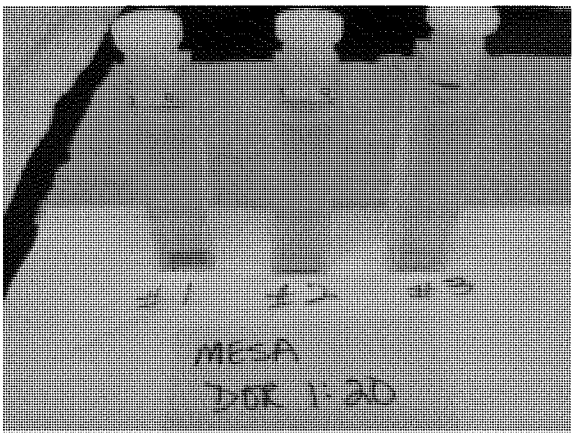
MESA
DATE 1-20

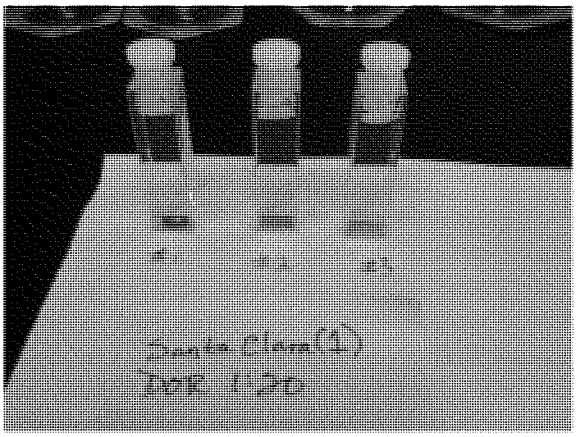

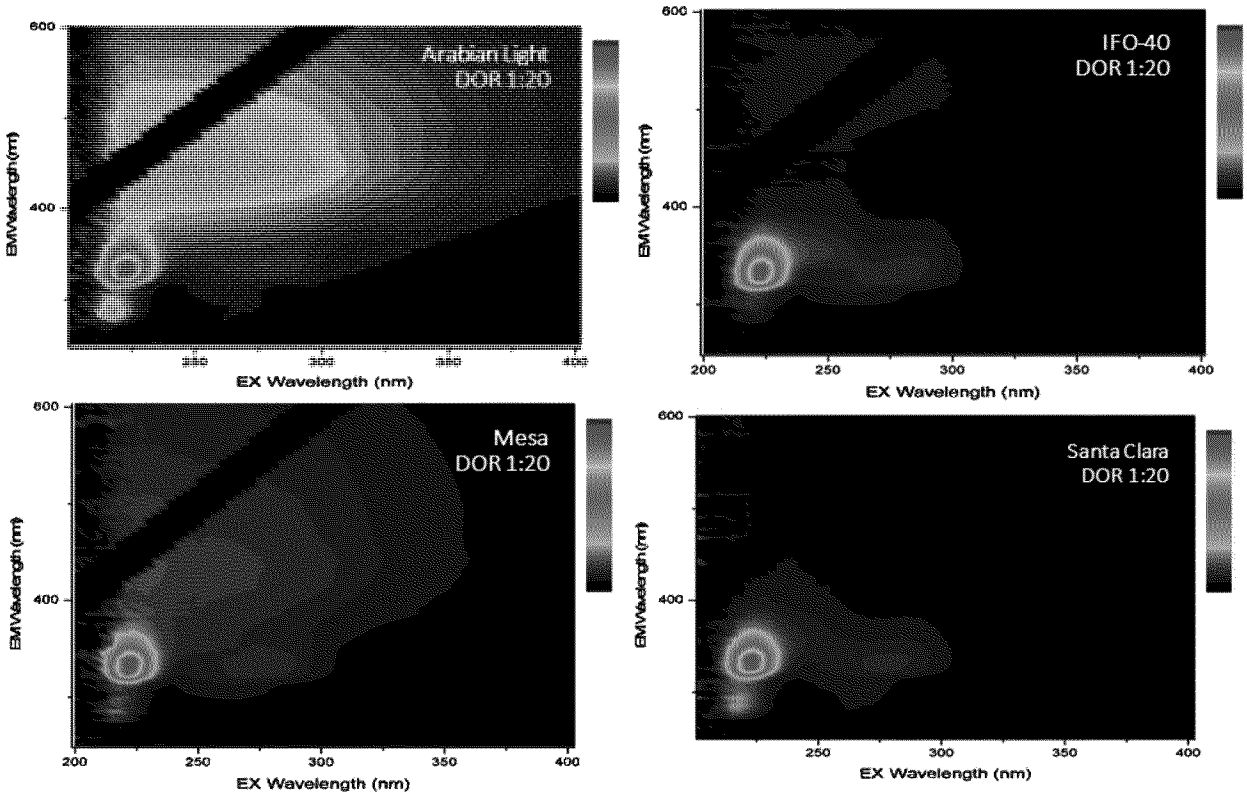

Figure 44. Photographs of pre-analysis samples and corresponding example EEMs of Type I (left) and II (right) oils for DOR = 1:20. Arabian Light is a light oil (API gravity > 31.1°) Mesa is a medium oil (API gravity 22.3 – 31.1°). IFO 40 and Santa Clara are heavy oil (API gravity < 22.3°).

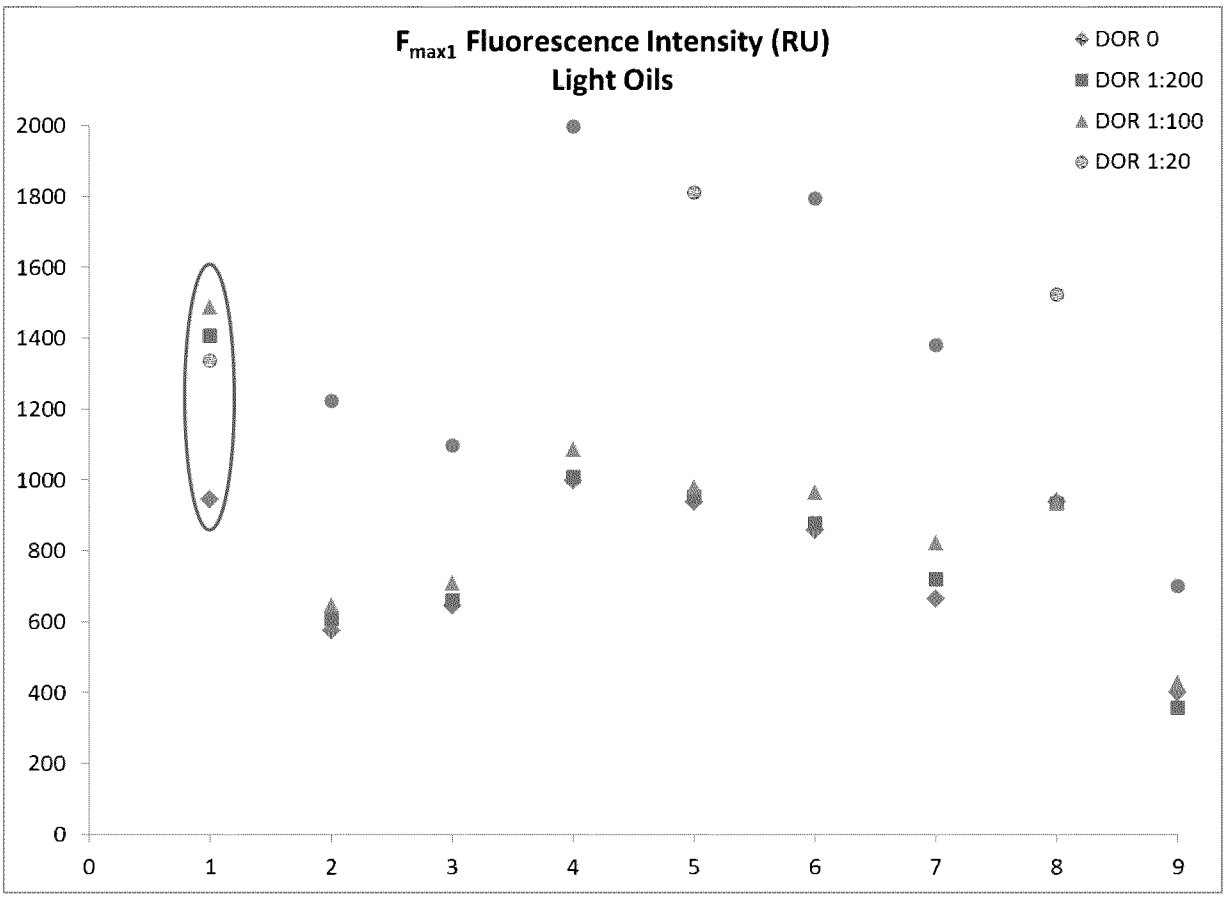

Figure 45. F_{max1} fluorescence for Light Oils (API gravity > 31°), in order of increasing density: 1. Scotian Shelf Condensate, 2. Federated, 3. Brent, 4. MC252—Discoverer Enterprise, 5. Hibernia, 6. MC252—generic, 7. Terra Nova, 8. Gullfaks, 9. Arabian Light. Note discrepancy in Scotian Shelf Condensate fluorescence pattern (circled) from that of all other Light Oils. It's particularly unusual that fluorescence intensity at highest DOR is lower than that at DORs 1:200 and 1:100.

ED_001324_00000298-00113

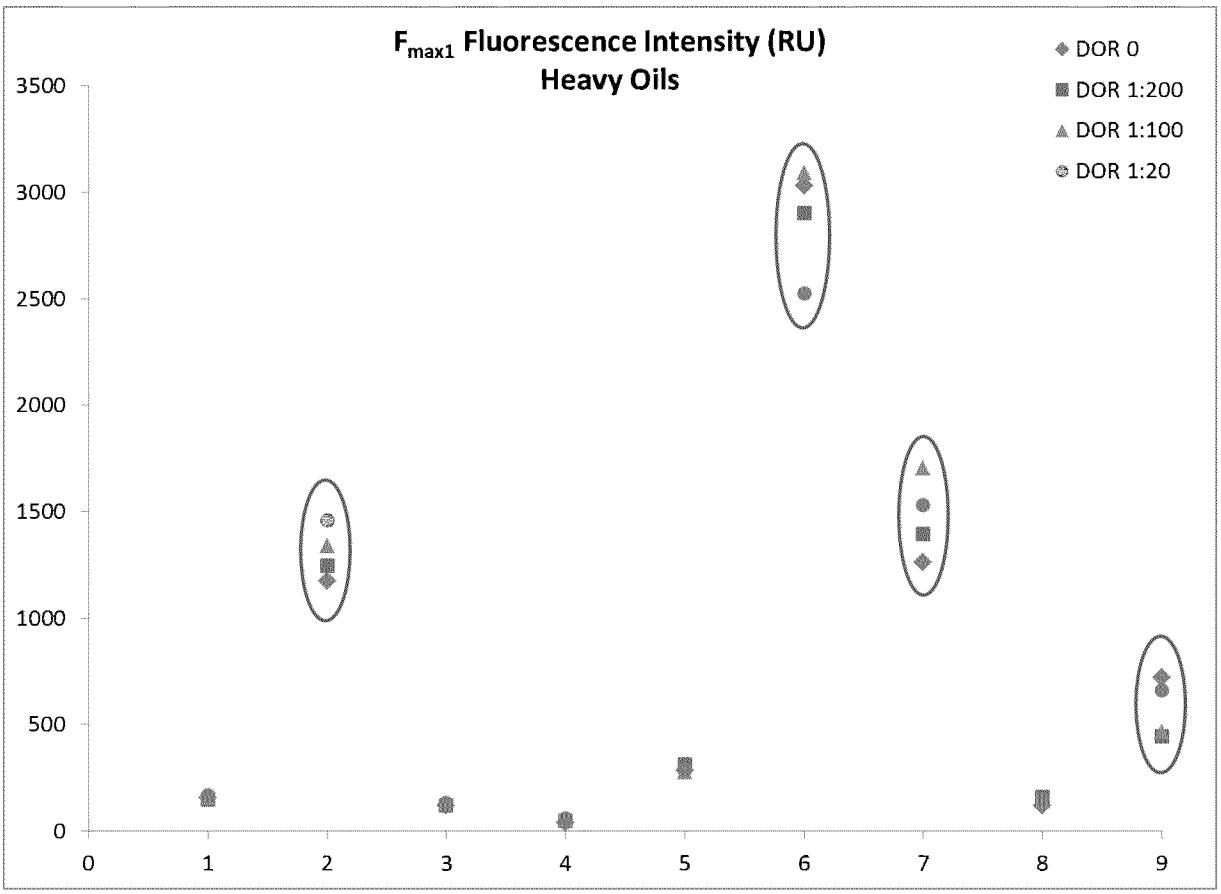

Figure 46. F_{max1} fluorescence for Heavy Oils (API gravity < 22.3°), in order of increasing density: 1. Santa Clara, 2. IFO 40, 3. Cold Lake Dilbit, 4. Access Western Blend Dilbit, 5. Hondo, 6. IFO 120, 7. IFO 180, 8. Belridge Heavy, 9. IFO 300. Note discrepancy in Intermediate Fuel Oils (circled) from that of all other Heavy Oils.

B.3.2 Fluorescence as a Function of Chemistry

Samples of dispersed oil in artificial seawater (DOR 0 and DOR 1:20 for each oil type), extracted into methylene chloride were analyzed via GC-MS. Total 2-3 ring PAHs, total 4-5 ring PAHs, and total alkanes (see Table 10) were each plotted against F_{max1}, F_{max2}, F_{max3}, and F_{max4}. Results showed best correlation between total 2-3 ring PAHs and fluorescence intensity. Both F_{max1} and F_{max4} had the best overall fit, with less well-correlated results for total 2-3 ring PAHs with F_{max2} and F_{max3}, perhaps due to the confounding presence of double peaks and sub-peaks in the latter

two. A linear relationship was found between concentration of total 2-3 ring PAHs and fluorescence intensity (F_{max1} and F_{max4}) at DOR 0, while a logarithmic relationship best modeled the fit at DOR 1:20 (Figures 47-48).

Table 10. Individual hydrocarbon compounds included in chemical analysis results reported as Total Alkanes, Total 2-3 ring PAHs and Total 4-5 ring PAHs

Total Alkanes:	**Total 2-3 ring PAHs:**	**Total 4-5 ring PAHs:**
n-decane	naphthalene	pyrene
undecane	methylnaphthalene	methylpyrene
dodecane	dimethylnaphthalene	dimethylpyrene
pentadecane	trimethylnaphthalene	trimethylpyrene
hexadecane	tetramethylnaphthalene	tetramethylpyrene
heptadecane	acenaphthene	naphthobenzothiophene
nonadecane	acenaphthylene	methylnaphthobenzothiophene
eicosane	fluorene	dimethylNBenzothiophene
tricosane	methylfluorene	trimethylNbenzothiophene
tetracosane	dimethylfluorene	tetramethylNbenzothiophene
n-nonacosane	trimethylfluorene	benz[a]anthracene
tricontane	dibenzothiophene	chrysene
n-heneicontane	methyldibenzothiophene	methylchrysene
dotriacontane	dimethyldibenzothiophene	dimethylchrysene
n-pentatriacontane	trimethyldibenzothiophene	trimethylchrysene
17α 7ime 21β 7imehopane	tetramethyldibenzothiophene	tetramethylchrysene
17β 7trametα 7trahopane	phenanthrene	benzo[b]fluoranthene
	anthracene	benzo[k]fluoranthene
	methylphenanthrene	benzo[e]pyrene
	dimethylphenanthrene	benzo[a]pyrene
	trimethylphenanthrene	perylene
	tetramethylphenanthrene	indeno[1,2,3-cd]pyrene
		dibenz[a,h]anthracene

ED_001324_00000298-00115

		benzo[ghi]perylene

Investigation of the chemistry – fluorescence intensity relationship at DOR 0 resulted in highest correlation between F_{max1} and 2-ring PAHs (R^2 = 0.82) and between F_{max3} and both 3 and 4-ring PAHs (R^2 = 0.87 and 0.81, respectively) across all oil types. It is important to note, however, that only 12 of the 25 oil types exhibited F_{max3} fluorescence at DOR 0.[2] These correlations support the fact that larger, more complex PAHs fluoresce at longer emission wavelengths. In examining the chemistry – fluorescence intensity relationships at DOR 1:20, all correlations were best described by a logarithmic rather than a linear curve. The best overall correlation shifted to that between F_{max3} and 2-ring PAHs (R^2 = 0.73), and the relationship between F_{max1} and 2-ring PAHs was only loosely correlated with R^2 = 0.54. Correlation between F_{max3} and 3-ring PAHs dropped to R^2 = 0.67, while there was only poor correlation between F_{max3} and 4-ring PAHs at R^2 = 0.29.

The effect of full dispersion (DOR 1:20) on dissolved hydrocarbons can be investigated by taking the ratio of total alkanes + PAHs at DOR 1:20 to total alkanes + PAHs at DOR 0—the Chemical Dispersibility Ratio (CDR). These ranged from a low of 0.8 for two heavy oils—Hondo and IFO 300—up to a maximum of 7.8 for Arabian Light. Although heavy oils tended to have lower CDRs and light oils tended to have higher ratios, oil density was not correlated with chemical dispersion. For example, the heavy oil Santa Clara (API Gravity 22.1°) had the third highest CDR (5.4), while Scotian Shelf Condensate, by far the the lightest oil (API Gravity 46.6°), had a CDR of only 2.2. Investigation of the effect of dispersion on fluorescence intensity can be similarly investigated by taking the ratio of F_{max1} fluorescence intensity at DOR 1:20 to that at DOR 0, resulting in the Fluorescence Dispersibility Ratio (FDR). This also shows a general increasing trend with increasing API Gravity, but only moderate linear correlation (R^2 = 0.55). Finally, considering the relationship between CDR and FDR, we also see a general, overall increasing trend, but poor linear correlation (R2 = 0.17).

[2] Oil types exhibiting Fmax3 fluorescence at DOR 0: Access Western Blend Dilbit, Alaska North Slope (both fresh and 10% weathered), Arabian Light, Brent, Federated, Gullfaks, Heidrun, Hibernia, MC252 (both Discoverer Enterprise and generic), and Terra Nova.

ED_001324_00000298-00116

All four Intermediate Fuel Oils (IFO 40, IFO 120, IFO 180, and IFO 300) as well as Scotian Shelf Condensate (SSC), showed fluorescence and chemistry anomalies that tended to skew overall results. . With respect to SSC, all other light oils (API Gravity < 22.3°) exhibited increasing fluorescence intensity with increasing DOR, culminating in a marked increase at DOR 1:20; however, SSC actually showed a significant decrease in fluorescence intensity at DOR 1:20, dropping to below the level exhibited at DOR 1:200 (Figure 45). Additionally, SSC was the only light oil which exhibited no F_{max3} fluorescence at any DOR. Chemically, SSC was also unusual, containing a very high proportion of 2-ring to 3-ring PAHs—52.2 for DOR 0 and 58.6 for DOR 1:20. With the exception of Santa Clara, with a 2-ring to 3-ring ratio of 31.9 at DOR 0, all other oil types had a ratio of 10 or less at both DOR 0 and DOR 1:20. SSC also contained no 4-ring or 5-ring PAHs, unlike all other oils with the exception of DOR 0 Santa Clara. All four of the Intermediate Fuel Oils fell into the heavy oil group (API Gravity > 31°), in which all other oils showed little to no increase in fluorescence intensity with increasing DOR as well as maximum F_{max1} intensity of just 60-288 RU. The IFOs, however, showed far greater F_{max1} intensity across the board (721-3031 RU) along with clear separation with increasing DOR. Like Scotian Shelf Condensate, IFO 120, IFO 180, and IFO 300 also exhibited a drop in F_{max1} intensity at DOR 1:20; in fact, IFO 120 F_{max1} at DOR 1:20 was actually 17% lower than at DOR 0. These same three IFOs also had the highest overall concentration of PAHs , and all four IFOs were the only oils to contain any anthracene. For all oil types, total alkanes as a function of fluorescence intensity was found to be only loosely correlated, as total concentration increased overall in relation to fluorescence intensity with no clear relationship.

ED_001324_00000298-00117

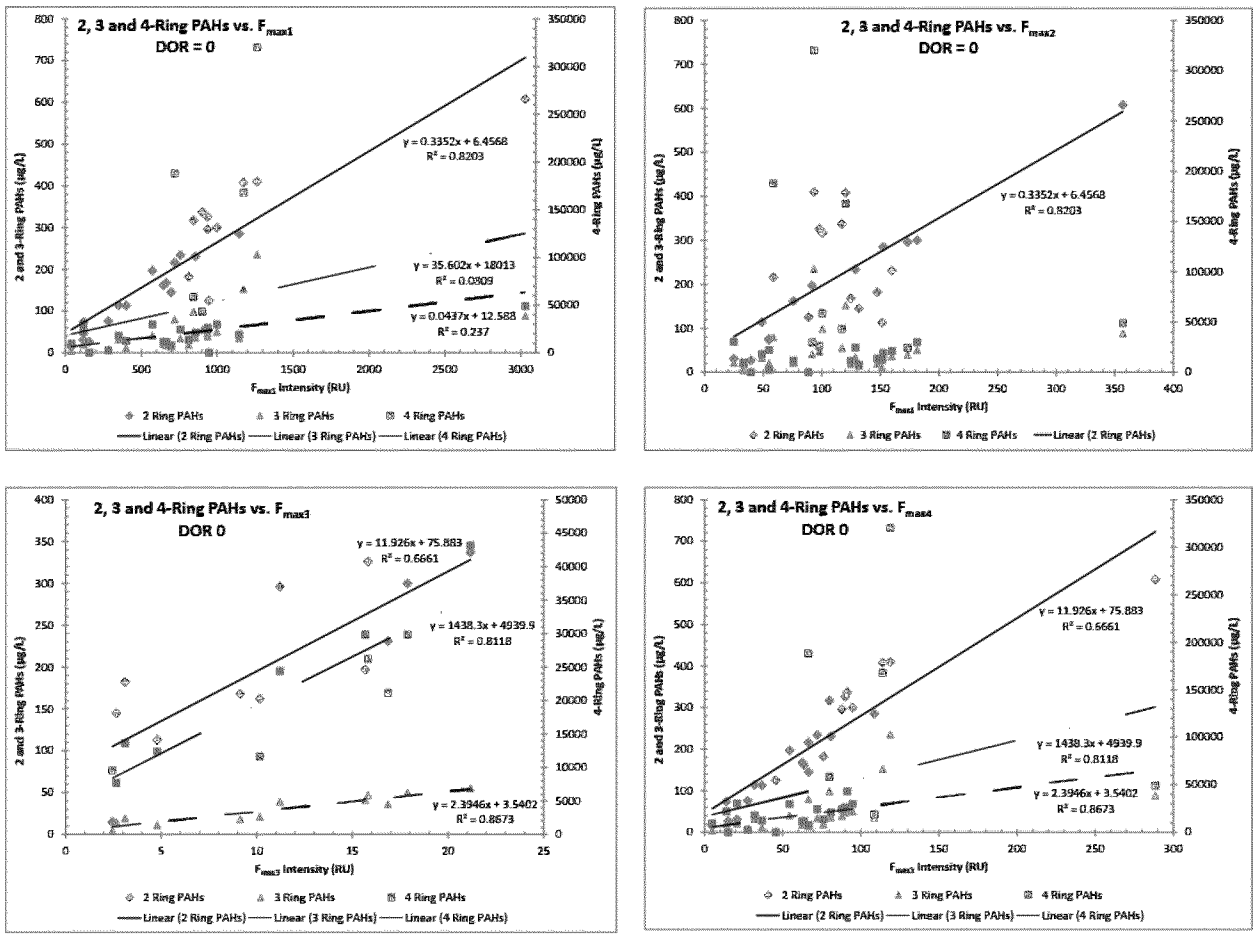

Figure 47. For all oil types at DOR 0, total concentration of 2, 3 and 4-ring PAHs (µg/L) against fluorescence intensity (RU) at F_{max1} (top left), against F_{max2} (top right), against F_{max3} (bottom left), and against F_{max4} (bottom right). Strong linear correlation between 2-ring PAHs and F_{max1} fluorescence, but little to no correlation between 3-ring or 4-ring PAHs and F_{max1} fluorescence intensity. Strong linear correlation between 3-ring PAHs and fluorescence intensity at F_{max3} as well as between 4-ring PAHs and fluorescence intensity at F_{max3}; moderately strong correlation between 2-ring PAHs and fluorescence intensity at F_{max3}.

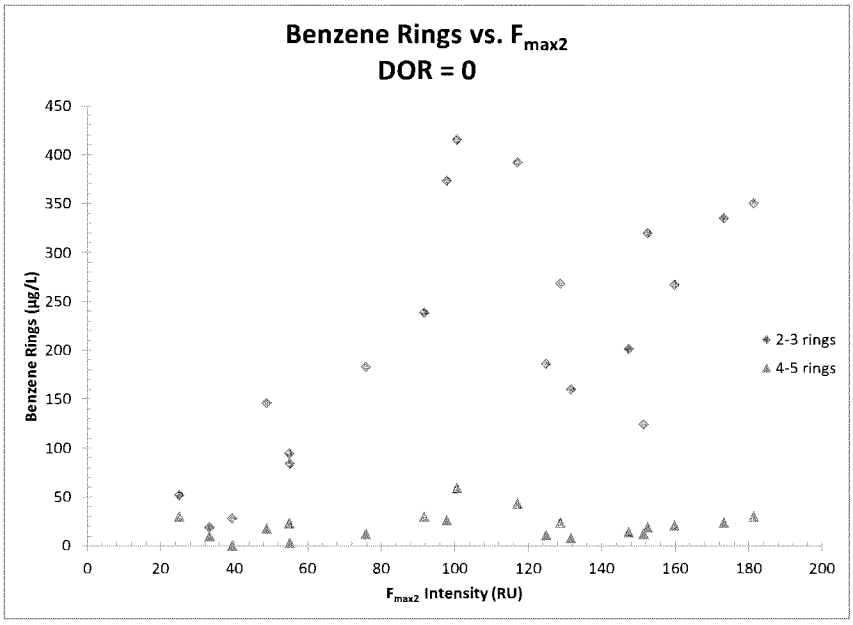
Benzene Rings vs. F_{max2}
DOR = 0
Benzene Rings (µg/L)
450
400
350
300
250
200
150
100
50
0
0
20
40
60
80
100
120
140
160
180
200
F_{max2} Intensity (RU)
2-3 rings
4-5 rings

ED_001324_00000298-00120

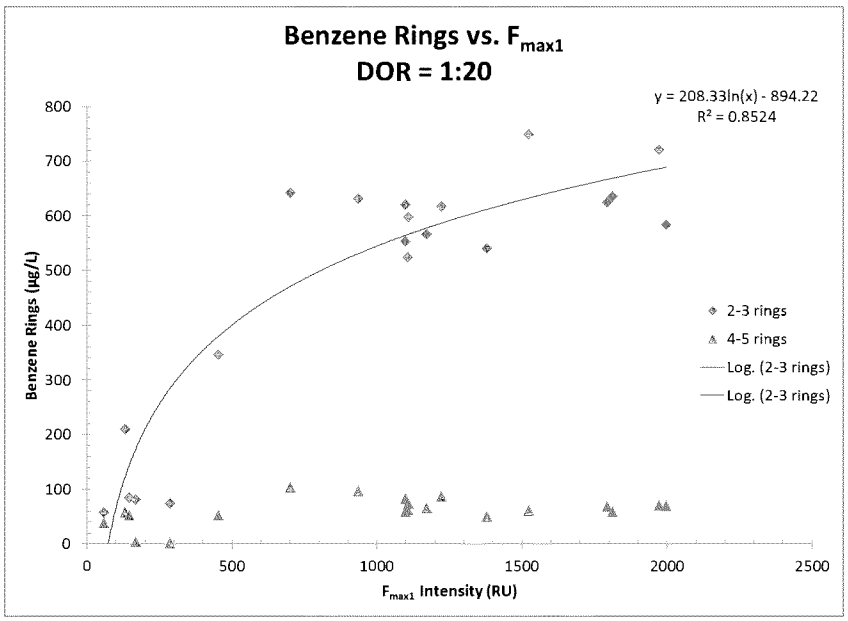
Benzene Rings vs. F_{max1}
DOR = 1:20
y = 208.33ln(x) - 894.22
R^2 = 0.8524
Benzene Rings (µg/L)
F_{max1} Intensity (RU)
2-3 rings
4-5 rings
Log. (2-3 rings)
Log. (2-3 rings)

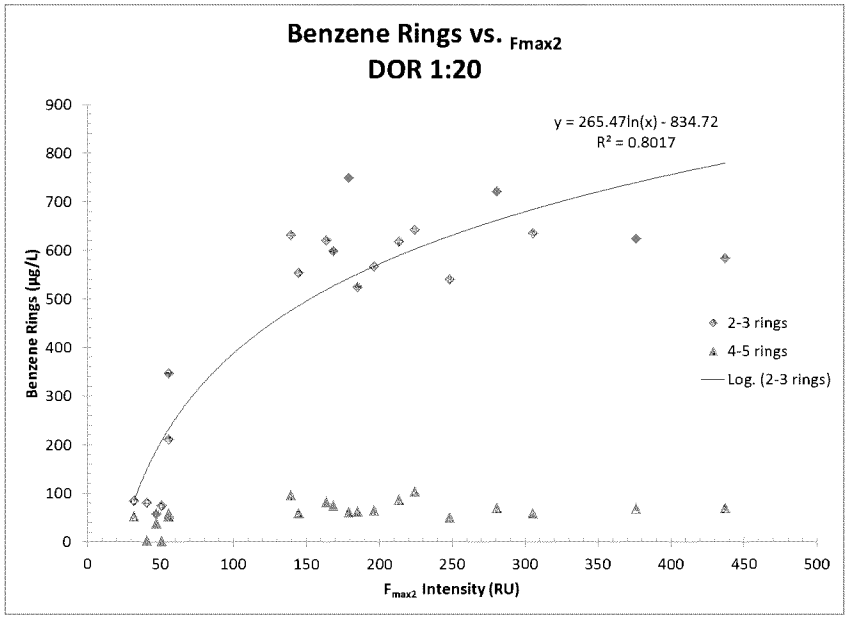
Benzene Rings vs. Fmax2
DOR 1:20
y = 265.47ln(x) - 834.72
R^2 = 0.8017
Benzene Rings (µg/L)
F_{max2} Intensity (RU)
2-3 rings
4-5 rings
Log. (2-3 rings)

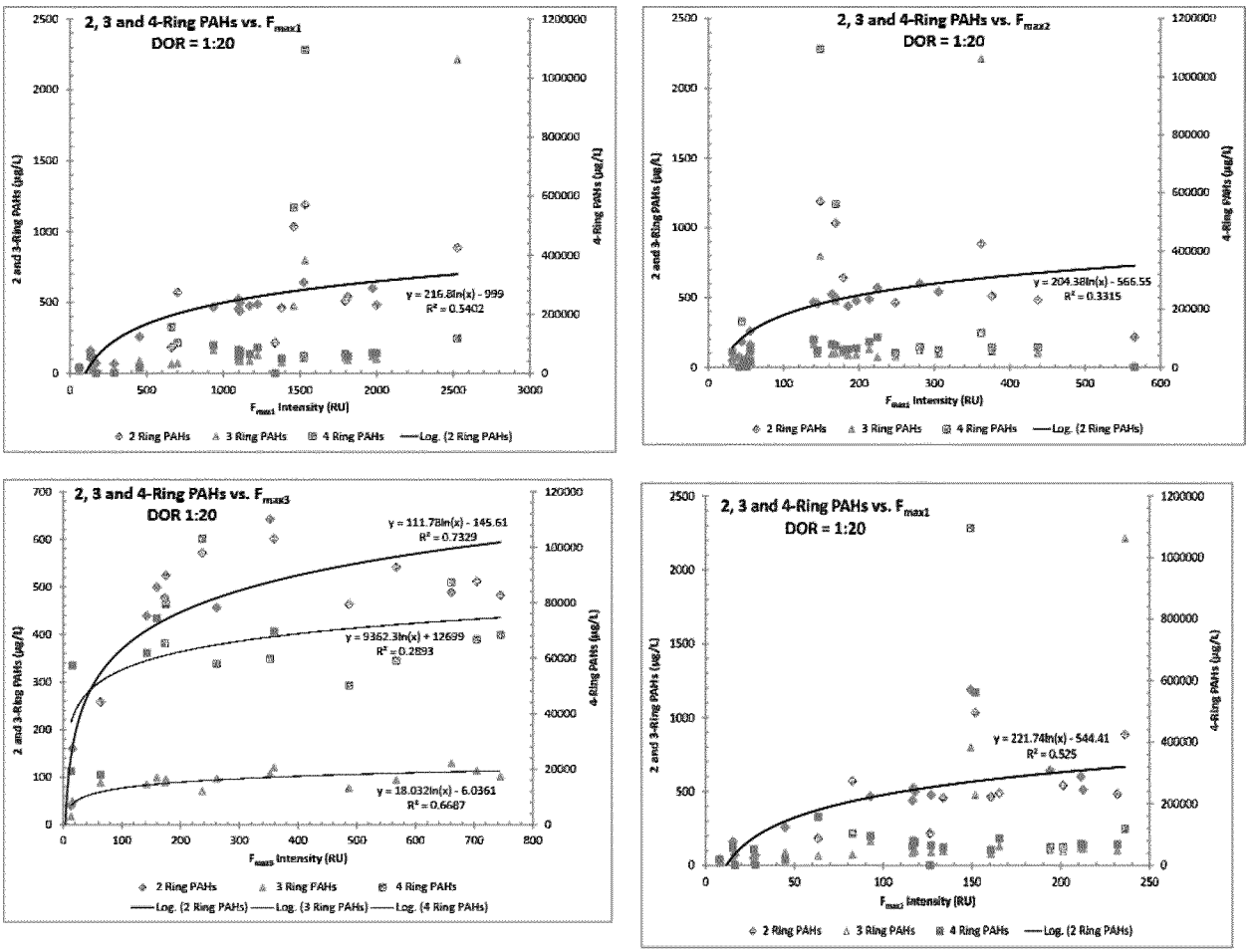

Figure 48. For all oil types at DOR 1:20, total concentration of 2, 3 and 4-ring PAHs (µg/L) against fluorescence intensity (RU) at F_{max1} (top left), against F_{max2} (top right), against F_{max3} (bottom left), and against F_{max4} (bottom right). A moderate logarithmic correlation is exhibited between 2-ring PAHs and fluorescence intensity (RU) at Fmax1, Fmax2, and Fmax4. A strong logarithmic correlation is shown between 2-ring and 3-ring PAHs and fluorescence intensity (RU) at F_{max3}, and only a weak logarithmic correlation between 4-ring PAHs and fluorescence at F_{max3}.

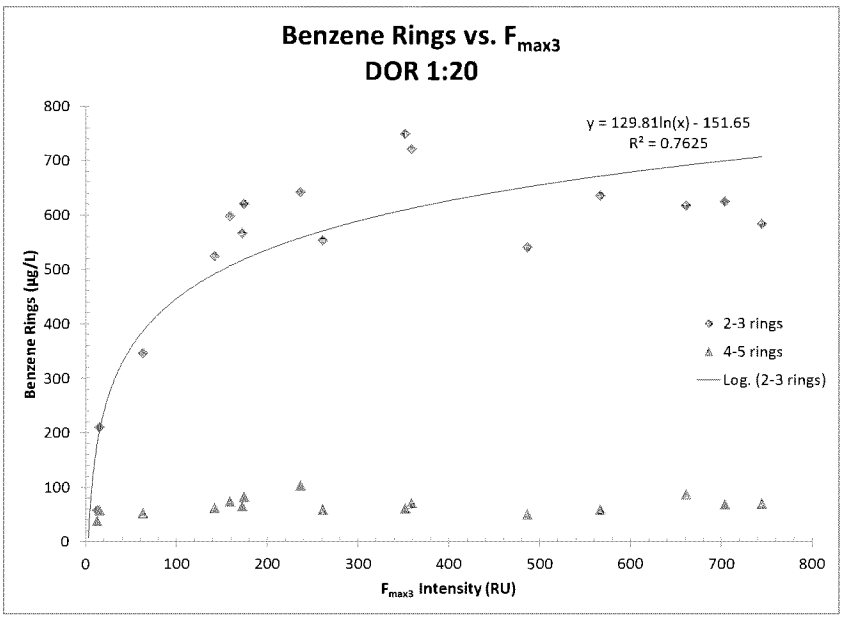
Benzene Rings vs. F_{max3}
DOR 1:20
y = 129.81ln(x) - 151.65
R^2 = 0.7625
Benzene Rings (µg/L)
F_{max3} Intensity (RU)
2-3 rings
4-5 rings
Log. (2-3 rings)
0
100
200
300
400
500
600
700
800

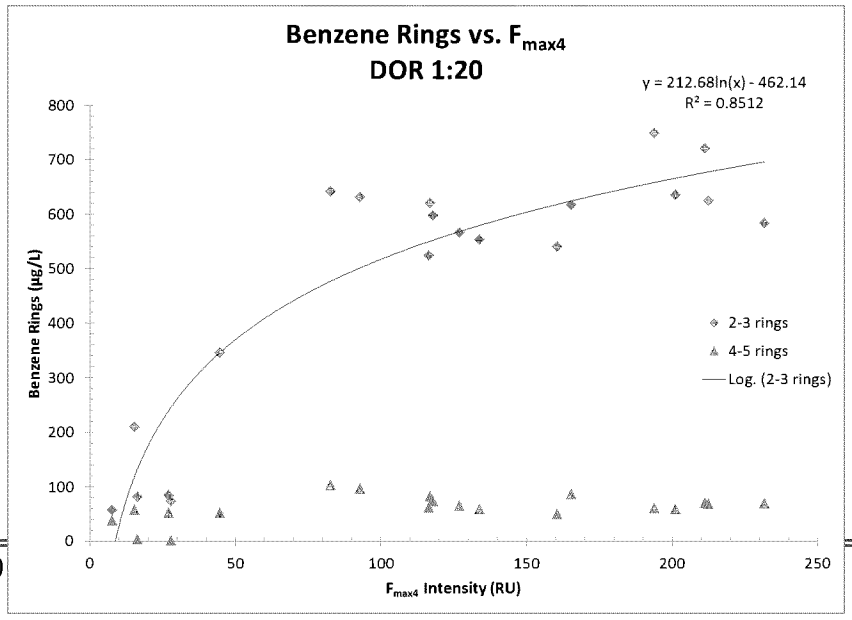
Benzene Rings vs. F_{max4}
DOR 1:20
y = 212.68ln(x) - 462.14
R^2 = 0.8512
Benzene Rings (µg/L)
F_{max4} Intensity (RU)
2-3 rings
4-5 rings
Log. (2-3 rings)
0
50
100
150
200
250
300
400
500
600
700
800

B.3.3 Flume Tank and Baffled Flask EEM Comparison

In addition to the EEMs generated from the BFT of 25 oil types, EEMS were also generated from the discrete sample collection during the flume tank experiments using South Louisiana Crude oil (SLC) in Task A of this project report. Samples for EEM analysis were collected and immediately analyzed on the same Horiba Aqualog at DFO using identical analysis protocols and data processing. A comparison of SLC MC252 EEMs for varying DOR from the BFT (left) and the flume tank (right) experiments are illustrated in Figure 51. Note that that the contour coloring for the peaks is identical between experiments, but the baseline color varied, where black was used for the BFT EEMs and blue used for tank EEMs, but the appearance of the blue color this is not to be confused with the presence of higher fluorescence in regions away from the peak fluorescence. Fluorescence Intensity Ratios (FIR) were calculated for the tank EEMs and found to be between 7.1 and 9.1 for DOR = 0, 1.3 and 4.3 for DOR = 1:100 and 0.6 and 0.8 for DOR = 1:20. This is follows the findings of Bugden et al., 2008 where a decrease in FIR is observed with the addition of dispersant. It is also consistent with the BFT EEMs which show a 4.9 for DOR = 0 and 0.4 for DOR = 1:20 (Supplemental Table A). These results indicate that FIR can be an indicator of dispersion effectiveness for SLC oil.

ED_001324_00000298-00124

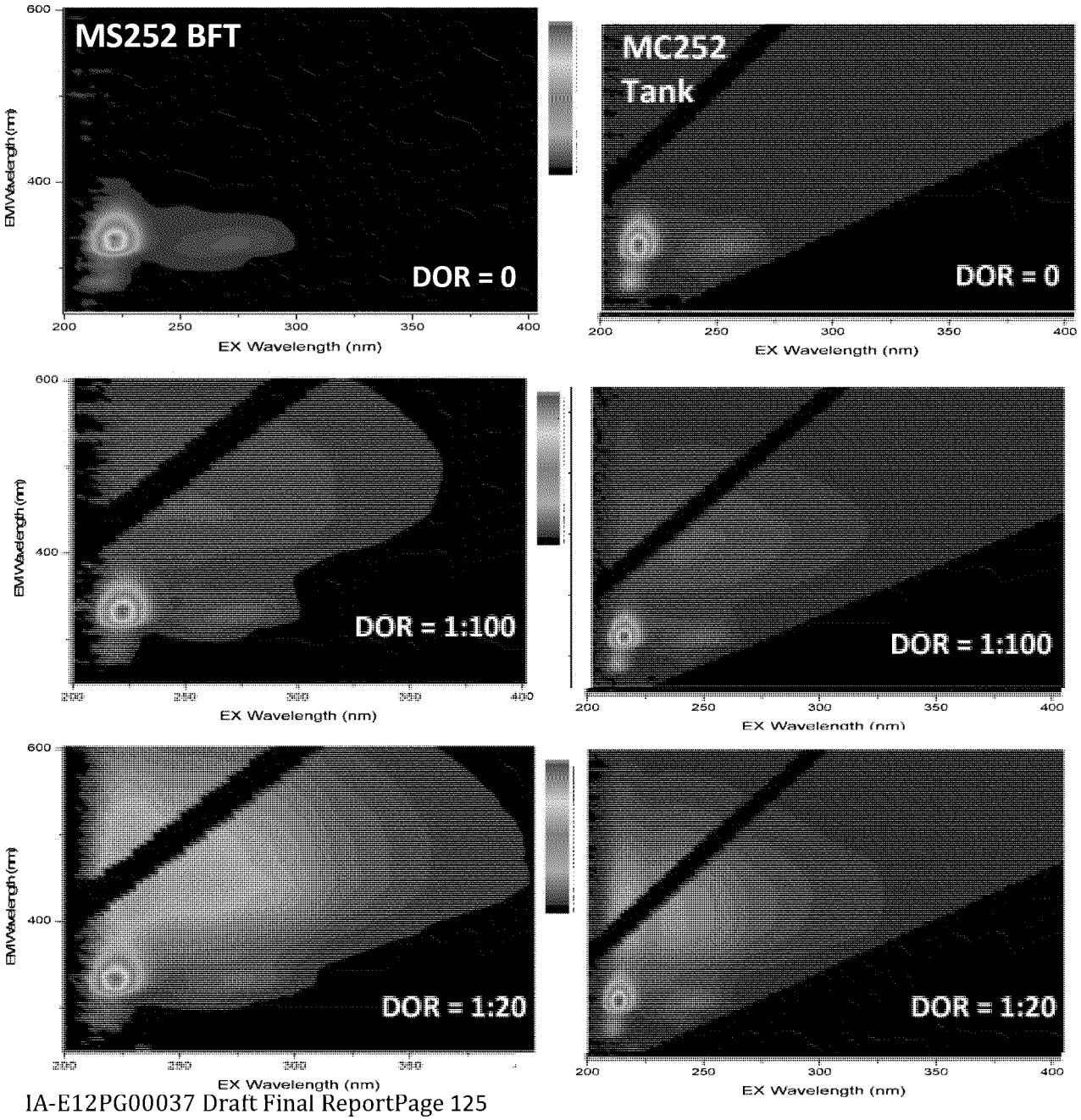
MS252 BFT
DOR = 0
MC252
Tank
DOR = 0
DOR = 1:100
DOR = 1:100
DOR = 1:20
DOR = 1:20
EM Wavelength (nm)
EX Wavelength (nm)
600
400
200
250
300
350
400

Figure 49. South Louisiana Crude MC252 EEMS from BFT (left panels) and tank experiments (right Panels) for DOR = 0, 1:100 and 1:20.

B.3.4 PARAFAC Modeling

DOR = 0

PARAFAC modelling was performed using PLS Toolbox software (Eigenvector, Inc.) and MATLAB (The MathWorks, Inc.) on all 25 oil types from the baffled flask experiments for DOR = 0 (Table 10). A five-factor model was fit to the dataset without application of any pre-processing options, then with application of constraints for non-negativity, EEM filtering (12nm First Order Rayleigh and 24nm Second Order Rayleigh), and normalization methods 1-Norm (area = 1) and inf-Norm (maximum = 1). The initial 5-factor model without any constraints explained 97.623% of the data, core consistency was high (92%), and residuals were low and randomly distributed; however, split half analysis showed 0% similarity between the splits and overall model. Further, Mode 2 (emission) factors 4 and 5 contained significant negative regions, factor 4 appeared to be modelling only noise, and factor 5 contained two significant and equal peaks, all indications of poor fit. Application of the non-negativity constraint and re-running the 5-factor model resulted in a slight reduction in percentage of data explained by the model (96.544%), and a slight reduction in core consistency (88%). Split half analysis resulted in only 0.8% agreement between splits and the overall model, while factor 4 now contained the two significant and equal peaks seen previously in factor 5, and factor 5 now appeared to be modelling only noise. Addition of EEM filtering as well as non-negativity to a third PARAFAC analysis resulted in a very slight increase to 96.717% of the data explained by the model and an increase in core consistency to 91%, but split half analysis dropped to 0% agreement between splits and the overall model; aforementioned problems with Mode 2 factors 4 and 5 remained as well. Application of 1-Norm (area = 1) normalization constraint along with non-negativity and EEM

ED_001324_00000298-00126

filtering and re-running the 5-factor model provided nearly identical results, with 96.876% of data explained, 87% core consistency, and the same problems with Mode 2 factors 4 and 5; however, split half analysis improved slightly to 4.6%. Changing the normalization method to inf-Norm (maximum = 1) method and re-running the 5-factor model resulted in 95.55% of data explained by the model and 81% core consistency, but problems with Mode 2 factors 4 and 5 remained. Split half analysis again resulted in 0% similarity between splits and the overall model. In order to find the optimal number of factors to fit the data, 4-factor models were run with non-negativity, EEM filtering, and each type of normalization applied separately, followed by 3-factor models taken through the same process. The 3-factor model with application of non-negativity, EEM filtering and normalization proved best overall. Both methods of normalization gave results within 1-3% on all measures of goodness of model fit; however, the model using the inf-Norm (maximum = 1) normalization method was selected as the more conservative method, preserving differences in spectral shape among oil types. The 3-factor model represented 95% of the data with 93% core consistency, good variation per component, and low, randomly distributed residuals. The split half analysis showed 75.2% similarity between splits and the overall model.

ED_001324_00000298-00127

Table 10. Oil Types used for PARAFAC Analysis

Type I	Type II
ANS	Access Western Blend Dilbit
ANS 10% weathered	Belridge Heavy
Arabian Light	Cold Lake Dilbit
Brent	Heidrun
Federated	Hondo
Gullfaks	IFO-40
Hibernia	IFO-180
MC252 – Discoverer Enterprise	Lago
MC252 – generic	Santa Clara
MESA	Vasconia
Sea Rose	
Terra Nova	

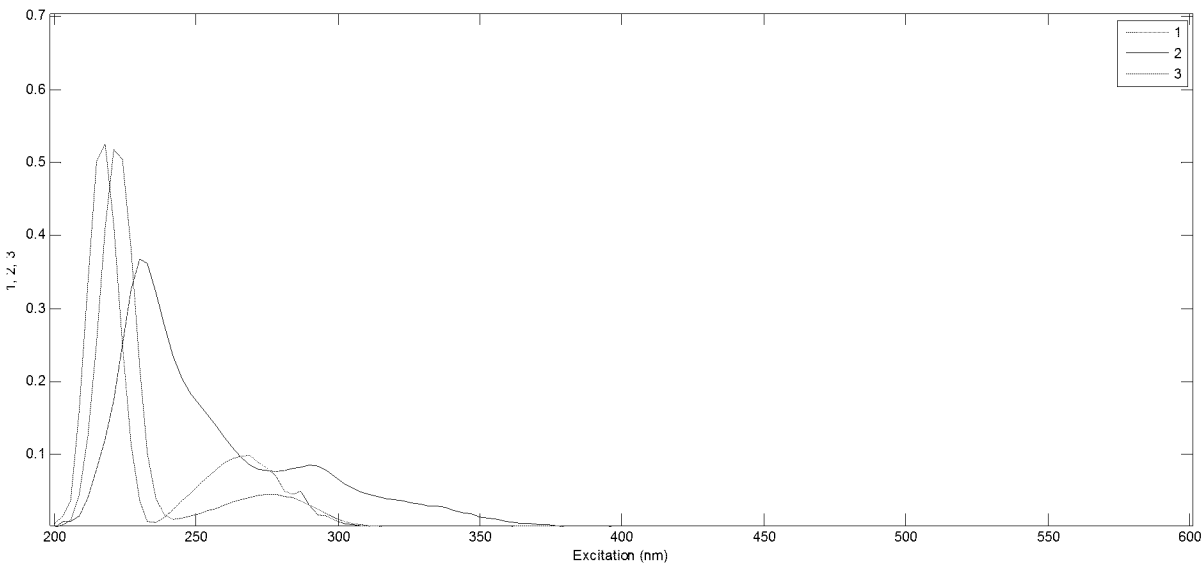

Figure 50. Graph of loadings for Mode 3 - excitation for all 22 oils at DOR = 0 resulting from 3-factor PARAFAC model.

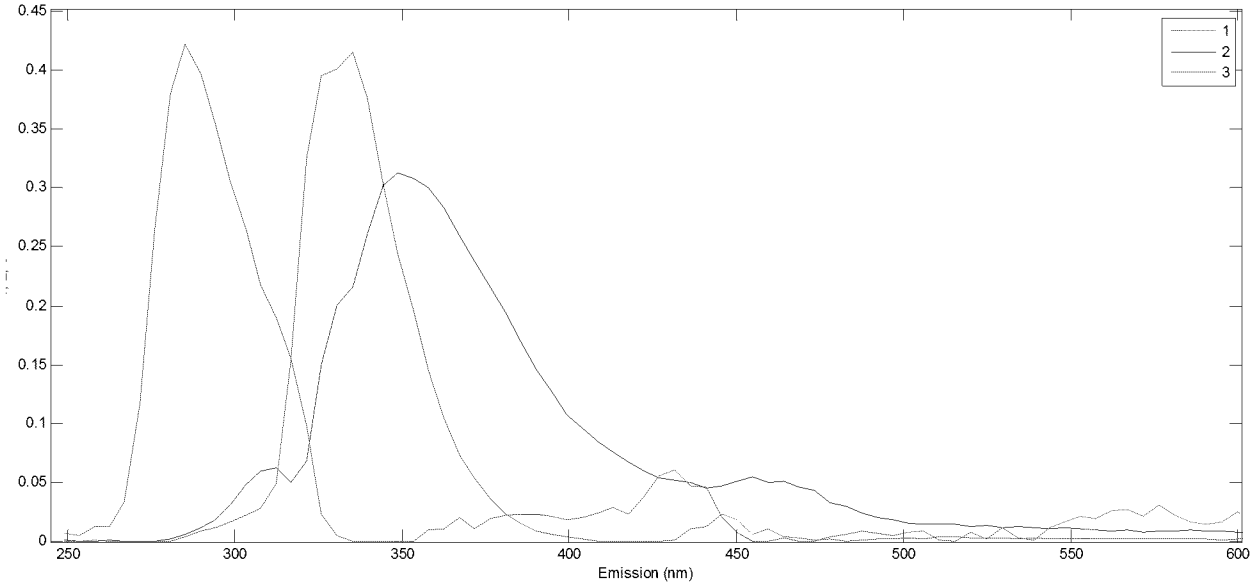

Figure 51. Graph of loadings for Mode 2 - emission for all 22 oils at DOR = 0 resulting from 3-factor PARAFAC model.

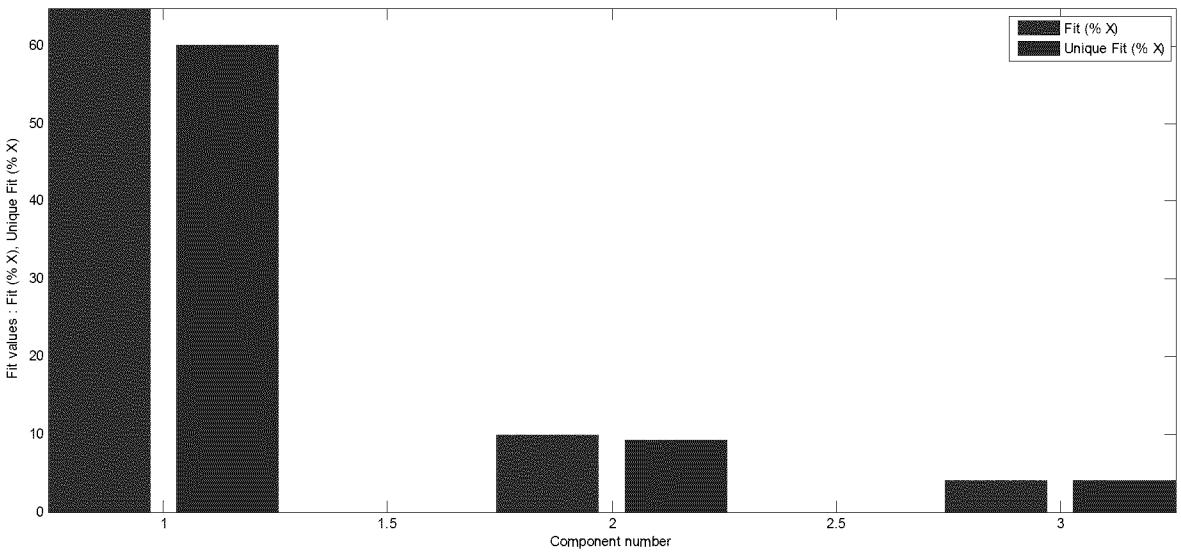

Figure 52. Fit (% X) vs. unique fit (% X) for 3-factor PARAFAC model run on all 22 oil types at DOR = 0.

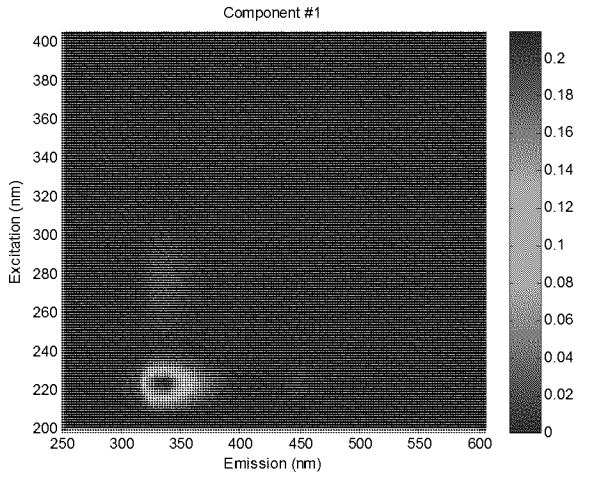

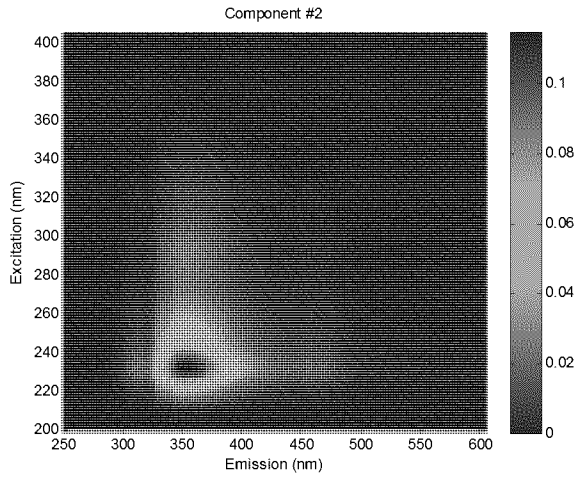

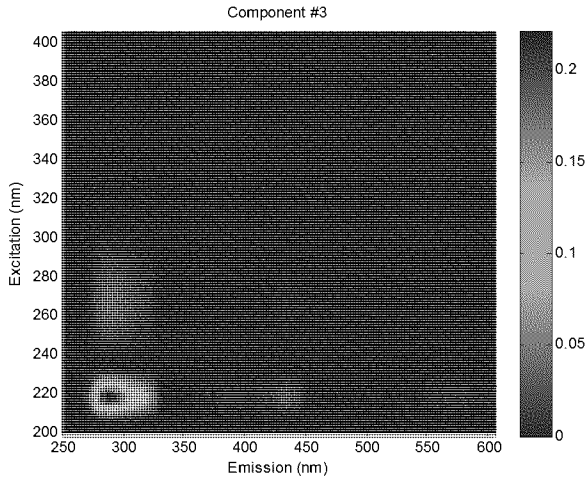

Figure 53. EEM views of factor 1 with Fmax at Ex/Em = 224/340nm (top left), factor 2 with Fmax at Ex/Em = 233/353nm (top right), and factor 3 with Fmax at ex/em = 218/290 (bottom).

DOR = 1:100

Sample files from the DOR = 1:100 baffled flask experiments (flask #1) were uploaded, and a five-factor PARAFAC model was performed using the previously determined optimal combination of pre-processing constraints—non-negativity, EEM filtering (12 and 24 nm for First and Second Order Rayleigh, respectively), and inf-Norm normalization. Core consistency was high (93%) and the model explained 96.7% of the data; however, variation per component

was very low for factor 5, and the loadings for Mode 2 (emission) showed factor 5 appeared to be modelling noise. Split half analysis showed similarity between splits and overall model of only 5.8%. Re-running the model with six factors resulted in a slight improvement to 96.9% of the data explained and good core consistency of 89%; however, both factors 5 and 6 appeared to be modelling noise and had low variation per component. Split half analysis failed, with 0% similarity between splits and the overall model. A four-factor model resulted in 96.6% of the data explained by the model and core consistency of 96%. Variation per component was good for all four factors, and loadings for Modes 2 and 3 contained only appropriately-shaped emission and excitation curves, respectively. Residuals were low and randomly distributed. Split half analysis was excellent, with similarity between splits and overall model of 83.5%.

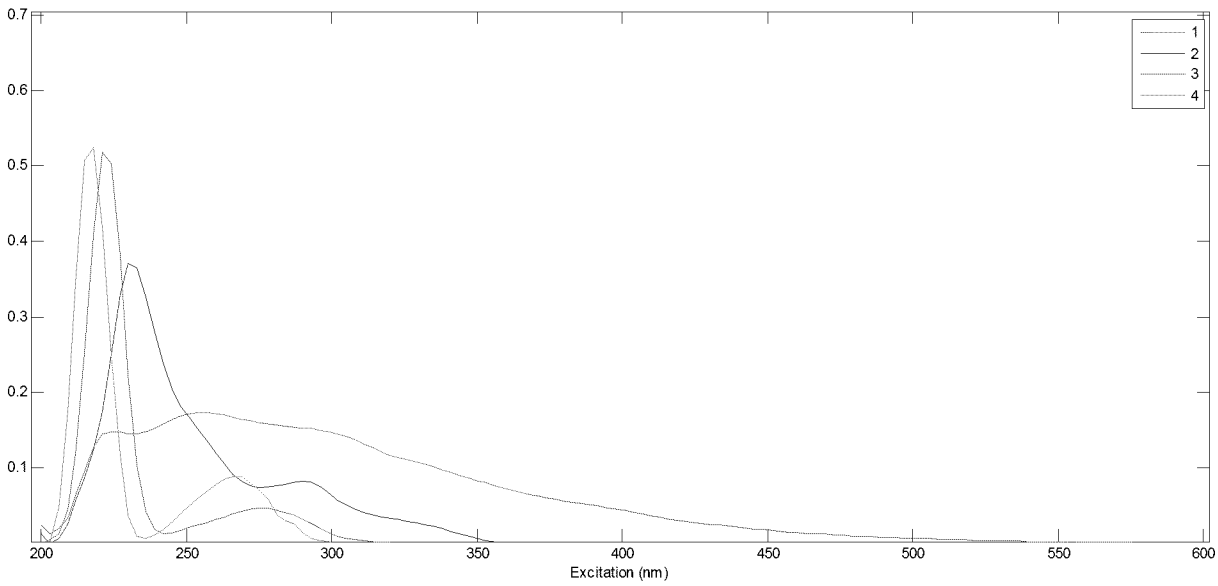

Figure 54. Graph of loadings for Mode 3 - excitation for all 22 oils at DOR = 1:100 resulting from 4-factor PARAFAC model.

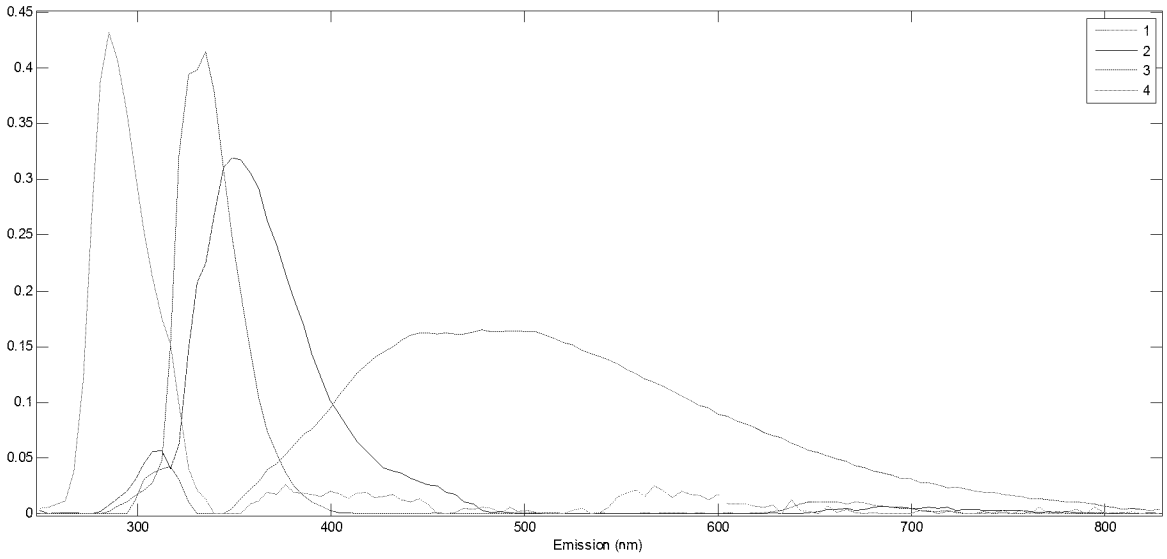

Figure 55. Graph of loadings for Mode 2 - emission for all 22 oils at DOR = 1:100 resulting from 4-factor PARAFAC model.

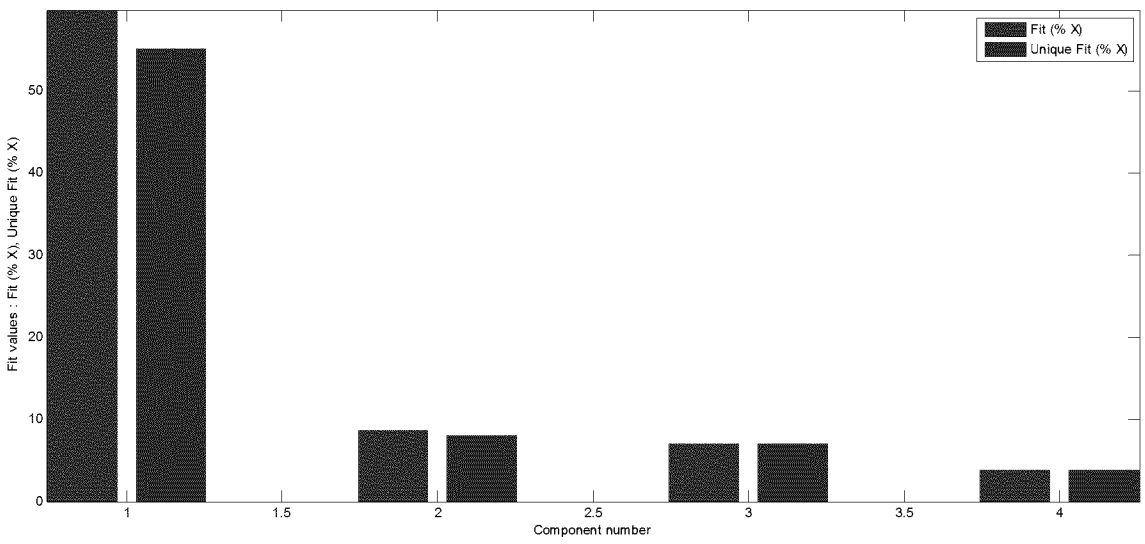

Figure 56. Fit (% X) vs. unique fit (% X) for 4-factor PARAFAC model run on all 22 oil types at DOR = 1:100.

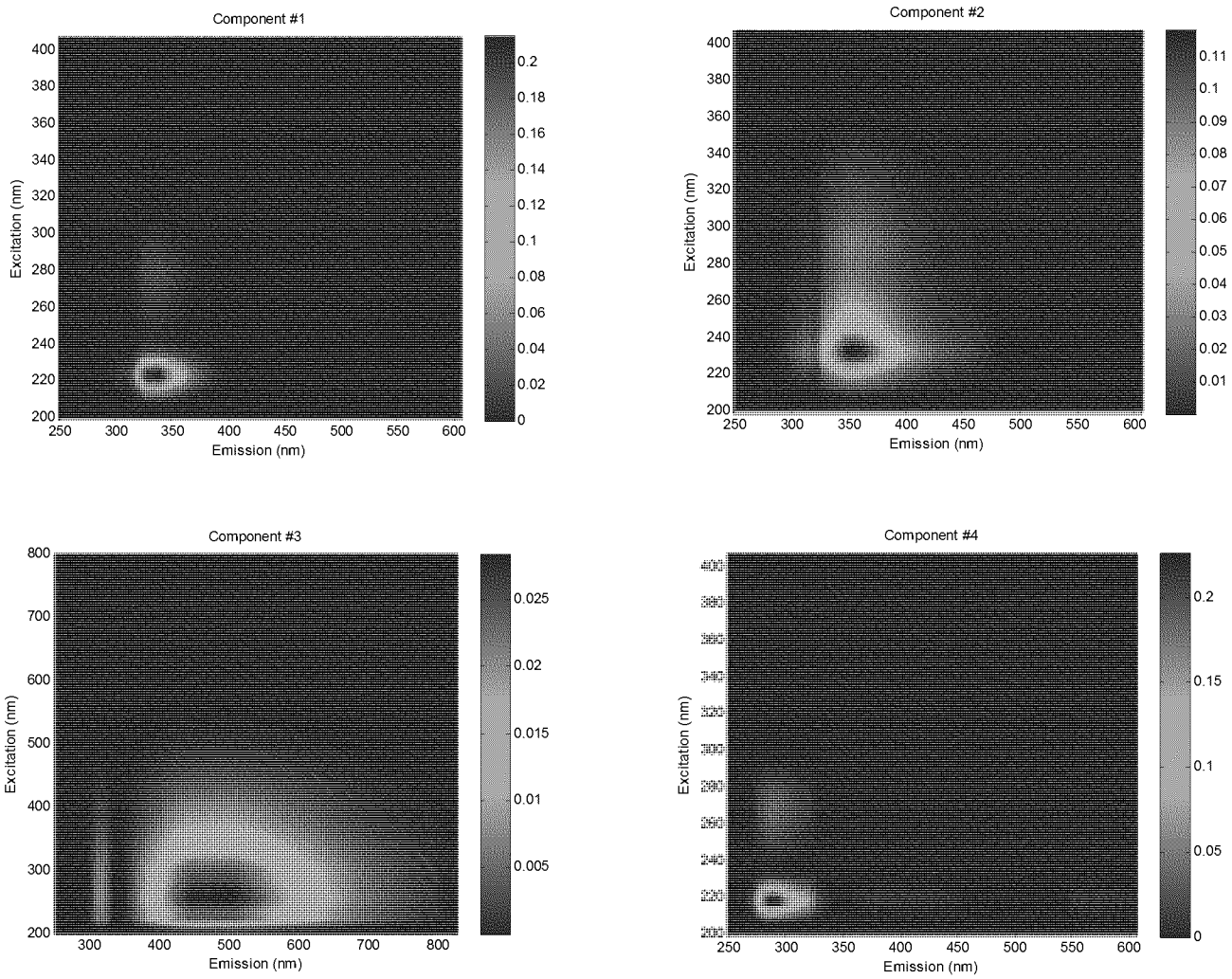

Figure 57. EEM view of factor 1 with Fmax at Ex/Em = 221/335nm (top left), factor 2 with Fmax at Ex/Em = 230/349 nm (top right), factor 3 with Fmax at Ex/Em = 254/445-506 nm (bottom left), and factor 4 with Fmax at Ex/Em = 218/285 nm (bottom right).

DOR = 1:20

Sample files from flask #1 of the DOR = 1:20 baffled flask experiments were loaded, and based

on results obtained in previous analyses, a five-factor model with non-negativity, EEM filtering (12 and 24nm First and Second Order Rayleigh, respectively), and inf-Norm normalization constraints was performed. Results showed 95.8% of the data was explained by the model with 87% core consistency and good variation per component; however, the relative percent difference between fit and unique fit for factor 1 was 55%. Residuals were low and randomly distributed and loadings for Mode 2 and 3 appeared to be valid emission and excitation curves. Unfortunately, split half analysis was 0% between splits and the overall model. In order to obtain better results, a six-factor model was performed; however, split half analysis was still 0%. Stepping through individual sample residuals showed an anomalously high negative peak in Arabian Light sample, so the data were reloaded with the sample file from baffled flask #2 for that oil type and a new five-factor model run. Results obtained showed 96.0% of the data explained by the model with 86% core consistency; however, split half analysis was still just 0.1%. Repeating the six-factor model with the new sample set resulted in 96.1% of data explained by the model and 87% core consistency; split half analysis revealed a 5.5% similarity between splits and the overall model. Running a seven-factor model resulted in an error message of <0% core consistency due to two or more components fitting the same feature. A four-factor model explained 95.6% of the model with 94% core consistency. Split half analysis resulted in 40.3% similarity between splits and overall model; however, visual inspection of the splits showed one peak significantly shifted and transformed from the model curve in split 2. These results indicate that it may be impossible to represent all 22 types of oil with one PARAFAC model. Visual inspection of the loadings for Mode 2 from the six-factor model suggest that there may be two underlying types, each with three factors, since there are three pairs of similar curves.

ED_001324_00000298-00134

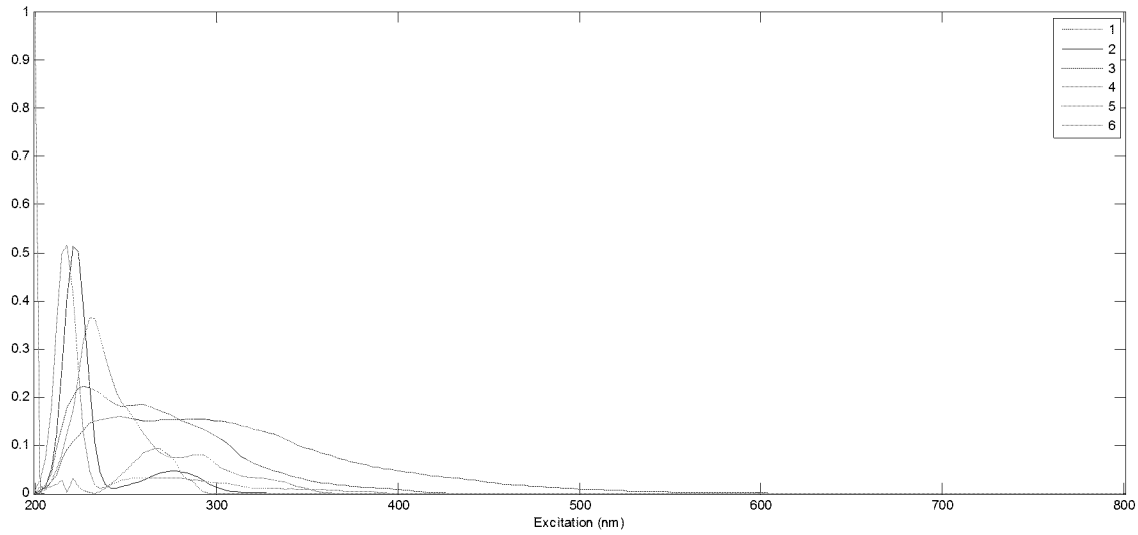

Figure 58. Mode 3 loadings - Excitation for six-factor PARAFAC model on all 22 oil types at DOR 1:20.

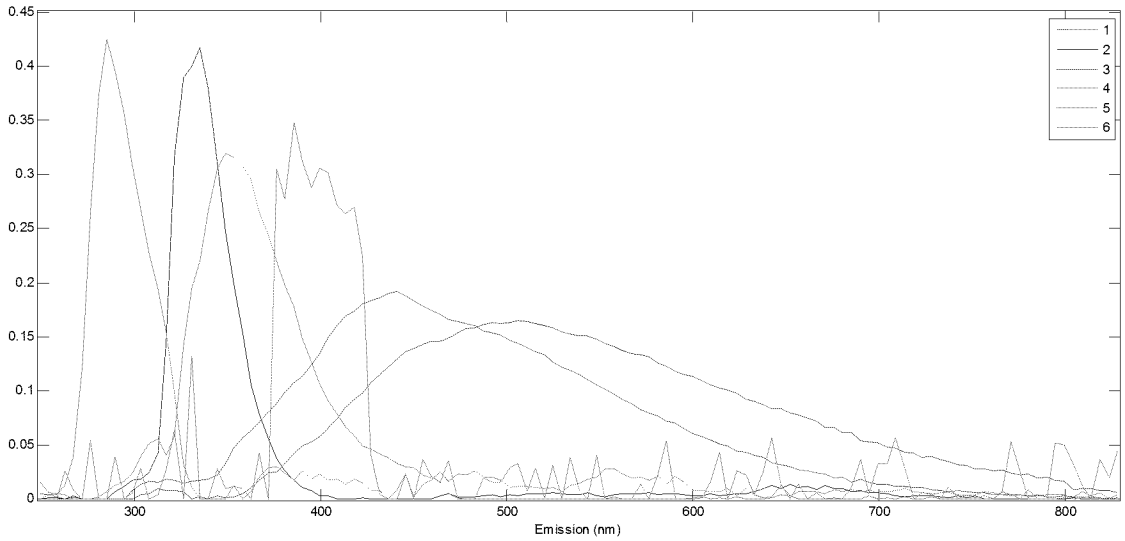

Figure 59. Mode 2 loadings - Emission for six-factor PARAFAC model of all 22 oil types at DOR = 1:20.

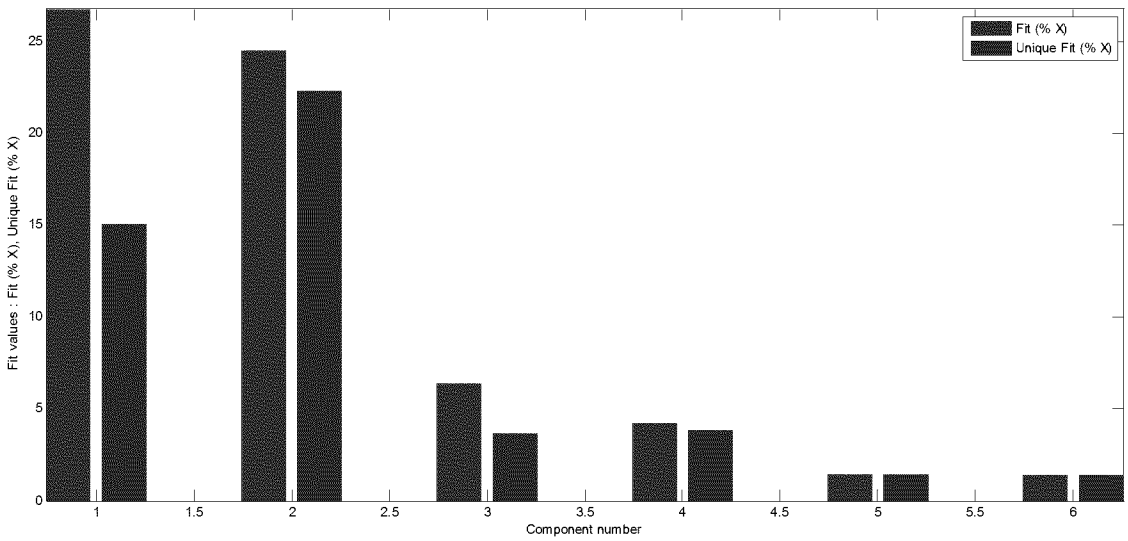

Figure 60. Fit (% X) vs. unique fit (% X) for six-factor PARAFAC model on all 22 oil types at DOR = 1:20.

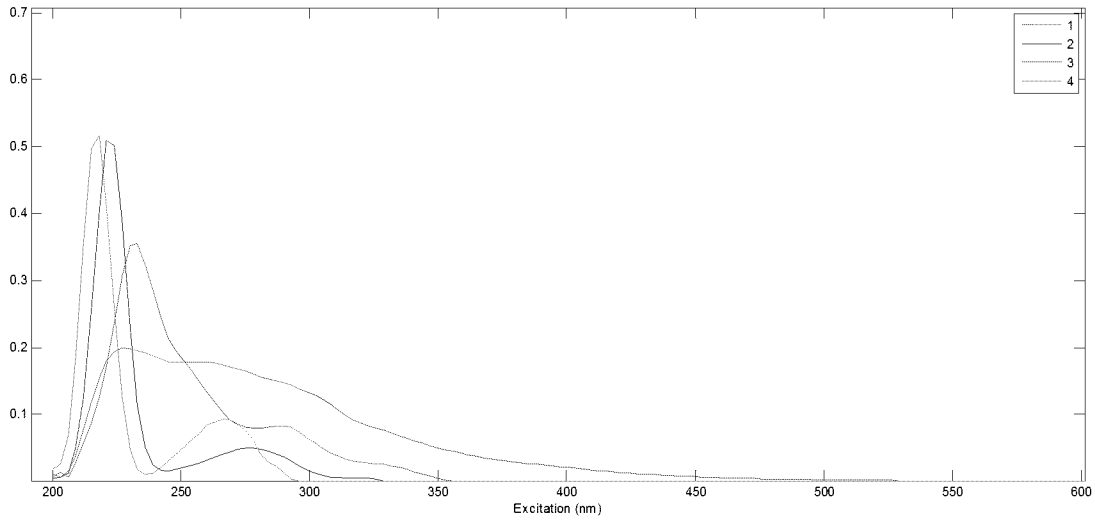

Figure 61. Mode 3 loadings - Excitation for five-factor PARAFAC model of all 22 oil types at DOR = 1:20.

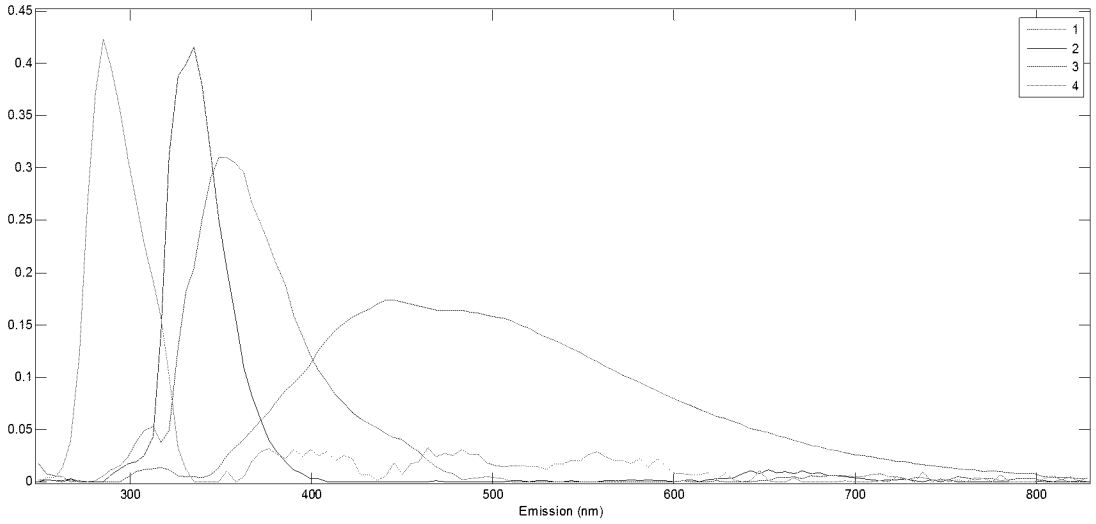

Figure 62. Mode 2 loadings - Emission for five-factor PARAFAC model of all 22 oil types at DOR = 1:20.

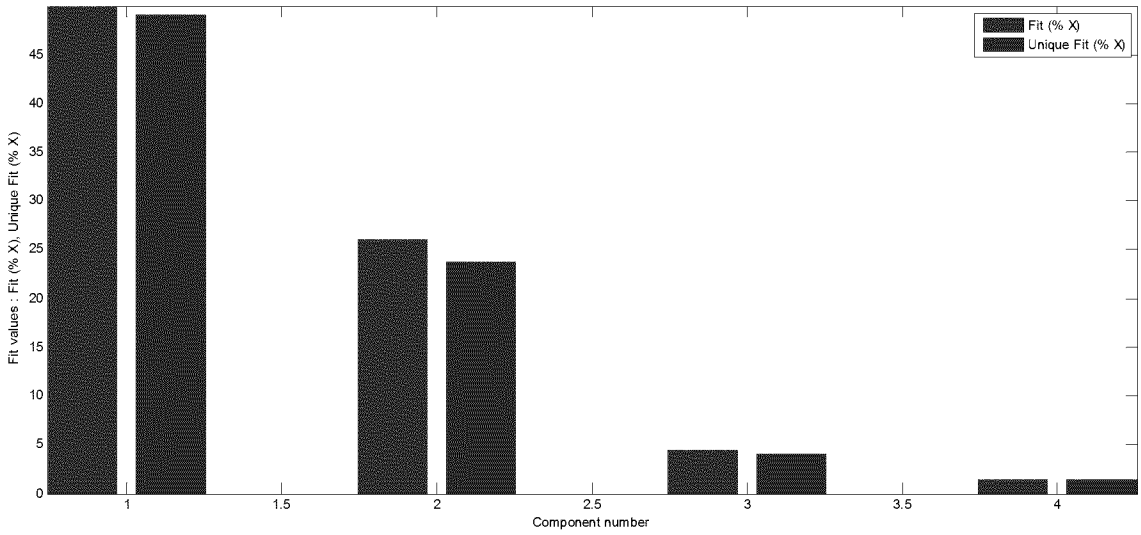

Figure 63. Fit (% X) vs. unique fit (% X) for five-factor PARAFAC model on all 22 oil types at DOR = 1:20.

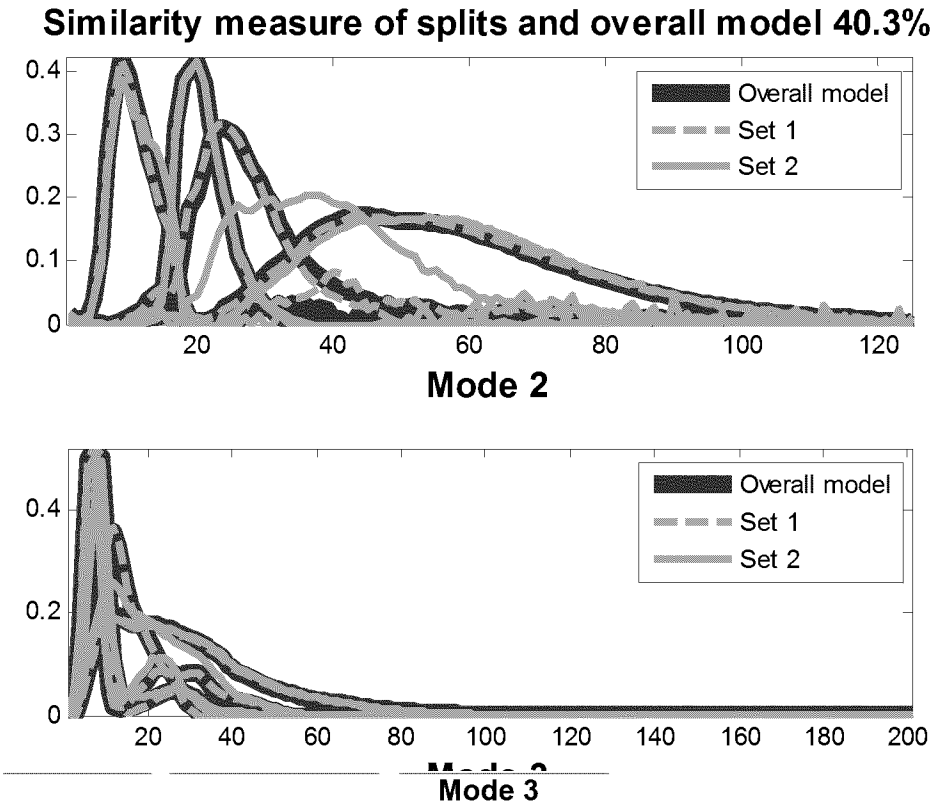

Figure 64. Similarity measure of split halves and overall model for 5-factor model.

DOR = 1:20, Oil Type I & II Comparison

The 22 types of oil can be grouped by the tendency for F_{max1} fluorescence intensity to markedly increase with increased DOR (Type I), and those with little to no increase in F_{max1} fluorescence intensity with increasing DOR (Type II). Since it was not possible to determine a definitive number of component factors using all 22 sample files from the DOR = 1:20 baffled flask experiments, PARAFAC analysis was performed separately on Type I and Type II oil samples.

Type I Oils

A four-factor model with the optimal pre-processing constraints of non-negativity, EEM filtering (12 and 24nm for First and Second Order Rayleigh, respectively), and info-Norm constraints was run on the twelve Type I oil samples (Table 3) by loading the DOR = 1:20 dataset and excluding Type II samples. Results showed the model characterized 95.9% of the data with 95% core consistency and low, randomly distributed residuals; however, the relative percent difference between fit and unique fit was high at 60% and 62% for factors 1 and 3, respectively. Factor 4 represented only 1.1% of the data and appeared to be modelling only noise from the graph of loadings for Mode 2 (emission). Split half analysis showed a 0% similarity between splits and the overall model. Re-running the model with three factors explained 95.7% of the data with 95% core consistency. Variation per component was problematic for factors 2 and 3, with relative percent difference between fit and unique fit of 61% and 62%, respectively. Further, in the graph of loadings for Mode 2 (emission) factor 3 appeared nearly identical to factor 2, just shifted to a slightly longer wavelength. Split half analysis was slightly improved over the four-factor model, with a 28.4% similarity between splits and model. Finally, re-running the model with two factors resulted in the best result with 95.0% of the data explained, 100% core consistency and good variation per component. Split half analysis showed an excellent 96.3% similarity between splits and the overall model. The graphs of loadings for Mode 2 and 3 appear to be reasonable emission and excitation spectra, respectively. Noted, however, is the appearance of minor double peaks in emission spectra at 308 nm for factor 1 and 294 nm for factor 2.

ED_001324_00000298-00139

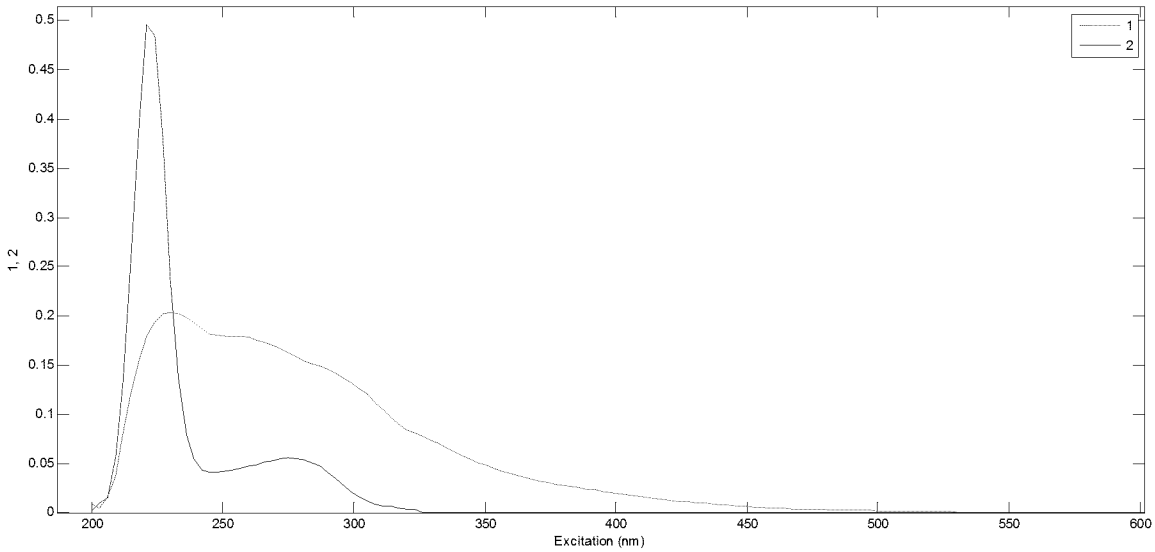

Figure 65. Mode 3 loadings - Excitation for two-factor PARAFAC model of Type I oils at DOR = 1:20.

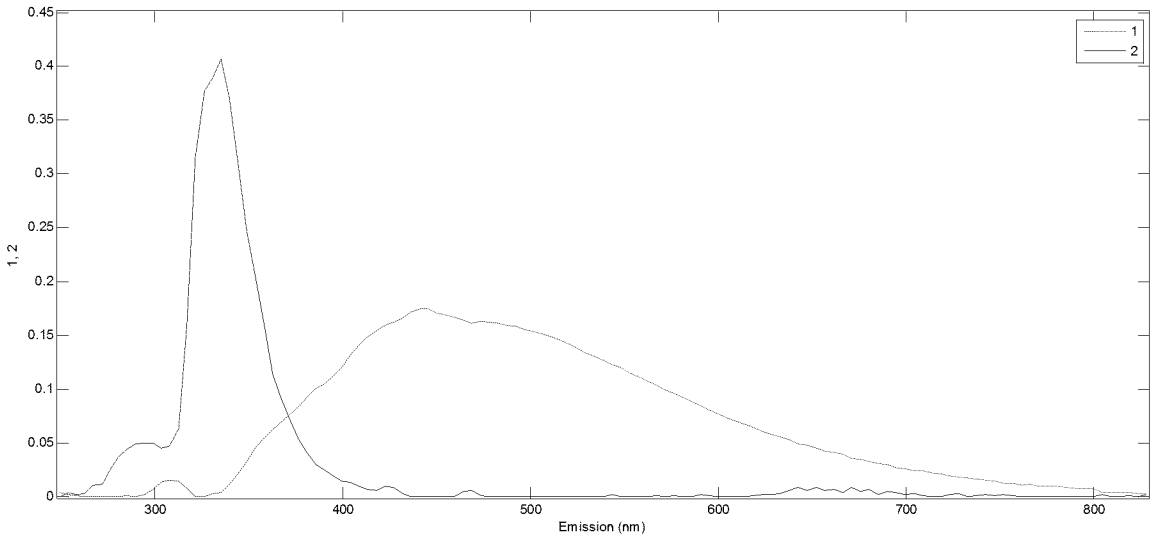

Figure 66. Mode 2 loadings - Emission for two-factor PARAFAC model of Type I oils at DOR = 1:20.

ED_001324_00000298-00140

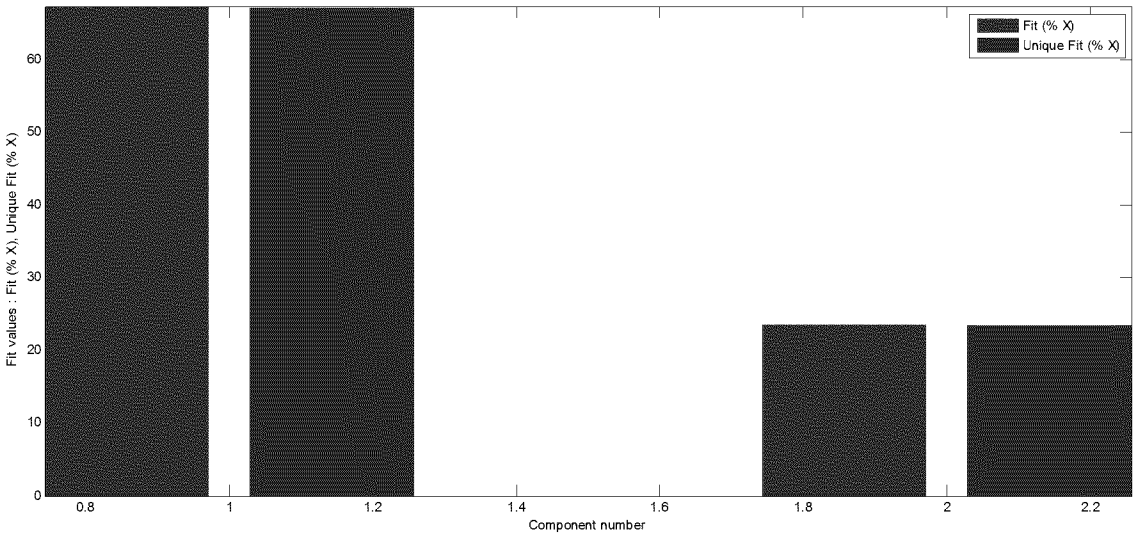

Figure 67. Fit (% X) vs. unique fit (% X) for two-factor PARAFAC model of Type I oils at DOR = 1:20.

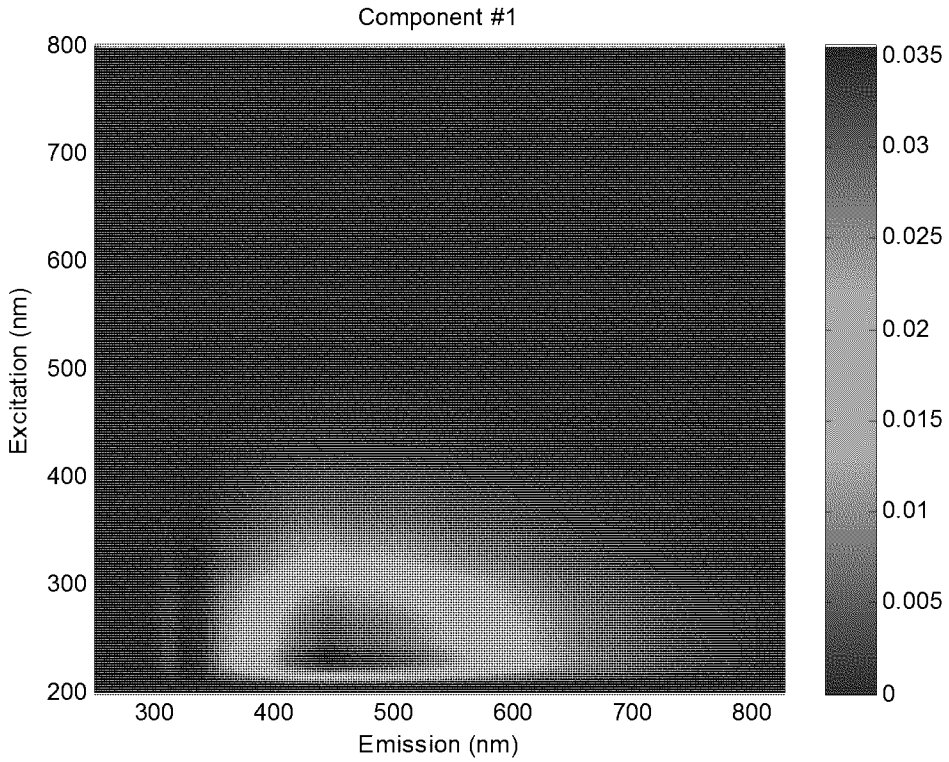

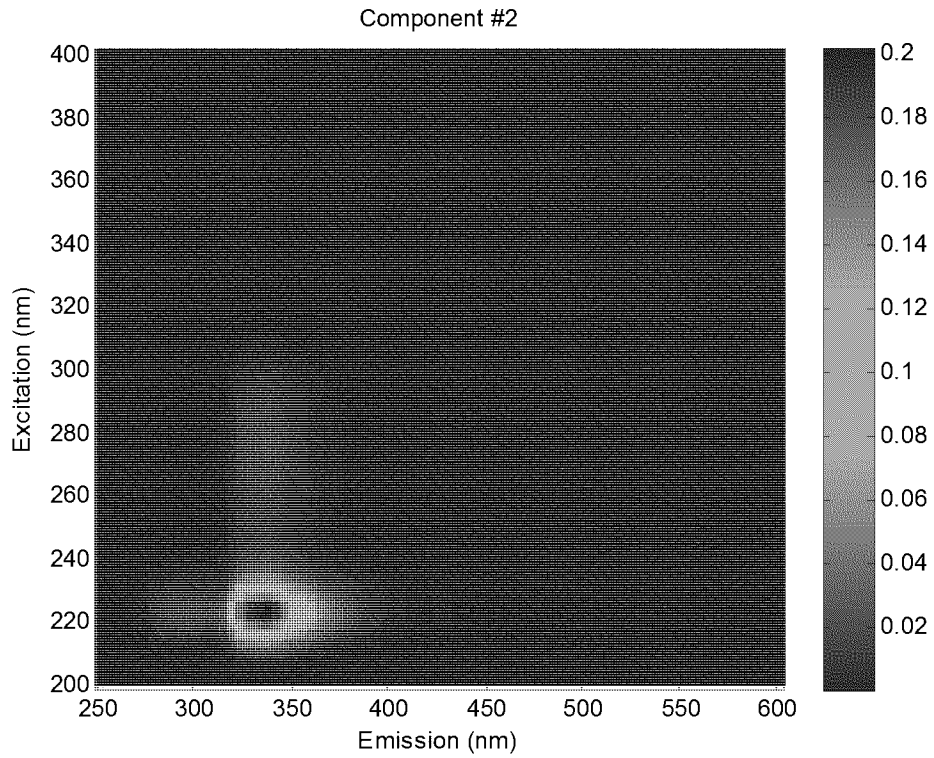

Figure 68. EEM view of factor 1 with F_{max} at Ex/Em = 230/445 nm (above), and factor 2 with F_{max} at Ex/Em = 221/335 nm (below)

Type II Oils

To initiate PARAFAC analysis with the group of ten Type II oil samples (Table 3), the same four-factor model with aforementioned three optimal constraints was performed. The model explained 95.9% of the data with 91% core consistency and low, randomly distributed residuals. Variation per component was good for all four factors. The graph of loadings for Mode 2 (emission) had the appearance of true emission profiles for factors 1-3; however, factor 4 contained a significant, broad double peak. Split half analysis resulted in a similarity measure of only 22.8% between splits and the overall model. Increasing the number of factors to five and re-running the model in an attempt to separate the two peaks noted in emission factor 4 did not appreciably improve results, with 96.1% of the data explained by the model and 90% core consistency. Variation per component showed factor 5 accounted for less than 1% of the data, and split half analysis yielded 0.3% similarity between splits and the overall model. Re-running the model with three factors resulted in the best result with 93.3% of the data explained by the model, 94% core consistency and good variation per component. Split half analysis showed 87.9% similarity between the splits and the overall model. Noted once again is the appearance of minor double peaks in emission spectra at 290 nm for factor 1, 303 nm for factor 2, and 312 nm for factor 3.

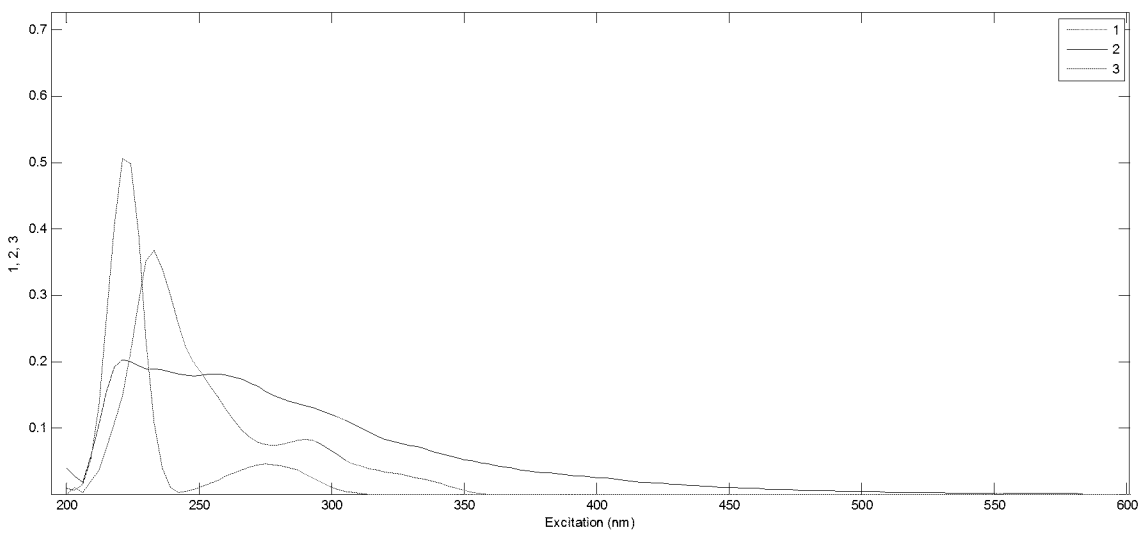

Figure 69. Mode 3 loadings - Excitation for three-factor PARAFAC model of Type II oils at DOR = 1:20.

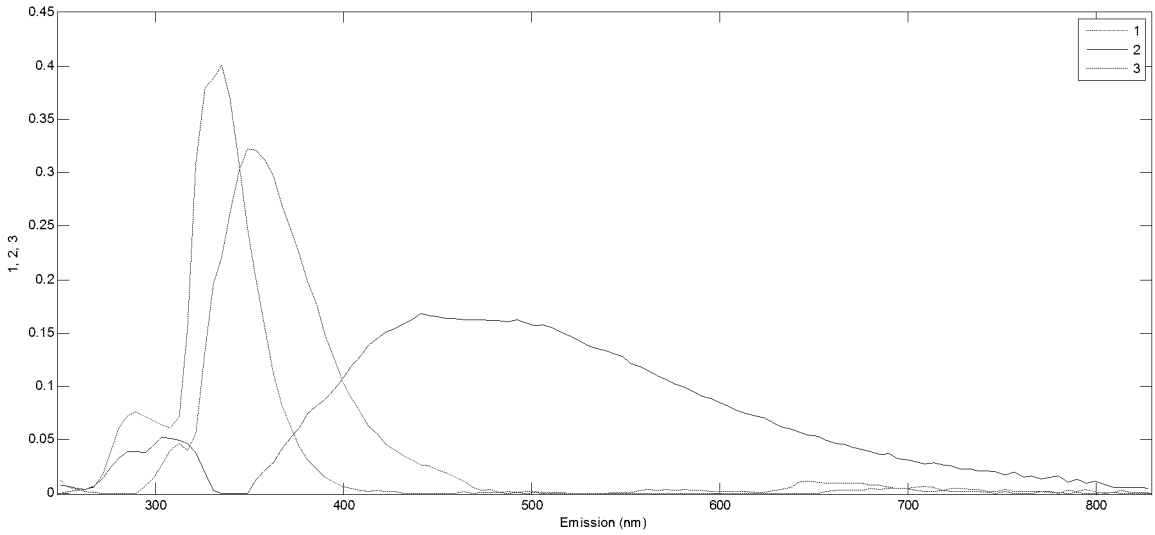

Figure 70. Mode 2 loadings - Emission for three-factor PARAFAC model of Type II oils at DOR = 1:20.

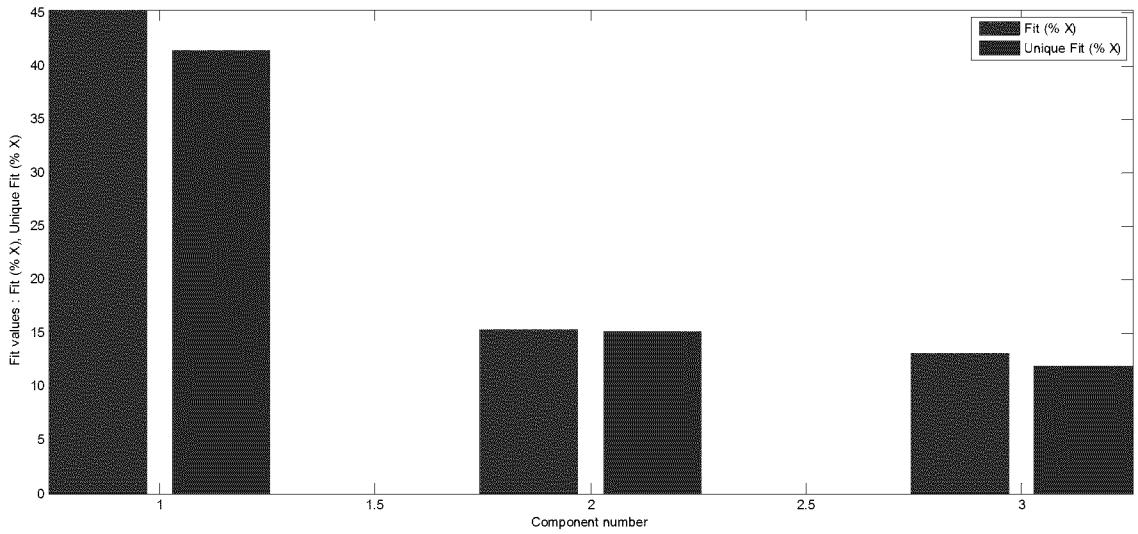

Figure 71. Fit (% X) vs. unique fit (% X) for three-factor PARAFAC model of Type II oils at DOR = 1:20.

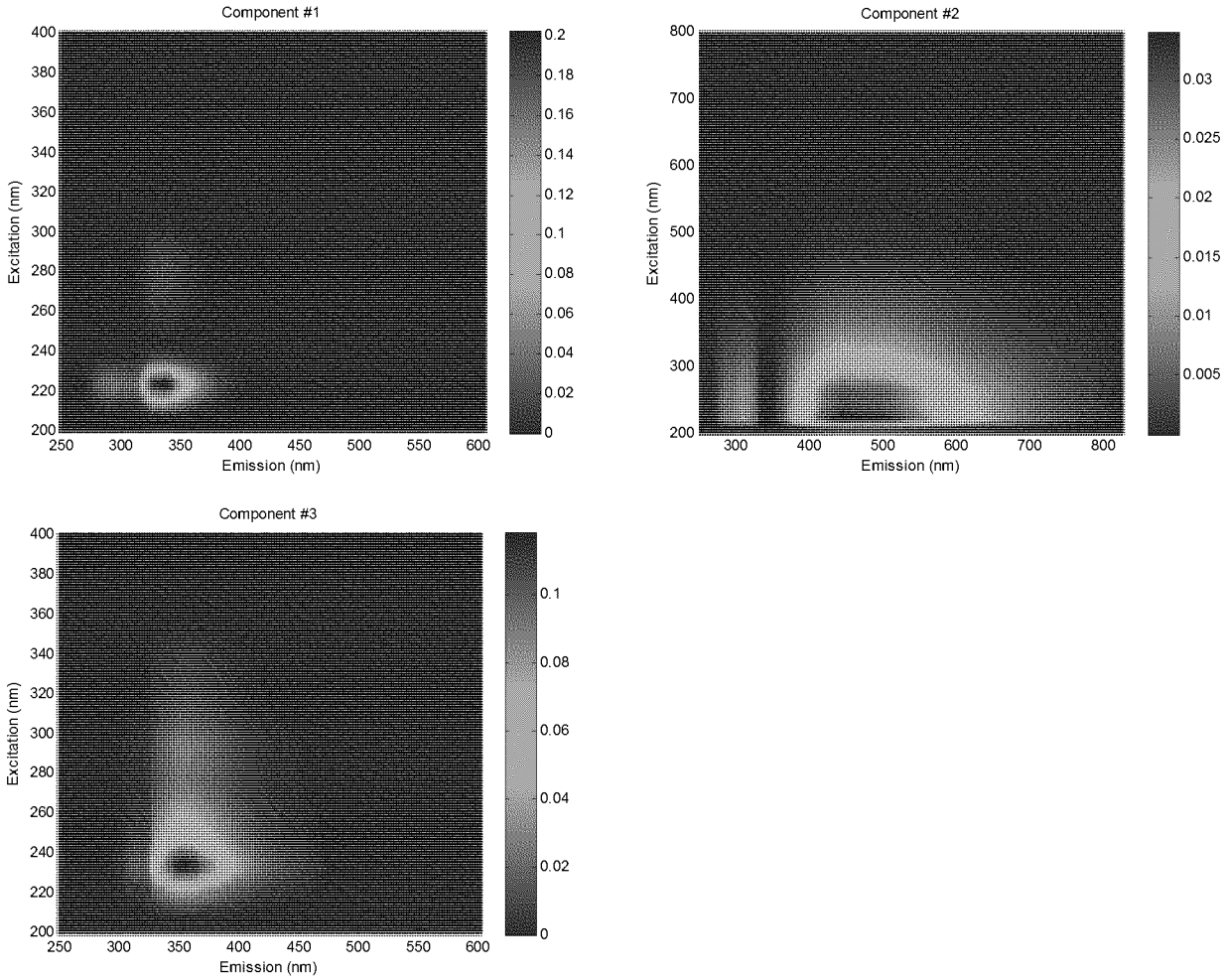

Figure 72. EEM view of factor 1 with Fmax at Ex/Em = 221/335 nm (top left), factor 2 with Fmax at Ex/Em = 221/492 nm (top right), and factor 3 with Fmax at Ex/Em = 233/349 nm (bottom left).

DOR = 1:100, Oil Type I & II Comparison

Type I Oils

Given the success with splitting samples into Type I and II groupings and improving the PARAFAC analysis in resolving difficulties in factor identification with DOR = 1:20 oil samples, this procedure was performed with DOR = 1:100 and DOR = 0 oil samples, as well. First analysis of the twelve Type I oil samples at this DOR was done using a three-factor PARAFAC model with the same three pre-processing constraints previously applied. The DOR = 1:100 dataset was loaded, and Type II oil samples were excluded from analysis. Results showed 97.8% of the data explained by the model with 88% core consistency. Variation per component was good, but fit vs. unique fit for factors 1 and 3 had a relative percent difference of 51%. Visual inspection of loadings graphs showed Mode 2 (emission) factors 1 and 3 were almost completely overlapping, the only difference being a minor double peak at 285 nm on factor 3. Similarity between splits and overall model was only 0.3%. Increasing the number of factors to four and re-running the model resulted in a slight increase in the data explained (98.2%); however core consistency dropped to 78%. Variation per component was essentially unchanged for components 1, 2 and 3, and less than 3% of the data was explained by factor 4. Split half analysis similarity between splits and the overall model was 0%. Dropping the number of factors to two and re-running the model resulted in 97.0% of the data explained by the model and 100% core consistency. Variation per component was good; however, over 75% of the fit was modelled by factor 1. Loading curves for both Mode 2 and Mode 3 looked very much like those for Type I oils at DOR = 1:20. Split half analysis resulted in only 22.6% similarity between splits and the model. The graph of data Set 2 and the model correlated nicely; however, the graph showed for data Set 1, factor 2 was not well correlated with the model in either Mode 2 (emission) or Mode 3 (excitation). Separation of oils into further sub-types may help to achieve a representative PARAFAC model.

ED_001324_00000298-00146

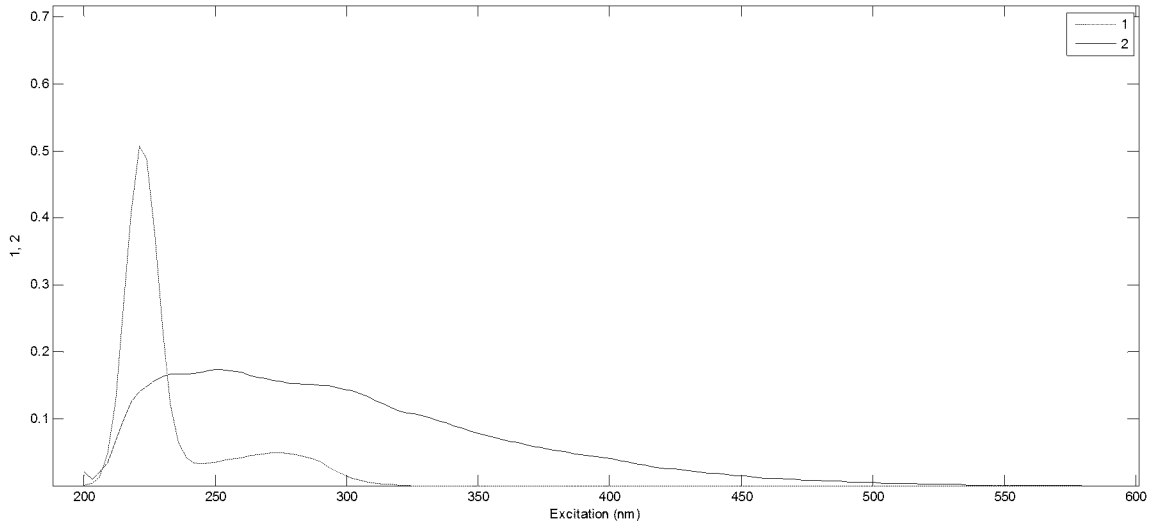

Figure 73. Mode 3 loadings - Excitation for two-factor PARAFAC model of Type I oils at DOR = 1:100.

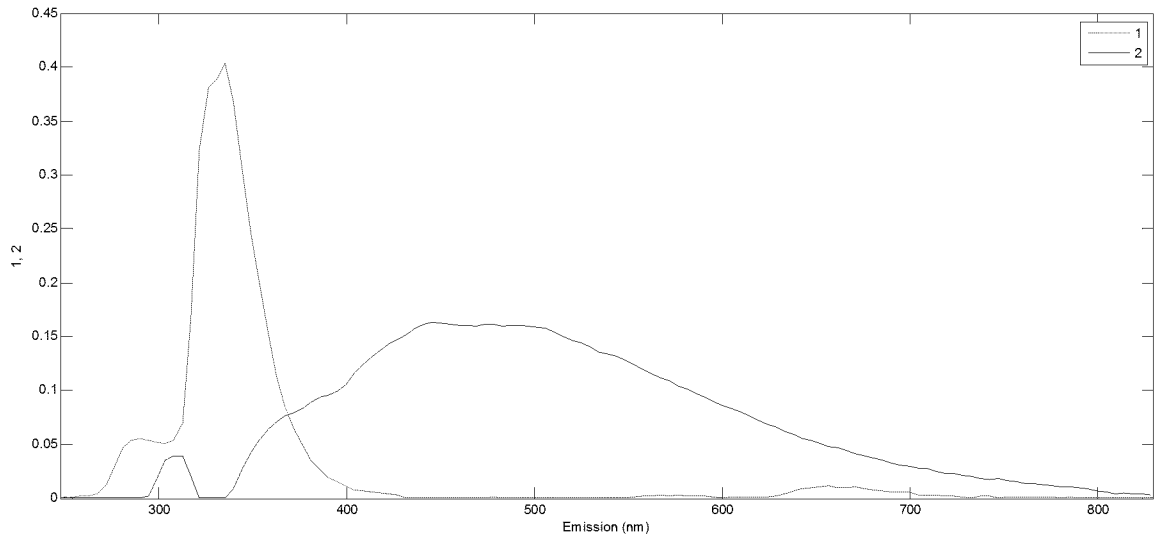

Figure 74. Mode 2 loadings - Emission for two-factor PARAFAC model of Type I oils at DOR = 1:100.

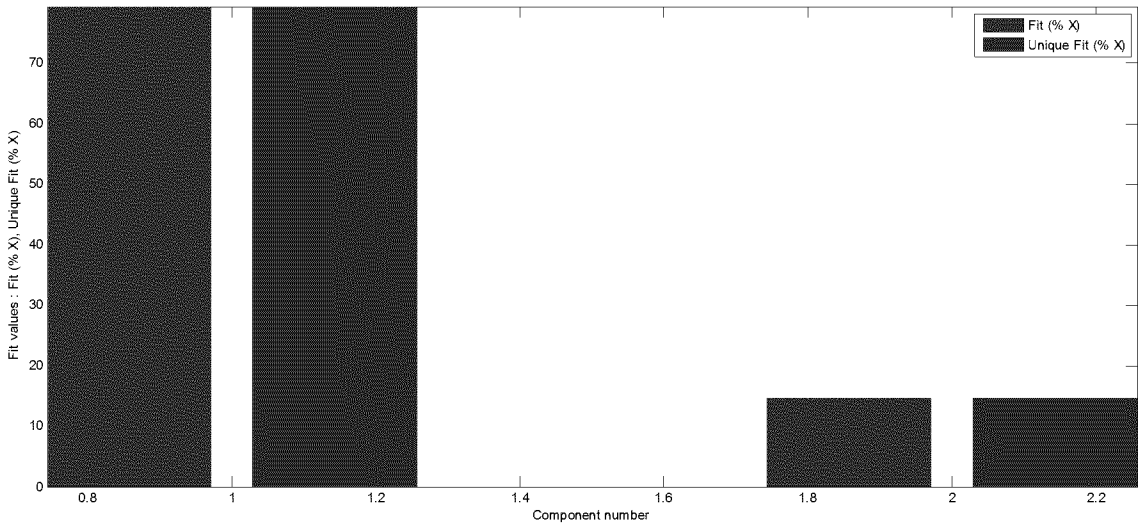

Figure 75. Fit (% X) vs. unique fit (% X) for two-factor PARAFAC model of Type I oils at DOR = 1:100.

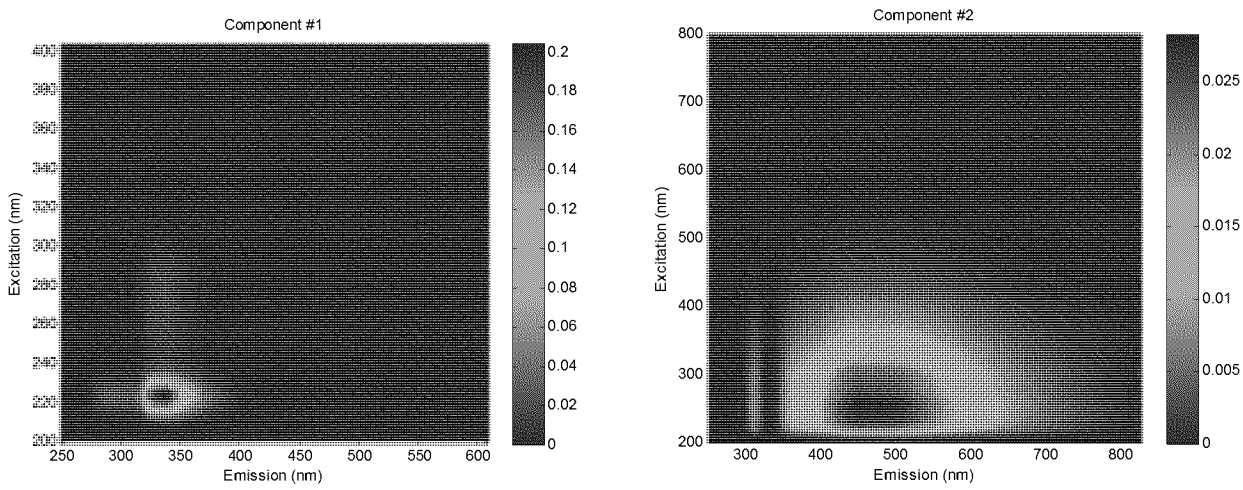

Figure 76. EEM view of factor 1 with F_{max} at Ex/Em = 221/335 nm (above), and factor 2 with F_{max} at Ex/Em = 251/445-500 nm (below).

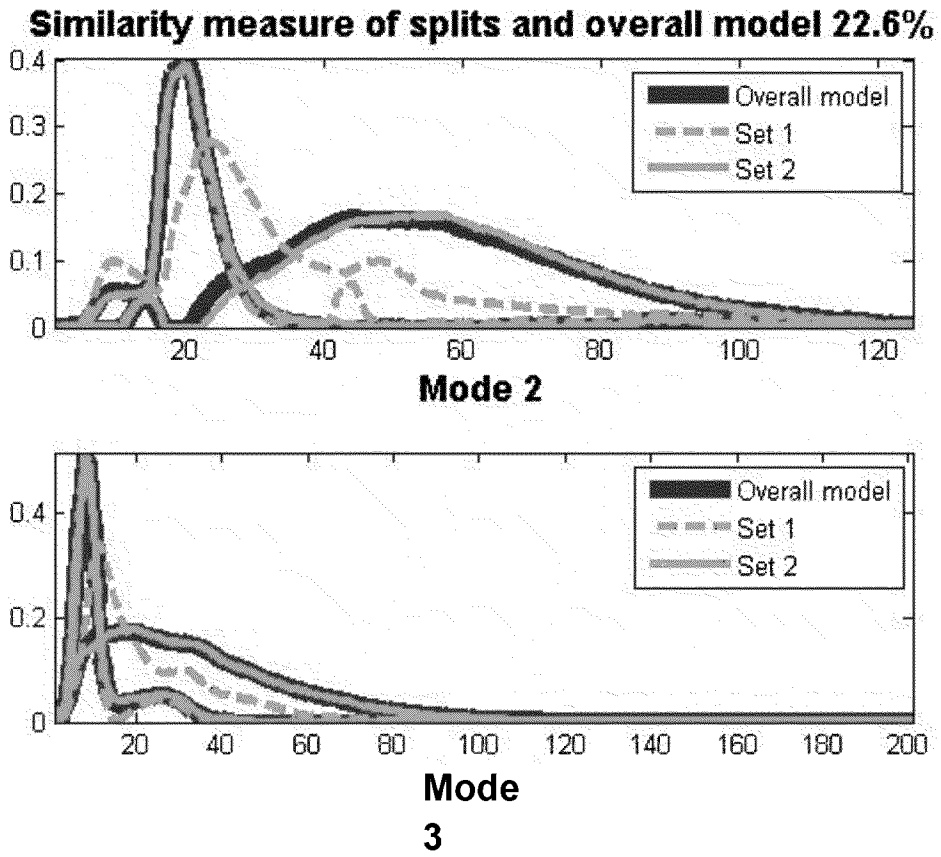

Figure 77. Similarity measure of split halves and overall model for 2-factor model.

Type II Oils

Based on results of PARAFAC modelling performed on DOR = 1:20 Type II oils, a three-factor model with the same previously applied pre-processing constraints was run on the DOR = 1:100 Type II oil samples. The model explained 94.7% of the data, and core consistency was 95%. Variation per component was very good, and loadings for both Mode 2 and 3 appeared to model reasonable emission and excitation spectra. Split half analysis had a somewhat low similarity of 62.7% between splits and the overall model. To find a better fit, a four-factor model was performed, and results showed a slight increase to 95.3% of data explained by the model, but a reduction to 56% in core consistency, and split half analysis similarity was only 1.8% between splits and the model. A two-factor model was then performed, resulting in 91.0% of the data explained by the model and core consistency of 100%. Split half analysis yielded similarity of 70.5% between splits and the overall model. While split half analysis was somewhat better for the two-factor model, the three-factor model represented a better percentage of the data while retaining high core consistency. It is clear from viewing the loadings graphs and EEM view of components that the three-factor model is capturing a true third component.

Two-factor Model

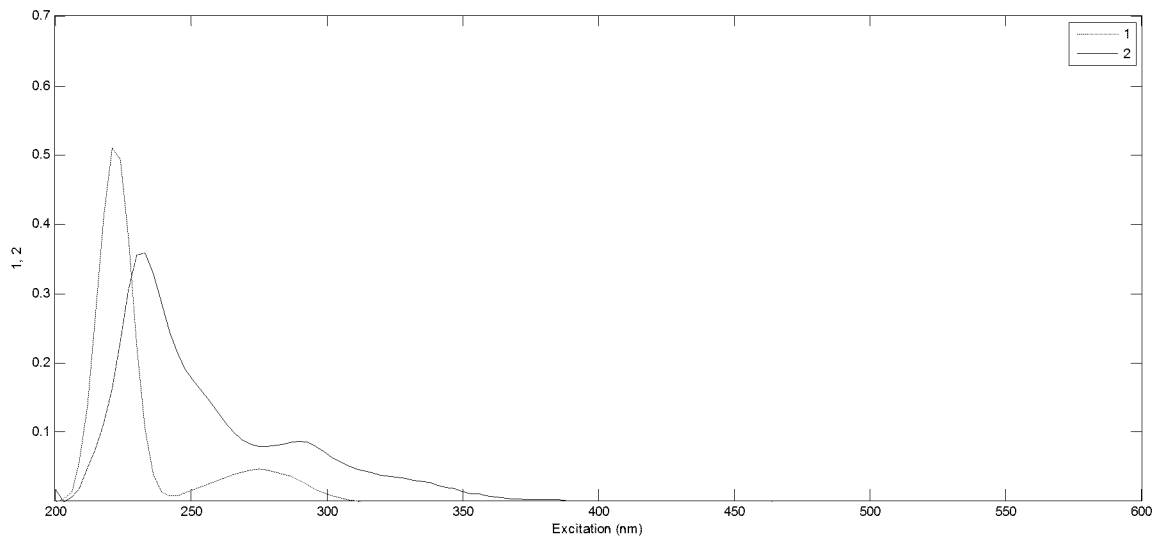

Figure 78. Mode 3 loadings - Excitation for two-factor PARAFAC model of Type II oils at DOR =

1:100.

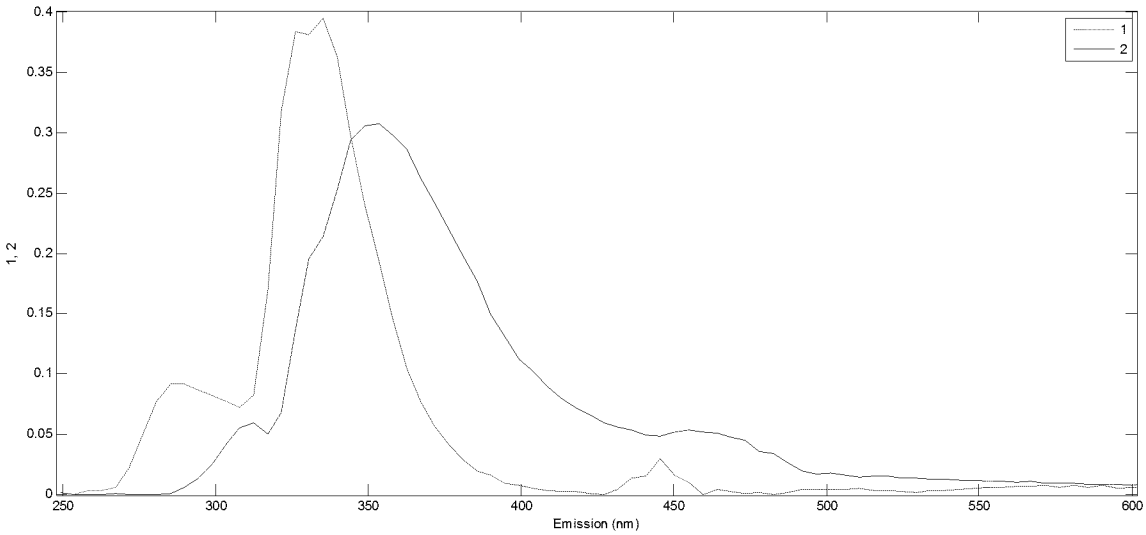

Figure 79. Mode 2 loadings - Emission for two-factor PARAFAC model of Type II oils at DOR = 1:100.

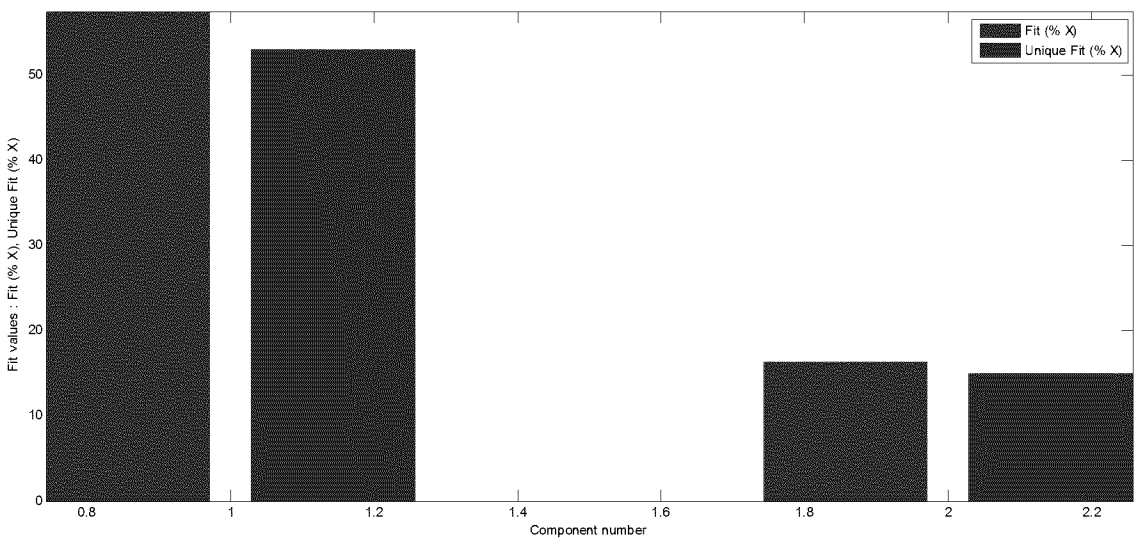

Figure 80. Fit (% X) vs. unique fit (% X) for two-factor PARAFAC model of Type II oils at DOR = 1:100.

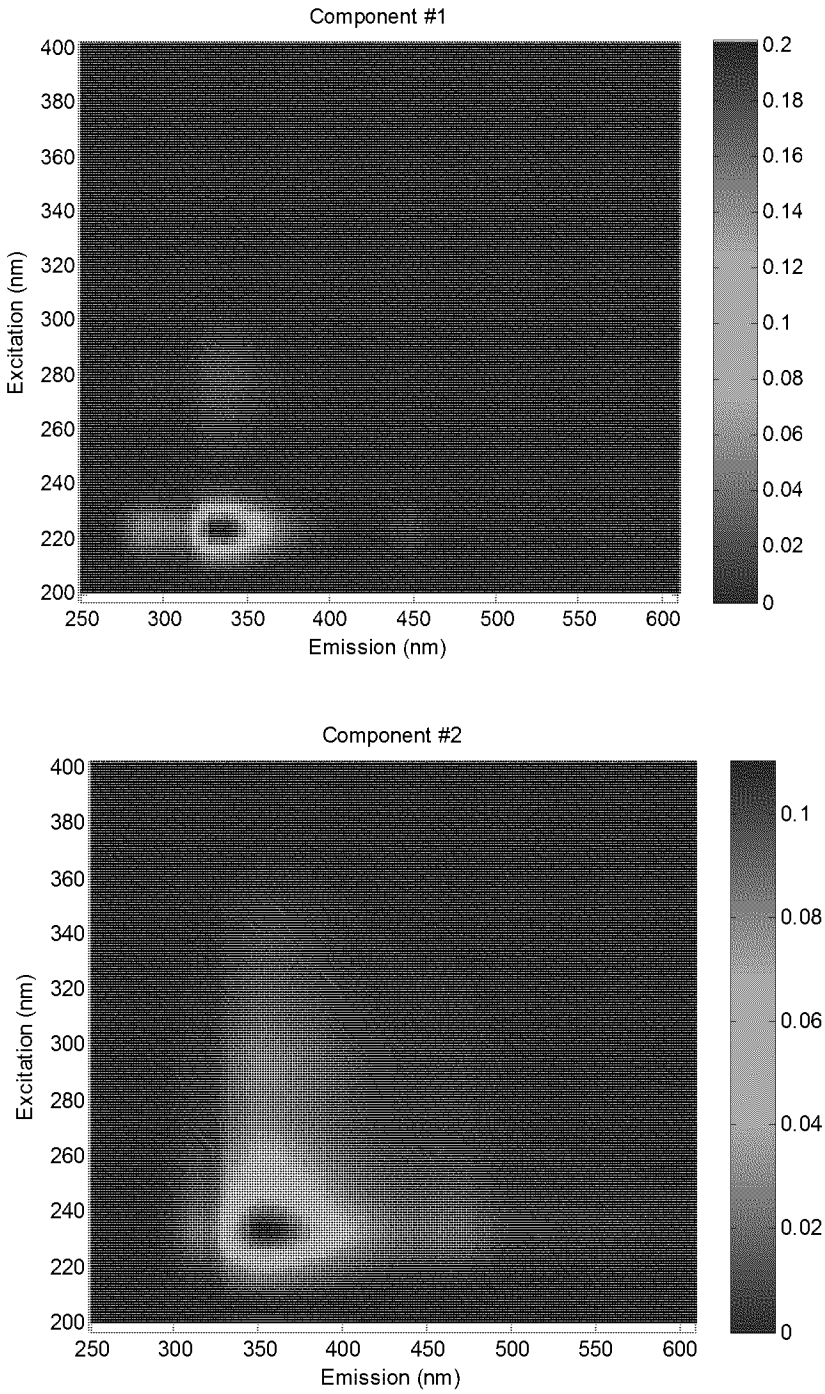

Figure 81. EEM view of factor 1 with F_{max} at Ex/Em = 221/335 nm (above), and factor 2 with F_{max} at Ex/Em = 233/353 nm (below).

Three-factor Model

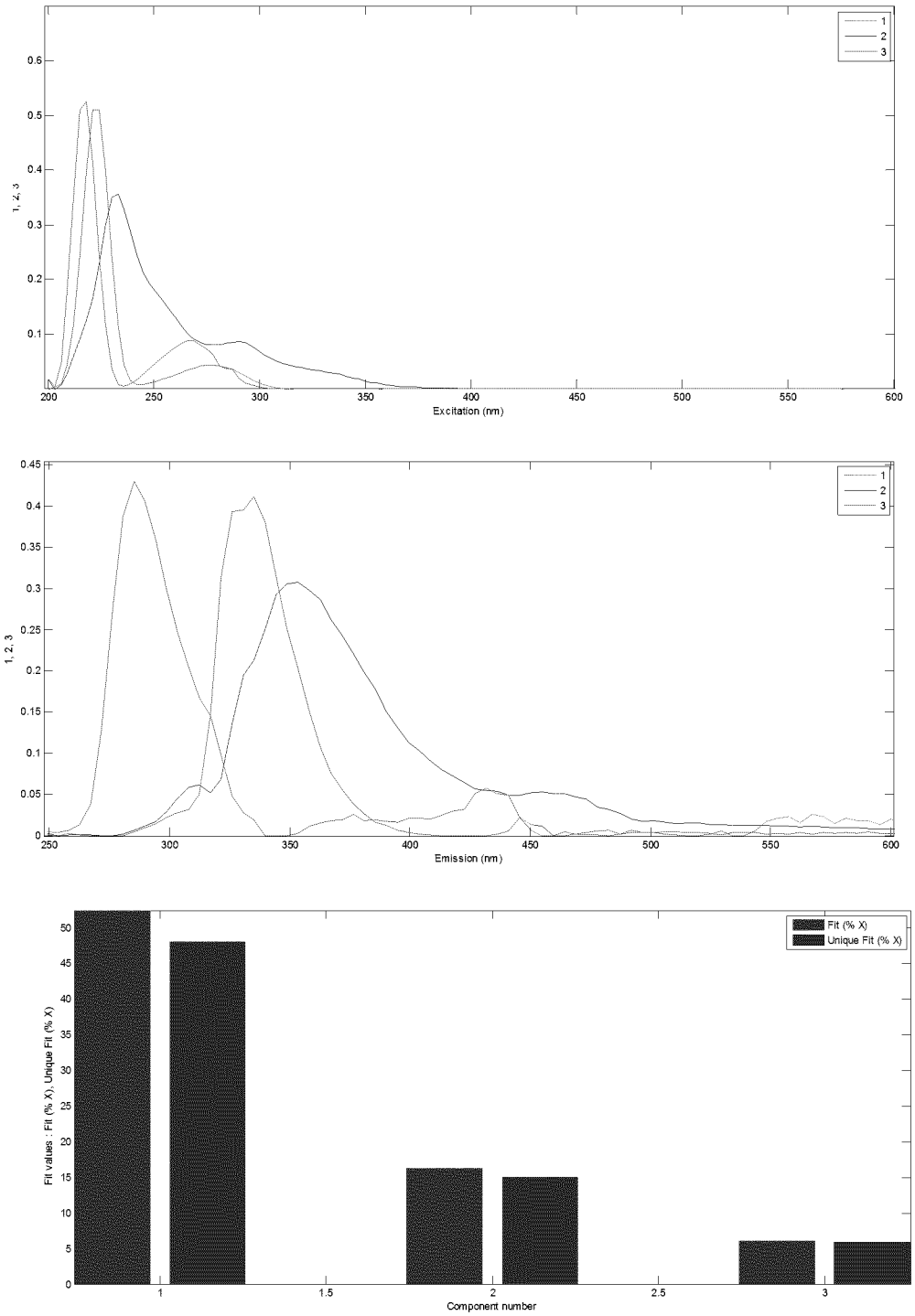

Figure 82. Mode 3 loadings - Excitation (top) and Mode 2 loadings - Emission (middle) for three-factor PARAFAC model of Type II oils at DOR = 1:100. Fit (% X) vs. unique fit (% X) for three-factor PARAFAC model of Type II oils at DOR = 1:100 (bottom).

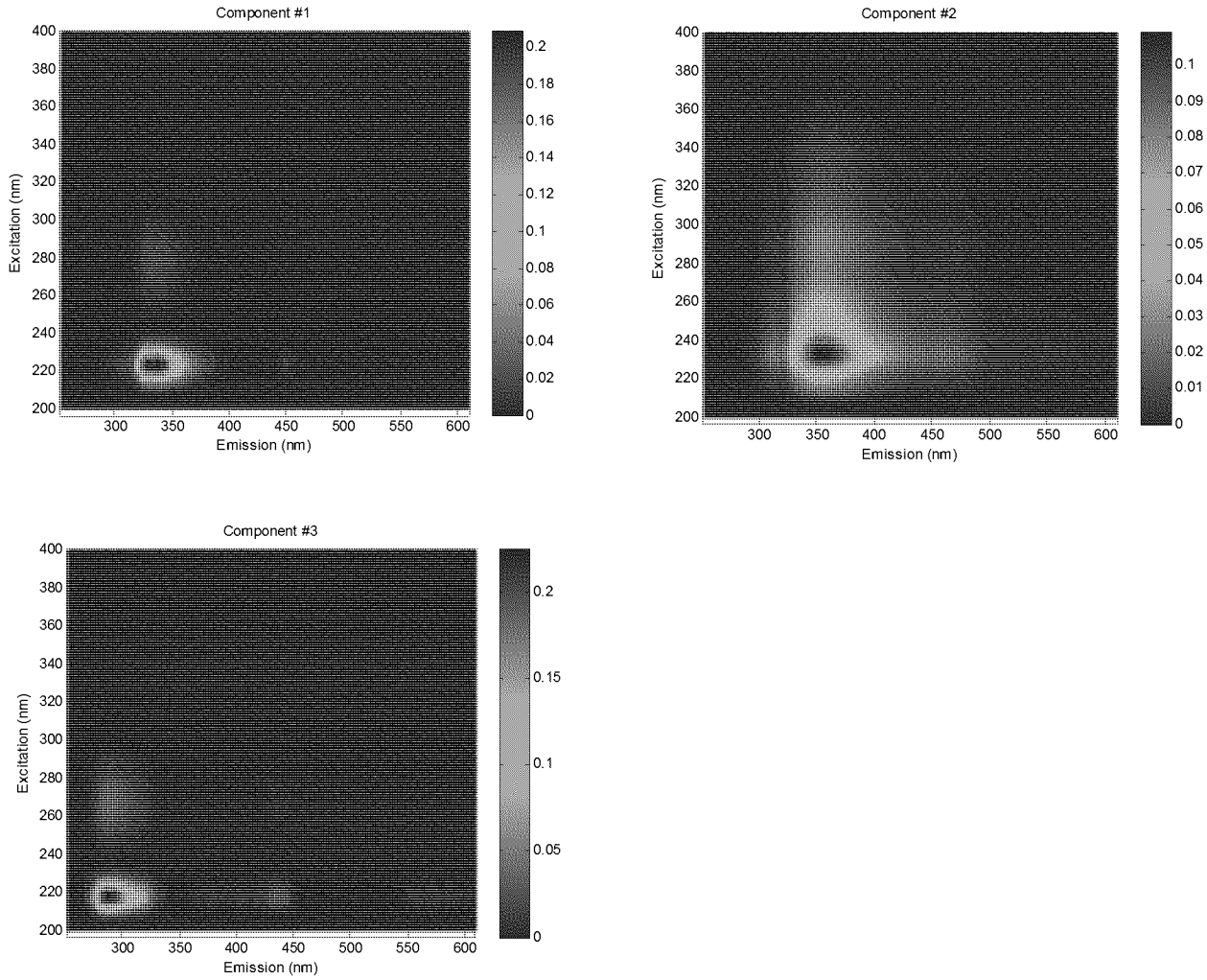

Figure 83. EEM view of factor 1 with Fmax at Ex/Em = 221/335 nm (top left), factor 2 with Fmax at Ex/Em = 233/353 nm (top right), and factor 3 with Fmax at Ex/Em = 218/285 nm (bottom left).

DOR = 0 – Type I Oils

To begin the analysis of Type I oil samples, the DOR = 0 dataset was loaded, and Type II oil sample files were excluded. A three-factor PARAFAC model with the previously selected pre-processing constraints was performed. Results explained 94.4% of the data, but core consistency was only 19%. Variation per component was not optimal, with a relative percent difference of 42% between fit and unique fit in both factors 1 and 2. While fit vs. unique fit for factor 3 was good, it only accounted for 2.4% of the model. Split half analysis resulted in similarity of 0.8% between the splits and the model. Re-running the model with four factors resulted in 94.7% of the data explained by the model and core consistency of only 33%. Variation per component was similar to that obtained with the three-factor model; however, the addition of factor 4 represented less than half of one percent of the data. Split half analysis yielded 0% similarity between splits and the overall model. Dropping the number of factors to two and running the model again resulted in 93.6% of the data explained by the model and 100% core consistency. Variation per component showed close to 90% of the data was modelled by factor 1 and less than 2% by factor 2. In addition, factor 2 displayed two separate and equal peaks in loadings for Mode 2 (emission), indicating a poor fit. Split half analysis resulted in 0.3% similarity between the splits and the overall model. It appears impossible to arrive at a satisfactory PARAFAC model for all Type I oils collectively; perhaps splitting these samples into at least two subgroups would improve resolution.

DOR = 0 – Type II Oils

Type I oil samples were then excluded from the DOR = 0 dataset, and a three-factor PARAFAC model with the previously selected pre-processing constraints was run on the Type II oil sample files. Results showed that 96.2% of the data was explained by the model, with 94% core consistency. Variation per component was good with only 7-8% relative percent difference between fit and unique fit in factors 1 and 2, and less than 1% difference in factor 3. Split half analysis showed 68% agreement between splits and the overall model. Four-factor and two-factor models, with the same constraints, were also run in an attempt to improve goodness-of-fit. The four-factor model resulted in 96.5% of the data explained by the model and 93% core

ED_001324_00000298-00155

consistency, but split half similarity between splits and overall model was only 0.1%. The two-factor model resulted in a drop in data explained by the model to 92.8% and an increase in core consistency to 100%. However, split half similarity between splits and model was 0.7%. Therefore, the three-factor model was selected as best overall. It was noted that the graphs of loadings and EEM views of factors were almost identical to those obtained with the three-factor PARAFAC model for all 22 oils at DOR = 0.

ED_001324_00000298-00156

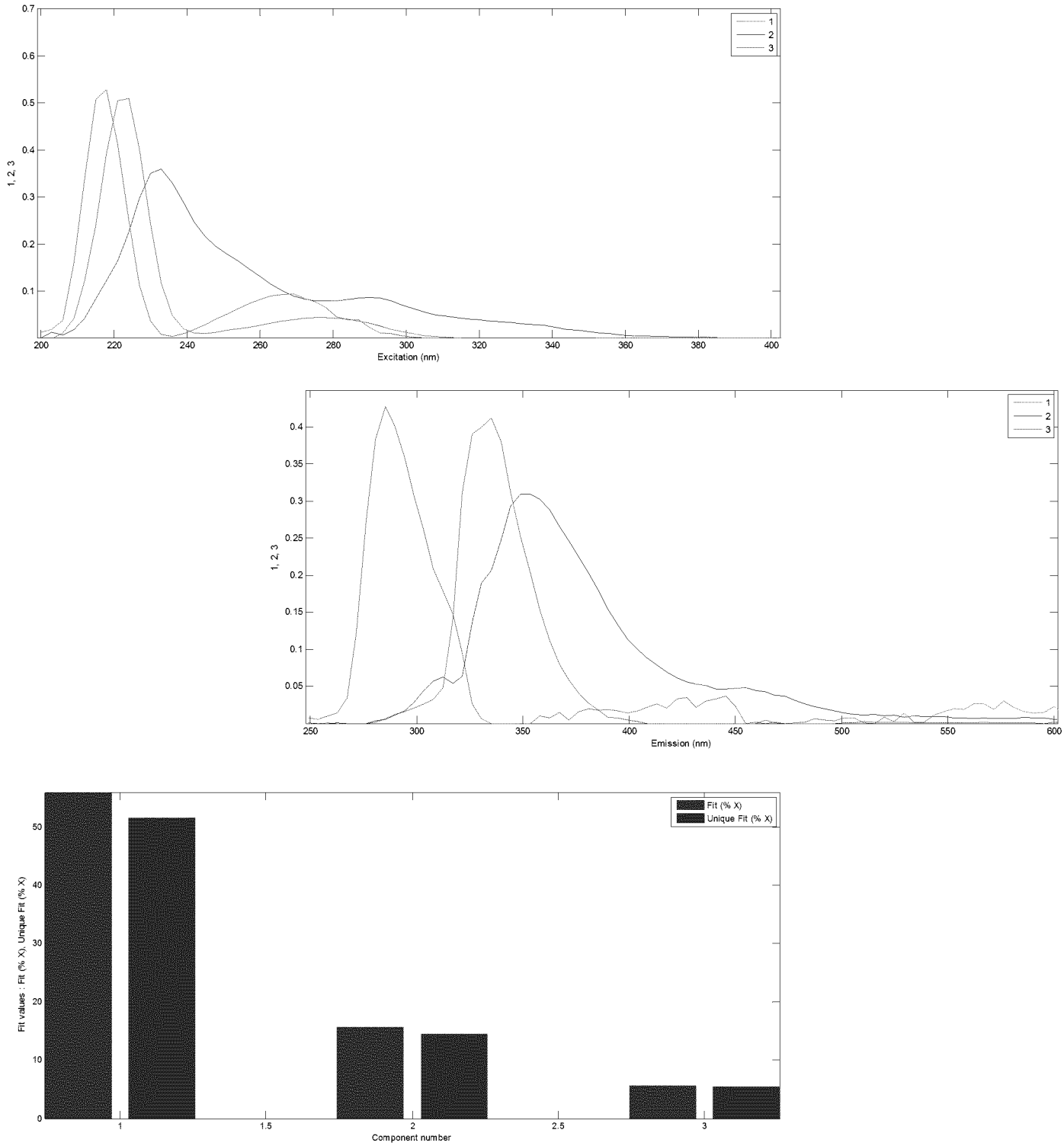

Figure 84. Mode 3 loadings -excitation (top), Mode 2 loadings – emission (middle) and fit (% X) vs. unique fit (% X) (bottom) for three-factor PARAFAC model of Type II oils at DOR = 0.

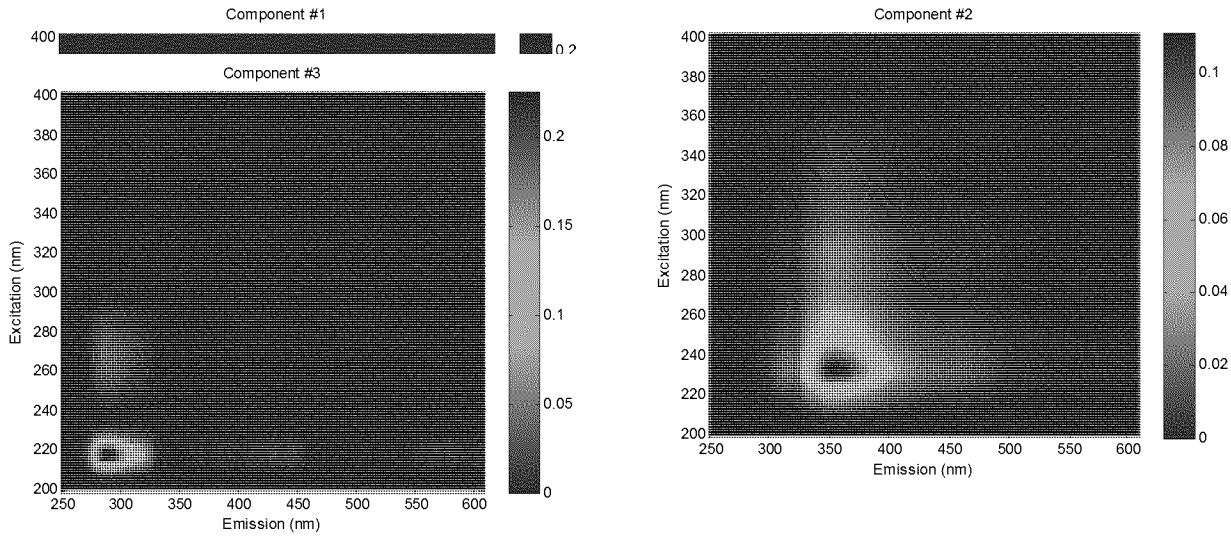

Figure 85. EEM view of factor 1 with Fmax at Ex/Em = 224/335 nm (top left), factor 2 with Fmax at Ex/Em = 233/353 nm (top right), and factor 3 with Fmax at Ex/Em = 218/285 nm (bottom left).

PAHs and Proteins

A four-factor PARAFAC model was run with non-negativity, EEM filtering (12nm First Order Rayleigh, 24nm Second Order Rayleigh), and inf-Norm normalization (maximum = 1). An error message was displayed indicating that two or more components could be fitting the same feature, and core consistency was <0%. Although variation per component was good, only 69.2% of data was explained by the model, sample 1 residuals were high, and Mode 1 Loadings showed samples 3 and 4 (pyrene and phenanthrene) clearly overlapping.

Table 11. Polycyclic Aromatic Hydrocarbons (PAHs) in dichloromethane, further dissolved in artificial seawater.

PAH	Original concentration	Amount added to seawater	Final concentration
Fluorene	1000 µL/mL	10 µL	100 µL /L
Phenanthrene	129.26 µg/mL	10 µL	12.9 µg/L
Anthracene	10 µg/mL	20 µL	2.0 µg/L
Pyrene	10 mg/mL	20 µL	2.0 mg/L

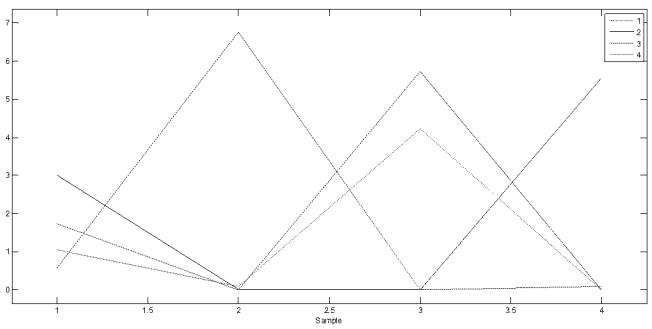

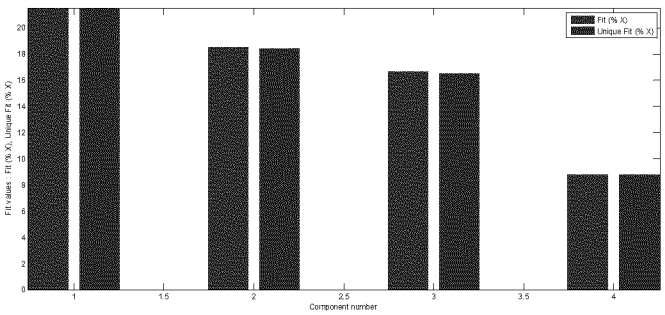

Figure 86. Mode 1 loadings (left), and Fit (% X) vs. unique fit (% X) (right), for PAHs.

Results of a three-component model had core consistency of 94%; however, only 61.7% of the data was explained by the model, and Mode 2 factor 3 appeared to be modelling noise. A two-component model explained only 53.5% of the data; however, core consistency was 100% and both Mode 2 emission factors appeared to be valid emission spectra.

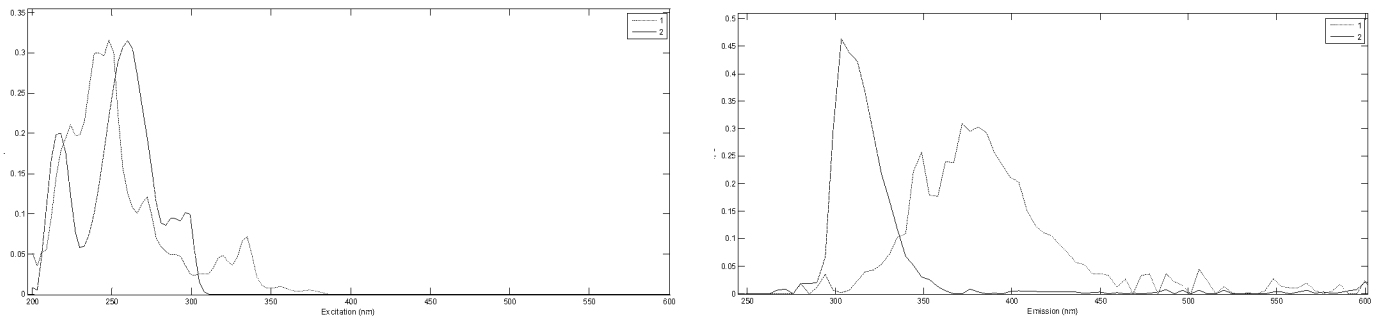

Figure 87. Mode 3 loadings - Excitation (left) and Mode 2 loadings - Emission (right) for two-factor PARAFAC model of PAHs.

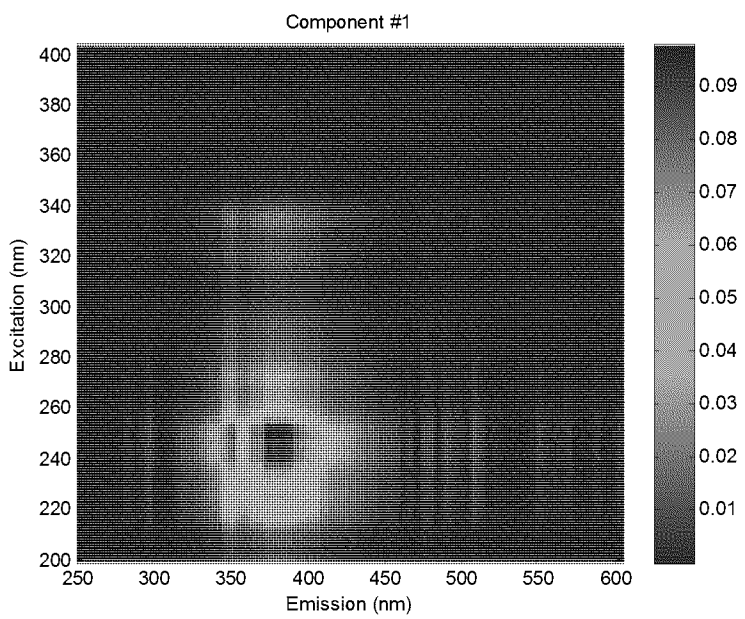

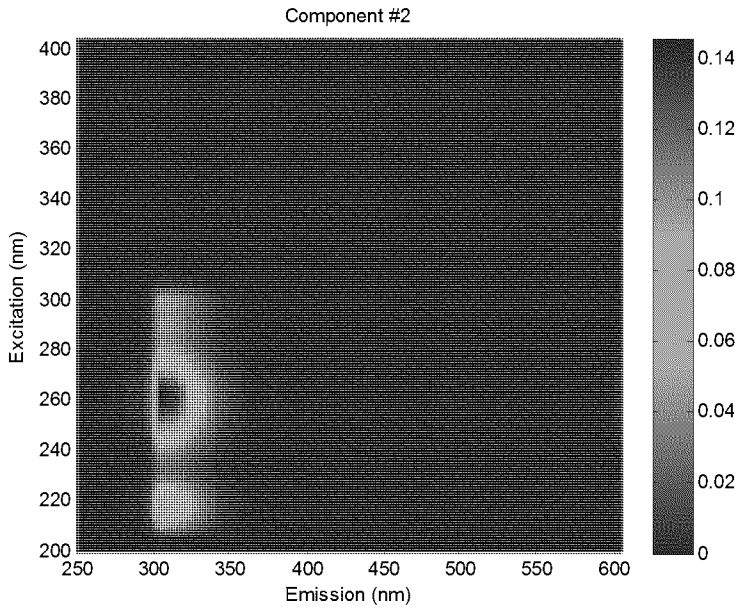

Figure 88. EEM view of factor 1 with F_{max} at Ex/Em = 251/376 nm (above), and factor 2 with F_{max} at Ex/Em = 263/308 nm (below).

Sample files of two proteins—tyrosine and tryptophan, 1ppm in artificial seawater, were also imported into SOLO, and a two-factor PARAFAC model was performed. Results showed that 99.2% of the data was explained by the model and core consistency was 100% with excellent variation per component and low, randomly distributed residuals. Loadings for Mode 2 (emission) and Mode 3 (excitation) show realistic spectra for these two proteins.

ED_001324_00000298-00161

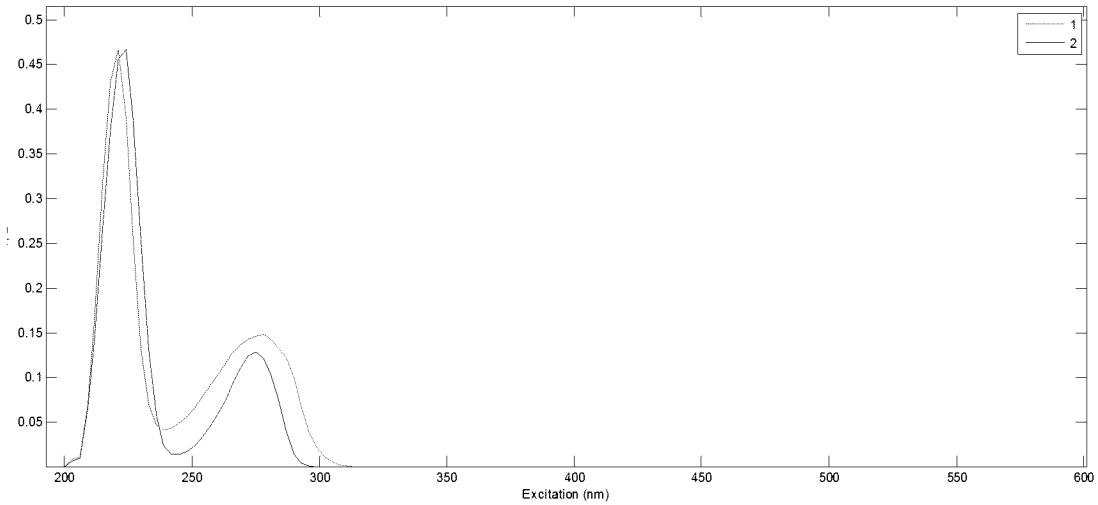

Figure 89. Mode 3 loadings - Excitation (above) and Mode 2 loadings - Emission (below) for two-factor PARAFAC model of proteins.

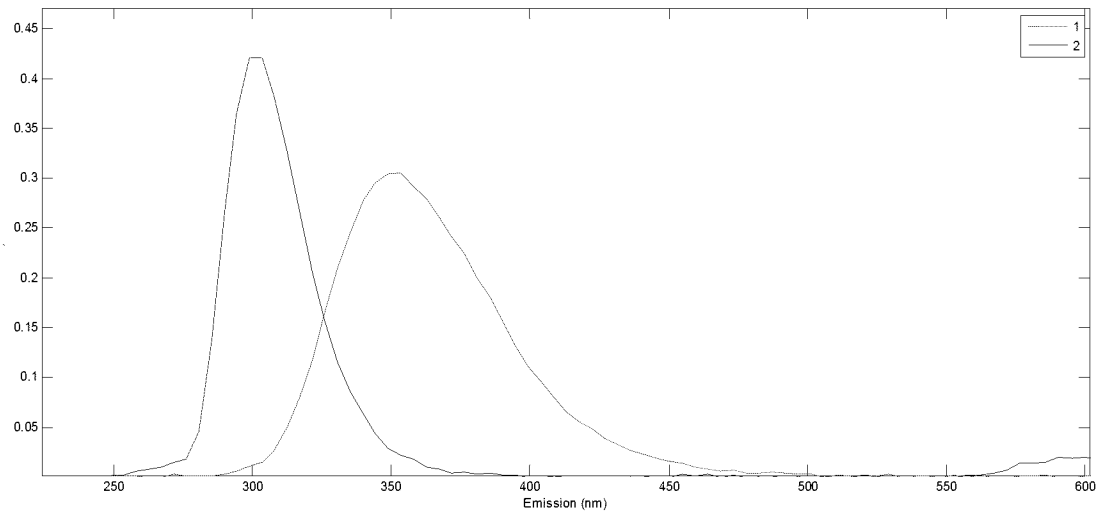

Comparing the results of PARAFAC analysis on PAHs with that on naturally-occurring proteins illustrates the complexity of the fluorescence signals displayed by PAHs vs. the strong, clear signals arising from proteins. Ideally, PARAFAC modelling of aqueous organic fluorophores would show little overlap between excitation and emission spectra and have a single emission peak (Murphy,et al. 2013); however, the molecular complexity of PAHs leads to convoluted fluorescence signals which creates a challenge for PARAFAC decomposition into component factors.

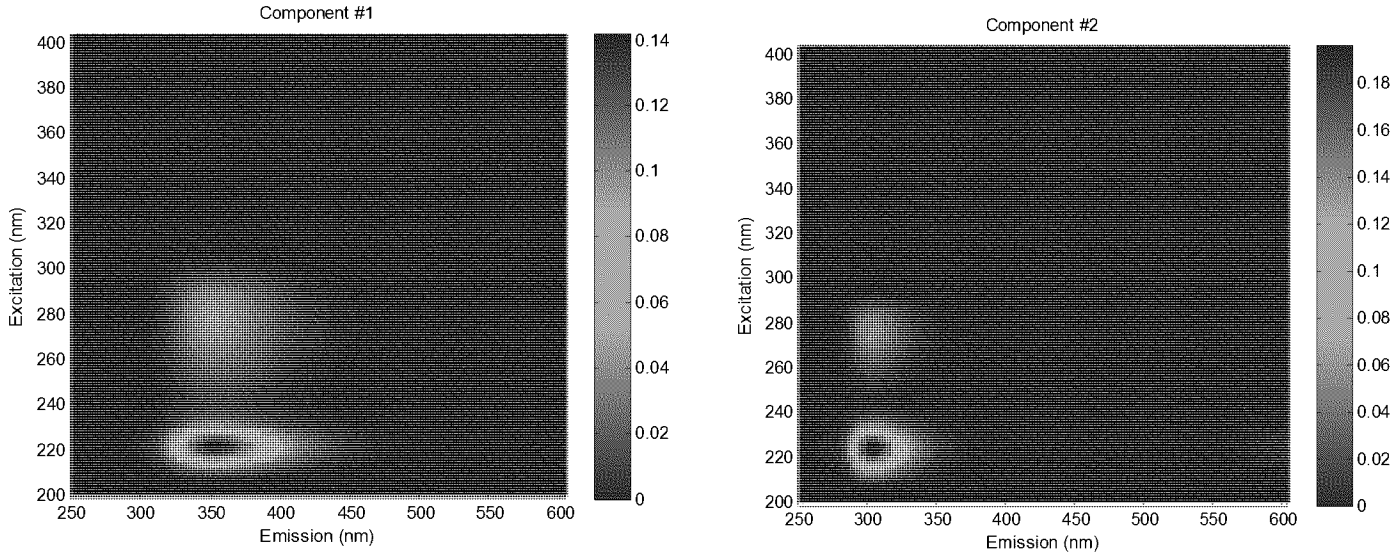

Figure 90. EEM view of factor 1 with F_{max} at Ex/Em = 221/353 nm (above) and factor 2 with F_{max} at Ex/Em = 224/300 nm (below).

REFERENCES

Alliance for Coastal Technologies Report (2008) Hydrocarbon sensors for oil spill prevention and response. Ref # [UMCES]CBL08-095, 28 pp.

Andersen, C. M., R. Bro (2003) Practical aspects of PARAFAC modeling of fluorescence excitation-emission data. J. Chemom., 17:200-217.

Bieroza, M., A. Baker, J. Bridgeman (2010) Classification and calibration of organic matter fluorescence data with multiway analysis methods and artificial neural networks: an operational tool for improved drinking water treatment. Envirometrics, 22: 256-270.

Boehme, J.R., PG. Coble, R.N. Conmy (2004) Examining CDOM fluorescence variability using

principal component analysis: seasonal and regional modeling of three-dimensional fluorescence in the Gulf of Mexico. Marine Chemistry, 89:3-14.

Bahram, M., et al. (2006). "Handling of Rayleigh and Raman scatter for PARAFAC modeling of fluorescence data using interpolation." Journal of Chemometrics 20(3-4): 99-105.

Bugden, J.B.C., C.W. Yeung, P.E. Kepkay, K. Lee (2008) Application of ultraviolet fluorometry and EEMS to fingerprint oil and chemically dispersed oil in seawater. Marine Pollution Bulletin, 56(4): 677-85.

CRRC Report (2010) Coastal Response Research Center Deepwater Horizon Dispersant USE Meeting Report, May 26-27, 2010, 108 pp.

Christensen, A.B. Hansen, J. Mortensen, O. Andersen (2005) Characterization and matching of oil samples using fluorescence and PARAFAC. Anal. Chem., 77:2210-17.

Coble, P.G. (1996) Characterization of marine and terrestrial DOM in seawater using EEM spectroscopy. Mar. Chem., 51: 325-346.

Coble, P.G. (2014) Aquatic Organic Matter Fluorescence. In Aquatic Organic Matter Fluorescence. Coble, P.G., Lead, L., Baker, A., Reynolds, D.M. and Spencer, R.G.M., Eds., Cambridge University Press, pp. 75-122.

Cole, M.G., T. King, K. Lee (2007) Analytical technique for extracting hydrocarbons from water using sample container as extraction vessel in combination with a roller apparatus. Anal. Chem., 77: 2210-17.

Conmy, R.N., P.G. Coble and C.E. Del Castillo (2004) Calibration and performance of the WetLabs' SAFIre *in situ* fluorometer using seawater. Contin. Shelf Res., 24: 431-42.

Conmy, R. N., et al. (2014a) Submersible Optical Sensors Exposed to Chemically Dispersed Crude Oil: Wave Tank Simulations for Improved Oil Spill Monitoring. Environ Sci Technol 48(3): 1803-1810.

Conmy, R.N., R.F. Chen, C.E. Del Castillo, B. Downing (2014b) Calibrations and Quality Control of *In situ* Sensors. In: Fluorescence Applications in Aquatic Science. Eds: A. Baker & P.G. Coble, Cambridge Univ. Press, 31 pp.

Fingas, M. (2011) Introduction to Oil Chemistry and Properties. In Oil Spill Science and Technology; Fingas, M., Eds; Elsevier. pp. 51-59.

Frank, U. (1978) A Review of Fluorescence Spectroscopic Methods for Oil Spill Source Identification. Toxicological and Environment Chemistry Rev., 2:163-185.

Fuller, C.B., J.S. Bonner, C.A. Page, G. Arrambide, M.C. Sterling, Jr., T. Ojo (2003) Field instruments for real time in-situ crude oil concentration measurements. A Conrad Blucher Institute, Texas A&M Corpus Christi Report, 10 pp.

Johansen, O., et al. (2013) Droplet breakup in subsea oil releases - Part 2: Predictions of droplet size distributions with and without injection of chemical dispersants. Marine Pollution Bulletin 73(1): 327-335.

Joint Analysis Group Report (2010) Review of Data to Examine Subsurface Oil in the Vicinity of DWH MC-252, May 19-June 19, 2010; 29 pp.

Kepkay, P., W. Young, J.B.C. Bugden, Z. Li, K. Lee (2008) Ultraviolet fluorescence spectroscopy (UVFS): A new means of determining the effectiveness of chemical dispersants on oil spills. International Oil Spill Conference. API, Washington D.C., Savannah, GA, pp. 639-44.

King, T.L., B. Robinson, C. McIntyre, P. Toole, S. Ryan, F. Saleh, M.C. Boufadel, K. Lee (2015) Fate of surface spills of cold lake blend diluted bitumen treated with dispersant and mineral fines in a wave tank. In: Environmental Engineering Science, Vol. 32, No. 3, 01.03.2015, p. 250-261.

Lee, K., Li, Z., Boufadel, M.C., Venosa, A.D. and Scott Miles, M. (2009) Wave tank studies on dispersant effectiveness as a function of energy dissipation rate and particle size distribution. Final report submitted to NOAA/CRRC/UNH. Pp67+ appendix.

Li, Z., Lee, K., King, T., Boufadel, M.C. and Venosa, A.D., (2008) Oil droplet size distribution as a function of energy dissipation rate in an experimental wave tank 2008 International Oil Spill Conference. Americal Petroleum Institute, Washington D.C., Savannah, GA, pp. 621-626.

Li, Z., Lee, K., King, T., Boufadel, M.C. and Venosa, A.D., (2009a) Evaluating Chemical Dispersant Efficacy in an Experimental Wave Tank: 2, Significant Factors Determining *In Situ* Oil Droplet Size Distribution. Environmental Engineering Science, 26(9): 1407-1418.

Li, Z., Lee, K., King, T., Boufadel, M.C. and Venosa, A.D., (2009b) Evaluating crude oil chemical dispersion efficacy in a flow-through wave tank under regular non-breaking wave and breaking wave conditions. Marine Pollution Bulletin, 58: 735-744.

Li, Z., Lee, K., King, T., Boufadel, M.C. and Venosa, A.D., (2010) Effects of temperature and wave conditions on chemical dispersion efficacy of heavy fuel oil in an experimental flow-through wave tank. Marine Pollution Bulletin, In Press, Corrected Proof.

Li, Z., K. Lee, T. King, P.E. Kepkay, O. Mikkelsen, C. Pottsmith (2011) Monitoring dispersed oil droplet size distribution at the GOM Deepwater Horizon spill site. International Oil spill Conference Proceedings, March 2011.

Masutani, S.M., E.E. Adams (2000) Experimental Study of Multiphase Plumes with Application to Deep Ocean Oil Spills," Final Report to U.S. Dept. of the Interior, Minerals Management Service, Contract No., 1435-01-98-CT-30946.

Murphy, K. R., et al. (2010). "Measurement of Dissolved Organic Matter Fluorescence in Aquatic Environments: An Interlaboratory Comparison." Environ Sci Technol 44(24): 9405-9412.

Murphy, K. R., C.A. Stedmon, D. Graeber, R. Bro (2013) Fluorescence Spectroscopy and mutli-way techniques, PARAFAC. Anal. Methods, 5: 6557-6566.

NOAA Technical Report NOS OR&R 25 (2010): Joint Analysis Group, Deepwater Horizon Oil Spill: Review of Preliminary Data to Examine Subsurface Oil in the Vicinity of MC252, May 19 – June 19, 2010, 168 pp.

Oil Budget Calculator (2010) NOAA Report Oil Budget Calculator: Deepwater Horizon, Federal Interagency Solutions Group, 217 pp.

NRC Report (2005) National Research Council Oil Spill Dispersants: Efficacy and Effects, Washington, DC, 400 pp.

Priaro, M. (2014) A Bitumen and Dilbit Primer. https://www.behance.net/gallery/16654901/A-BITUMEN-AND-DILBIT-PRIMER (accessed June 10, 2016).

Stedmon, C.A., S. Markager, R. Bro (2003) Tracing dissolved organic matter in aquatic environments using a new approach to fluorescence spectroscopy. Mar. Chem., 82: 239-54.

Stedmon, C.A., R. Bro (2003) Characterizing dissolved organic matter fluorescence with parallel factor analysis: a tutorial. Limnol. Oceanogr. Methods, 6: 572-579.

Venosa, A.D., D.W. King, G.A. Sorial (2002a) The Baffledd Flask Test for Dispersant Effectiveness: A Round Robin Evaluation of Reproducibility and Repeatability. Spill Science &Technology Bulletin, 7(5-6): 299-308.

Venosa, A.D., K. Lee, M.T. Suidan, S. Garcia-Blanco, S. Cobanli, M. Moteleb, J.R. Haines, G. Tremblay, M. Hazelwood (2002b) Bioremediation and Biorestoration of a Crude Oil-Contaminated Freshwater Wetland on the St. Lawrence River. Bioremediation Journal,6(3):261-281.

Wickley-Olsen, E., Boufadel, M.C., King, T., Li, Z., Lee, K., Venosa, A.D. (2007) Regular and breaking waves in wave tank for dispersion effectiveness testing. In: Proceedings of the 30th Arctic and Marine Oil spill Program (AMOP) Technical Seminar, Edmonton, AB, Canada. Environment Canada, Ottawa, Ontario, Canada, pp. 161–187.

Zepp, R. G., et al. (2004). "Dissolved organic fluorophores in southeastern US coastal waters: correction method for eliminating Rayleigh and Raman scattering peaks in excitation-emission matrices." Marine Chemistry 89(1-4): 15-3.

Zhao, L., et al. (2014). "Evolution of droplets in subsea oil and gas blowouts: Development and validation of the numerical model VDROP-J." Marine Pollution Bulletin 83(1): 58-69.

ED_001324_00000298-00167

B.3.4 PARAFAC Modeling

Originally designed to model complexity in the field of psychometrics (Carroll and Chang, 1970; Harshman, 1970), parallel factor analysis (PARAFAC, also known as canonical decomposition or CANDECOMP) was first employed in the analysis of fluorescence data within the next ten years (Appellof and Davidson, 1981). Over the past twenty years, PARAFAC has been widely embraced by chemometricians and used to tease apart the overlapping fluorescence components of complex chemical mixtures containing fluorescent substances ranging from proteins and pigments to pesticides and PAHs (Andersen and Bro, 2003). More recently, PARAFAC analysis has been used in the analysis of the fate and transport of dispersed oil from the Deepwater Horizon Oil Spill (Mendoza, et al., 2013; Zhou, et al., 2003).

Presented with hundreds of complex fluorescence EEM data sets containing [samples x excitation x emission] data, PARAFAC analysis can reduce this complexity to [samples x intensity at a few important wavelength pairs] (Murphy, et al., 2014). In the past, this information gathering was often done via time-consuming "peak-picking" whereby EEMs were visually inspected for apparent F_{max} location, then fluorescence intensity data at that excitation/emission point was copied and pasted into a spreadsheet for further analysis. PARAFAC provides the capability to turn that somewhat qualitative task into a more quantitative exercise; however, careful preparation of the data is critical in order to obtain a meaningful outcome. PARAFAC analysis also allows the consideration of minor fluorescence peaks, which may have been overwhelmed by high-intensity major peaks, but may be no less important in the analysis of EEM results. More importantly, PARAFAC analysis allows for direct comparison to chemical composition upon successful modelling of an EEM data set (Murphy, et al., 2014). The steps that must be undertaken for successful PARAFAC analysis are: (1) importing raw data and assembling the dataset; (2) preprocessing to correct biases, remove scatter and normalize; (3) exploring the dataset to remove possible outliers and develop preliminary models; (4) validating the model by determining the proper number of components and evaluating model fit; (5) interpreting results (Murphy, et al., 2013).

Clearly, the fluorescence profiles of the 25 oil types in the BFT analysis are related to the underlying complexity of the chemical compounds that comprise them (Figure ??). In an attempt to identify those connections, PARAFAC analysis was performed on the fluorescence data. The PLS Toolbox (Eigenvector, Inc.) was used within MATLAB (MathWorks, Inc. 2014b) to accomplish this task. After importing raw data and assembling datasets, three constraints were applied to all samples: normalization, EEM filtering, and non-negativity. Normalization was done to compensate for the wide variation in fluorescence intensity across oil types (F_{max1} = 39.6 RU for Access Western Blend Dilbit to F_{max1} = 3090.2 RU for IFO 120) in order to prevent samples with high fluorescence intensity values from skewing the model. Further, normalization of maximum intensity to 1 (inf-Norm) was chosen rather than normalization of the entire area of fluorescence (1-Norm) to preserve differences in spectral shape. EEM filtering was applied in order to remove artifacts of the fluorescence analysis process known as first and second order Rayleigh scatter. This was accomplished by interpolating data across those regions (12 nm for first order Rayleigh and 24 nm for second order Rayleigh); zero values were also assigned to sub-Rayleigh wavelengths since fluorescence emission takes place at wavelengths above excitation due to Stokes shift. Raman scatter, the other light-related artifact which must be removed before PARAFAC analysis can

be performed, was accomplished as sample analysis was done by subtracting that day's sample blank from each sample. Finally, after running several PARAFAC test models using 4, 5, 6 and 7-component s on a dataset containing the DOR 0 sample from flask #1 of all 25 oil types, data between excitation at 200 nm and 212 nm was excluded. The inherent "noise" typically found at excitation < 240 nm, related to the low intensity of xenon lamps in that region, led to this decision. Excluding data at excitation and emission wavelengths above 680 nm was also employed in order to improve processing results since no fluorescence information of value was contained in that region.

The biggest challenge in PARAFAC modelling is in determining the most appropriate number of component factors. While it is important to ensure separation of all individual factors, it is also critical not to select too many components in order to avoid over-fitting the data. Bro suggests several ways of doing this in his PARAFAC tutorial (1997): comparison of the resulting factor profiles with background knowledge of expected components, consideration of the residuals, and split half validation of the model. The latter has also been recommended by other researchers (Harshman and Lundy, 1994; Murphy, et al., 2013). Split half analysis is accomplished by dividing the data into two independent subsets and applying the model to each of the subsets. In theory, if the correct number of components has been selected, the two halves of the data should each fit the model well; however, Murphy cautions that a relatively large data set is necessary in order for this to hold true (2013). Smilde, et al., (2004) also caution that some phenomenon observed in a data subset which does not match the overall model may just be present in that particular random half of the data. Thus, we might anticipate that split half validation will work better with samples within oil weight subdividions than with the dataset containing all 25 oil types as a whole. Bro and Kiers (2003) have also advised using core consistency of the model to validate that the correct number of components have been selected. All of these methods were employed for the following analyses by first noting the percentage of data fit by the model, next checking the core consistency of the model, then inspecting residuals, inspecting the loadings for Mode 3 (excitation) and Mode 2 (emission), and inspecting EEMs of each component. Finally, split half analysis was done. In all cases, several models were run with different numbers of components to ensure selection of the most appropriate model.

All 25 Oil Types

DOR 0

Initially, a five-component model was fit to the dataset, followed by 4-, 6- and 7-component models. Best overall fit was obtained with the six-component model, which explained 99.504% of the data. Core consistency was 52%, and split half validation was 56.4% (shown below). Review of residuals showed they were minimal with random distribution, inspection of plots of Mode 2 and Mode 3 loadings, as well as EEMs of individual components all supported choice of the 6-factor model for best fit.

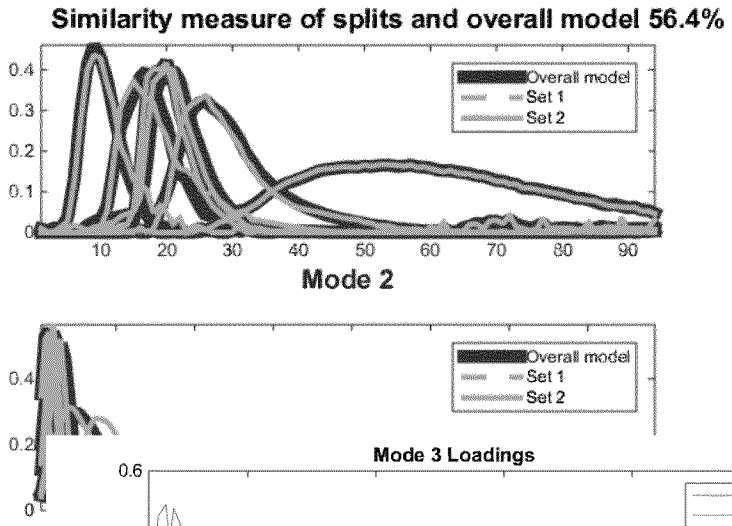

Figure ??. Example of split half validation for the 6-component model of 25 oil types at DOR 0 showing individual fit of data splits (Set 1, left; and Set 2, right) compared to overall model for Mode 2 (top) and Mode 3 (bottom) loadings.

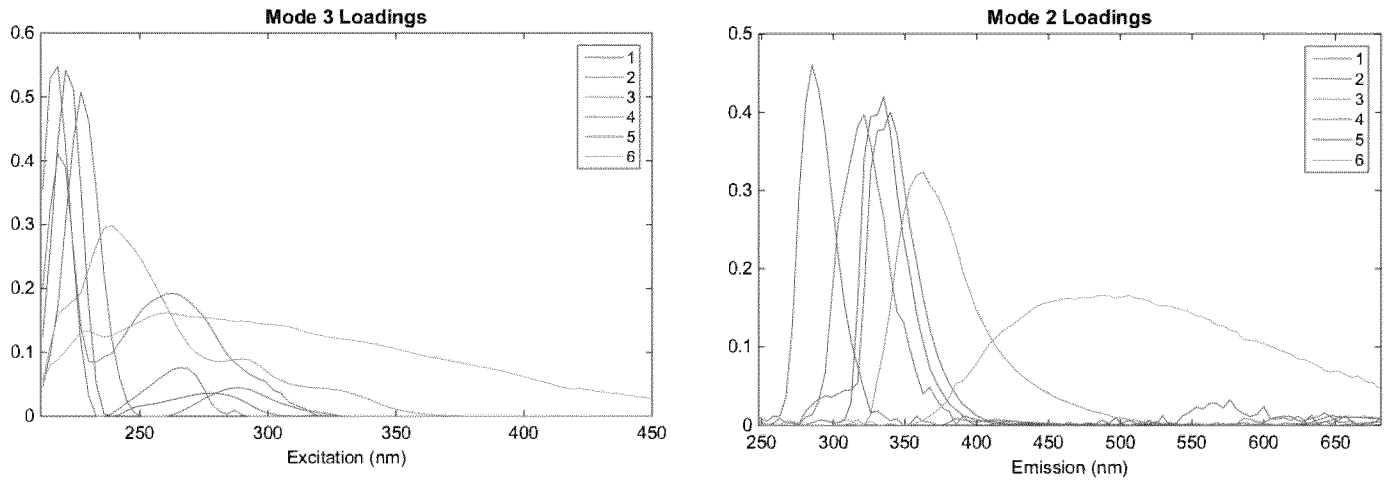

Figure ??. Mode 3 Loadings(Excitation) and Mode 2 Loadings (Emission) for all 25 oil types—DOR0 using 6-component model. Note difference in x-axis scales. Although components are tightly spaced, all appear as separate and distinct peaks.

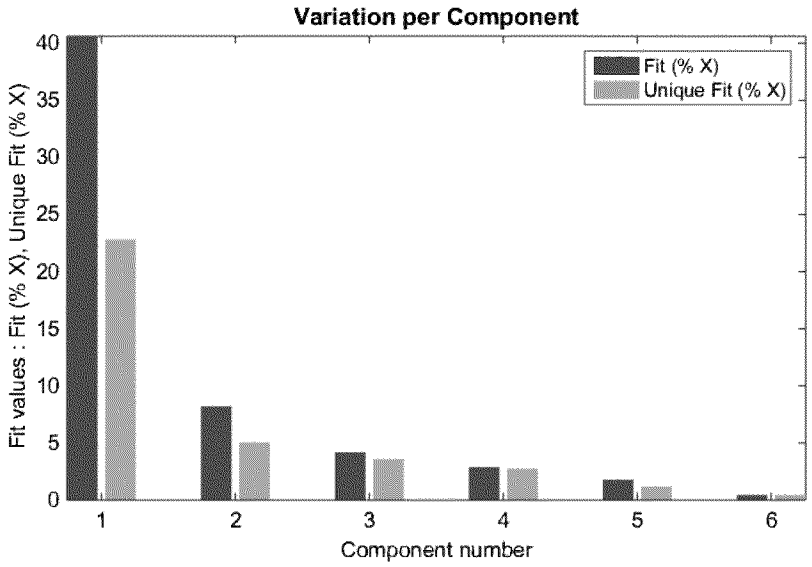

Figure ??. Variation per Component shows Component 1 accounted for >20% to 40% (unique fit and fit) of the data, while Component 2-contributed 5-10% (unique fit and fit) and Components 3-6 accounted for 5% or less of the data, respectively. While Component 6 accounted for a very low percentage of the data, the 6-component model was still a better fit to the data than the 5-component model.

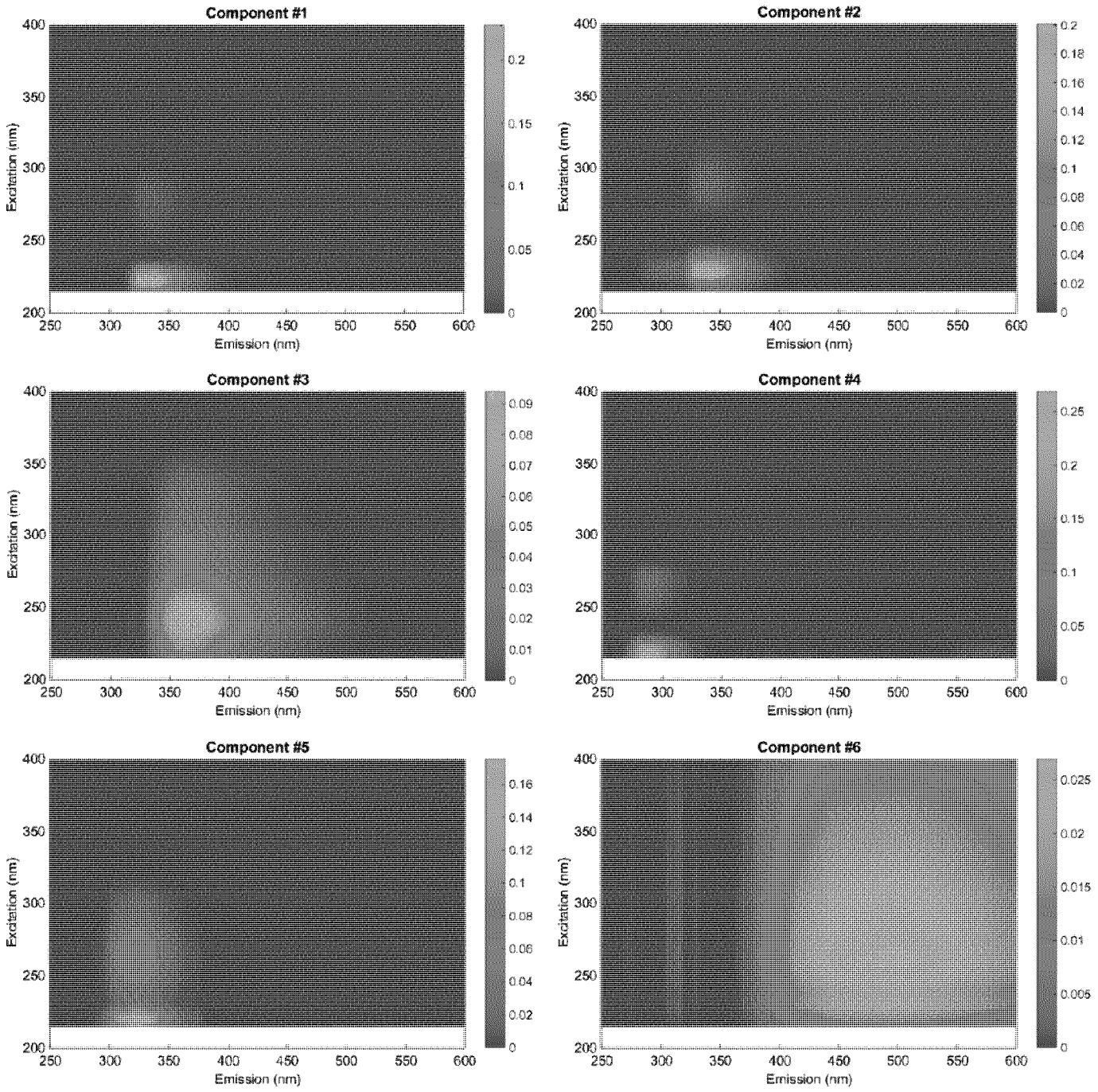

Figure ??. EEM views of the six components of PARAFAC model for 25 oil types at DOR 0. Component #1: F_{max} = Ex 224nm/Em 335nm; Component #2: F_{max} = Ex 230nm/Em 340nm; Component #3: Fmax = Ex 239nm/Em 363nm; Component #4: Fmax = Ex 218nm/Em 290 nm; Component #5: Fmax = Ex 221nm/Em 322nm; Component #6: Fmax = Ex 260nm/Em 474-511nm

DOR 1:100

A six-component model was fit to the dataset containing all 25 oil types at DOR 1:00 since that was the best fit for the DOR 0 dataset, followed by a 7-component model, which returned an error warning that two or more components may be fitting the same feature, as well as core consistency <0%. Finally, a 5-component model was fit to the dataset. Interestingly, for the DOR 1:100 dataset, the 5-component model proved to be the best fit, explaining 99.353% of the data with core consistency of 72% and split half validation of 75.8%. Residuals were minimal and randomly distributed, and visual inspection of loadings and component EEMs led to acceptance of the 5-component model.

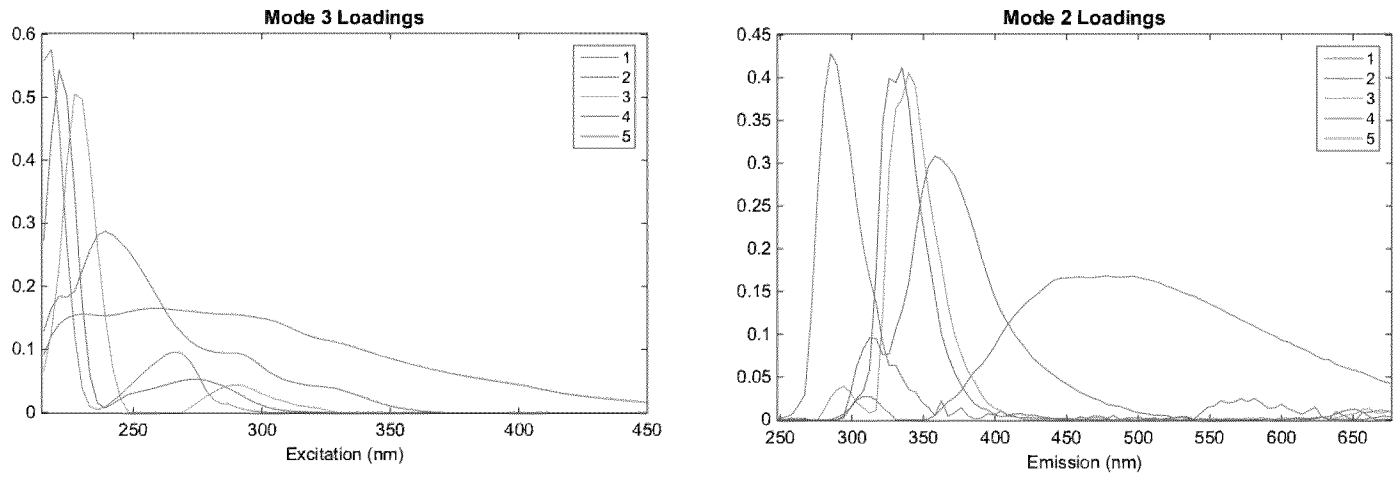

Figure ??. Mode 3 Loadings (Excitation) and Mode 2 Loadings (Emission) for all 25 oil types—DOR 1:100 using 5-component model. Note difference in x-axis scales. Although components are tightly spaced, all appear as separate and distinct peaks.

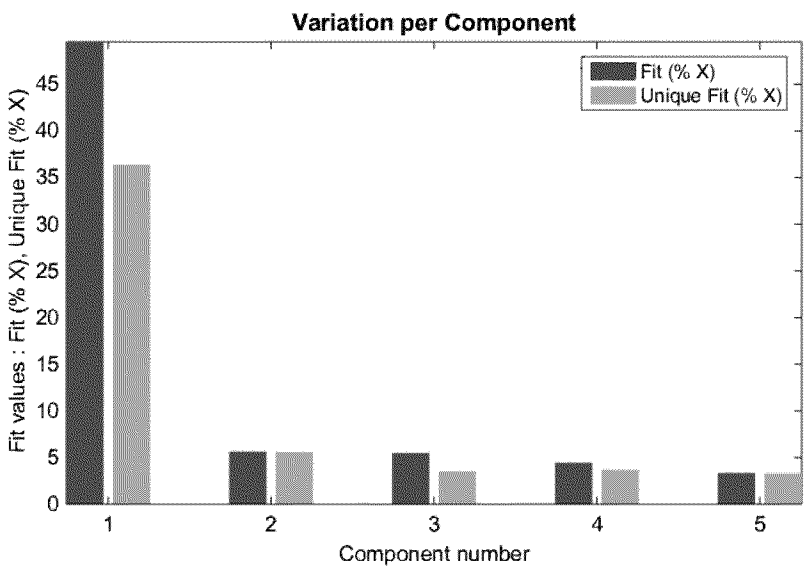

Figure ??. Variation per Component shows Component 1 accounted for >35% to almost 50% (unique fit and fit) of the data, while Components 2-5 accounted for 5% or less of the data, respectively.

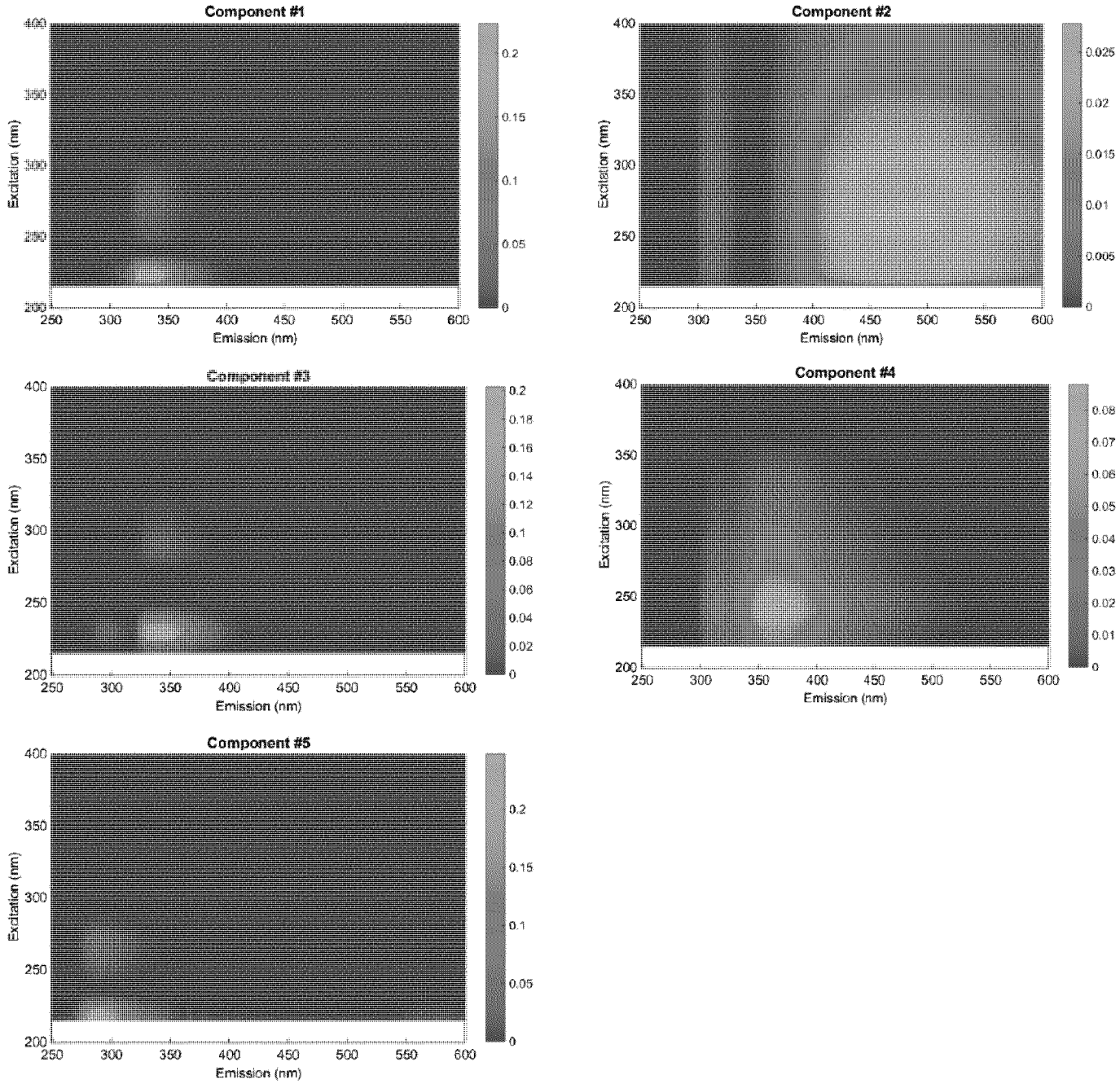

Figure ??. EEM views of the five components of PARAFAC model for 25 oil types at DOR 1:100. Component #1: F_{max} = Ex 224nm/Em 335nm; Component #2: F_{max} = Ex 254-266nm/Em 455-501nm; Component #3: F_{max} = Ex 230nm/Em 344nm; Component #4: F_{max} = Ex 242nm/Em 363 nm; Component #5: F_{max} = Ex 218nm/Em 290nm.

DOR 1:20

Once again, a six-component was fit to the dataset containing all 25 oil types at DOR 1:20; however, an error message warning that two or more components may be fitting the same data was displayed, and the core consistency was <0%. Fitting a 5-component model to the data, however, resulted in 98.891% of the data explained by the model as well as core consistency of 84% and a split half validation of 84%. Overall, residuals were minimal and randomly distributed; however, residuals appeared to occur at somewhat higher wavelengths than at other DORs. Visual inspection of loadings and component EEMS led to final acceptance of the 5-component model.

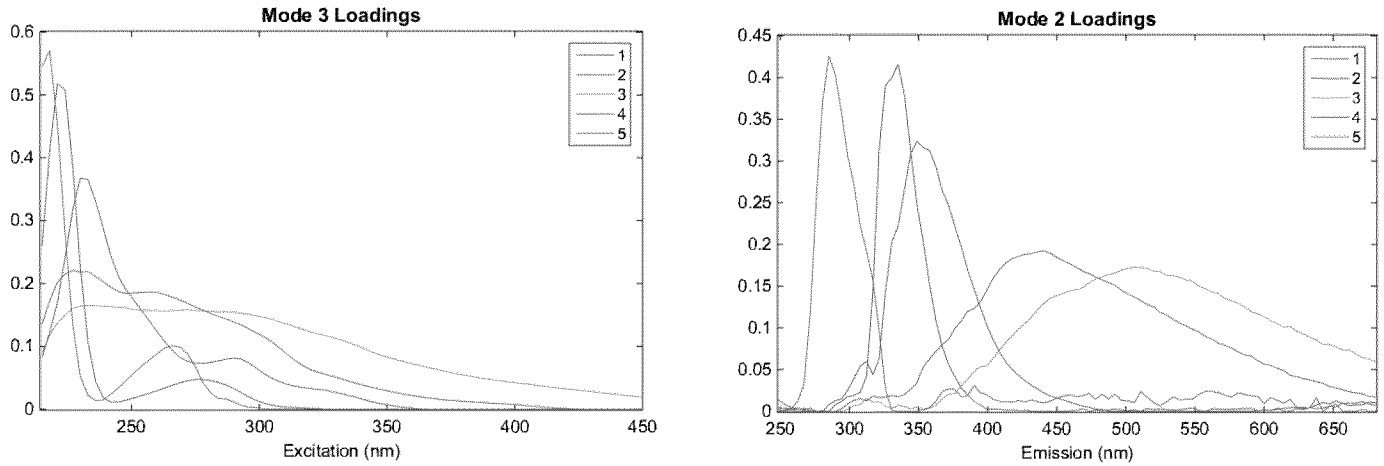

Figure ??. Mode 3 Loadings (Excitation) and Mode 2 Loadings (Emission) for all 25 oil types—DOR 1:20 using 5-component model. Note difference in x-axis scales. Effect of full dispersion appears to broaden and shift emission peaks to longer wavelengths.

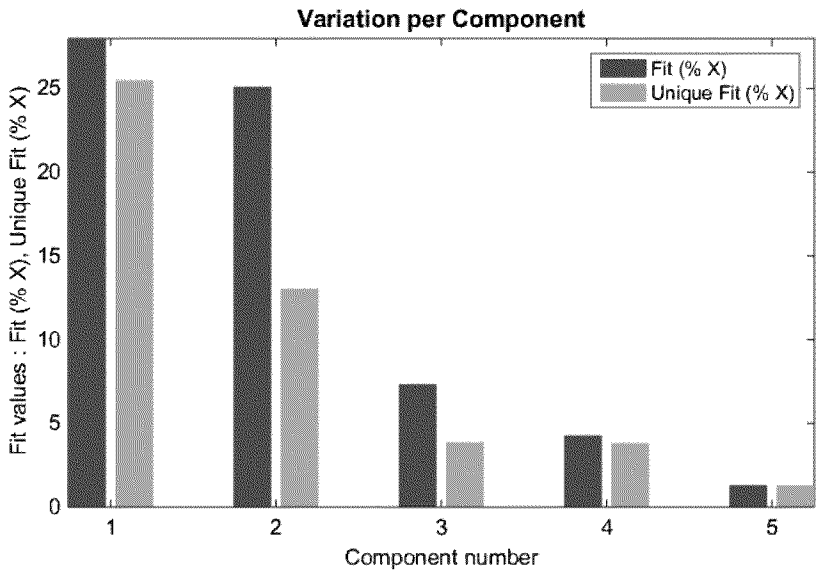

Figure ??. Variation per Component shows Component 1 accounted for 25 to 30% of the data (unique fit and fit) while Component 2 has increased to >10% to 25% (unique fit and fit) of the data. Contribution from Component 3 and 4 have increased, as well.

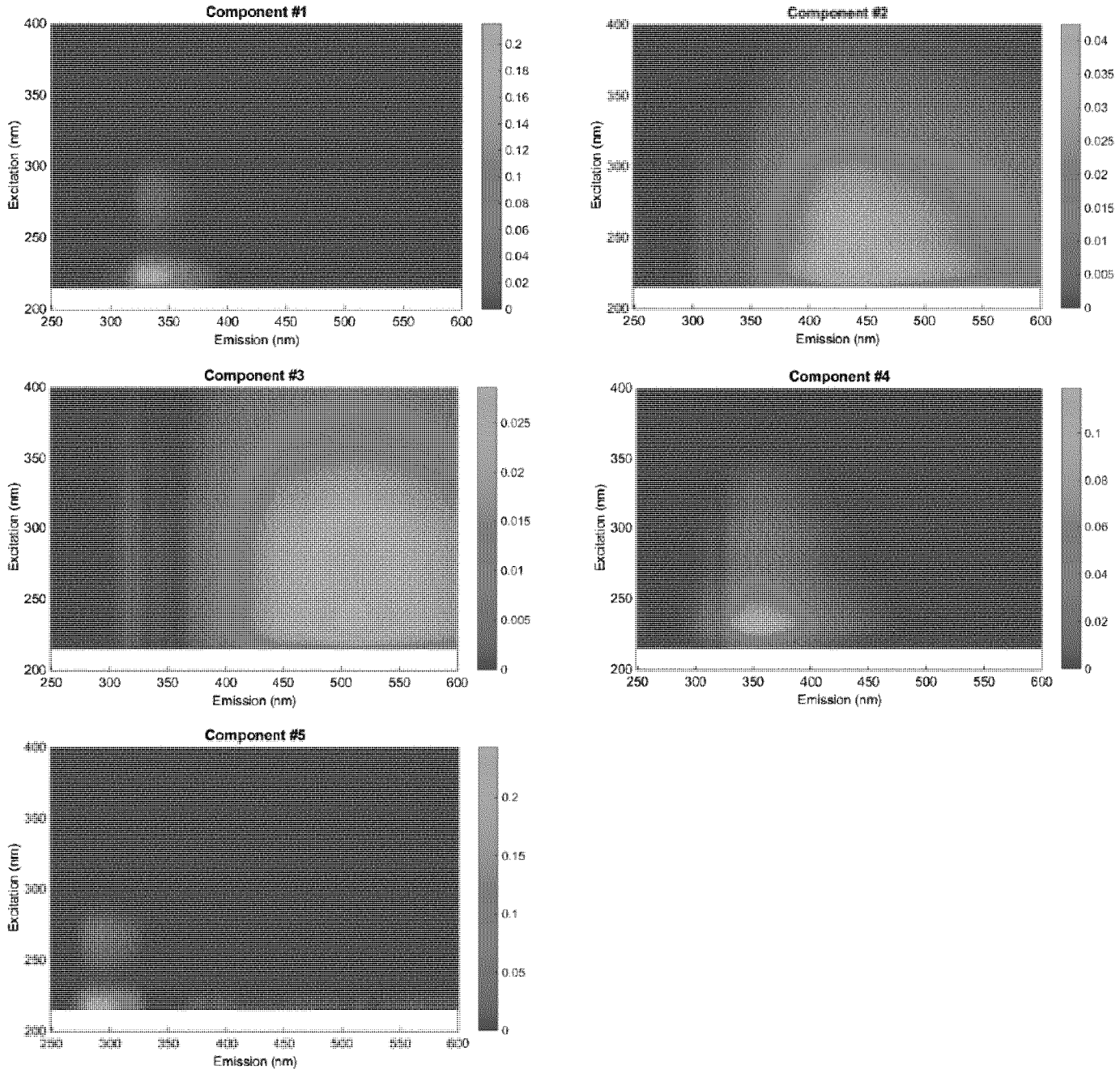

Figure ??. EEM views of the five components of PARAFAC model for 25 oil types at DOR 1:20. Component #1: F_{max} = Ex 224nm/Em 335nm; Component #2: F_{max} = Ex 233-266nm/Em 432-450nm; Component #3: F_{max} = Ex 230-242nm/Em 501-520nm; Component #4: F_{max} = Ex 233nm/Em 349nm; Component #5: F_{max} = Ex 218nm/Em 290nm.

Conclusions

PARAFAC analysis of EEM datasets for the 25 oil types at DOR 0, DOR 1:100 and DOR 1:20 show interesting changes in fluorescence intensity with increasing dispersion. However, we see a decrease in distinct components from six at DOR 0 to five at DOR 1:100 and 1:20. From analysis of plots of Mode 3 (Excitation) and Mode 2 (Emission) Loadings, it appears that increased dispersion results in a broadening and shift to longer emission wavelengths as well as in a larger contribution of fluorescence intensity at higher wavelengths. Upon examination of the EEMs of each component, several other patterns emerge. Even with the minimal dispersion at DOR 1:100, contribution to the overall model from a broad fluorescence peak which provided the least contribution to the overall model at DOR 0--Component #6—became second in importance at DOR 1:100, albeit with a contribution to the model of only about 5%. Upon full dispersion at DOR 1:20, this broad, high-wavelength peak retained importance to the model of approximately 5-7%; however, another broad, but slightly lower wavelength peak appeared as Component #2 with 12-25% contribution to the overall model. Throughout the entire analysis, Component #1 at Ex 224nm/Em 335nm remained the most important contribution to the model, which confirms this fluorescence region as the best target for detecting oil in the marine environment. However, since the region represented by Component #2 in the DOR 1:20 dataset becomes a major contribution to the model only upon effective dispersion, the FIR ratio (Bugden et al., 2008) can be used to track this important parameter.

References to add:

Appellof, C.J., and E.R. Davidson (1981) Strategies for Analyzing Data from Video Fluorometric Monitoring of Liquid Chromatographic Effluents. J. Anal. Chem. 53:2053-2056.

Bro, R. (1997) PARAFAC. Tutorial and applications. Chemometrics and Intelligent Laboratory Systems. 38:149-171.

Bro, R., and H.A.L. Kiers (2003) A new efficient method for determining the number of components in PARAFAC models. J. Chemometrics 17:274-286.

Carroll, J.D. and J.-J. Chang (1970) Analysis of Individual Differences in Multidimensional Scaling via an N-Way Generalization of "Eckart-Young" Decomposition. Psychometrika 35:283-319.

Harshman, R.A. (1970) Foundations of the PARAFAC procedure: Models and conditions for an "explanatory" multimodal factor analysis. UCLA Working Papers in Phonetics 16:1-84.

Harshman, R.A. and M.E. Lundy (1994) PARAFAC: Parallel factor analysis. Computational Statistics & Data Analysis 18:39-72.

Mendoza, W.G., D.D. Riemer, R.G. Zika (2013) Application of fluorescence and PARAFAC to assess vertical distribution of subsurface hydrocarbons and dispersant during the Deepwater Horizon oil spill. Environmental Science Processes & Impacts 15:1017-1030.

Murphy, K.R., Bro, R., Stedmon, C.A. (2014) Chemometric Analysis of Organic Matter Fluorescence. In: Aquatic Organic Matter Fluorescence. Eds: Coble, P.G., Lead, J., Baker, A., Reynolds, D.M., Spencer, R.G.M. Cambridge University Press, pp.339-375.

Smilde, A., Bro, R., Geladi, P. (2004) Validation and Diagnostics. In: Multi-way Analysis With Applications in the Chemical Sciences. John Wiley & Sons, Ltd. Pp. 145-173

Zhou, Z, Guo, L., Shiller, A.M., Lohrenz, S.E., Asper, V.L., Osburn, C.L. (2003) Characterization of oil components from the

Deepwater Horizon oil spill in the Gulf of Mexico using fluorescence EEM and PARAFAC techniques. Marine Chemistry 148:10-21.

To: Conmy, Robyn[Conmy.Robyn@epa.gov]
From: Schubauer-Berigan, Joseph
Sent: Thur 6/23/2016 9:23:29 PM
Subject: RE: QAPP signature
G-LRPCD-0030110-QP-1-0_160531_final_JSB.pdf

Here you go.

Joseph P. Schubauer-Berigan, Ph.D.
Chief, Environmental Stressors Management Branch
USEPA, Office of Research and Development
National Risk Management Research Laboratory
26 W. Martin Luther King Drive
Cincinnati, OH 45268
schubauer-berigan.joseph@epa.gov
Office 513-569-7734

Cell 513-516-5904
FAX 513-569-7620

From: Conmy, Robyn
Sent: Wednesday, June 22, 2016 8:02 AM
To: Schubauer-Berigan, Joseph <Schubauer-Berigan.Joseph@epa.gov>
Subject: QAPP signature

Hi Joe,

Can you please sign the attached QAPP and send back to me to have Pegasus sign?

Thanks,

Robyn

<>/<>/<>/<>/<>/<>/<>/<>/<>/<>/<>/<>/<>/<>/<>/<>/<>/<>

Robyn N. Conmy, Ph.D.

Research Ecologist

USEPA/NRMRL/LRPCD

26 West MLK Drive

Cincinnati, Ohio 45268

513-569-7090 (office)

513-431-1970 (EPA mobile)

727-692-5333 (Personal mobile)

conmy.robyn@epa.gov